

Bond University

DOCTORAL THESIS

DNA Typing Methods for Highly Degraded Samples

Hughes-Stamm, Sheree

Award date:
2013

[Link to publication](#)

General rights

Copyright and moral rights for the publications made accessible in the public portal are retained by the authors and/or other copyright owners and it is a condition of accessing publications that users recognise and abide by the legal requirements associated with these rights.

- Users may download and print one copy of any publication from the public portal for the purpose of private study or research.
- You may not further distribute the material or use it for any profit-making activity or commercial gain
- You may freely distribute the URL identifying the publication in the public portal.

Take down policy

If you believe that this document breaches copyright please contact us providing details, and we will remove access to the work immediately and investigate your claim.



DNA TYPING METHODS FOR HIGHLY DEGRADED SAMPLES

Sheree Hughes-Stamm

Faculty of Health Sciences & Medicine
Bond University

A thesis submitted in total fulfilment of the requirements of the degree of
Doctor of Philosophy by Research

July 2012

ABSTRACT

Highly degraded biological samples may be encountered in cases of mass disasters, missing persons cases, and forensic casework. As biological tissue degrades, DNA becomes progressively more fragmented and a decrease in the ability to gain an accurate DNA profile results. The successful typing of highly degraded DNA can be further complicated by also having chemical modifications (DNA damage). Such highly degraded samples often produce incomplete or no STR profiles. Alternate genotyping strategies such as mini-STRs and SNPs have proven to be more successful in profiling such difficult samples and were therefore investigated in this thesis.

A quantitative PCR (qPCR) assay that can simultaneously quantify total human nuclear DNA, male DNA and the extent of DNA degradation was examined in this study. By considering the amount of DNA and the degradation ratio of a sample, a general prediction of genotyping success using STR, mini-STR and SNP analysis could be made, thereby determining which genotyping method may be more informative and maximising the evidentiary value of each sample.

Bone and tooth samples were subjected to one of five harsh environmental conditions to produce skeletal samples of varying levels of preservation. These included surface exposure, burial, immersion in saltwater or freshwater, and extreme heat. Overall, the DNA was most susceptible to degradation from UV exposure, extensive microbial activity and extreme heat. Two commercial STR kits (AmpFISTR® NGM™ and PowerPlex® ESI 16) were used to amplify these samples and showed that both kits performed well with low and moderately degraded samples. However, with highly degraded samples, more complete STR profiles were consistently obtained using the PowerPlex® ESI 16 kit. The improved performance of the PowerPlex® ESI kit with highly degraded samples was also seen when STR-typing 200 year old skeletal remains recovered from the HMS Pandora shipwreck. An alternative method for retrieving dentine from teeth for DNA analysis was investigated. The quality and amount of amplifiable DNA per milligram of powder were both significantly higher than when the entire tooth root was powdered for DNA extraction.

A 96-plex GoldenGate® Genotyping SNP assay comprised of SNPs known to have association with hair, eye or skin colour was evaluated for forensic use. The assay performed well with high molecular weight genomic samples, but a significant reduction in the SNP call rate and accuracy was observed with whole genome amplified samples, and samples that were degraded and/or in low amounts. A pilot study testing the predictive power of the same 96-plex pigmentation SNP panel found that ancestry determination for the three major population groups (Caucasian, African American and Hispanic) was robust. The prediction of eye colour was reasonably accurate, but the ability to determine hair and skin colour was weaker and yielded more inconsistent results when blind tested.

Finally, in an attempt to improve the quality of highly degraded DNA template prior to multiple displacement amplification (MDA) and STR-typing, several methods of DNA repair were investigated. Linear ligation to increase template length and circularisation of fragmented samples to create a more ideal template for MDA were both unsuccessful, and failed to produce more complete STR profiles. Commercial DNA repair cocktails and WGA kits also failed to yield any consistent improvement in the genotyping of degraded samples. A marked variation in DNA quantity values was observed when determining the amount of MDA end product using qPCR. The amount of MDA product measured was dependant on which locus was used for detection during qPCR. These data reflected the inherent amplification bias that occurs during the MDA process, and highlighted the importance of choosing suitable loci for qPCR quantification of MDA product and genotyping whole genome amplified samples.

DECLARATION

This thesis is submitted to Bond University in fulfilment of the requirements for the degree of Doctor of Philosophy by Research.

This thesis represents my own original work towards this research degree and contains no material which has been previously submitted for a degree or diploma at this University or any other institution, except where due acknowledgement is made.

Sheree Hughes-Stamm

July, 2012

ACKNOWLEDGEMENTS

I would first like to thank the Faculty of Health Sciences and Medicine (HSM) at Bond University for the financial support to successfully complete this doctoral research. In addition, the provision of my Australian Postgraduate Award Scholarship by Bond University and the Australian Government provided the stipend which enabled me to undertake these postgraduate studies. Additional funding for this research was provided by the United States National Institute of Justice (NIJ), and the Technical Support Working Group (TSWG) of the United States Government National Interagency Research and Development Program for Combating Terrorism. In addition, substantial in-kind support was provided by Illumina, Inc. in the form of long-term loan of the BeadExpress™ scanner, custom primer design, and the provision of all bead-plates and reagents.

I must also acknowledge both the HSM faculty and Bond University Graduate School of Research for the provision of substantial funds to attend one national and two international forensic science conferences in order to present works from this thesis. I would also like to thank the Australian and New Zealand Forensic Science Society for providing additional financial support to attend one international and two national forensic symposia to present results of this research.

I would like to sincerely thank my supervisors Professor Angela van Daal and Associate Professor Kevin Ashton for their continual support, advice and encouragement. They have been true mentors, guiding my learning, having confidence in my abilities and pushing my boundaries. I also owe a big thank you to Professor Kuldip Bedi, Associate Professor Walter Wood and Associate Professor Gillian Renshaw who all encouraged me to undertake this PhD. They have been strong advisors in both my academic and personal lives even before the inception of this degree.

Much thanks and gratitude must also be extended to the fellow higher degree research students within our forensic genetics research group at Bond University, namely Kelly Grisedale, Mark Barash, Kat Sanders and Olga Kondrashova. They have made this journey enjoyable by adding fun and laughter into each working day and

providing the most fantastic support throughout my studies. I will always value their friendship. I know the strong professional relationships we have built during these last few years will continue, and we will hopefully participate in collaborative research in the future.

Sincere thanks must also be extended to several professionals who have made this research possible; Dr. Ray Randle, an orthopaedic surgeon and Dr. John Cosson, a maxillo-facial surgeon at John Flynn Private Hospital who have kindly provided the bone and tooth samples used in this study. Dr. Frauke Warnke, a dentist from the School of Dentistry and Oral Health, Griffith University also assisted me greatly with the physical process of extracting dentine and X-ray imaging the teeth. In addition, the fieldwork required for this research was conducted on a plot of land donated specifically for this study by Mr Tim Connolly, the Director of New Haven Funerals. I wish to thank all four of these wonderful people for their continual support, and for being so generous with their time and resources.

On a personal note, I must thank from the bottom of my heart my husband Shaun and children Tiarne and Brayden who have been extremely supportive of my every endeavour throughout these studies. They have sacrificed substantial amounts of attention and quality family time, and have never complained when I have been away travelling for weeks at a time.

One very special person in my life, fellow PhD student and best friend, Nicola Beckett has been there for me to laugh and cry with over the past four years. We have travelled the world together attending forensic conferences and she has been my rock and greatest supporter. I could have given up numerous times if not for her inspirational pep talks.

Finally, I wish to thank my parents. Since I was a little girl my Dad has always told me that I could do anything I wanted to in this world, and has always been extremely proud of everything I have ever done. My mother is a jewel in my life, and without her endless generosity and love, it would not have been possible to complete these studies.

TABLE OF CONTENTS

ABSTRACT	i
DECLARATION	iii
ACKNOWLEDGEMENTS	iv
TABLE OF CONTENTS	vi
LIST OF TERMS AND ABBREVIATIONS	x
DEFINITIONS AS APPLIED TO THIS DOCUMENT	xi
LIST OF FIGURES	xii
LIST OF TABLES	xvii
1 CHAPTER ONE.....	1
1.1 Introduction	2
1.2 Factors Influencing the Success of DNA Profiling.....	4
1.2.1 Environmental Insults.....	4
1.2.2 DNA Damage	4
1.2.3 DNA Degradation	7
1.2.4 PCR Inhibitors.....	7
1.3 Highly Degraded Remains in Natural and Mass Disasters	8
1.3.1 Bone	9
1.3.2 Teeth	11
1.4 Genetic Markers for Identity Testing.....	13
1.4.1 Short Tandem Repeats (STRs)	15
1.4.2 Mini-STRs.....	17
1.4.3 Mitochondrial DNA (mtDNA)	19
1.4.4 Single Nucleotide Polymorphisms (SNPs)	21
1.4.5 Markers of the Future	26
1.5 DNA Quantification and Assessment of Degradation.....	27
1.6 Alternate Technologies for Challenging Samples	33
1.6.1 Ancient DNA Techniques.....	33
1.6.2 Optimised Extraction.....	33
1.6.3 Low Copy Number (LCN) Methods.....	34
1.6.4 Whole Genome Amplification (WGA)	37
1.6.5 Repair Strategies	47
1.6.6 PCR Enhancers.....	50
1.7 Project Aims	51

2	CHAPTER TWO.....	53
2.1	INTRODUCTION.....	58
2.2	MATERIALS and METHODS.....	59
2.2.1	Sonication.....	59
2.2.2	Capillary Electrophoresis.....	59
2.2.3	Quantitative PCR (qPCR).....	59
2.2.4	Genotyping.....	61
2.3	RESULTS and DISCUSSION.....	62
2.3.1	qPCR Degradation Assay.....	64
2.3.2	Mixtures.....	67
2.3.3	Genotyping.....	69
2.4	CONCLUSIONS.....	76
3	CHAPTER THREE.....	78
3.1	INTRODUCTION.....	80
3.1.1	Case Study: HMS Pandora Remains.....	85
3.2	MATERIALS AND METHODS.....	86
3.2.1	Biological samples.....	86
3.2.2	Fieldwork Plot.....	87
3.2.3	Environmental Monitoring.....	88
3.2.4	Surface Remains.....	90
3.2.5	Buried Remains.....	91
3.2.6	Burnt Remains.....	92
3.2.7	Water Immersion.....	93
3.2.8	Pandora Remains.....	94
3.2.9	Genetic Analysis.....	94
3.3	RESULTS and DISCUSSION.....	101
3.3.1	Environmental Observations.....	101
3.3.2	Taphonomic Observations.....	108
3.3.3	DNA Degradation.....	152
3.3.4	Genotyping.....	155
3.3.5	Comparative Genotyping of Two Dentine Extraction Methods from Teeth.....	160
3.3.6	Case Study – HMS Pandora Remains.....	175
3.3.7	STRBoost®.....	182
3.4	CONCLUSIONS.....	193

4	CHAPTER FOUR.....	197
4.1	INTRODUCTION.....	199
4.2	METHODS.....	204
4.2.1	Samples.....	204
4.2.2	Whole genome amplification (WGA).....	206
4.2.3	SNP Analysis.....	207
4.3	RESULTS AND DISCUSSION.....	211
4.3.1	96-SNP Multiplex Assay.....	211
4.3.2	Sensitivity Study.....	216
4.3.3	Whole Genome Amplification (WGA) Protocol Study.....	217
4.3.4	Challenging Samples.....	220
4.3.5	Phenotype and Ancestry Prediction.....	227
4.4	CONCLUSION.....	253
5	CHAPTER FIVE.....	256
5.1	INTRODUCTION.....	257
5.2	General Materials and Methods.....	260
5.2.1	DNA Extraction and Quantitation.....	260
5.2.2	DNA Degradation.....	260
5.2.3	Assessment of DNA Repair.....	261
1.	Polymerase Chain Reaction (PCR) Quadruplex Assay.....	261
2.	Commercial Forensic STR PCR Amplification Kits.....	263
5.3	Whole Genome Amplification.....	263
5.3.1	Materials and Methods.....	264
5.3.2	Results and Discussion.....	265
5.4	Linear Ligation + MDA.....	272
5.4.1	Material and Methods.....	274
5.4.2	Results and Discussion.....	275
5.5	CircLigase™.....	281
5.5.1	Materials and Methods.....	281
5.5.2	Results and Discussion.....	282
5.6	PreCR®.....	291
5.6.1	Materials and Methods.....	292
5.6.2	Results and Discussion.....	294
5.7	Restorase®.....	299
5.7.1	Materials and Methods.....	299

5.7.2	Results and Discussion	301
5.8	REPLIg-FFPE	304
5.8.1	Materials and Methods	305
5.8.2	Results and Discussion	305
5.9	Alternative DNA Quantitation	310
5.9.1	Materials and Methods	312
5.9.2	Results and Discussion	313
5.10	Conclusions	317
6	CHAPTER SIX.....	320
6.1	Introduction	321
6.2	Comparative Genotyping of Degraded Samples.....	322
6.3	Genotyping of Environmentally Challenged Samples	323
6.3.1	Comparative Dentine Extraction from Teeth.....	324
6.3.2	Skeletal Remains from HMS Pandora.....	324
6.4	Pigmentation SNP Panel	325
6.5	DNA Repair	328
6.6	Future Directions	330
6.7	Final Conclusions.....	331
6.8	Summary.....	333
7.	REFERENCES	334
8.	APPENDICES	357

LIST OF TERMS AND ABBREVIATIONS

DNA	Deoxyribonucleic acid
dsDNA	Double stranded DNA
ssDNA	Single stranded DNA
nDNA	nuclear DNA
gDNA	genomic DNA
mtDNA	mitochondrial DNA
ng	Nanograms
pg	Picograms
µL	Microlitres
nt	Nucleotides
indels	Insertion/deletion polymorphisms
STR	Short Tandem Repeats
mini-STR	mini-Short Tandem Repeats
SNP	Single Nucleotide Polymorphisms
AmpFLP	Amplified fragment length polymorphisms
VNTR	Variable Number Tandem Repeat
AIMs	Ancestry Informative Markers
RFLP	Restriction Fragment Length Polymorphism
H ₂ O	Water
HMW	High Molecular Weight
AP	Apurinic/aprimidinic
ABI	Applied Biosystems Inc.
PCR	Polymerase Chain Reaction
MDA	Multiple Displacement Amplification
WGA	Whole Genome Amplification
DOP-PCR	Degenerate oligonucleotide primed PCR
RCA	Rolling Circle Amplification
RCA-RCA	Restriction and Circularisation-Aided Rolling Circle Amplification
PEP	Primer Extension Pre-amplification
PGD	Preimplantation Genetics and Diagnosis
IPC	Internal PCR Control
LCN	Low Copy Number
LTDNA	Low Template DNA
SWAGDAM	Scientific Working Group on DNA Analysis Methods
ANZFSS	Australia and New Zealand Forensic Science Society
ENFSI	European Network of Forensic Science Institutes
EDNAP	European DNA Profiling group
ICMP	International Commission for Missing Persons
PHR	Heterozygote peak height ratios

DEFINITIONS AS APPLIED TO THIS DOCUMENT

Degraded DNA	Double stranded DNA broken into small fragments.
DNA Degradation	The process of the DNA double helix breaking into smaller fragments.
Damaged DNA	Minor destruction of DNA molecule inducing modifications and lesions such as apurinic/apyrimidinic sites, nicks, cross-linkages, oxidative damage etc.
Decomposition	Breakdown of human remains and biological tissues after death.

LIST OF FIGURES

CHAPTER ONE

FIGURE 1.1	DIAGRAMATIC REPRESENTATION OF A HUMAN MOLAR [60]	12
FIGURE.1.2	OVERVIEW OF THE POLYMERASE CHAIN REACTION (PCR).....	14
FIGURE 1.3	TYPICAL STR PROFILES FROM HMW AND DEGRADED DNA SAMPLES.	16
FIGURE.1.4	MINI-STR PRIMER AND MULTIPLEX KIT DESIGNS.....	17
FIGURE 1.5	REAL-TIME PCR AMPLIFICATION CURVES.....	29
FIGURE 1.6	FLOWCHART DEPICTING THE CHOICE OF DNA STRATEGY AFTER QUANTIFICATION WITH THE QPCR ASSAY. [191].....	32
FIGURE 1.7.	SCHEMATIC REPRESENTATION OF THE HYPERBRANCHED STRAND- DISPLACEMENT AMPLIFICATION REACTION OF MDA [274]	41
FIGURE 1.8	ROLLING CIRCLE AMPLIFICATION (RCA).	45
FIGURE 1.9	OUTLINE OF RCA–RCA (RESTRICTION AND CIRCULARIZATION-AIDED ROLLING CIRCLE AMPLIFICATION) OF DAMAGED AND PARTIALLY DEGRADED FFPE SAMPLES	46
FIGURE 1.10.	OVERVIEW OF THE FFPE REPLI-G PROCESS.	49

CHAPTER TWO

FIGURE 2.1	FRAGMENT ANALYSIS OF ARTIFICIALLY DEGRADED SAMPLES USING THE QIAXCEL SYSTEM	63
FIGURE 2.2	SENSITIVITY OF THE QUADRUPLEX QPCR ASSAY IN ASSESSING DNA DEGRADATION [#]	65
FIGURE 2.3	SENSITIVITY STUDY AND COMPARATIVE SUCCESS RATES OF LOCI RETRIEVAL.	71
FIGURE 2.4	AMPFLSTR [®] PROFILER PLUS [®] PCR AMPLIFICATION KIT LOCUS DROP-OUT [#] RATES COMBINED OVER ALL TEMPLATE AMOUNTS (2NG-15.2PG) OF UNDEGRADED AND DEGRADED SAMPLES.	73
FIGURE 2.5	COMPARISON OF THE COMBINED SUCCESS OF THE SMALLEST LOCI (≤150BP) IN EACH OF THE PROFILER PLUS AND MINIFILER KITS WITH THE FULL 53SNP PANEL.	74
FIGURE 2.6.	COMPARISON OF SUCCESSFUL LOCI RETRIEVAL AND ASSOCIATED MATCHING PROBABILITY (PM) VALUES GENERATED BY AMPFLSTR [®] PROFILER [®] PLUS, MINIFILER [™] AND SNP ANALYSIS OF EXTREMELY DEGRADED DNA. US CAUCASIAN POPULATION.....	75

CHAPTER THREE

FIGURE 3.1	DENTAL ANATOMY.	82
FIGURE 3.2	EXTRACTION OF DENTAL PULP.	83
FIGURE 3.3	ANATOMY OF THE LOWER LIMB AND BONY ELEMENTS USED IN THIS STUDY	86
FIGURE 3.4	FÉDÉRATION DENTAIRE INTERNATIONALE (FDI).....	87

FIGURE 3.5 RESEARCH PLOT SETUP	88
FIGURE 3.6 ENVIRONMENTAL DATA LOGGERS IN SITU.	89
FIGURE 3.7 SURFACE SAMPLES.....	90
FIGURE 3.8 SET UP OF BURIED SAMPLES.	91
FIGURE 3.9 BURNT REMAINS.....	92
FIGURE 3.10 SET UP OF SKELETAL SAMPLES IN FRESH WATER AND SALT WATER TANKS.	93
FIGURE 3.11 THE LEVEL AT WHICH TOOTH ROOTS WERE REMOVED FOR DNA EXTRACTION.	96
FIGURE 3.12 INSTRUMENTS AND PROCESS INVOLVED IN THE FILING METHOD TO EXTRACT DENTINE FOR DNA PURIFICATION.....	97
FIGURE 3.13 RELATIVE HUMIDITY AND AMBIENT TEMPERATURE ON SITE.....	102
FIGURE 3.14 RECORDED SOIL TEMPERATURE OF THE BURIAL TRENCHES.	103
FIGURE 3.15 WATER TEMPERATURE DATA.	105
FIGURE 3.16 ONE WEEK OF SURFACE EXPOSURE.	109
FIGURE 3.17 TWO WEEKS OF SURFACE EXPOSURE.....	110
FIGURE 3.18 THREE MONTHS OF SURFACE EXPOSURE.....	112
FIGURE 3.19 SIX MONTHS OF SURFACE EXPOSURE.	114
FIGURE 3.20 NINE MONTHS OF SURFACE EXPOSURE.	115
FIGURE 3.21 12 MONTHS OF SURFACE EXPOSURE.	116
FIGURE 3.22 18 MONTHS OF SURFACE EXPOSURE.	117
FIGURE 3.23 24 MONTHS OF SURFACE EXPOSURE.	118
FIGURE 3.24 BONE SAMPLES BURIED FOR ONE WEEK.....	119
FIGURE 3.25 TWO WEEKS OF BURIAL.....	120
FIGURE 3.26 TWO BONE SAMPLES BURIED FOR THREE MONTHS SHOWING THE SUPERIOR AND INFERIOR SURFACES BEFORE AND AFTER WASHING.	122
FIGURE 3.27 BONE AND TEETH BURIED FOR SIX MONTHS.	124
FIGURE 3.28 NINE MONTHS OF BURIAL.	125
FIGURE 3.29 BONE AND TEETH RECOVERED AFTER 12 MONTHS OF BURIAL.....	126
FIGURE 3.30 18 MONTHS OF BURIAL.	128
FIGURE 3.31 BONE AND TOOTH SAMPLES BURIED FOR 24 MONTHS.....	130
FIGURE 3.32 FRESH WATER TANKS AFTER ONE WEEK OF SAMPLE INCUBATION	131
FIGURE 3.33 SUBMERGED FOR ONE WEEK IN FRESHWATER.....	132
FIGURE 3.34 TWO WEEKS SUBMERGED IN FRESHWATER.	134
FIGURE 3.35 FOUR WEEKS SUBMERGED IN FRESHWATER.	136
FIGURE 3.36 SKELETAL SAMPLES AFTER FOUR WEEKS SUBMERGED IN FRESHWATER.	137
FIGURE 3.37 SIX WEEKS SUBMERGED IN FRESHWATER.....	138
FIGURE 3.38 EIGHT WEEKS OF INCUBATION IN FRESHWATER.	139
FIGURE 3.39 TWO WEEKS SUBMERGED IN SALTWATER.....	141
FIGURE 3.40 ONE MONTH SUBMERGED IN SALTWATER	143
FIGURE 3.41 THREE MONTHS SUBMERGED IN SALTWATER.....	144

FIGURE 3.42	SIX MONTHS SUBMERGED IN SALTWATER.....	145
FIGURE 3.43	BONES EXPOSED TO LOW LEVELS OF HEAT.....	146
FIGURE 3.44	BONES EXPOSED TO MODERATE LEVELS OF HEAT.....	147
FIGURE 3.45	BONE EXPOSED TO HIGH LEVELS OF HEAT.....	148
FIGURE 3.46	SAMPLES EXPOSED TO EXTREME HEAT.....	149
FIGURE 3.47	SAMPLES EXPOSED TO EXTREME HEAT (~700°C) AND DIRECT FLAMES FOR A PROLONGED PERIOD (30 MINUTES).....	151
FIGURE 3.48	AVERAGE LEVELS OF DNA DEGRADATION OF FIELDWORK SAMPLES...	154
FIGURE 3.49.	COMPARATIVE STR PROFILING SUCCESS OF THE AMPFLSTR® NGM™ AND POWERPLEX® ESI 16 AMPLIFICATION KITS WITH DEGRADED SAMPLES.....	157
FIGURE 3.50	COMPARATIVE LINEAR CORRELATION ANALYSIS OF ALLELE DROPOUT RATE AND MEAN LOCUS LENGTH OF BOTH POWERPLEX® ESI 16 AND AMPFLSTR® NGM™ KITS.....	159
FIGURE 3.51	X-RAYS OF TEETH BEFORE AND AFTER FILING OF ROOT CANALS FOR DENTIN POWDER.....	160
FIGURE 3.52	COMPARATIVE YIELD OF AMPLIFIABLE DNA PER MG OF DENTINE POWDER.....	163
FIGURE 3.53	THE SUCCESS OF STR PROFILES FROM DNA RECOVERED VIA TWO METHODS FROM TEETH	165
FIGURE 3.54	STR PROFILES OF TOOTH SAMPLES 3, 4 AND 7 USING THE 'ALL ROOT' AND 'FILING' METHODS OF DENTINE EXTRACTION.	172
FIGURE 3.55	PANDORA BONE AND TOOTH SAMPLES.....	176
FIGURE 3.56	DENTAL X-RAYS OF PANDORA TEETH.....	177
FIGURE 3.57	CLASSIC STR PROFILE FEATURES OF HIGHLY DEGRADED SAMPLES WERE ROUTINELY SEEN IN THE PANDORA SKELETAL SAMPLES.....	179
FIGURE 3.58	AVERAGE PROFILING SUCCESS AND HETEROZYGOTE PEAK HEIGHT RATIOS OF DNA EXTRACTS FROM PANDORA SAMPLES.	182
FIGURE 3.59	STR PROFILES FROM SURFACE EXPOSED BONE SAMPLES WITH AND WITHOUT THE ADDITION OF STRBOOST.....	184
FIGURE 3.60	PANDORA SAMPLES WITH AND WITHOUT STRBOOST®.	186

CHAPTER FOUR

FIGURE 4.1	AN OVERVIEW OF THE ILLUMINA GOLDENGATE GENOTYPING ASSAY WORKFLOW.....	200
FIGURE 4.2	ILLUMINA VERACODE TECHNOLOGY.....	201
FIGURE 4.3	EXAMPLES OF GOOD AND POOR GENOTYPE CLUSTERING PATTERN FOR INDIVIDUAL SNPS	209
FIGURE 4.4	AN EXAMPLE OF THE DIFFERENCE IN CLUSTERING PATTERNS BETWEEN GENOMIC AND WGA SAMPLES.....	211

FIGURE 4.5 THE OBSERVABLE RUN-TO-RUN VARIABILITY IN CLUSTERING AND RFU VALUES.	215
FIGURE 4.6 SNP TYPING SUCCESS OF ENVIRONMENTALLY CHALLENGED SAMPLES WITH AND WITHOUT WGA.	224
FIGURE 4.7 THE SNP SUCCESS OF DEGRADED SAMPLES WITHOUT WGA BY THE AMOUNT OF TEMPLATE	226
FIGURE 4.8 PROPORTION OF SAMPLES USED FOR STATISTICAL MODELLING OF EACH CHARACTERISTIC INVESTIGATED.....	228
FIGURE 4.9 COMPARISON OF THE STATISTICAL MODELS USED TO PREDICT EYE COLOUR	233
FIGURE 4.10 STATISTICAL MODELS FOR THE PREDICTION OF EYE COLOUR.....	235
FIGURE 4.11 STATISTICAL MODELS FOR THE PREDICTION OF EYE COLOUR.....	237
FIGURE 4.12 COMPARISON OF THE STATISTICAL MODELS FOR THE PREDICTION OF SKIN COLOUR.....	238
FIGURE 4.13 STATISTICAL MODELS FOR THE PREDICTION OF SKIN COLOUR.	241
FIGURE 4.14 STATISTICAL MODELS FOR THE PREDICTION OF SKIN COLOUR.	241
FIGURE 4.15 COMPARISON OF THE STATISTICAL MODELS FOR THE PREDICTION OF HAIR COLOUR.	242
FIGURE 4.16 STATISTICAL MODELS FOR THE PREDICTION OF HAIR COLOUR.....	244
FIGURE 4.17 COMPARISON OF THE STATISTICAL MODELS FOR THE PREDICTION OF ANCESTRY	247
FIGURE 4.18 STATISTICAL MODELS FOR THE PREDICTION OF ANCESTRY.....	248
FIGURE 5.1 OVERVIEW OF THE SIX DNA REPAIR METHODS INVESTIGATED IN THIS THESIS PRIOR TO MDA AND/OR STR TYPING.....	259

CHAPTER FIVE

FIGURE 5.2 MDA PRODUCT FROM VARYING DNA TEMPLATE VOLUMES.....	265
FIGURE 5.3 STR-TYPING OF HMW DNA WITH AND WITHOUT MDA.....	266
FIGURE 5.4 TESTING FOR PCR INHIBITION DUE TO EXCESSIVE MDA REAGENTS.....	268
FIGURE 5.5 THE EFFECT OF ETHANOL PRECIPITATION OF MDA PRODUCT PRIOR TO STR AMPLIFICATION.	269
FIGURE 5.6 STR RESULTS OF MDA PRODUCT WITH AND WITHOUT SPIN COLUMN FILTRATION AND SAMPLE DILUTION PRIOR TO PCR.....	271
FIGURE 5.7 AGAROSE GEL ELECTROPHORESIS OF MDA PRODUCT FROM DEGRADED AND HMW DNA TEMPLATE.....	273
FIGURE 5.8 WORKFLOW OVERVIEW OF THE LINEAR LIGATION OF DEGRADED DNA SAMPLES PRIOR TO MDA AND STR-TYPING	274
FIGURE 5.9 GEL ELECTROPHORESIS OF DEGRADED SAMPLES TREATED WITH T4 DNA LIGASE AND WHOLE GENOME AMPLIFIED.	275
FIGURE 5.10 THE AVERAGE FRAGMENT LENGTHS OF THE DEGRADED SAMPLE BEFORE AND AFTER LINEAR LIGATION	276

FIGURE 5.11	STR RESULTS OF MDA AND T4 DNA LIGATED SAMPLES WITH A) 10NG AND B) 1NG DNA TEMPLATE.....	278
FIGURE 5.12	QUADRUPLEX PCR RESULTS OF DEGRADED DNA SAMPLES REPAIRED WITH T4 DNA LIGASE PRIOR TO MDA AND STR-TYPING.	280
FIGURE 5.13	WORKFLOW OVERVIEW OF CIRCULAR LIGATION OF DEGRADED DNA SAMPLES.....	282
FIGURE 5.14	CIRCULARISATION OF THE CONTROL OLIGO PROVIDED IN THE CIRCLIGASE™ KIT.	283
FIGURE 5.15	CIRCULARISATION OF HIGHLY DEGRADED DNA.....	283
FIGURE 5.16	THE EFFECT OF T4 POLYNUCLEOTIDE KINASE (PNK) TREATMENT OF DEGRADED DNA AND T4 DNA LIGATED TEMPLATES PRIOR TO CIRCULARISATION AND MDA.....	285
FIGURE 5.17	MDA YIELD USING LINEAR AND CIRCULAR LIGATED SAMPLES AS TEMPLATES.....	286
FIGURE 5.18	MDA YIELD OF CIRCLIGASE™ TREATED TEMPLATE WITH AND WITHOUT FILTRATION PRIOR TO AMPLIFICATION.	287
FIGURE 5.19	MDA YIELD OF CIRCLIGASE™ PRODUCT WITH AND WITHOUT SAMPLE PURIFICATION PRIOR TO A 1 HOUR OR 20 HOUR INCUBATION.....	288
FIGURE 5.20	STR-TYPING OF DEGRADED DNA SAMPLES TREATED WITH T4 DNA LIGASE, CIRCLIGASE™ AND MDA PRIOR TO PCR.....	289
FIGURE 5.21	RESULTS OF PCR AMPLIFICATION OF CIRCLIGASE™ TREATMENT WITH AND WITHOUT THE ADDITION BETAINE PRIOR TO MDA.	290
FIGURE 5.22	ARTIFICIALLY DEGRADED SAMPLES USED FOR PRECR® TREATMENT PRIOR TO MDA AND/OR STR TYPING.....	292
FIGURE 5.23	WORKFLOW OVERVIEW FOR THE REPAIR OF DEGRADED SAMPLES USING PRECR® PRIOR TO MDA AND STR-TYPING.	293
FIGURE 5.24	OPTIMISATION OF PRECR® REPAIR CONDITIONS.....	295
FIGURE 5.25	STR AMPLIFICATION OF DNASE I AND UV DEGRADED SAMPLES PRETREATED WITH PRECR® REPAIR MIX.	295
FIGURE 5.26	STR RESULTS OF PRECR® AND MDA TREATED SAMPLES USING THE POWERPLEX ESI 16 STR AMPLIFICATION KIT.	297
FIGURE 5.27	DEGRADED DNA SAMPLES USED FOR RESTORASE® TREATMENT PRIOR TO MDA AND/OR STR TYPING.....	300
FIGURE 5.28	SAMPLE WORKFLOW OVERVIEW OF THE DNA REPAIR USING RESTORASE® DNA POLYMERASE PRIOR TO MDA AND STR-TYPING.....	301
FIGURE 5.29	STR GENOTYPING SUCCESS OF DEGRADED SAMPLES WITH AND WITHOUT RESTORASE® TREATMENT.....	302
FIGURE 5.30	AGAROSE GEL ELECTROPHORESIS OF DEGRADED SAMPLES BEFORE AND AFTER FFPE REPLI-G AMPLIFICATION.....	306
FIGURE 5.31	STR QUADRUPLEX RESULTS COMPARING A TWO AND EIGHT HOUR FFPE REPLI-G INCUBATION.	307

FIGURE 5.32	STR PROFILE SUCCESS OF DEGRADED SAMPLES WITH AND WITHOUT REPLIC-FFPE AMPLIFICATION.....	309
FIGURE 5.33	SCHEMATIC REPRESENTATION OF THE CHROMOSOME LOCATIONS OF EACH LOCUS USED FOR QUANTITATION OF MDA PRODUCT.	311
FIGURE 5.34	COMPARATIVE QUANTITATION RESULTS USING DIFFERENT LOCI FOR DETECTION OF DNA BEFORE AND AFTER MDA.	314
FIGURE 5.35	COMPARATIVE DEGRADATION RATIOS BEFORE AND AFTER MDA.....	315
FIGURE 5.36	IDEOGRAMS INDICATING THE CHROMOSOME LOCATIONS OF RPPH1 AND RNU LOCI.	316

LIST OF TABLES

CHAPTER TWO

TABLE 2.1 PCR AMPLICON LENGTH, FLUORESCENCE LABELS, PRIMER AND PROBE CONCENTRATIONS OF EACH TARGET SEQUENCE INCLUDED IN THE QUADRUPLEX QPCR ASSAY.....	60
TABLE 2.2 SENSITIVITY DATA OF THE QUADRUPLEX QPCR ASSAY AND DEGRADATION RATIOS WITH UNDEGRADED AND DEGRADED SAMPLES.....	66
TABLE 2.3 QUANTIFICATION RESULTS OF MALE AND FEMALE MIXED SAMPLES INDICATING MALE:FEMALE RATIOS GENERATED BY THE QUADRUPLEX ASSAY.....	68

CHAPTER THREE

TABLE 3.1 THE MODE AND DURATION OF ENVIRONMENTAL EXPOSURE TO EACH OF THE TEETH INVESTIGATED.....	96
TABLE 3.2 PCR CYCLING CONDITIONS OF BOTH AMPFLSTR® NGM™ (APPLIED BIOSYSTEMS) AND POWERPLEX® ESI 16 (PROMEGA) AMPLIFICATION KITS.....	99
TABLE 3.3 MEASURED PH OF THE SOIL COLLECTED AT EACH BURIAL TRENCH BEFORE SAMPLE PLACEMENT AND AFTER HARVEST.....	104
TABLE 3.4 MEASURED SALINITY AND PH OF THE SALTWATER TANK.....	106
TABLE 3.5 MEASURED SALINITY AND PH OF THE FRESHWATER TANK.....	107
TABLE 3.6 MEDIAN LENGTH OF AMPLICONS AT EACH LOCUS IN BOTH AMPFLSTR® NGM™ AND POWERPLEX® ESI 16 AMPLIFICATION KITS.....	158
TABLE 3.7 TOOTH SAMPLES AND ENVIRONMENTAL INSULT APPLIED TO EACH.....	162
TABLE 3.8 COMPARATIVE YIELD OF DENTINE POWDER, TOTAL AMPLIFIABLE DNA AND THE AMOUNT OF DNA RETRIEVED PER MILLIGRAM OF POWDER VIA THE TWO METHODS TESTED.....	162
TABLE 3.9 YIELD OF AMPLIFIABLE DNA FROM THE PANDORA BONE AND TOOTH SAMPLES.....	178
TABLE 3.10 THE NUMBER OF ADDITIONAL ALLELES WHICH WERE DETECTED AND ASSIGNED TO A CONSENSUS PROFILE AFTER AMPLIFICATION WITH STRBOOST®.....	187
TABLE 3.11. CONSENSUS STR PROFILES FROM PANDORA SAMPLES.....	189

CHAPTER FOUR

TABLE 4.1 SAMPLE NUMBERS (N =917) AS CATEGORISED BY PHENOTYPE.....	205
TABLE 4.2. OCCURRENCE OF POORLY PERFORMING AND EXCLUDED SNPS.....	213
TABLE 4.3 SENSITIVITY RESULTS.....	216
TABLE 4.4 COMPARISON OF THREE WGA PROTOCOLS.....	218
TABLE 4.5 COMPARISON OF TWO SPLIT AND POOL METHODS.....	219

TABLE 4.6	COMPARISON OF METHODS FOR SUBOPTIMAL SAMPLES INTO THE SNP ASSAY WITH AND WITHOUT WGA.	220
TABLE 4.7	SNP-TYPING RESULTS FROM DEGRADED FIELDWORK BONE SAMPLES....	222
TABLE 4.8	THE NUMBER OF DNA SAMPLES GENOTYPED AND SUBSEQUENTLY USED FOR THE GENERATION OF PREDICTIVE MODELS FOR EACH PHENOTYPE.	229
TABLE 4.9	THE COMPARATIVE SNP PERFORMANCE	230
TABLE 4.10	THE 24 SNPS REMOVED FROM ANALYSIS DUE TO MORE THAN 5% MISSING DATA.	231
TABLE 4.11	INFORMATION ON 46 DNA VARIANTS REPORTED TO BE STRONGLY ASSOCIATED WITH HAIR COLOUR.	245
TABLE 4.12	BLIND TESTING OF THE PREDICTIVE MODELS FOR EACH PHENOTYPE. ...	250

CHAPTER FIVE

TABLE 5.1	DNA REPAIR METHODS USED IN THIS STUDY.....	258
TABLE 5.2	PCR AMPLICON LENGTH AND PRIMER SEQUENCES AND CONCENTRATIONS OF EACH TARGET SEQUENCE INCLUDED IN THE QUADRUPLEX PCR ASSAY.	262
TABLE 5.3	TYPES OF DAMAGE REPAIRED BY PRECR®. [301]	291

1 Chapter

Introduction and Literature Review

1.1 Introduction

In the aftermath of any mass disaster one of the most important and immediate considerations is victim identification. Devastating natural phenomena such as the 2004 tsunami near Sumatra and earthquakes, accidents such as fires and plane crashes [1, 2] along with intentional acts such as the 2001 World Trade Centre attacks [3, 4], wars, bombings and acts of genocide all result in large numbers of fatalities. In these circumstances forensic personnel are charged with the responsibility of identifying hundreds or even thousands of bodily remains.

Conventional methods of identification include visual identification, fingerprints, biological profiling (forensic anthropology) and dental matching. However, these methods can be inadequate when remains are highly fragmented and decomposed. In cases of fatalities involving intense heat, velocity or advanced decomposition, the remaining elements are usually bone and teeth. While DNA identification can be made from all human tissues, the DNA in these compromised samples is often highly degraded. The occurrence of several mass fatalities in the last decade has necessitated the rapid improvement of DNA techniques used in the identification of highly degraded human remains.

Current forensic DNA typing methods use between 9 and 21 short tandem repeat (STR) markers of nuclear DNA (nDNA) ranging from 100-500bp in length to generate an individual profile. A DNA profile can be obtained from common forensic samples such as blood, buccal swabs and semen, due to the relatively large amounts of intact DNA. However in circumstances in which DNA is in very low amounts and/or is highly degraded, DNA profiles are difficult to obtain. Mitochondrial DNA (mtDNA) has been relied on to generate a victim profile from these difficult sample types. Although a reliable means of identification, the discriminatory power offered by a mtDNA profile is relatively low compared to that generated by analysing nDNA. Therefore, scientists in the field are predominately focusing on analysing nDNA from these highly degraded samples. This includes the optimisation of various extraction techniques to maximise DNA yield from a sample, and more effective amplification and detection methods [5, 6].

Genetic profiling relies on primers and enzymes (DNA polymerases) to recognise, bind and amplify strands of DNA during the polymerase chain reaction (PCR) which exponentially replicates many copies of a particular sequence. The industry standard method of DNA profiling utilizes short tandem repeats (STRs) ranging from 100-500bp [7]. This process commonly fails to produce a result with highly degraded remains due to the fragmentation of the genome into small pieces. The more extensive the sample degradation, the smaller the fragments of DNA, and the less likely a full DNA profile will be obtained.

One approach to increasing the success of DNA typing of highly degraded DNA is to decrease the target amplicon size. The smaller the target for PCR, the more likely the sequence will be intact and detected, leading to greater profiling success. There has been significant advancement in methodologies used to genotype such fragmented samples. Mini-STRs which reduce amplicon length by moving primers closer to the target region (~70-280bp) have proven to be a useful tool for genotyping degraded samples [8]. Single nucleotide polymorphisms (SNPs) may provide the greatest success due to their very short amplicon lengths (ranging from 45-80bp) [9-11]. The comparative success of these genotyping methods in profiling highly degraded samples will be examined.

In addition to degradation, DNA in forensic samples may also be damaged due to the exposure to harsh environmental insults such as UV light, heat, water immersion and decomposition of tissues. Structural DNA damage can include oxidation, hydrolysis, pyrimidine dimers, DNA-DNA and DNA-protein cross-linkages. Environmental samples may also contain substances from the local substrate (eg. humic acid from soil, microbial DNA) which co-extract with the target DNA and adversely affect PCR amplification. DNA damage and inhibitory agents can interfere with PCR amplification and therefore decrease the genotyping success of such challenging samples.

Alternatively, if one could repair the damage and/or fragmentation of the DNA, an increase in genotyping success should also result. The optimal outcome would be that DNA could be repaired to a level when conventional STR typing is successful.

Strategies such as DNA repair, whole genomic amplification (WGA) and PCR enhancement will be investigated.

1.2 Factors Influencing the Success of DNA Profiling

1.2.1 *Environmental Insults*

The extent of biological decomposition depends primarily on two factors: time and environmental conditions [12]. Forensic samples are commonly exposed to harsh environmental conditions which affect the degree of sample preservation. After cell death, the DNA begins to degrade. Degradative processes accumulate with time, while environmental conditions such as temperature, humidity and pH modify the rate and aggressiveness of the degradation [13]. Fire, immersion in water, burial in soil [14] and microbial infestation are all elements which influence the decomposition of remains and the degradation of DNA. An increase in temperature and humidity leads to a growth in microbial numbers and increased DNase activity [15, 16]. DNA damage is caused by a combination of factors rather than any single environmental insult.

1.2.2 *DNA Damage*

Some forms of structural modification and DNA damage may be general in nature, where others are caused by exposure to a specific source. Regardless of the source, DNA damage may significantly interfere with PCR amplification and therefore decrease genotyping success. DNA damage is a multi-factorial process which collectively gives rise to very challenging samples from which to gain a genetic profile for identification. Forms of DNA damage include oxidation, hydrolysis, pyrimidine dimers, cytosine deamination and DNA-DNA and DNA-Protein cross-linkages. Of these various forms, oxidation, hydrolysis and pyrimidine dimers are common in forensic samples.

1.2.2.1 Oxidation

Oxidative damage mediated by free radicals will result in modified bases [17]. The major site of oxidative attack on the DNA bases are the carbon-carbon double bonds of both pyrimidines, and the imidazole ring of purines, both leading to fragmentation [17, 18]. Damage includes modifications of sugar residues, conversion of cytosine and thymine to hydantoin, removal of bases and crosslinkages [19]. Reactive oxygen species such as superoxide and hydrogen peroxide are generated by ionizing radiation or microbial metabolism of anaerobic bacteria that colonise post-mortem tissue [19]. Oxidative base products block replication during PCR as standard *Taq* DNA polymerase cannot bypass the lesions [20].

1.2.2.2 Hydrolysis

The most vulnerable bond to damage in DNA is the N-glycosyl bond that attaches the base to the deoxyribose backbone. Hydrolysis of this bond results in the loss of a base leaving an apurinic/apyrimidinic (AP) site that eventually forms a nick [21]. Because the reactive species is H₂O, the vast majority of forensic samples exposed to moist environmental conditions accumulate many AP sites. Hydrolytic cleavage and oxidation are accelerated by heat and humidity [22]. Such conditions are commonly encountered in cases of natural and mass disasters, such as the recovery of victims of flooding, tsunami and waterlogged burial sites in tropical climates.

Typical PCR polymerases stall at an AP site preventing further replication [23]. AP sites break down into nicks creating single strand breaks. If these single stranded breaks occur on both strands within a distance of 10-20 base pairs, neither the hydrogen bonds between the bases nor the chromatin structure are strong enough to keep the strands together and result in double-stranded breaks [24]. Partial or complete failure of amplification may result. The pH of the aqueous environment also affects the degree of DNA damage since the rate of acid-catalysed depurination leading to strand breaks is pH dependant [25].

Dehydration provides DNA a measure of protection against damage. It is hypothesised that this is due to a change in the conformational state of the DNA and the reduction of normal cellular chemistry and damage due to microbial growth [26]. To ensure the preservation of DNA evidence, the air-drying of reference buccal swabs and evidence blood-spot samples prior to storage is routine forensic practise.

1.2.2.3 Ultraviolet Exposure

Pyrimidine dimers are pairs of adjacent thymine (T) or cytosine (C) bases that crosslink when DNA is exposed to ultraviolet light [21]. Photochemical exposure induces the formation of covalent linkages by localized reactions on the C=C, or T=T double bonds which stall DNA polymerase and arrest replication during PCR [27]. Other photo-lesions are formed on UV exposure such as purine and pyrimidine oxidation products [28]. However, the predominant UV induced damage to DNA in bloodstains appears not to be pyrimidine dimers (as with living tissues), but single strand breaks [26]. However, it is likely a combination of damage types is responsible for common profile loss in evidentiary samples exposed to the elements.

1.2.2.4 Microbial Digestion

Colonisation by microbial fauna and flora (including fungi, mould and algae) are common contaminants of skeletal material recovered from a crime scene or mass disaster. Microorganism growth has been shown to be a significant cause of DNA damage leading to the non-typeability of forensic samples [24]. Microorganisms secrete digestive enzymes which introduce DNA damage via reactive oxygen species and double stranded breaks. Microbial metabolism products have been shown to increase the rate of DNA strand breakage 25-fold [25]. Heat and humidity promote microbial growth, and therefore are environmental factors that play important roles in sample, and more specifically DNA preservation.

1.2.3 DNA Degradation

Whilst the mechanisms of DNA degradation may differ, the end result is universal; fragmentation of the double helix into smaller and smaller pieces as it degrades [13]. This makes amplification of DNA difficult and most commonly results in partial or no DNA profiles. Although DNA may be subjected to many forms of damage, fragmentation due to single and double strand breaks is thought to be the major cause of partial profiles in degraded samples [26]. Once the average DNA fragment length is reduced to below 300bp, a significant loss of genetic information occurs due to the lack of suitable template DNA for amplification [29].

After death, blood ceases to perfuse tissues with oxygen and nutrition which leads to a drop in cellular adenosine triphosphate (ATP) production. The level of intracellular ATP determines which of the two processes of cell death a particular cell will undergo; apoptosis or necrosis. Apoptosis is an energy dependant programmed cell death characterised by loss of the plasma membrane, condensation of cytoplasm and extensive fragmentation of DNA into oligomers of approximately 180bp via activation of endogenous endonucleases [30]. Necrosis is a passive metabolic collapse including increased cell volume, swollen organelles, and chromatin condensation. Rupture of membranes and organelle breakdown follow and the released lysosomal enzymes generate a random DNA degradation pattern [31]. Regardless of the mode of cell death, DNA is broken into small lengths by endogenous enzymes generating highly degraded samples for downstream genetic analysis. These degradative processes are influenced by factors such as temperature [32], oxygen levels and microbial activity [33].

1.2.4 PCR Inhibitors

The presence of inhibitory agents in a sample may also offer a challenge for PCR amplification. PCR inhibition is the most common cause of amplification failure when adequate amounts of DNA are present [31]. Substances from the sample substrate may be co-extracted with the target DNA (textile dyes from denim [34], humic acid from soil [35], microbial DNA [36]), or be present within the sample itself (fatty acids

from bone [36], haeme in blood [37], melanin in hair [38]). Amplification of a sample containing inhibitors leads to the loss of alleles from larger STR loci or complete failure of all loci. These results are similar to, and may be mistaken for severely degraded samples [19]. Inhibitors may negatively affect primers, cell lysis during extraction [39], or reduce polymerase activity [40]. Strategies to overcome PCR inhibitory effects include dilution of the extract to reduce the inhibitor [41], the addition of more *Taq* DNA polymerase, the use of more robust and tolerant DNA polymerases [42], sample clean up devices (such as spin columns). PCR enhancers such as bovine serum albumin (BSA) [43] and PCRBoost™ [44] have also proven to neutralise inhibiting compounds.

Quantitative real-time PCR (qPCR) is the method of choice for quantifying the amount of DNA in a sample. This assay can simultaneously detect the presence of inhibitors by including an internal PCR control (IPC). The IPC is commonly a synthetic oligonucleotide that is co-amplified with the DNA samples. A reduction in the reaction efficiency, fluorescence values and a delay in amplification are indicators that a particular sample may contain inhibitors [45].

1.3 Highly Degraded Remains in Natural and Mass Disasters

Extensive reviews have been published documenting the challenges of DNA profiling that are encountered in the wake of a mass disaster [3, 8, 46-48]. Methods of sample collection and storage, DNA extraction, quantification and profiling technologies are reviewed, and improvements are suggested based on lessons learnt from collaborative experience.

Conventional methods of identification such as fingerprints and dental matching can be inadequate in the case of mass disasters due to the decomposition and disarticulation of human remains. DNA analysis is then the most appropriate tool of victim identification. Unlike fingerprints or dental features, DNA-based identity testing is not restricted to any particular body part. Therefore DNA profiling is able to re-associate separated or co-mingled remains typical of mass graves and high impact

disasters such as plane crashes or explosions [2, 49]. Due to the varying environmental conditions to which mass disaster samples are often exposed, the quality of the remains retrieved for identification will vary from apparently pristine to highly decomposed [46].

DNA profiling methods used in mass disaster victim identification (STR and mtDNA typing) are well established. However during the victim identification effort following the World Trade Center tragedy in 2001 these DNA methods sometimes (2% of cases) failed due to the extremely degraded state of the remains [47]. Alternate technologies have been developed in an effort to increase the chances of obtaining a genetic profile from such challenging samples. These include mini-STRs [3], indels (insertion/deletion polymorphisms) [50] and SNPs [51].

1.3.1 Bone

Often in the event of a mass disaster or the identification of a long-deceased individual, only skeletonised remains are recovered. The fact that bone and teeth are inevitably the only surviving material for DNA testing [52] is evidence that these tissues are to a certain extent able to resist the damaging effects of time and environmental insults. Bone is therefore a vital source of DNA for identification purposes, particularly in cases of fully skeletonised remains and mass disasters.

Bone is a dynamic tissue comprised of ground substance and collagen fibres which provide structural framework and flexibility, whilst inorganic mineral salts give strength and rigidity. Inorganic hydroxyapatite constitutes approximately 70% of bone tissue and it is this portion of the tissue that is targeted for DNA extraction. It is believed that this tough mineral component of bone provides a physical barrier or protection for DNA enclosed within the bone cells (osteocytes) [53]. It has also been postulated that dense crystallised aggregates of bone matrix [54] or the adsorption of DNA to hydroxyapatite and/or collagen [55] may stabilise and provide added protection for endogenous DNA. Although the histological structure of bone tissue may confer protection of the endogenous DNA, DNA yield from bone tissue is generally

very low. This is likely due in part to the low density of osteocytes within the mineralised matrix. In addition, research has shown that many of these cells are pycnotic or in karyolysis [56]. Significantly improved DNA yield from bone using an extraction method which employs total demineralisation supports this theory [53, 57].

The level of DNA preservation in skeletal remains can be variable and the success of obtaining a full DNA profile depends substantially on the type of bone available for testing [41]. Dense femoral sections or intact teeth are considered optimal sources with one study showing an approximate 90% success rate (recovery of 12 or more loci in a 16-plex kit) from these sample [41]. However, other samples such as vault, cranial bones and vertebrae had substantially lower recovery rates [41]. The dense cortical bone of weight-bearing leg bones yielded the highest success rates (femur 87%) compared to long bones of the arms (humerus 46%, radius 25% and ulna 23%). DNA profiling success rates differed substantially when sampling other skeletal elements [52]. This suggests that certain skeletal elements contain more nucleated cells and may be better than others in protecting, and therefore providing DNA for typing. Bone selection for DNA analysis is therefore an important factor for successful identification.

Bone tissue is one of the most challenging, time-consuming and labour intensive biological samples from which to extract DNA [58] This is due to the difficulty of preparing and sampling the skeletal material before DNA extraction, and the presence of PCR inhibitors. Traditional sampling procedures include decontamination, cutting and sanding, pulverisation of bone into powder by blenders and grinders with liquid nitrogen and organic or silica-based extraction. These methods are robust and have been utilised on forensic casework and disaster victim identification with success [59]. However when analysing extremely degraded remains, the amount DNA available is often extremely low. It is therefore not surprising that superior extraction techniques which maximise DNA yield from skeletal samples are being investigated. Ancient DNA research laboratories have developed new methods which maximise DNA recovery from bone [60-62], and forensic labs have adapted several ancient DNA techniques to suit forensic needs [13]. In addition to improving extraction methods from severely degraded skeletal samples, other research has focused on modifying DNA amplification

methods in order to improve the DNA profiling success of such challenging samples [63].

1.3.2 Teeth

Teeth are the hardest tissue in the human body [64] and are resistant to adverse conditions such as humidity, heat, high temperature and microbial action [65, 66]. It is not surprising that teeth along with bones are often the sole remains of a long deceased individual. Teeth have traditionally been used as a source of DNA when all other tissues are lost or have failed to yield enough useable DNA for identification. Dental pulp is encased in extremely tough dental enamel and is therefore a protected source of both mitochondrial and nuclear DNA for genotyping.

Dental enamel is acellular and is therefore not a source of DNA, but sufficient quantities of DNA are found in the crown dentine and root (Fig. 1.1) to support DNA extraction and downstream analysis. The root [67] and cementum [68] have been shown to produce the highest yields of DNA. The pulp and dentine form a structural and functional unit with mature odontoblasts lining the root canals with cellular projections extending into the dentine [69]. Dentine is a preferred target for DNA isolation as it is protected beneath a layer of cementum and enamel. It is hypothesised that these protected cells will present the optimal source of DNA from teeth. Despite teeth providing such a valuable source of DNA from very ancient and/or degraded remains little is known about the relative amounts of DNA within different regions of teeth, or the potential impact of sampling methods on the resulting quality and quantity of DNA extracted from preserved teeth [68].

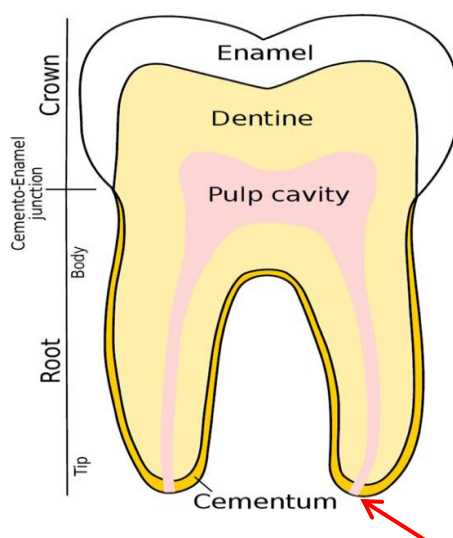


Figure 1.1 Diagrammatic representation of a human Molar [60]

A typical human tooth consists of a crown covered by enamel, a pulp cavity encased by dentine tissue and one to four roots. Each root is lined by a cementum layer and has an apical foramen (arrow) at the tip to allow for the passage of nerves and blood vessels into the pulp cavity.

Methods described in the literature to extract material from teeth for DNA isolation include grinding the whole tooth [70], the root [5], sectioning of the tooth [71, 72], endodontic access to pulp cavity and dentine via the crown [73], and a non-powdering method by simply soaking the whole tooth in extraction buffer overnight [74]. Maximal yield of dental DNA is achieved by grinding the entire tooth into a powder for extraction. However this gives rise to two main disadvantages. Firstly, the tooth is completely destroyed eliminating any further radiographic, morphologic or restorative analysis which may be required. This is an important consideration, as minimal sample damage is often a requirement for the analysis of ancient and museum remains. Secondly, a significant increase in PCR inhibition and DNA degradation is observed over extracts from pure dental pulp [71]. The inclusion of sub-optimal dental tissue in the grinding and extraction processes leads to a more highly degraded DNA sample. This problem may be overcome by sampling only those portions of the tooth which provide ample DNA of sufficient quality for successful genotyping.

1.4 Genetic Markers for Identity Testing

Protein-based genetic markers were the first system used for biological identity testing more than 25 years ago [75]. This pioneering method had several limitations. Stability of proteins in most tissues exposed to harsh environmental conditions is poor, resulting in insufficient amounts of protein available for testing. In addition, the power of discrimination is very low and individualisation is not possible [76]. The forensic community turned to DNA polymorphisms as alternative markers to protein based systems as DNA offered several advantages. In addition to the vast amount of variability at the DNA level which could be exploited for identity purposes, DNA is present in all biological tissues and is relatively stable in forensic samples.

DNA was first applied to a forensic setting in the late 1980's using restriction fragment length polymorphism (RFLP) typing of variable number of tandem repeat (VNTR) loci [77, 78]. RFLP provided the high power of discrimination required for human identity testing, but successful profiling required relatively large amounts (10-25ng) of intact DNA. Fragment lengths of up to 10,000bp were required. This method was therefore not applicable to evidence samples which were degraded and/or in amounts well below the requirement for successful RFLP analysis.

RFLP analysis was replaced by PCR-based assays more than a decade ago [79]. The polymerase chain reaction (PCR) is a method used to amplify particular regions of DNA from biological tissues. This process is used to replicate a specific region of the genome over and over again to produce millions of copies of a particular sequence. The target region is defined by oligonucleotides (primers) complementary to the 3' ends of the target sequence, and amplified with a DNA polymerase. This enzymatic process involves 30-40 cycles of heating and cooling to provide the required conditions for strand denaturation, primer binding, and extension of primers by the polymerase (Fig. 1.2).

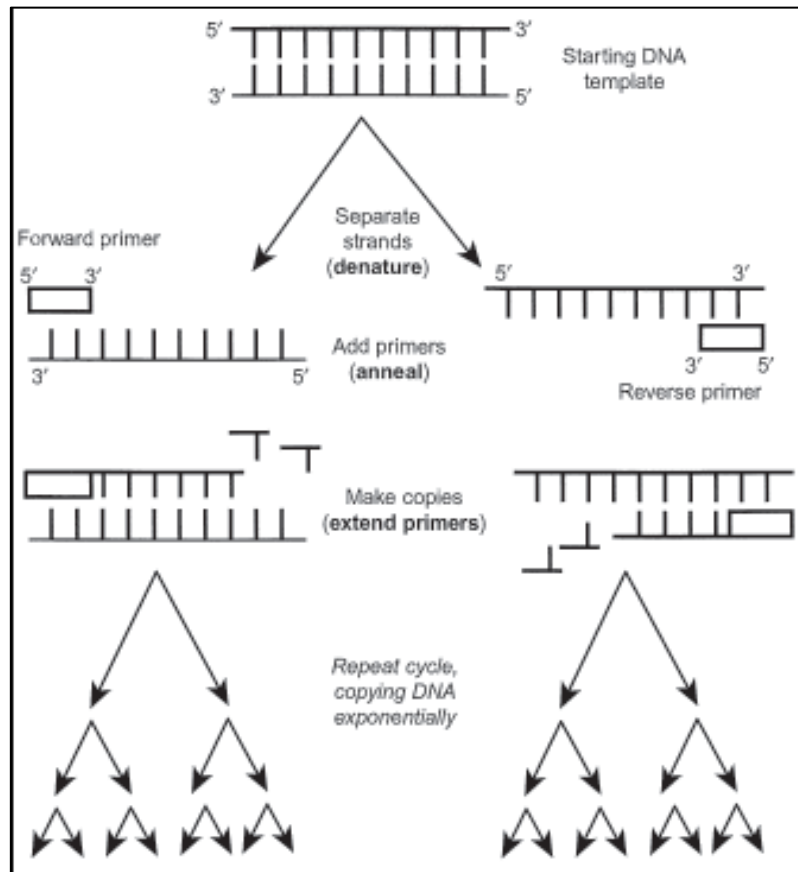


Figure.1.2 Overview of the polymerase chain reaction (PCR).

During each cycle, the double stranded DNA is heated to separate the two strands. The sample is then cooled to allow primers to bind to the target regions. Finally the temperature is again raised to enable the DNA polymerase to extend the primers and replicate the complimentary strand. The cycle is repeated 30-40 times with the number of DNA molecular fragments doubling each cycle. (Figure taken from [80])

PCR can yield a complete DNA profile from relatively minute amounts of sample (>100pg). The first PCR-based systems used for identity testing were founded on SNP variation. Sequence polymorphisms at the HLA-DQA1 locus and other loci (LDLR, GYPA, HBGG, D7S8 and Gc) were typed using allele specific oligonucleotide (ASO) hybridization [76]. These SNP-based assays were highly sensitive, but did not provide the high power of discrimination that VNTR/RFLP afforded, and due to the bi-allelic nature of SNPs individual contributions to a mixture sample were difficult to interpret [76].

In the early 1990's amplified fragment length polymorphisms (AmpFLP) were used for forensic identity testing. This PCR-based method amplified VNTR loci such as D1S80, ApoB, D17S30 (YNZ22) and COL2A1 which were separated on a polyacrylamide gel and visualised using silver staining [81, 82]. Although this method was faster than RFLP, it still required relatively large amounts of intact DNA (>5ng).

By the end of the 1990's, short tandem repeat (STR) or microsatellite loci (a sub class of VNTR markers) had replaced early genetic markers used in PCR-based methods. STRs were a significant advantage over RFLP and VNTRs due to their smaller amplicon size (100-500bp), high degree of polymorphism and semi-automated workflow [76]. STRs are currently the gold standard method of forensic identity testing.

1.4.1 Short Tandem Repeats (STRs)

Short tandem repeats (STRs) are small stretches of DNA typically between two and seven nucleotides in length, which repeat a variable number of times within a particular region in the genome [83]. The number of times the repeat occurs at each site (locus) is variable between unrelated individuals. An individual STR profile is the combination of 9-21 loci which segregate independently from one another.

Amplification of STR targets using PCR results in amplicons ranging between 100-500bp in length [7]. Commercially produced multiplex STR kits are used in most forensic laboratories as they simplify and standardise procedures. Such assays are extremely robust, accurate and possess very high powers of discrimination. The continuous development of commercial autosomal STR kits has contributed to a worldwide standardization and validation of this technology [8].

1.4.1.1 Limitations of STRs for Highly Degraded Samples

STRs are the markers used for routine human identity testing within the forensic community. Despite their high powers of discrimination and robustness, STR assays often fail when genotyping extremely degraded samples. As DNA degrades, it breaks

into smaller and smaller pieces. The larger loci (>200bp) are therefore the first to be affected, and are commonly lost. This results in partial STR profiles with the largest alleles and/or loci dropping out, in what is termed the 'ski-slope effect'. (Fig. 1.3). The development of primers that result in shorter amplicons, known as mini-STRs, have helped to improve the profiling success of highly degraded samples (see Section 1.4.2).

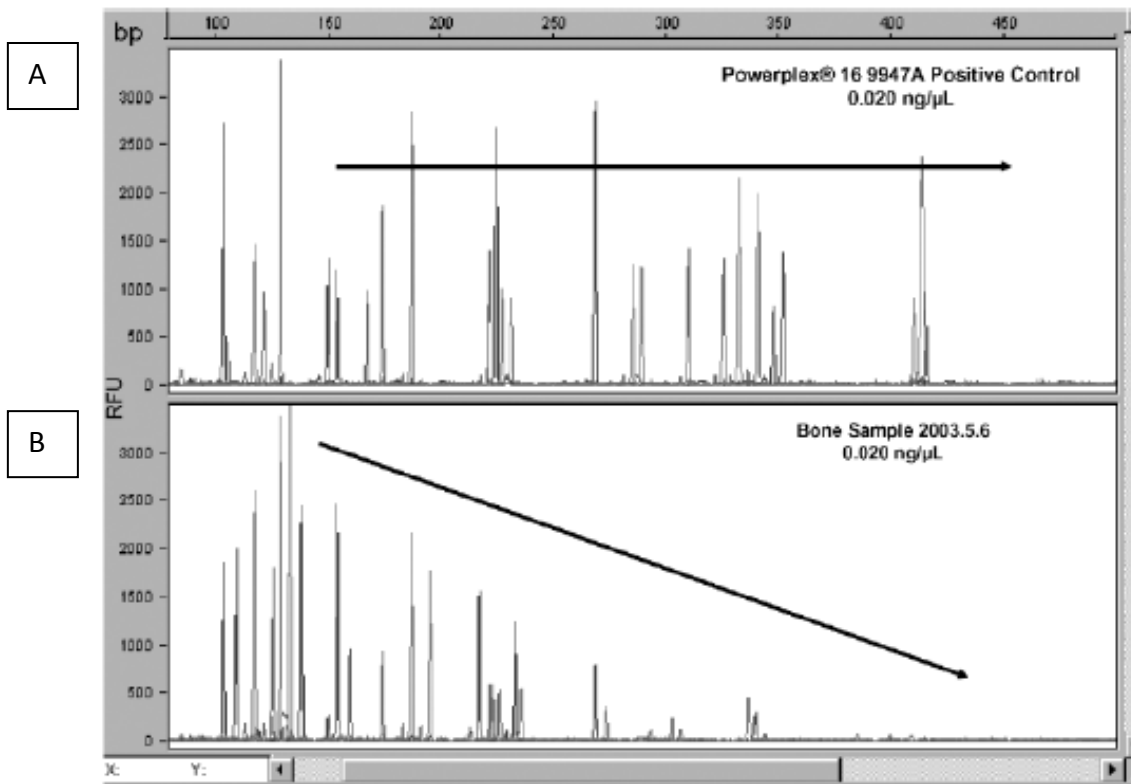


Figure 1.3 Typical STR profiles from HMW and degraded DNA samples.

A) STR profile of a non-degraded control sample shows successful amplification of all loci. B) The profile from a degraded bone sample shows a reduction in fluorescence intensity, and complete drop out of the larger STR loci. This phenomenon is commonly referred to as the 'ski-slope' effect. [84]

1.4.2 Mini-STRs

The premise of mini-STRs is very simple; move the primer binding sites closer to the target repeat units to create the smallest amplicons possible [84-86] (Fig. 1.4). This provides the greatest chance of success when attempting to amplify highly fragmented DNA. A direct relationship between amplicon size and profile success rates has been demonstrated [13, 29, 87]. As the level of sample degradation rises, longer loci fail to amplify.

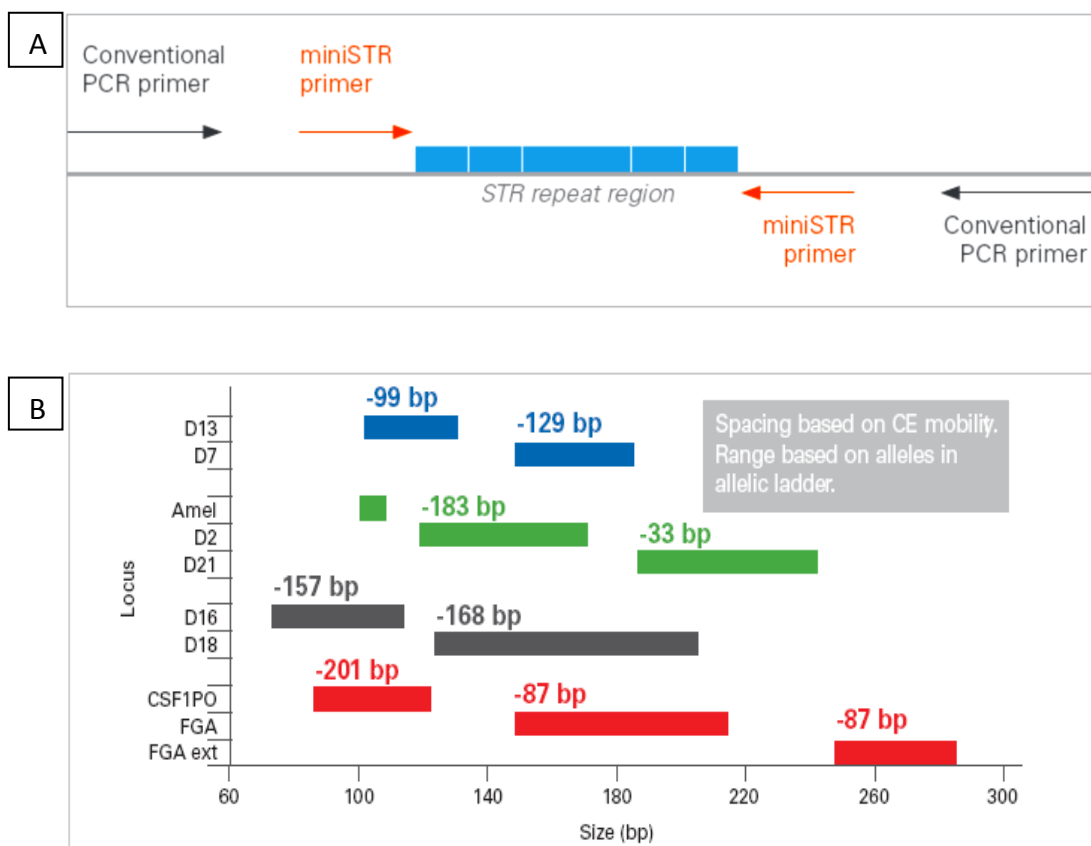


Figure.1.4 Mini-STR primer and multiplex kit designs.

A) PCR primers are re-designed to anneal closer to each repeat region in order to achieve the smaller amplicons (mini-STRs) B) AmpFISTR® MiniFiler™ (Applied Biosystems) kit multiplex configuration indicating the reduction in amplicon size compared to the Identifiler® kit (Applied Biosystems).[88]

Mini-STRs have proven superior to standard STR testing for small amounts of degraded DNA [89, 90]. A greater than three-fold increase in more complete or even full profiles from degraded samples were seen when standard STR kits failed [8].

Studies on highly degraded samples showed that all mini-STR loci below 120bp appeared resistant to the most aggressive degradation [13] whilst those above 150bp failed more readily [91]. The European DNA Profiling (EDNAP) collaborative study concluded that mini-STR systems were a more effective tool over traditional STR and existing SNP systems for analysing highly degraded samples. Their recommendation was to adopt the three mini-NOC1 loci, D10S1248, D14S1434 and D22S1045, developed by the US National Institute of Standards and Technology (NIST) [85, 92] as European standards.

The commercial AmpFISTR[®] MiniFiler[™] PCR amplification kit was developed by Applied Biosystems in 2007. It amplifies eight autosomal loci and the sex determination locus amelogenin. This kit permits size reduction on eight of the longer STR loci amplified in the AmpFISTR[®] Identifier[®] Kit and five in the AmpFISTR[®] SGMPlus[®] kit. Therefore database compatibility with existing database samples processed with commercial STR megaplexes is preserved. MiniFiler[™] has been shown to increase the retrieval of additional STR information from ancient [93] or degraded and inhibited forensic samples in which standard STR genotyping failed to produce complete profiles [94]. An additional benefit for the analysis of highly degraded samples and samples with low amounts of DNA, is the increased sensitivity of the MiniFiler[™] kit.

1.4.2.1 Limitation of Mini-STRs

The major disadvantage of mini-STRs is that fewer loci can be simultaneously amplified in a multiplex and separated by capillary electrophoresis. As primers have been moved as close as possible to the repeat region, the wide size range of amplicons has been decreased and all loci have the same general size of ~100-150bp [92]. As fragments are separated by length during capillary electrophoresis, a limited number of mini-STR loci can be separated in each dye channel.

It has been argued that higher powers of discrimination are obtained by a partial STR profile compared to a full mini-STR profile [41]. A study of the comparative success of STR and mini-STR analysis on highly degraded skeletal material concluded that a 16-plex where the six largest STR loci drop out still provided more genetic information than a mini-STR 6-plex with 100% amplification success [41]. However, the AmpFISTR® MiniFiler™ PCR amplification kit with eight loci may provide a useful and powerful tool for genotyping degraded samples. A probability of identity value of 8.21×10^{-11} may be generated from a full MiniFiler™ profile compared to a partial AmpFISTR® Identifiler® profile (seven loci under 200bp) value of 6.10×10^{-08} (US Caucasian population) [88]. The probability of identity values would vary substantially depending on the level of sample degradation and therefore how many loci drop out from the STR profile. The strongest power of identity possible for any degraded sample may be achieved with a combined partial AmpFISTR® Identifiler® STR profile and complete MiniFiler™ profile.

Although mini-STRs demonstrate superior performance over conventional STRs in the analysis of samples which are degraded and/or in very low amounts, full profiles are often not produced due primarily to extreme fragmentation of DNA. This level of DNA degradation may be encountered in ancient remains, forensic or mass disaster cases, leaving many victims unable to be identified.

1.4.3 Mitochondrial DNA (mtDNA)

Forensic scientists have conventionally relied on mitochondrial DNA (mtDNA) to generate a victim profile from very difficult samples which fail with standard STR and mini-STRs analyses due to insufficient template [95, 96]. In addition to being extremely degraded, genomic DNA in skeletal remains is usually found in very low quantities. Mitochondria are organelles that are present in very high copy number within each cell (100s-1000s), compared to just one copy of genomic DNA [97]. The circular structure of mtDNA is thought to make it less susceptible to exonuclease activity than linear genomic DNA [83]. Both the relative abundance of mtDNA and its more protected circular nature may explain its superior survival rate [83] and enable

greater success of amplification in highly degraded samples such as bone and teeth. mtDNA sequencing was the primary identification tool used to identify individuals from bones recovered from American war casualties [98] and was also employed during the World Trade Centre tragedy in cases of extreme sample degradation [99].

Mitochondrial variation is exploited for forensic identity testing by sequencing the two hypervariable regions (HV1 and HV2) of the mtDNA control region [98, 100]. These regions do not code for vital cell functions and therefore nucleotide variability and polymorphisms between individuals are more abundant [83]. Unlike nuclear DNA (nDNA), mtDNA is maternally inherited, and barring mutation, the sequence of all siblings and maternal relatives is identical [101]. This characteristic is beneficial for tracing maternal lineages, missing persons or mass disaster cases where maternal relatives can provide reference samples.

Mitochondrial markers produce haplotypes with only one allele per locus. As a result statistical calculations for random match probabilities do not provide as high a power of discrimination as autosomal markers. Haplotypes are presented as differences from the universal reference sequence known as the Cambridge or Anderson's Reference Sequence (rCRS) [102]. A number of HVI and HV2 haplotypes have been found to be very common within certain populations. For example, between 38% [103] and 50% [104] of all European Caucasians belong to the super haplogroup H.

The concept of re-designing primer sets in order to decrease amplicon size in autosomal markers (i.e. mini-STRs) has also been applied to mtDNA analysis with success [105]. Although a very reliable means of identification, the discriminatory power offered by a mtDNA profile is relatively low compared to that of nDNA. Current mitochondrial analysis is technically difficult, expensive and time consuming although more recently developed alternative technologies offer more rapid means for mtDNA analysis such as next generation sequencing [106] and mass spectrometry [107, 108]. Because of the greatly reduced power of discrimination of mtDNA typing, it is not surprising that the research focus is leaning towards improving retrieval of genetic information from nDNA for highly degraded samples.

1.4.4 Single Nucleotide Polymorphisms (SNPs)

STR loci exhibit length variation. Single nucleotide polymorphisms (SNPs) are base substitutions, insertions or deletions that occur at single positions in the genome which show sequencing, not length variation. SNPs occur at a rate of approximately 1 SNP/1000bp [109, 110], and constitute almost 90% of all human genomic variation [111]. Millions of SNPs are spread across the human genome on all 22 autosomal chromosomes, both sex chromosomes (i.e X-SNPs and Y-SNPs), as well as on mitochondrial DNA (mt-SNPs). The abundance of SNPs provides a potential wealth of information for human identification purposes.

An important feature of SNPs is a relatively low mutation rate ($\sim 10^{-8}$ per replication) [112] compared to STRs ($\sim 10^{-3}$ - 10^{-5}) [113]. The low mutation rate means SNP loci have a positive association with population or ancestral groups as they are stable genetic markers over long periods of time. SNP loci are well suited for kinship and/or pedigree analysis and also offer the potential to infer ethnicity and/or phenotypic characteristics.

1.4.4.1 Forensically Important SNPs

The utility of SNPs within the field of forensic science may be broadly divided into two applications; identification and intelligence [114].

1.4.4.2 Forensic Identification

The SNPforID consortium was established in 2003 with the principal goal of developing SNP-based DNA analysis tools that would have comparable discriminating power and ease of use to existing STR based technologies for identification [114]. The most substantial advantage SNPs offer identity testing is with highly degraded remains, where the resultant DNA fragments are smaller than the required length for STR typing. For SNP loci it is possible to design PCR primers that provide amplicons of 45-55bp (SNP + length of two primers) [11]. The significant reduction in amplicon length should maximise the number of loci retrieved from highly degraded samples.

The best SNPs for identity testing are those with the highest heterozygosity (i.e. 50% for bi-allelic markers) and low F_{st} values (low population heterogeneity), as fewer loci will be needed to reach high levels of discrimination [76]. Several SNP assays have been designed as potential panels for identification of individuals [11, 115-121]. The SNPforID consortium developed a 52 SNP panel [122] which demonstrated a mean match probability of 5.0×10^{-19} in the populations studied (compared to AmpFISTR® Identifiler® kit 5.0×10^{-18}) [123]. The SNPforID multiplex assay was later modified to a 49-SNP multiplex assay with improved sensitivity (100pg input DNA) and overall robustness [124].

Another category of SNPs which are useful for identity testing are lineage informative SNPs. Due to the lack of recombination and low mutation rate of SNPs that reside on the mtDNA genome and Y chromosome, these lineage markers are informative for tracing human migration patterns [125], or kinship analysis, particularly where reference and unknown samples are separated by several generations. The most likely forensic use of lineage SNPs is in missing person cases and mass disaster identifications [76]. SNPs may also be utilised to resolve ambiguous STR relationship results [126, 127], increase information from the X chromosome [128, 129], or further define common Y chromosome [125, 130] and mtDNA haplotypes [131, 132].

1.4.4.3 Forensic Intelligence

SNP markers linked to biogeographical ancestry and physical traits have been sought as a source of forensic intelligence ([133] reviewed in [134]). Information regarding ethnic origin of a DNA sample may be gleaned from a category of SNPs referred to as ancestry informative markers (AIMs) [135]. These markers occur at very different frequencies between populations [136, 137] and can indicate ancestral origin of a person. Several panels of AIMs have been developed which assign ancestry to major bio-geographical groups and various subsets thereof [135, 138] (reviewed in [76]). While ethnicity may indirectly suggest the general appearance of a suspect, AIMs are unable to accurately predict appearance.

The most obvious descriptors of an individual's appearance are colouring, height and facial features [76]. All are highly heritable [139, 140] and therefore the genetic basis of such traits may be exploited for possible forensic intelligence. The introduction of genome-wide association studies has provided a vehicle for identifying genes involved in complex traits such as external visible traits [141, 142]. Most studies have focused on the pigmentation of skin [143-146], hair [147-149], eye colour [150-155] and height [156, 157]. Of all the traits studied to date, eye colour is the most accurately predictable [134]. The IrisPlex system was developed as a single multiplex assay based on SNaPshot™ chemistry using six of the most predictive SNPs from six pigmentation genes for the prediction of eye colour [158]. This system has already been validated for forensic use [159]. The same authors recently created a singleplex predictive assay for eye and hair colour (HIrisPlex) by adding 18 more DNA variables (SNPs and indel) to the six IrisPlex SNPs [160]. The Office of the Chief Medical Examiner (OCME) of the city of New York has also recently tested a SNP panel for eye and skin colour predictability [161].

Numerous SNPs have been identified as being strongly associated with external visible characteristics. The key genes found to be predictive of hair, skin and/or eye colour include the HERC2, MC1R, OCA2, SLC24A5, SLC45A2 (MATP), ASIP, IRF4, MYO5A and TYR genes [158, 162-164]. Melanin is the main pigment of eye, skin and eye colour and therefore is intuitive that these genes are largely associated with melanin synthesis or localisation [162]. Many pigmentation SNPs are also highly associated with ancestry and therefore several recent studies have focused on combining both sets of markers into a single panel of predictive SNPs [133, 165, 166]. This approach is known as forensic DNA phenotyping [134]. Both biogeographical and phenotypic information regarding a suspect or missing person could provide valuable information for investigative leads.

1.4.4.4 SNPs and Highly Degraded Samples

The principle advantage of SNPs for forensic analysis of highly degraded samples is the ability to design short amplicons (potentially 45-55bp [11]). This feature alone highlights the potential of SNPs as an alternate method for identification from highly

fragmented DNA. SNP genotyping systems targeting very short markers (average 69bp) have been successfully applied to the most degraded samples from the World Trade Center remains [8, 51] and other disasters involving fire and explosives [48] when STR analysis produced incomplete or no profiles at all.

A case report involving a highly decomposed and badly charred femur has demonstrated that the collective power of a full 52 SNP profile was better than a partial STR profile [91]. By utilising the validated SNaPshot™ (Applied Biosystems) primer extension multiplex set, a full profile was obtained. Moreover the 52 SNPs gave a much higher average random match probability of 3.7×10^{-21} as compared with 8.2×10^{-11} using the commercial Mini-Filer™ amplification kit. The SNP primers used in this case were designed to produce amplicons below a 115bp size limit [85, 116, 167]. The same degraded sample was genotyped with three different mini-STR multiplexes generating amplicons between 58-293bp in length and two STR kits producing 100-365bp amplicons. Each conventional STR set failed to amplify any detectable alleles, whilst only partial profiles were obtained with the mini-STR sets. This case study reinforces the strong association between reduced amplicon size and the improvement of quality and completeness of profiles obtained from extremely degraded DNA.

Additional support for the advantage of SNP analysis over STR and mini-STRs for identification of highly degraded samples is provided by a study showing a complete failure of STRs, a 44% success rate with Mini-Filer™ and 100% success with SNP typing [13]. The improved SNPforID 49-SNP multiplex assay was also shown to retrieve full profiles from small amounts (100pg) of degraded samples which failed to resolve any (or very few) STR loci. Mean match probabilities ranged from 10^{-14} – 10^{-21} [118]. This same SNPforID assay was able to profile degraded samples with the highest match probability of 1.1×10^{-15} compared to the 10^{-6} when those samples were profiled with a STR amplification kit (SEfiler) [168].

SNPs have been proposed as complements to traditional STR and mini-STR profiling for analysis of highly degraded samples [76, 114]. Coupled with the ability to obtain

genetic information regarding ancestral origin and phenotypic characteristics, SNPs may become a valuable addition to human identification testing.

1.4.4.5 Limitations of SNPs

SNP genotyping is not a new technology for identity testing, and was in fact the first PCR-based system to be utilised for forensic DNA testing [169]. SNPs are much less informative per locus for identity testing compared with STR markers due to the bi-allelic nature of most SNPs. Therefore to match the statistical power of discrimination of traditional STR multiplexes (9-16 STRs), 45-60 SNPs would be required [170-172]. However this may become largely irrelevant if a full SNP profile can be obtained from highly degraded material using large-scale multiplexes and simple, easily adopted genotyping systems [91, 116].

Large multiplex reactions may lead to poor amplification efficiency and make it difficult to gain accurate and reproducible profiles [173]. A possible solution to this problem is to run tandem PCR reactions of several SNP multiplexes each consisting of a smaller subset of loci. With this approach, the sample size needs to be large enough to be split between PCR reactions. Improved multiplexing of SNP assays has potentially overcome what was once considered a substantial limitation. A multiplex assay with 52 [116] and 49 [124] SNPs for human identification demonstrates that it is possible to construct large, sensitive multiplex PCR assays for forensic applications. These assays have been shown to produce full SNP profiles from degraded samples which yielded partial profiles using STR markers using as little as 100pg DNA.

Another limitation of SNPs involves the interpretation of mixtures or multiple donor samples. Because SNP markers have at most two alleles per locus, assigning profiles to individual contributors may become problematic [76]. The ability to obtain quantitative information from allele calls is important when attempting to decipher mixtures [170]. Although more difficult than STR analysis, the interpretation of mixed samples is possible with SNP typing. Mixtures were able to be identified (even in degraded samples) to a 1:40 ratio using the *SNPforID* assay [168]. The absence of stutter artefacts present in STR analysis is a benefit for some SNP interpretation

scenarios [174]. More recent advancements in SNP typing technology such as electrospray ionization mass spectrometry have overcome the limitation of mixture interpretation within SNP profiles [9, 100, 175]

1.4.5 Markers of the Future

The repertoire of genetic markers used for forensic identity testing has evolved substantially. General agreement exists within the international forensic community that STRs will continue to be the markers of choice for the foreseeable future because of their robustness and widespread use in national databases [7, 170, 176, 177].

The primary reason to add or change markers within databases is to increase the chances of amplifying highly degraded DNA rather than to increase the discriminating power of current techniques [173]. In 2006, the European DNA Profiling Group (EDNAP) and the European Network of Forensic Science Institutes (ENFSI) recommended that existing core loci be re-engineered to enable small amplicon detection (<130bp) and the inclusion of three new mini-STR loci (D10S1248, D14S1434, D22S1045) [178]. Mini-STRs and Y-STRs may be used in conjunction with conventional STR markers to provide added information in specific circumstances. Mini-STRs provide additional benefit in the typing of degraded material whereas Y-STRs aid in the analysis of mixed (male/female) samples.

Recent work has investigated the utility of SNPs within human nucleosome regions as a superior set of SNP markers for use with extremely degraded samples [179]. A nucleosome core particle consists of 146bp of DNA wrapped around a histone octamer in 1.65 turns of a flat, left-handed superhelix [180]. There is evidence that the histone-DNA complexes found in nucleosomes offer protection from external agents involved in DNA degradation processes [181, 182]. A set of 18 autosomal SNPs from nucleosomic regions were identified and combined into a single multiplex assay for forensic identification purposes [179]. This assay gave a slightly higher success rate than the SNP_{for}ID 29-SNP multiplex assay (6%) and a more substantial improvement than MiniFiler™ (24%) when analysing highly degraded casework samples.

Another set of short amplicon binary markers (SABs) have been recently investigated for potential use in forensic DNA profiling [50, 183, 184]. Insertion/deletion polymorphisms (indels) are typically analysed in amplicons of less than 160bp and therefore considered ideal for the analysis of highly degraded samples [185]. Indels have also been shown to be particularly useful for low template samples showing extremely low quantification values ($\sim 10\text{pg}$) [183]. This study found that the combined SAB marker sets (50 SNPs and 38 indels) showed a 10-fold improvement compared with commercial STR and mini-STR amplification kits when typing severely degraded skeletal material. In isolation, the Random Match Probabilities (RMP) for the 38 indels ranged from $10^{-7} - 10^{-19}$, and RMP values for the 50 SNPs ranged from $10^{-11} - 10^{-24}$. Well preserved bone samples yielding full 15 marker STR profiles showed highly discriminating RMP values ($10^{-13} - 10^{-21}$) [183]. However, STR profiling of the most degraded samples gave values RMPs ranging from $10^{-2} - 10^{-3}$, and increased to $10^{-26} - 10^{-32}$ when the SAB data was added. Despite this improvement in power of discrimination using the indel markers, comparable RMPs can be achieved by using larger SNP panels.

1.5 DNA Quantification and Assessment of Degradation

Following the collection of an evidentiary sample, DNA is extracted and the amount of human DNA is routinely measured. This ensures that the correct amount of template is added to the PCR reaction for genotyping. Commercial STR amplification kits used in forensic laboratories require 0.5-2ng of template DNA for optimal results. Too much DNA leads to artefacts in STR profiles such as off-scale (pull-up peaks), split peaks (due to incomplete adenylation) and enhanced stutter, whilst too little may produce stochastic effects such as allele drop-out.

In cases of mass fatalities or environmentally challenged forensic samples, the total number of genome copies and the available copies suitable for PCR are often not the same, suggesting that DNA quality should also be evaluated. The most important information required from the quantification process is not a measure of total human

DNA in a sample, but the amount of amplifiable DNA. Therefore methods to assess both the amount and condition of DNA in a sample are important.

A PCR reaction may fail due to DNA degradation and/or inhibition, making a method that can simultaneously assess both the quality and quantity of template present in an extracted sample beneficial in deciding how to proceed [83]. Early quantitation methods involved UV absorbance or staining of a gel with ethidium bromide. In addition to consuming much of the available sample, these methods lacked specificity and sensitivity which may lead to overestimation of DNA quantity. Improved methods have been developed that overcome these problems.

From the 1990's to early 2007, many forensic laboratories used slot blot hybridisation for DNA quantification. Genomic DNA was captured on a nylon membrane followed by the addition of probes (radioactive, chemiluminescent or colorimetric). A direct visual comparison between the unknown sample and DNA standards was made to determine the amount of DNA in each sample. The process was laborious, consumed sample, and lacked sensitivity [186]. In 2004, the commercial product QuantiBlot™ (Applied Biosystems) was released and became the most common method for measuring DNA prior to PCR amplification in forensic laboratories. PicoGreen™ was another method used for quantitation of forensic samples [187]. This method is based on fluorescent detection where intercalating dyes are incorporated into any double stranded DNA which may result in an overestimation of amplifiable DNA for downstream genotyping.

QuantiBlot™ (and hybridisation-based systems) have been superseded by real-time quantitative PCR (qPCR) assays for the quantification of DNA in forensic labs [188, 189]. The advent of qPCR overcame the limitations of more traditional quantification methods. qPCR was first described by Higuchi et al. [190] as a process that detects amplified product at the end of each PCR cycle by measuring the intensity of the fluorescent probes as the reaction proceeds. An amplification curve is generated with three distinct phases (Fig. 1.5A):

- i) the initial “lag” phase, where the exponential amplification occurs
- ii) “exponential” phase, when PCR is occurring efficiently

iii) “linear or plateau” stage, when reactants are becoming exhausted.

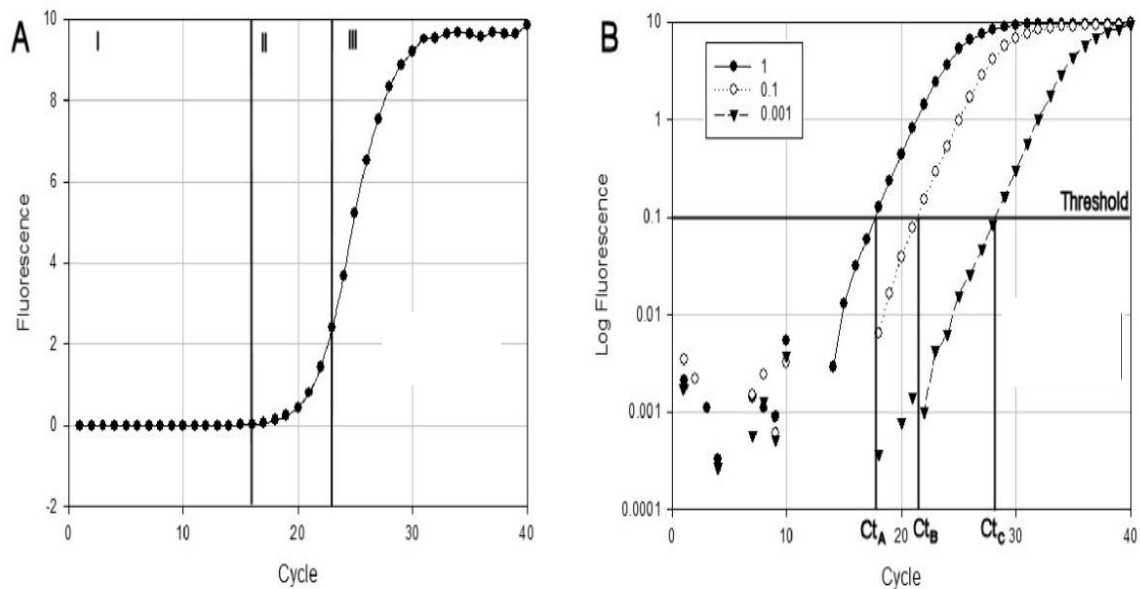


Figure 1.5 Real-time PCR Amplification Curves

A) The three phases of PCR amplification. I – the initial “lag” phase, II – the “exponential” phase and III – the “linear or plateau” phase. B) The cycle threshold (Ct) is set within the “exponential” phase of amplification when a linear relationship is established. [191]

The cycle threshold (Ct) is a set point within the exponential phase of amplification when a linear relationship can be established between the log of the concentration of DNA and the number of PCR cycles (Fig. 1.5B). The amount of initial DNA template in an unknown sample is calculated from the Ct by the use of a standard curve derived from a dilution series of known DNA quantitation standards.

Real-time PCR assays can be based on the detection of fluorescent intercalating dyes (SYBR™ Green), TaqMan® probes or primer quenching. Based on the amplification of a single or multi-copy targets the concentration of amplifiable DNA can be measured with high degrees of accuracy and sensitivity [192].

The Quantifiler™ Human DNA Quantification kit was developed in 2007 and validated for forensic testing by Applied Biosystems Inc. [193]. It provides analysts with a measure of amplifiable total human DNA quantity (lower limit of 20pg) by amplifying a

62bp nuclear target (hTERT). The kit detects PCR inhibition by including a synthetic internal PCR control (IPC) target. A delay in the IPC cycle threshold (C_T) value differentiates null amplifications due to inhibition from those simply due to insufficient quantities of template DNA. This is an important feature for the analysis of forensic casework samples.

Advancement in quantitation kits for human identity testing was made with the addition of a Y-chromosome target (SRY) to the qPCR assay. This allowed simultaneous determination of the amount of male DNA and the total amount of nDNA in a sample. This measure is of particular importance when analysing mixed male and female samples (eg. sexual assault samples). By quantifying the male component of a mixed sample a more accurate determination of the amount of sample required for successful STR amplification of that male contributor is achieved. Several commercial kits (Quantifiler™ Y Human, Quantifiler® Duo Human DNA (Applied Biosystems) and Plexor® HY system (Promega)) have been used by forensic laboratories to simultaneously quantify the amount of the total human DNA and male component in each sample. This added information allows the selection of the optimal STR chemistry (autosomal or Y-STR) to streamline workflow whilst increasing downstream analysis success rates. These kits are able to detect male DNA from samples with male/female mixtures with a DNA ratio greater than 1:1000 male/female DNA [193, 194]. An IPC is included in both kits to detect any PCR inhibition. Protocols for commercial qPCR assays are straightforward, labour-saving and amenable to automation [195], all considerations for routine forensic application.

The primary purpose of commercial quantification kits is to measure the amount of amplifiable human DNA in a sample prior to PCR. However, these kits do not assess the level of DNA degradation in a sample. A pre-PCR screening assay which can simultaneously measure the quantity of DNA and assess the level of degradation of a sample would be useful in determining which genotyping method (STR, mini-STR, mitochondrial analysis) may be most informative. As a result an increase in laboratory efficiency by minimising the number of samples requiring re-analysis and a more prudent use of limited samples may be achieved [196].

This review will discuss several qPCR assays which have been designed to provide post-extraction sample assessment. The amount of information that can be gleaned from a single quantification reaction, such as the total nDNA and/or mtDNA quantity, amount of male DNA, the degree of degradation and/or presence of inhibitors has increased.

Assays amplifying one mtDNA and one nDNA target provide a qualitative assessment of DNA degradation. Amplification failure or success of the nuclear target would indicate whether STR or mtDNA typing would be more informative for a particular sample [36, 197-199]. These methods were found to be reliable indicators of downstream genotyping success in extremely degraded samples. However in order to predict whether a moderately degraded sample would benefit more from STR or mini-STR analysis, methods of assessing DNA degradation required refinement.

In 2006 a multiplex qPCR assay was designed to amplify two nuclear DNA sequences of different lengths, allowing for a more sensitive assessment of DNA degradation and quantification of amplifiable DNA [195]. The inclusion of an internal PCR control (IPC) in this triplex was a substantial advance in the evolution of pre-PCR screening assays. The IPC allowed the detection of PCR inhibitors and the differentiation of failed amplifications due to inhibition from those simply due to insufficient quantities of template DNA. A 170-190bp TH01 STR amplicon and 67bp CSF1PO STR amplicon was produced. An empirical ratio of relative amounts of short to long amplicons provided a quantitative estimate of the degree of degradation present in each sample. Rigorous testing on simulated casework samples showed the assay to be a reliable indicator of the degree of DNA degradation, DNA quantity and inhibition whilst sacrificing minimal DNA extract. Importantly, this study also demonstrated the utility of the assay to predict the downstream genotyping success of STR analysis, showing a general concordance between the qPCR degradation ratio and reduction in STR peaks detected.

This assay was improved by adding a Y-chromosome target, thereby making a quadruplex which detects the amount of total human DNA, male DNA, DNA degradation and the presence of PCR inhibitors in forensic samples [196]. This useful

diagnostic tool for sample assessment could improve the first-pass success rate for STR genotyping, thus minimising the consumption of extracted DNA and maximising throughput. This assay would be useful for identifying those samples that would be analysed more successfully with sample clean-up procedures or alternate genotyping tools such as mini-STRs (Mini-Filer™), Y-STRs (Y-filer™), SNPs or sample clean up rather than conventional STR typing [195] (Fig. 1.6). An advance on this assay was designed which in addition to dual nuclear (different sizes), and Y-chromosome targets also included two mitochondrial amplicons [200]. This assay therefore simultaneously provided information regarding the total amount of human DNA, the male component, and more severe levels of degradation.

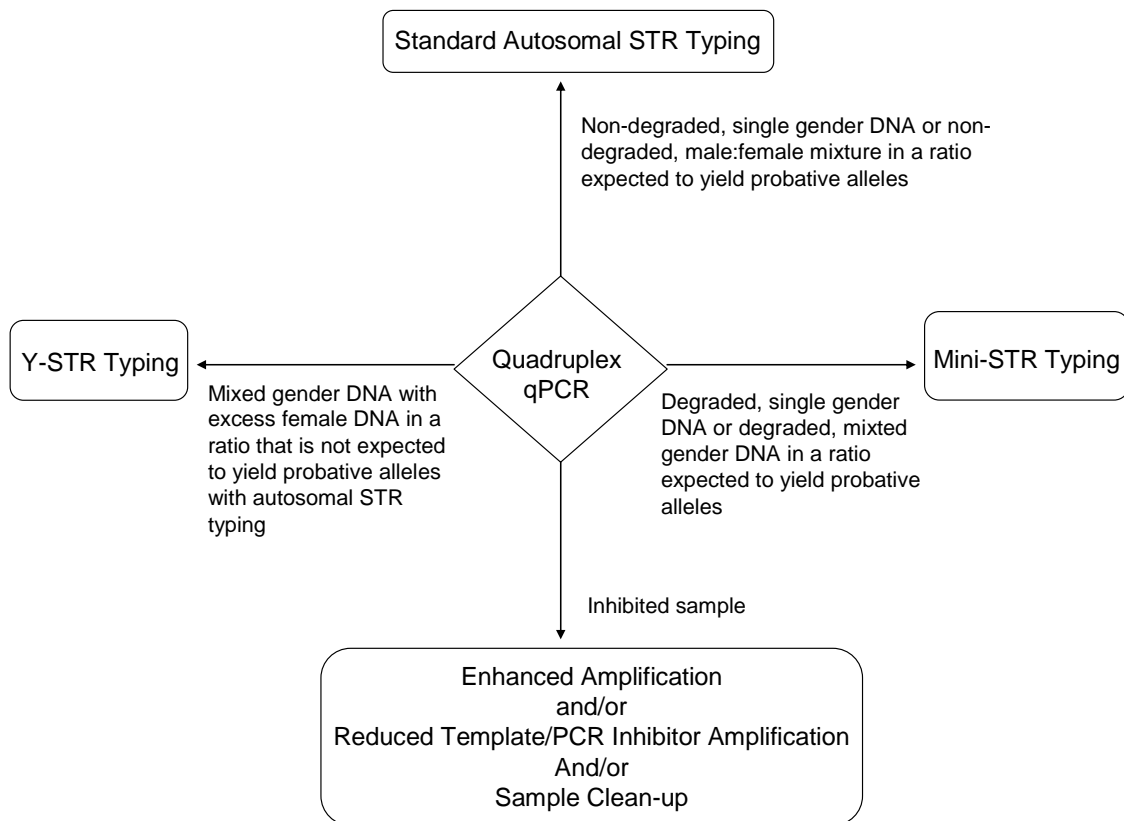


Figure 1.6 Flowchart depicting the choice of DNA strategy after quantification with the qPCR assay. [191]

More recently, alternate approaches to DNA quantification of degraded and low template samples have been published. Several *Alu*-based assays have been investigated [201-203]. These assays target multicopy *Alu* repeat DNA sequences providing a much lower level of detection (4pg) than single-copy gene assays such as the Quantifiler systems (25pg). One of the assays also included a Y-target to measure the male component of a sample [202]. The most recent of these assays [203] was designed to assess the level of DNA degradation with the amplification of two targets of different sizes within the *Alu* sequence (63 and 246bp). A recent study comparing single and multi-copy quantification assays reported that the single copy approach provided better accuracy whilst the multi-copy approach produced better sensitivity [204].

1.6 Alternate Technologies for Challenging Samples

1.6.1 Ancient DNA Techniques

Geneticists analysing ancient samples routinely deal with the many problems that present when testing DNA that is low in quality and quantity. This commonality links the fields of ancient DNA and forensic science. Much research has been carried out by molecular archaeology laboratories in an attempt to improve sample preparation and DNA extraction [60, 205], amplification methods from small quantities of ancient DNA [206] and DNA repair methods [207, 208]. Several techniques have been modified for the analysis of highly degraded forensic samples with success [13].

1.6.2 Optimised Extraction

Modified extraction protocols to maximise DNA yield from ancient bone samples [5, 62, 209] and from war remains [53, 59] have been well documented. Improvement in results using optimised DNA extraction methods for extremely degraded samples have been reported [5, 13, 61, 210]. When run in parallel, DNA extracted via standard forensic protocols has been shown to amplify poorly compared to samples extracted using an ancient DNA protocol (22.2% vs. 44% respectively with Mini-Filer™ and 85%

vs. 100% with SNP typing) [13]. The increased amount and possibly the quality of DNA retrieved from samples using the ancient DNA methods provided more template DNA for PCR which led to the improved success of both genotyping systems. The increased DNA yield with the ancient DNA protocol was also found to help overcome inhibition by allowing greater levels of dilution.

Standard bone extraction techniques used in forensic laboratories involve incubation of powdered bone in extraction buffer, collection of the supernatant and disposal of the remaining pellet of undissolved bone powder. However, a novel protocol which utilises complete demineralization of the undissolved bone sample has been shown to maximise DNA recovery [53]. Areas of extensive mineralisation with bone tissue provide physical barriers to the extraction reagents and therefore limit release of DNA molecules. Destruction of such dense crystal aggregates are likely to permit access to protected endogenous DNA [54]. Several studies have shown the total demineralisation method to significantly improve DNA quantity and quality from old skeletal material compared to standard extraction methods [53, 57, 211].

Improved extraction techniques are being investigated in order to maximise profiling success from skeletal material. These include methods for bone [63, 212-217] and ancient remains [55, 218], remains found in freshwater [219], non-destructive, non-powdering methods for bone and teeth [74, 220], buried [211] putrefied [221] and burnt [91, 222, 223] remains.

1.6.3 Low Copy Number (LCN) Methods

Forensic evidence samples sometimes present in trace amounts. These low template DNA (LTDNA) samples are generally defined as those with a DNA template amount less than 0.1ng or when PCR starts to exhibit exaggerated stochastic effects [224, 225]. The lower limits of sensitivity of commercial STR multiplex kits ranges 0.25-0.5ng, with an optimum input of 0.5-2ng DNA per reaction, and not more than 28-30 cycles of amplification [123, 226].

Although some degraded samples may present with sufficient quantities of DNA, this does not always reflect the amount of amplifiable DNA needed for successful PCR of STR markers. A highly degraded sample may contain ample DNA, but only one or two copies of relatively intact DNA. It is for this reason that highly degraded DNA samples commonly mimic true low template samples, and why LCN PCR methods are often employed in the analysis of such samples. This situation adds weight to the suggestion that DNA quality and quantity should both be evaluated independently [227].

Since the late 1990s much research has focused on the use of LTDNA within a forensic context. The ability to generate a DNA profile from as little as two or three cells enthused many law enforcement bodies and has led to an increase in the analysis of 'touch' DNA [79]. LCN profiling differs from standard DNA profiling by the number of cycles used during PCR amplification [224]. By increasing the number of cycles from 28 to 34, the chance of amplifying the few copies present in the DNA extract is improved [173]. However, this potential benefit must be carefully weighed against the substantial limitations that are associated with LCN conditions. Most importantly the increased risk of contamination, along with exaggerated stochastic effects such as allele drop-out/drop-in, increased peak height imbalance and stutter must all be considered when interpreting LCN profiles [224, 228, 229]. The interpretation and limits of these effects are based on internal laboratory validation [230, 231]. Even with such complications it has been suggested that by abiding by robust guidelines, such profiles may be interpreted [228]. Others argue that due to the incomplete and unreliable nature of LCN profiling any identifications resulting from LCN typing should be used as investigative tools only [232].

DNA profiles have been obtained from tools and firearms [233], fingerprints [234-236], hair [237], bone [209], saliva and sweat traces [238] by increasing PCR cycle number up to 40 cycles. However, comparative studies of LCN methods concluded that the optimal cycle number was 34 and little was gained by increasing the cycle number further. It did not improve sensitivity but in fact increased artefacts due to stochastic effects [228, 229]. Other work suggests that in the majority of LCN cases, slightly

better results were obtained with 28 cycles, and four to six more cycles after the addition of more *Taq* DNA polymerase [225, 239].

Alternative approaches to the standard 34-cycle LCN PCR have been suggested [240]. With a combination of PCR product clean-up, increased sample loading and injection time and voltage, STR profiles have been reported from 28-cycle PCR with the same, or better quality and sensitivity as those generated from 34-cycle PCR [241, 242]. Post-PCR purification of LCN PCR products prior to capillary electrophoresis (CE) and increased CE injection settings have been investigated as means of increasing PCR sensitivity without increasing PCR cycle number [243]. Significant increases in fluorescent signal intensity have been observed in purified PCR product over that of unpurified samples. The increased occurrence of undesirable artefacts was in accordance with other published data [228, 229, 239]. One problem which may result from increased cycle numbers during PCR and/or increased injection parameters is over-amplification and over-loaded profiles for the major component of mixtures, making mixture interpretation more difficult [244]. By extending the primer annealing time from one to 20 minutes during PCR, it was hypothesised that the few DNA molecules present in the LTDNA sample are more effectively used as templates. The data showed lower drop-out rates, increased peak heights and improved detection of mixtures [244].

Mini-STR assays tested on artificially degraded DNA samples utilised a 32 cycle protocol representing an intermediate between standard and LCN conditions [173]. The combination of both the small amplicons targeted and the increased cycle number appeared to contribute to increased success rates. Even greater profiling success may be achieved using SNP analysis as shorter amplicons than mini-STRs markers are targeted.

1.6.4 Whole Genome Amplification (WGA)

Fundamental to DNA identification is the availability of genomic DNA of adequate quality and quantity. The ability to faithfully amplify DNA from a limited source would be advantageous to any field. 'Immortalisation' of precious samples would enable multiple analyses of the material and create an archive for future investigation (eg. re-testing for the defence). Such technology would be of benefit not only to the forensic community but also to the fields of embryonic disease diagnosis, stem cell research, molecular anthropology and microbial genome detection in bioterrorism [245]. WGA randomly amplifies the entire genome. This process differs from PCR which targets specific regions.

WGA techniques have been predominately used to amplify high molecular weight clinical samples that are limited in quantity, although some work on high-quality forensic samples has also been conducted [246, 247]. Most important to the forensic community are studies investigating the utility of WGA methods on DNA of low quality and quantity [248-250]. As described, LCN techniques have provided some improvement in genotyping success from highly degraded samples. However if the quantity of starting DNA can be increased, the problems that result from low levels of template DNA should be avoided.

WGA methods generate long DNA fragments from small amounts of starting template DNA (nanograms), demonstrating a high yield and fidelity with complete coverage of the genome [251]. The main challenge of WGA is obtaining a balanced and faithful replication of all chromosomal regions without the loss of, or preferential amplification of, any genomic loci or alleles. Genotyping requires the accurate replication of both alleles at each locus of interest during WGA. Imbalanced amplifications can lead to genotyping errors due to allele dropout or low quality data, resulting in inaccurate or low genotyping success rates [252].

In principle, WGA could be executed from a single cell. Although successful WGA from single cells (6-7pg) has been reported, results are inconsistent, with allele drop-outs being a significant problem [253, 254]. Because only a single copy of each locus is

available, near perfect reproducibility is essential for a robust and useful single-cell WGA protocol [255]. Even a study demonstrating reliable SNP analysis coupled with MDA from a small number of cells (1-10) recommends that accuracy and resolution could be significantly enhanced with increasing the MDA template amount [256]. It is generally recommended that a minimum of 1-10ng (~150-1500 diploid cells) of genomic DNA be used for routine WGA to ensure that a significant number of templates representing all alleles are available for amplification [257-259]. Considering standard PCR requires 0.5-1ng of template for optimal amplification, this recommended lower limit will need reducing.

As with any technique involving the amplification of DNA, the risk of contamination must be considered. This is of particular concern for WGA methods because of the high product yield from minute starting amounts of DNA. The random nature of WGA means that any exogenous DNA would also be amplified and may even supersede successful amplification of the target DNA [249].

In the search for a reliable and robust WGA method for genotyping STR and SNP markers, several methods have been investigated.

1.6.4.1 PCR Based Methods

Early WGA methods involved PCR amplification of the genome using primers directed at repeat interspersed sequences (eg. Alu-repeats) [260] or linker-adapter based amplification methods using universal PCR primers [261]. Other PCR based approaches include random or partly degenerate primers and *Taq* DNA polymerase. Two PCR-based WGA methods previously investigated for clinical use have also been studied for forensic application [246, 248, 249].

The primer extension preamplification (PEP) technique involves a high number of PCR cycles using *Taq* DNA polymerase and completely degenerate 15-mers to amplify DNA [262, 263]. The degenerate primers can anneal to regions internal to products amplified in previous cycles, thereby creating shorter and shorter fragments with each cycle [251]. An improved-PEP method (I-PEP) may improve the yield and fidelity of

amplicon products [264]. However, PEP-based methods produce short products, suffer from incomplete coverage, uneven amplification of loci and a relatively high error rate (compared to other WGA methods) [262]. These are therefore not ideal for forensic purposes.

Degenerate oligonucleotide primed-PCR (DOP-PCR) uses partially degenerate primers (defined sequences at its 5'-end and 3'-end with a random hexamer sequence between them) that bind during several low temperature annealing cycles at many sites throughout the genome [265]. After these low stringency cycles the annealing temperature is raised increasing priming specificity. LL-DOP-PCR (long products from low quantities) is a modified DOP-PCR method which amplifies longer products (0.5-10kb compared to 0.2-2kb standard DOP-PCR) from DNA quantities of ~1ng [251]. Longer products are produced by increasing the annealing and extension times and a higher fidelity is achieved due to the 3'-5' exonuclease activity of *Pwo* DNA polymerase. In addition, significantly better coverage for microsatellites is achieved compared to conventional DOP-PCR methods [251].

The introduction of bias during PCR amplification results in the loss or uneven representation of loci or alleles within a locus and is a serious concern for genotyping. Variation in the extent of amplification bias has been observed with PCR-based WGA methods. Amplification biases of 10^2 - 10^4 and 10^3 - 10^6 -fold have been demonstrated using PEP and DOP-PCR respectively [262]. As a result allele dropout and genotyping miscalls are observed and in extreme cases regions of the genome are completely lost [259]. Both PEP and DOP-PCR have been refined to increase the fidelity and the length of the amplification products [262]. However, all current PCR-based WGA methods suffer from incomplete and uneven genome coverage, significant amplification bias, generation of short amplicons, and high error rates compared to non-PCR WGA methods [262, 266].

1.6.4.2 Non-PCR Based Methods

Non-PCR based WGA methods rely on the bacteriophage Φ 29 DNA polymerase which replicates the circular single stranded viral genome. In contrast to *Taq* DNA polymerases, the Φ 29 DNA polymerase is capable of protein-primed initiation [267]. DNA polymerisation occurs via an isothermic strand displacement method which has significant advantages over PCR-based methods. Φ 29 DNA polymerase is a highly processive, strand displacing enzyme which generates higher yields and longer length products compared to *Taq* DNA polymerase [268]. It also has 3'-5'-exonuclease activity providing proofreading capabilities [269]. Φ 29 DNA polymerase has an error rate of 10^{-6} - 10^{-7} [270] in contrast to native *Taq* DNA polymerase, which has an error rate of 3×10^{-3} [271]. The application of Φ 29 DNA polymerase to a linear template is termed Multiple Displacement Amplification (MDA) (Figure 1.7) whilst amplification of a circular template is termed Rolling Circle Amplification (RCA) (Figure 1.8).

1.6.4.3 Multiple Displacement Amplification

Multiple displacement amplification (MDA) represents the most reliable and efficient WGA protocol developed to date [272]. MDA relies on isothermal amplification utilising the high processivity and strand displacement abilities of Φ 29 DNA polymerase and the use of random hexamer primers [270, 273]. Primers anneal to multiple sites along the linear DNA template and serve as initiation sites for the Φ 29 DNA polymerase-mediated replication. As the replication proceeds along the template, it reaches the initiation site for other replication events. These strands are displaced, allowing replication to continue. The displaced strands then serve as new template molecules for initiation of subsequent DNA replication resulting in hyperbranched amplification of long fragments (Fig. 1.7). These fragments may be up to 70kb in length, although the average size is 10kb [249], compared to <3kb fragments produced via PCR-based WGA. MDA favours more equal representation of sequences because each priming event is propagated over very long distances in the genome, and the number of initiation events is lower than PCR-based methods [274].

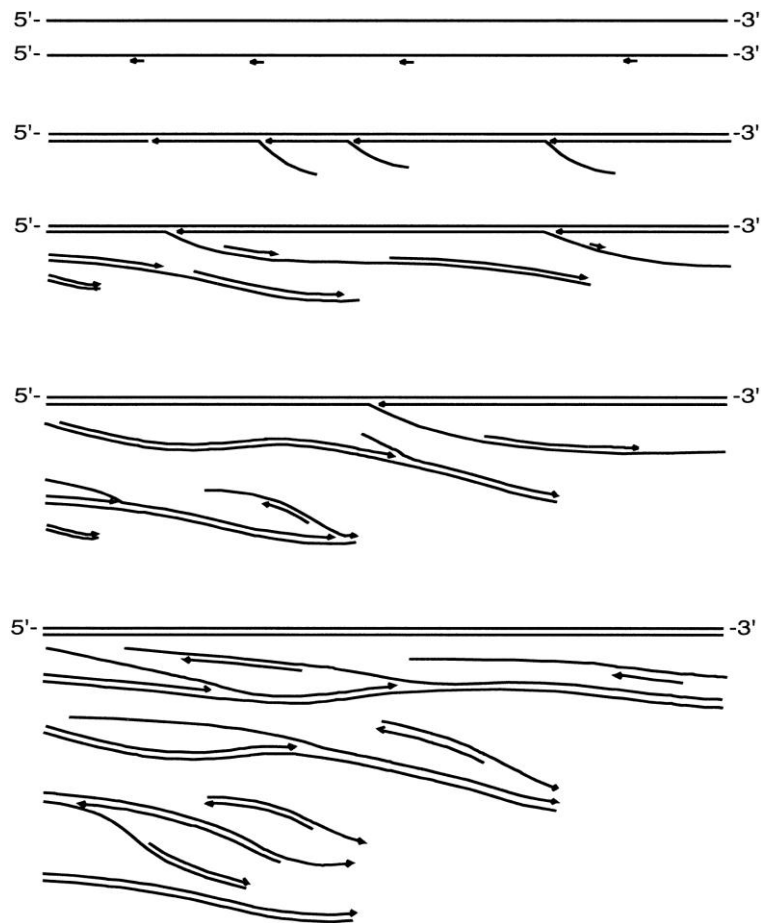


Figure 1.7. Schematic representation of the hyperbranched strand-displacement amplification reaction of MDA [274]

Random hexamer primers anneal to DNA template and are extended by $\Phi 29$ DNA polymerase. Replication proceeds along the template, and when the enzyme reaches the initiation site for other replication events the strand is displaced. This allows replication to continue as the displaced strands then serve as new template molecules for initiation of subsequent DNA replication. This process results in hyperbranched amplification of long fragments.

MDA generally produces a much higher yield of product compared to PCR-based methods. MDA reactions are self-limited, and therefore the product yield will depend more heavily on the reaction conditions and amount of reagents as opposed to the amount of input DNA [258]. Consequently, varying DNA concentrations in the initial sample will plateau during MDA, producing uniform end-product DNA concentrations. MDA generates efficient yields of DNA with an average of 225-350ng/ μ l [275]. Although WGA yield is not correlated with the amount of input DNA, the proportion of the successfully typed STR profiles has been shown to generally decrease when the starting DNA amount is reduced [246, 276]. Strong allelic imbalance and dropouts

have been shown to appear with a starting template of 0.1-0.25ng with consistent and reliable STR typing obtained using >0.5-5ng genomic DNA [246, 275]. These results suggest that the sensitivity and specificity of MDA may depend on the amount of starting DNA. These studies were carried out on high molecular weight DNA. The added complication of DNA degradation was not investigated.

The reported minimum amount of DNA required to overcome stochastic effects during MDA varies from as little as 0.07ng [253] to 0.5ng [275], to 3ng [252]. The amount of input DNA recommended by commercial MDA kits to minimise amplification bias and produce accurate and reproducible results is 5-10ng. However, that is not to say that MDA cannot be performed with less DNA. The utility of MDA for forensic purposes would be dependent on the ability to reproducibly and accurately genotype samples from <100pg template DNA. Limited success has been achieved with MDA (followed by STR, SNP analysis and sequencing) on single cells [247, 277], mitochondrial DNA [278] and clinical samples [279]. However, other studies have shown frequent allele dropout and significantly high levels of amplification bias [253, 254]. A recent study has shown better DNA typing results directly from single cells compared to pre-treatment with WGA [280]. As expected, amplification bias decreases with increasing template amount.

The amplification bias observed with MDA is much lower compared to other WGA methods [246, 257, 281]. An average three to sixfold bias between genomic loci has been observed in MDA products [259, 274, 282] compared to a 10^3 - 10^6 -fold amplification bias using DOP-PCR and a 10^2 - 10^4 -fold bias with PEP [258]. Although significantly lower levels of amplification bias are observed with MDA over that of PCR-based WGA methods, the bias can cause genotyping or copy number discrepancies [268]. A reduction in amplification has been shown to occur in regions of the genome with high repetitive DNA (centromeres and telomeres) and also in regions with large numbers of long interspersed elements (LINEs) and/or short interspersed elements (SINEs) [259]. It is proposed that these areas are under-amplified due to the exhaustion of complementary primers within the reaction [258].

With very small numbers of cells, pooling of MDA products has been suggested to correct for stochastic variations [283]. Pooling replicate DNA samples prior to analysis of STRs and SNPs in as little as 100 micro-dissected cells showed 82 - 100% accuracy [284]. Pooling replicate MDA products was also shown to improve SNP genotyping results in samples with low amounts or poor quality DNA [283]. Pooling of three replicate MDA reactions gave a small improvement in both call rate and STR genotyping accuracy [284, 285]. Alternatively, the combination of two MDA reactions (with and without denaturation) reduced locus and allelic bias significantly, aiding in copy number analysis and subsequent genotyping [268]. However, one must consider whether it may be more beneficial to perform one MDA reaction with more template DNA as opposed to splitting the extract into replicates and then re-pooling MDA products to even out the effects of amplification bias.

In addition to amplification from purified genomic DNA, MDA can also be performed directly from biological samples such as whole blood, buccal cells, tissue cultured cells, or laser-captured micro-dissected tissue [259, 284]. This feature may be of benefit to the forensic community for the direct amplification of trace evidence samples where DNA extraction and the potential loss of DNA may be avoided.

An issue with MDA is the production of non-specific product during amplification, as seen in negative controls. In the absence of DNA template, MDA (and other WGA methods) can produce spurious products visible by agarose gel electrophoresis [246, 249, 257, 274]. The products are likely to stem from the prolific DNA amplification by Φ 29 DNA polymerase and have been shown to contain substantial amounts of single-stranded DNA, primers and free nucleotides [249]. Such spurious products have been found not to yield PCR product, and do not interfere with downstream genotyping [246, 257]. However, this makes simple gel electrophoresis (or any method that assays overall DNA content) unsuitable for assessing the success of WGA procedures. Therefore allele-specific, PCR based techniques should be utilised [249]. Recent improvements to remove the spurious product in negative controls have been made to

the GenomiPhi V2 Amplification kit (GE Healthcare Life Sciences) and this is therefore no longer a problem.

MDA and Degraded Samples

The performance of MDA is dependent on the quality of the template DNA [274]. While WGA appears to work well on pristine DNA samples, its use with samples of low-quality DNA and limited amounts may be restricted [249]. Commercial MDA kits such as REPLI-g (QIAGEN) and GenomiPhi V2 recommend template DNA to be >2kb in length with some fragments >10kb for optimal results. The amplification efficiency of MDA rapidly diminishes as the molecular weight of the starting material decreases. Highly fragmented DNA has fewer binding sites per target molecule for initiation of replication resulting in fewer hyperbranching events and overall much lower yield [274].

Documented performance of MDA from degraded template DNA varies markedly. Some studies have reported MDA to produce typeable DNA from samples which previously failed [286] as well as less amplification bias [258] and higher amplification yield compared to PCR-based WGA methods [252]. Others have shown strong allelic imbalance [287], and a decrease in the number of alleles observed post-MDA [250]. In general, genotyping sub-optimal forensic samples (dried blood, hair, bone) post-MDA was considered unreliable [249].

Furthermore an amplification procedure that uses random primers to increase DNA quantity will reduce DNA fragment size with each progressive priming event. Any given primer will anneal randomly along the entire length of the target molecule. The resultant product pool will average a 50% reduction in size compared with the starting material [249]. Subsequent rounds will continue the trend in size reduction. While this would not be a concern when ample high molecular weight (HMW) template is available, MDA of highly fragmented DNA can only generate smaller product from already short templates. It has also been suggested that the hyperbranching

amplification used in MDA may prove to be inefficient with highly fragmented DNA [274].

Although MDA has been successful in the analysis of minute amounts of HMW DNA, its ability to accurately amplify degraded DNA in low quantity warrants further investigation. One measure of WGA success would be its ability to accurately genotype extremely degraded DNA (<200bp), or from template amounts less than 100pg in samples that would otherwise fail using conventional STR and mini-STR methods. MDA appears to be the most promising WGA method. However further improvement is required for its application to highly degraded samples before its use on forensic casework can be recommended.

1.6.4.4 Rolling Circle Amplification (RCA)

RCA also relies on bacteriophage Φ 29 DNA polymerase which in vivo replicates the circular single stranded viral genome (Fig. 1.8). Like MDA, RCA utilises the high processivity and strand displacement abilities of Φ 29 DNA polymerase and random hexamer primers in an isothermic amplification. The only difference is a circular template as opposed to a linear DNA molecule is amplified.

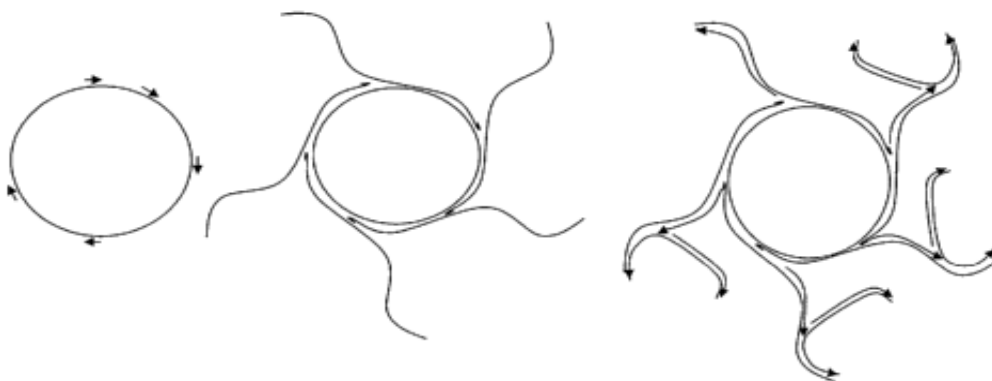


Figure 1.8 Rolling circle amplification (RCA).

Single stranded circular DNA is primed with random hexamer primers. The Φ 29 DNA polymerase extends while displacing the strand upstream. Priming of the displaced strand, extension and further branching results in hyperbranching and exponential amplification. (from <http://patents1.ic.gc.ca/cipo/cpd/en/patent/2607532/summary.html>)

1.6.4.5 Restriction and Circularisation-Aided Rolling Circle Amplification (RCA-RCA)

RCA-RCA involves a combination of restriction enzyme cleavage and isothermal Φ 29 DNA polymerase-mediated amplification of a circular template DNA molecule. It has been utilised successfully to amplify DNA from formalin-fixed samples [288]. In this method, the DNA is first cleaved by a restriction enzyme with the aim of producing two cuts between successive DNA damage sites and then treated with T4 DNA ligase to induce circularisation of the digested DNA. Subsequent treatment with exonuclease destroys any remaining linear template. The resulting circles are denatured and amplified using Φ 29 DNA polymerase (Fig. 1.9) [258].

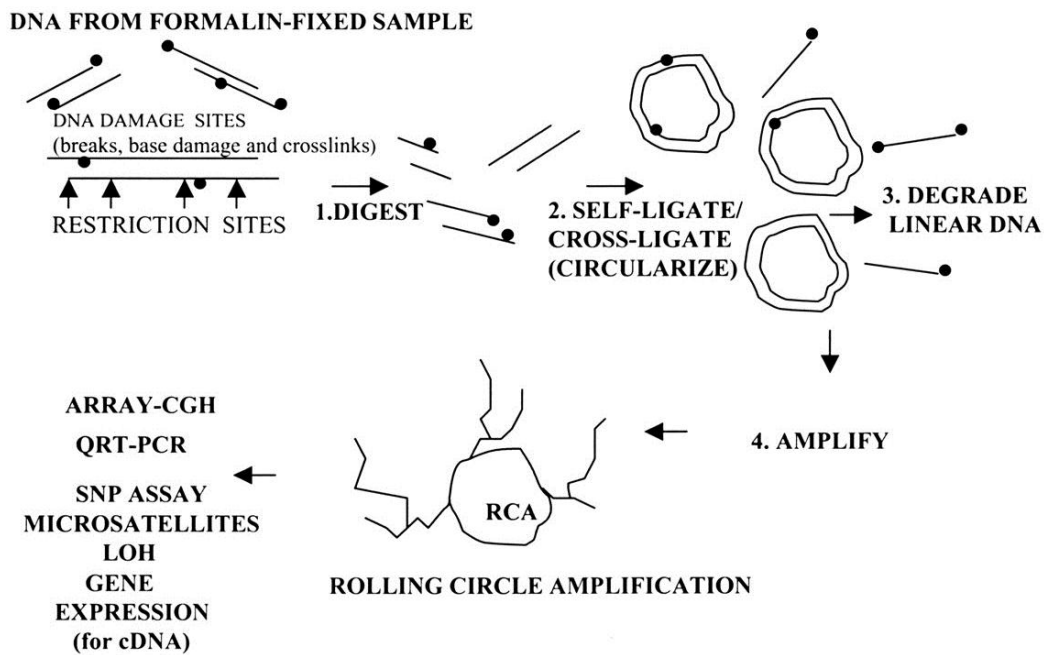


Figure 1.9 Outline of RCA-RCA (Restriction and Circularization-Aided Rolling Circle Amplification) of damaged and partially degraded FFPE samples

1. DNA is digested with a restriction enzyme. 2. Cuts between DNA damage sites (•) generate intact DNA fragments that can be circularised with T4 ligase. 3. Noncircular DNA is eliminated via exonuclease. 4. Circular DNA is denatured to enable RCA. [288]

The success of RCA-RCA relies on generating two cuts by the restriction enzyme within the degraded fragment. It can be expected that for highly degraded DNA this becomes increasingly difficult. The choice of a more frequent cutter (eg. four-base restriction enzyme) should achieve maximum sample recovery and amplification from highly degraded samples. However it is a concern that cutting already small fragments with restriction enzymes into smaller pieces, and digesting non-circularised fragments would lead to the loss of potential template. Due to the much smaller targets required for SNP-typing, this may not be as great a concern. This method would not appear to provide any advantage over MDA for whole genome amplification of highly degraded samples in very low amounts.

1.6.5 Repair Strategies

Improvements in the genotyping success of challenging forensic samples may result if DNA could be repaired prior to WGA, STR or SNP-typing. Several commercial DNA repair products have been investigated by forensic laboratories in order to improve DNA-typing of highly degraded, damaged and low template samples.

1.6.5.1 Ligation + MDA

Fragments of DNA (<2kb) are unsuitable templates for WGA [289]. The inability of Φ 29 DNA polymerase to prime from extremely short fragments may be the predominant reason that MDA fails to amplify such highly degraded samples. T4 DNA enzyme ligates dsDNA through the formation of a phosphodiester bond between a 5' phosphate and a 3'hydroxyl group. T4 DNA ligase may be used to ligate small fragments of dsDNA together forming concatamers. This should increase the length of template molecule which may then be a suitable template for MDA. However, initial studies have shown that T4 ligation of both double and single stranded template to be inefficient [290, 291].

1.6.5.2 *CirLigase™ + RCA*

The bacteriophage Φ 29 DNA polymerase replicates its circular single stranded viral genome. Therefore the circularization of highly fragmented DNA (<200bp) may provide a more suitable template for Φ 29 DNA polymerase via Rolling Circle Amplification (RCA). *CirLigase™* (Epicentre® Biotechnologies) efficiently circularises short ssDNA templates (>30bases) with almost no formation of linear or circular concatamers. *CirLigase™* has been shown to successfully circularise ssDNA fragments prior to RCA for applications such as genome walking [292], RNA sequencing [293] and WGA [294]. Initial pilot studies optimising *CirLigase™* conditions for low amounts of fragmented DNA have shown promising results [295, 296].

Although beyond the scope of this review, several other repair technologies aiming to improve DNA profiling from degraded samples have been published such as ligase detection reaction with PCR [297], bead hybridisation [298], and pre-PCR reaction assays [299, 300].

1.6.5.3 *PreCR™*

PreCR™ (New England BioLabs®) is a commercial cocktail of enzymes that repairs DNA lesions such as nicks, abasic sites, thymidine dimers and oxidative damage [301]. Hydrolysis (resulting in AP sites and nicks) and pyrimidine dimers are forms of damage that are common in environmentally challenged forensic samples. Initial studies evaluating the effect of *PreCR™* treatment on UV damaged samples showed an increased retrieval of STR loci and peak height values [302, 303].

1.6.5.4 *Restorase®*

Restorase® (Sigma-Aldrich) is a commercial cocktail designed to facilitate repair and provide reliable amplification of damaged DNA. *Restorase* combines a DNA repair enzyme with a high-quality long PCR DNA polymerase blend *AccuTaq* to repair damaged DNA sites which improves amplicon specificity and yield [304]. This product has been investigated as an alternate polymerase for DNA typing of very difficult forensic samples [305, 306].

1.6.5.5 REPLI-g-FFPE

Formalin-fixed paraffin-embedded (FFPE) tissues have been successfully used as a viable source of DNA for clinical analysis [307] and forensic cases [308, 309]. DNA within biological tissues which is formalin-fixed undergoes chemical modifications that degrade and fragment DNA [310] to lengths shorter than 300bp [311]. Genotyping and DNA sequence analysis of these samples can be limited by the small amount of sample available. A process which can amplify small amounts of highly degraded template to yield enough HMW product for successful analysis would be of great benefit to the molecular, medical and forensic sciences. A commercial WGA kit (REPLI-g FFPE, Qiagen) has been developed to amplify such highly damaged and fragmented samples. A ligation reaction randomly joins DNA fragments in preparation for the WGA reaction (Fig. 1.10). The WGA master mix contains the proprietary REPLI-g Midi DNA Polymerase and undergoes a two to eight hour isothermal reaction. The REPLI-g FFPE Kit is recommended for use with genomic DNA with average DNA fragments >500 bp in length. The end product is suitable for most downstream genotyping methods such as STR, SNP and sequencing assays. However, it should be noted that the manufacturer states that best genotyping results are obtained when amplicons of approximately 100 bp or smaller in size are targeted [312].

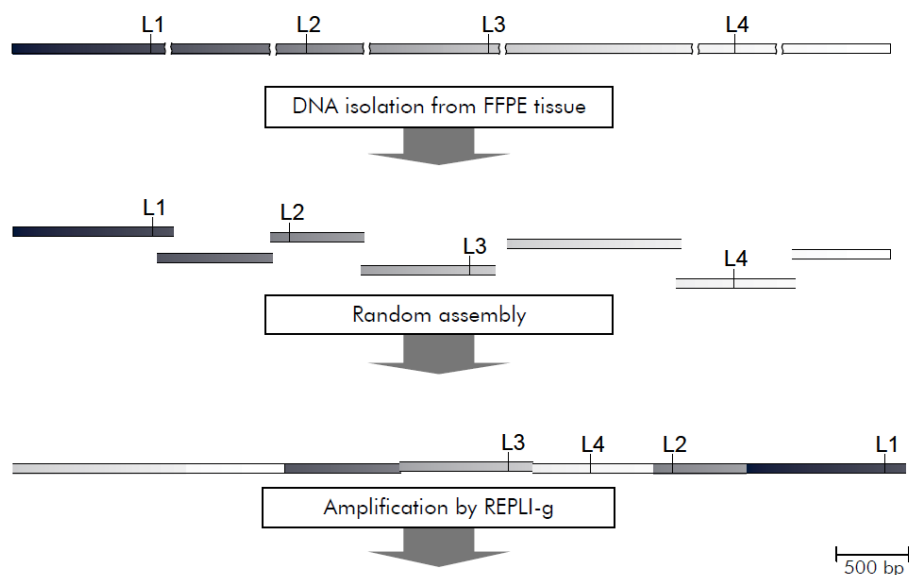


Figure 1.10. Overview of the FFPE REPLI-g process.

DNA fragments are randomly ligated together to form a longer template for the REPLI-g whole genome amplification reaction.

1.6.6 PCR Enhancers

An alternative approach to improving genotyping results from suboptimal samples is not to repair the DNA template, but to enhance the efficiency of the PCR reaction. Two methods which have been investigated by forensic laboratories are based on the principle of reducing the available reaction volume.

1.6.6.1 Molecular Crowding

By creating crowded reaction conditions an increase in intermolecular DNA ligation and binding of polymerases to DNA has been demonstrated [313, 314]. The inclusion of “stuffer DNA” or a polymer such as polyethylene glycol (PEG) during MDA reactions of HMW DNA (1-0.005ng) significantly decreased amplification bias and increase the number of detectable alleles in downstream STR genotyping [315]. Crowding of MDA or RCA reactions may facilitate more interaction between primers, Φ 29 polymerase and the DNA template and improve amplification.

1.6.6.2 PCR/STRBoost™

PCRBoost™ and STRBoost™ (Biomatrix Inc.) are novel reagents that can enhance PCR fivefold or more by improving sensitivity and specificity of amplification of genomic DNA [316]. An initial study has shown PCRBoost™ to increase the recovery of alleles from DNA with inhibitors, a “touch” sample and one ancient bone sample [44]. Additionally, successful amplification from thermally degraded samples with PCRBoost™ added to the PCR has also been reported [317]. This ‘boosting’ reagent is added directly to the PCR reaction mix and therefore requires no alteration to the STR kit used or cycling protocols. STRBoost™, has been more recently developed by Biomatrix specifically to improve STR results of challenging and low level samples [318]. Initial results have shown STRBoost™ to increase the number of detectable alleles, enhancing peak heights and overcoming the inhibitory effects of humic acid and indigo [319]. However, significant and consistent improvement in genotyping from highly degraded samples treated with PCRBoost™ or STRBoost™ has not been demonstrated.

1.7 Project Aims

The overarching aim of this research was to investigate various genotyping approaches for highly degraded DNA samples such as those resulting from natural, mass and missing person cases. Forensic markers such as STRs, mini-STRs and SNPs were used to examine the genotyping success of degraded samples, and a newly developed SNP panel was used to assess the potential for gaining phenotypic information from suboptimal DNA samples. In addition, this study explored the potential of several DNA repair and PCR enhancement strategies in order to improve downstream genotyping of such degraded samples.

The specific aims of this thesis were:

AIM 1: To evaluate the ability of a real-time qPCR assay to assess the level of DNA degradation in a sample and predict downstream genotyping success.

AIM 2: To investigate the comparative genotyping success of highly degraded samples using STR, mini-STR and SNP methods.

AIM 3: To create a collection of mock forensic skeletal samples which mimic the types of samples which may result from a mass disaster or missing person case:

- a) Bone and teeth would be exposed to environmental insults such as surface and burial conditions, submerged in fresh and saltwater and subjected to intense heat and fire.
- b) DNA extracted from these fieldwork samples should incur various types of DNA damage, and vary in the degree of DNA degradation.

AIM 4: To use the real-time qPCR assay (from Aim 1) to assess the level of degradation and inhibition of the mock forensic skeletal samples.

AIM 5: To compare the genotyping success of the environmental skeletal samples using two standard forensic STR amplification kits.

AIM 6: To investigate a novel technique to extract dentine from teeth in order to yield better quality DNA and generate more complete downstream STR profiles.

AIM 7: To investigate whether STR-typing of 200 year old bones and teeth from a shipwreck would be successful.

AIM 8: To explore the utility of a new 96-plex SNP assay on the BeadExpress (Illumina) for:

- c) the success and accuracy of the assay using genomic, WGA and degraded samples.
- d) the ability of the SNP assay to predict hair, eye and skin colour (pilot study).

AIM 9: To investigate the potential of several DNA repair methods and commercial PCR enhancement products in order to improve STR-typing of highly degraded samples.

2 Chapter Two

Assessment of DNA Degradation and the Genotyping Success of Highly Degraded Samples

ADDENDUM

This chapter has been published in the International Journal of Legal Medicine:

Assessment of DNA degradation and the genotyping success of highly degraded samples. Sheree R. Hughes-Stamm, Kevin J. Ashton and Angela van Daal. 2011, Volume 125, Number 3, Pages 341-348

Contributions of Authors:

Sheree Hughes-Stamm:

- All bench work
- All data analysis
- Preparation of manuscript

Kevin Ashton:

- Editing of manuscript

Angela van Daal:

- Assistance with experimental design and interpretation of results
- Editing of manuscript

2.1 INTRODUCTION

In the case of natural and mass disasters, missing persons and forensic casework, highly degraded biological samples are encountered. Conventional methods of identification such as fingerprint, forensic anthropology and dental matching can be inadequate when remains are highly fragmented and decomposed. DNA typing using industry standard short tandem repeats (STRs) often becomes the principle means of identification [51]. DNA becomes progressively more fragmented as biological tissue degrades and this results in a decreasing ability to gain a complete STR profile [13]. The successful genotyping of samples exhibiting very high levels of DNA degradation can be further complicated by the availability of only minute quantities of material. Such highly degraded samples commonly produce incomplete or no STR profiles and therefore the less informative mitochondrial DNA typing or less reliable low copy number typing are sometimes used for these samples [320]. The most favoured approach to increasing the success of DNA typing of highly degraded samples is to decrease the target amplicon size. Based on the principle that the smaller the target for PCR, the more likely the sequence will be intact and detected, much focus has been placed on designing reduced-length amplicon (~70-280bp) STR multiplexes (mini-STRs) by moving primers closer to the target region [321]. Mini-STRs have proven to be a useful tool for genotyping degraded samples [8, 41, 322, 323]. The European DNA Profiling (EDNAP) collaborative study recommended that existing STR loci be reengineered to provide smaller amplicons and three new mini-STR loci be added to the European core loci for the purpose of increasing the chances of amplifying highly degraded DNA [173]. However, single nucleotide polymorphisms (SNPs) may provide the greatest genotyping success for degraded samples due to their potentially very short amplicon lengths (45-80bp) [9, 11, 76, 173, 324].

Multiplex real-time quantitative PCR (qPCR) assays which simultaneously quantify total human genomic DNA, male DNA, the extent of DNA degradation and the presence of PCR inhibitors have been previously described [195, 196]. Further to Hudlow *et al*, 2008 [196] we report a capillary gel electrophoresis method of assessing DNA degradation in addition to a qPCR assay. We also investigate the comparative

genotyping success of highly degraded samples using STR, mini-STR and SNP typing systems. This type of study should prove valuable as a diagnostic tool for choosing which DNA typing systems may be the most informative whilst minimizing sample consumption

2.2 MATERIALS and METHODS

2.2.1 Sonication

DNA was extracted from whole blood (n=4) using QIAamp[®] Blood Maxi Kit (Qiagen, Hilden, Germany). Degraded samples were generated by sonication (Branson SLPt Sonifier[®], Danbury, CT, USA). The sonicator probe was treated with 10% bleach and UV irradiation before and after each sample. DNA extract (0.5-1mL) was sonicated on ice with 3/32" Microtip at 30% amplitude for up to 25 mins in cycles of 30 secs. Three size ranges were generated, <200bp (extremely degraded), 200-400bp (highly degraded) and >400bp (moderately degraded).

2.2.2 Capillary Electrophoresis

DNA samples were analysed via capillary electrophoresis using a High Resolution gel cartridge on a QIAxcel system (Qiagen, Hilden, Germany). Aliquots (1-3µL) of neat DNA extract were combined with DNA dilution buffer (Qiagen) to 10µL total volume. The QIAxcel system produces a digital gel image and an electropherogram for fragment analysis.

2.2.3 Quantitative PCR (qPCR)

Degradation assessment utilised a modified quadruplex qPCR assay previously described [196]. The four targets included two autosomal (TH01 and CSF), one male-specific target (SRY) and a synthetic oligonucleotide internal PCR control (IPC). PCR product was detected using dual labelled hydrolysis probes (TaqMan MGB[®], Applied Biosystems, Foster City, CA and TaqMan[®], Operon, Huntsville, AL). The assay was

performed on the Rotor-Gene 6000 (Qiagen) real-time thermocycler in a 20 μ L reaction volume using QuantiTect Multiplex PCR Mastermix (Qiagen). Modifications to the previously published assay include 5'dyes and primer concentrations (Table 2.1). Primer and probe sequences were unchanged as in Hudlow *et al.* except for the SRY probe ([Cy3.5]TTGCCCTGCTGATCTGCCTCCC[BHQ2A]) [196]. The two-step qPCR protocol consisted of an initial 15min 95°C polymerase activation step, followed by 40 cycles of 60 sec of denaturation (94°C) and 90 sec of combined annealing/extension (60°C). Pre-quantified, high molecular weight human genomic male DNA (Promega, Madison, WI) was used as a qPCR quantification standard and no template controls were included to monitor contamination. The ability of the assay to quantify the amount of male DNA in a background of female DNA was assessed by combining male and female DNA (1:1, 1:10, 1:100 and 1:1000). Both undegraded high molecular weight (HMW) and degraded mixture samples were tested. HMW mixtures utilised Human Genomic Male DNA (Promega, Madison, WI), and female K562 DNA (Promega, Madison, WI). Moderately degraded male and female DNA were used to generate degraded mixture samples.

Table 2.1 PCR amplicon length, fluorescence labels, primer and probe concentrations of each target sequence included in the quadruplex qPCR assay.

Target	Amplicon Length (bp)	Dye	Primer Concentration (nM)	Probe Concentration (nM)
SRY	137	Cy3.5	600	200
CSF	67	FAM	400	100
TH01	~170-190	Cy5	600	200
IPC	77	VIC	100	200

2.2.4 Genotyping

The AmpFISTR® Profiler Plus®, and AmpFISTR® MiniFiler™ PCR Amplification kits (Applied Biosystems) were used for STR and mini-STR genotyping respectively. PCR was performed in 25µL reaction volumes on a GeneAmp 9700 thermocycler (Applied Biosystems) with cycling protocols as per kit manufacturer instructions. Electrophoresis was performed on a 3130 Genetic Analyser (Applied Biosystems). Samples were prepared for fragment analysis as per AmpFISTR® Profiler Plus®, and AmpFISTR® MiniFiler™ PCR Amplification kit recommendations. Data analyses were performed using GeneMapper ID v 3.2.1 software (Applied Biosystems) with a 50 relative fluorescence units (RFU) peak amplitude threshold for all dyes. A partial profile was defined as the loss of one or more alleles or loci. SNP analysis (53 SNPs – S1) was performed in 4 separate multiplex reactions (in triplicate) using Sequenom Mass Array with iPLEX GOLD chemistry by the Australian Genome Research Facility (AGRF, St. Lucia, QLD). PCR cycling conditions consisted of denaturation at 94°C for 4mins, followed by 45 cycles of 94°C for 20 sec, 56°C for 30 sec and 72°C for 1 min, with a final extension at 72°C for 3 mins. The shrimp alkaline phosphatase incubation was at 37°C for 40 min and 85°C for 5 mins. The iPLEX single base extension reaction consisted of 94°C for 30sec, followed by a 200-short-cycle program of one loop of five cycles (94°C for 5 sec and 52°C for 5 sec) sitting inside a loop of 40 cycles with 80°C for 5 sec and then a final extension at 72°C for 3 minutes. The 53 SNP panel used was not designed for human identification purposes. It is an assay previously used in our laboratory and was utilised in this study solely to determine the success rate of SNP typing from highly degraded samples. As such, no population data were used. Instead an average heterozygosity value of 0.45 was assumed to estimate the type of matching probability (pM) that could be expected from SNPs chosen for identification purposes (SNPs with high heterozygosity values). The pM of each locus was determined by adding together the square of each possible genotype. With the assumption of locus independence and Hardy-Weinberg equilibrium, the pM for the set of SNPs was calculated as the product of the pM for each individual marker. Statistical analyses were performed using Microsoft Office Excel 2007 and SPSS Statistics 17.0.

2.3 RESULTS and DISCUSSION

A series of artificially degraded samples ranging from moderate to extreme levels of degradation was achieved with 5 min, 15 min and 25 min sonication respectively. Degradation was assessed in a two-step process. The QIAxcel system (Qiagen) produces a digital gel image for fragment analysis (Fig. 2.1A). The electropherogram provides a profile of the fragment composition of each sample (Fig. 2.1b). Samples with greater than 90% of fragments sized below 200bp were considered extremely degraded. Those samples with more than 90% of fragments sized between 200bp and 400bp were considered highly degraded and samples with greater than 90% of fragments sized above 400bp were considered moderately degraded (Fig. 2.1). These size ranges were used to test the genotyping success of the STR (100-400bp) mini-STR (~100-250bp) and SNP (~80-120bp) genotyping methods. The QIAxcel system provided a rapid, cost effective (less than 50c/sample) screening method for assessing sample quality.

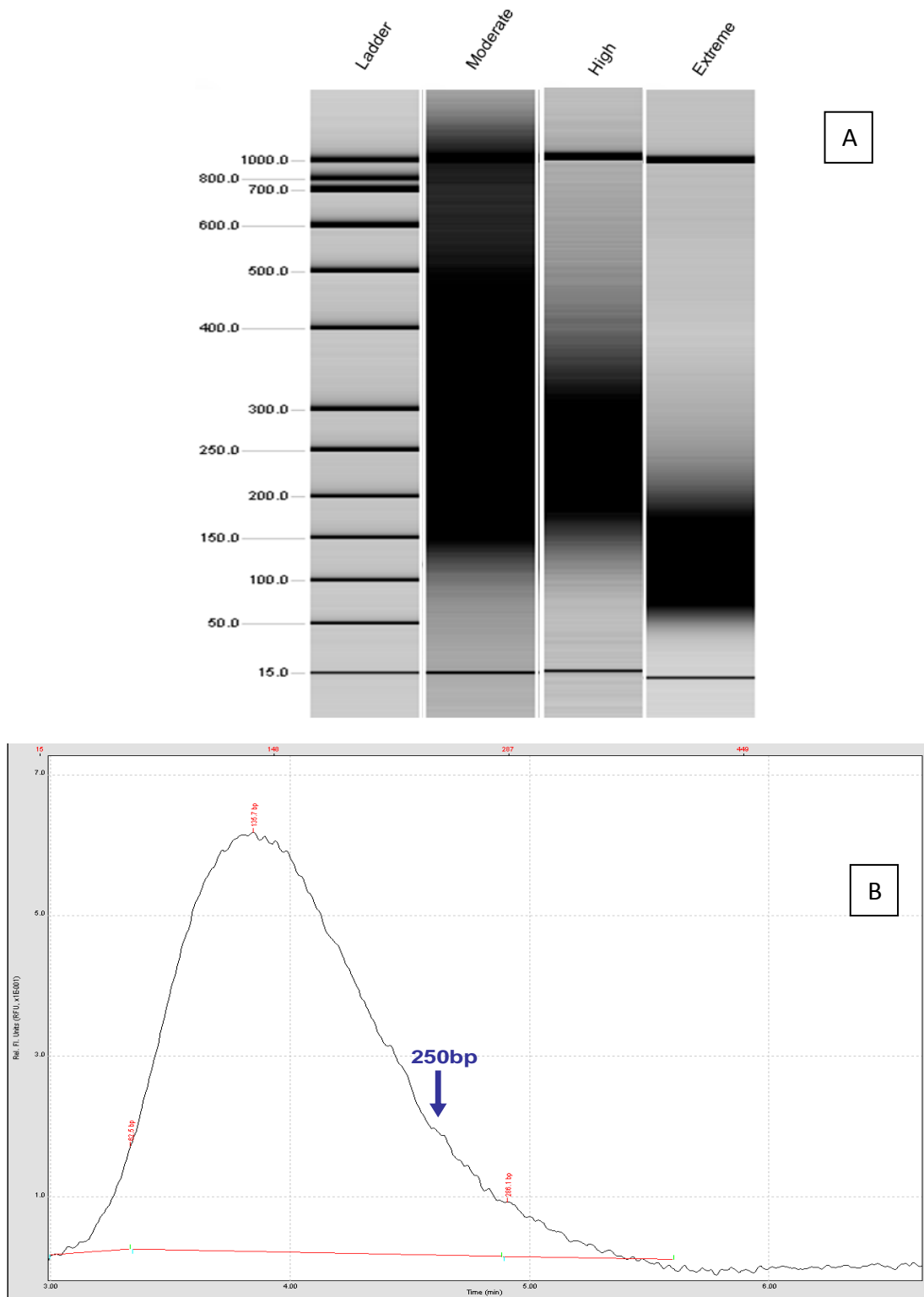


Figure 2.1 Fragment analysis of artificially degraded samples using the QIAxcel system

A) Digital gel image showing the range of fragments sizes in samples which were classified with moderate, high or extreme levels of degradation. B) A digital electropherogram of an extremely degraded DNA sample.

2.3.1 qPCR Degradation Assay

The modified quadruplex qPCR assay was able to simultaneously quantify total human DNA, male DNA and the extent of PCR inhibition and DNA degradation with reasonable accuracy and sensitivity. Calibration curves for each assay, namely; TH01, SRY, CSF, IPC showed good linearity with R^2 values above 0.99. Between assay reproducibility was assessed with three separate assays each in triplicate and data for each sample were used to calculate the mean and standard deviation.

To assess the sensitivity of the assay DNA template amounts ranging from 2ng – 15.6pg were used. Precise quantification, as indicated by standard deviations in C_T of less than one cycle was achieved for all four targets to 62.5pg. These results are concordant with the reported lower limit of 44pg of Hudlow *et al.* [196]. Quantification of DNA at 15.6pg was unreliable showing wide variation or failure to detect. This is consistent with stochastic effects expected at such low levels of template (reviewed in [232]). At 15.6pg of template TH01 was the most common failure (63%) followed by SRY (54%) and CSF (18%). These results are consistent with expectations based on the amplicon length of the targets (TH01; 170-190bp, SRY; 137bp, CSF; 67bp). The failure to detect these amplicons may be due to a combination of stochastic effects and lack of intact template at such low amounts. All targets of undegraded DNA were detected at 15.6pg but the failure to detect at this template level increased as the sample quality decreased (44% moderately, 66% high and 77% extremely degraded samples).

The ability of the CSF-TH01-SRY-IPC assay to indicate the level of DNA degradation in a sample was evaluated. As expected the degradation ratio (CSF quantity/ TH01 quantity) increased as the level of degradation increased (Fig. 2.2). No statistically relevant correlation between the degradation ratio and sample quality was observed. This is not surprising however given the testing of only three levels of DNA degradation, in addition to undegraded DNA.

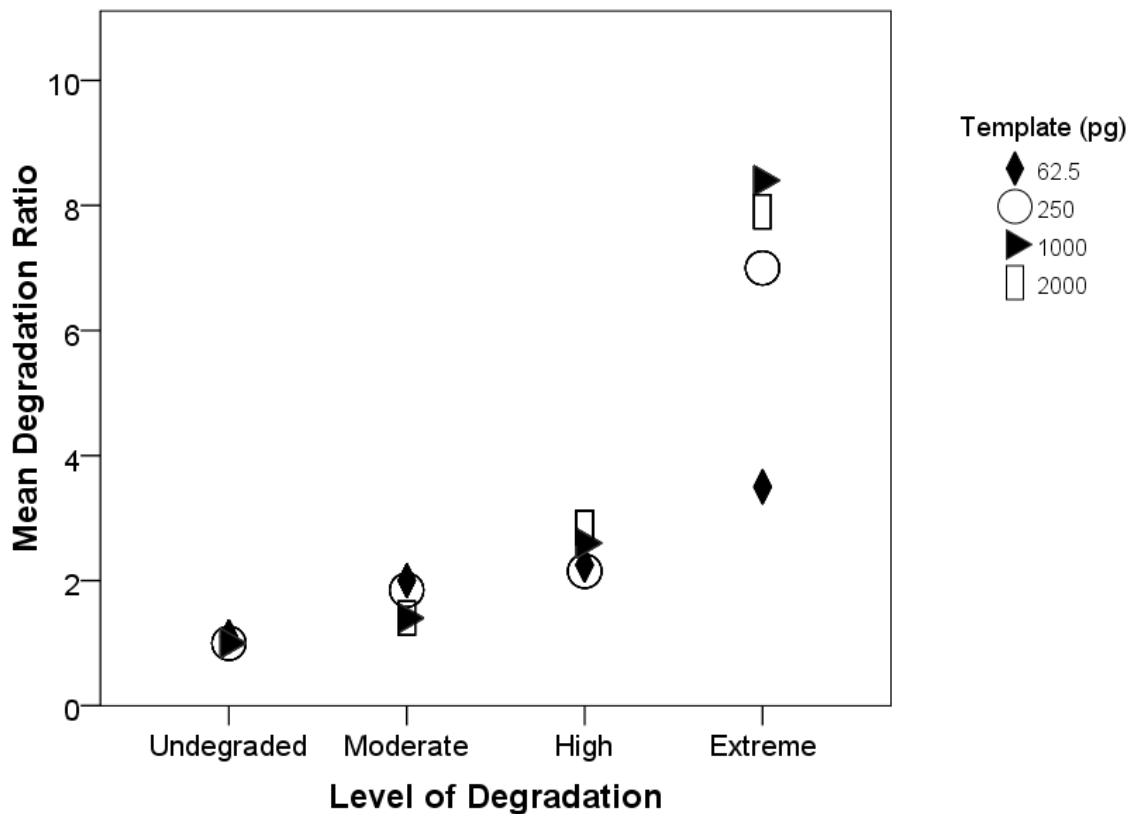


Figure 2.2 Sensitivity of the quadruplex qPCR assay in assessing DNA degradation[#]

[#]A ratio of 1 indicates equal amplification of both long and short PCR targets. A ratio >1 indicates greater amplification of the smaller target and therefore possible DNA degradation.

To assess the sensitivity and accuracy of the CSF-TH01-SRY-IPC assay to predict the degree of degradation, DNA template amounts from 2ng – 15.6pg were tested (Table 2.2). The assay produced reliable degradation ratios to a lower limit of 15.6pg in high quality samples and to a level of 62.5pg for all degraded samples. This is likely because while CSF was detected at 15.6pg TH01 was often not detected at all, making it impossible to generate a ratio.

Table 2.2 Sensitivity data of the quadruplex qPCR assay and degradation ratios with undegraded and degraded samples.

Level of Degradation	Template amount (pg)	Mean Quantity TH01 (pg) ^a	Mean Quantity CSF (pg) ^a	Mean Degradation Ratio ^{a,b}
Undegraded	1000	1010 (42)	1015 (35)	1
	250	280	290	1
	62.5	50	55 (7)	1.1 (0.14)
	15.6	15 (7)	22 (3)	1.46 (0.35)
Moderate	2000	1150 (95)	1720 (303)	1.467 (0.115)
	1000	480 (30)	660 (40)	1.4
	250	83 (5)	160 (26)	1.9 (0.264)
	62.5	23 (5)	46 (10)	2
	15.6	7 (5)	8 (5)	1.14
High	2000	513 (20)	1480 (90)	2.899 (0.057)
	1000	246 (15)	693 (130)	2.8 (0.4)
	250	60 (10)	147 (23)	2.5 (0.754)
	62.5	10 (3)	40 (17)	2.25 (0.353)
	15.6	0	7 (5)	c
Extreme	2000	173 (5)	1447 (80)	8.333 (0.702)
	1000	83 (5)	717 (80)	8.6 (0.346)
	250	23 (5)	157 (35)	6.766 (1.078)
	62.5	7 (2)	40 (10)	3.5 (0.707)
	15.6	0	10 (5)	c

^a Standard Deviation shown in brackets

^b Degradation ratio = quantity TH01/quantity CSF

^c Degradation ratio not possible due to lack of detection of TH01 amplicon

It should be noted that the combination of extreme DNA degradation and low template amounts (<250pg) resulted in an apparent overestimation of sample quality (Fig 2.2 and Table 2.2). This may be explained by the fact that extreme degradation effectively decreases the amount of intact template and exacerbates the stochastic effects which result from amplification of low template samples.

2.3.2 Mixtures

The ability of the qPCR assay to quantify a minor male component of a mixture was investigated. Known mixtures were prepared using HMW standards and highly degraded DNA in ratios from 1:1 to 1:1000 to simulate low copy number female:male mixture samples. Each mixture was then quantified with the TH01-CSF-SRY-IPC assay in triplicate. The male component was kept constant at 20pg as this was considered the lower limit of detection of the assay. Table 2.3 indicates that the quadruplex assay was able to detect male DNA to a lower limit of 20pg in a 1:1000 mixture. However a large standard deviation was commonly observed which may be expected for amounts below 100pg due to stochastic effects. This is also consistent with variation observed in previous studies [196]. It should be noted that a consistently higher male:female ratio (quantity of SRY/quantity TH01) was also observed in degraded mixtures compared to the corresponding HMW samples. This may indicate a relative resistance of the Y chromosome (or at least the region where SRY gene is located) to degradation. An alternate explanation is that this difference is accounted for by the smaller amplicon size of SRY (137bp) vs TH01 (170-190bp) and/or reduced competition of reagents.

Table 2.3 Quantification results of male and female mixed samples indicating male:female ratios generated by the quadruplex assay.

Ratio	Template DNA (pg/rxn)			Mean Quantity TH01 (pg/rxn) ^a		Mean Quantity SRY (pg/rxn) ^a		Mean Male:Female Ratio ^{a,b}	
	Total	Male	Female	Undegraded	Degraded	Undegraded	Degraded	Undegraded	Degraded
1:1	40	20	20	40	20	23 (4)	15 (5)	0.575 (0.075)	0.75 (0.354)
1:10	220	20	200	190 (77)	170 (8)	28 (8)	30 (10)	0.147 (0.048)	0.176 (0.071)
1:100	2020	20	2000	1680 (440)	790 (14)	30 (18)	30	0.018 (0.003)	0.038 (0.004)
1:1000	20,020	20	20,000	20,280 (1490)	7435 (750)	29 (2)	25 (7)	0.001 (0.0001)	0.003 (0.001)

^a Standard deviation shown in brackets

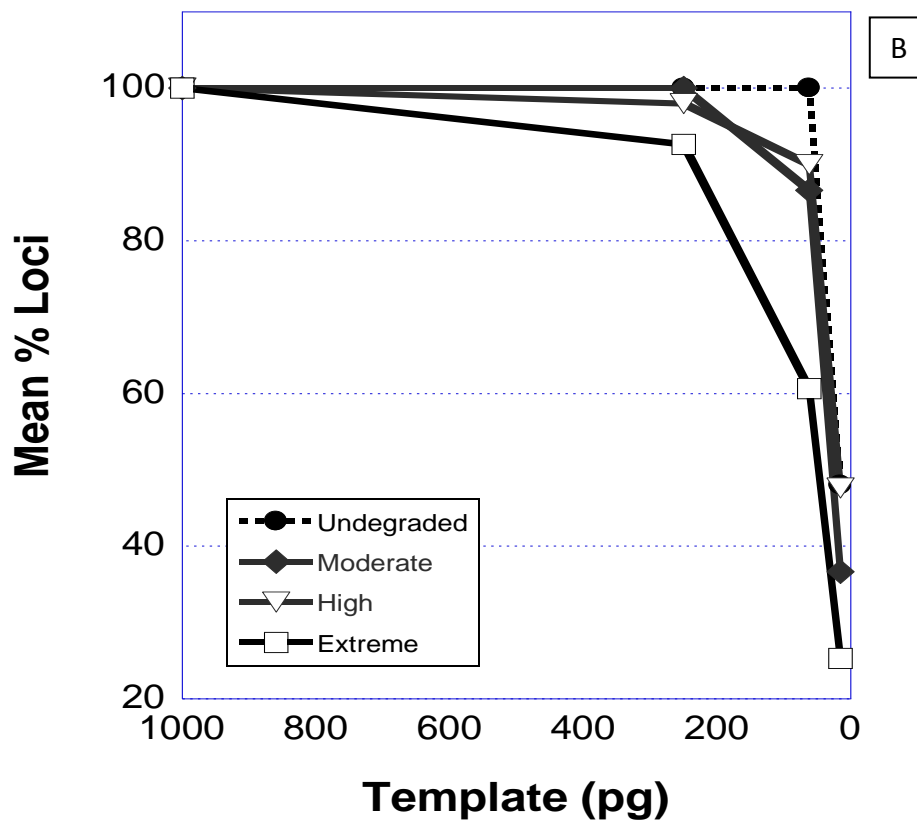
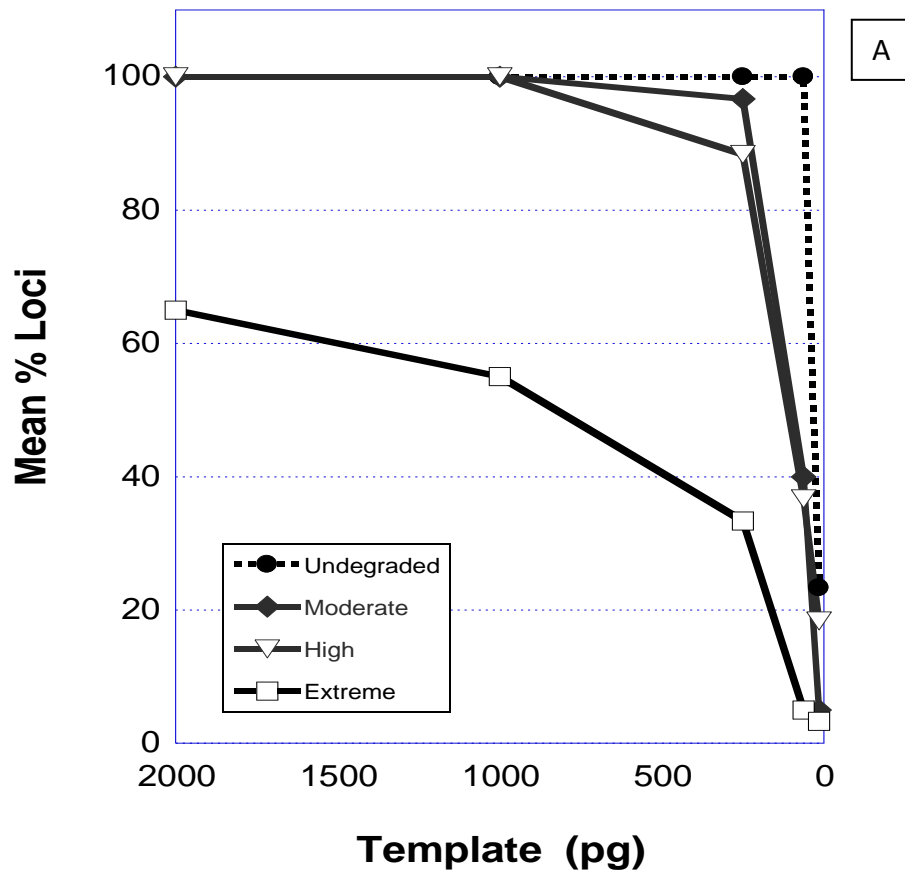
^b Male:female ratio = quantity SRY/quantity TH01

2.3.3 Genotyping

Sensitivity and comparative studies of genotyping success rates across STR, mini-STR and SNP typing were performed using intact and degraded samples. Evaluation of differentially degraded samples identified that overall SNP analysis provided the highest rate of loci retrieval compared to AmpFISTR® Profiler Plus® and AmpFISTR® MiniFiler™ amplification kits.

All typing methods performed well with intact single source DNA in amounts as low as 62.5pg (Fig. 2.3). Significant improvement was observed in the genotyping success of undegraded DNA using SNP analysis or mini-STRs over STR typing at 15.6pg (72% vs 48% vs 23% respectively). The AmpFISTR® MiniFiler™ PCR amplification kit is known to offer increased sensitivity over STR kits (0.2-0.6ng vs 1-2.5ng) [325]. Smaller amplicon size, enhanced kit chemistry, increased cycle number and differing cycling conditions contribute to this improvement in performance [326]. These results indicate that mini-STR and, in particular SNP typing would probably provide a better alternative to STR profiling for routine low copy number (LCN) samples in addition to highly degraded DNA.

Within the recommended input range of commercial STR kits (1-2.5ng) complete profiles were achieved with moderate and highly degraded DNA. However amplification of extremely degraded samples in this template range resulted in partial profiles (55-65% loci). An almost two-fold improvement in genotyping success with MiniFiler™ and SNP typing over that of Profiler Plus® was observed with these samples (Fig. 2.3B & C). Complete typing success was seen with MiniFiler™ and SNP typing compared to only 55-65% with Profiler Plus® STR typing. It should be noted that all MiniFiler™ profiles showed evidence of off-scale alleles and pull-up artefacts with DNA amounts greater than 250pg. This may be expected due to the increased cycle number and sensitivity of kit chemistry.



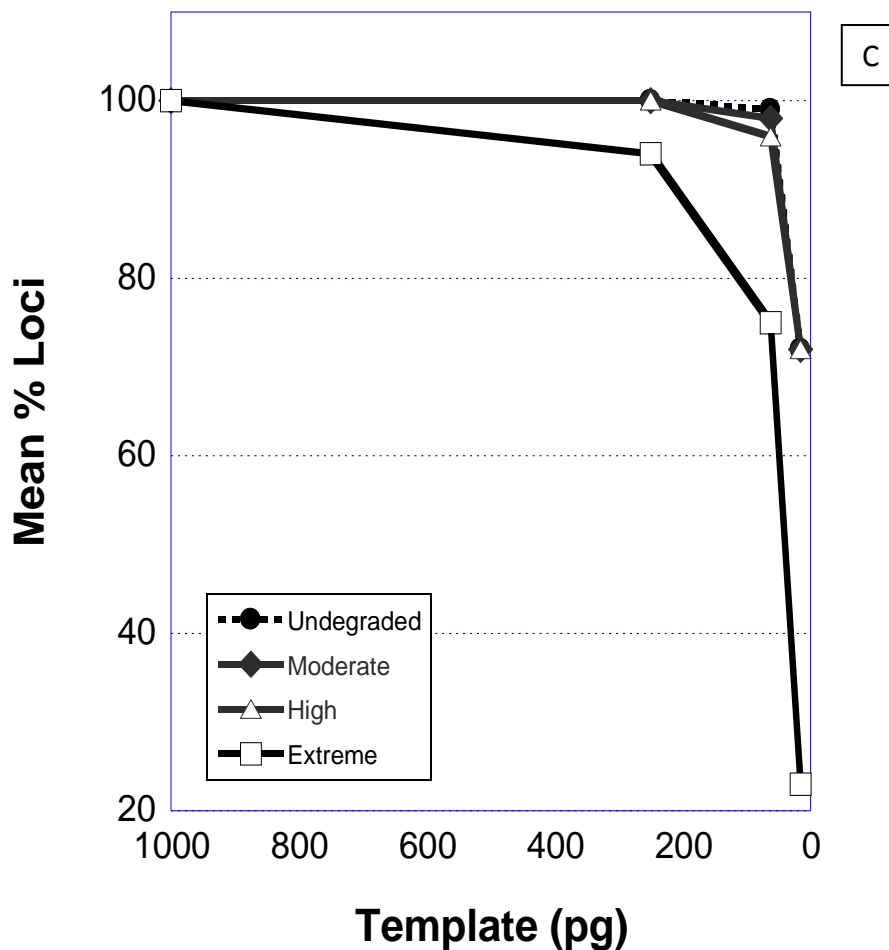


Figure 2.3 Sensitivity study and comparative success rates of loci retrieval.

The success of genotyping HMW and differentially degraded DNA samples was measured as the mean percentage of loci correctly called. The same samples were comparatively genotyped with three systems: (A) Profiler Plus®, (B) MiniFiler™ and (C) SNP analysis.

A substantial reduction in genotyping success is observed with all degraded samples below 250pg. Mini-STRs and SNPs showed considerable increases in loci retrieval across all input amounts <1ng compared to STRs (Fig. 2.3). These results support previous studies demonstrating the enhanced performance and sensitivity of the AmpFISTR® MiniFiler™ amplification kit [325, 326] and SNP genotyping [13, 116, 305, 324] for typing degraded samples. This may be attributed to reduced amplicon size, improved kit chemistry, genotyping platforms or a combination of all factors. Although MiniFiler™ yielded more complete profiles from template amounts <250pg compared with Profiler Plus®, the MiniFiler™ profiles showed an increase in baseline artefacts and allele drop-in.

SNP analysis yielded the highest overall rate of loci retrieval for all samples tested with the one exception being extremely degraded DNA in very low amounts (15.6pg). This result may be explained by a combination of exacerbated stochastic effects and possible limitations of the SNP platform used. Of all SNP mis-calls, 71% were due to failure of detection and 29% were false homozygotes due to allelic dropout. 80% of all SNP genotyping mis-calls occurred with 15.6pg DNA. The SNPs analysed ranged in length from 82-120bp with a mean length of 99bp. As expected, the success rate of loci retrieval increased as the number of loci in each multiplex reaction decreased. The 26 loci multiplex on average retrieved 89.8% of the SNP loci, the 15 loci multiplex 91.9%, the 10 loci multiplex 93% and the duplex assay successfully called 95.6% of the loci. The five least successful SNPs (70-80% correct) were not only in the largest multiplex, but included SNPs in the three larger reactions. There was no correlation between SNP amplicon length and genotyping success. Primer and assay design is therefore an equally important contributor to the success of SNP typing of highly degraded samples as amplicon size.

AmpFISTR® Profiler Plus® showed a considerable decline in retrievable loci as sample quality and template amount decreased (Fig. 2.3A). As expected the longer amplicons were more susceptible to locus drop-out as the level of degradation increased (Fig. 2.4). The four longest loci included in the Profiler Plus® kit (D18, D7, FGA and D21) showed ≥80% locus drop-out with extremely degraded DNA with template amounts ranging from 2ng down to 15.6pg. As expected due to reduced length, the four longest target loci in the AmpFISTR® MiniFiler™ kit (FGA, D7, D18 and D21) showed comparatively reduced locus dropout rates of 40%, 27%, 27% and 13% respectively.

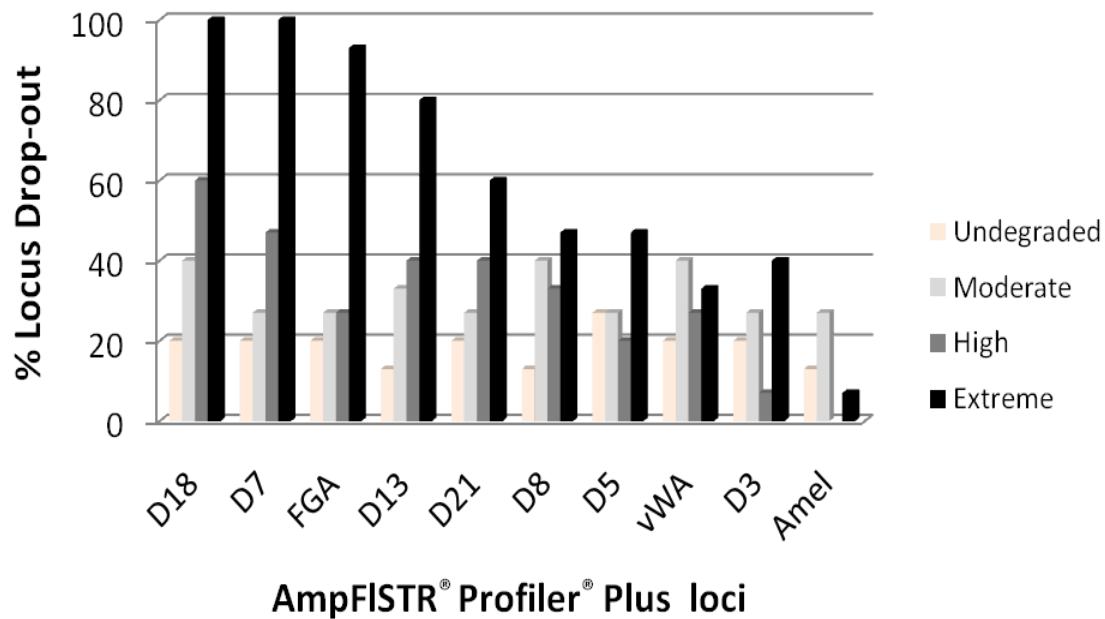
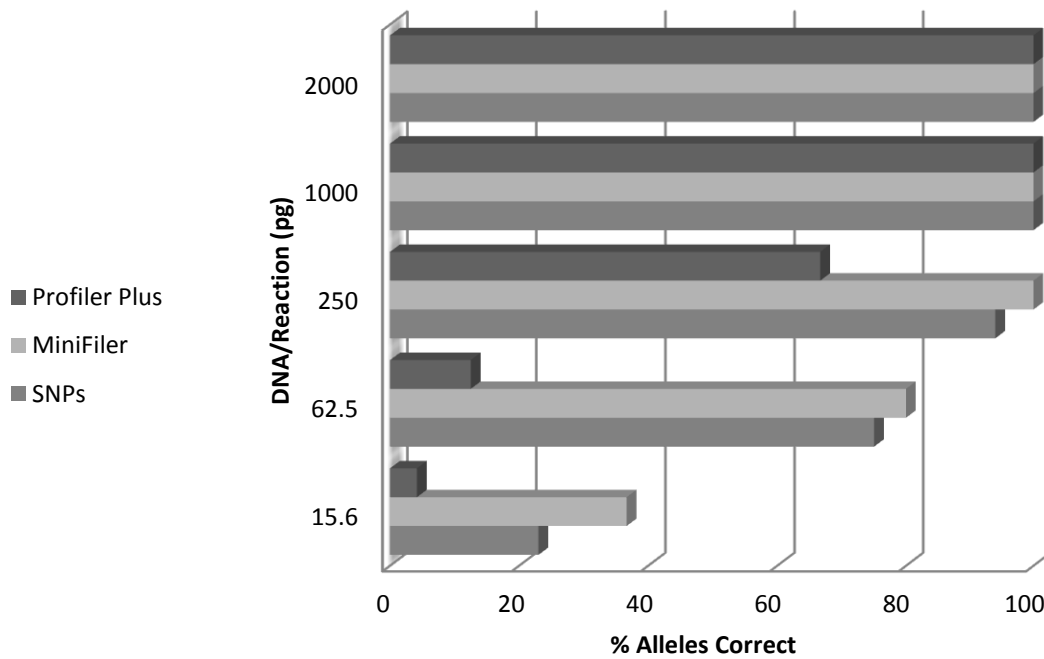


Figure 2.4 AmpFISTR® Profiler Plus® PCR Amplification kit locus drop-out# rates combined over all template amounts (2ng-15.2pg) of undegraded and degraded samples.

when both alleles at a given locus drop-out

An interesting comparison is the success rates of STRs, mini-STRs and SNPs of equivalent size. The success of retrieval of the smallest loci ($\leq \sim 150\text{bp}$) in the Profiler Plus (Amelogenin, D3S1358, D5S818, D8S1179) and MiniFiler kits (Amelogenin, CSF, D13S317, D16S539, D2S1338) are compared to that of the SNP panel ($< 120\text{bp}$) with extremely degraded samples (Fig. 2.5). At input amounts of $\geq 1\text{ng}$, all typing methods yielded 100% alleles. At lower amounts (250, 62.5, 15.6pg), the small loci of the Profiler Plus kit showed a much higher allele dropout rate (33.6%, 87.5%, 95.8% respectively) than those of the SNP assay (6%, 25% and 77% respectively) and MiniFiler kit (0%, 20%, 63.3%). This comparison suggests that regardless of amplicon size, the robustness of assay design and chemistry have a significant impact on the profiling success of highly degraded samples. When comparing similar sized amplicons across the three assays, the small loci of the MiniFiler kit performs the best. However, when considering the success rates of the kits as a whole, SNP typing provided the highest rate of loci retrieval from highly degraded samples presumably because all of the loci are small amplicons.



^a Profiler Plus loci (Amelogenin, D3S1358, D5S818, D8S1179)

^b MiniFiler loci (Amelogenin, CSF, D13S317, D16S539, D2S1338)

^c All 53 SNPs included (<120bp)

Figure 2.5 Comparison of the combined success of the smallest loci (≤ 150 bp) in each of the Profiler Plus and MiniFiler kits with the full 53SNP panel.

It has been suggested that lower match probability (pM) values may be obtained with a partial STR profile compared to a full mini-STR profile [41]. This may be the case with low or moderate levels of DNA degradation when >80% loci are retained. However our results show that consistently lower pM values were obtained with MiniFiler™ than those generated from partial Profiler Plus® profiles with $\leq 60\%$ loci (Fig. 2.6). The MiniFiler™ kit is designed to function as an adjunct to STR typing kits for challenging samples. Therefore maximal matching probabilities may be achieved with a combined partial STR profile and a complete mini-STR profile. Analysis of the 53 SNP panel described in this paper (assumed average heterozygosity of 0.45) generated pM values significantly lower than complete MiniFiler™ profiles (1.2×10^{-24} vs 8.2×10^{-11}). The pM values obtained with $\geq 70\%$ of this 53 SNP set successfully genotyped are as discriminatory as a full 15-plex STR kit (AmpFISTR® Identifiler PCR kit, Applied Biosystems) (8.8×10^{-19} vs 5.01×10^{-18} [123]). These results suggest that SNP analysis

could provide not only greater genotyping success, but also greater powers of discrimination when typing severely degraded and/or DNA in low amounts.

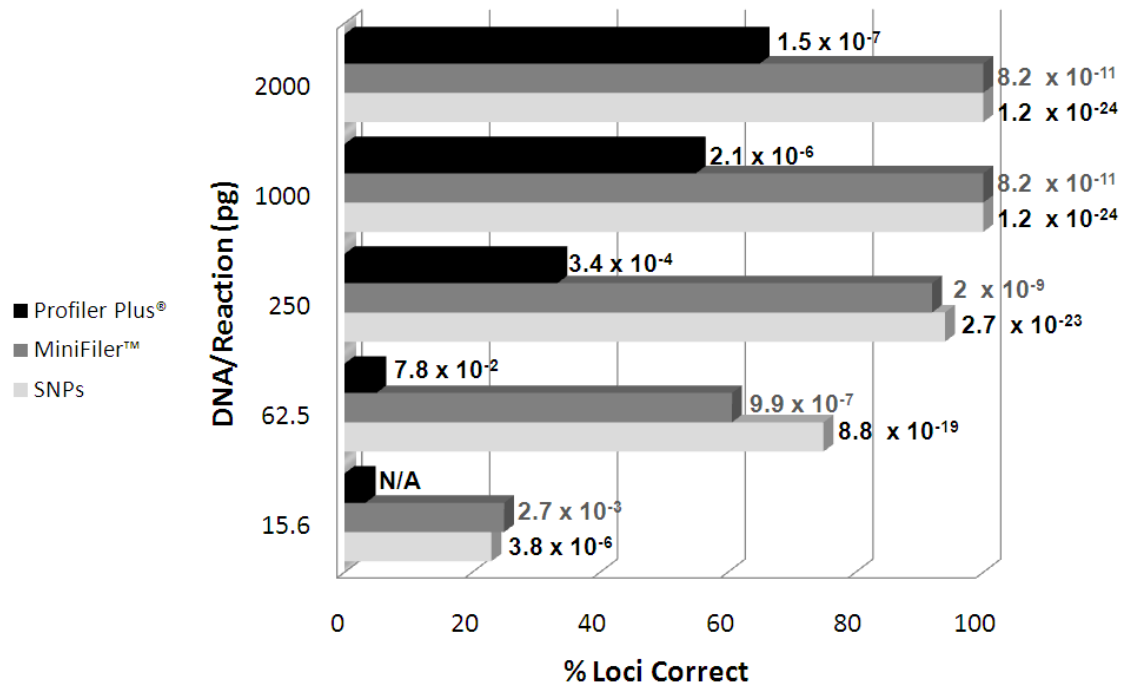


Figure 2.6. Comparison of successful loci retrieval and associated matching probability (pM) values generated by AmpFISTR® Profiler® Plus, MiniFiler™ and SNP analysis of extremely degraded DNA. US Caucasian population.

While a statistical correlation between the degradation ratio generated by the qPCR quadruplex and downstream genotyping success was not observed, a general trend is seen which may assist in the prediction of the genotyping success of each method. This lack of statistical correlation is to be expected since only three levels of DNA degradation plus intact DNA were tested. Samples with amounts of DNA >1ng, and low degradation ratios (<2.5) would be expected to yield complete profiles with all three typing methods. However samples with the same low degradation ratios but <1ng template would be predicted to generate more complete profiles using MiniFiler™ or SNP analysis. An extremely high degradation ratio (>7) would predict low success with Profiler Plus® amplification regardless of template amount. Such extremely degraded samples would generate more complete profiles with MiniFiler™ amplification or SNP typing. SNP analysis would be expected to generate the most complete genetic profile from all degraded samples in low amounts (≤250pg). The

broad prediction of genotyping success using STR, mini-STR and SNP analysis could assist in the choice of method and thereby maximise the genetic information gleaned from challenging samples.

2.4 CONCLUSIONS

Levels of DNA degradation were assessed with the QIAxcel capillary electrophoresis system and a quadruplex qPCR assay. The QIAxcel provides a rapid, cost effective screening method and the more sensitive quadruplex qPCR assay was able to simultaneously quantify total human DNA, male DNA as well as the extent of DNA degradation. Minute amounts of male DNA in a background of female DNA were able to be detected and showed some evidence of protection to DNA degradation. By considering the amount of DNA and the degradation ratio of a sample, a general prediction of genotyping success using AmpFISTR[®] Profiler Plus[®], MiniFiler[™] kits and SNP analysis can be made. This assay could assist in determining which genotyping method may be more informative thereby maximising the evidentiary value of each sample. For good quality and moderately degraded samples in amounts within the recommended input amounts for PCR, STR profiling would be the most appropriate choice. However in cases of extreme degradation and/or template amounts below 250pg, mini-STR or SNP analysis should yield significantly more complete profiles and generate lower match probabilities. Although not currently used for routine human identification by the forensic community, SNP typing has been suggested as an adjunct to traditional STR and mini-STR profiling for analysis of highly degraded samples [9, 324]. The results of this study demonstrate the substantial improvement in loci retrieval of extremely degraded and low level samples via SNP analysis with the potential to generate comparable powers of discrimination to mini-STR profiles. Coupled with the ability to obtain genetic information regarding ancestral origin and phenotypic characteristics (reviewed in [76]), SNPs could become a valuable addition to human identification testing.

DNA becomes progressively more fragmented as biological tissue degrades resulting in decreasing ability to gain a complete DNA profile. Successful identification of samples exhibiting very high levels of DNA degradation may be complicated by presenting in minute quantities. The industry standard method for human DNA identification utilising short tandem repeats (STR) may produce partial or no DNA profile with such samples. We report a comparative study of genotyping using STRs, mini-STRs and single nucleotide polymorphisms (SNPs) with template at different levels of degradation in varying amounts. Two methods of assessing quantity and quality of a DNA sample prior to genotyping were investigated. The QIAxcel capillary gel electrophoresis system provided a rapid, cost effective screening method for assessing sample quality. A real-time quantitative PCR (qPCR) assay was able to simultaneously quantify total human DNA, male DNA, DNA degradation and PCR inhibition. The extent of DNA degradation could be assessed with reasonable accuracy to 62.5pg and genomic targets could be quantified to a lower limit of 15.6pg. The qPCR assay was able to detect male DNA to a lower limit of 20pg in a 1:1000 background of female DNA. By considering the amount of DNA and the degradation ratio of a sample, a general prediction of genotyping success using AmpFISTR® Profiler Plus®, MiniFiler™ kits and SNP analysis can be made. The results indicate mini-STRs and SNP markers are usually more successful in typing degraded samples and in cases of extreme DNA degradation ($\leq 200\text{bp}$) and template amounts below 250pg, mini-STR and SNP analysis yielded significantly more complete profiles and lower match probabilities than corresponding STR profiles.

3 Chapter Three

Mock Forensic Skeletal Remains and Case Study

ADDENDUM

Contributions to Chapter 3:

Sheree Hughes-Stamm:

- Experimental design
- All fieldwork and laboratory bench-work
- All data analysis
- Author of the chapter

Angela van Daal:

- Assistance with experimental design and interpretation of results

Frauke Warnke:

- Filing of dentine powder from teeth
- X-ray imaging of teeth

Nicolene Lottering:

- Assistance with fieldwork sample collection
- Assistance with environmental data collection (weather observations, photography and salinity testing)

Walter Wood:

- Assistance with fieldwork design and initial set-up of equipment and samples.

3.1 INTRODUCTION

The aim of this chapter was to create a collection of mock forensic skeletal samples mimicking the types of samples which may result from a mass disaster or missing person case. In cases of fatalities involving intense heat, velocity or advanced decomposition, the human remains from which a positive identification are made are usually bone and teeth. Due to the inability to use other conventional methods such as fingerprints and visual identification, DNA analysis is the most appropriate method for obtaining an identification in such cases. However, the DNA in these compromised samples is often damaged and/or highly degraded and may present a challenge for conventional genotyping methods.

Forensic samples such as skeletal remains, blood, saliva and semen stains are sometimes exposed to harsh environmental conditions which affect the degree of DNA preservation. The extent of decomposition depends primarily on two factors: time and environmental conditions [12]. After cell death, the DNA begins to degrade and progressively breaks into smaller fragments. The degradation accumulates with time, while environmental conditions such as temperature, humidity and pH modify the rate and extent of the degradation [13]. Fire, immersion in water, burial in soil and microbial infestation are all elements which influence decomposition of remains and affect the degenerative effects on DNA. Samples exposed to harsh environmental insults cause a plethora of DNA damage in addition to fragmentation. No one environmental factor is solely responsible for damaging DNA in typical forensic samples. This complex DNA damage differs from the double stranded breaks generated by sonication in the artificially degraded samples used previously in this study (Chapter 2).

In this study, bone and tooth samples were exposed to various environmental insults to create mock forensic skeletal samples which are differentially damaged and degraded. These samples were used to evaluate comparative genotyping techniques (also Chapter 4). The environmental conditions simulated in this study included surface exposure, burial, water immersion (fresh and salt), heat and fire exposure.

The level of degradation of these environmentally challenged samples was assessed in order to identify conditions which may induce greater degradation to DNA in bone and teeth. Samples were genotyped using two commercially available STR amplification kits (AmpFISTR® NGM™ (Applied Biosystems) and PowerPlex® ESI 16 (Promega)), in order to assess the impact of the DNA damage. These kits are widely used within the forensic community for human identification purposes and therefore a brief comparative study of the success of these two kits for genotyping environmentally challenged samples was undertaken.

Teeth have traditionally been used as a source of DNA when all other tissues are decomposed or have failed to yield sufficient DNA for identification. This is because often teeth are the only skeletal elements containing adequate DNA for identification or analysis of highly degraded or ancient remains [327, 328]. Dental pulp is encased in tough, highly mineralised dental enamel thereby better protecting DNA.

One technique used to generate dentin powder for DNA extraction involves grinding the entire tooth [41, 329]. However this approach has two main disadvantages. Firstly, the tooth is completely destroyed eliminating any further radiographic, morphologic or restorative analysis. Secondly, a significant increase in PCR inhibition and DNA degradation is observed compared with extracts from pure dental pulp [71]. With rigorous sanding and cleaning of the external surfaces of the tooth contamination may be minimised or eliminated.

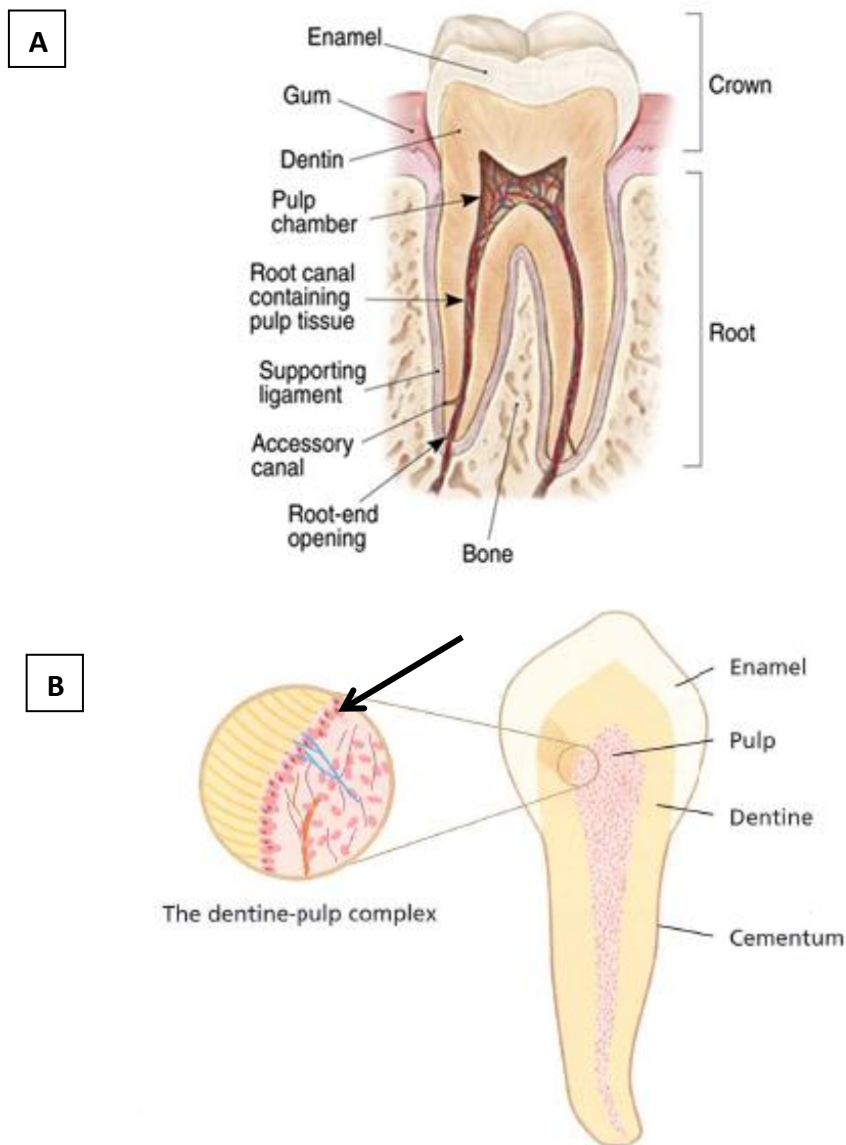


Figure 3.1 Dental Anatomy.

A) The anatomy of a typical tooth consisting of a crown, root and pulp chamber [330]. B) Nucleated odontoblasts (arrow) line the pulp cavity and root canals have cytoplasmic processes which extend into the dentine forming the dentine-pulp complex [331].

The inclusion of sub-optimal dental tissue in the grinding and extraction processes leads to a more highly degraded DNA sample. This problem may be overcome by sampling only those portions of the tooth which provide ample DNA of sufficient quality for successful genotyping. Dental enamel is acellular but sufficient quantities of DNA are found in the crown dentine, pulp chamber and root to support downstream analysis. One study [64] found the pulp to contain the most DNA, while another [67] found the root to produce the highest yield of DNA.

The pulp and dentin form a structural and functional unit with mature odontoblasts lining the root canals and projecting into the dentin (Fig. 3.1B) [69]. Dentin is a preferred target for DNA isolation as it is protected beneath a layer of cementum and enamel and should therefore be the optimal source of DNA from teeth. It is surprising given that teeth provide such a valuable source of DNA from ancient and/or degraded remains, that little is known about the relative amounts of DNA within different regions of teeth, or the potential impact of sampling methods on the resulting quality and quantity of DNA extracted from preserved teeth [68].



Figure 3.2 Extraction of dental pulp.

A) A dental drill (bur) is used to create a hole in the occlusal surface of the crown. B) Access to the pulp cavity and root canals. [73]

Techniques used to access the pulp cavity and/or dentine from the root canal include sectioning the tooth either vertically [71, 72] or horizontally at the enamel-cement (crown-root) junction [69]. Both techniques can be difficult and both destroy tooth morphology. A third and more conservative approach has been described in the literature [73, 332]. This method avoids total tooth destruction by drilling a hole in the occlusal (superior) surface of the crown with a dental bur (drill) (Fig. 3.2). Once a hole is created, the pulp is extracted using a scooping tool. Whilst the crown morphology is disturbed, the tooth itself remains whole. Although these techniques have shown comparable or better results [52, 332, 333] than grinding the entire tooth, a comparison with grinding the whole root (minus the enamel/crown) has not been

investigated. The alternate methods to grinding the whole tooth require specialised dental skill, equipment and endodontic material.

This study investigated two different methods for isolating dentine powder solely from the root of a tooth for DNA analysis. The first method involved the removal and grinding of the entire root into a powder with a freezer mill. The second technique involved the manual use of endodontic files to scrape the dentin lining the root canal thereby generating a powder from which to extract DNA. This second method avoids the physical pulverisation of dentine into a powder and the possible heat damage during drilling and/or grinding.

Endodontic files are routinely used by dentists for procedures such as root canal therapy, treatment of dental abscesses and removal of fractured root tips [334]. The file cleans and shapes the root canal to produce a clean environment to receive a root canal filling material. These procedures involve drilling a hole in the crown and approaching the root from the occlusal surface. It was hypothesised that by applying this same principle, but approaching the root canal via the root-end opening (apical foramen), drilling (and therefore heat) would be avoided, and a cleaner, richer and more pristine source of dentine for DNA extraction would be obtained. Powder containing higher amounts of DNA would be retrieved, whilst PCR inhibitors and contaminating exogenous DNA could be minimised.

3.1.1 Case Study: HMS Pandora Remains

The skeletal remains from a 200 year old shipwreck were used as a case study to demonstrate the utility of DNA extraction and STR-typing strategies on old, environmentally challenged, and degraded remains. The *HMS Pandora* was sent from England in 1790 to capture and imprison the 25 mutineers who had over-run Captain Bligh's *HMS Bounty*. A year later, 14 of the men were captured in Tahiti and were locked in a small cell on the quarter deck referred to as 'Pandora's box'. The *Pandora* then set sail for Timor in pursuit of the *Bounty* and the remaining eleven mutineers. The *Pandora* struck the Great Barrier Reef off the northern tip of Queensland and sank, resulting in the loss of 31 lives.

The *Pandora* shipwreck was discovered in 1977. Subsequent excavations, between 1986 and 1995-1998, led to the discovery of human remains, with over 200 human bones and bone fragments found. These skeletal remains were thought to come from three men, affectionately named 'Tom', 'Dick' and 'Harry'. Based on forensic anthropological analysis, postcranial bones were assigned to each skull. This case study examined whether STR profiles could be obtained from bone (humerus/tibia/ilium) and tooth samples from each of these three skeletons. The comparative performance of two commercially available and widely used STR-typing kits for human identification (AmpFISTR[®] NGM[™] (Applied Biosystems) and PowerPlex[®] ESI 16 (Promega)) was assessed.

3.2 MATERIALS AND METHODS

3.2.1 Biological samples

Two reference buccal swabs were collected from each donor by the surgeon, nurse or dentist. Swabs were allowed to air-dry prior to storage at room temperature until processed. Bone was collected by an orthopaedic surgeon during routine knee replacement surgery. Bone samples (n=92) consisted of a wedge of bone from the femoral condyles and the complete tibial plateau (medial and lateral condyles) (Fig. 3.3). Samples were deemed surgical waste and ethics approvals were granted by John Flynn Hospital (08/05) and Bond University Human Research Ethics Committee (RO-743). Donors were supplied with an explanatory form and signed an informed consent form (Appendix 2).

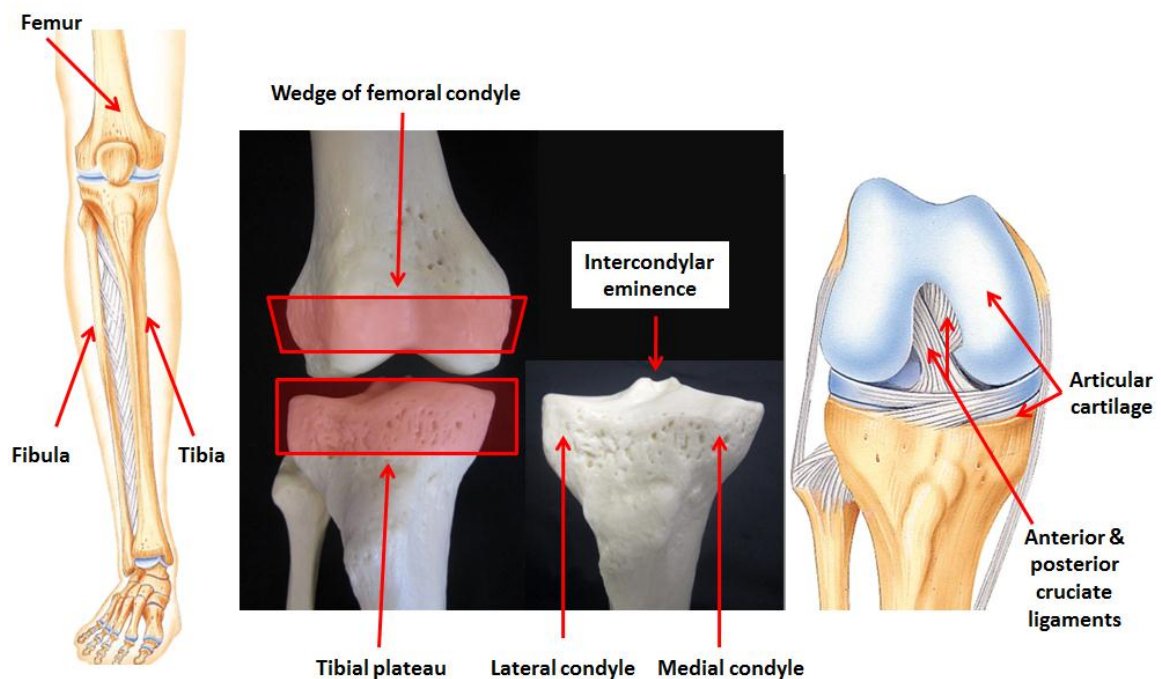


Figure 3.3 Anatomy of the lower limb and bony elements used in this study

A) The long bones of the lower limb B) Sections of bone were removed for this study from the femoral condyles and tibial plateau.(shaded red) during routine knee replacement surgery. C) The anatomical features of the tibial plateau and the associated articular cartilage and ligaments.

Teeth (n=50) were collected by a maxillo-facial surgeon from dental extractions. All teeth were classified by a qualified dentist using the Fédération Dentaire Internationale (FDI), World Dental Federation notation (ISO-3950 notation) (Fig. 3.4). Teeth were prioritised for inclusion in fieldwork as follows; unrestored molars, restored molars, unrestored premolars and restored premolars. Bone and tooth samples were stored at -80°C until required. All samples were assigned a unique barcode identifier.

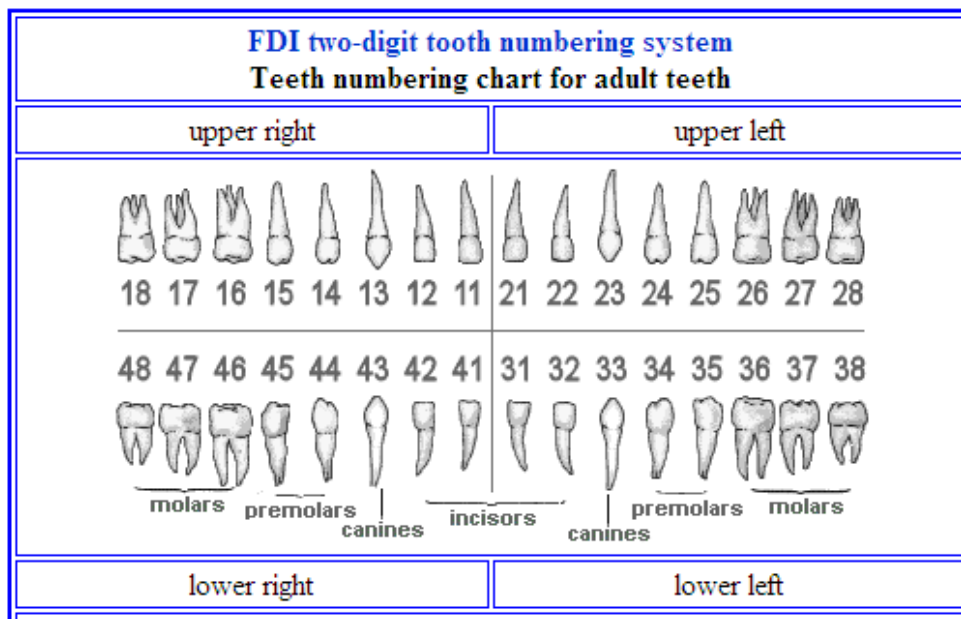


Figure 3.4 Fédération Dentaire Internationale (FDI)

The World Dental Federation notation chart used to identify the teeth used in this study [335]

3.2.2 Fieldwork Plot

A plot of land (9.5m x 9.5m) was donated by New Haven Funerals (Yatala, Gold Coast, Queensland) for the duration of this project. The local Gold Coast environment is classified as a humid subtropical climate (Köppen climate classification (*Cfa*)). The plot is attached to the onsite crematorium building and secured from the public and large scavenging animals by a 1.8m high fence and locked gate. The fenced area housing the samples is on a gentle slope (running from north to south) and is exposed to direct sunlight for the majority of the day with light shade provided by surrounding trees

morning and afternoon. The plot consisted of six surface cages, six burial trenches and two water tanks (freshwater and saltwater) (Fig. 3.5). Three data-loggers were used to monitor local environmental and sample conditions (temperature and humidity).

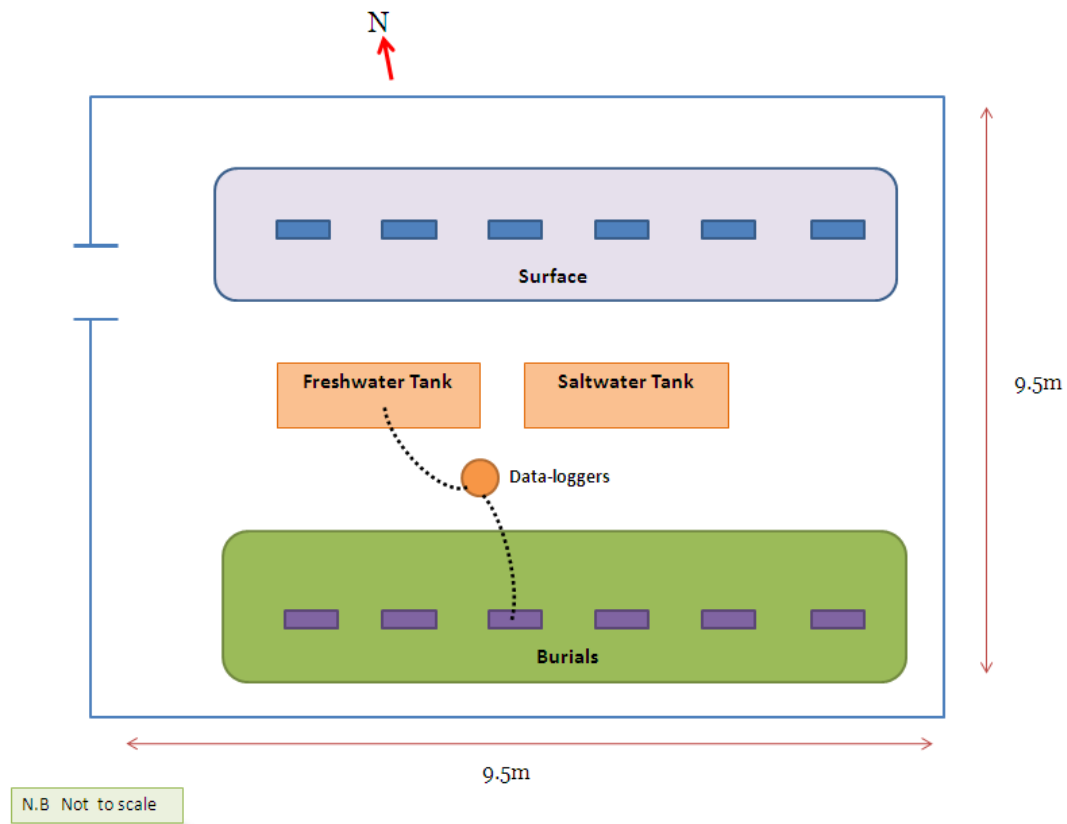


Figure 3.5 Research plot setup

Bone and teeth were placed in one of six cages on the surface or one of the six trenches used to bury samples for up to 24 months. Skeletal samples were also placed in one of two tanks (freshwater or saltwater) for up to six months. Dataloggers attached to a wooden stake in the centre of the research plot were used to record ambient temperature and humidity, and the temperatures of the water tanks and burial trenches via probes (dotted lines).

3.2.3 Environmental Monitoring

Local environmental conditions were recorded with three automatic data-loggers (Tinytag 2, Gemini Data-loggers)(Fig. 3.5 & 3.6). All three units were anchored to a wooden stake in the centre of the research plot protected from direct sunlight and precipitation by a white plastic bucket (Fig. 3.6B). One data-logger recorded ambient temperature and humidity every three hours. Another data-logger recorded soil temperature every six hours via a probe buried at the bottom of trench number three.

Water temperature was recorded every three hours by the third data-logger via a probe placed at the bottom of the fresh water tank. A daily weather report containing recorded temperatures, humidity and rainfall was also obtained from the Australian Bureau of Meteorology, Gold Coast Seaway weather station with (Appendix 2).



Figure 3.6 Environmental data loggers in situ.

A) Data-loggers were anchored to a wooden stake in the centre of the research plot and B) covered by a white bucket for protection from direct sunlight and rain. C) Long probes monitored the temperature of the freshwater tank.

3.2.4 Surface Remains

Samples were randomly allocated into one of six groups (cages) each with five bone samples and one set of teeth. Each bone sample originated from a separate donor. The tibial plateau and an additional bony element (wedge of femoral condyle) from each donor were used. One set of two teeth were assigned to each cage. Both teeth in each cage originated from the same donor. Teeth were housed within a plastic collar to restrict movement within the cage (Fig. 3.7A). Each sample (intercondylar eminence superiorly orientated) was placed approximately 5cm apart and separated within the cage by stainless steel pegs (Fig. 3.7B).

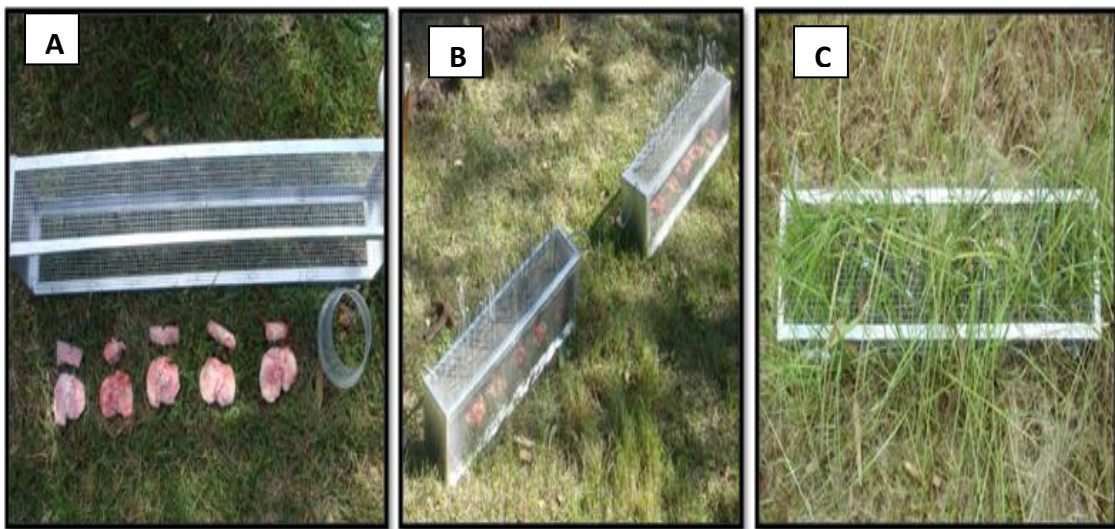


Figure .3.7 Surface samples.

A) Initial setup consisted of five bone and one tooth sample in each cage. B) The six cages were placed over the samples and pegged down to protect from scavenger interference. C) Natural grass growth was allowed through the cages throughout the study.

Grass was trimmed from around each cage as required, but was allowed to grow undisturbed over time within each cage (Fig. 3.7C). Samples were harvested at various time periods ranging from one week to 24 months.

3.2.5 Buried Remains

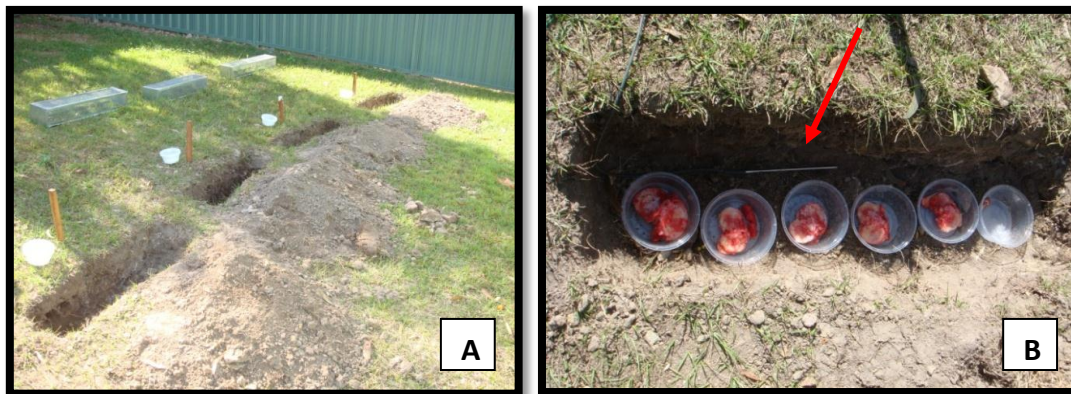


Figure 3.8 Set up of buried samples.

A) Empty trenches in preparation for sample placement. B) Sample setup within each trench showing the position of the data-logger probe recording soil temperature (arrow).

Samples were randomly allocated into one of six groups (trenches) each with five bone samples and one set of teeth. Each sample was housed in a plastic container (intercondylar eminence superiorly orientated) and placed on the bottom of a trench (Fig. 3.8B) and backfilled with the same soil removed whilst digging the trench. Trench depth ranged from 180 – 260mm. Samples were harvested at the same time as the surface remains ranging from one week to 24 months. Solid bedrock was located at approximately 280-300mm below the surface. A temperature data-logger probe (Tinytag 2, Gemini Data-loggers) was placed on the bottom of trench three (180mm deep) recording soil temperature every six hours. The local soil is loose and dry with an initial average pH of 6.47. Soil samples were also collected from the base of the trench after sample harvest for pH measurement. The pH was measured by adding 8g soil to 50mL distilled water and mixed vigorously for one minute. Each sample was allowed to settle for exactly five minutes and measured with an UltraBasic portable pH meter (Denver Instruments, Germany).

3.2.6 *Burnt Remains*

Bones (n=12) were exposed to varying degrees of heat exposure in a cremation oven (Power-Pak II, Industrial Equipment & Engineering Co., Orlando, Florida, USA) to simulate a range of burnt skeletal remains (Fig. 3.9A). Samples were exposed to combinations of low (~150°C), moderate (~350°C), high (~550°C), extreme (~700°C) and prolonged extreme heat (30 minutes) with direct flame. Samples were not burnt to the point of cremation (600-800°C for 90-120 minutes), as all organic matter is fully destroyed at such intense and prolonged heat. Samples were placed (superiorly orientated, Fig. 3.9B) in an oven of a specific temperature, and harvested at various time points (4-30 minutes).



Figure 3.9 Burnt remains.

A) The cremator oven used to burn the bone and tooth samples in this study. B) Bone samples were placed on a metal plate with the articular surfaces facing up prior to heat exposure C) Those same samples (in B) after high heat (~550°C) for 20 minutes.

3.2.7 Water Immersion

Two 80L fish tanks (60cmx46cmx45cm) were used to simulate fresh and saline aquatic conditions. Bone (n=30) and tooth (n=10) samples were placed in plastic containers (with lids) and placed either on the bottom of the tank or suspended from the wire mesh covering the tank (Fig. 3.10). Holes were drilled into the bases and lids of each container. Freshwater from the onsite dam was used to fill both tanks. Table salt (3kg) was dissolved in the saline tank to simulate saltwater conditions (approximately 3.5% sodium chloride).

Water levels were regularly monitored with more water added if significant evaporation was observed, or more salt after heavy rainfall. Water samples were routinely collected and tested off site to ensure salinity fell within a range of 2.5% to 4.5%. The amount of salt added to the tanks was adjusted accordingly. Water temperature was recorded every three hours via a probe attached to an automatic data-logger (Tinytag 2, Gemini Data-loggers) placed at the bottom of the fresh water tank.



Figure 3.10 Set up of skeletal samples in fresh water and salt water tanks.

Bone and tooth samples were placed in labelled plastic containers and either placed on the floor or suspended from wire mesh covering each tank.

3.2.8 Pandora Remains

Genetic analysis was performed on three sets of skeletal samples from the *HMS Pandora* shipwreck. These samples were provided by the Queensland Museum. Each set consisted of one bone fragment and one molar. All samples had been removed for DNA processing approximately ten years ago and stored at -80°C. These remains were determined to originate from three individuals referred to as 'Tom', 'Dick' and 'Harry' by the original case anthropologist [336]. All three molars were classified by a qualified dentist using the Fédération Dentaire Internationale (FDI), World Dental Federation notation (ISO-3950 notation) (Fig. 3.4).

3.2.9 Genetic Analysis

3.2.9.1 Reference Samples

DNA was extracted from both reference buccal swabs from each donor using the QIAGEN EZ1 tissue kit on the QIAGEN EZ1 robot (in separate runs) as per manufacturer's instructions. All DNA extracts were stored at -30°C until quantification and genotyping.

3.2.9.2 Bone Samples

Each group of fieldwork samples consisted of two to five biological replicates per time period. Initial assessment of each time period was done with two bone samples. All bone samples were scrubbed with disposable toothbrushes and sterile water to remove dirt, dead grass and any mould on the surface. After the initial cleaning process, all handling of bone and tooth samples, extraction and PCR set-up was carried out in a dedicated low template DNA laboratory. Sample cleaning and preparation was performed in a fume hood washed with 20% bleach and 70% ethanol before and after each sample. All tubes, distilled water, utensils and equipment were washed with 20% bleach, 70% ethanol and UV irradiated for at least 30 minutes prior to use. All samples were scrubbed with sterile brushes to remove as much dirt and debris as possible. Any

soft tissue remaining on the bone samples was removed with a sterile scalpel. Samples were placed in sterile autoclave bags or conical tubes and placed in an oven (30°C) overnight to dry. The surface of the bone (and any foreign material and contamination) was sanded using a rotary power tool (Dremel Stylus™, USA). The samples were broken into small pieces using a sterile chisel or cutting disc and placed in a sterile 50mL conical tube. The bone chips were washed to remove any contaminants or inhibitors such as dirt, fat and foreign DNA. The wash series consisted of four steps; 20% bleach, two washes of sterile water and 100% ethanol each incubated for in 25mL for five minutes in a shaking incubator (900rpm at 22°C). Bone chips were placed in sterile paper bags or conical tubes and dried at 30°C overnight. If after drying traces of fat or oil were observed, bone chips were washed again with 100% ethanol (five minutes in shaking incubator, 900rpm at 22°C) and redried at 30°C overnight. The ethanol washing and drying process was repeated until no visible trace of fat or oil was evident. Bone chips were ground into a fine powder using a liquid nitrogen freezer mill (6770 SPEX, USA). The freezer mill cycle conditions consisted of a ten minute pre-cool, 2x one minute crush, 2x one minute cool. To monitor contamination, control samples were taken by swabbing the crushing cylinder prior to processing.

3.2.9.3 Teeth

An X-ray (Planmeca intra; 63kV, 8mA, 0.125 seconds) of each tooth was taken prior to treatment in order to assess the condition of the root and dental cavity. Teeth were soaked in 20% bleach for 5 minutes then 100% ethanol for 5 minutes prior to drying at 30°C overnight. Samples (n=7) used to compare the efficiency of the two methods consisted of two molars from each same individual, each being treated in one of two methods. Each tooth was exposed to one of the environmental insults tested in this study (Table 3.1)

Table 3.1 The mode and duration of environmental exposure to each of the teeth investigated.

Sample ID	Tooth numbers (FDI notation)	Environmental Exposure
1	38, 48	Buried for 12 months
2	28, 48	Buried for 24 months
3	26, 46	Surface Exposure for 12 months
4	28, 18	Surface Exposure for 24 months
5	38, 48	Saltwater for 6 months
6	15, 25	Freshwater
7	28, 18	Extreme Fire Exposure

Teeth were processed in one of two ways:

A) 'All Root' Method

The roots were completely removed from the crown with a sterile chisel (Fig. 3.11). All root material was ground to a powder using the same freezer mill protocol as previously described for bone samples (Section 3.2.9.2).

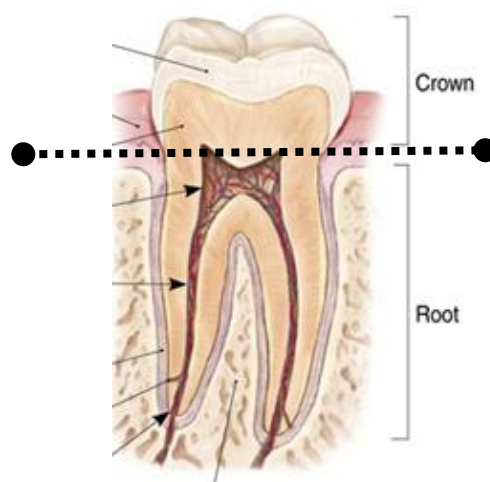


Figure 3.11 The level at which tooth roots were removed for DNA extraction.

Teeth were sectioned at the cemento-enamel junction (dotted line) with a sterile chisel, and the entire root was ground into a fine powder for DNA extraction.

B) Filing Method

The tips of each root (approximately 1-2mm) were removed with a Dremel Stylus™ drill and cutting wheel attachment to improve access to the root canal. Teeth were sprayed with 20% bleach and 100% ethanol, allowed to air-dry or dried at 30°C. Dentin and pulp were extracted via the roots of each tooth by a qualified dentist. A series of Hedström endodontic files (Sizes 08 – 80) (Fig. 3.12A and B) were used to scrape the dentin from inside each root and pulp cavity. The file series increase in diameter in order to progressively widen the root canal and generate powdered dentin (Fig. 3.12C and D). The powder (~50-100mg) was collected on sterile sheets of foil and transferred to 50mL tubes for DNA extraction. A second X-ray of each tooth was taken post-treatment.

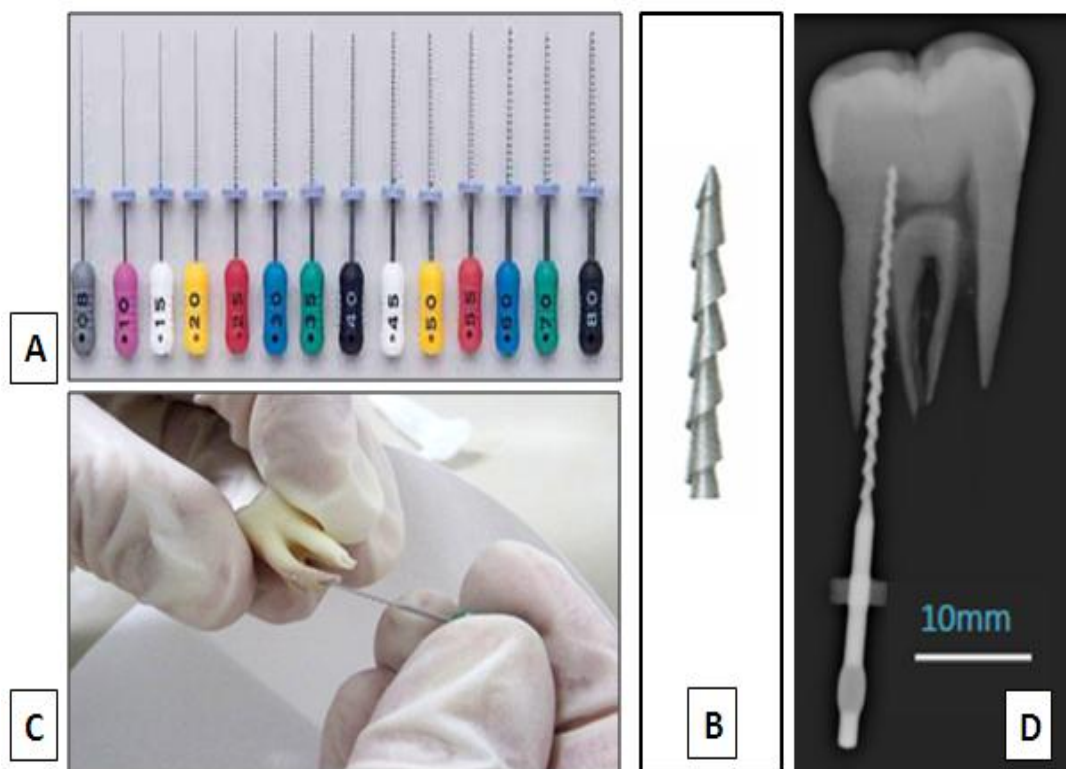


Figure 3.12 Instruments and process involved in the filing method to extract dentine for DNA purification.

A) A series of endodontic files were used to widen the root canals and generate powdered dentine. B) A schematic diagram of the spiralled blade of the Hedström files. C) Files were repeatedly inserted into the root canal via the apex of the root. D) An X-ray post-treatment with the file in situ showing the extent of access to the root canal and pulp cavity using this method.

3.2.9.4 DNA Purification

Bone tissue (0.5-0.8g) and tooth powder (0.06-0.3g) were digested using a modified total demineralisation method [337] and extracted using the QIAGEN Blood Maxi kit [59, 215]. Powder was incubated in a digestion buffer: 10mL ATL Buffer (QIAGEN), 5mL 0.5M EDTA, 150 μ L Proteinase K (20mg/mL) and 200 μ L 1M DTT (half volumes for tooth powder) at 56°C for 24 hours in a shaking incubator. An additional 5mL 0.5M EDTA was added (bone and tooth powder) and returned to the shaking incubator at 56°C for a further 24 hours. 15mL AL buffer (QIAGEN) and 150 μ L Proteinase K (20mg/mL) (half volumes for tooth powder) was added and incubated at 70°C for one hour in a shaking incubator. Samples were centrifuged at 1000g for 5 minutes and the supernatant was transferred to new tubes. For the remainder of the process both bone and tooth samples were treated identically. The supernatant was mixed with 15mL 100% Ethanol and added to QIAGEN Blood maxi spin columns. The columns were centrifuged for three minutes at 2000g, washed with 10ml AW1 buffer and centrifuged again. The filter was washed with 10mL AW2 buffer and centrifuged again at 2000g for three minutes. Residual AW2 buffer was removed by further centrifugation at 2000g for 10 minutes. DNA was eluted by adding 3mL AE buffer preheated to 72°C and centrifuged at 2000g for three minutes. The elution process was repeated by running eluate back through the filter for maximal concentration. All samples were concentrated by centrifugation for 3minutes at 4000g in Amicon Ultra-4 columns (Millipore) to a final volume of 200-400 μ L. Samples were further concentrated using a 30 minute centrifugation in a Speedvac (Thermo scientific) at the medium heat setting. The Pandora bone samples were concentrated using Microcon YM-30 filters (Millipore) to simultaneously concentrate and minimise PCR inhibitor carry over (~80 μ L final volume).

3.2.9.5 Quantification

The quantity and quality of DNA recovered from the skeletal remains was assessed using the real-time quantitative (qPCR) quadruplex assay described in Chapter 2 of this thesis. This assay simultaneously quantifies total human DNA, male DNA, PCR inhibition and the level of DNA degradation of a sample prior to genotyping. DNA

extract (3µL) of all skeletal samples was added to each quantification assay. Samples were analysed in duplicate for quantification and subsequent STR profiling.

3.2.9.6 Genotyping

Samples were genotyped using both AmpFISTR® NGM™ (Applied Biosystems) and PowerPlex® ESI 16 (Promega) amplification kits as per manufacturer instructions. All reference samples were genotyped with 0.5ng input template. The target input amount of DNA for each bone and tooth sample was also 0.5ng. However if the DNA concentration was measured at <0.03ng/µL, the maximum sample volume possible per reaction (17.5µL) was added. PCR was performed in 25µL reaction volumes on a GeneAmp 9700 (Applied Biosystems) as per recommended cycling conditions (Table 3.2).

Table 3.2 PCR cycling conditions of both AmpFISTR® NGM™ (Applied Biosystems) and PowerPlex® ESI 16 (Promega) amplification kits.

PCR Step	AmpFISTR® NGM™	PowerPlex® ESI 16
Initial incubation	95°C for 11 minutes	96°C for 2 minutes
Cycle	29 cycles:	30 cycles:
	94°C for 20 seconds	94°C for 30 seconds
	59°C for 3 minutes	59°C for 2 minutes
72°C for 90 seconds		
Final Extension	60°C for 10 minutes	60°C for 45 minutes
Soak	4°C	4°C

A commercial PCR enhancer (STRBoost[®], Biomatrica, San Diego, USA) was used in STR-typing of the most degraded samples in this study. The samples tested with STRBoost[®] were the surface bone samples exposed to the environmental elements for six to 24-months (n=7) and the 200 year old Pandora shipwreck remains (n=3). STR reactions were performed as per the manufacturer instructions by replacing 10% of the reaction volume with the STRBoost[®] mastermix. The amount of template added to each STR reaction was 0.5ng for all surface exposed bone samples. Due to the low concentrations of the Pandora samples, the maximum volume (17.5µL) was added to each STR reaction. Reactions were run in duplicate due to the limited amount of DNA template and STRBoost[®] product available.

Electrophoresis was performed on a 3130 Genetic Analyser (Applied Biosystems). Samples were prepared for fragment analysis as per AmpFISTR[®] NGM[™] and PowerPlex[®] ESI 16 PCR amplification kit recommendations. Data analyses were performed using GeneMapper ID v 3.2.1 software (Applied Biosystems) with a 50 relative fluorescence units (RFU) peak amplitude threshold for all dyes. The stutter threshold was 15%. For the *HMS Pandora* remains where no reference profiles were available, a consensus approach was employed. An allele was assigned to a particular locus when observed at least twice across replicates. In addition, concordance was sought between the tooth and bone profiles from each individual.

3.3 RESULTS and DISCUSSION

Bone and tooth samples were subjected to various environmental insults to mimic the types of forensic skeletal samples which may result from natural or mass disasters or missing persons cases. The primary focus of this fieldwork was to subject bone and teeth to elements such as heat, water, burial and surface exposure to create differentially damaged and degraded samples. The DNA isolated from these decomposed remains was used to evaluate forensic DNA typing methods from such challenging samples.

This study was not designed as an investigation into the taphonomy of skeletal elements under various environmental conditions. Nor was it an aim of this study to describe any correlation between the post-mortem interval (time since death) and the morphological features of the remains. However a brief description of the samples at each time period is presented in order to appreciate the condition of the samples from which DNA was sourced. These observations include gross morphological changes to the bone and teeth and the associated micro-environments. Routine fieldwork data such as weather information, water and soil temperatures, pH and salinity measures are also described.

3.3.1 *Environmental Observations*

3.3.1.1 *Weather Data*

Ambient temperature and relative humidity were measured using an on-site data-logger every six hours for 24 months. Additional weather data such as rainfall and wind gust were also obtained from local weather observations by the Australian Bureau of Meteorology (Gold Coast Seaway) (Appendix 2).

As expected, temperatures measured onsite fluctuated seasonally with a minimum of ~12°C and a maximum of ~31°C for the time period (Fig. 3.13). While the temperatures recorded at the Gold Coast seaway ranged from 7°C to 37°C. This difference in temperature range is likely due to the difference in location, with the

research plot situated approximately 32 km inland (NW) from the Gold Coast seaway. Relative humidity fluctuated between 40 – 98% RH on site (Fig. 3.13) whilst ranging from 19 – 100% RH at the Gold Coast Seaway (Appendix 2).

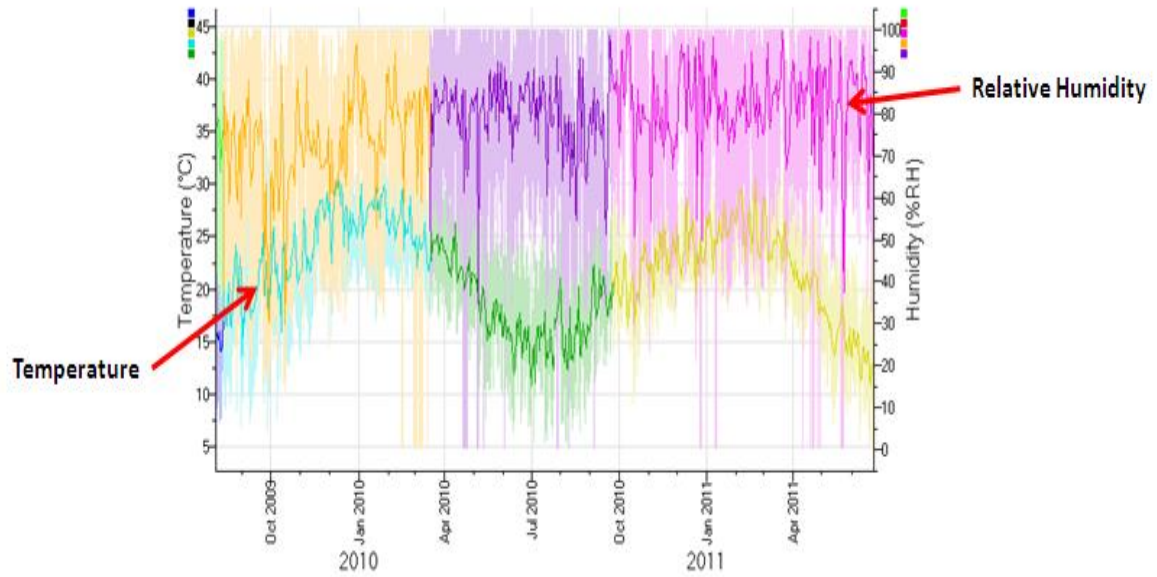


Figure 3.13 Relative humidity and ambient temperature on site.

Data from the onsite datalogger showed a seasonal fluctuation in ambient temperature and relative humidity over the 24 month period of this study.

3.3.1.2 Soil Data

The temperature of the soil was recorded by a data-logger probe for the duration of the study. The probe was located at the bottom of trench three at a depth of 180mm and recorded the temperature every six hours. The temperature fluctuated seasonally with a minimum of $\sim 13^{\circ}\text{C}$ in winter 2011 and a maximum of $\sim 32^{\circ}\text{C}$ in summer 2010 (Fig. 3.14).

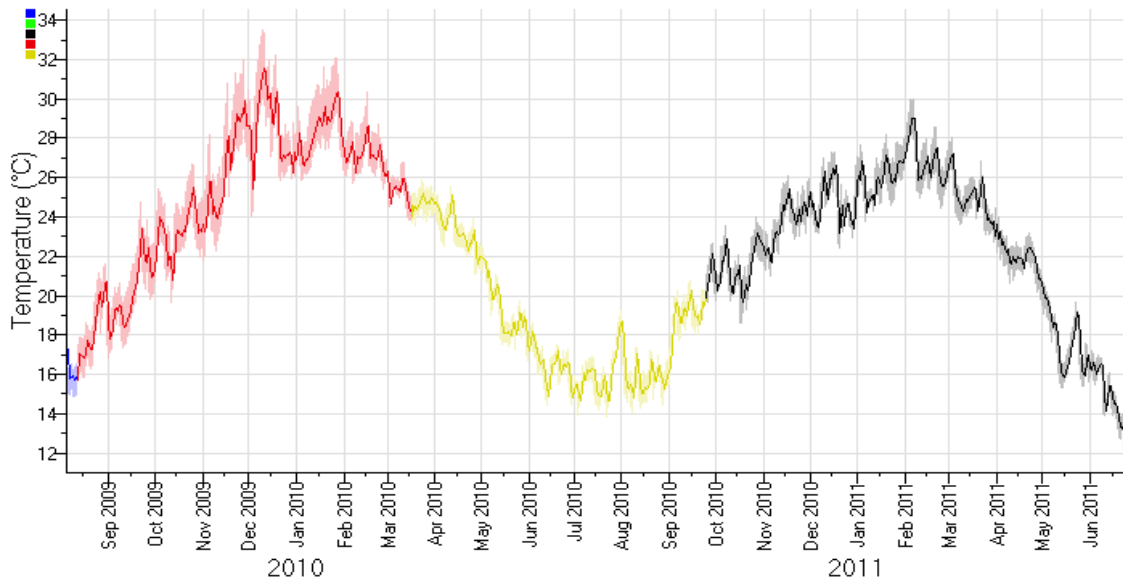


Figure 3.14 Recorded soil temperature of the burial trenches.

Data recorded by a datalogger probe placed at the bottom of a burial trench showed a seasonal fluctuation in soil temperature over the 24 month period of this study.

The pH of the soil was also tested for each burial trench before and after sample harvest. The initial pH of the six trenches ranged between 6.3 and 6.8. The soil pH measured at the time of bone and tooth harvests ranged between 6.1 and 6.7 (Table 3.3) No significant changes in soil pH were observed. However a small initial decrease in pH was observed within the first six weeks. Most commonly an increase in pH is observed in the early stages of decomposition [338-340]. An increase in soil pH results when the decomposition juices formed during the processes of putrefaction and autolysis of soft tissue and internal organs leech into the underlying soil. The fact that an increase in soil pH was not seen in this study is not surprising as only small bony fragments were used, and the decomposition fluids were minimal since bone samples were de-fleshed. In addition, the samples were placed in plastic containers thereby reducing the leakage of any fluids into the burial soil.

Table 3.3 Measured pH of the soil collected at each burial trench before sample placement and after harvest.

Trench	Initial pH	pH at Harvest	Time of burial
1	6.4	6.2	1 week
2	6.3	6.2	6 weeks
3	6.7	6.7	10 weeks
4	6.4	6.4	3 months
		6.5	6 months
5	6.8	6.7	9 months
		6.7	12 months
6	6.3	6.4	18 months
		6.3	24 months

3.3.1.3 Water Tanks

Two tanks were used to incubate bone and tooth samples for periods of up to six months. Both tanks were placed within the research plot and were fully exposed to the elements. The tanks were filled with unfiltered fresh water from the on-site dam. The water temperature was measured every three hours via a probe attached to an automatic data-logger placed at the bottom of the fresh water tank (Tinytag 2, Gemini Data-loggers). The six month study was conducted during the warmer months of October to March. The water temperature fluctuated within a range of 14 - 35°C with an average of approximately 26°C. These water temperatures fluctuated more widely than the measured ambient temperature, as measured by the on-site data-logger, which showed a minimum of 16°C and a maximum of 30°C for the same time period (Fig. 3.15).

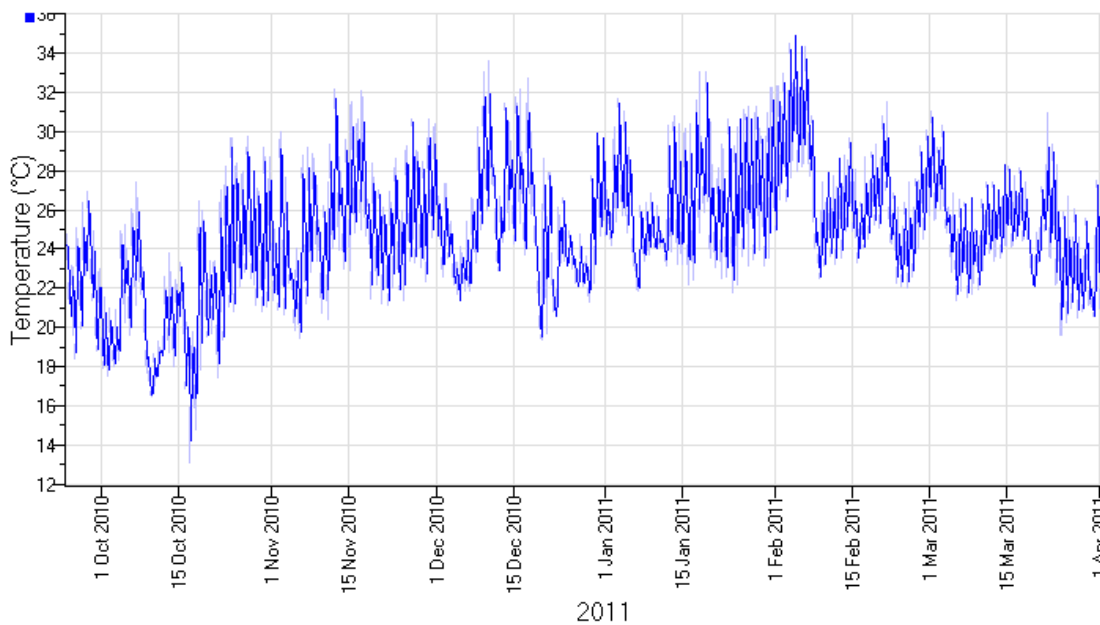


Figure 3.15 Water temperature data.

Data recorded by the data-logger probe at the bottom of the freshwater tank show the expected seasonal fluctuation in water temperature over the six month period of this study.

Salt was added to one of the tanks to be within a salinity range of 30 000 – 39 000ppm. The average salinity of seawater is 35 000ppm or 3.5% sodium chloride [341]. The salinity was monitored each week for the first three months, and then fortnightly for the remaining three months and adjusted accordingly. Additional measures were taken after heavy rain to compensate for dilution of the salt. The salinity range was kept between 24 700 – 39 400ppm for the duration of the study, and the pH ranged between 6.8 – 7.2 (Table 3.4).

Table 3.4 Measured salinity and pH of the saltwater tank.

Time (weeks)	pH	Salinity (ppm)
1	6.8	30 500
2	6.8	28 300
3	6.8	29 400
4	6.8	29 950
5	6.8	39 400
6	6.8	36 650
7	6.8	33 050
8	6.8	32 200
9	6.8	33 400
10	6.8	32 700
11	6.8	34 600
12	6.8	24 700
15	6.9	29 050
18	6.8	31 100
20	6.8	33 500
22	6.8	24 930
24	6.9	29 800
26	7.2	31 100

The freshwater tank was filled with unfiltered water directly from an on-site dam. It was designed to mimic a semi-stagnant body of freshwater such as a pond, dam, marshland, small lake or waterhole (Salinity range between 0 and 1000ppm) [341]. Due to excessive algae accumulation, the tank was emptied each week, cleaned out, and water replaced. The pH and salinity was monitored once a week for the duration of this study (12 weeks). Salinity fell within the range defined as freshwater (<1000ppm) measuring 144 – 787ppm (Table 3.5).

Table 3.5 Measured salinity and pH of the freshwater tank.

Time (weeks)	pH	Salinity (ppm)
1	6.8	201
2	6.8	149
3	6.8	311
4	6.8	787
5	6.8	537
6	6.7	277
7	6.9	288
8	6.8	144
9	6.8	361
10	6.9	240
11	6.8	380
12	7	647

3.3.2 Taphonomic Observations

Bone and teeth were exposed to one of five environmental insults; surface exposure, burial, saltwater, freshwater and extreme heat. Samples were left on the surface or buried in trenches from periods of one week to 24 months. Samples were submerged in freshwater for up to eight weeks or in saltwater for up to six months. Bone and teeth were placed in a cremator oven and exposed to varying degrees of heat for up to 30 minutes. Samples were subjected to these conditions in order to create mock forensic skeletal samples of varying levels of preservation such as those which may be recovered from mass disaster or missing person cases. The DNA extracted from these environmental samples was expected to vary in the types and degree of DNA damage and degradation.

The taphonomic observations made during this study are briefly described. The aim of this section is to document the visual changes that occurred to the samples as a result of the different environmental insults. As the bone and tooth samples used in this study had minimal amounts of adherent soft tissue, the conventional processes and stages of body decomposition did not apply. However changes in sample preservation, odour, microbial growth and the local environment are presented.

3.3.2.1 Surface

Samples were placed directly on the grass in October (autumn) (Fig. 3.16A). After one week of exposure to sunlight the small amount of soft tissue (remnants of the crucial ligaments and articular cartilage) were moderately desiccated (Fig. 3.16B & C). The ligaments were dry on the surface, but retained some moisture internally. Any articular cartilage on the tibial plateau was also moderately dehydrated. These mummification events would be expected in warm and dry conditions such as those the bones had been exposed to.

The wedge of cancellous bone from the femoral condyle, and the inferior surface of the tibial plateau were moist and greasy. Green mould was seen on the inferior surface (Fig. 3.16D). The grassy area directly under the bone samples was starting to

turn brown. This was likely due to the lack of sunlight to the grass under the bones, but may also be due to small amounts of decomposition fluids leeching from the bones. No offensive odour was detected with any of the surface remains throughout the study.

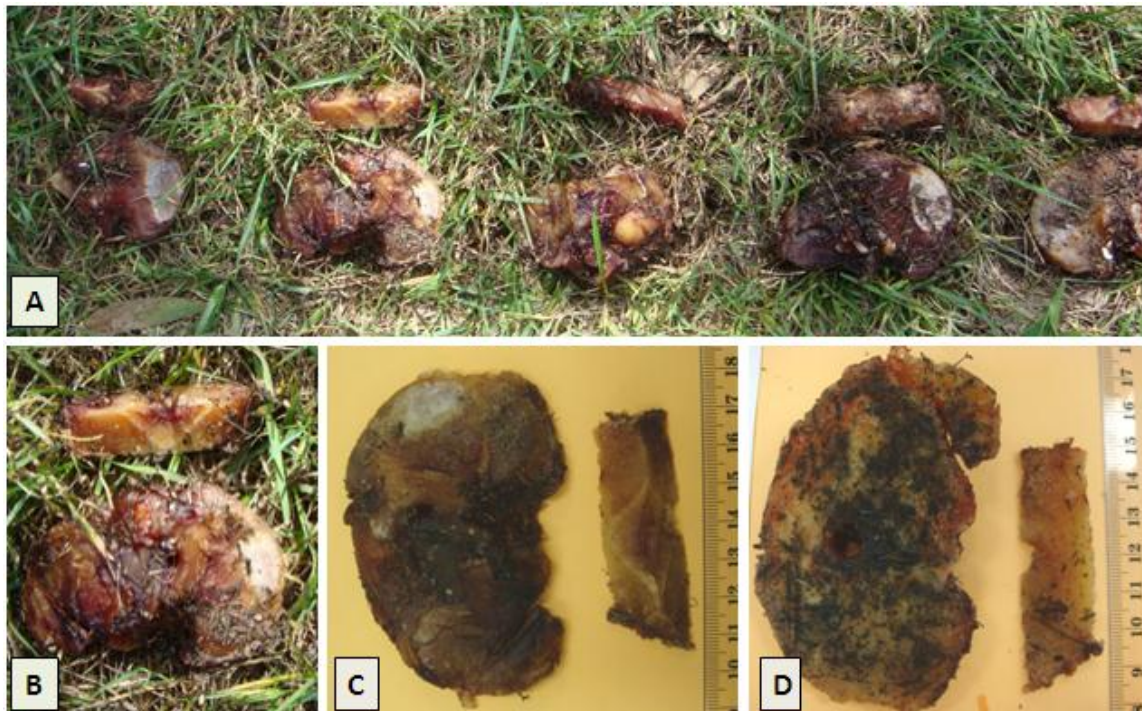


Figure 3.16 One week of surface exposure.

A) Fives sets of bone samples were placed in each cage. Two bone fragments from each individual were used. B,C) Bone showing signs of exposure with cartilage and soft tissue desiccated on the superior surface, D) Green mould on the inferior surface of the tibial plateau.

After a further week of surface exposure (2 weeks total) the samples did not appear to advance in decomposition but continued to dry out. When samples were removed, a distinct area of dead grass and a black oily residue was seen on the grass beneath each bone (Fig. 3.17A). This area is known as a cadaver decomposition island (CDI) [342]. During the early stages of cadaver decomposition, purge fluids escape from the body and flow into the soil. The chemical components are by-products of autolysis (self-digestion of cells) and putrefaction (anaerobic digestion of proteins by endogenous bacteria). The degradation of protein, lipids and carbohydrates will produce carbon, nitrogen and phosphorous-rich products which leech into the underlying soil [343]. This increase in soil nutrients within the cadaver decomposition island is associated with an increase in soil microbial and biomass and activity. Although whole cadavers

were not used in this study, small amounts of fluids from the decomposing fatty bone marrow and soft tissues may have created the small islands. The black oily residue is thought to be a combination of the decay fluid and black mould, with microbial growth using the fluids as a metabolic substrate.

All soft tissue on the bone samples was completely dried and the articular cartilage in the tibial plateau was dry and cracked (Fig. 3.17C). The cancellous bone on the inferior surface was still greasy and moist. After two weeks, the teeth were completely dry, devoid of any soft tissue and appeared to have been slightly bleached white due to the sunlight exposure (Fig. 3.17B).



Figure 3.17 Two weeks of surface exposure.

A) Black residue seen on the grass under each sample. B) Teeth located in the grass. C) Bone samples with soft tissue on the superior surface showing signs of desiccation.

After three months of surface exposure all remnants of the desiccated ligaments were gone. However, small amounts of extremely dry and cracked articular cartilage were still visible on the tibial plateau. Although not observed, it was thought that the removal of any remaining flesh could be attributed to small scavengers such as ants. Distinct black CDIs were present under and surrounding each bone sample (Fig. 3.18A & B). Black mould growth had increased and was now seen on all surfaces of each bone sample (Fig. 3.18). Small focal spots of white and yellow mould infiltrated the trabecular bone on the inferior surface of all bone samples (Fig. 3.18D). A larger area of white mould growth surrounding the intercondylar eminence was seen on one sample (Fig. 3.18C). These mould colonies were unable to be completely removed during the washing process despite scrubbing with a toothbrush (Fig. 3.18E & F). Complete removal (visually) was only achieved by sanding the bone surfaces prior to DNA extraction.



Figure 3.18 Three months of surface exposure.

A) Black mould was seen on all surfaces of each bone and B) in the CDIs under each sample. C) and D) Black and white and yellow mould colonised the bone surfaces. E) and F) Moulds were unable to be completely removed with washing alone.

After six months of surface exposure the grass in each cage had grown to completely cover the samples (Fig. 3.19A). Each bone sample was covered by dirt and grass seeds (Fig. 3.19B). The long grass created a shade canopy which limited the amount of direct sunlight on the samples. This coverage may have allowed for the retention of more moisture in the samples than if they had been completely exposed to sunlight. This shade would also have provided a favourable environment for more prolific growth of mould and fungi. The fifth and sixth months of surface exposure also coincided with more rainfall than the previous four months (Appendix 2).

All surfaces of the bones were covered by a thick black 'mat' of dirt, decaying grass, black, green and white mould (Fig. 3.19D). It appeared that these mould species were colonising the moist dirt and decaying vegetation rather than the bone surface itself. After cleaning, all dirt, grass, and focal spots of white and green mould were removed (Fig. 3.19E). However, the more extensive black mould growth had infiltrated the trabecular bone on the inferior side and as a result was only removed with sanding. Bone samples were thin, slightly moist and greasy. One bone sample was broken during the washing process (Fig. 3.19E&F). Teeth were dry and intact with no visible microbial growth associated with them (Fig. 3.19C).

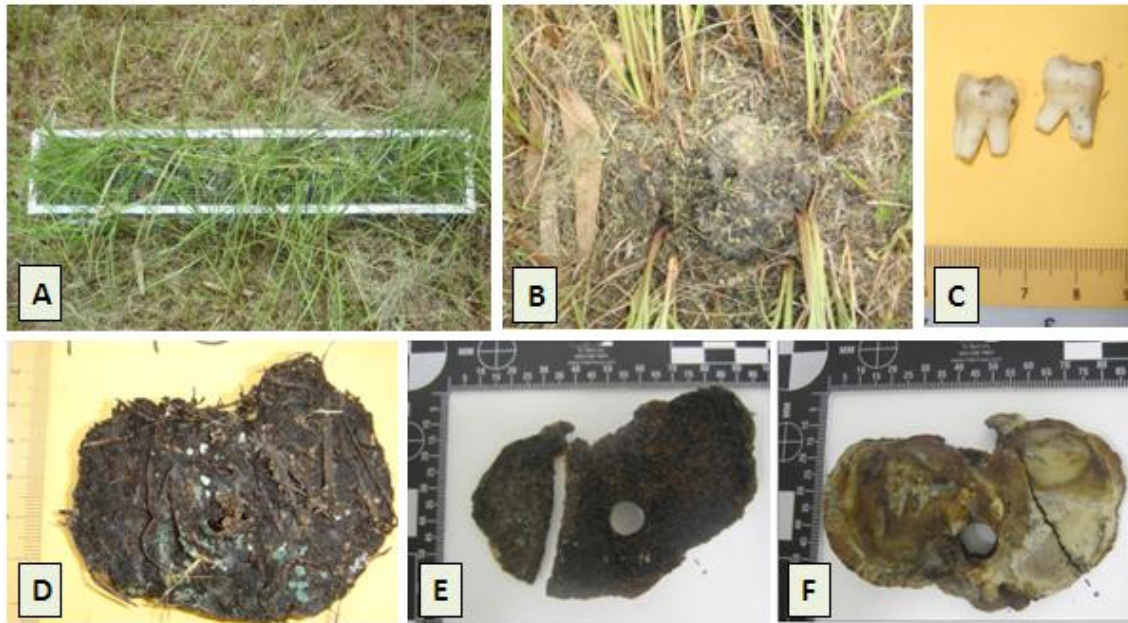


Figure 3.19 Six months of surface exposure.

A) Grass growing around the samples and through the cage. B) Bone sample in situ after grass is cleared, C) Tooth samples, D) Bone sample covered in dirt, dead grass with small colonies of mould, E) Bone sample cleaned showing black mould on the inferior surface and a fracture (broken during washing process) F) Superior surface of the bone sample with complete removal of soft tissue and the majority of articular cartilage.

After nine months of surface exposure the bone samples were all partially buried by dead vegetation and dirt (Fig. 3.20A). The superior bone surface was dry with dirt and grass adhered (Fig. 3.20B) whilst the inferior surface was slightly moist with a film of black sticky mould (Fig. 3.20C). After scrubbing, the dirt was removed leaving a clean articular surface devoid of all soft tissue and articular cartilage (Fig. 3.20D). However, the black mould on the inferior surface of the bone was not able to be completely removed until sanding.

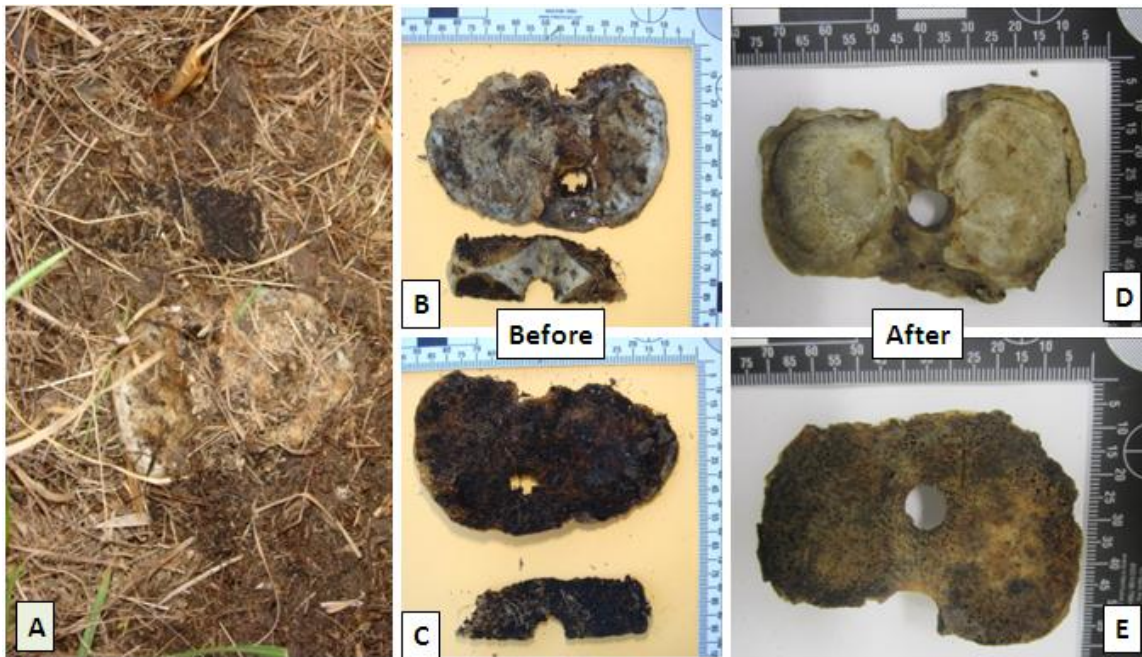


Figure 3.20 Nine months of surface exposure.

A) Bone sample in situ covered in dead grass (surrounding foliage cleared). Sample before washing showing B) dirt and lack of soft tissue on the superior surface and C) black mould on the inferior surface. After washing the D) superior surface is devoid of soft tissue and cartilage and E) most of the mould on the inferior surface is removed during the washing process, however small areas harbour black mould growth.

After 12 months of surface exposure, the skeletal samples continued to dry out and had no remaining soft tissue or cartilage (Fig. 3.21A & C). The inferior bone surface was dry, but slightly sticky due to the mould growth. Three different types of mould growth were seen; black, white and yellow spots (Fig. 3.21B). The mould had infiltrated the trabecular bone as scrubbing with a toothbrush was only able to remove the very superficial layer of growth. The discolouration patterns caused by infiltration of mould into the trabecular bone are still visible after vigorous washing (arrows, Fig. 3.21D).

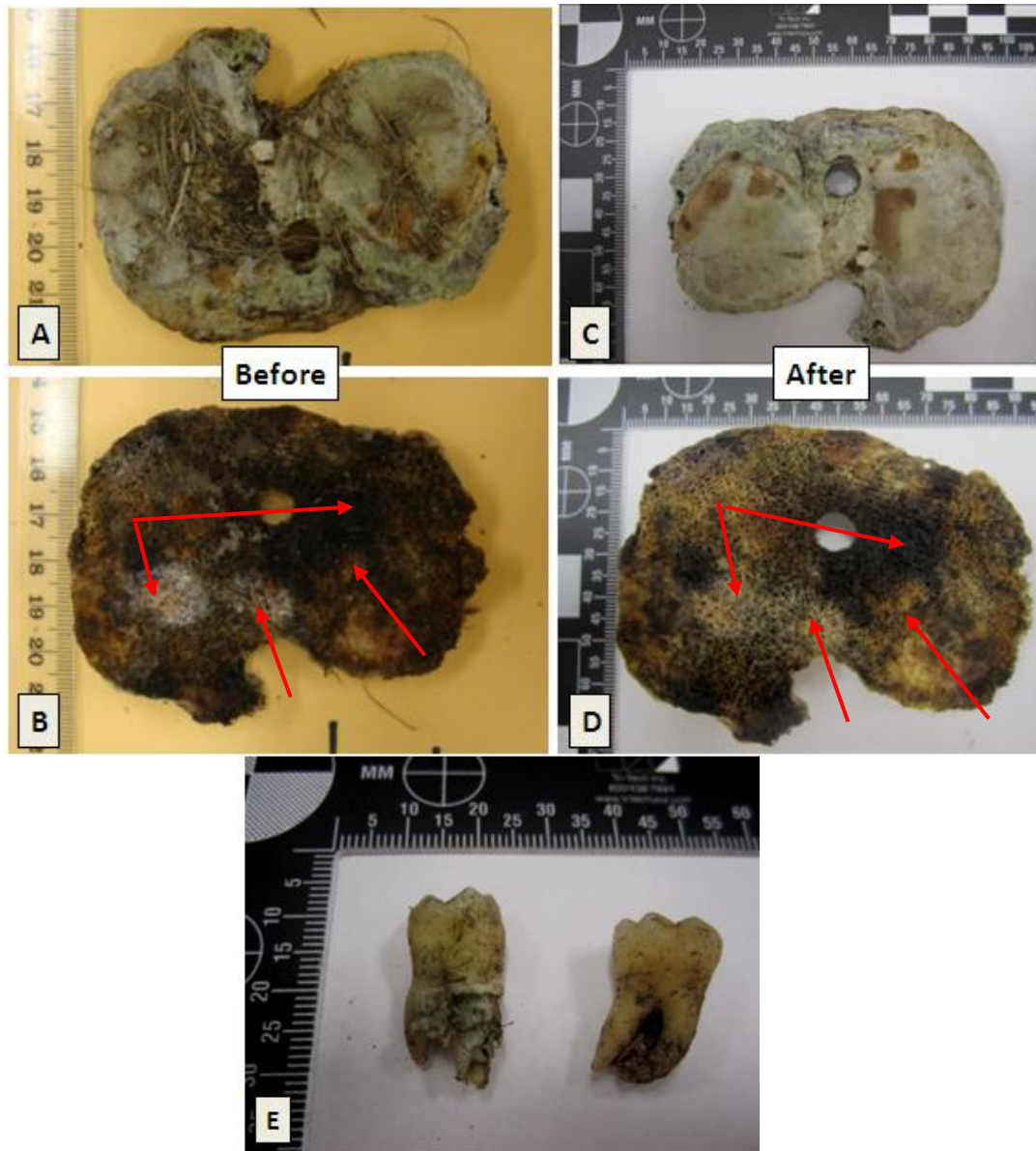


Figure 3.21 12 months of surface exposure.

Bone sample prior to washing with A) grass adhered to the superior surface and B) black, white and yellow mould colonies on the inferior surface (arrows). After washing the C) superior surface is completely devoid of all soft tissue and appears to be slightly bleached and D) remnants of the mould colonies remain within the cancellous bone on the inferior surface. E) Teeth with fragments of bony tissue adhering to the roots remained attached.

After 18 months, the grass had grown in a dense mass through the cage to a height of approximately 60cm. (Fig. 3.22A). Samples were not easy to locate even once the foliage was removed as they were partially buried by the surrounding dirt (Fig. 3.22B). Bone tissue was dry and samples were completely covered in dirt. Grass roots of up to 40mm had infiltrated the cancellous bone on the inferior surface (Fig. 3.22D). After scrubbing each bone sample with a toothbrush, most of the dirt and roots were removed from the surface. Remaining dirt and root matter was removed during the sanding process which followed the wash step. No mould was seen in the dirt adhering to the bones, or the surface of these bones themselves.

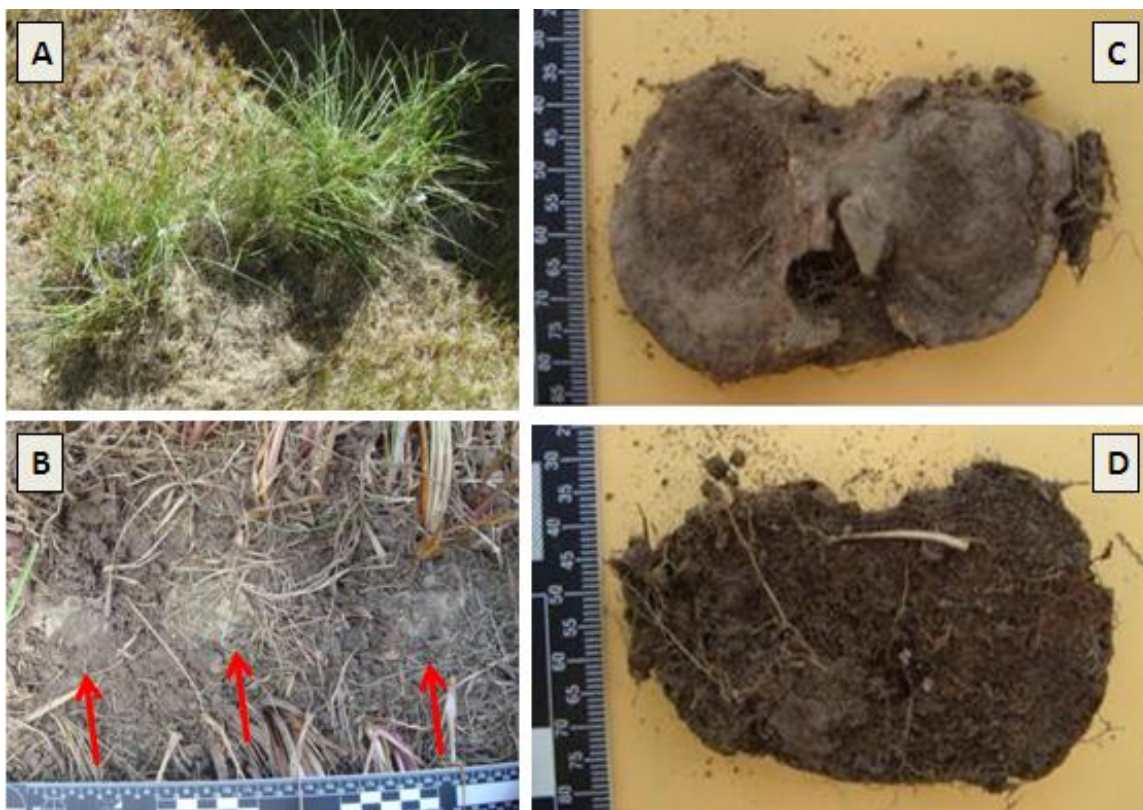


Figure 3.22 18 months of surface exposure.

A) Extensive grass growth through the cage. B) Bone samples in situ (arrows) covered by dirt and dead grass (surrounding foliage removed). C) Superior view of bone sample and D) roots extending into the cancellous bone on the inferior surface.

Samples exposed to the elements for 24 months appeared to be in a similar condition as those samples retrieved at 18 months. The dense grass surrounding the bone samples had grown through the cage to a height of approximately 90cm (Fig. 3.23A). Samples were not easy to locate even once the foliage was removed as they were almost completely covered in dirt. Bone samples were very dry and brittle on the edges. A green colouring was seen on the superior surface and surrounding the intercondylar eminence (Fig. 3.23B). This staining was not seen on surface bone samples retrieved at any other time period and was thought to be green algae. This discolouration could not be removed during the washing process but was sanded from the surface prior to extraction. The cancellous bone on the inferior surface was heavily infiltrated with grass roots and clots of dirt (Fig. 3.23C). The teeth were intact and dry with dirt firmly attached to the external surface, particularly around the roots (Fig. 3.23D).



Figure 3.23 24 months of surface exposure.

A) Growth of grass through the samples and cage. B) Green colouring on the superior surface of bone. C) Root infiltration of the inferior bone surface. D) Three molars.

3.3.2.2 Buried

Bone samples harvested after one week of burial in soil were very moist. The decomposition fluids had leached into the surrounding soil forming muddy clumps of soil which coated the outside of each sample. Extensive white mould growth was seen on the inferior surface of each sample and formed a sticky mat between the two bone fragments in each container (Fig. 3.24B). The mould seemed to colonise the moist surfaces of bone samples where decomposition fluids would accumulate. The mould was easily removed from the bone surface during the washing process.

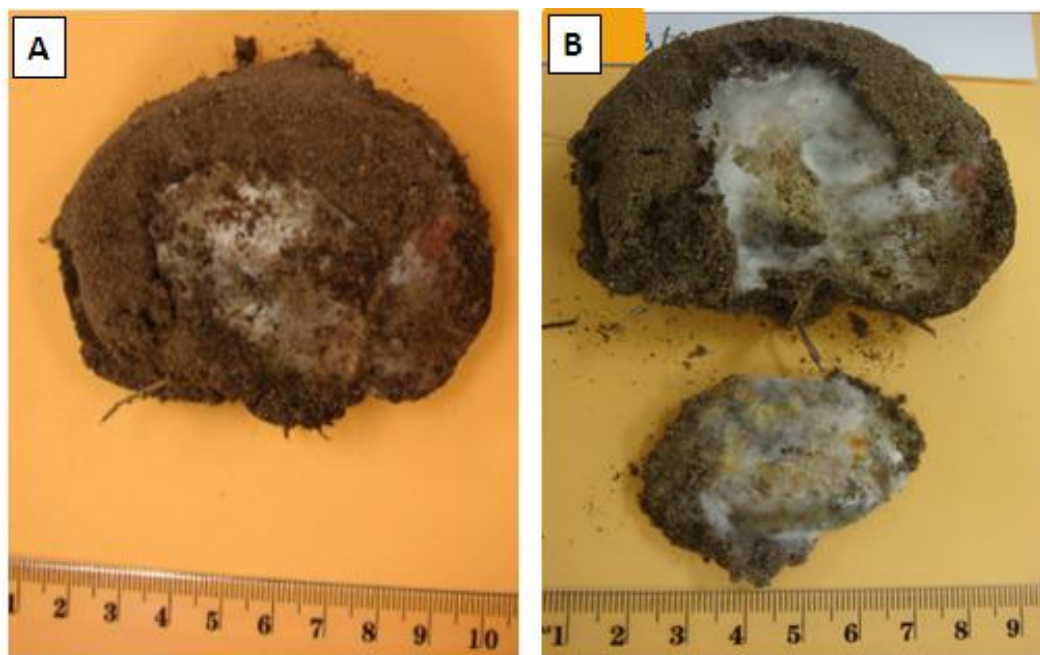


Figure 3.24 Bone samples buried for one week.

A) The two bone samples were very moist, stuck together with white mould and encased in a clump of dirt. B) Extensive mould growth was seen between the two bone surfaces.

After two weeks of burial the bone samples were still very moist. The decomposition fluids leaching from the bone could be seen in the soil of each container (Fig. 3.25A & E). The plastic containers retained the fluids and therefore had kept the samples more moist than if the fluids had been allowed to diffuse into the surrounding soil. The same white mould seen in the samples buried for one week showed more extensive growth in these samples. The filamentous mould was growing between bone fragments, and also extended further into the soil within each container (Fig. 3.25A & F). The white filaments were attached to the bone surface itself. However, all remnants of this mould were completely removed during the washing process prior to DNA extraction. The teeth recovered were dry and intact (Fig. 3.25D).

An insect larva had burrowed into the moist soil surrounding one bone sample (Fig. 3.25B & C). This larva was thought to be a Pasture wireworm (common beetle larva) which feeds on plant roots and grubs in the soil. This larva was not associated with the bone, nor involved in the decomposition process. No decomposition odour was present with these samples.

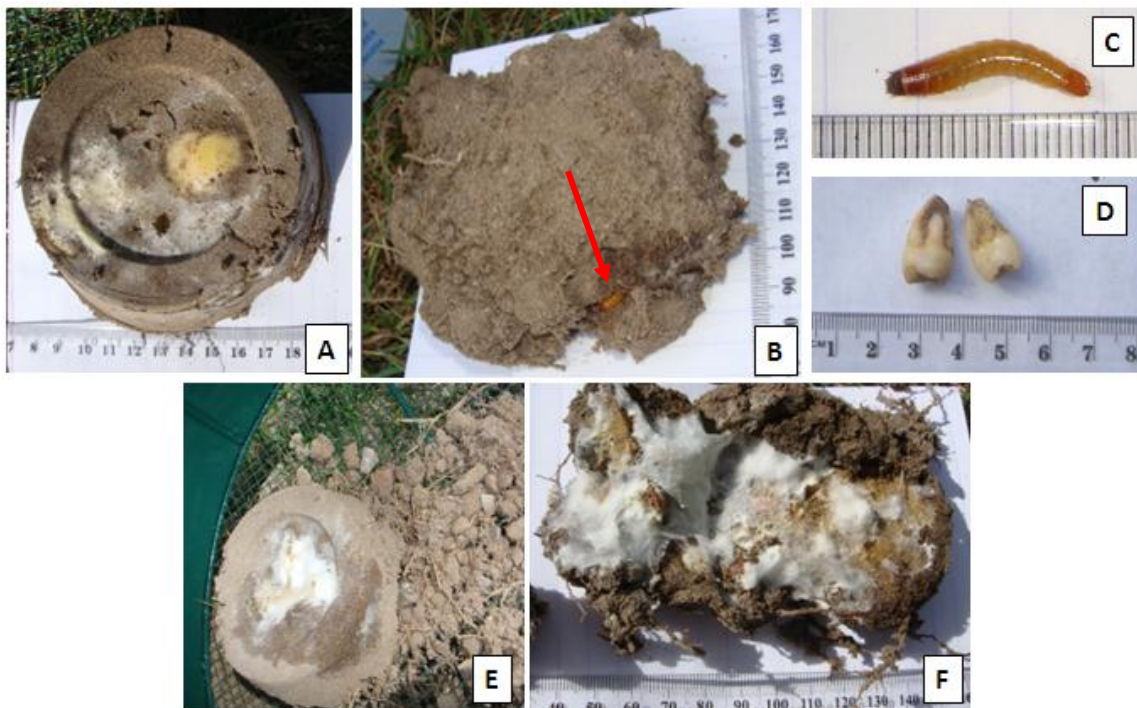


Figure 3.25 Two weeks of burial.

A) and E) Bone samples were encased in soil moist with decay fluid, displaying extensive white mould growth throughout the surrounding dirt. B) and C) a small larva was found inside the sample container. D) Two teeth were recovered intact. F) The white mould was thickest at the moist bony surfaces in contact with each other.

Decomposition of the bone samples had noticeably advanced after three months of burial. The samples were encased in a moist shell of compacted soil (Fig. 3.26A) with some samples having roots embedded in the dirt. These roots did not extend into the trabecular bone at all and were removed with the dirt during washing. One sample had many small insect eggs deposited on the soil surrounding the bone (Fig. 3.26E). These eggs were also removed during the cleaning process. The inferior surface of the bone was very moist and sticky. This was due to a combination of decomposition fluids, mud, bacterial and mould growth. Some samples showed yellow and black mould on the inferior surface (Fig. 3.26B) whilst others had a creamy biofilm (Fig. 3.26F) on the surface. After cleaning, the mould residue was removed from the surface. However, the discolouration due to the mould remained on the bone indicating that the mould had infiltrated the trabecular bone.

After cleaning, remnants of dried and cracked articular cartilage and cruciate ligaments were present on the superior bone surfaces. The distinctive black mould residue was seen covering the remaining soft tissues. This mould could not be removed during the washing process, but was completely removed with sanding of the bone surface prior to DNA extraction. A slight decomposition odour was present with these remains.

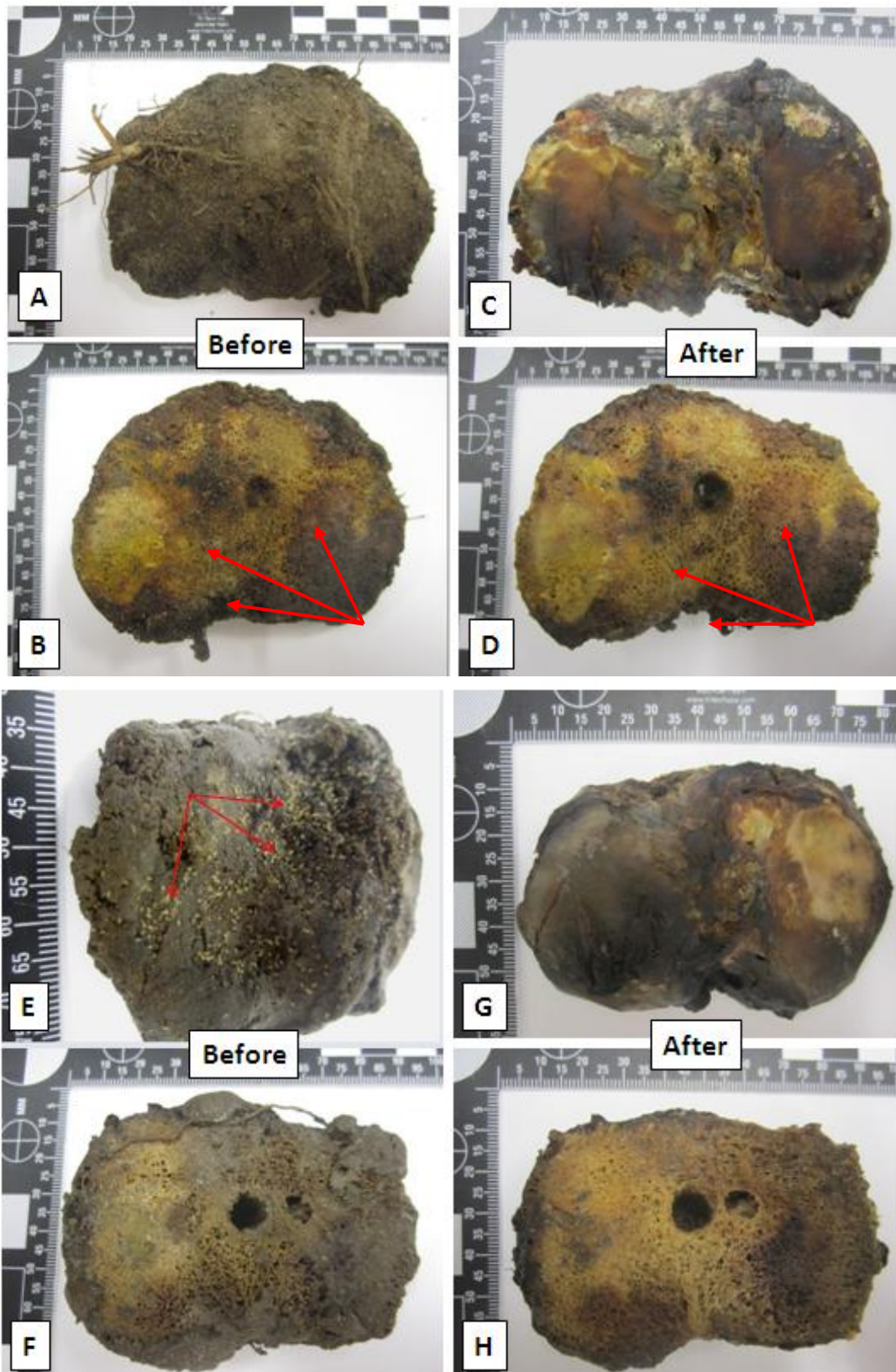


Figure 3.26 Two bone samples buried for three months showing the superior and inferior surfaces before and after washing.

Bone samples were encased in moist soil with A) grass roots, and E) small insect eggs in one case. B) Black and yellow mould were seen on the inferior surfaces. F) A creamy biofilm was seen on the inferior bone surface. C), D), G) and H) Eggs and plant roots were removed with washing, but the mould could not be completely removed. C) and G) show the dried remnants of articular cartilage and black mould which could not be removed with washing alone.

After six months, the classic surface features of burial were evident. These included a loss of vegetation, slight depression and disturbance of the soil (Fig. 3.27A) at the burial site. In addition, the roots from surrounding grass were extending across the trench from the walls (Fig. 3.27B). The presence of roots growing into gravesites and skeletal remains is a significant taphonomic marker. The type of plant and the length of roots have been used to determine the post mortem interval of buried remains [344]. The soil in the trench was dry and starting to compact.

Both of the samples retrieved at this time point showed extensive root infiltration of each container. The grass roots had formed a circular ring around the bottom of each container (Fig. 3.27C & E). However, the two bone samples displayed a difference in the amount of fluid leaching from each sample. One sample and the soil within the container was mostly dry (Fig. 3.27C) whilst the soil surrounding the other sample was still moist (Fig. 3.27E). This difference may be attributed to the fact that the second sample was in direct contact with the plastic container and therefore more the decomposition fluids which leached from the bone was retained rather than being absorbed by the surrounding soil.

Both samples were encased by moist soil and significant root growth. The roots were growing in the dirt adhering to the sample (Fig. 3.27F & G). After washing and scrubbing with a brush, most of the dirt and root matter were removed. However, the roots had infiltrated the cancellous bone on the inferior surface of each sample. These small roots were tightly lodged within the trabecular spaces and were unable to be removed during the washing process alone. These were removed during the sanding step prior to DNA extraction.

After washing, the bone samples were slightly greasy with the remnants of mould colonisation on the inferior surfaces (Fig. 3.27H). No soft tissue (articular cartilage or ligament) was adhered to the superior surface (Fig. 3.27I). No odour was present with these remains.



Figure 3.27 Bone and teeth buried for six months.

A) Surface depression of burial trench with disturbed vegetation. B) Roots from surrounding grass extend across the trench (arrows). C) and E) Roots from surrounding vegetation had infiltrated the sample container forming a ringed root mass in the bottom of each container. D) Intact tooth. F) and G) Bone samples were encased in dirt and fine roots prior to washing. H) and I) All dirt and roots were removed with scrubbing with a sterile brush. No soft tissue remained on the superior surface.

No significant advancement in decomposition was observed from six to nine months. The bone was still quite greasy with moist dirt adhering to the samples. However, a significant increase in root infiltration of the trabecular bone was evident with roots up to 50cm being tightly lodged within the trabecular spaces (Fig 3.28).

In addition to black mould on the inferior surface, a white mould spot was seen on the superior surface (arrow, Fig. 3.28B). All dirt, mould and root matter was removed by washing and then sanding the bony surfaces prior to DNA extraction. No soft tissue or odour was present.

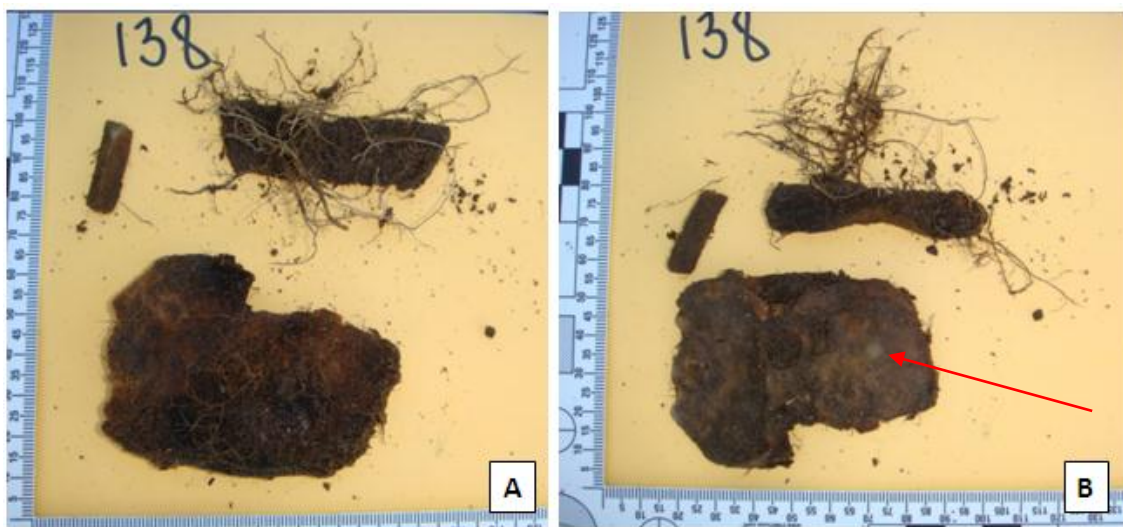


Figure 3.28 Nine months of burial.

A) Trabecular bone was heavily infiltrated with grass roots and B) a spot of white mould was seen on the tibial plateau (arrow).

After twelve months of burial the bone samples were only slightly moist with dirt adhering to the surfaces. Root growth was extensive, forming a thick ring of root mass in each container (Fig. 3.29C) and infiltrating the cancellous bone (Fig. 3.29A & B). One of these roots was much thicker than the others measuring over 110mm in length. No soft tissue or odour was present. The teeth recovered were dry and intact, although one of the teeth had a carie in the crown prior to burial. (Fig. 3.29F & G).

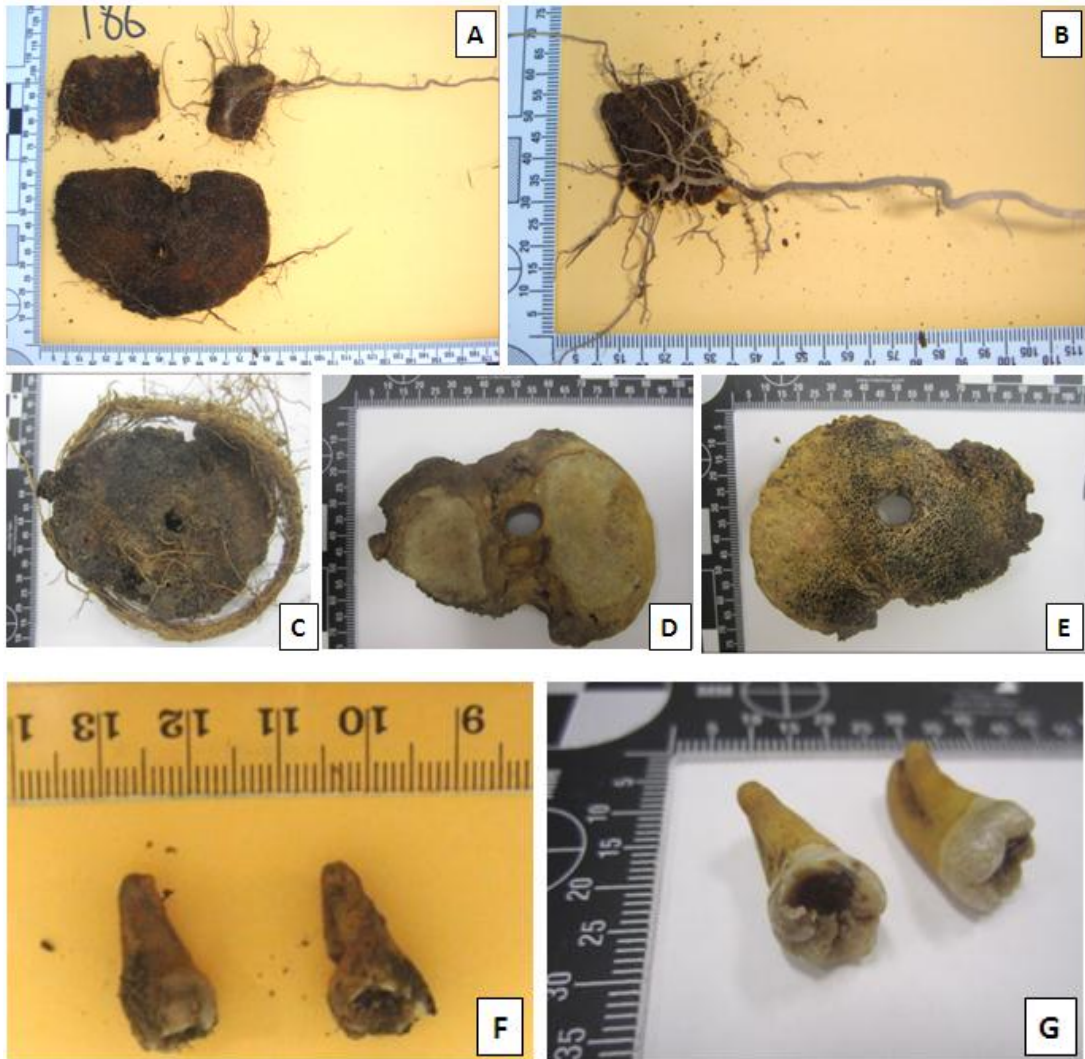


Figure 3.29 Bone and teeth recovered after 12 months of burial.

A) and B) The cancellous bone was heavily infiltrated by grass roots. C) A thick ring-shaped mass of roots were seen at the bottom of each container. D) and E) After washing, bone samples were devoid of all dirt, and soft tissue. E) Some black discoloration persisted on the inferior bone surface. Two teeth were recovered intact; F) before washing and G) after washing displaying the one tooth carie which was present prior to burial.

After 18 months of burial, the trench surface outline was difficult to detect. The surface depression was very shallow and the surrounding grass had reclaimed the area (Fig 3.30A). The soil was very dry and compact making it difficult to dig and retrieve the samples (Fig 3.30B). A ring of root mass was present in each container (Fig. 3.30C). The soil surrounding each sample was dry and in small clumps. Any fluids resulting from decomposition and/or mould colonisation had now dried. The bone surfaces were devoid of soft tissue and mould. This dry environment is not favourable for growth of local microbial, mould or fungi.

Extensive root growth was present in the soil surrounding each sample and infiltrated the trabecular bone itself (Fig. 3.30D - F). Small roots were tightly embedded in the cancellous bone on the inferior surface and small foramina (holes) on the superior surface (Fig. 3.30H). These roots were only removed with sanding. No soft tissue or odour was present.

After 24 months of burial the soil surrounding each sample was loose and dry. A ring of root matter was present within the container housing each sample (Fig. 3.31A). Extensive root growth was also observed surrounding each bone sample. Teeth were dry and intact (Fig. 3.30B). Bone samples were dry and fragile. One sample broke upon handling (Fig. 3.30D), and the edges of all samples crumbled slightly during cleaning. No remnants of soft tissue, mould or odour was present.

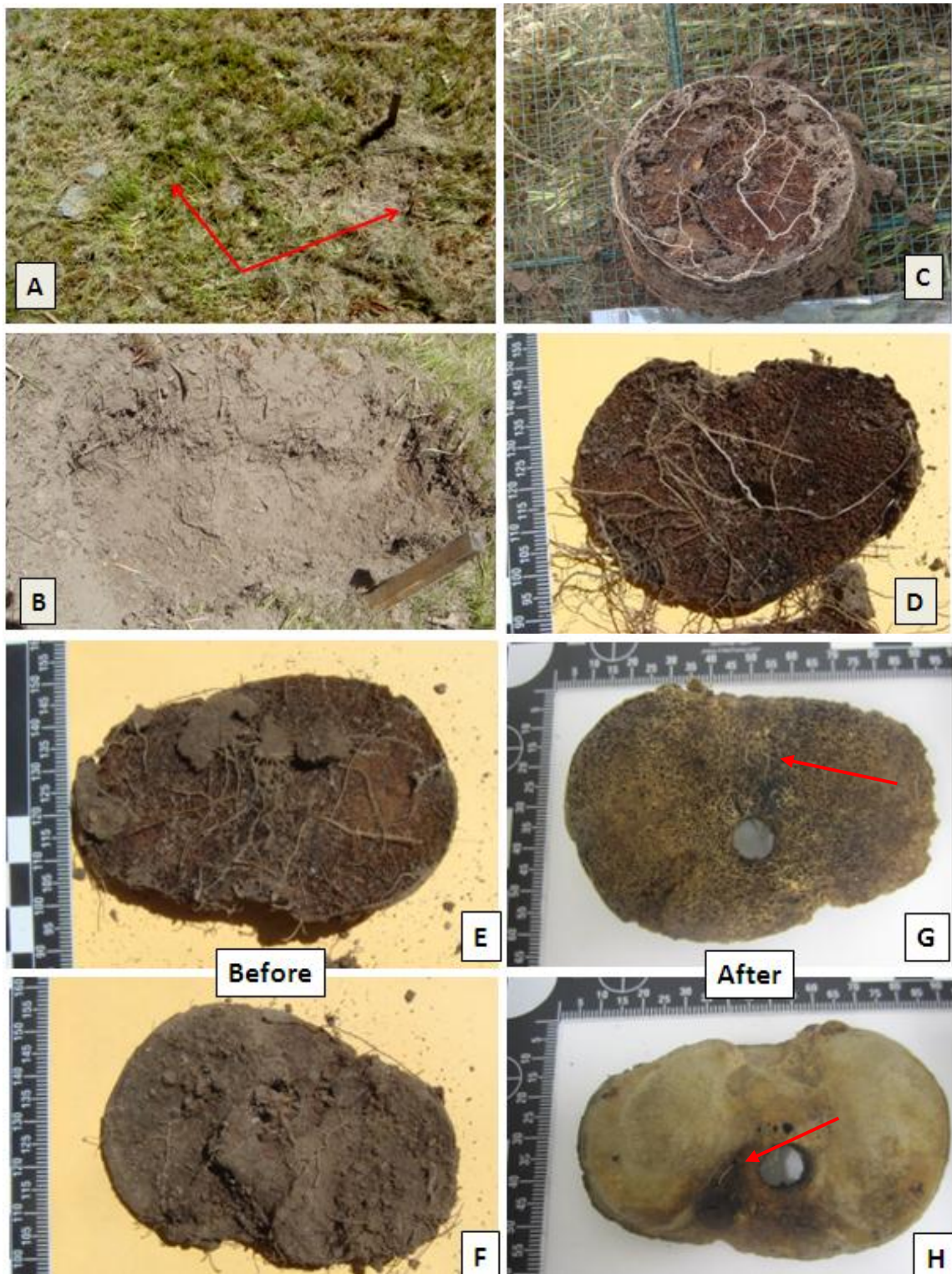
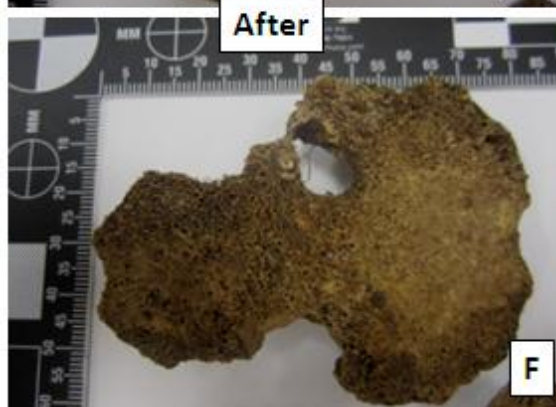
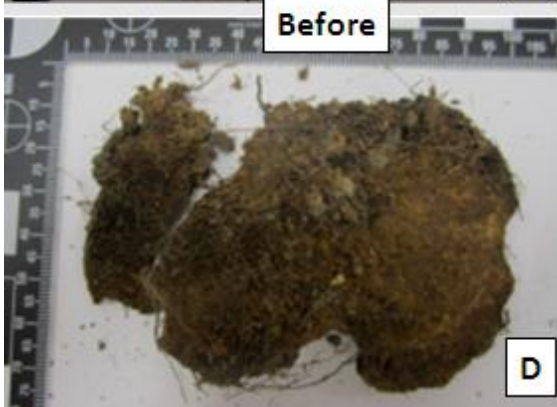


Figure 3.30 18 months of burial.

A) Surface appearance of the burial trench showing a shallow depression and recovering vegetation making defining the trench boundaries (arrows) difficult to define. B) Soil was dry and compact with significant root growth across the trench. C) A ring-shaped root mass was seen in each sample container. D) and E) Extensive root growth across the bony surfaces. F) Bone samples were covered in dirt and grass roots. After washing G) and H), the majority of dirt and root matter was removed. However fine roots deeply penetrated the G) cancellous bone (arrow), and H) small foramina on the superior surface (arrow) which could not be removed solely with washing and scrubbing.



Before

After

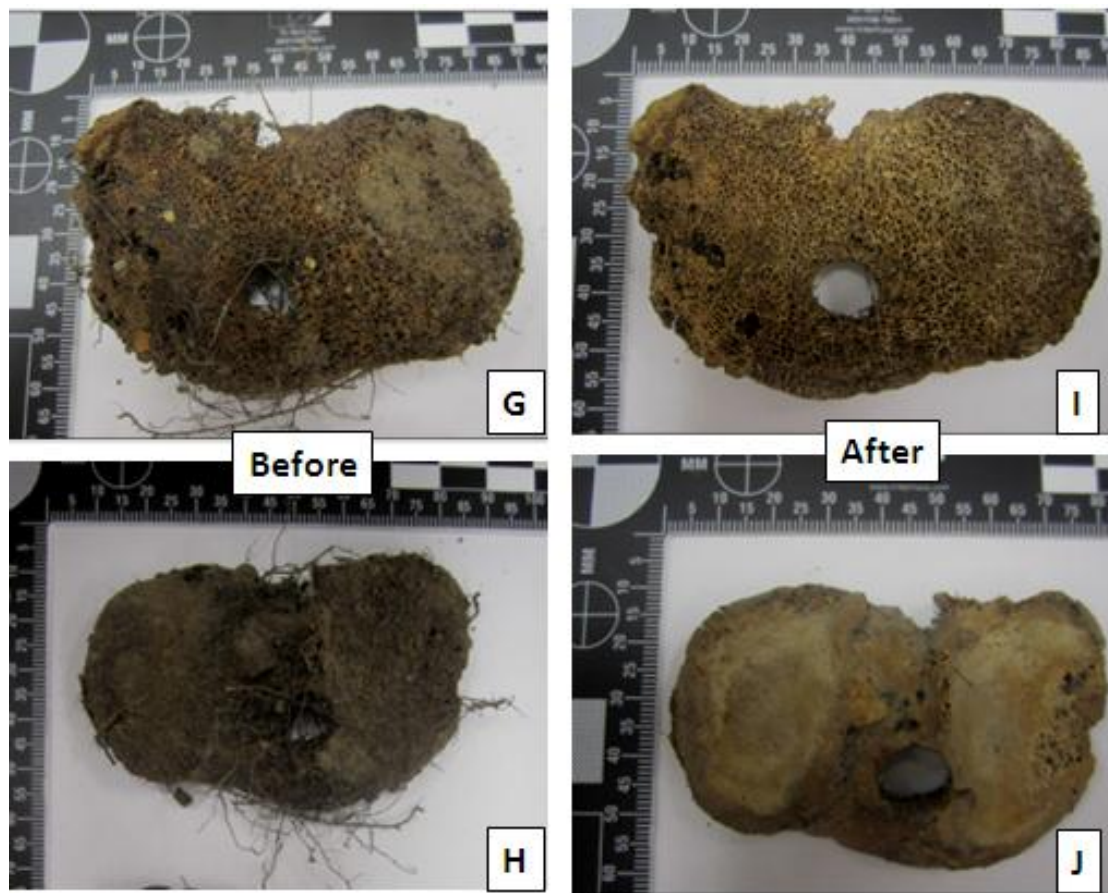


Figure 3.31 Bone and tooth samples buried for 24 months.

A), C), E), G) Bone samples before being washed showing dirt and root infiltration. A) Roots formed a ring shape around the bottom of each container. One sample C) – F) broke during sample handling. After washing and scrubbing E), F), I) and J) show the bones are dry and fragile. B) Teeth were recovered intact.

3.3.2.3 Fresh Water

Bone and tooth samples were incubated in tanks filled with freshwater pumped from a local dam for up to three months (Fig. 3.32A). The water was changed weekly in order to reproduce the conditions of a semi-stagnant body of water such as a dam, pond, water-well, marsh, or small lake. The water had a yellow-brownish colouration which is characteristic of water from a dam, weir or bore.

After one week of submersion, the water was beginning to go cloudy and a grey biofilm had developed on the water surface (Fig. 3.32B). A small amount of green algae had also started growing on the bottom of the tank and on the outside of the sample containers (Fig. 3.33A). A very slight odour was detected. This was presumed to be due to gaseous by-products from microbes in the bio-film on the water surface.

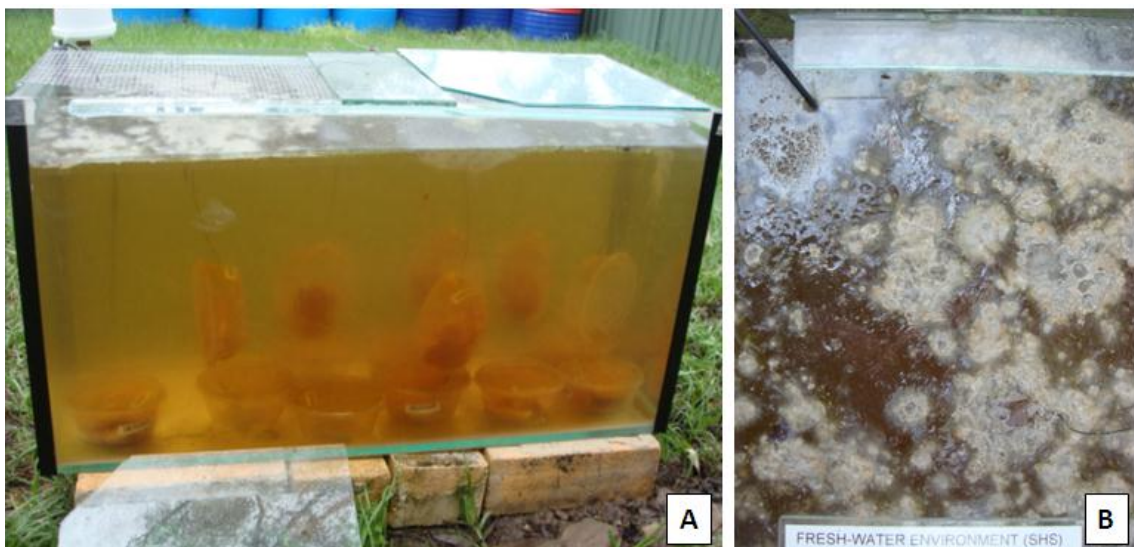


Figure 3.32 Fresh water tanks after one week of sample incubation

A) Samples in the freshwater cage. B) A grey biofilm was seen on the water surface.

The bone samples harvested at one week showed no signs of discolouration or decomposition. The samples were spotted with small (<1mm – 6mm), pale yellow, spherical appendages (Fig. 3.33B & C). These growths on the bony surfaces were most likely algal or yeast colonies (Royal Botanical Gardens Australia, personal communication, August 2012). The colonies did not extend into the bone tissue itself and were easily removed during the washing process prior to DNA extraction.

Bone samples were greasy due to the fatty bone marrow starting to leach from the spaces within the trabecular bone. The articular cartilage and cruciate ligaments were soft with no signs of decomposition (Fig. 3.33A). After washing and scrubbing each sample, it was necessary to remove as much of the cartilage and ligamentous material using a sterile scalpel prior to drying and sanding in preparation for DNA extraction.

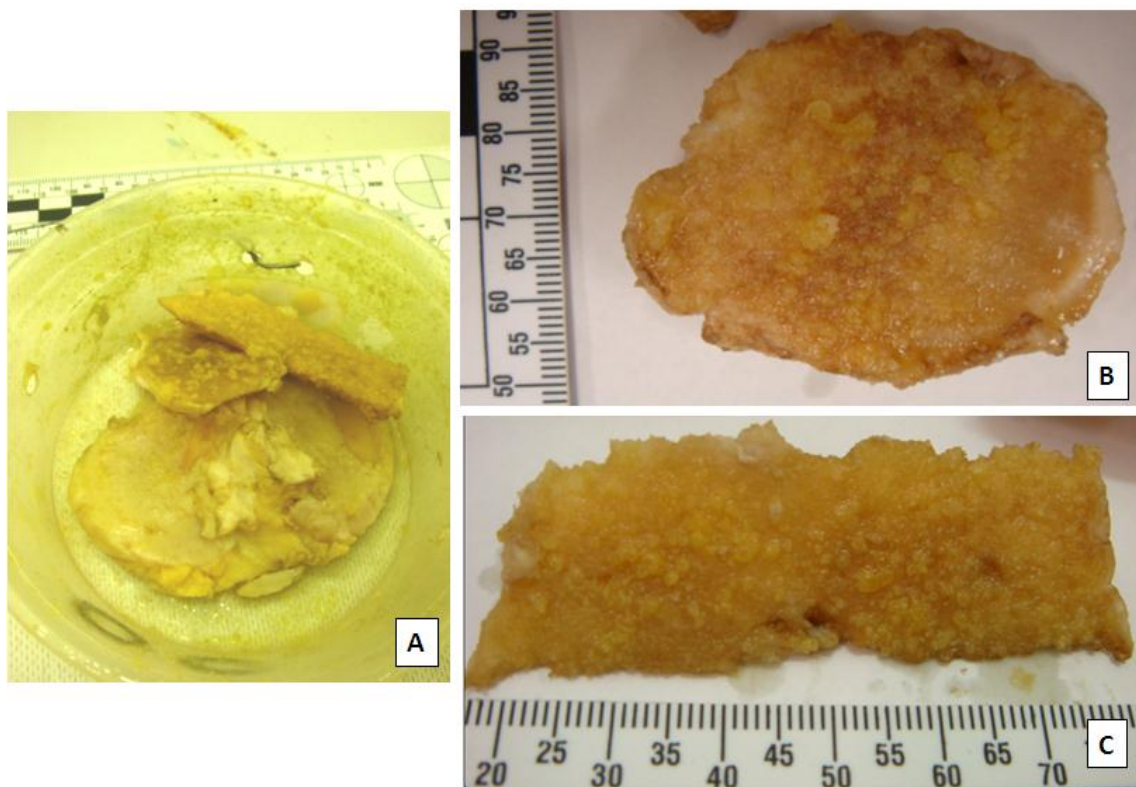


Figure 3.33 Submerged for one week in freshwater.

A) Green algal growth inside container and covering bone samples. All soft tissues are present. Soft yellow bulbous microbial/algal growth on B) inferior bony surface and C) wedge of femoral bone.

After two weeks of incubation in freshwater, the grey bio-film which was seen on the water surface a week earlier was not present. However, a thin oily residue was noted on the water surface (Fig. 3.34A). This may have been due to dissolved fat leaching from the bone samples. A significant increase in algal growth was evident with a thin layer of brownish-green algal slime covering the bottom of the tank. All sample containers were lined inside and out with the greenish algae (Fig. 3.34B).

The bulbous encrustations on the bone surfaces persisted after two weeks of incubation (Fig. 3.34C-E). These algal growths were larger (up to 16mm in diameter) and covered the bone surface more densely. The growths ranged in colour from white to yellow. It was thought that the fat leaching from the trabecular spaces in the bone may have contributed to the more yellow colour. These growths were soft, and crumbled when touched.

The odour present whilst retrieving the samples from the water tank was more pronounced. The offensive odour was significantly stronger after four weeks of incubation, and became more and more pungent as the study progressed. It was thought that the odour was predominately due to the algal and microbial colonisation of the tank with stagnant water.

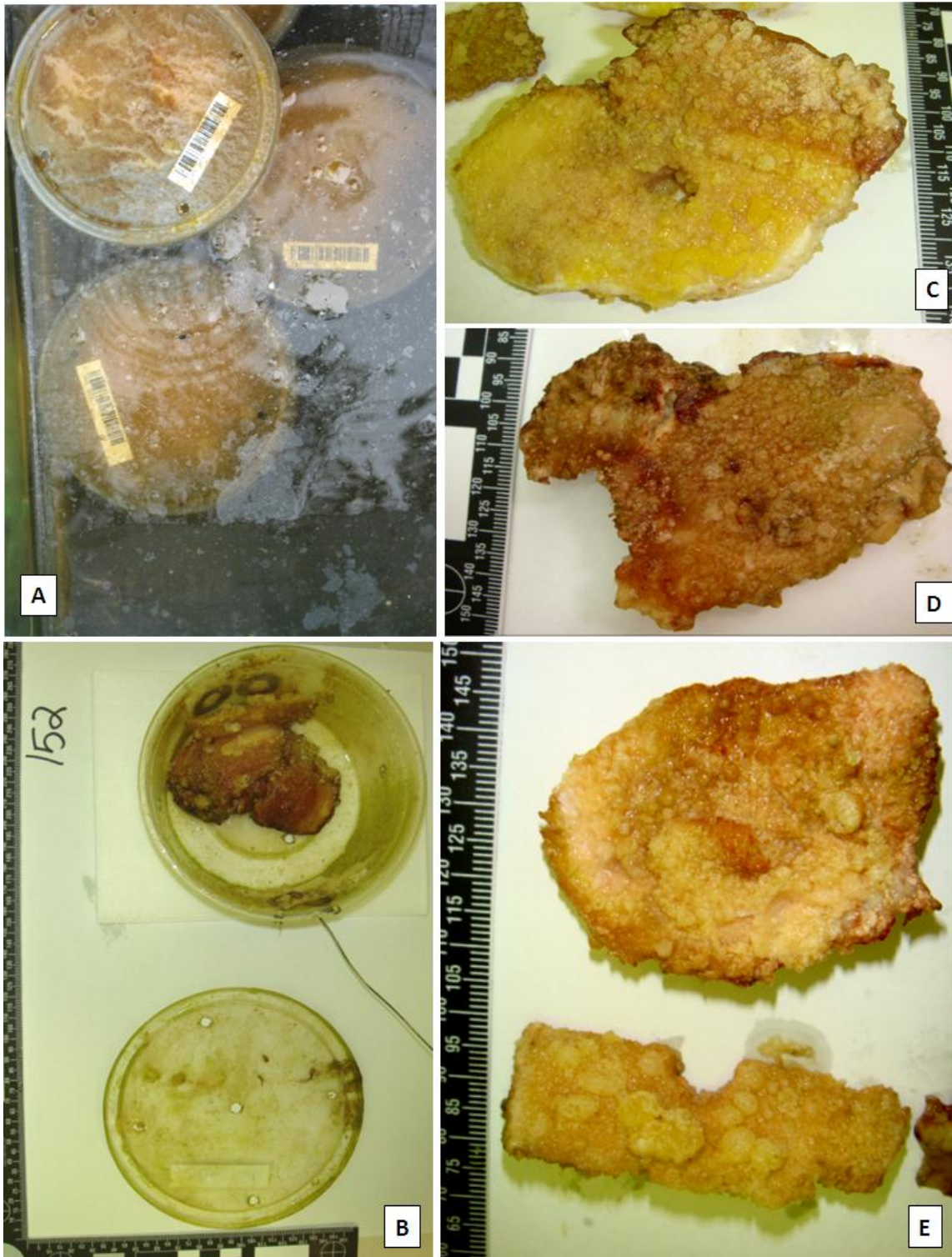


Figure 3.34 Two weeks submerged in freshwater.

A) and D) extensive algal growth inside tank and containers, B) Soft tissue preserved on tibial plateau with half the surface covered in a reddish, yellow microbial film, C), E) and F) Cancellous bony surfaces were covered with pale yellow bulbous growths.

After one month of incubation in freshwater, the tanks and sample containers were lined with bright green and red algal films (Fig. 3.35A – D). The green algae were widespread, lining the glass tank, plastic containers and samples, whilst the red algae were more restricted to the insides of the sample containers and bones. All soft tissues (articular cartilage and ligaments) were still attached. Each sample in the container was coated with the green-red algal slime (Fig. 3.35D). The long filamentous strings of algae blocked the water pump filter during the water change process. Manual syphoning of tank water was performed for the remainder of the study.

After four weeks of freshwater incubation, the same white and yellow bulbous colonies were still seen attached to the bone surface. However, these round growths were now harder and more brittle to the touch and often discoloured due to the green and red slime (Fig. 3.36A-C). These encrustations were also more difficult to remove. Simple scrubbing with a brush was ineffective at removing them entirely. Sanding of the bone surface was required to completely clean the bone surface. This suggests that the algae/microbes may have infiltrated the superficial layers of bone. Teeth recovered at four weeks were intact and covered in green algae (Fig. 3.36D).

After six weeks of being submerged in freshwater the overall algal and/or microbial growth had increased significantly. All plastic containers and bone samples were covered in a thick layer of green and red slime (Fig. 3.37A, C & D). This slime was very thick and completely encased all of the bone samples. In comparison, the tooth container only presented with a thin layer of green algae on the plastic container. These observations would lead to the conclusion that the green algae was widespread within the tank coating all surfaces, but the red algae was more specific to the organic matter in the tank. This mixture of red and green slimy bio-film is consistent with various algal blooms in bodies of stagnant water (Royal Botanical Gardens Australia, personal communication, August 2012).

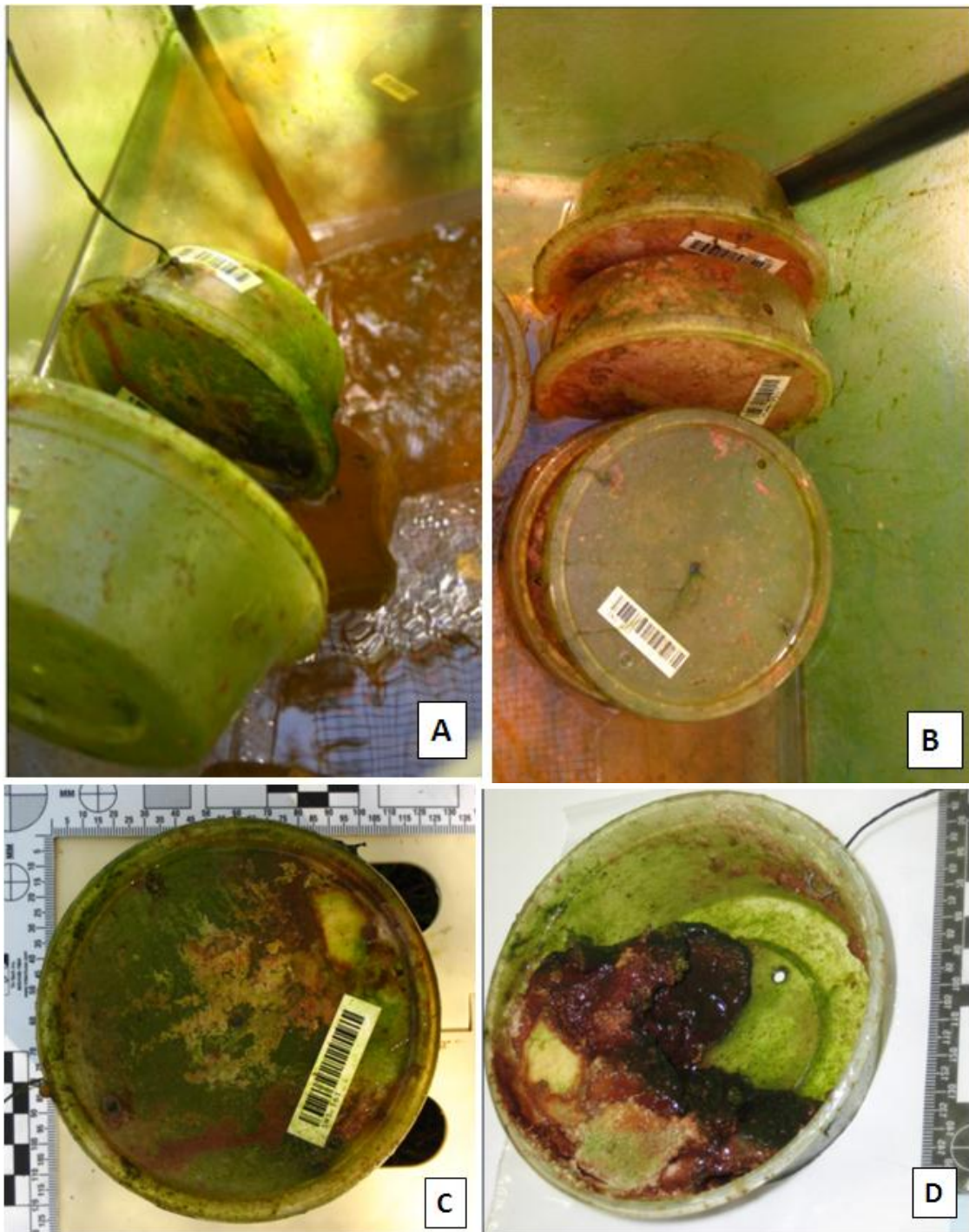


Figure 3.35 Four weeks submerged in freshwater.

A) and B) Extensive growth of red and green algae inside the tank and, C) and D) inside each container.

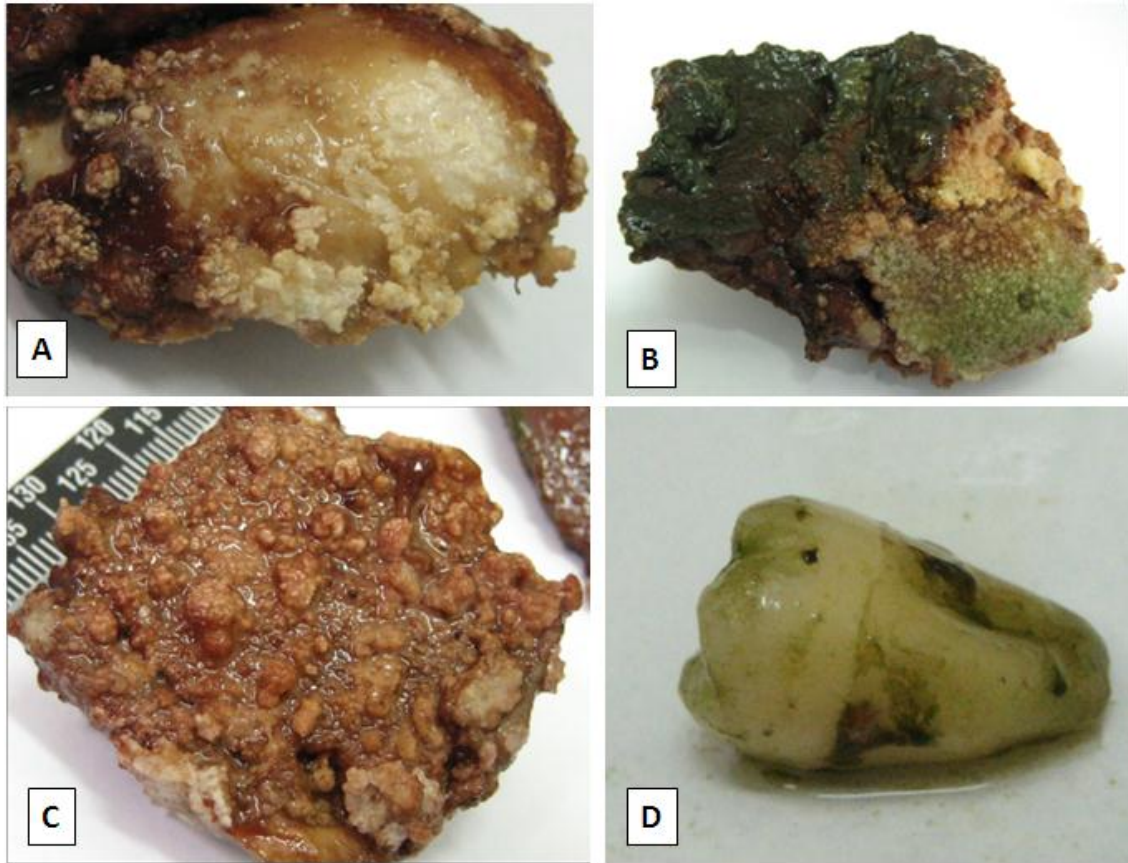


Figure 3.36 Skeletal samples after four weeks submerged in freshwater.

Bone samples showing various microbial and/or algal growths, A) White crusty growths, B) green algae, and C) pale bulbous growths. D) Algal growth on tooth.

The waterlogged samples were soft and greasy with remnants of articular cartilage and cruciate ligaments still attached and fully encased in the thick bio-film (Fig. 3.37C - E). The inferior surfaces of the bones were covered with the same whitish coloured bulbous growths seen on all samples submerged in freshwater during this study (Fig. 3.37F) and were only completely removed by sanding the bone surface. The tooth recovered was intact, slightly darker in colour and covered in green algae (Fig. 3.37G).

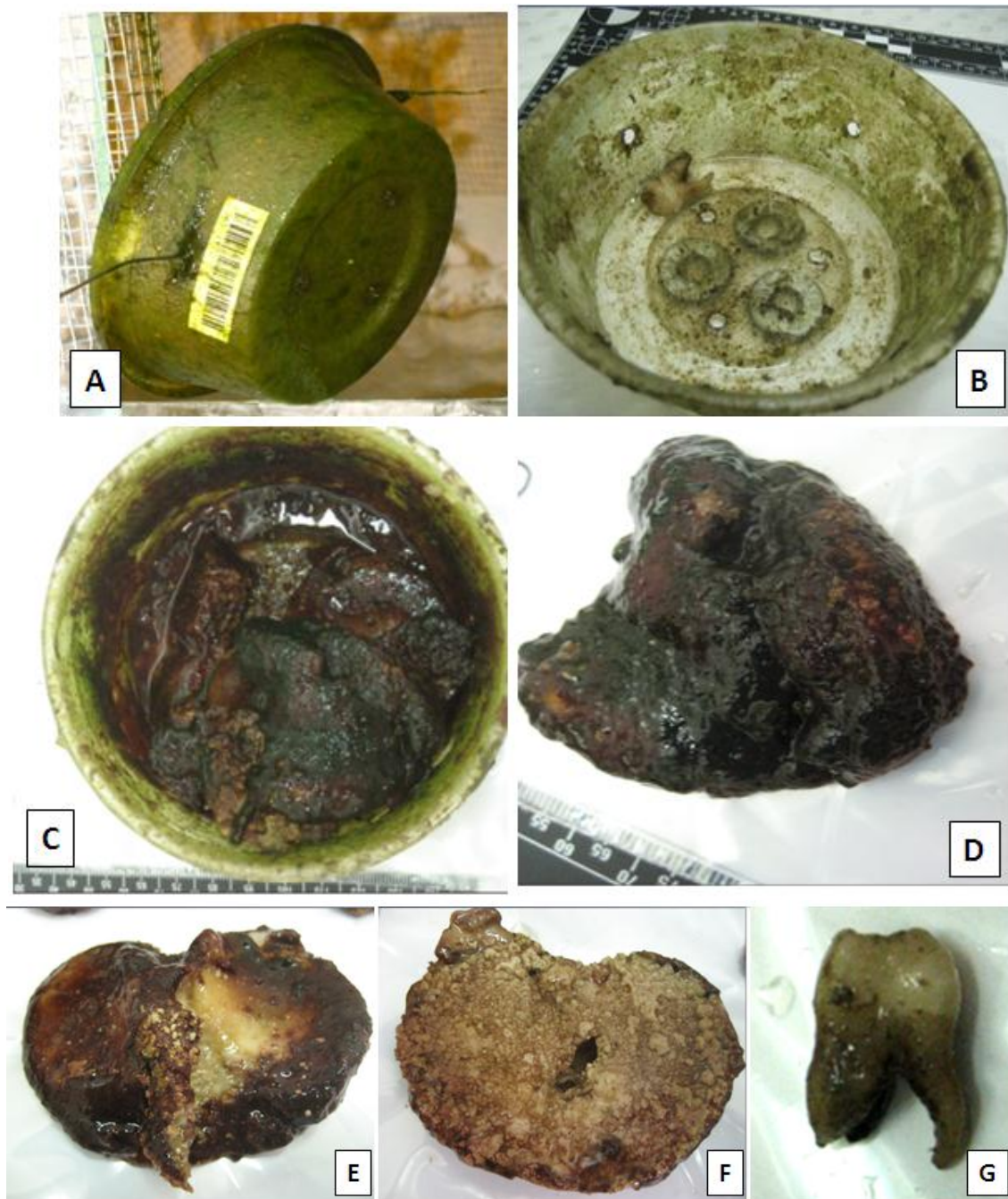


Figure 3.37 Six weeks submerged in freshwater.

Extensive green and red algal growth was seen on and inside A), B), C) each container. C) – E) show a thick reddish green biofilm on all samples. F) The inferior bony surface was the site of soft creamy coloured bulbous growths. G) Algal growth was on the intact molar recovered.

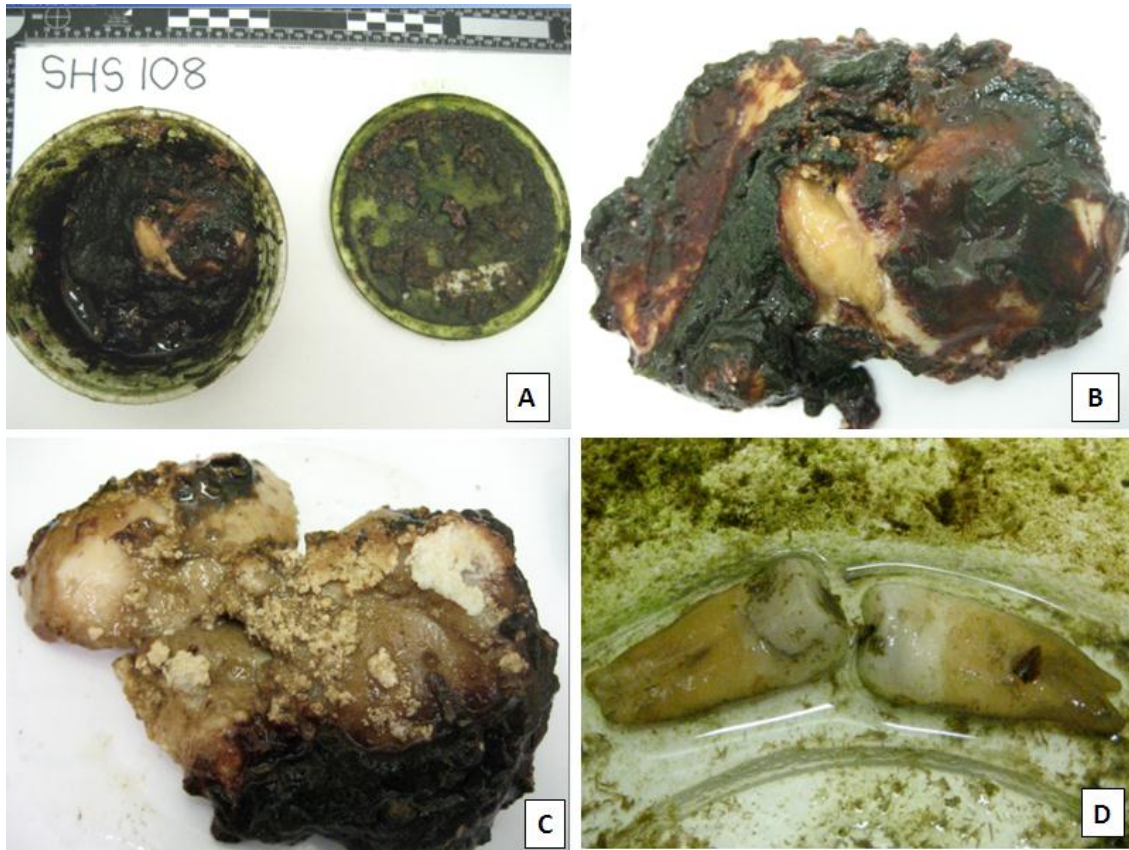


Figure 3.38 Eight weeks of incubation in freshwater.

A) and B) Each sample container and bone sample was covered in a thick reddish, green biofilm. C) A whitish crumbly substance (Adipocere) was seen on the soft tissue remnants of one bone. The two teeth recovered had some green algae adhered to the external surface.

After eight weeks of freshwater immersion, bone samples continued to be covered in the same thick green and red biofilm (Fig. 3.38A &B). The waterlogged bone samples were greasy with all remnants of soft tissue adhered firmly to the bone. A greyish white crumbly material was present on the superior surface of the bone samples (Fig. 3.38C). This substance is termed adipocere or “grave wax” and is commonly found on decomposing remains recovered from moist environments [345]. The waxy substance forms from the hydrolysis and hydrogenation of the neutral fats in adipose (fat) tissue into insoluble, resistant lipid residues [346, 347].

Adipocere formation may initiate within hours post-mortem [348]. However, visible adipocere accumulation has been reported in the literature to occur in approximately six weeks after death [349, 350]. The results of this study support those observations. The timing of adipocere onset can vary greatly from a few days to several months [351-353]. The key factors in adipocere formation include moisture (from the microenvironment surrounding the remains or from the body itself), mildly alkaline pH, warm temperature and anaerobic conditions [354]. It is presumed that abundant adipose tissue is necessary for adipocere formation with no indication in the literature that adipocere could form on de-fleshed bones with very little fat and soft tissue. However a recent study has shown visible adipocere accumulations on sections of de-fleshed femur buried in soil for up to 18 months [347]. Adipocere was observed on the surface of bone samples submerged in freshwater for eight weeks in this thesis, and supports the notion that there is enough residual fatty tissue and lipids present in de-fleshed bones to initiate adipocere formation.

3.3.2.4 Salt Water

Bone and teeth were submerged in saltwater for periods of up to six months in order to mimic human remains which may be recovered from marine conditions. It is understood that decomposition occurs more slowly in saltwater environments than in freshwater due to the reduction of bacterial action because of the salt concentration [355]. It was therefore decided to increase the period of submersion of samples in this study from two months (freshwater samples) to six months in salt water. Overall, the samples showed relatively good levels of preservation for the entire six months.

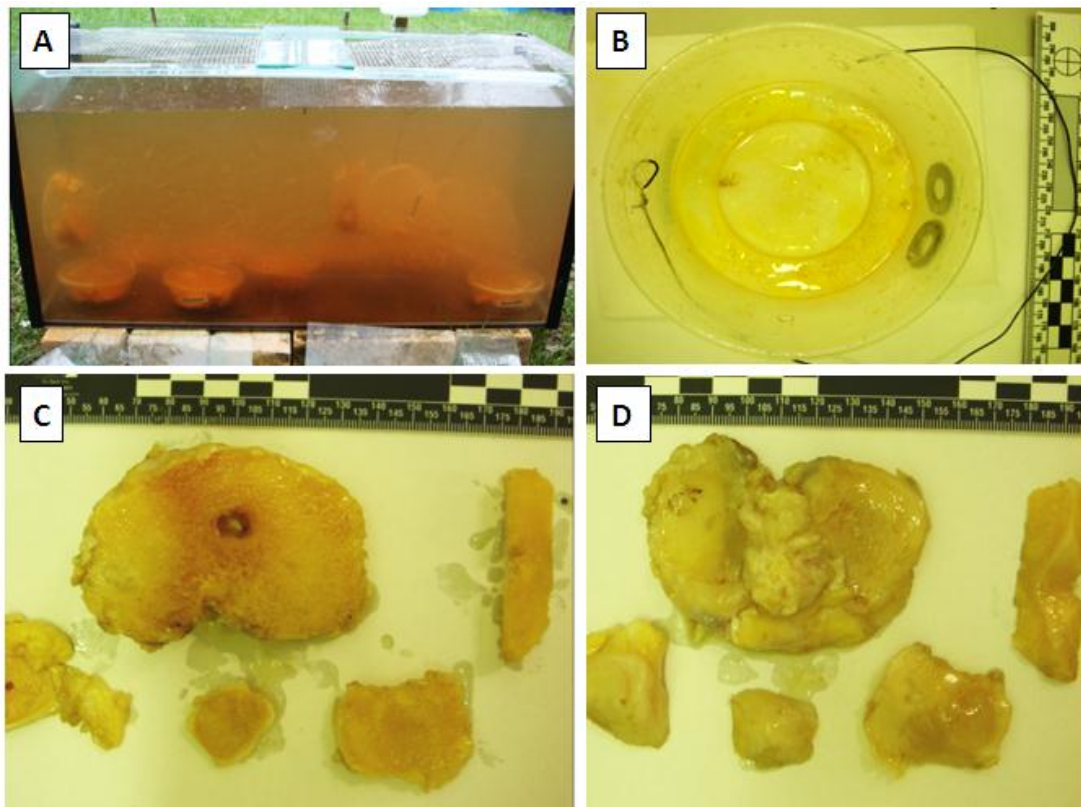


Figure 3.39 Two weeks submerged in saltwater.

A) Sample containers in the saltwater tank B) An oily residue was seen in each sample container. Bone samples were well preserved with no visible damage to the C) inferior or D) superior surfaces. Soft tissue was still present on the articular surface of the tibial plateau.

After two weeks of incubation in salt water, the tank water was murky in appearance (Fig. 3.39A) with a very slight odour. In the bottom of each sample container a significant amount of yellow oily substance was observed (Fig. 3.39B). This was due to the leaching of dissolved fat tissue from the spaces within the trabecular bone. All soft tissue (cruciate ligaments and articular cartilage) was well preserved (Fig 3.39C & D). No discolouration of bone tissue, microbial or algal activity was evident.

After one month of incubation in salt water, a thick oil slick was seen on the surface (Fig. 3.40A). This oil was due to the continued leakage of dissolved fats from the bone samples. This layer was removed prior to pumping water from the tank and retrieving the sample containers (Fig. 3.40B). A second layer of loose fatty material covered the bottom of the tank.

Within each container, bone samples were coated with a thick layer of yellow fatty material (Fig. 3.40 C & D). This substance was easily removed by wiping with a tissue and washing with warm water. The bone samples were well preserved with no visual discolouration and all soft tissues were still adhered to the bone (Fig. 3.40E). No visible microbial or algal growth was noted.

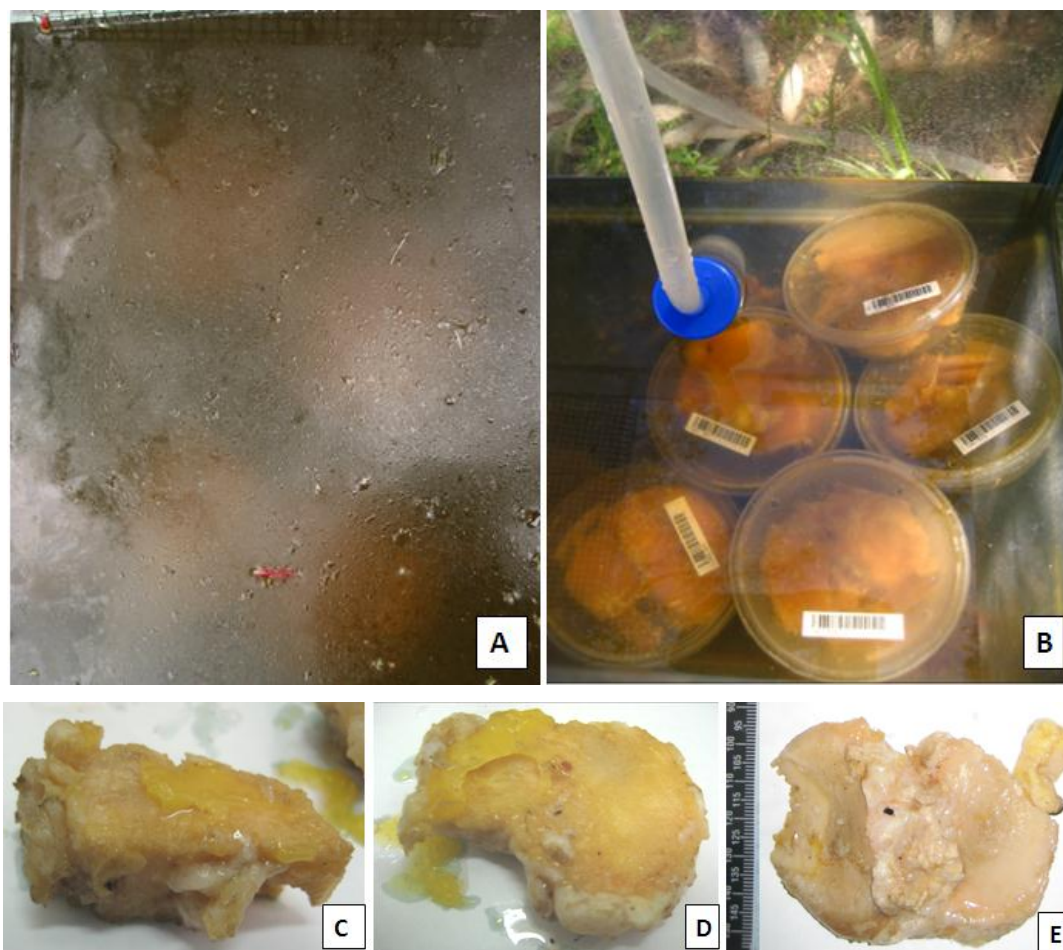


Figure 3.40 One month submerged in saltwater

A) An oily residue was seen on the water surface. B) Sample containers sit on the bottom of the saltwater tank during each water change. D & E) A thick yellow, fatty residue is seen on the surface of bone fragments. E) Well preserved sample showing no discolouration or loss of soft tissue.

Significant taphonomic changes to the water and bone samples had occurred after three months of submersion in salt water. The layer of lipid globules on the water surface was thinner. However, the thick fatty substance on the bottom of the tank persisted. An increase in overall microbial activity was observed. A brownish residue covered the plastic sample containers and the bone samples within (Fig. 3.41A & B). This may be due to algal and/or bacterial growth. This bio-film was a different colour than the slimy growths seen with freshwater samples, which suggests that different microbial and/or algal species had colonised the two sets of samples. This is not surprising given the increased salt concentration of the marine samples.

The cruciate ligaments and articular cartilage were intact and did not show any signs of decomposition. However, a noticeable colour change had occurred. The waterlogged bony tissue had become significantly darker, particularly on the inferior surface (Fig. 3.41C). The trabecular bone on the inferior surface (Fig. 3.41C) and the femoral wedge (Fig. 3.41D) was spotted with whitish spherical growths of up to 8mm in diameter. These were consistent in appearance and texture to the algal or yeast growths seen in the freshwater samples after two weeks of incubation.

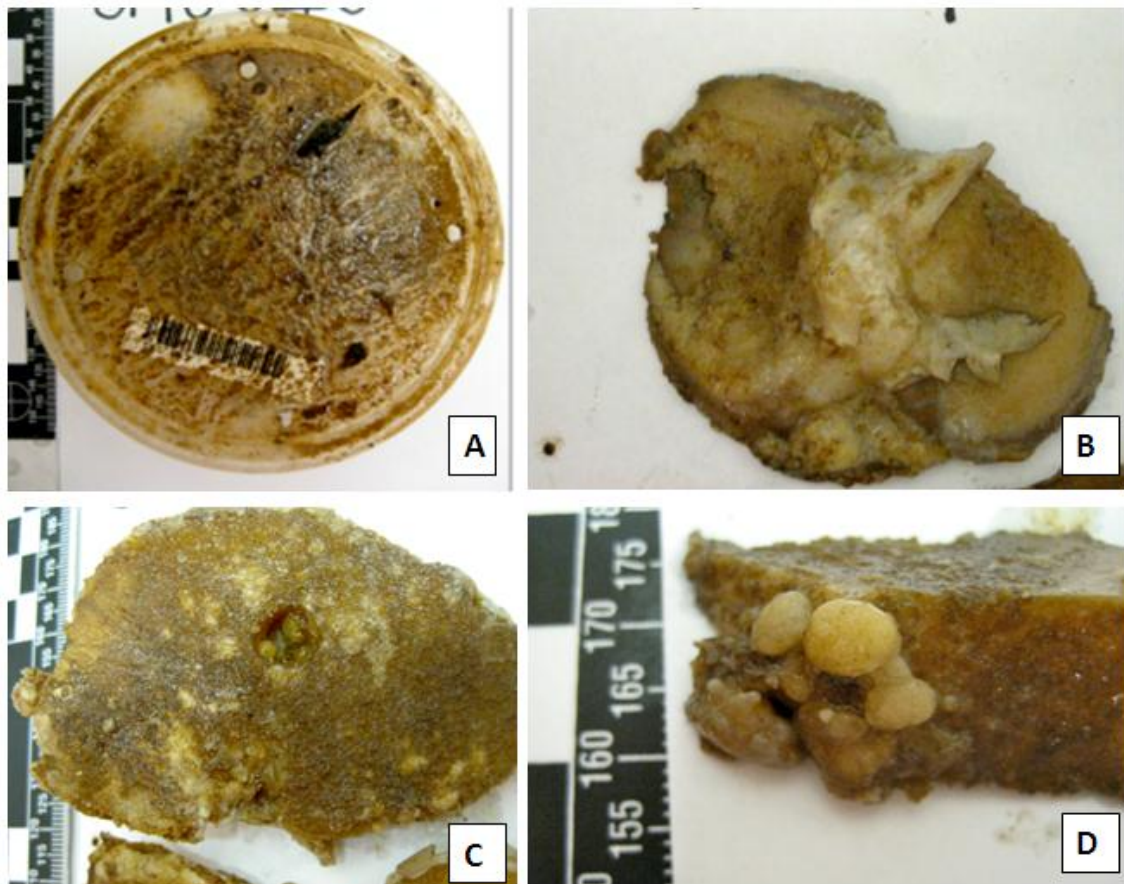


Figure 3.41 Three months submerged in saltwater.

A) Greenish brown algal film on and inside each sample container. B) Bone sample with the soft tissue still well preserved. C) and D) Small, cream-coloured bulbous focal growths are seen on the cancellous bone surfaces.

After six months of saltwater incubation, the oily residue on the water surface was no longer present. However, the thick creamy layer on the tank floor persisted, and the water was very murky. Overall microbial growth had continued to increase. The greenish brown residue lined the inside of each container and covered all bone and tooth samples (Fig. 3.42A - C). This substance was not slimy like that seen in the

freshwater samples but pasty and slightly greasy in texture. This material was thought to be a mixture of lipids from the decomposing bone tissue and the various microbes using those fats as a nutritional source. The cream coloured growth was found on the inferior surfaces of all bone samples (Fig. 42D) and was easily removed during the standard washing process prior to DNA extraction. The remnants of both cruciate ligaments were still anchored to the bone, but had started to decompose and lose their anatomical architecture. The articular cartilage on the superior surface was still present and coated with the greenish brown bio-film. This material had stained the soft tissues and was unable to be removed with washing. The structural integrity of the bone tissue was completely intact and greasy.

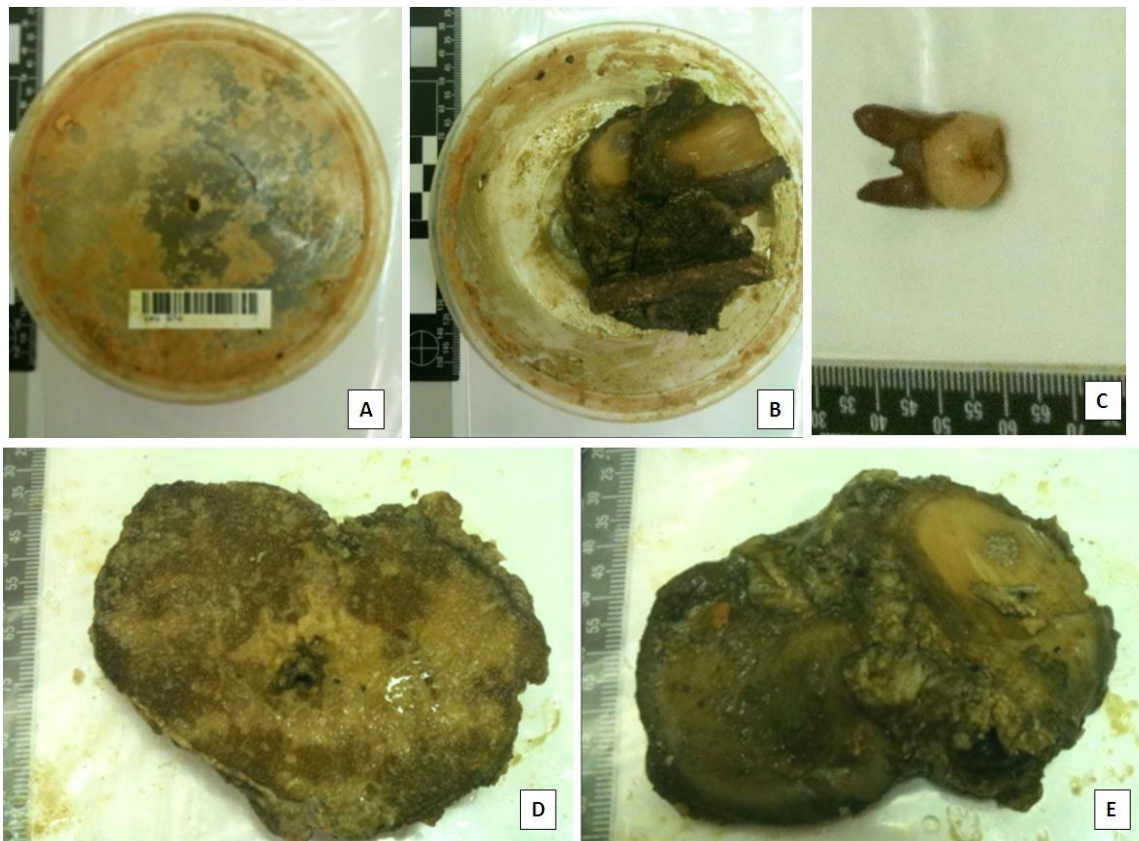


Figure 3.42 Six months submerged in saltwater.

A) and B) A Reddish brown creamy residue was seen inside sample containers, and C) and D) on all bone sample surfaces. C) The molar was recovered intact. D) A soft cream coloured growth was seen on the inferior bony surface. E) Soft tissue was present on the articular surface of the bone and was discoloured.

3.3.2.5 Heat

Bones were exposed to five levels of heat treatment: 1. low (~150°C), 2. moderate (~350°C), 3. high (~550°C), 4. extreme (~700°C) and 5. prolonged extreme heat with direct exposure to the flame. Those bones exposed to low levels of heat (Fig. 3.43) showed charring and blackening of the edges of the bony fragments and any attached soft tissues (remnants of the anterior and posterior cruciate ligaments, fibrous joint capsule and articular cartilage). These soft tissue elements whilst burnt on the edges were still pliable and relatively soft. The inferior/interior surfaces of the fragment showed very little heat damage to the cancellous bone. However, much oil from the melting bone marrow was seen oozing from the bones during the heating process (Fig. 3.43C). With this degree of heat and exposure, the samples were still well preserved, moist and greasy.

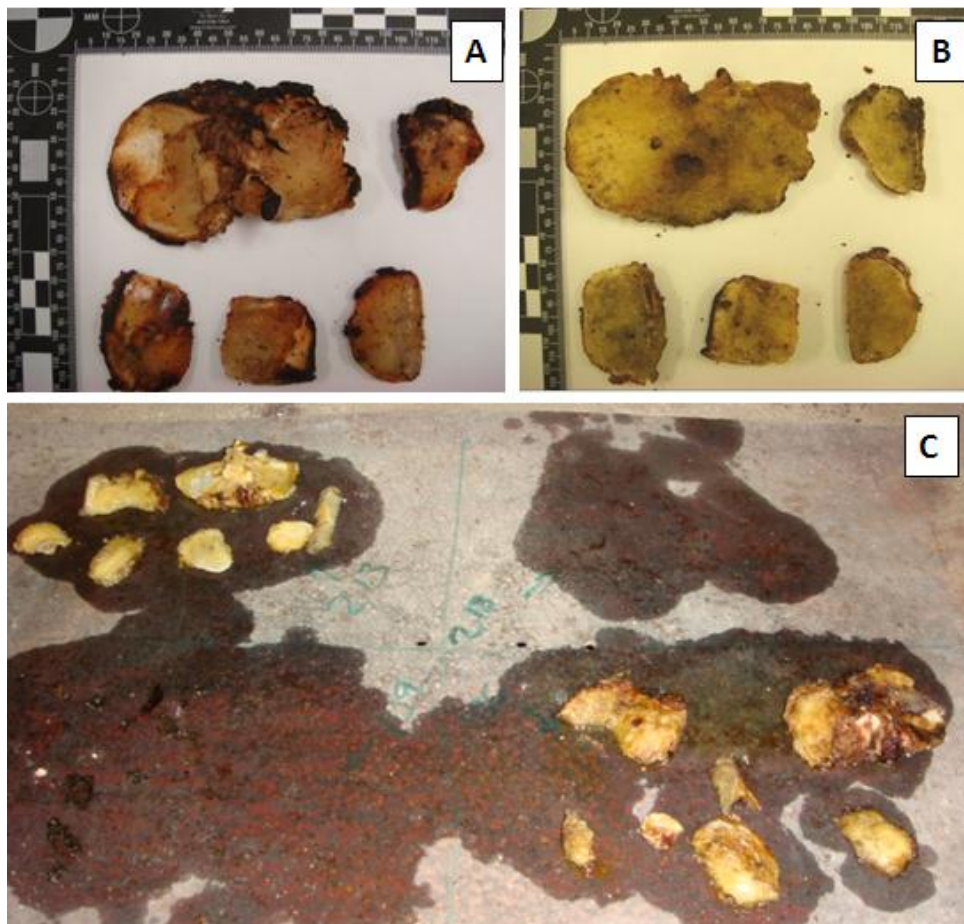


Figure 3.43 Bones exposed to low levels of heat.

- A) External surface and B) internal bony surface of one set of bones showing charring on the edges.
- C) Fatty bone marrow leached from samples during the heating process.

With a moderate amount of heat (~350°C), samples (Fig. 3.44) displayed more extensive burning and slightly more blackening of both the internal and external surfaces than those exposed to lower heats. Any remnants of soft tissue were burnt to the point of being hard and crisp. The articular cartilage dried and cracked extensively (Fig. 3.44B & D). Bony fragments were still intact and greasy. The surface of the cancellous bone was charred black, but still well preserved underneath.

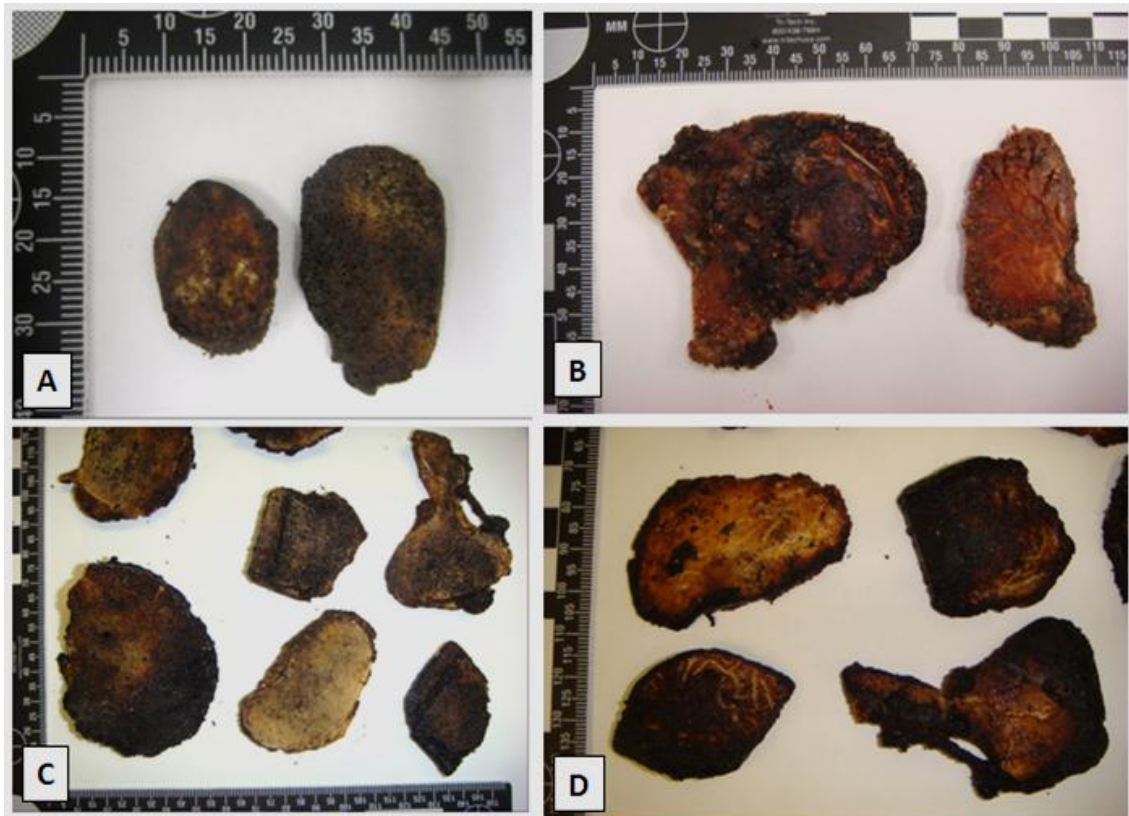


Figure 3.44 Bones exposed to moderate levels of heat.

Four different sets of bony fragments (A-D) show significant charring at the edges and inferior surfaces. B) and D) Cracking of the articular cartilage was seen.

Bones exposed to high temperatures (~550°C) showed a marked increase in heat damage (Fig. 3.45). All remnants of soft tissue and articular cartilage had been consumed and destroyed. The vast majority of both the external and internal surfaces were blackened and charred. The burnt bony surface was drier and crumbled slightly at the edges upon handling. Surface damage was deeper than seen with bones exposed to less intense heat. However when the charred surface was sanded back prior to DNA extraction, moist and greasy bone appeared to be well protected underneath.

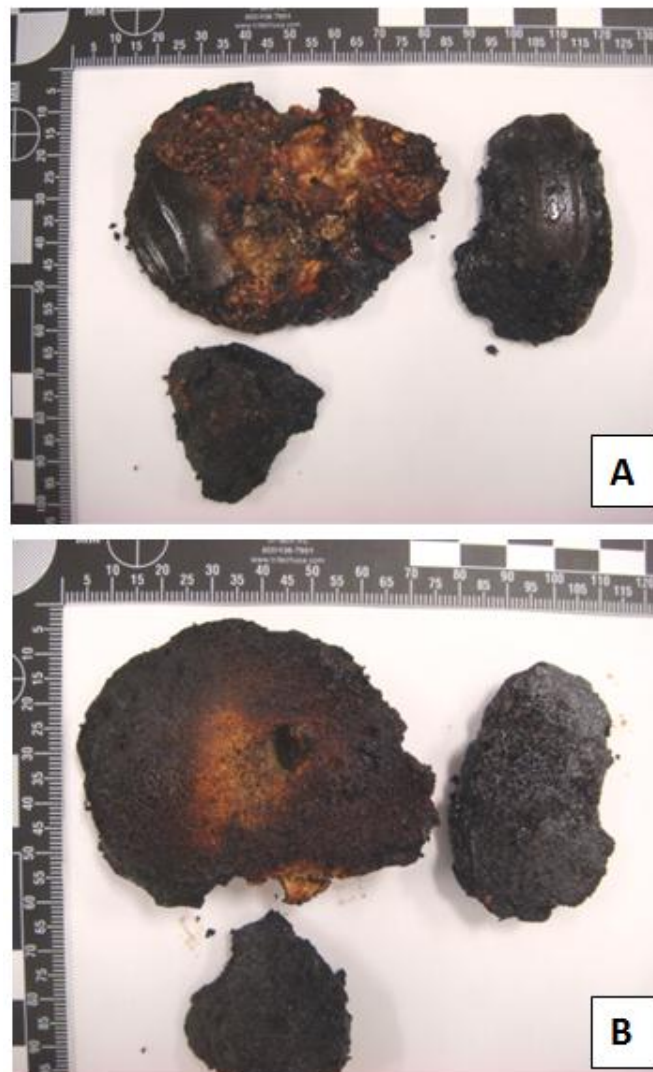


Figure 3.45 Bone exposed to high levels of heat.

Bones exposed to high levels of heat showing high degree of charring on both the A) external and B) internal surfaces.

Bones exposed to extreme levels of heat (~700°C) were completely blackened and charred over all surfaces (Fig. 3.46). The burnt surfaces were very dry and brittle. The edges crumbled completely when handled. The depth of charring was deeper than those bones exposed to less intense heat. However upon sanding away of the charred surfaces, a small amount of moist, greasy bone tissue was exposed. The teeth were burnt on the under-side resting on the metal plate. The crowns of the teeth cracked and several small pieces of enamel chipped off at the edges (Fig. 3.46D).

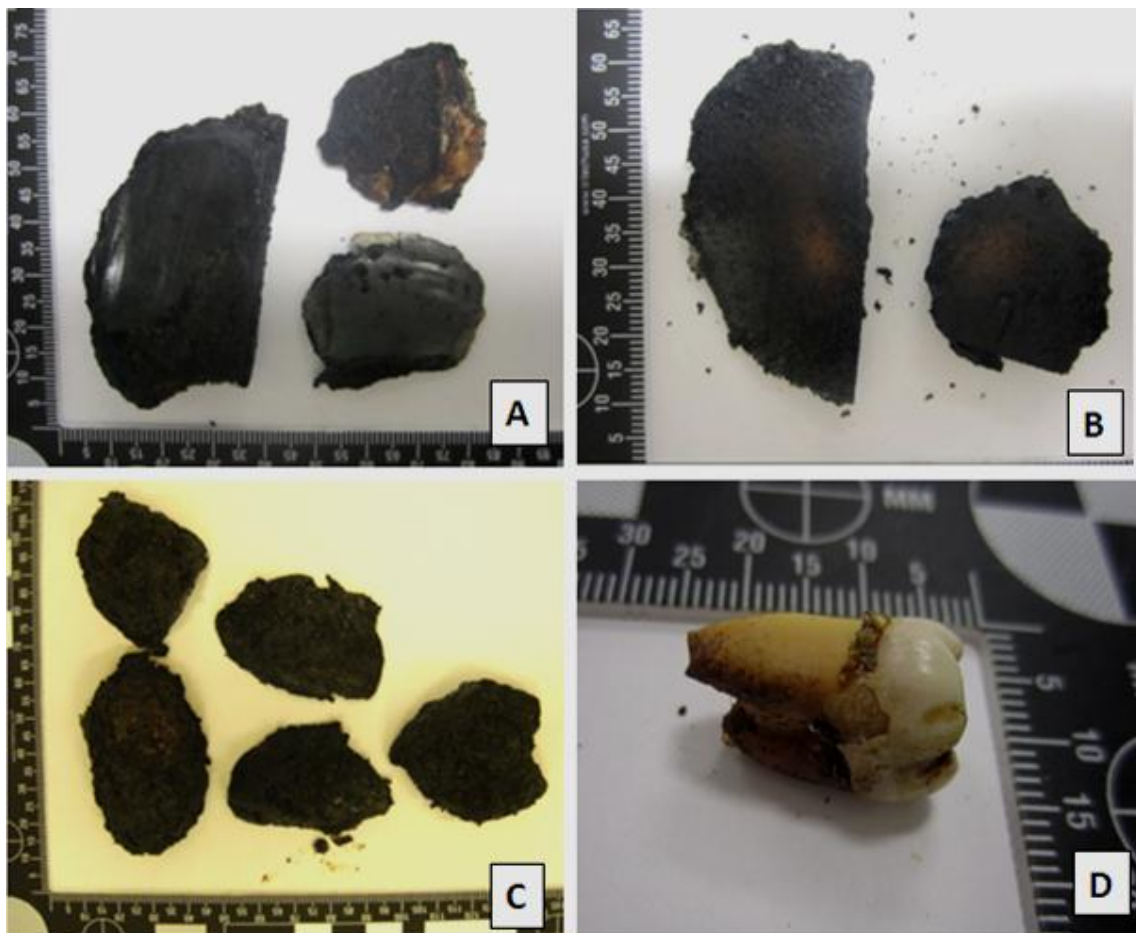


Figure 3.46 Samples exposed to extreme heat.

Bones exposed to extreme heat show extensive charring over the entire A) external and B), C) internal bony surfaces. D) The enamel on the tooth exposed to extreme heat had chipped during the heating process.

Prolonged exposure (30 minutes) to extreme temperatures almost completely destroyed the bony tissue and architecture. All fragments showed extreme charring and some displayed the whitish grey colouring of early calcination on the edges which is characteristic of exposure to very high temperatures (Fig. 3.47A). The bony surface was extremely dry and brittle and crumbled to ashes when handled. These samples disintegrated when washed and prepared for sanding. One sample withstood the rigours of sanding to yield one small, thin sliver of bone for DNA extraction (approximately 1cm²). This fragment was ground into a powder in the freezer mill and digested. However, when the silica spin column was centrifuged during the extraction process, the suspended fine ash particles clogged the filter. The samples were therefore discarded.

The teeth exposed to this extreme level of heat also showed extensive damage (Fig. 3.47D). The roots were completely charred and the tips showed signs of early calcination. The enamel on the crown completely shattered and exploded away from the underlying dentine. These teeth disintegrated during the initial cleaning process and therefore DNA extraction was not performed on these samples.

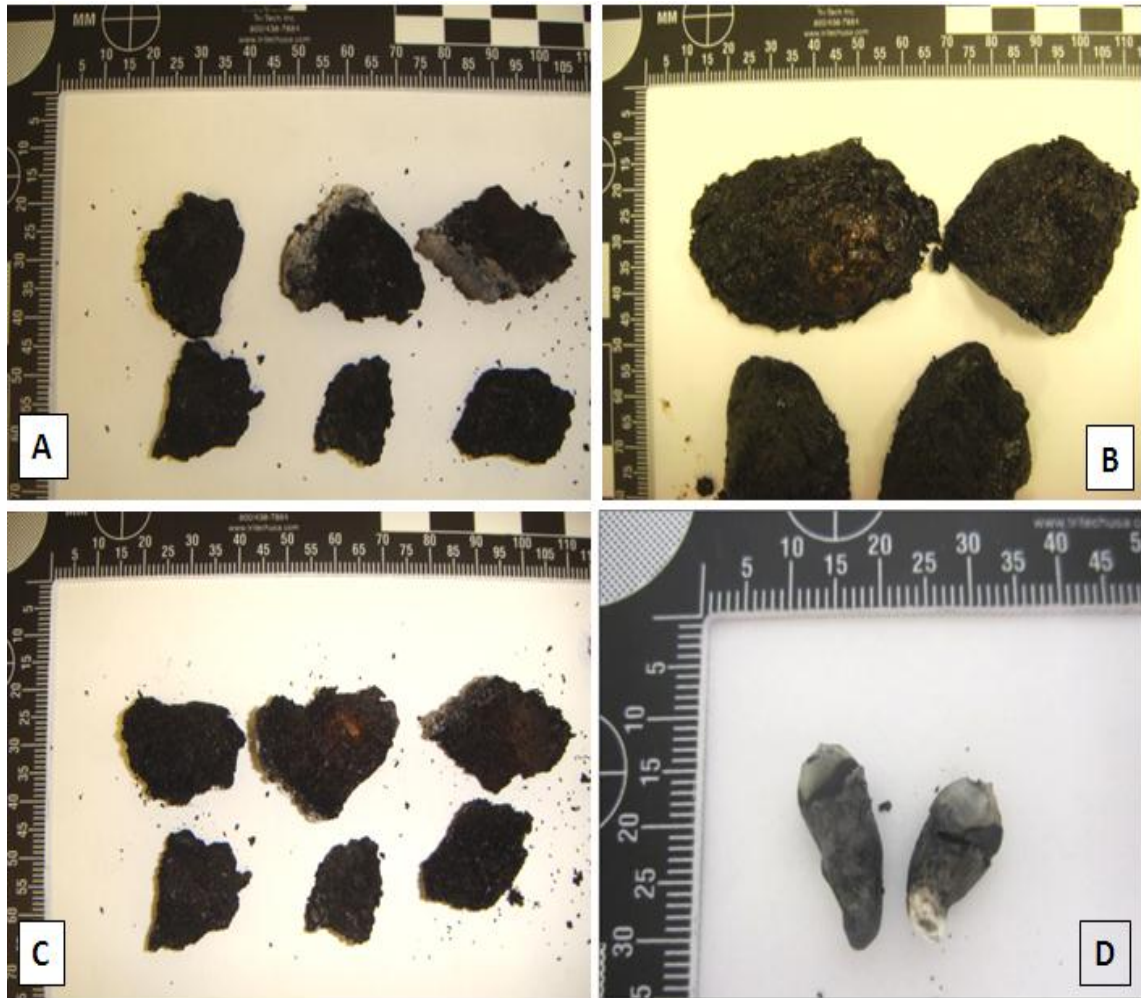


Figure 3.47 Samples exposed to extreme heat (~700°C) and direct flames for a prolonged period (30 minutes).

A)-C) Bone samples were badly charred with exposure to prolonged extreme heat. D) Teeth exposed to extremely high temperatures for a prolonged period of time lost all enamel from the crown, and the white root tips showed signs of calcination.

3.3.3 DNA Degradation

Skeletal samples were exposed to various environmental insults in order to create a set of damaged and degraded bone samples which mimic the range of environmental conditions seen with forensic skeletal samples. The level of DNA degradation and PCR inhibition was assessed for each sample using the quantitative PCR multiplex assay described in Chapter 2.

The level of sample preservation was reasonably constant within and across each environmental challenge except those samples which were left on the surface (Fig. 3.48) Surface samples showed the heaviest and most variable levels of degradation (degradation ratios ranging from 3.5-9.1) (Fig. 3.48A). However no correlation between the length of exposure and degradation ratio was observed.

Relatively low levels of degradation (degradation ratios between 1.5 and 2) were observed with buried and saltwater samples regardless of the time of exposure. Freshwater and heat-exposed samples yielded DNA which was somewhat more degraded (ratios between 2 and 3.5) with ratios rising slightly with increased time of environmental insult. These data support findings that DNA degrades faster in freshwater than in salt water [356].

Bones exposed to prolonged extreme heat exposure were so badly charred that they crumbled completely when handled. Samples either disintegrated during cleaning and sanding prior to extraction, or they clogged up the spin column filter during the DNA isolation procedure.

Exposure to sunlight inflicted the most damaging effect on DNA within the bone samples (ratios ranging from 3.5-9.1) (Fig. 3.48A). It is well understood that UV radiation indirectly damages DNA by creating free radicals (UV-A) and directly by crosslinking adjacent cytosine and thymine bases creating pyrimidine dimers (UV-B) [21]. These types of damage can lead to nicks and double-stranded breaks in the DNA affecting downstream PCR amplification.

The majority of the damage occurred early (within the first time period tested) and then plateaued over the remaining time period examined (Fig. 3.48). These results support the notion that DNA damage and degradation is a complicated process, more heavily influenced by the type of environmental insult (pH, UV exposure, temperature, bacterial and fungal colonisation etc.) than the length of time alone.

PCR inhibition as measured by a delay in the cycle threshold (Ct) of the internal PCR control in the real-time PCR degradation assay was not observed during amplification of the environmentally challenged samples (data not shown).

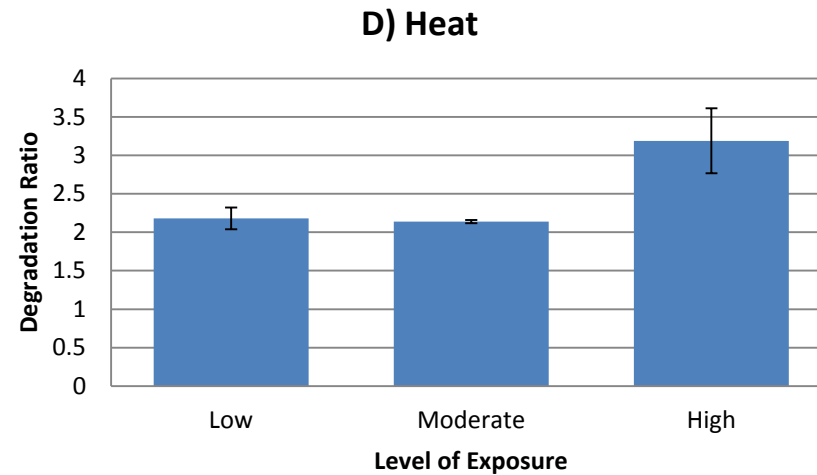
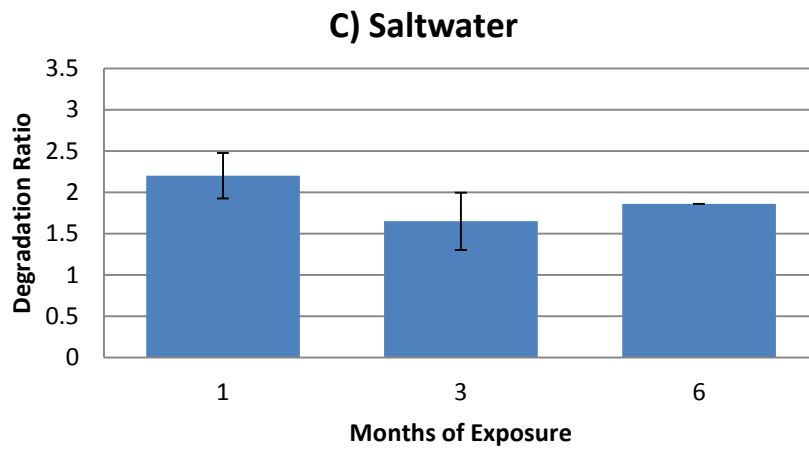
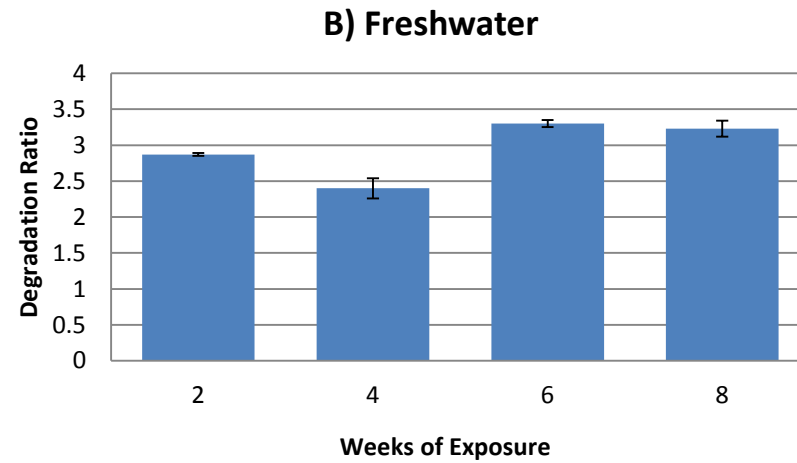
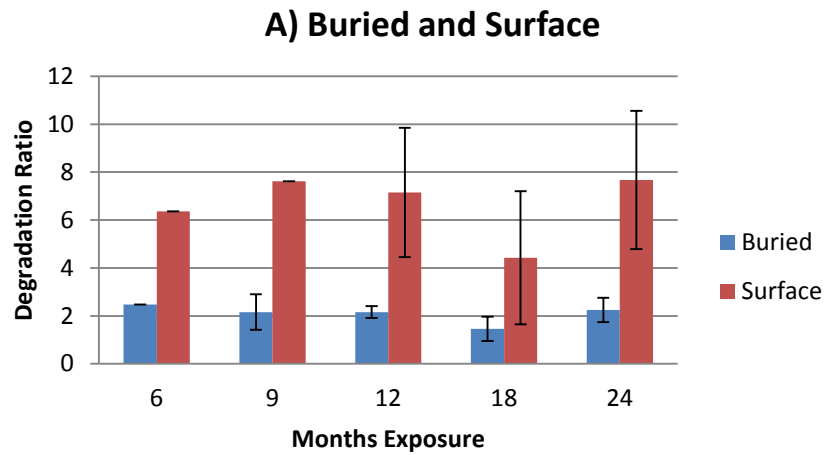


Figure 3.48 Average levels of DNA degradation of fieldwork samples.

DNA degradation of fieldwork samples exposed to a) burial and surface conditions, b) freshwater, c) saltwater and d) heat as assessed by a quantitative real-time PCR multiplex assay. Data presented as means \pm SEM.

3.3.4 Genotyping

The comparative success rates of STR genotyping of environmentally challenged skeletal samples using AmpFISTR® NGM™ (Applied Biosystems) and PowerPlex® ESI 16 (Promega) amplification kits was investigated. Both STR kits contain 15 loci plus the amelogenin locus (Appendix 2) and performed equally well with the less degraded samples (Fig. 3.49). Both STR kits amplify the same 16 loci (including amelogenin) but primer design has resulted in the same loci being different lengths in the two kits. For example, D18S51 is approximately 260-350bp in the NGM kit and reduced to 130-220bp in the ESI kit. In order to maximise the success of genotyping degraded forensic samples, the majority of loci are designed to be less than 250bp in length (PowerPlex® ESI 16 with 9 of the 16 and AmpFISTR® NGM 11 of the 16) (Appendix 3).

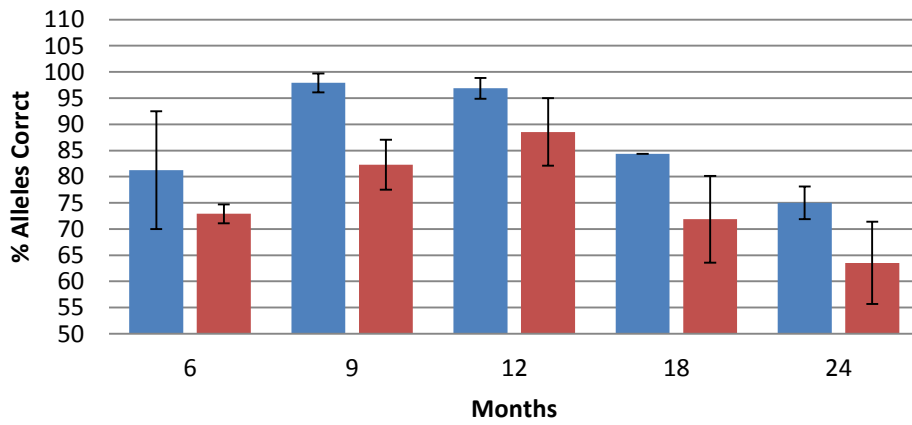
Complete and concordant STR profiles were obtained for all bone samples stored in saltwater for up to six months and all samples exposed to heat and fire (data not shown). Comparable kit performance (98-100% successful allele recovery) was observed with all freshwater (Fig. 3.49C) and all buried samples except one (24 months exposure) (Fig. 3.49B). A 10% decrease in alleles were detected using the NGM™ kit in those buried samples compared to the same samples using the PowerPlex® ESI 16 kit. As samples became more degraded, the difference in performance of the two STR kits became more evident. On average, 10-15% more alleles were recovered from the most degraded set of samples (surface remains) using the PowerPlex® kit versus the NGM™ kit (Fig. 3.49A).

These results suggest that the PowerPlex® ESI 16 amplification kit chemistry is more tolerant to DNA degradation and/or damage than the AmpFISTR® NGM kit. The extra cycle (30 vs 29 cycles) in the PowerPlex® kit may also provide an advantage over the NGM kit when amplifying poor quality samples.

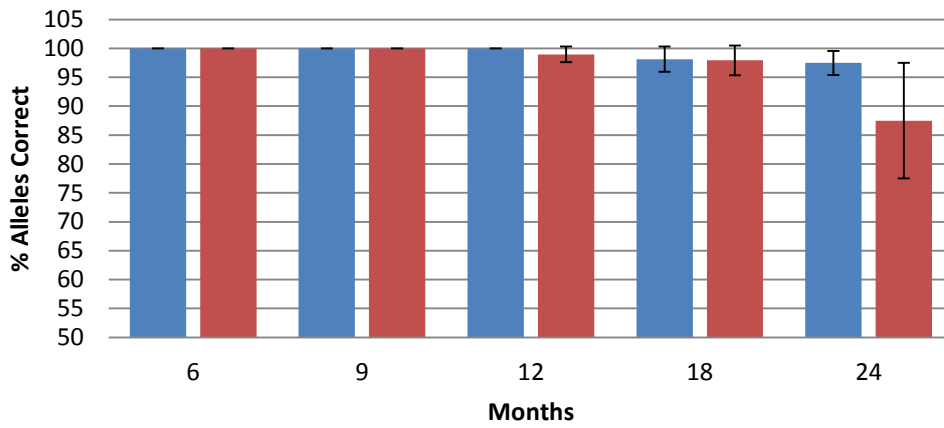
No statistical correlation between time of exposure and STR success was observed. However, a general trend of decreased allele recovery might be expected if this research was performed over longer time periods and/or samples were subjected to more aggressive environmental insults.

Previous studies [357, 358] have investigated whether the quantity and/or quality of DNA is correlated with the visual condition of a bone. Results of one study [357] concluded that neither skeletal nor individual bone appearance is a reliable indicator of mtDNA typing success. Although Misner *et al.* (2009) examined different bone types and used mtDNA as an indicator, the conclusions seem to hold true for the bony elements genotyped using nuclear DNA STR typing in this thesis. All bone samples subjected to various degrees of heat yielded complete profiles, and the STR success of samples subjected to burial and water conditions were good despite the variety of states of decomposition of the samples. Although environmental factors such as moisture, pH, micro-organisms and time are considered to have an effect on bone decomposition (and the DNA within) [358], the type of bone assayed is considered by some to be the most important factor in genotyping success [52, 357].

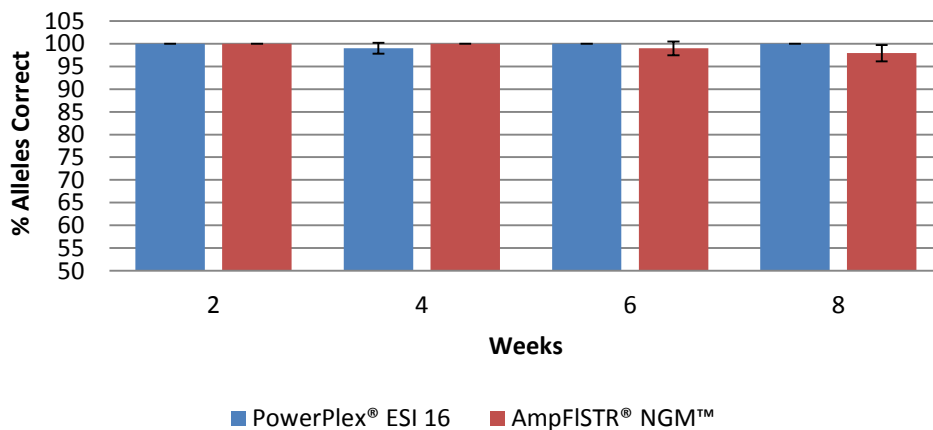
A. Surface



B. Buried



C. Freshwater



■ PowerPlex® ESI 16 ■ AmpFISTR® NGM™

Figure 3.49. Comparative STR profiling success of the AmpFISTR® NGM™ and PowerPlex® ESI 16 amplification kits with degraded samples.

Degraded samples were exposed to A) surface, B) burial, or C) freshwater. Data presented as mean ± SEM.

The most degraded set of environmental samples (surface exposed, n=7 in triplicate) were used to investigate the relationship between allele dropout and amplicon length between the two kits. Locus length was expressed as the median length of alleles amplified at each locus and graphed from smallest to longest (Table 3.6). Allele dropout was calculated as the number of times an allele had dropped out at each locus in the total number of alleles expected at that locus across all 21 amplifications per kit (expressed as a percentage).

Table 3.6 Median length of amplicons at each locus in both AmpFISTR® NGM™ and PowerPlex® ESI 16 amplification kits.

NGM		ESI	
Locus	Median length (bp)	Locus	Median length (bp)
D2S441	100	Amelogenin	90
D22	102	TH01	91
Amelogenin	103	D8	102
D10	104	D16	112
D8	145	D3	128
D19	148	vWA	152
D3	156	D18	165
vWA	175	FGA	186
TH01	195	D19	192
D1	200	D21	229
D21	210	D1	244
D12	254	D2S1338	260
FGA	256	D10	304
D16	260	D12	313
D18	296	D22	326
D2S1338	310	D2S441	364

N.B. Only highlighted loci showed allele dropout.

Allele dropout in the NGM kit was observed in loci once the median amplicon length was ≥ 175 bp, and ≥ 229 bp in the ESI kit (Table 3.6). The rate of allele dropout increased more steeply with the NGM kit compared to the ESI kit after approximately 200bp (Fig. 3.50). The allele dropout rates were also much higher overall with the NGM kit compared to the ESI kit. An interesting observation was that even though the ESI kit has a more large loci (>300bp) than the NGM kit, these loci demonstrated lower dropout rates than smaller loci in the NGM kit. These data suggest that successful STR

kit performance is not only determined by locus length, but also the robustness of kit chemistry and possibly primer design.

Linear regression was performed to investigate the statistical relationship between the median locus size and the allele dropout rates of both kits (Fig. 3.50). Loci with no allele dropout were not included in the analysis. The D2S1338 locus in the NGM amplification showed a very low rate of dropout and was removed from the regression analysis as an outlier (Fig. 3.50). Amplification of the same samples with the two kits resulted in different linear correlation coefficients. The higher R^2 value (0.9) with the AmpFISTR® NGM™ amplifications show that the allele dropout was more strongly correlated with the allele length. The AmpFISTR® NGM™ kit was therefore more susceptible than the PowerPlex® ESI 16 kit to allele dropout as the length of the targets increased.

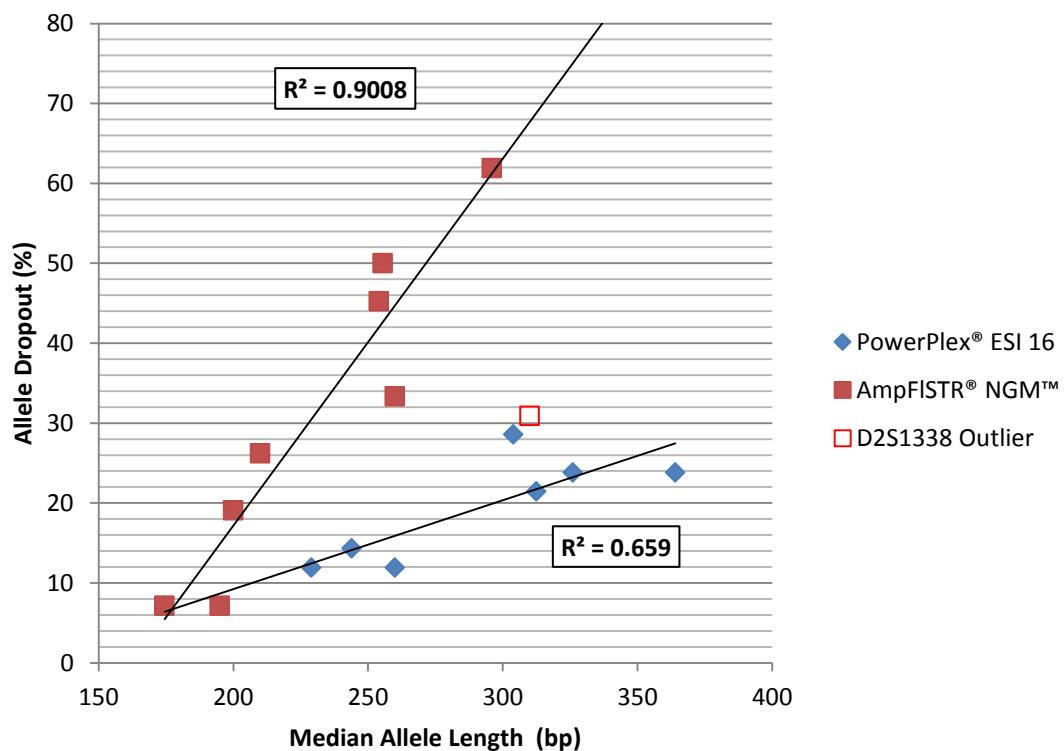


Figure 3.50 Comparative linear correlation analysis of allele dropout rate and mean locus length of both Powerplex® ESI 16 and AmpFLSTR® NGM™ kits.

3.3.5 Comparative Genotyping of Two Dentine Extraction Methods from Teeth

The optimal method for extracting high quality dentine powder from teeth (n=7) for DNA purification was investigated. A novel method of extracting powder was explored as an alternative to the currently employed method of cutting the root from the crown and grinding the entire root into a powder in a freezer mill or blender cup. Endodontic files were used to scrape the inside of each root canal to retrieve powdered dentine (targeting protected DNA nucleated cells) for DNA extraction. X-rays of each tooth before and after the process demonstrate the widening of each root canal (Fig. 3.51).



Figure 3.51 X-rays of teeth before and after filing of root canals for dentin powder.

The apical root tips were removed for access to the root canals. Roots canals were significantly wider and shorter after filing for dentine powder.

A wide variation in the quality and quantity of DNA extracted from teeth of different individuals recovered from the same environmental conditions has been reported [359]. Several factors may be responsible for the variation observed in the quantity and quality of dentin powder and resultant DNA in this study:

- a. Sample to sample variation. The amount of accessible (and viable) dentine between molars from the same individual may differ significantly.
- b. Dental anatomy. Roots which were excessively curved and narrow, or had irregular deposits of dentine made access to higher portions of the root canal and pulp cavity (and therefore the superior sites for pristine DNA-rich tissue) more difficult.
- c. The technical process of dentine removal itself. Dentine powder was manually scraped from inside the tooth roots. The amount of dentine powder physically recovered from each tooth during this filing process will vary (0.05 – 0.14mg in this study).
- d. Environmental exposure. The teeth tested were exposed to different environmental conditions which may differentially affect the DNA quality inside each tooth.

As expected, more tooth powder was obtained using the total root method compared to the filing method (Table 3.8). However, when the amount of amplifiable DNA from both methods was quantified, the trend was opposite (Table 8). Four of the seven samples yielded an increase in the total yield of amplifiable DNA using the filing method compared to the total root method (average 6-fold (+/-3-fold) increase). Two samples (1 and 6) yielded less amplifiable DNA using the filing method than the total root method and one sample (5) produced comparable amounts. Biological variation between the teeth and/or the small sample size may also contribute to the difference in DNA yield. The amount of total DNA was not quantified in this study, as it was deemed more informative to determine how much amplifiable DNA was obtained from each method for downstream STR-typing.

Table 3.7 Tooth samples and environmental insult applied to each.

Sample ID	Environmental Exposure
1	Buried for 12 months
2	Buried for 24 months
3	Surface Exposure for 12 months
4	Surface Exposure for 24 months
5	Saltwater for 6 months
6	Freshwater for 2 months
7	Extreme Fire Exposure

Table 3.8 Comparative yield of dentine powder, total amplifiable DNA and the amount of DNA retrieved per milligram of powder via the two methods tested.

Sample	Amount of dentine powder (mg)		Total Amplifiable DNA (ng)	
	Filing Method	Total Root Method	Filing Method	Total Root Method
1	0.10	0.28	17.93	34.94
2	0.09	0.32	2.61	0.26
3	0.07	0.30	0.42	0.13
4	0.14	0.25	5.49	0.89
5	0.06	0.28	0.10	0.09
6	0.05	0.35	0.48	0.64
7	0.05	0.50	0.18	0.00

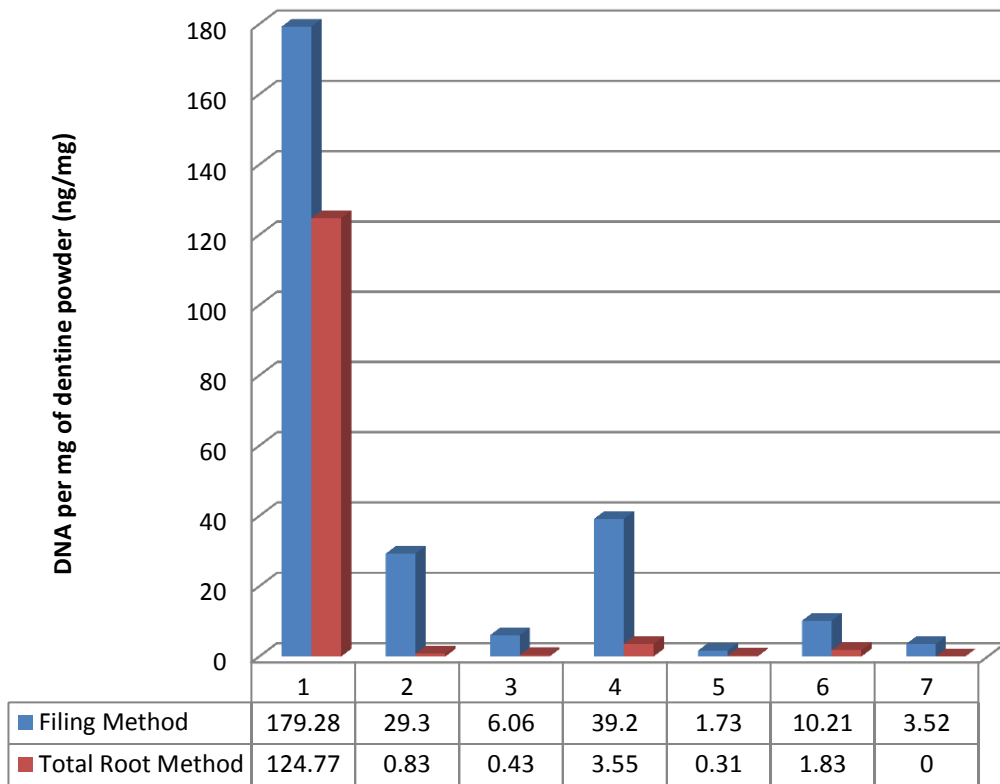


Figure 3.52 Comparative yield of amplifiable DNA per mg of dentine powder.

The efficiency of DNA extraction using two different methods was compared. The listed values indicate the yield of amplifiable DNA (ng) per milligram of dentine powder from each set of environmentally challenged teeth via the two methods.

An interesting comparison is the DNA yield per milligram of dentine powder extracted. This is an indication of efficiency in the recovery of amplifiable DNA with the two different powdering methods. All samples yielded more amplifiable DNA per milligram of powder using the filing method (Figure 3.52). However the increase in DNA yield was variable over the seven samples (ranging from 1.5 to 35.5-fold). These results support that the filing method targets the DNA-rich region of the root canal and therefore results in a higher proportion of nucleated cells per milligram of powder. Despite the fact that grinding the entire tooth generates more powder, and in general more DNA, the filing method is more efficient at retrieving amplifiable DNA. The sub-optimal powder generated by crushing the entire root may contain PCR inhibitors which reduce the efficiency of the PCR reaction during quantification. However, no significant delay in cycle threshold (Ct) of the internal PCR control was observed with

the 'all root' samples versus the 'filing method' samples. A decrease in DNA quantity and quality may also result from the harsh physical nature of the crushing process. The entire root is pulverised by mechanical force into a powder. Although performed under liquid nitrogen, the heat generated and the high crushing forces may damage the DNA within the tooth. These data suggest that it is counterproductive to grind the entire tooth root for DNA analysis.

Sample 1 yielded substantially more DNA than all other teeth in this study regardless of the method used to extract the dentine (Table 3.8). These data suggest two possibilities; the first being biological variation, meaning that this individual had a higher amount of DNA-rich tissue in her teeth than the other individuals investigated, or the second being environmental. This tooth was buried for a period of 12 months and therefore may have been protected from the harsh environmental effects such as sunlight, humidity and microbial action which may degrade the DNA. However, teeth are thought to be resistant to these adverse conditions [65, 66, 360]. Due to the small numbers in this study no explanation for the DNA yields could be drawn.

Results of the degradation assay showed that all tooth samples yielded low amounts of DNA (5–437pg/ μ L). As a result of the low concentrations of amplifiable DNA, the degradation ratios generated by the qPCR assay are not accurate, and is not a reliable measure of sample quality.

The quality of DNA recovered from teeth using both methods was assessed via STR analysis. The average number of correct alleles detected (Fig. 3.53A), and the average peak height ratio (PHR) of each sample profile (Fig. 3.53B) were the two key indicators measured. The filing method yielded more consistent and overall better results than those seen with the all root method. Much wider variation in both allele recovery and PHR was observed with the all root samples.

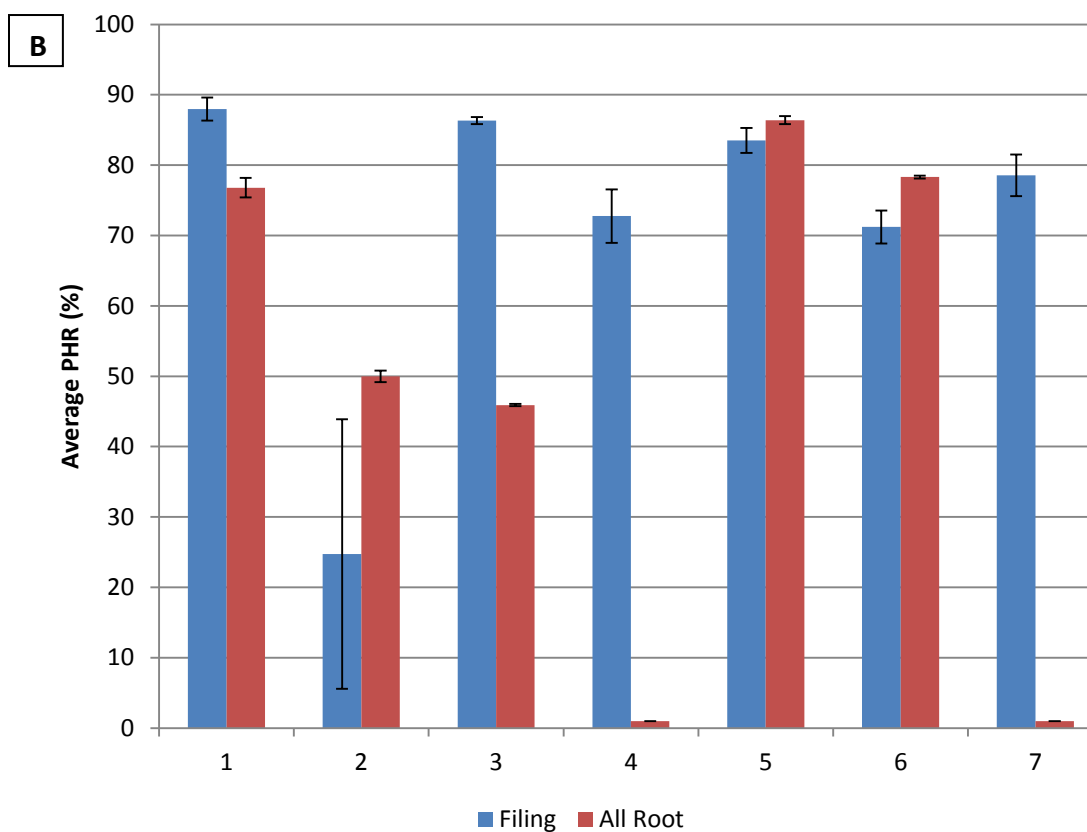
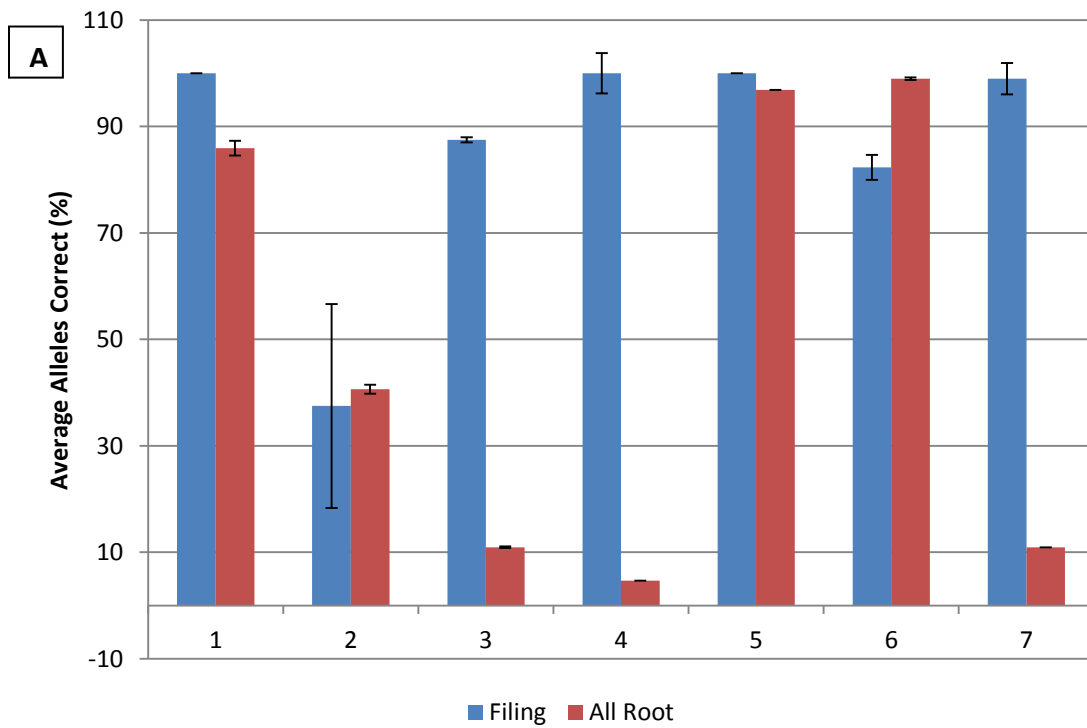


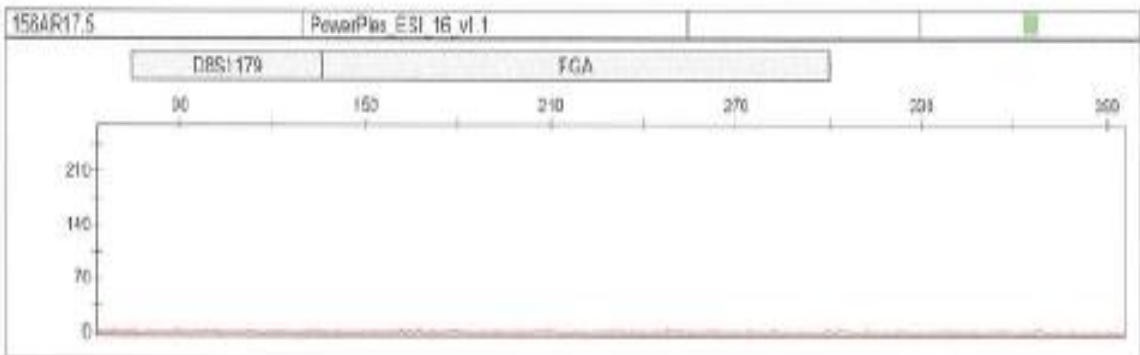
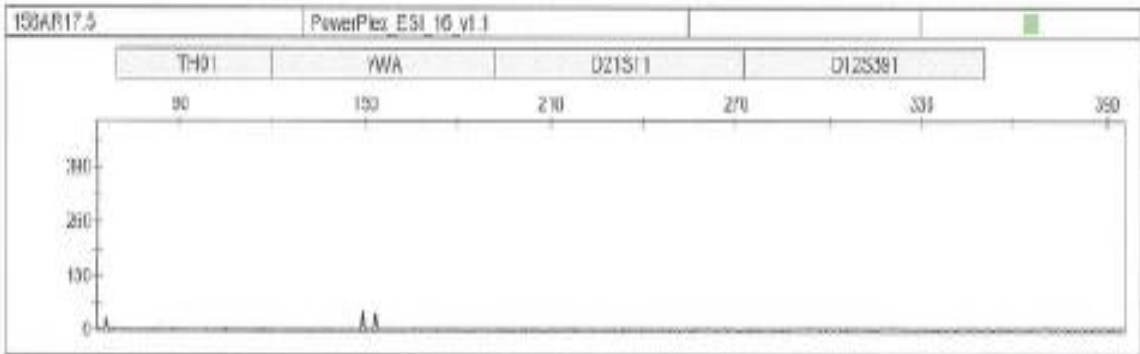
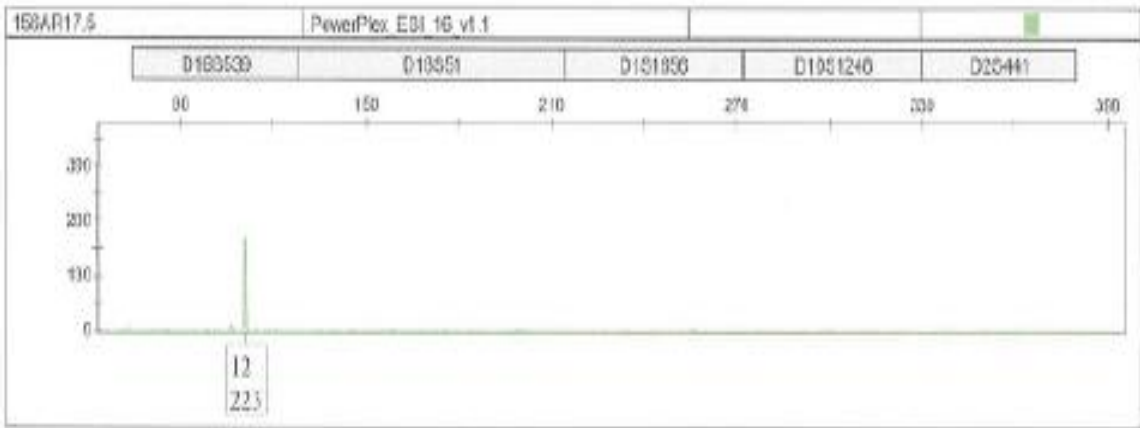
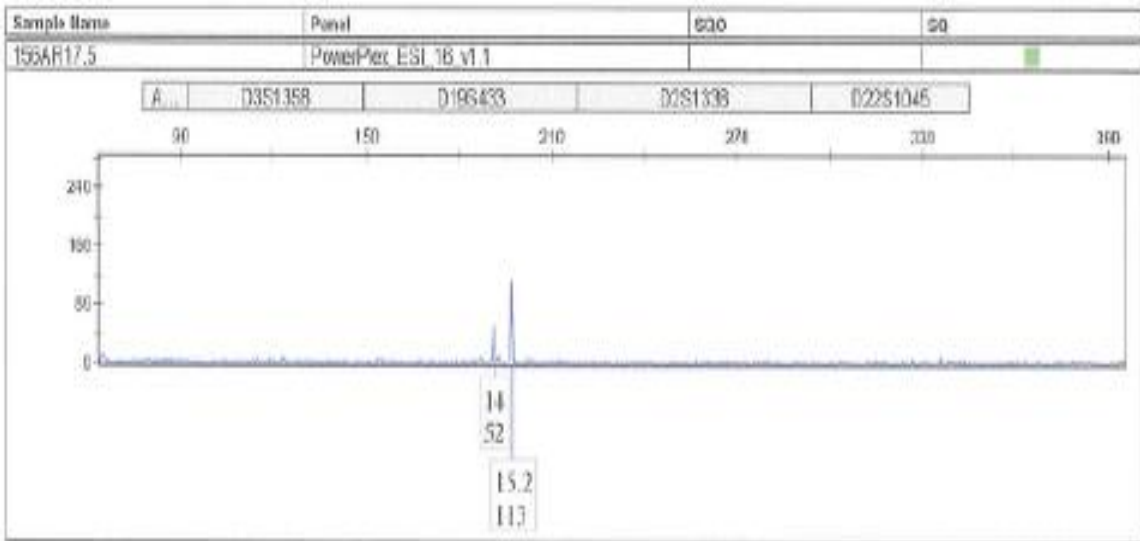
Figure 3.53 The success of STR profiles from DNA recovered via two methods from teeth

Comparative DNA quality from teeth via the two methods tested as measured by A) average number of alleles recovered and B) average peak height ratio (PHR) of each STR profile. Data presented as mean \pm SEM.

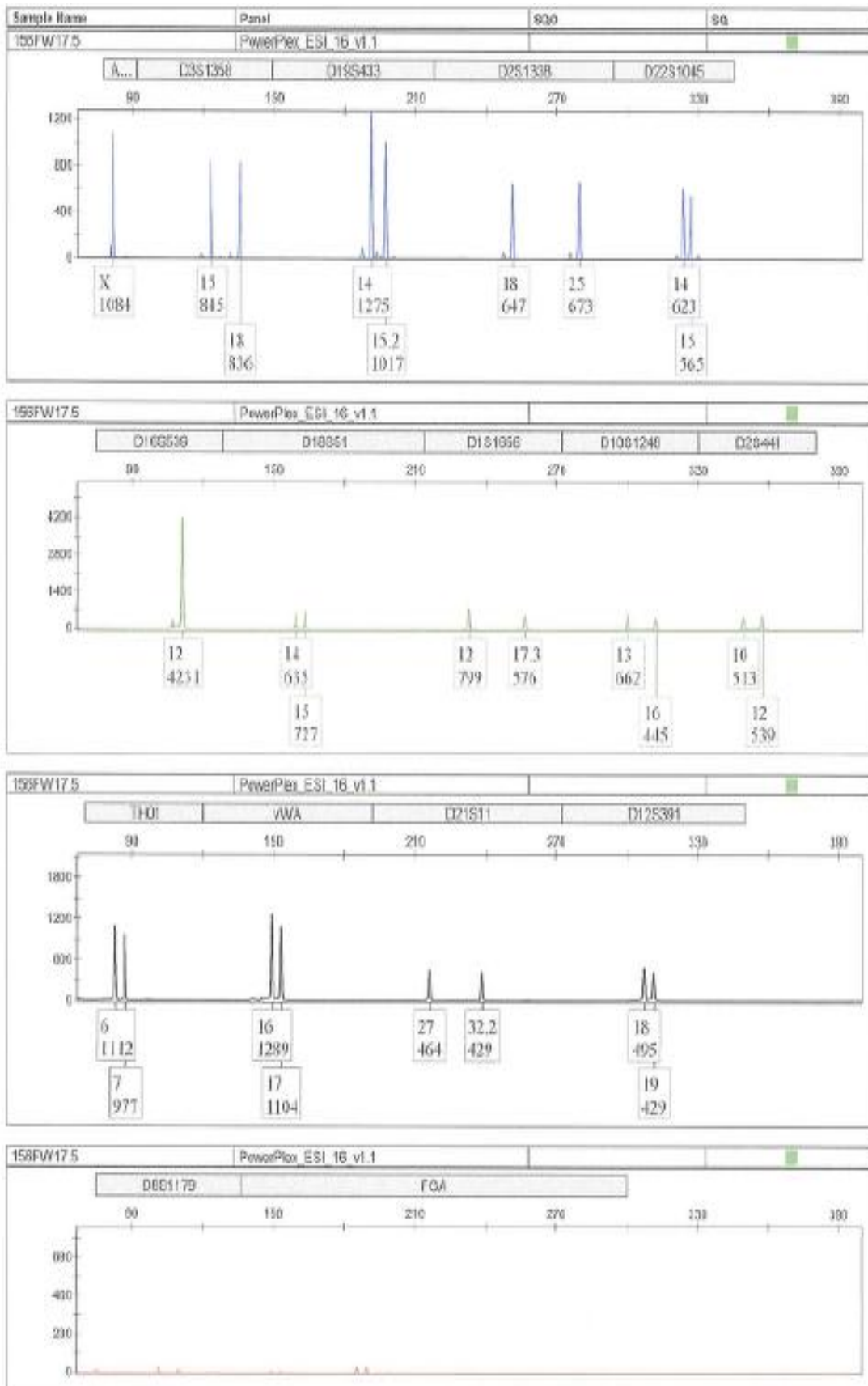
In five of the seven teeth (1, 3, 4, 5 and 7) the filing method generated significantly more complete STR profiles than the all root method. In three of those five samples (samples 3, 4 and 7) a complete (or near complete) profile was obtained with the filing method when $\leq 10\%$ of alleles were recovered by grinding the entire root (Fig. 3.54). The STR profiles from the same three teeth displayed considerable allelic imbalance using the all root method (0-40% average PHR).

The 'all root' samples showed wide variation in the average PHR. Three of the seven 'all root' samples showed average PHR $>70\%$ ($\pm 5.2\%$) and two with 40-50% ($\pm 2.9\%$). A profile PHR of 0% was calculated for one of the remaining two samples when only one allele was detected at heterozygote loci. An average PHR could not be calculated for the remaining sample as not a single allele was detected. The filing method generally produced more balanced profiles than the all root method. Six out of the seven 'filed' samples produced profiles with an average PHR $>70\%$ ($\pm 7\%$). One filed tooth (sample 2) had an average PHR of 25% (SEM=19%). The wide standard error of the mean seen in both the PHR and number of alleles recovered from the 'filed' sample of tooth 2 (Fig. 3.53) is due to different profiling results from the duplicate STR reactions. Due to the total consumption of the DNA extract from this tooth sample, the STR reaction could not be repeated.

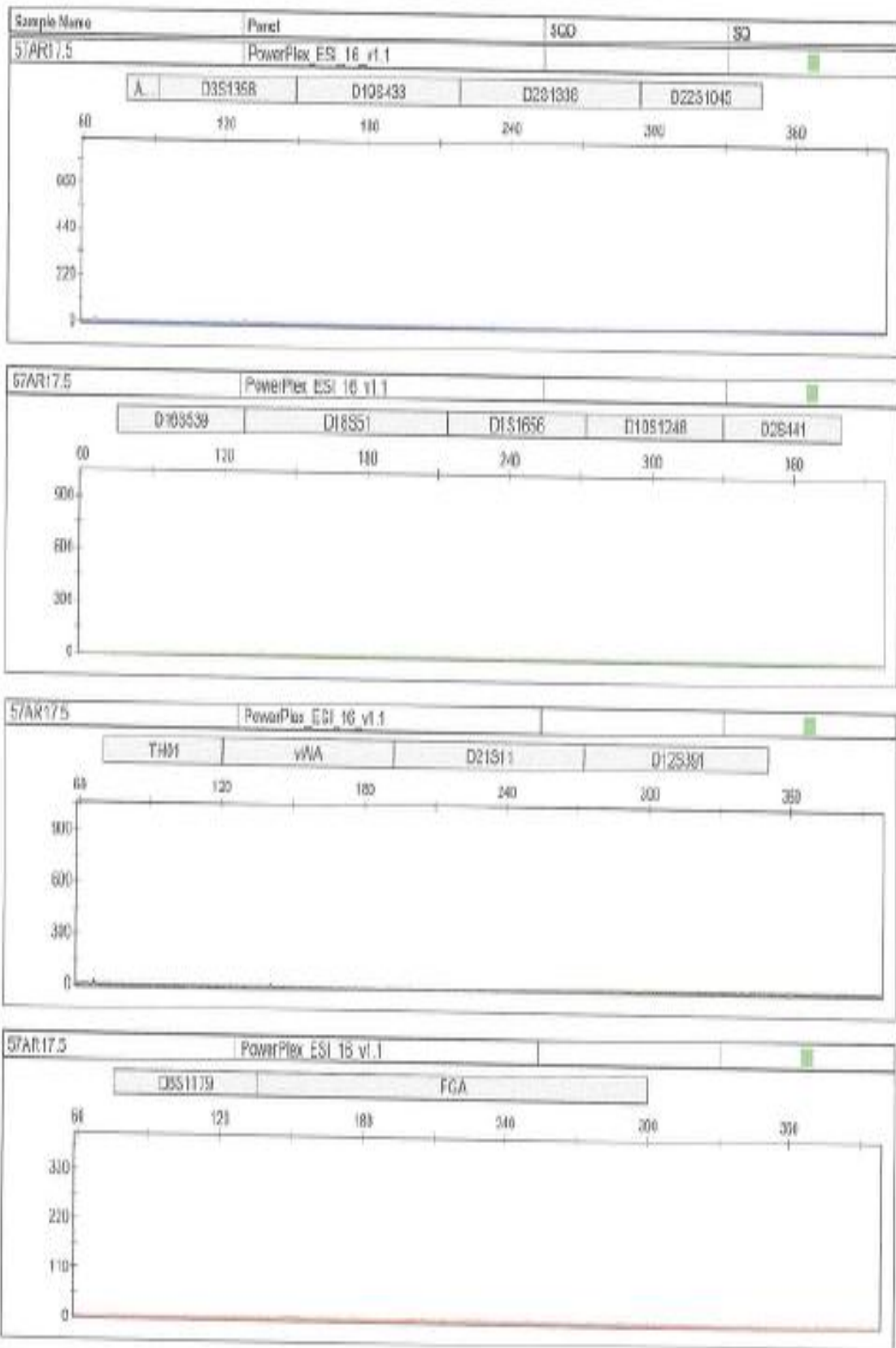
Sample 3 – All root method



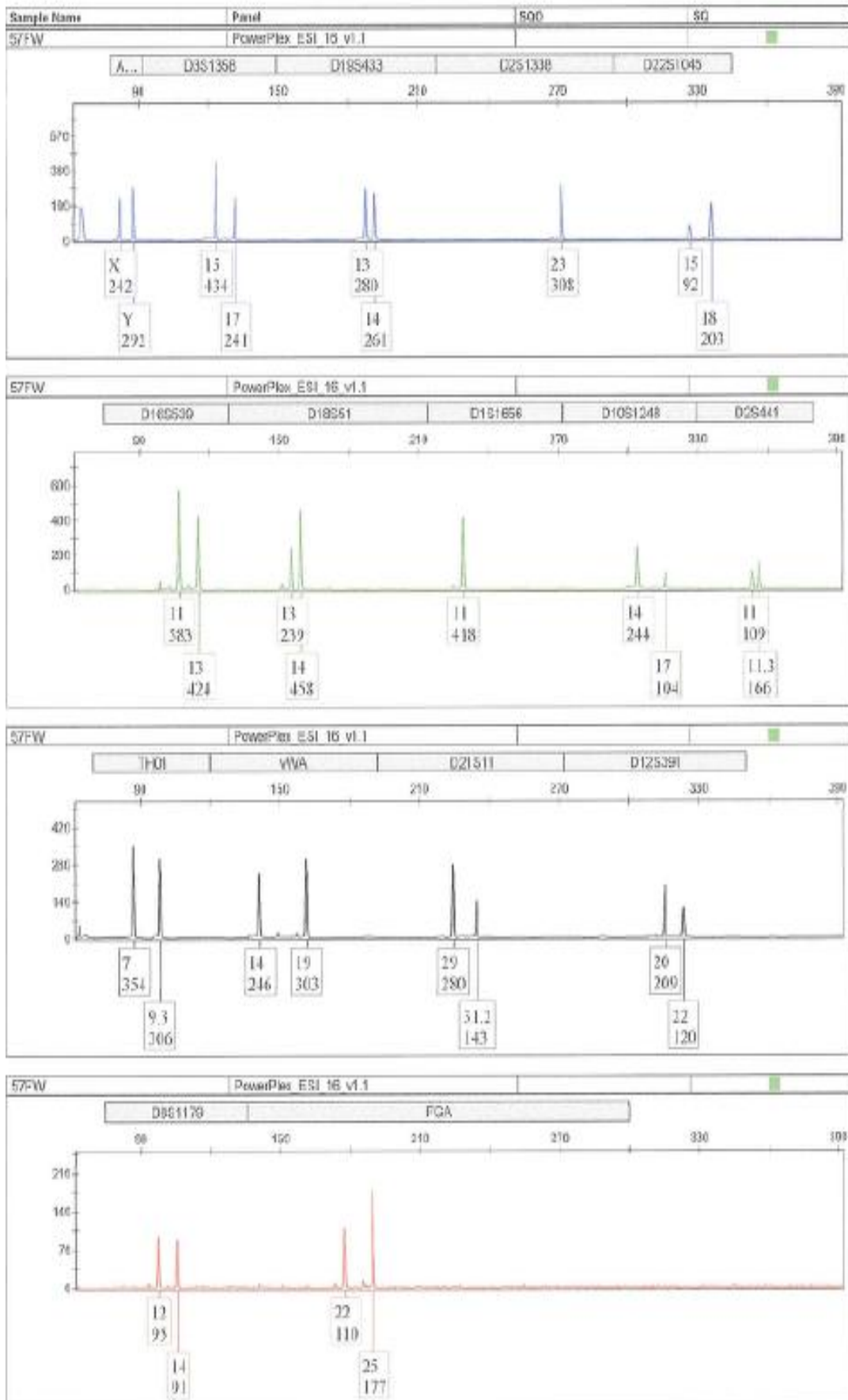
Sample 3 – Filing method



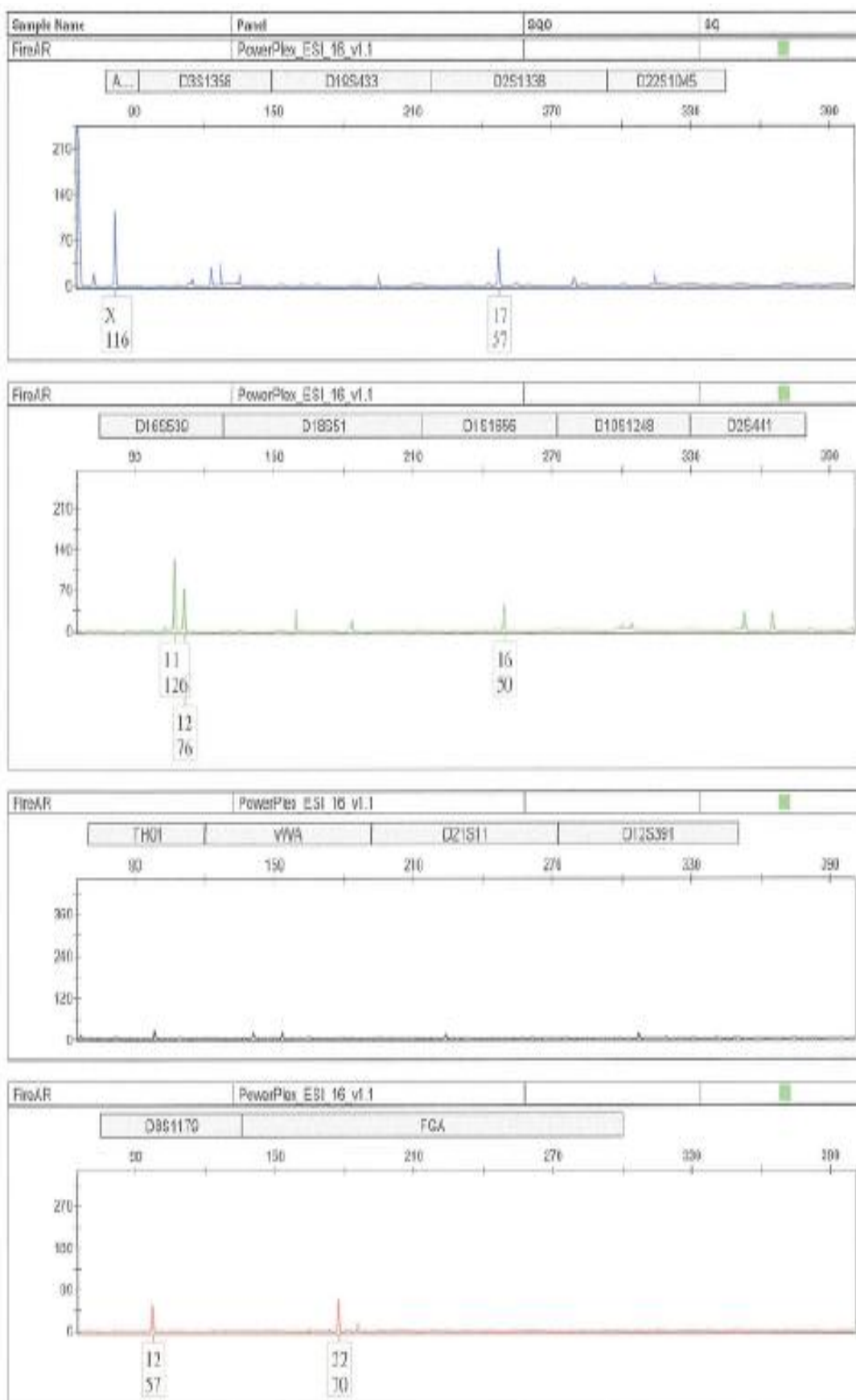
Sample 4 – All root method



Sample 4 – Filing method



Sample 7 – All root method



Sample 7 – Filing method

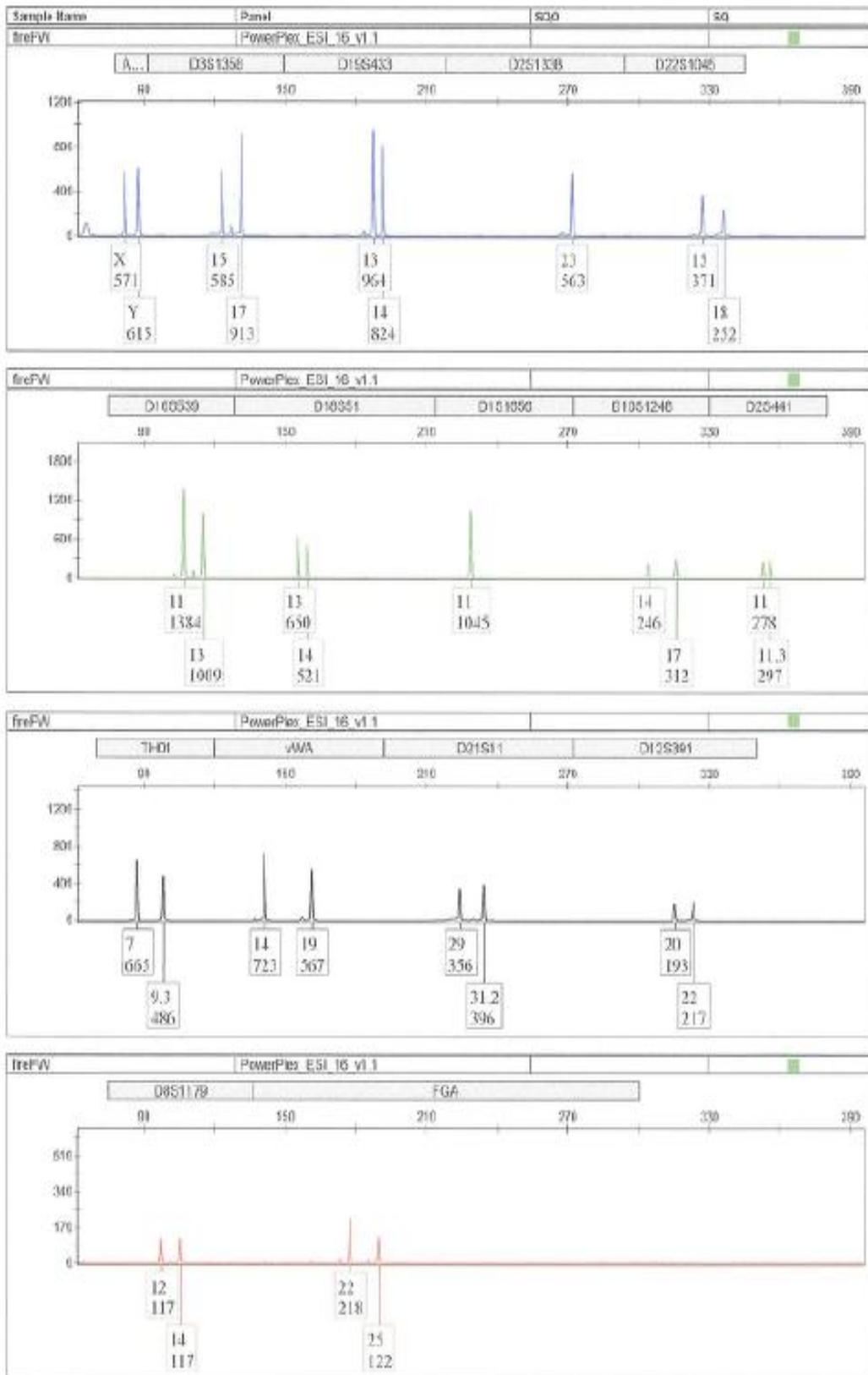


Figure 3.54 STR Profiles of Tooth samples 3, 4 and 7 using the 'all root' and 'filing' methods of dentine extraction.

The occurrence of drop-in alleles was monitored to assess the risk of contamination of both methods. More contamination was observed with the 'all root' samples. In a total of 14 profiles (448 alleles) for each method (in duplicate), ten (2.2%) drop-in alleles were seen in 'all root' profiles as opposed to three (0.6%) in the 'filing' profiles. This result was surprising due to the substantially more direct handling of each tooth during the filing process. The most likely explanation is that the decontamination washing process of the whole teeth prior to grinding was not adequate to remove all exogenous DNA. Of the three drop-in alleles seen in the 'filing' method, two were consistent with handler profiles.

Results of this study suggest that the filing method is superior to grinding the entire root for extracting dentine powder from teeth. DNA of greater quality and quantity was recovered which in turn led to improved STR profiles. These results support a previous study which showed poorer STR profiles from crushing the entire tooth or root compared with another form of endodontic access to the root canal (via the crown) for removing pulp and dentine [73]. A recent study [68] has shown a four to five times higher yield of mtDNA from tooth cementum compared to dentine in ancient human molars. This finding is surprising since currently cementum has been largely ignored as a source of DNA. In fact, common protocols (not used in this study) call for sanding of the external surface of the roots (cementum) prior to processing. The largest concentration of cementum is located at the root tip [68]. This is an important consideration, as the very tip of the root was removed during the filing method to allow for easier access to the root canal with the endodontic files. It is therefore possible that a significant source of good quality DNA may have been lost in this study. These practises of sanding and external root surface and root tip removal should be re-examined for future research into improved DNA extraction methods from teeth.

Less contamination was also seen with the filing method. However, this may not hold true if the decontamination process of whole teeth is improved and optimised to ensure all inhibitors and exogenous DNA is removed prior to processing. The manual process of removing dentine with endodontic files was laborious and more time consuming than grinding the entire root (2-3 hours vs 40 minutes). The significantly

longer time required for extracting dentin powder from teeth may not be a major concern for casework or research when the demand for DNA extractions from teeth is infrequent. However, when large numbers of tooth samples are required for processing and genotyping (such as in a mass disaster situation), the extra time required per sample would not make this method attractive. The combined benefits of retaining tooth morphology and the more complete and evenly balanced STR profiles outweighs the disadvantages of the additional time and skill required to perform the filing process. Based on these results the filing method was used to extract dentine from the 200 year old Pandora teeth.

3.3.6 Case Study – HMS Pandora Remains

Bone and tooth samples submerged in the Pacific Ocean for over 200 years presented a 'real-life' set of highly degraded samples to genotype. Three sets of skeletal samples (named 'Tom', 'Dick' and 'Harry' by the researchers who recovered the remains) were available for analysis. The samples from 'Tom' consisted of three small bone cores from the ilium, and one molar (tooth no.37/38) (Fig. 3.55C). The sample available from 'Dick' was one section of the humerus and one molar (tooth no.47) (Fig. 3.55B). Two sections of the tibia and one molar (tooth no.47) were retrieved from 'Harry' (Fig. 3.55C).

All three teeth had been extracted from the mandible by a previous researcher and appeared to be in good condition and absent of caries. The tooth from 'Tom' was cleanly extracted, although a visible darkening of the roots was noted (Fig. 3.55A). The molar from 'Dick' was intact with a small amount of osseous tissue still adhered between the roots which dislodged during processing. The tooth from 'Harry' was excised from the mandible in situ, together with the surrounding bony tissue. The molar was firmly anchored within the alveolar socket with the roots appearing to be completely calcified. The apex of both roots were cut during the original removal process with the openings of each root canal cemented closed.

Powdered dentine was retrieved from each 'Tom', 'Dick' and 'Harry' tooth (0.105g, 0.125g and 0.14g respectively) using the filing method described in Section 3.2.9.3. The inner lining of the root canals were scraped with endodontic files to produce a fine powder. This process resulted in the widening of each root canal (Fig. 3.56). Most importantly the crown and other morphological and radiological features useful for identification and individualisation were preserved.

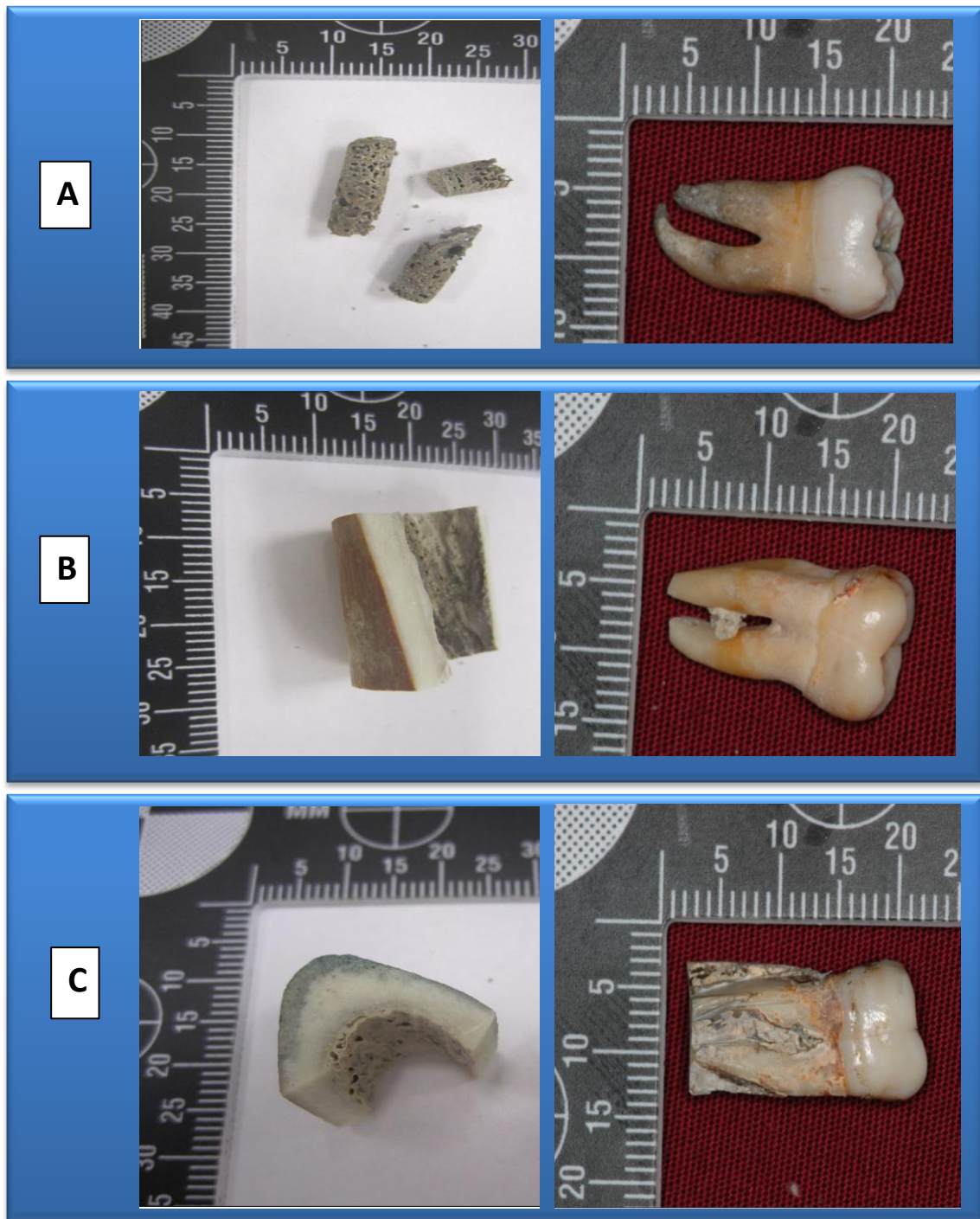


Figure 3.55 Pandora bone and tooth samples.

Samples are referred to as A) 'Tom'; three bone cores from the ilium, B) 'Dick'; section of the humerus, and C) 'Harry'; section of tibia. One molar from each skull was provided for analysis.

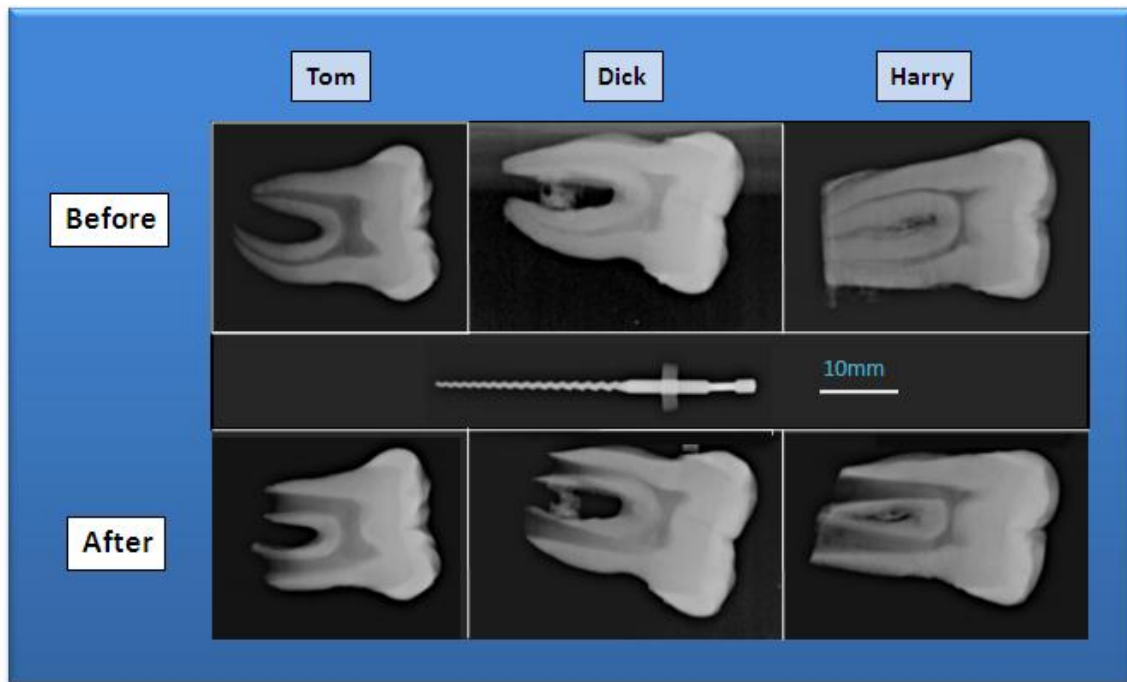


Figure 3.56 Dental X-rays of Pandora teeth.

X-ray images of tooth samples from 'Tom', 'Dick' and 'Harry' before and after removal of dentine powder using the filing method. Note the widening of the root canals.

Quantification

The amount of amplifiable genomic DNA (as measured by the qPCR degradation assay described in Chapter 2) from all samples was low (Table 3.9). On average a more than three-fold increase in DNA was seen from the three tooth samples compared to the bone samples (Table 3.9). Both the bone and tooth samples from 'Tom's' remains yielded the least DNA (1 and 2pg/ μ L respectively). The extremely low yield from the bone sample is primarily due to the suboptimal source material. Three small spongy bone cores from the ilium were available for extraction from 'Tom' compared to the compact bone samples from the humerus and tibia for 'Dick' and 'Harry'. It is well documented that higher DNA yields are routinely obtained from compact bone versus spongy bone [47, 52, 358, 361]. This variation in DNA yield is most likely due to histological differences between spongy and compact bone. The osteocytes of compact bone are housed within many concentric layers of calcified matrix (hydroxyapatite and collagen) conferring relative protection from external insults

compared to osteocytes found within the thin trabeculae of spongy bone devoid of the protective layers of bone matrix [357].

However, this does not explain the much lower yield from Tom's tooth. Approximately the same amount of powder (~0.1g) was extracted from each of the three teeth, but the DNA yield was significantly lower than that of the other two teeth. Differences in DNA yield may be a result of variation in the final volume after the spin column concentration treatments (up to 2-fold difference). However, a more likely explanation may be significant tissue damage. A darkening of the roots in Tom's tooth was noted prior to powdering. Although the cause of this discoloration is unknown, it may indicate ante-mortem death of the tooth roots which would leave fewer (and possibly more degraded) resident odontoblasts, and therefore a poorer source of viable DNA.

Table 3.9 Yield of amplifiable DNA from the Pandora bone and tooth samples.

Source	Bone (pg/ μ L)	Tooth (pg/ μ L)
Tom	1	2
Dick	15	42
Harry	28	108

Because very low amounts of DNA were present, the assessment of DNA degradation for each sample via the real-time PCR degradation assay was not reliable. No evidence of PCR inhibition was indicated by the internal PCR control (IPC) included in the degradation assay for any of the skeletal samples.

STR Genotyping

Despite the low DNA concentration of all samples, STR-typing of the 200 year old remains resulted in STR profiles. Profiles from the Pandora remains displayed the typical features of degraded samples such as the decrease in fluorescence of longer amplicons (or “ski-slope” effect), allelic imbalance, and increased allele and locus dropout (Fig. 3.55). The alleles which were lost most frequently were the larger (>250bp) loci in each kit.

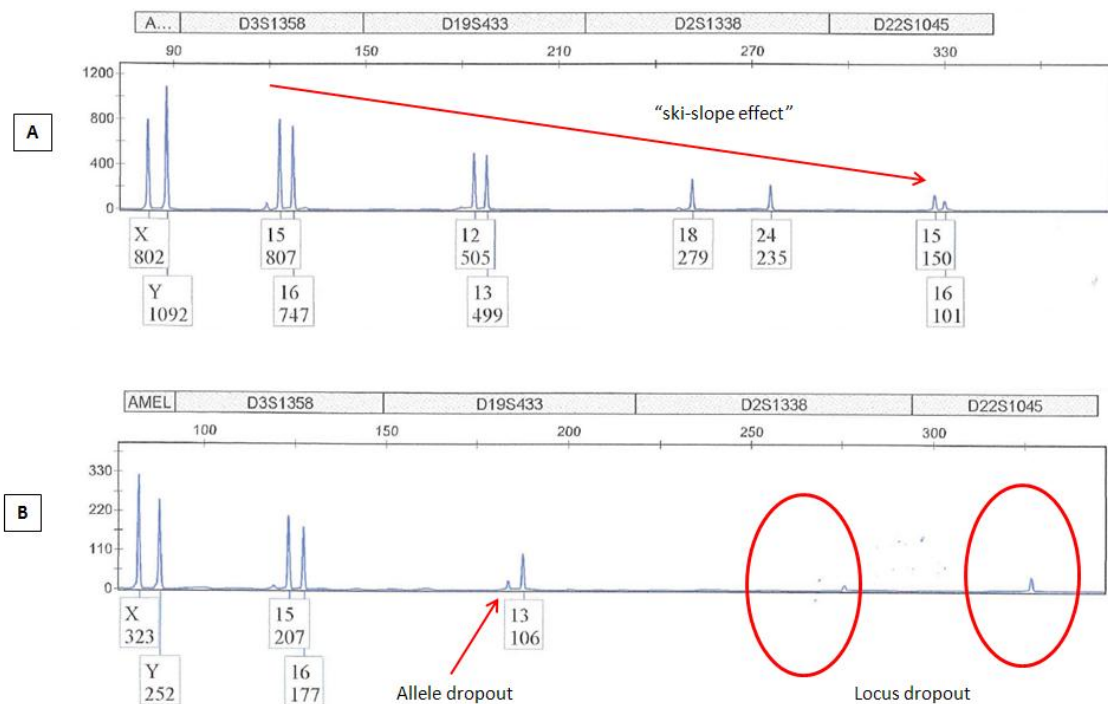


Figure 3.57 Classic STR profile features of highly degraded samples were routinely seen in the Pandora skeletal samples.

STR profiles generated with the PowerPlex® ESI 16 amplification kit from A) ‘Dick’s’ tooth and B) ‘Dick’s’ bone samples.

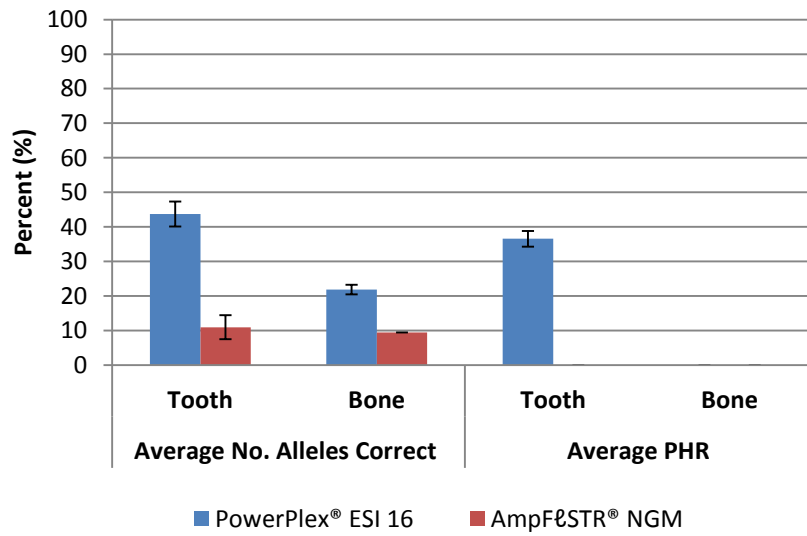
The tooth samples yielded more complete STR profiles than the bone samples. Complete consensus profiles were obtained from the teeth assigned to ‘Dick’ and ‘Harry’ using both STR kits tested (Table 3.11 and Appendices 4C & F). However the tooth from ‘Tom’ yielded an average of only 10.9% total alleles with the AmpFISTR® NGM kit and 43.7% with the PowerPlex® ESI 16 amplification kit. The partial profiles obtained from ‘Tom’s’ tooth are likely explained by the much lower yield of DNA from

that particular tooth compared to 'Dick' and 'Harry' (2pg/ μ L versus 42 pg/ μ L and 108 pg/ μ L respectively) (Table 3.9). In addition to fewer alleles, the STR profiles obtained from Tom's tooth displayed lower average peak height intensities (87 RFU vs 615 RFU and 1200 RFU) and heterozygote peak height ratios (PHR) than the other two teeth (approximately 30% versus, 70% and 80%). These data may also indicate a higher level of DNA degradation in this sample. The marked decrease (0% vs 37%) in the average PHR of Tom's tooth STR profiles generated with AmpFISTR[®] NGM kit compared to the PowerPlex[®] ESI 16 amplification kit (Fig. 3.58) is a result of the much higher level of allele dropout seen with the NGM kit. In fact, the AmpFISTR[®] NGM kit failed to detect both alleles at even one heterozygotic locus.

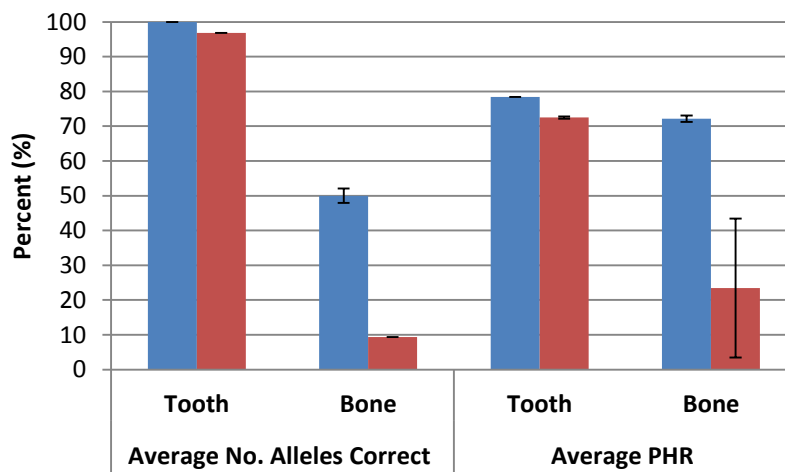
The STR profiling success of the Pandora bone samples was mixed (Appendices 4A-H). More complete and evenly balanced STR profiles were consistently obtained from samples profiled with the PowerPlex[®] ESI 16 amplification kit compared to those with the AmpFISTR[®] NGM kit (Fig. 3.58). The sub-optimal bone samples from 'Tom' resulted in extremely low DNA yield (Table 3.9) and poor STR results (Appendices 4G & H). More than twice the average number of alleles was obtained using the PowerPlex[®] ESI 16 amplification kit (21 vs 9%) (Fig 3.58A). The average PHR of Tom's bone STR profiles could not be calculated since all alleles at the heterozygous loci failed to amplify. More than twice the number of alleles were recovered from Harry (95% vs 44%), and five times more from Dick (50% vs 9%) with the PowerPlex[®] ESI 16 kit (Fig. 3.58). In addition to generating more complete STR results, the ESI profiles were also more balanced than those generated using the NGM kit. Substantial improvement in allele balance was observed in ESI profiles with Dick (72% vs 24% average PHR) and less marked with Harry's bone sample (65% vs 52%).

These results suggest that the PowerPlex[®] ESI 16 amplification kit chemistry is more sensitive to low amounts of template and more tolerant of DNA degradation and/or damage than the AmpFISTR[®] NGM kit. The extra PCR cycle in the PowerPlex[®] ESI 16 kit may contribute to these improved STR results.

A. Tom



B. Dick



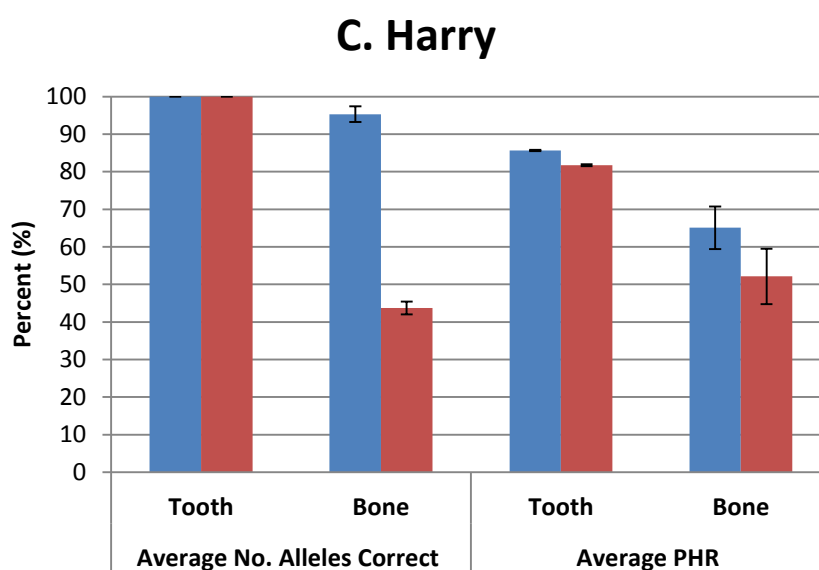


Figure 3.58 Average profiling success and Heterozygote peak height ratios of DNA extracts from Pandora samples.

Data is presented as the mean \pm SEM

3.3.7 STRBoost®

3.3.7.1 STRBoost® with Environmental Samples

The most degraded set of environmental samples (surface remains) were used to test if the commercial PCR enhancer STRBoost® (Biomatrix) could improve the quality of STR profiles. STRBoost® was used in combination with both AmpFISTR® NGM™ and PowerPlex® ESI 16 amplification kits.

Results were mixed and inconsistent. In fact, the data suggest no correlation between the number of alleles recovered (Fig 3.59A) from the highly degraded samples and the addition of STRBoost®. The addition of STRBoost® to both amplification kits sometimes yielded slightly more alleles with some samples, but resulted in less alleles with others. Little difference in STRBoost® performance was observed between the two kits.

The data do not support an improvement in STR profile quality as measured by the average heterozygote peak height ratio (Fig 3.59B). Changes in allelic balance across STR profiles due to STRBoost® also appear to be random in nature. No change in average profile PHR was seen in relation to either amplification kit.

To adequately assess if the addition of STRBoost® to commercial forensic amplification kits can improve STR profiles from highly degraded samples, larger sample numbers would be required.

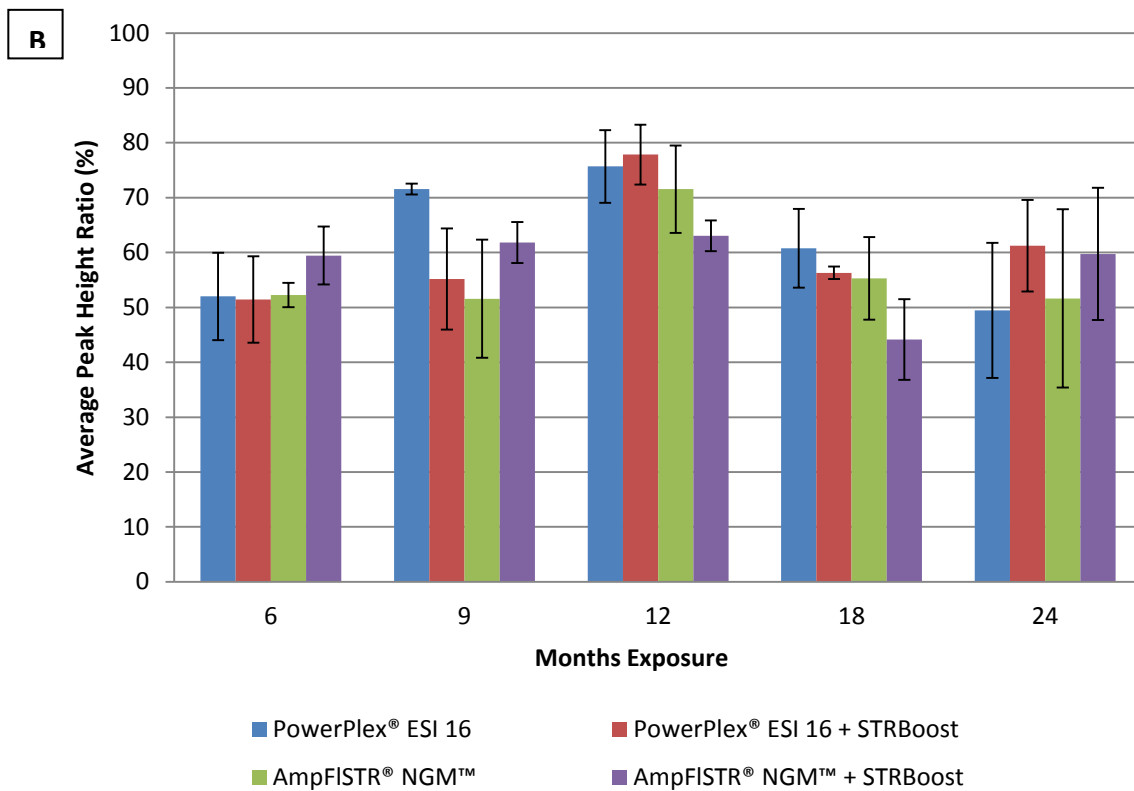
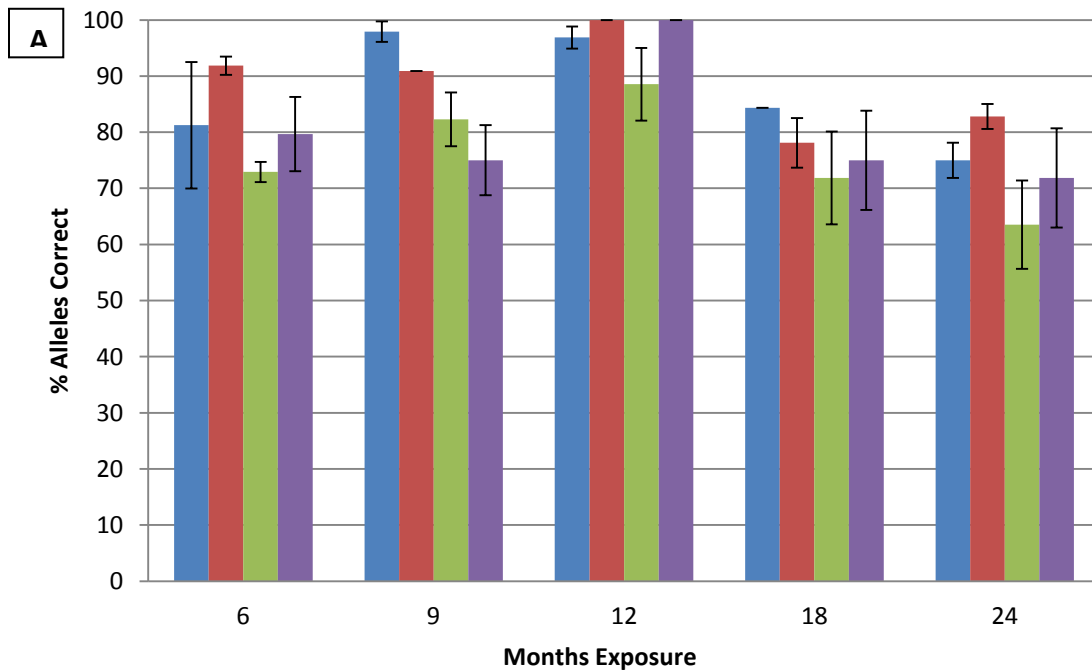


Figure 3.59 STR profiles from surface exposed bone samples with and without the addition of STRBoost.

Comparison of STR profiles from with and without the addition of STRBoost® using the AmpFISTR® NGM™ and PowerPlex® ESI 16 amplification kits. A) Average number of alleles correctly called and B) Average heterozygote peak height ratios. Data is presented at the mean ± SEM.

3.3.7.2 STRBoost® with Pandora Remains

STRBoost® (BioMatrica) was used to investigate if any additional alleles could be recovered from the Pandora samples yielding partial profiles (all three bone samples and Tom's tooth). Due to the limited volume of DNA extract available for genotyping, samples were only run in duplicate. A small increase in the average number of alleles was observed when samples were amplified with STRBoost® (Fig. 3.58). However this result was not consistent across replicates, with two samples showing no improvement in allele calls and one tooth sample yielding less alleles. Often alleles which amplified well during routine STR typing were lost completely with STRBoost®, but additional alleles were recovered at other loci.

No significant improvement or reduction in profile quality (as measured by average heterozygote peak height) was observed across the samples amplified with STRBoost®. Neither is any correlation seen between allele recovery and DNA quantity or profile quality. The data do not suggest that STRBoost® works more efficiently in combination with either the ESI or NGM kits to recover alleles.

As there were no reference samples for the Pandora remains, a consensus approach was used to assign alleles at each locus and generate a STR profile for each sample. This approach was considered appropriate since the profiles are known to be single source. An allele was assigned to a particular locus when observed at least twice across replicates. A significant difference in the completeness of profiles with all four methods (PowerPlex® ESI 16 and AmpFISTR® NGM kits with and without STRBoost®) was observed (Table 3.11).

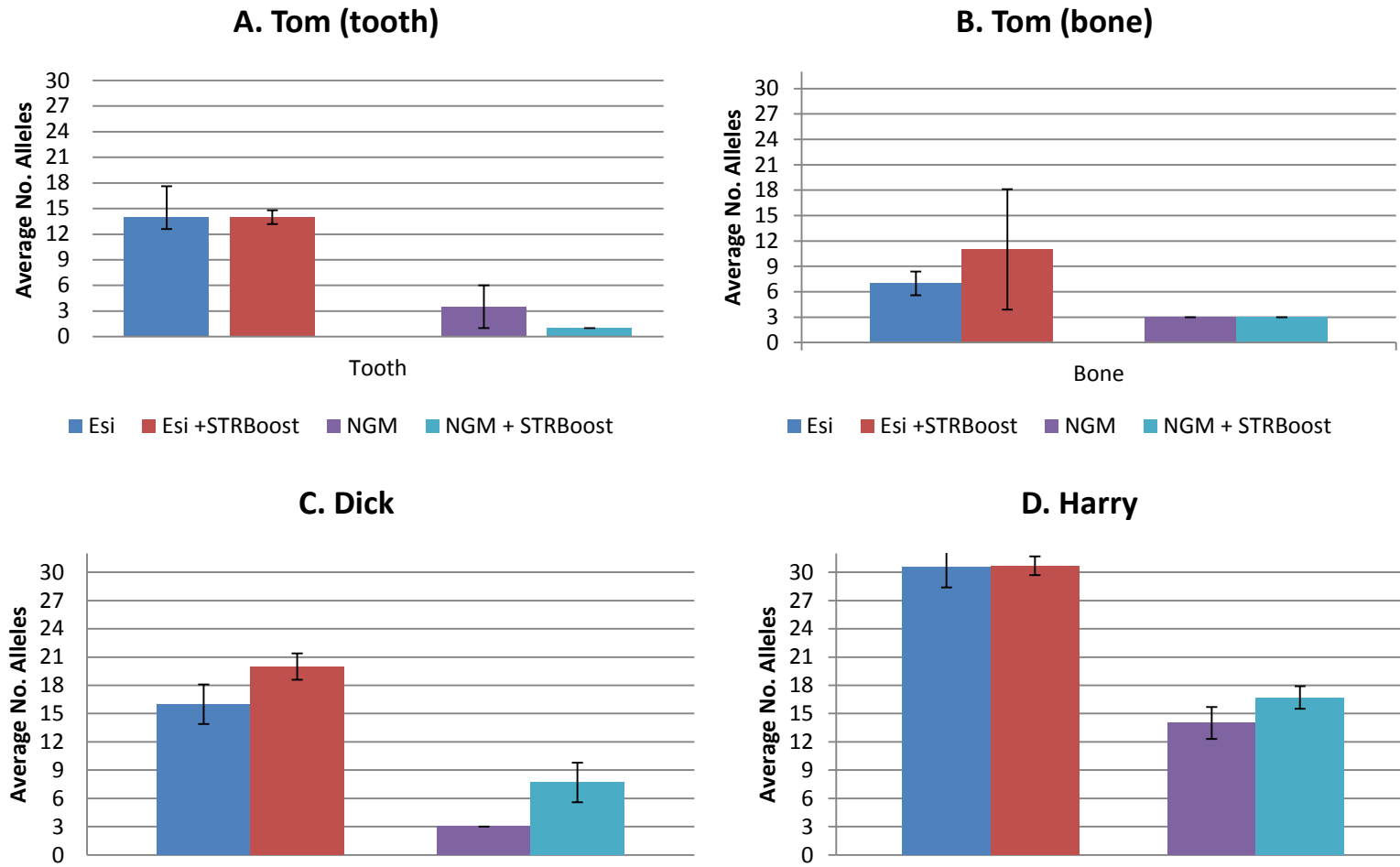


Figure 3.60 Pandora samples with and without STRBoost®.

The average number of alleles amplified from A.Tom’s tooth, and bone samples from B. Tom, C. Dick, and D. Harry using the PowerPlex® ESI 16 and AmpFISTR® NGM amplification kits with and without STRBoost®. Data is presented as mean ± SEM.

Overall, the PowerPlex® ESI 16 generated more complete profiles than the AmpFISTR® NGM kits. Complete consensus profiles were assigned to the teeth of Dick and Harry with both kits, whilst all three bone samples and ‘Tom’s tooth generated partial profiles. Three samples failed to amplify with the NGM kit without STRBoost® (Dick’s bone and Tom’s bone and tooth samples) (Table 3.11).

STRBoost® increased the number of alleles detected using the consensus method for all samples which yielded partial profiles without STRBoost®. The most valuable improvement was seen when amplification with the STR kit alone failed. In these three cases, STRBoost® added to the NGM kits resulted in nine additional alleles with ‘Dick’s bone sample, one with ‘Tom’s bone and four with ‘Tom’s tooth. Six additional alleles were able to be added to the consensus profile for ‘Dick’s bone sample using the ESI kit, and two additional alleles were seen in ‘Harry’s bone samples amplified with both kits (Table 3.10).

Table 3.10 The number of additional alleles which were detected and assigned to a consensus profile after amplification with STRBoost®.

Kit	Tom		Dick		Harry	
	Tooth	Bone	Tooth	Bone	Tooth	Bone
PowerPlex® ESI 16	2	2	N/A	6	N/A	2
AmpFISTR® NGM	4	1	N/A	9	N/A	2

N/A = PCR not performed as STR profiles were already complete

As expected, the most complete profile was obtained by pooling the STR results from all four methods from each sample and then employing the consensus approach across all 10-20 amplifications. A complete STR profile for ‘Dick’s bone and partial profiles for the other two bone fragments and ‘Tom’s tooth were obtained using this method.

Concordance between the STR profiles of the bone and tooth samples from each individual was expected. ‘Tom’ and ‘Dick’ samples were concordant across all loci. However the STR profiles from ‘Harry’s bone and tooth samples were not a ‘match’. ‘Harry’s bone sample was in fact concordant with ‘Dick’s STR profile (Table 3.11 and

Appendix 4). It was assumed that one of two scenarios was responsible for this result. Firstly, the original bone sample harvested from Dick's tibia was mislabelled as Harry's, or secondly, Dick's tibia was incorrectly re-associated to Harry's remains. In order to distinguish these possibilities, the original skeletal remains in the Queensland Museum were re-sampled and a new bone sample was taken from 'Harry's' tibia. This sample was processed identically to all the other bone samples in this study. The STR profile from this sample was concordant with Dick's profile. Therefore Harry's tibia had been incorrectly re-associated more than ten years ago, and actually belongs to Dick.

In an attempt to gain the most complete STR profile possible for each individual, all 14 -24 amplifications of bone and tooth samples were examined together. An increase in the number of alleles that could be assigned to profiles was achieved. By applying this pooled consensus approach across all 14 amplifications (bone and teeth), an additional 25% and 47% alleles were able to be assigned compared to 'Tom's tooth and bone samples in isolation. In order to gain the most complete STR profile for 'Dick', data from both bone fragments belonging to 'Dick' were combined (10 bone profiles which were originally assigned as 'Harry's' bone, and 'Dick's 10 profiles). When generating the consensus profile for 'Dick's bone in this combined manner, a complete STR profile was obtained (an additional 22% alleles compared to Dick's original bone sample) (Table 3.11).

These STRBoost® results were not reproducible. Multiple STRBoost® amplifications resulted in additional alleles being detected. However, performing more PCR reactions (>five) without STRBoost® may also provide similarly improved results. The use of STRBoost® resulted in the amplification of additional alleles from the 200 year old Pandora bones.

Table 3.11. Consensus STR profiles from Pandora Samples.

‘Tom’ Consensus Profiles

Sample	Amel	D3S135 8	D19S43 3	D2S133 8	D22S104 5	D16S53 9	D18S5 1	D1S1656	D10S124 8	D2S44 1	TH0 1	Vwa	D21S1 1	D12S39 1	D8S117 9	FGA
Bone																
ESI	X,x	14,x									8, 8					21, x
ESI STRBoost			13, x				x, 13				8, 8					21, x
NGM																
NGM STRBoost					15, x				13, 14							
TOTAL BONE^a		14,x	13, x		15, x		13, x		14, x		8, 8					21, x
Tooth																
ESI	X, x	14, 18	13, 15	x, 25		13, 14					8, 8				10, x	21, x
ESI STRBoost	X, x		x, 15	25, x		13, 14	x, 13	13, x			8, x	18, x		x, 21		21, x
NGM																
NGM STRBoost									13, x							
TOTAL TOOTH^a	X, Y	14, 18	13, 15	x, 25		13, 14			13, x		8, 8	18, x		x, 21	10, x	21, x
Combined Bone and Tooth^c	X,Y	14, 18	13, 15	x, 25	15, x	13, 14	13, x	13,x	13, 14		8, 8	14*, 18	30.2*, x	18*,21	10,13*	21, x

x Allele not called

^a Consensus profile generated from the 10 amplifications across the four different methods

^b Consensus profile generated from the 4 reactions using both amplification kits (2rxn/kit)

^c Consensus profile generated from the 14 amplifications across the four different methods of both the bone and tooth samples combined

*Allele seen at least twice across all profiles examined, but not twice in any one method

‘Dick’ Consensus Profiles

Sample	Amel	D3S135 8	D19S43 3	D2S133 8	D22S104 5	D16S53 9	D18S5 1	D1S1656	D10S124 8	D2S44 1	TH0 1	Vwa	D21S1 1	D12S39 1	D8S117 9	FGA
Bone																
ESI	X,Y	15, 16				11, 11	13, 13				6, 7	17, 18				22, 22
ESI STRBoost	X,Y	15, 16	12,13		x, 16	11, 11	13, 13				6, 7	17, 18	29,x		9, 12	22, 22
NGM																
NGM STRBoost	X, x				15, 16				13, 14	11, x				X, 18	9, 12	
TOTAL BONE^a	X,Y	15, 16	12, 13		15, 16	11, 11	13, 13		13, 14	11, x	6, 7	17, 18	29,x	X, 18	9, 12	22, 22
Tooth																
ESI	X, Y	15, 16	12, 13	18, 24	15, 16	11, 11	13, 13	15, 17.3	13, 14	11, 15	6,7	17, 18	29, 30	17, 18	9, 12	22, 22
NGM	X, Y	15, 16	12, 13	18, 24	15, 16	11, 11	13, 13	15, 17.3	13, 14	11, 15	6,7	17, 18	29, 30	17, 18	9, 12	22, 22
TOTAL TOOTH^b	X, Y	15, 16	12, 13	18, 24	15, 16	11, 11	13, 13	15, 17.3	13, 14	11, 15	6,7	17, 18	29, 30	17, 18	9, 12	22, 22
Combined Bone and Tooth^c	X, Y	15, 16	12, 13	18, 24	15, 16	11, 11	13, 13	15, 17.3	13, 14	11, 15	6,7	17, 18	29, 30	17, 18	9, 12	22, 22

x Allele not called

^a Consensus profile generated from the 10 amplifications across the four different methods

^b Consensus profile generated from the 4 reactions using both amplification kits (2rxn/kit)

^c Consensus profile generated from the 14 amplifications across the four different methods of both the bone and tooth samples combined

*Allele seen at least twice across all profiles examined, but not twice in any one method

‘Harry’ Consensus Profiles

Sample	Ame I	D3S135 8	D19S43 3	D2S133 8	D22S104 5	D16S53 9	D18S5 1	D1S1656	D10S124 8	D2S44 1	TH0 1	Vwa	D21S1 1	D12S39 1	D8S117 9	FGA
Bone																
ESI	X, Y	15, 16	12, 13	18, 24	15, x	11, 11	13, 13	x, 17.3	13, 14	11, x	6, 7	17, 18	29, 30	17, 18	9, 12	22, 22
ESI STRBoost	X, Y	15, 16	12, 13	18, x	15, 16	11, 11	13, 13	15, 17.3,16 [#]	13, 14	11, x	6, 7	17, 18	29, 30	17, 18	9, 12	22, 22
NGM	X, Y	15, x			15, 16	11, 11			13, 14	11, 15		17, 18			9, 12	
NGM STRBoost	X, Y	15, x	12, 13		15, 16	11, 11			13, 14	11, 15		17, 18			9, 12	
TOTAL BONE^a	X, Y	15, 16	12, 13	18, 24	15, 16	11, 11	13, 13	15, 17.3, 16[#]	13, 14	11, 15	6, 7	17, 18	29, 30	17, 18	9, 12	22, 22
Tooth																
ESI	X, Y	14, 17	13, 14	17, 25	11, 16	11, 13	12, 14	16, 17	14, 15	10, 11	7, 8	18, 20	30, 31	15, 20	10, 14	20, 22
NGM	X, Y	14, 17	13, 14	17, 25	11, 16	11, 13	12, 14	16, 17	14, 15	10, 11	7, 8	18, 20	30, 31	15, 20	10, 14	20, 22
TOTAL TOOTH^b	X, Y	14, 17	13, 14	17, 25	11, 16	11, 13	12, 14	16, 17	14, 15	10, 11	7, 8	18, 20	30, 31	15, 20	10, 14	20, 22
Combined Bone and Tooth	Different Individuals															

x Allele not called

^a Consensus profile generated from the 10 amplifications across the four different methods

^b Consensus profile generated from the 4 reactions using both amplification kits (2rxn/kit)

[#] Contamination seen in at least two profiles examined in any one method

Combined 'Dick' Consensus Profiles

Sample	Amel	D3S135 8	D19S43 3	D2S133 8	D22S10 45	D16S53 9	D18S5 1	D1S1656	D10S12 48	D2S44 1	TH0 1	Vwa	D21S1 1	D12S39 1	D8S117 9	FGA
Bone																
ESI	X,Y	15, 16	12,13	18,24	15,x	11, 11	13, 13	X, 17.3	13, 14	11, x	6, 7	17, 18	29,30	17, 18	9, 12	22, 22
ESI STRBoost	X,Y	15, 16	12,13	18, x	15, 16	11, 11	13, 13	15, 16 [#] , 17.3	13, 14	11, x	6, 7	17, 18	29,30	17, 18	9, 12	22, 22
NGM	X,Y	15,x			15, 16	11, 11			13, 14	11,15		17, 18			9, 12	
NGM STRBoost	X, x	15,x	12,13		15, 16	11, 11			13, 14	11, 15		17, 18		X, 18	9, 12	
TOTAL BONE^a	X,Y	15, 16	12, 13	18,24	15, 16	11, 11	13, 13	15, 16[#], 17.3	13, 14	11, 15	6, 7	17, 18	29,30	17, 18	9, 12	22, 22
Tooth																
ESI	X, Y	15, 16	12, 13	18, 24	15, 16	11, 11	13, 13	15, 17.3	13, 14	11, 15	6,7	17, 18	29, 30	17, 18	9, 12	22, 22
NGM	X, Y	15, 16	12, 13	18, 24	15, 16	11, 11	13, 13	15, 17.3	13, 14	11, 15	6,7	17, 18	29, 30	17, 18	9, 12	22, 22
TOTAL TOOTH^b	X, Y	15, 16	12, 13	18, 24	15, 16	11, 11	13, 13	15, 17.3	13, 14	11, 15	6,7	17, 18	29, 30	17, 18	9, 12	22, 22
Combined Bone and Tooth^c	X, Y	15, 16	12, 13	18, 24	15, 16	11, 11	13, 13	15, 17.3	13, 14	11, 15	6,7	17, 18	29, 30	17, 18	9, 12	22, 22

x Allele not called

^a Consensus profile generated from the 20 amplifications across the four different methods (10 amplifications from the bone sample previously assigned as 'Harry')

^b Consensus profile generated from the 4 reactions using both amplification kits (2rxn/kit)

^c Consensus profile generated from the 24 amplifications across the four different methods of both the bone and tooth samples combined

[#] Contamination seen in at least two profiles examined in any one method

3.4 CONCLUSIONS

Bone and teeth were exposed to one of five environmental insults in order to create a set of mock forensic skeletal samples similar to those resulting from mass disasters or missing person cases. Samples were subjected to surface exposure, burial, saltwater, freshwater and extreme heat to create samples of varying levels of preservation. Environmental parameters such as rainfall, relative humidity and temperature were measured. Data reflect the expected seasonal variation in temperatures and rainfall for the sub-tropical climate in which this research was performed.

Bones exposed to the surface for up to 24 months went through various stages of mould infestation and desiccation of soft tissues. Bone samples buried in soil remained moist with various mould species colonising the samples over the course of the study. With exposure to low and moderate heat all of the samples were well preserved. With high and extreme temperatures, bone samples demonstrated extensive charring on the external surfaces, but the underlying tissue was quite well preserved. Prolonged exposure to extreme heat reduced the small bone and teeth samples close to charcoal and were unusable for DNA analysis. Compared to a human body (in situ), these samples were not encased in flesh, and therefore were unprotected from direct heat and flames.

Samples submerged in freshwater decomposed quicker than those in saltwater due to the favourable environment for microbial and algal growth. The freshwater samples were heavily encrusted with whitish-yellow algal growths within two weeks and were totally enveloped in green and red algal slime from four weeks. Adipocere deposits developed at eight weeks of freshwater incubation. Saltwater samples were well preserved with thick fatty deposits encasing the samples at one month and similar whitish-yellow growths appearing at three months. However, no green or red algal blooms were observed, nor did adipocere form on any saltwater samples. Decomposition of remains in aquatic environments is poorly understood and there is a deficiency of research into the differences in decomposition due to fresh or saltwater.

To replicate skeletal remains recovered from fires, bone and teeth were subjected to low (~150°C), moderate (~350°C), high (~550°C), extreme (~700°C) and prolonged extreme heat with direct flames.

The DNA extracted from these environmental samples varied in the degree of DNA damage and degradation. As measured by the real-time qPCR multiplex assay, the most degraded samples were those exposed to the surface and UV light with degradation ratios ranging from 3.5 to 9.1. Bones submerged in salt water or buried showed low levels of degradation (1.5-2), while freshwater and heat-treated samples were more degraded with ratios between 2 and 3.5. From these data, DNA was most susceptible to degradation from three elements: UV exposure, extensive microbial activity and extreme heat.

The variable level of DNA degradation observed with the environmental samples was reflected in the STR profiling success of these samples. Two commercial STR kits (AmpFISTR® NGM™ and PowerPlex® ESI) were used to assess the amplification of challenging samples. Both kits performed well with low and moderately degraded samples. However, with the highly degraded samples, a significant difference in profile success was observed between the two kits. On average, 10-15% more alleles were recovered from samples using the PowerPlex® ESI kit. No statistical correlation between the time of exposure, DNA degradation and profiling success was observed. However, data suggest that the majority of DNA damage occurs early and then plateaus. In addition, no correlation to the visual appearance or degree of decomposition of the bone samples and the STR-typing success was evident.

Three sets of bone and tooth samples (one bone segment and one tooth per individual) recovered from the 200 year old ship-wreck *HMS Pandora* provided an interesting case study for the genotyping of degraded skeletal material. The remains were considered to be from three individuals. Despite low concentrations of DNA in all bone and tooth samples, STR profiles were generated using both AmpFISTR® NGM™ and PowerPlex® ESI amplification kits. All profiles showed the classic signs of degradation. However in

general, the PowerPlex® ESI kit produced more complete and balanced profiles from the degraded samples than the AmpFISTR® NGM™ kit.

These results suggest that the PowerPlex® ESI 16 amplification kit is more sensitive to low amounts of template and more tolerant to DNA degradation and/or damage than the AmpFISTR® NGM kit. Concordance between the STR profiles of the bone and tooth samples from each individual was expected. 'Tom' and 'Dick' samples were concordant across all loci. However the STR profiles from 'Harry's bone and tooth samples were not a 'match'. 'Harry's bone sample was in fact concordant with the STR profile from 'Dick's tooth, and re-sampling confirmed that the bone had been incorrectly re-associated to the wrong individual by the anthropologist over ten years ago.

The commercial PCR enhancer (STRBoost®) was used in an effort to improve the STR profiles of the Pandora remains and the most degraded set of environmental samples. Results were mixed and inconsistent. No reliable improvement in STR profile quality was seen in the surface exposed bone samples as measured by the number of alleles correct and the heterozygote peak height balance. By using a consensus approach to assign alleles over numerous replicates, between one and nine additional alleles were able to be assigned to the Pandora profiles when amplified with STRBoost®.

An alternative method of filing the inside of the root canal for dentine as an optimal source of DNA for genotyping was investigated. Although a more laborious process that results in less dentine powder recovery, the amount of DNA per milligram of powder was significantly higher with the filing method. In addition, the quality of the DNA was superior since the number of alleles detected and the peak height ratios of the STR profiles were also greater.

In conclusion, forensic casework such as missing persons and mass disasters often require DNA analysis from bone and tooth samples. STRs are the traditional markers used for DNA identification and they work well with routine forensic samples. Improvements to commercial forensic STR kits have enabled more successful

amplification from samples with degraded and low amounts of DNA. However, some extremely degraded samples or very low amounts of DNA are still problematic. The use of SNPs may be a better approach for the genotyping of such challenging samples. SNPs can also potentially provide additional genetic data such as ancestry and phenotypic information.

4 Chapter Four

Utility of forensic phenotype SNP panel on challenging samples

ADDENDUM

Contributions to Chapter 4:

Sheree Hughes-Stamm:

- Experimental design
- All laboratory bench-work
- Data analysis
- Author of the chapter

Angela van Daal:

- Assistance with experimental design and interpretation of results
- Editing of chapter

Mark Barash:

- Assistance with the GoldenGate® assay and SNP genotyping data analysis

Philipp Bayer:

- Statistical analysis of phenotypic SNP data

Kelly Grisedale:

- WGA of database DNA samples prior to phenotypic SNP analyses

Wenjie Lui:

- Collation of candidate SNPs for the pigmentation SNP panel from literature

4.1 INTRODUCTION

Due to the compromised nature of environmentally challenged and degraded samples, conventional short tandem repeat (STR) genotyping can result in a partial profile or no profile at all. The forensic community has responded to this problem by designing mini-STR assays with smaller amplicons (<200bp) [86] and kits with more robust chemistry to overcome inhibition and increase sensitivity [326]. These innovations have resulted in a significant improvement in the genotyping success from challenging samples [89]. However, SNP analysis promises even better genotyping results from highly fragmented DNA samples [13]. The principle advantage of SNPs is their short amplicon length (potentially 45-55bp) [11].

Many different SNP technologies are available for genotyping. The majority of SNP genotyping assays can be classified based on the molecular mechanism employed: allele specific hybridization (ASO), primer extension, minisequencing, oligonucleotide ligation and invasive cleavage [172]. Detection methods for product analysis include fluorescence, luminescence and mass spectrometry. When deciding which platform to employ for forensic work, the three main considerations are; 1) the amount of DNA template required, 2), throughput capacity and 3) multiplexing capabilities. For this study, the Illumina GoldenGate Genotyping Assay for VeraCode was considered suitable due to its medium-scale multiplexing capacity (96 SNPs in a single well of a standard 96-well microplate). While this SNP assay recommends a relatively high amount of DNA template per sample (250ng), likely success with a reduction in the amount of DNA input was proposed (Illumina, personal communication).

The Illumina GoldenGate Genotyping Assay uses two allele-specific oligonucleotides (ASOs) with different nucleotides at the 3' ends to discriminate between the two SNP alleles. The two ASO primers are Cy3- and Cy5-labeled to discriminate between alleles. A third primer or locus specific oligonucleotide (LSO), including an address sequence (IllumiCode) unique for each SNP, anneals downstream of the ASO (Fig. 4.1). This third unlabelled primer anneals to a sequence common to all LSOs.

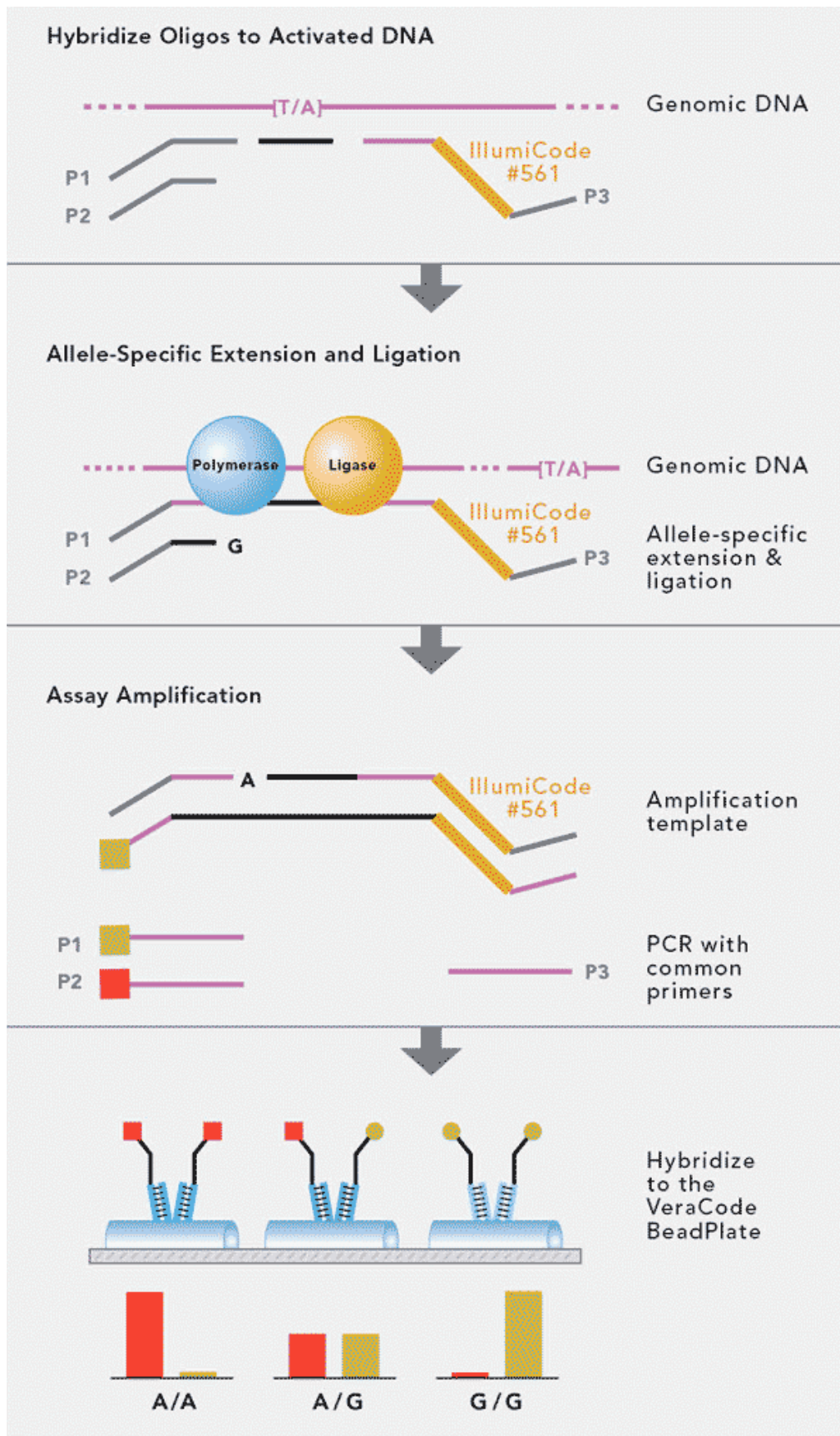


Figure 4.1 An overview of the Illumina GoldenGate Genotyping assay workflow.

After annealing, a DNA polymerase extends the ASOs which is then ligated to the LSO, simultaneously generating PCR template for the 96 SNPs. The templates are then amplified using a set of three primers common to all SNP sites. The resultant amplicons are hybridised to VeraCode glass beads carrying complementary sequences to the IllumiCodes. A unique digital holographic code is contained within each VeraCode silica glass bead. This code allows for tracking of multiplexed markers. The BeadExpress™ is a two-colour laser detection system that allows high-throughput reading of multiplexed VeraCode Assays. The microbeads are washed over a grooved plate where they align within the grooves (Fig. 4.2A). Once aligned, the BeadExpress™ scans the plate with red and green fluorescent lasers which are detected by the optical system (Fig. 4.2B). Cy3/Cy5 fluorescence ratios are calculated and used to determine the SNP genotypes.

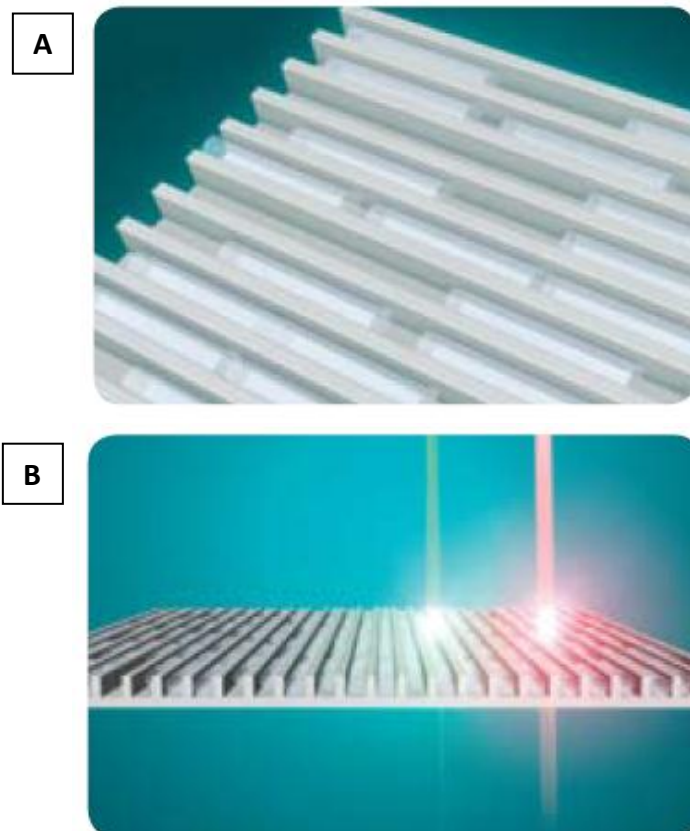


Figure 4.2 Illumina Veracode technology.

A) VeraCode beads aligned within the grooves of the BeadExpress plate. B) Each bead is scanned with green and red fluorescent lasers.

Forensic casework samples often present with limited amounts of DNA template. If samples are below the optimal concentration for direct SNP analysis (~250ng/sample), they would require whole genome amplification (WGA) to produce sufficient quantities of DNA for SNP typing. WGA would also allow for additional testing and subsequent archiving. One of the limitations of the WGA process is uneven amplification and therefore not a faithful representation of the entire genome. This most commonly results from the under-amplification of certain regions of the genome such as telomeres and centromeres [258, 272] or regions containing repetitive elements [362] and regions of higher than average G-C content [363]. This imbalance may result in sub-optimal genotyping downstream due to allelic imbalance or complete loss of loci. Indeed, a study has found that MDA DNA for SNP typing via the GoldenGate® assay is feasible, but warranted caution regarding SNP selection based on SNP distance to telomere and local G-C content [279].

In order to assess the viability of WGA prior to SNP genotyping, the effect of WGA on downstream SNP typing of samples was assessed. Of the different types of WGA, multiple displacement amplification (MDA) represents the most reliable and efficient WGA protocol developed to date [272]. MDA relies on isothermal amplification utilising the high processivity and strand displacement abilities of Φ 29 DNA polymerase and the use of random hexamer primers. Although the amplification bias observed with MDA is much lower compared to other WGA methods [257, 364] MDA has been shown to suffer from significant imbalance resulting in downstream genotyping errors with degraded samples and very low template amounts (1-10 cells) [256, 363]. However, reports are inconsistent with some studies reporting successful amplification from single-cells [247, 253, 277] and improved genotyping from suboptimal forensic samples [250] prior to genotyping.

In addition to the standard kit protocol, two modified MDA methods were investigated to determine whether either of these techniques may reduce the allelic imbalance effects of WGA, and therefore produce better quality SNP results than the standard protocol. The first method involved splitting and re-pooling the sample prior to SNP testing. This approach is similar to that used for LCN typing, except the reaction is split

rather than the DNA sample. It was hypothesised that splitting the total reaction volume into multiple small aliquots during WGA and then re-pooling product prior to SNP typing may balance out any amplification bias generated within each individual WGA reaction. The second method subjected the sample to heating and cooling cycling conditions. As SNP targets are relatively short (~120bp), the long hyperbranching amplicons generated by the Φ 29 DNA polymerase may not be required, and may in fact contribute to the amplification bias. The hypothesis was that primers are forced off the template and back on to another random site in an attempt to generate multiple initiation events and create a more even coverage of the genome.

This study forms an initial evaluation of an Illumina GoldenGate 96-plex SNP assay on the Illumina BeadExpress platform for forensic analysis. The utility of the assay for degraded and environmentally challenged DNA samples was investigated. The SNP panel tested consists of 96 phenotypic SNPs which were chosen for known associations with hair, skin and eye colour. The most obvious descriptors of an individual's appearance are colouring, height and facial features [76]. All are highly heritable [139, 140] and therefore the genetic basis of such traits may be exploited for possible forensic intelligence. Research of such relevant phenotypic SNPs has focused on pigmentation of skin [143-145], hair [147, 148, 160] and eye colour [150, 151, 154, 155, 158, 159]. With such information, a forensic assay may be developed by multiplexing a number of physical characteristic SNPs in order to provide investigative leads to narrow the pool of suspects. This will be particularly beneficial for investigations of missing persons, where DNA typing of skeletal remains can be augmented with information regarding the physical appearance of the person from whom the remains originated.

The primary goal of this study was not to investigate the ability of the SNP panel to predict phenotype, but rather to assess the performance of the SNP platform in terms of its ability to reliably genotype samples of varying quantity and quality. Pilot data from a small subset of samples (n=552) are presented to demonstrate the potential of this SNP panel to predict hair, skin or eye colour. An additional 365 US population samples were genotyped for the prediction of ancestry.

4.2 METHODS

4.2.1 Samples

DNA samples were sourced from two databases:

1. In-house (Bond University) database: 552 DNA samples with known eye, hair, skin colour and ancestry data recorded.
2. Health Science Center, University of North Texas (UNT), Fort Worth, USA DNA database: 365 DNA samples across the three major US population groups; Caucasian, African American and Hispanic.

Degraded samples (n=35) were sourced from sub-optimal buccal swabs or environmentally challenged fieldwork samples (Chapter 3). Bone samples (tibial plateau) were exposed to five insults: 1) saltwater for 6 months, 2) freshwater for 2 months, 3) burial for up to 24 months, 4) surface exposure for up to 24 months and 5) heat exposure of low (~350°C), moderate (~550°C) and high (~700°C) temperatures. The level of degradation and inhibition were simultaneously assessed with the multiplex real-time PCR assay described in Chapter 2. Degraded samples were SNP typed with and without WGA amplification to investigate comparative success rates.

Pigmentation phenotype was assigned to all Bond University DNA samples by researchers over a period of 10 years using the same data collection form (Appendix 6). Ancestry was self nominated by the volunteer. Only ancestry (no pigmentation data) was supplied by UNT for the US population samples. However, in order to boost sample numbers for more robust statistical modelling, all African American samples were further assigned pigmentation data for dark skin and black hair. All appropriate ethical approvals have been granted for this project (RO-510).

Table 4.1 Sample numbers (n =917) as categorised by phenotype.

	Trait	No. Samples
Ethnicity	African American	181
	Caucasian	453
	Hispanic	167
	Other* or Unknown**	116
	No. Samples with Phenotypic data	801
	Total No. Samples	917
Skin	Fair	215
	Average	177
	Olive	80
	Dark	237
	Other* or Unknown**	208
	No. Samples with Phenotypic data	709
	Total No. Samples	917
Eyes	Blue	176
	Brown	205
	Green	77
	Hazel	88
	Other* or Unknown**	371
	No. Samples with Phenotypic data	546
	Total No. Samples	917
Hair	Blonde	96
	Brown	287
	Red	45
	Black	298
	Other* or Unknown**	191
	No. Samples with Phenotypic data	726
	Total No. Samples	917

* Categories not used for prediction analysis ** Phenotype data unknown

4.2.2 Whole genome amplification (WGA)

DNA (10-80ng) was added to Illustra GenomiPhi V2 DNA Amplification kits (GE Healthcare, Buckinghamshire, UK) and processed in one of three ways:

1) Recommended protocol

The GenomiPhi V2 kit recommends a minimum of 10ng pristine template per reaction for optimal genome representation [365]. Illumina recommends a minimum of 50ng/sample input into WGA prior to SNP analysis [366]. The standard protocol consisted of 1µL DNA (10-80ng) added to 9µL sample buffer, denatured at 95°C for 3 minutes followed by addition of 9µL Reaction Buffer and 1µL Enzyme Mix. Isothermic amplification was performed at 30°C for 90 minutes and the reaction was terminated by heat inactivation at 65°C for 10 minutes.

2) Split and pool method

Split and pool samples were prepared in one of two methods for isothermic amplification:

- a) Reaction volume of 20µL was split into 4 aliquots of 5 µL each.
- b) Double volume (40µL) reaction split into 8 separate aliquots of 5µL each.

Individual aliquots were subjected to isothermic amplification as per the standard kit protocol. Aliquots were subsequently pooled together and mixed prior to SNP analysis.

3) Cycling method

Samples amplified by the cycling method were prepared as per the standard protocol but were subjected to a 30-cycle PCR-amplification of 30°C for 10 seconds and 40°C for 5 seconds.

For SNP analysis, 1µL of neat WGA product (for each WGA approach described above) was added per reaction.

DNA extracts from buccal swabs and bone samples were found to vary in quantity and quality. Buccal swab extracts ranged from 0.3-20ng/ μ L and bone samples 0.02-300ng/ μ L. WGA was performed in double volumes on these samples in one of two ways to maximise the amount of template into each reaction:

1) Non-split WGA

10 μ L DNA (5-200ng) was added to 10 μ L sample buffer, denatured at 95°C for 3 minutes, followed by the addition on 18 μ L Reaction Buffer and 2 μ L Enzyme Mix. Isothermic amplification was performed as described in section 4.2.2.

2) Split and pool method

The double volume reaction was split into 8 separate aliquots as per described in section 4.2.2 split and pool method 2b.

4.2.3 SNP Analysis

Approximately 115 SNPs known to be associated with pigmentation phenotype were selected (Liu and van Daal, unpublished data) and submitted to Illumina for multiplex primer design using the Illumina® Assay Design Tool (ADT). Oligonucleotide pool assay (OPA) multiplex primer sets were designed and manufactured by Illumina for 96 of the SNPs (Appendix 7). Of the 96 SNP regions to be amplified, 94 were 121bp, and the other two 103bp and 93bp respectively. Each SNP was assigned a score (0-1.1) according to how well it is expected to perform, with higher values indicating a greater likelihood of a successful SNP genotype assignment [367] (Appendix 8). This allows for preferential selection of SNPs for inclusion in the assay. Illumina recommend avoiding SNPs with a Final_Score <0.4, as inclusion may decrease the overall assay performance. Eight SNPs with scores below 0.4 were considered essential for inclusion in the forensic pigmentation SNP panel because of known strong associations with hair phenotypes (Appendix 8). These SNPs are in the MC1R, OCA2, ASIP, SLC24A4, EDA2R, GPR143 and TCHHL1 genes.

SNP analysis was performed using the 96-plex GoldenGate® Genotyping Assay and the BeadExpress™ (Illumina, San Diego, USA). Input amounts of DNA ranged from 10-250ng/sample (in duplicate or triplicate). For the phenotype study, the majority of samples used were SNP typed directly from HMW gDNA with 100-250ng of DNA. However, a selection (n=60) of gDNA samples from the in-house database were whole genome amplified using the split and pool method (as described in 4.2.2) prior to genotyping. gDNA controls were included to check concordance of WGA treated samples. DNA samples from the UNT database were slightly degraded in transit, and therefore all samples were SNP typed directly (20ng-250ng of DNA input) without WGA.

Data analyses were performed using GenomeStudio™ Genotyping software (Illumina, San Diego, USA). Several indices were used to determine the performance of each SNP, the confidence of each SNP call, and the assay performance as a whole,. The call rate for each SNP indicates the proportion of samples assigned a genotype at each locus. The GenTrain Score (GTS) indicates how well separated and tight the clusters of the different genotypes are for each SNP. GenCall Score is a quality metric that indicates the reliability of each genotype call (0-1). The 50% GenCall Score (p50 GC) for a particular locus represents the 50th rank for all GenCall scores for that locus respectively [368].

SNPs were considered to be performing well if the GenTrain score was >0.3, the GenCall 50 was >0.4 and call rate was >90%. SNPs were considered to perform poorly if the call rate was 50-90%, but the GenTrain score was >0.3, and the GenCall 50 was >0.4. SNPs were excluded if the samples did not separate into well-defined clusters (Fig. 4b) (GenTrain Score <0.3), if more than 50% samples showed <0.15 relative fluorescence unit (RFU) (Fig. 4c), or if the overall call rate for that SNP was less than 90%.

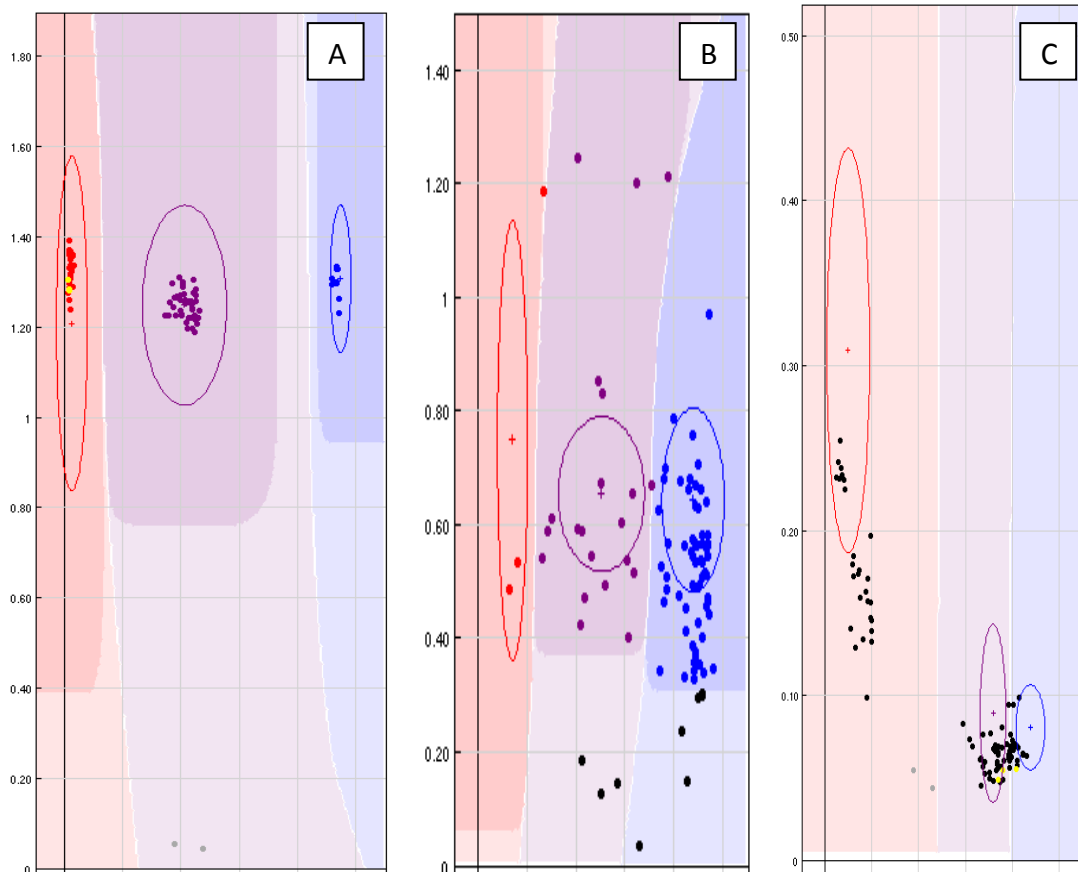


Figure 4.3 Examples of good and poor genotype clustering pattern for individual SNPs

A) Good separation of clusters defining the three possible genotypes. SNP were excluded from analysis due to B) poor separation of clusters, or C) less than 50% of samples at a particular locus fall below 0.15 RFU.

Individual samples were excluded from analysis at a particular SNP if the RFU value was below 0.15 or the GenCall value was less than 0.25. Samples were considered good quality if the call rate was 98-100%, moderate if 95-97% and acceptable if 90-94%. All samples with call rates >90% were included for genotyping. Samples were excluded from analysis of the entire assay if the call rate was below 90%.

A correct genotype was determined by sample replicate concordance. The consensus approach was employed with a genotype being called when seen at least twice in the triplicate analyses. In the case of samples with degraded references, the consensus approach involved calling a genotype when it was concordant with the reference and at least one other sample. Sequencing was not performed to confirm genotyping accuracy due to financial and time restraints.

A total of 917 samples were genotyped for the pigmentation study. Two types of statistical analyses were performed. The most strongly associated SNPs for each phenotypic trait (p-value <0.5) were identified using an open-source software package (GAPIT) developed for genome wide association studies (GWAS) [369], and the other was used to model the prediction of each trait. For each pigmentation trait and ethnicity, a forward stepwise conditional logistic regression was performed on a subset of samples (n=817) using PASW Statistics 18 (SPSS, Inc., 2009, Chicago, IL). As many SNPs as possible were used to build a predictive model for each phenotypic trait. In each step of the regression, all possible SNPs were tested to see if any additional SNP improved the predictive power of the model by measuring the R^2 value of the predictive model. In this way, several SNPs were grouped inside a model to predict the variation of each trait. However, it must be noted that R^2 values do not strictly apply to logistic regression analysis, and therefore a pseudo- R^2 (Nagelkerke) value was used to provide a general indication on the goodness-of-fit of each predictive model. A better indication is one based on a comparison of predicted and observed values from the fitted model [340]. In addition, low pseudo- R^2 values with logistic regression are the norm [340].

SNPs which had more than 5% of data missing were removed from statistical analysis. The algorithm used for the logistic regression analysis removed samples if even one datum point (genotype or phenotype) used to generate the predictive model was missing. To ascertain the validity of the models' predictions, logistic regressions were run on 100 additional blind samples. The rate of false positives, false negatives were also calculated.

4.3 RESULTS AND DISCUSSION

4.3.1 96-SNP Multiplex Assay

The performance of each SNP within the 96-SNP multiplex assay was tested for use with various types of DNA template:

- 1) pristine genomic DNA (n=306, 140 biological samples in duplicate or triplicate)
- 2) whole genome amplified DNA (n=342, 117 individuals in duplicate or triplicate)
- 3) degraded samples (n= 3 x 35 individuals)

The assay performed well with genomic samples in high amounts (250ng DNA per sample) reproducibly showing tight clusters and acceptable call rates (>90%). SNP typing of WGA samples routinely produced more diffuse clusters at more loci than gDNA samples (Fig. 4.4).

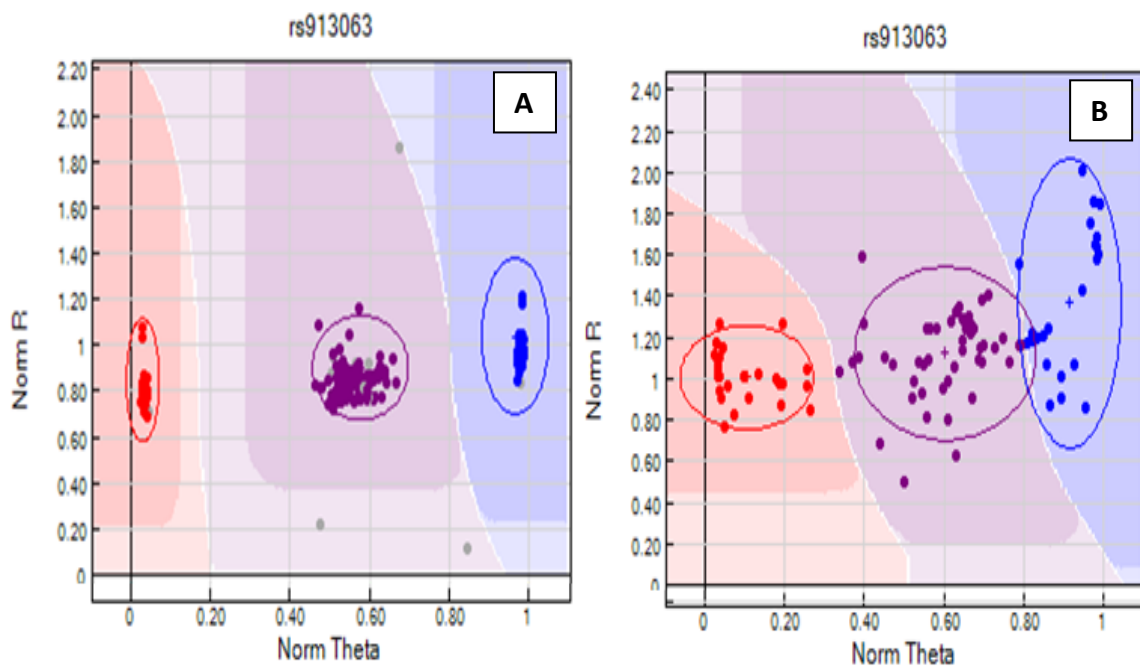


Figure 4.4 An example of the difference in clustering patterns between genomic and WGA samples.

The same DNA samples were SNP-typed A) before and B) after MDA. The clustering of the three possible genotypes at SNP rs913063 is a typical example of the more diffuse clustering when samples were whole genome amplified prior to SNP-typing.

Compared to gDNA samples, there was almost twice the rate of miscalls (average 0.06% vs 0.11%), and a higher number of SNPs performed poorly or required exclusion (8 vs 14 SNPs) with WGA samples (Table 4.2). This is likely due to the inherent amplification bias and/or stochastic effects from the WGA process.

Based on the data in Table 4.2, fifteen SNPs have been identified as requiring further evaluation or exclusion based on performance. Seven SNPs (rs3212355, rs3212359, rs1110400, rs2228479, rs3212361, rs1805008, rs6867641) performed poorly or required exclusion from both genomic and WGA sample analyses. The remaining eight SNPs showed poor performance with WGA samples but accurately genotyped with gDNA. The degree of poor performance with WGA varied. One of the eight SNPs (rs6152) always performed poorly with WGA samples. This is most likely because this SNP is located in a GC rich region (~70%), relatively close to the centromere (of the X chromosome) [335]. Five of the eight SNPs (rs885479, rs1408799, rs3212360, rs6625163, rs12855916) were observed to perform poorly, or were excluded only once during this study (2 SNPs with gDNA, 3 with WGA samples) (Table 4.2). Further investigation would be recommended before any conclusions could be made regarding the robustness of these eight SNPs within the panel.

The assay design involves each SNP being assigned a Final_Score (0 – 1.1), and Illumina recommend SNPs ranked <0.4 not be included in the multiplex assay. However, eight separate runs of the SNP-panel demonstrated that the predictive score is not necessarily an accurate reflection of the performance and success of each SNP (Table 4.2). Eight of the 96 SNPs in the panel were assigned a Final_Score of <0.4 (Appendix 8). Of these eight, only three were found to routinely fail and require exclusion from analysis, whilst five consistently performed well in the assay, and one required further investigation. Conversely, although the majority of SNPs (90.6%) with Final_Scores >0.4 performed well, it was not a guarantee of good performance. Within the group of 10 SNPs which routinely performed poorly or required exclusion in this study, seven had Final_Scores >0.4.

Table 4.2. Occurrence of poorly performing and excluded SNPs

Chrm	Gene	Illumina Final_Score	SNP	Rate Observed (%)					
				Both gDNA & WGA		gDNA Plates (n = 4)		WGA Plates (n = 4)	
				Excluded	Poor	Excluded	Poor	Excluded	Poor
16	MC1R	0.36	rs3212355	100		100		100	
16	MC1R	0.34	rs3212359	87.5		100		75	
16	MC1R	0.41	rs1110400	75		75		75	25
16	MC1R	0.49	rs2228479	75		75		75	25
16	MC1R	0.62	rs3212361	62.5		50		75	25
16	MC1R	0.33	rs1805008	50		25		75	
16	MC1R	0.76	rs33932559						75
16	MC1R	0.49	rs885479						25
16	MC1R	0.42	rs3212360					25	
X	EDA2R	0.10	rs12855916					25	
X	AR	0.99	rs6625163			25			
X	AR	1.10	rs6152						100
5	SLC45A2	0.84	rs6867641		100		100		100
11	TPCN2	0.97	rs35264875						50
9	TYRP1	0.95	rs1408799					25	

Six of the seven SNPs requiring assay exclusion are located within the MC1R gene on Chromosome 16. This is likely due to the large number of SNPs located closely to each other leading to problems with primer design, binding and therefore polymerase extension during PCR amplification. In addition MC1R has a higher (63% versus 40%) GC content than a typical human gene [370]. This difficulty was predicted with three of the six MCR1 SNPs allocated Final_Scores below the recommended threshold (0.4), and the relatively low scores of the other three SNPs (Final_Scores 0.4-0.6). These SNPs could possibly be resolved by high resolution melt (HRM) PCR analysis or sequencing the MC1R gene.

The SNP assay exhibited substantial run-to-run variability with respect to relative cluster positions and average RFU intensities (Fig. 4.5). Although this made the use of genotype cluster positions at the same SNP across different runs more difficult and time consuming, accurate genotyping was still possible. The variance is thought to be primarily due to differences in sample quality, but differences in assay chemistry and OPAs over time may also contribute. A slight difference in general assay performance was observed between fresh and older reagents. However this was not thought to significantly affect genotyping results. As expected, these observations were exaggerated in WGA sample plates due to the effects of amplification bias inherent in the WGA process.

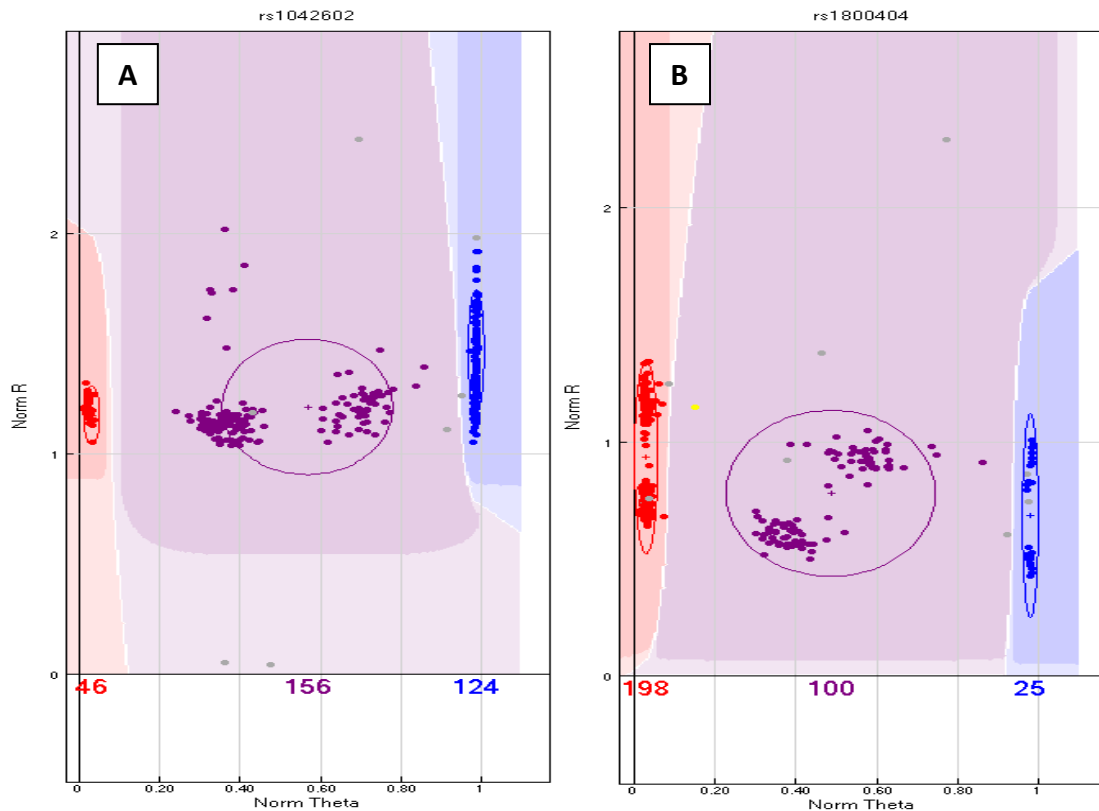


Figure 4.5 The observable run-to-run variability in clustering and RFU values.

Two different SNP plates (n=96 each) combined for analysis. With both SNPs A) rs1042602, and B) rs1800404 two distinct populations can be seen. The heterozygote cluster in A) and all three genotype clusters in B) are evidence of inter-run variability. Note the theta shift between the heterozygote samples in image A, and the difference in RFU values between the two sets of samples in image B.

Due to the superior performance of the SNP typing of non-WGA samples, it was considered preferable to genotype samples without WGA if possible. As DNA database and forensic samples are often limited and in low concentrations, it is vital to input minimal DNA into each reaction. However, as is the case for many forensic casework or degraded samples, this option is not always possible, and WGA is a pre-requisite.

4.3.2 Sensitivity Study

Pristine genomic DNA samples (n=10 individuals) were SNP typed to determine the lower limit of accurate genotyping with the 96-plex GoldenGate® Genotyping Assay. Samples were run in duplicate or triplicate (N=138 technical replicates) over three plates, with DNA amounts from 10 - 250ng.

Table 4.3 Sensitivity Results

Call rate	Percentage of Samples (%) via DNA input amount (ng/reaction)				
	250	125	50	20	10
98-100%	97.2	96.2	100	96.2	91.7
95-97	2.8	3.3		3.33	8.3
90-94%	0	0	0	0	0
< 90% Excluded	0	0	0	0	0
Miscalls (% of total genotypes called)	0	0	0	0.041	0.05
Av p50 GC	0.74	0.73	0.73	0.73	0.68
No. Samples	36	26	26	26	24

n= 10 Biological samples, 138 technical samples

The reliability of SNP calls was consistently high across all amounts of DNA as demonstrated by the average p50GC values, which reflect the tightness of the genotype clustering (Table 4.3). The assay showed reproducible and highly accurate results with as little as 50ng sample. The recommended input amount of DNA (250ng/sample) yielded the highest proportion of samples with 100% call rate. However, if samples are considered to perform well with a call rate threshold of >98%, then the assay was successful to a lower limit of 20ng, as >95% of all samples reached the SNP call rate threshold of 98%. With DNA amounts less than 50ng, genotyping

miscalls were observed. At 20ng DNA the proportion of samples generating a 100% call rate drops to 53.8% (96% of samples with a call >98% call rate) and low levels of miscalls were detected (0.041% of genotypes called). At 10ng, the call rate of samples within the 98-100% range dropped to 91.7% and a slightly elevated miscall rate of 0.05% of all genotype calls was observed. In addition, the slightly lower p50GC value suggests that 10ng input of DNA produces a wider distribution of samples within each genotype cluster. However the vast majority (99.95%) of the samples are still correctly called if an allele is assigned at a particular locus. Based on these data, SNP typing was performed on genomic DNA samples at input amounts of 50-250ng per sample.

4.3.3 Whole Genome Amplification (WGA) Protocol Study

Two modifications to the recommended protocol for the GenomiPhi V2 DNA Amplification kit were investigated to seek the optimal method for WGA prior to SNP typing. In addition, the difference in performance of the SNP assay by adding WGA treated samples with or without dilution (1 μ L of the neat (200-400ng), or a 1:10 dilution) of WGA product as template was tested.

Sample performance was variable across the three methods using either neat (200–400ng) or 1:10 dilution (20-40ng) of the WGA product into the SNP assay. No difference in SNP results was observed between the two input amounts with the standard WGA protocol. In WGA samples amplified with the cycling conditions, the 1:10 dilutions resulted in more samples with higher call rates than the corresponding undiluted samples (Table 4.4). However, the opposite trend was observed with the split and pool method. With this latter method, a significant improvement in call rate was observed with the undiluted split and pool WGA samples over those same samples diluted 1:10.

Table 4.4 Comparison of three WGA protocols

Call rate (%)	Percentage of Samples (%) via Method					
	WGA Std		WGA S/P		WGA Cycling	
	neat	1:10	neat	1:10	neat	1:10
98-100	83.3	83.3	100	88.9	90	100
95-97	0	0	0	11.1	10	0
90-94	16.7	16.7	0	0	0	0
<90 Excluded	0	0	0	0	0	0
Miscalls (% of total genotypes called)	0.3	0.3	0	0.4	0	0
No. Samples	12	12	9	9	10	10

n= 3 Biological samples, 62 technical samples.

In order to determine which WGA method resulted in optimal downstream SNP typing, the data from the best performing WGA input (neat or 1:10 dilution) of each method were compared. Overall the standard WGA protocol resulted in the poorest SNP typing results compared to split/pool and cycling methods with the lowest call rate (83.3%) and the greatest percentage of miscalls (0.3%). Both alternate WGA methods resulted in 100% of samples having 98-100% call rates. However, it should be noted that the undiluted split and pool samples produced the highest proportion of samples with a perfect 100% call rate (ie. 67% of samples at 100%, and 33% of samples with a call rate of 98-99%).

The slightly improved SNP-typing performance of WGA samples which have been split and pooled over those with the standard and cycling methods is most likely due to a more balanced amplification of the genome. However, STR-typing of split-and-pooled and cycling WGA product (1ng and 10ng WGA template) has shown no significant difference in allelic balance with STR loci between the different WGA methods (unpublished data, Grisedale and van Daal).

The split and pool WGA method for database samples (≥ 10 ng of DNA) provided the best genotyping results. These data support previous work stating that pooling of

MDA product from two or three separate amplifications significantly reduced any allele amplification bias during WGA [371]. The number of aliquots per sample was investigated to assess whether amplification bias may be reduced with an increased number of sub-sample reactions. WGA performed with eight sub-sample reactions compared to five aliquots, both pooled prior to SNP typing, generated significantly better SNP results (Table 4.5). This is measured by an increased percentage of samples (83.3% vs 64.6%) with call rates >98%, a decreased number of samples requiring exclusion (3.3% vs 8.3%) and less miscalls (0.08% vs 0.1%).

Table 4.5 Comparison of two Split and Pool methods

Call rate (%)	WGA Split and Pool Method (% of samples)		Genomic DNA (% of samples)
	5 aliquots	8 aliquots	
98-100	64.6	83.3	81.3
95-97	18.8	10	18.8
90-94	8.3	3.3	0
<90 Excluded	8.3	3.3	0
Miscalls (% of total genotypes called)	0.1	0.08	0
No. Samples	48	30	16

n= 25 biological, 94 technical samples (one plate)

Based on the data shown in Table 4.5, all genomic samples (10-80ng template) that were amplified by WGA were subject to the 8-aliquot split and pool method prior to SNP typing with an input of 1µL of undiluted WGA product per sample.

4.3.4 Challenging Samples

The majority of reference buccal swabs and environmental samples in this study were degraded and/or in amounts considered too low ($\leq 2\text{ng}/\mu\text{L}$) for direct SNP analysis. The samples were subjected to WGA to generate sufficient template to complete all genotyping requirements. The recommended minimum input of DNA by the kit manufacturer is 10ng for WGA, and 50ng for SNP typing. Theoretically the short amplicons (<121bp) of the SNP assay should allow good genotyping results from highly fragmented DNA samples. The ability of this assay to SNP type degraded and low template samples with and without WGA was explored.

Quantification of reference buccal swabs collected from bone donors showed low amounts of DNA with moderate degradation (degradation ratios 2.2-3.3). It is assumed that swabs were not allowed to sufficiently air-dry before storage resulting in DNA degradation. Although splitting WGA reactions into eight smaller reactions proved beneficial when amplifying 10-80ng of pristine template (4.3.3), it was hypothesised that splitting degraded and low quantity (<10ng) samples would decrease the quality of template produced for downstream SNP analysis. Prior to analysing the environmentally challenged bone samples, the poor quality extracts from reference buccal swabs were used to test the effect of splitting sub-optimal DNA template into several smaller sub-reactions for WGA on downstream SNP-typing.

Table 4.6 Comparison of methods for suboptimal samples into the SNP assay with and without WGA.

Call rate (%)	WGA Method (% of samples)		Genomic (% of samples)
	Non split WGA	Split and Pool	
98-100	0	0	66.7
95-97	42.3	11.5	29.2
90-94	34.6	42.3	4.2
< 90 Excluded	23.1	46.2	0
Miscalls (% Of total number genotypes)	0.08	1.5	0.06
Av p50 GC	0.65	0.59	0.65
No. Samples	26	26	24

n= 13 biological, 76 technical samples (one plate)

The same volume of neat DNA extract from degraded buccal swabs was added to each WGA reaction or the SNP assay without WGA. The best results were obtained without WGA, with 66.7% of samples considered to perform well (Table 4.6). Neither WGA method was successful, both failing to generate a single sample with a call rate of 98-100%. Of the two WGA methods the non-split method performed better than the splitting method with 42.3% vs 11.5% samples respectively considered acceptable. Twice the number of samples (46.2% vs 23.1%) required exclusion with the split and pool method compared to the non-split method. Furthermore, almost twice the occurrence of miscalls (1.5% vs 0.08%) were observed with the split and pool method over those seen with the non-split WGA samples. This value of miscalls (1.5%) is understated due to the inability to reliably assign a genotype to a further 6.3% of all allele calls. In these cases, the consensus approach failed to assign a genotype for those loci. In the majority of cases (44.9%), the genomic sample was called as a heterozygote and the two different WGA methods yielded opposing homozygote products at those loci. In 31.9% of unresolved cases two different genotypes were evenly represented, and in the remaining 23.2% the genomic samples alone were yielding non-concordant calls. These phenomena were not seen with any of the pristine genomic samples tested in this study. These data suggest that the amplification bias inherent in the WGA process is significantly exaggerated with samples of low quality and quantity. One allele is preferentially amplified during WGA creating product that is significantly unbalanced leading to a decrease in downstream SNP typing accuracy.

Although both WGA methods performed relatively poorly with suboptimal samples compared to direct SNP typing, the non-split WGA method was the better of the two. This result is not surprising given that splitting an already low amount of template into even smaller amounts is counter-intuitive. It has been shown that low level samples (<100pg) split into several sub-reactions during WGA generate STR profiles with increased heterozygote imbalance, more allele and locus drop out than if the WGA reaction was not split (unpublished data, Grisedale and van Daal). As a result of the combined SNP and STR data, the non-split WGA method was used to amplify the environmentally challenged bone samples.

Given the poor results with the buccal swabs, it was not surprising that the SNP typing of highly degraded bone samples was not very successful, particularly since various forms of DNA damage would also be expected. Almost half of samples (47.6%) required exclusion from the assay (Table 6). This poor performance was made significantly worse by WGA prior to SNP analysis with 71.4% of samples excluded. A substantial difference in the average GeneCall scores was observed between the reference, genomic bone and WGA bone samples (p50 GC: 0.65, 0.56, 0.44 respectively) (Table 6). This indicates that compared to reference genomic samples, the reliability of allele calls when they are made is generally lower for the degraded bone samples and even less when those degraded samples are whole genome amplified prior to SNP typing. An approximate 7.5-fold increase of miscalled genotypes and a 2-3-fold increase in the number of loci unable to be reliably assigned a genotype were seen with these environmentally challenged bone samples (Table 4.7).

Table 4.7 SNP-typing results from degraded fieldwork bone samples

Call rate (%)	Genomic Samples (% of samples)		WGA treated Bone Samples (% of samples)
	Reference [#]	Bone Samples	
98-100	57.1	30.9	11.9
95-97	40	16.67	11.9
90-94	0	4.8	4.8
< 90 Excluded	2.9	47.6	71.4
Average Call Rate	97.9	78.0	55.7
Median Call Rate	98.9	93.1	77.6
Miscalls (% of total number genotypes)	0.2	1.6	1.5
Unable to assign a genotype (% of total number genotypes)	0.3	1.2	0.7
Av p50 GC	0.65	0.56	0.44
No. Samples	35	42	42

Buccal swabs

n= 22 Biological samples, 119 Technical samples

Of the 190 genotypes where an allele could not be assigned with confidence (2.2% of total number of genotypes), the majority (76.3%) were due to non-concordance between the reference genotypes (duplicates) and the genotype calls in the corresponding samples (with or without WGA). For example, a non-concordant reference pair (any combination of AA/AT/TT or No-call (NC)) would be seen in conjunction with the non-WGA samples being called AA, and the WGA samples TT. The fact that many of the reference buccal swabs yielded DNA low in quantity and quality (presumably due to inadequate drying after collection) was the primary reason for loci not being called.

Due to the low quality reference samples, all genotypes at questionable loci were assigned using the consensus method. For 5.8% of alleles not called, the reference sample was a heterozygote and the WGA and non-WGA samples were genotyped as the two different homozygotes (eg. reference AT, with the WGA samples AA and non-WGA, TT). Of the 190 loci unable to be genotyped, 12.6% were due to non-concordance within the bone replicates (eg. Reference TT, bone sample duplicates AA, AT). Of these 12.6% uncalled loci, 9.5% were observed in the non-WGA samples and 3.2% within the WGA samples. The fact that non-WGA samples produced non-concordant genotypes three times more often than WGA samples suggests that the DNA degradation and damage itself is the major contributor to SNP failure with these samples.

Variation in overall performance was observed between the types of environmental exposure (Fig 4.6). Using call rate as the primary measure of success, the samples exposed to heat yielded the most complete SNP profiles with all three heat treatments producing average call rates above 98% (Fig. 4.6a). This may be explained by the fact that sufficient amounts of good quality DNA were able to be extracted from these samples. As a result, it was possible to input the optimal 125-250ng template to the SNP assay. These bone samples were extremely charred on the outside, but the osseous tissue internally was well protected and therefore DNA quality was preserved within that tissue.

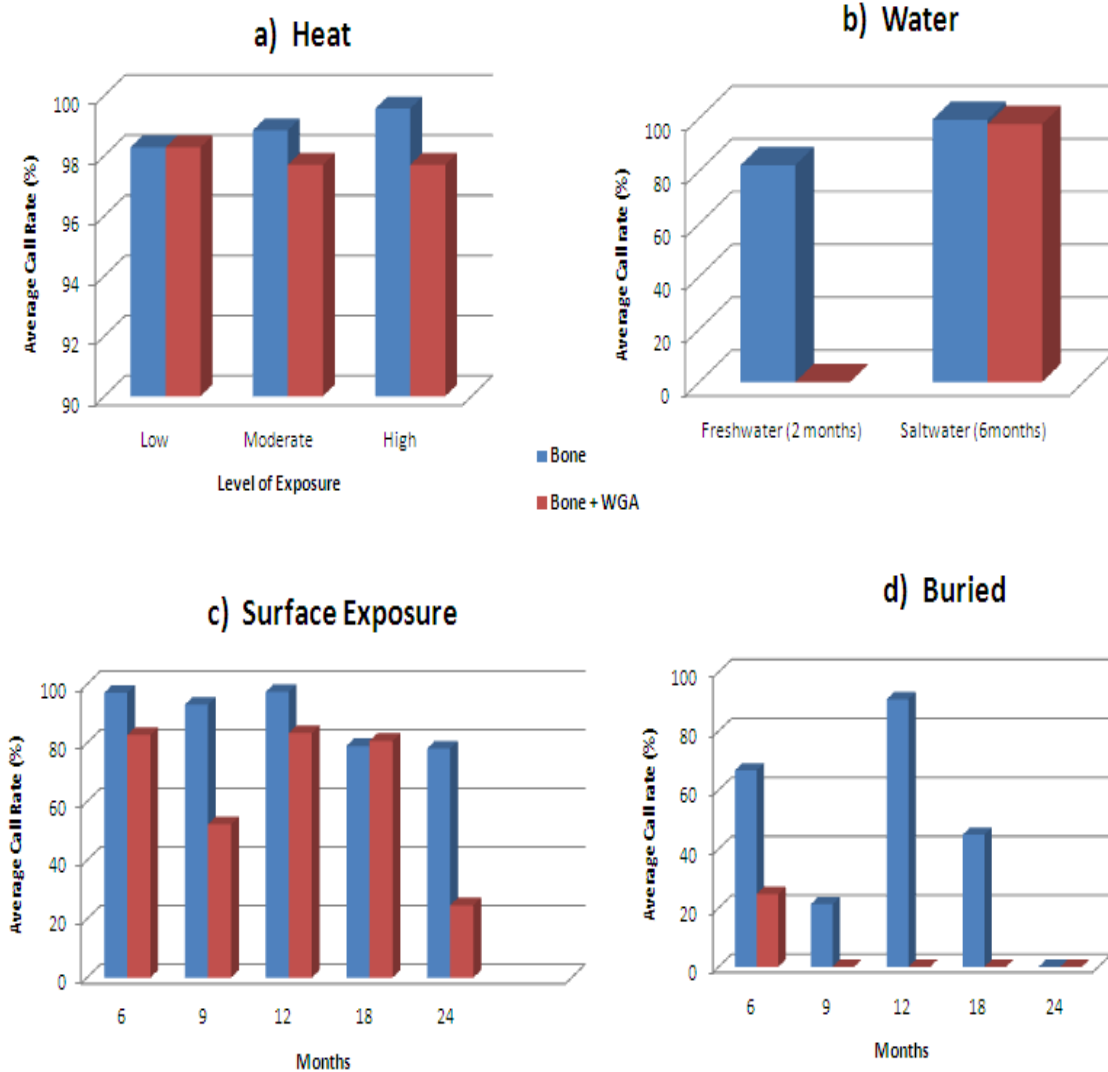


Figure 4.6 SNP typing success of environmentally challenged samples with and without WGA.

The average SNP call rate of a) heat treated , b) freshwater and salt water, c) surface and d) buried bone samples. Each bone sample was directly SNP-typed, or whole genome amplified prior to SNP-typing.

Freshwater samples decomposed much faster than saltwater samples showing extensive colonisation by microbes and algae. As a result these bones were incubated for only two months as opposed to six months for the saltwater samples (see Chapter 3). Even with a longer exposure period, the saltwater samples yielded higher SNP call rates than the freshwater samples (99.4% vs 82.2% respectively) (Fig. 4.6b). It is known that saltwater slows the rate of cadaveric decomposition by suppressing bacterial growth [355]. These SNP data suggest that the saltwater environment may also preserve DNA within bone tissue. This notion is supported by STR data where

more complete profiles were obtained from bone samples incubated in saltwater compared to those in freshwater (Chapter 3, section 3.3.4).

The average genotyping success of surface samples was consistent for up to one year exposure (approximately 95%). However a 15% decrease in call rate was seen in samples with 18 and 24 months exposure (Fig. 4.6c), which brings the rate below 90% and therefore not considered reliable for genotyping.

The buried samples generated the poorest and the most variable SNP profiles (0-90% call rates) (Fig. 4.6d). Interestingly, DNA from buried remains was measured by the qPCR degradation assay as being mildly degraded (ratio of 2.3) and therefore the very poor SNP-typing results from these samples was surprising. The DNA from surface remains was significantly more degraded (qPCR ratio 6.2) and not surprisingly produced inferior STR profiles (data presented in Chapter 3, Fig. 3.48, 3.49). However, in contrast, the surface samples generated better SNP results to those of the buried samples. The poor SNP-typing of the buried samples is more likely due to the amount of DNA than the effect of burial. The buried samples yielded the least amount of DNA of all the fieldwork samples and therefore present the least amount of template for SNP typing (Fig 4.7). More DNA was retrieved from the surface remains and therefore more template could be added to the SNP assay (2.5-85ng vs 0.15-2.5ng). This suggests that the negative effects of DNA damage and degradation may be partially compensated for by the addition of more template into the SNP assay. This notion is intuitive given that DNA degradation in essence decreases the amount of suitable template for genotyping. The fact that STR kits are designed for optimal performance with much less input DNA (0.5-1ng vs 250ng), and are more tolerant to inhibitors and degraded DNA template, may also explain this difference in SNP and STR success from the same samples.

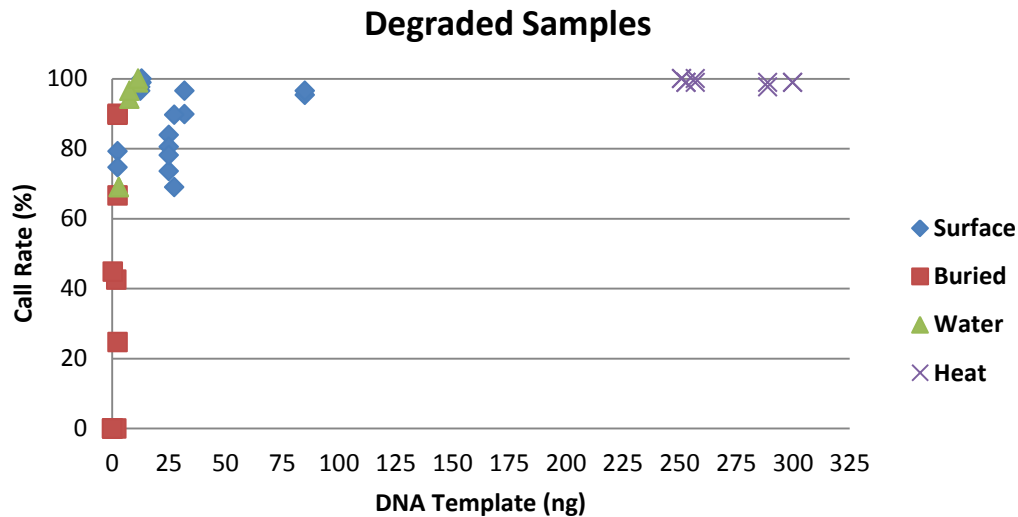


Figure 4.7 The SNP success of degraded samples without WGA by the amount of template

The average SNP call rate (%) was plotted against the amount of gDNA template from environmentally challenged bone samples.

No strong trend in regards to length of environmental exposure and SNP success was observed. This suggests that other factors such as the differences in micro-environments, efficiency of DNA purification and the biological sample itself may be equally influential on SNP performance. It is understood that the rate of human decomposition is significantly influenced by local environmental factors, and that differential decomposition may occur due to variation in microenvironments [372]. It is logical however that a general decrease in sample quality (and therefore SNP analysis) over time would be observed. The lack of such a trend in the results of this study may be due to the very small sample size available for analysis.

Regardless of the mode of environmental insult, genotyping was universally more successful without WGA prior to SNP-typing. These data suggest that WGA (or the methods investigated in this work) of low DNA quality and quantity creates template DNA which is unsuitable for reliable SNP typing.

4.3.5 Phenotype and Ancestry Prediction

Eye, skin and hair colour are highly heritable visual traits [141]. Such traits are important in a forensic context as they form key descriptors of an individual, at least in Caucasian populations. In addition to these external visual characteristics (EVCs), the assignment of ancestry to a person (or DNA sample) can also provide important information. The ability to determine EVCs and ancestry from DNA can be of assistance in solving missing person cases, identifying mass disaster victims, providing intelligence information for crime scene samples when no suspect is identified, or giving a 'face' to historical skeletal remains.

The main goal of this pilot study was to investigate the predictive value of the 96-plex SNP panel (described in section 4.2.3) for hair, skin, eye colour and ancestry. 915 individuals from various population groups (primarily Caucasian, African American and Hispanic) were genotyped. These samples varied in DNA quantity and quality. Forward stepwise conditional logistic regression was used to build predictive models for each phenotype and ancestry. The logarithm used to generate the predictive models (in SPSS) is not tolerant of missing data. As a result, samples were removed if even one datum point (genotype or phenotype) used to generate the predictive model was missing. Therefore if a model requires nine SNPs, samples must have a genotype for all nine SNPs, and the phenotype data for that trait assigned. This led to a high percentage of samples (~20%) in each trait failing to meet the strict requirements for inclusion in the statistical modelling (Fig. 4.8 and Table 4.8).

Proportion of samples used for statistical analysis

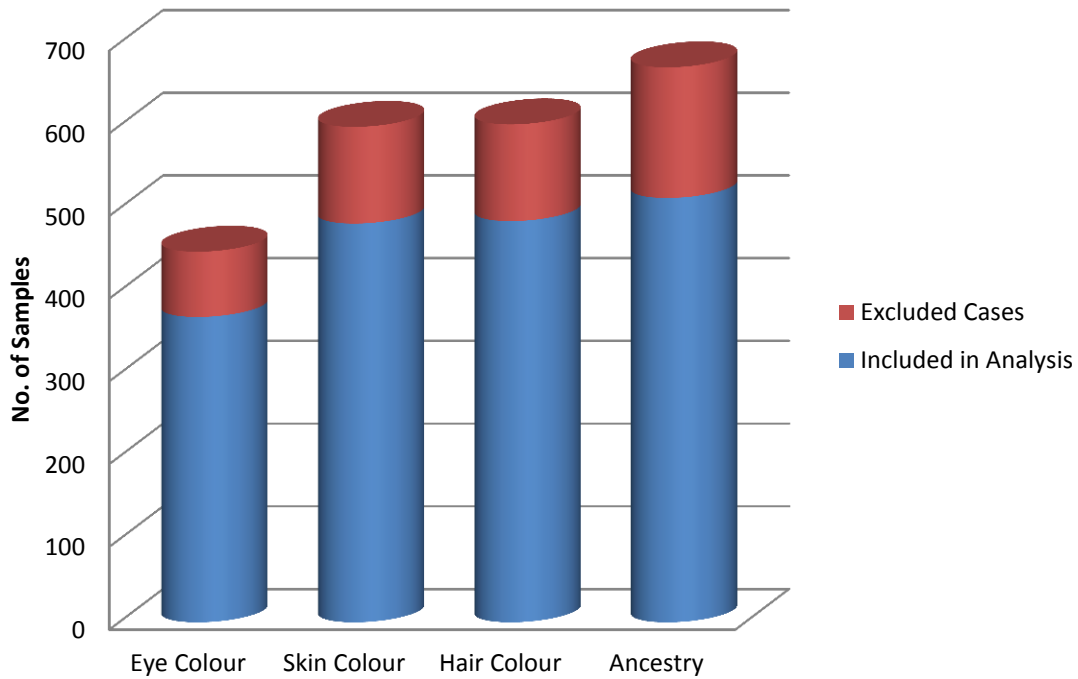


Figure 4.8 Proportion of samples used for Statistical modelling of each characteristic investigated.

The high number of samples excluded from statistical modelling may be due to substantial inter-run variability between the plates (as previously described in section 4.3.1). This variability resulted in the number of SNPs being excluded each run ranging 1 to 12 of the 96 SNPs during the data quality control and clean-up process prior to the statistical analysis. The major influences on the performance of the GoldenGate® Genotyping assay were sample quality and quantity. The population samples used in this study varied widely in both the amount of DNA (50ng – 250ng per sample) and the quality of the template (HMW genomic DNA, slightly degraded gDNA, and whole genome amplified samples) used for genotyping.

Table 4.8 The number of DNA samples genotyped and subsequently used for the generation of predictive models for each phenotype.

	Trait	No. Samples			Used for Prediction (%)
		^a Complete Dataset	^b Available Dataset	^c Used for Prediction	
Ethnicity	African American	181	160	119	74.38
	Caucasian	453	371	298	80.32
	Hispanic	167	140	96	68.57
Skin	Fair	215	175	142	81.14
	Average	177	147	122	82.99
	Olive	80	67	57	85.07
	Dark	237	210	161	76.67
Eyes	Blue	176	146	115	78.77
	Brown	205	167	142	85.03
	Green	77	60	52	86.67
	Hazel	88	75	60	80.00
Hair	Blonde	96	76	60	78.95
	Brown	287	233	190	81.55
	Red	45	38	33	86.84
	Black	298	255	202	79.22
^a Total number of samples genotyped					
^b No. of samples available for predicting models after 100 random samples were removed					
^c No. of samples used to generate predictive models					

The initial performance assessment of the 96-plex SNP panel (Table 4.2, section 4.3.1) was a reasonably good indicator of the genotyping success using the larger and more heterogeneous set of samples. All seven SNPs which failed in the initial evaluation also failed in this study (Table 4.9). Similarly, the five SNPs which were flagged for further investigation in the initial assessment were all excluded from the phenotype prediction analysis. Only one of the three SNPs which performed poorly in the initial study required exclusion from these analyses. However, it is a concern that 11 SNPs which performed well in the evaluation study had to be excluded from analysis in the prediction of phenotype and ancestry due to missing phenotype data or poor call rates.

The number of SNPs requiring exclusion varied markedly from plate to plate reflecting differences in sample quality. Samples were from several different sources, and as a result varied in the amount and quality of DNA available for genotyping. The run-to-run variation resulted in a more wide-spread exclusion of genotype data and SNPs which were ‘zeroed’. This result had the detrimental flow-on effect of increasing the number of samples removed from the logistic regression analysis as the algorithm removes samples if one datum point (genotype or phenotype) used to generate the predictive model is missing.

Table 44.9 The comparative SNP performance

Recommendation^a	No. SNPs Predicted^a	No. SNPs Excluded^b
Well Performing	81	11
Further Investigation	5	5
Poorly performing	3	1
Exclude	7	7

^a Results of initial SNP assay evaluation in section 4.3.1

^b Results of the phenotype and ancestry prediction study in section 4.3.5

Because the algorithm used for statistical analysis was not tolerant to missing data, SNPs with more than 5% of data missing (more than 5% of samples were not assigned a genotype for that particular SNP) were disqualified from statistical analysis. This threshold resulted in 24 of the 96 SNPs (25%) being removed (Table 4.10).

Table 4.10 The 24 SNPs removed from analysis due to more than 5% missing data.

SNP	Gene	Predicted SNP Performance*	Illumina Final_Score [#]
rs1110400	MC1R	Exclude	0.412
rs3212361			0.622
rs3212355			0.362
rs1805008			0.332
rs3212359			0.344
rs2228479			0.489
rs3212360		Further Investigation	0.421
rs885479			0.421
rs6867641	SLC45A2	Exclude	0.837
rs1426654		Well performing	0.628
rs12855916	EDA2R	Further Investigation	0.1
rs1041668		Well performing	1.1
rs4827380			1.1
rs1485682			1.1
rs6152	AR	Poor performing	1.1
rs6625163		Further Investigation	0.994
rs1800404	OCA2	Well performing	1.1
rs1800407			1.1
rs1408799	TYRP1	Further Investigation	0.949
rs2733832		Well performing	1.1
rs2424984	ASIP	Well performing	1.1
rs1894704	HPS4	Well performing	1.1
rs11803731	TCHHL1	Well performing	0.322
rs3768051	LYST	Well performing	0.912

* As predicted from panel evaluation in section 4.3.1 (Table 4.2)

[#] Illumina designate Final_Scores (0-1.1). Scores >0.4 are predicted to fail, and are therefore recommended by Illumina to be excluded from the assay.

Eight of the SNPs excluded from analysis are located within the MC1R gene on chromosome 16 (discussed in section 4.3.1). Three SNPs (rs2296151, rs41273937 and rs11547464) were removed from analysis because they were monomorphic. The global minor allele frequencies for these SNPs are low (0.008, 0.001 and 0.004 respectively). No SNP variation has been reported between Caucasian and African population groups with a minor allele frequency (MAF) of 0 being reported (dbSNP website). Twenty seven SNPs in total were removed from statistical analysis (24 due to poor performance or missing data, and 3 due to being monomorphic.)

4.3.5.1 Statistical Modelling

It was not an aim of this research to conduct a comprehensive association study. However, a pilot study was undertaken to assess the potential of the 96-SNP panel to predict hair colour, eye colour, skin colour and ancestry. Two methods of statistical analyses were used. The first method identified individual SNP associations. Strongly associated SNPs for each phenotypic trait (p -value < 0.5) were identified using an open-source software package (GAPIT) developed for genome wide association studies (GWAS) (Appendix 9). The second analysis was used to model the prediction of each trait. This involved logistic regression (PASW Statistics 18) where each step of the regression, all possible SNPs were tested to see if any could improve on the predictive power of the model towards the trait by measuring the Nagelkerke pseudo- R^2 value of the predictive model (Appendix 10). If a SNP improved the percentage correct of the model, the SNP was included. In this way, several SNPs were grouped inside a model to predict the variation of each trait. The final Nagelkerke R^2 value of each model is a general indication of the strength of the association. However, the most reliable measure for the robustness of the model is a comparison between the predicted and actual outcomes.

4.3.5.1.1 Eye Colour

Of all human pigmentation traits, the genetic basis of eye colour is the most fully understood and can be predicted with the highest accuracy. This study evaluated the 96-plex SNP panel (section 4.2.3) for those SNPs which may be predictive of blue, brown, green and hazel eye colours. Statistical models were generated for the prediction of all four eye colours (Figure 4.9). The predicted accuracies were all approximately 85% using three SNPs for predicting green eyes and six SNPs each for the other three colours (Fig. 4.10).

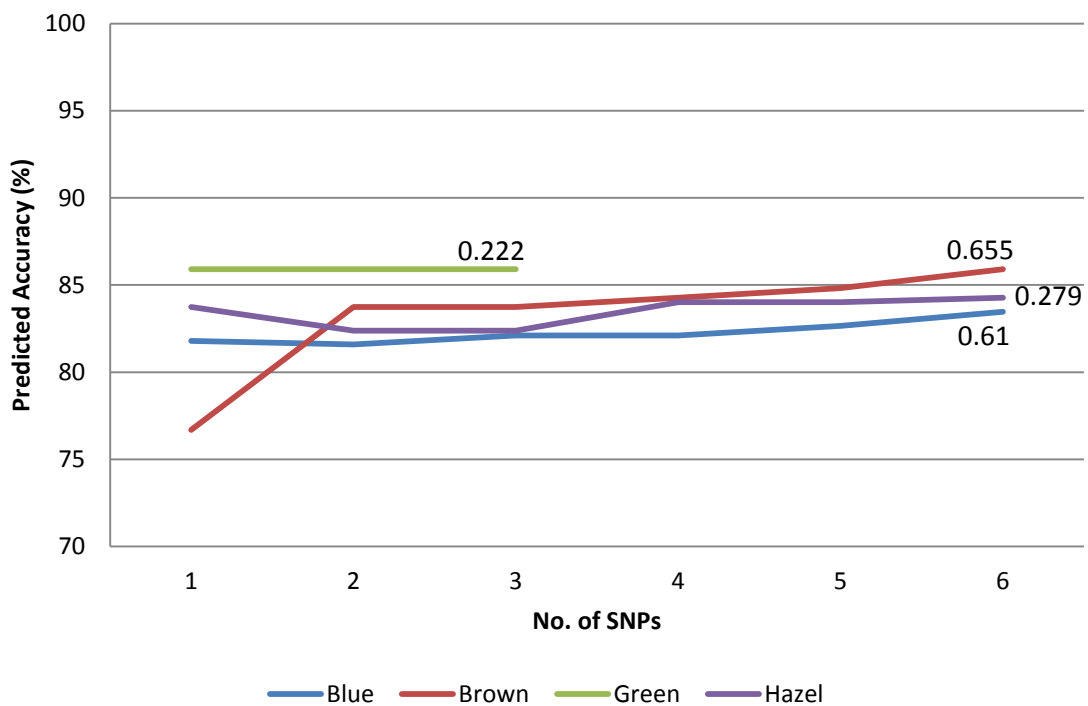
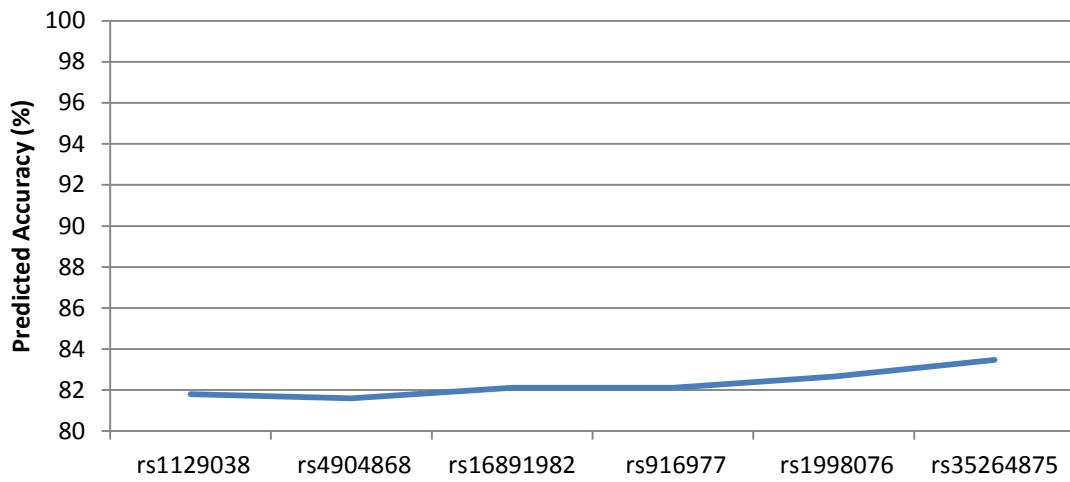


Figure 4.9 Comparison of the statistical models used to predict eye colour

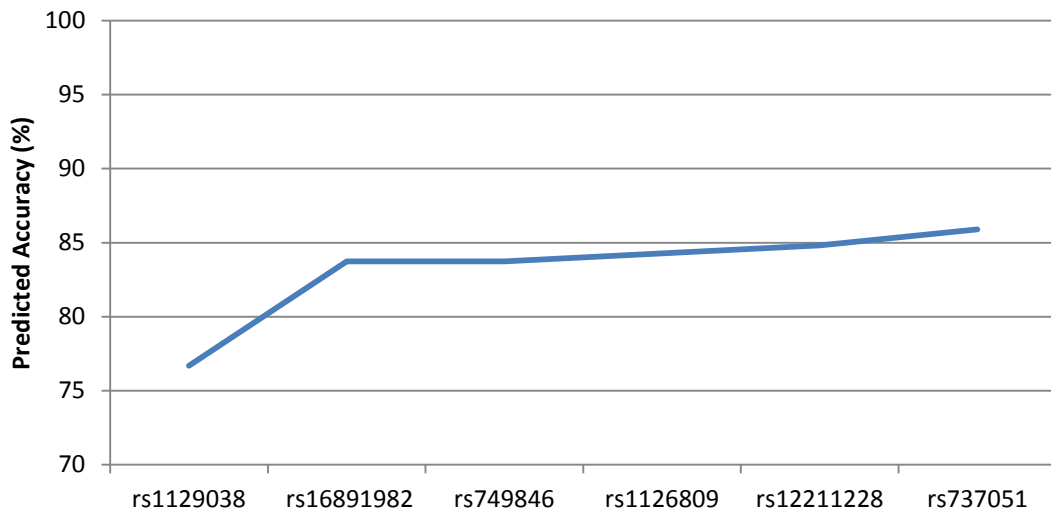
The predicted accuracy of each statistical model for each eye colour is compared. Values displayed are Nagelkerke R^2 values for each model indicating the goodness-of-fit.

Interestingly, even though the predictive accuracy of all colours was similar, the statistical models for blue and brown eye colours were much more robust than the other two colours (R^2 values 0.6 versus 0.2) (Fig. 4.9). The predicted accuracy of blue and brown eye colour was lower than expected given that other studies have shown accuracies of 88-100% [155, 158, 373]. Those studies were performed with approximately 400-6000 individuals.

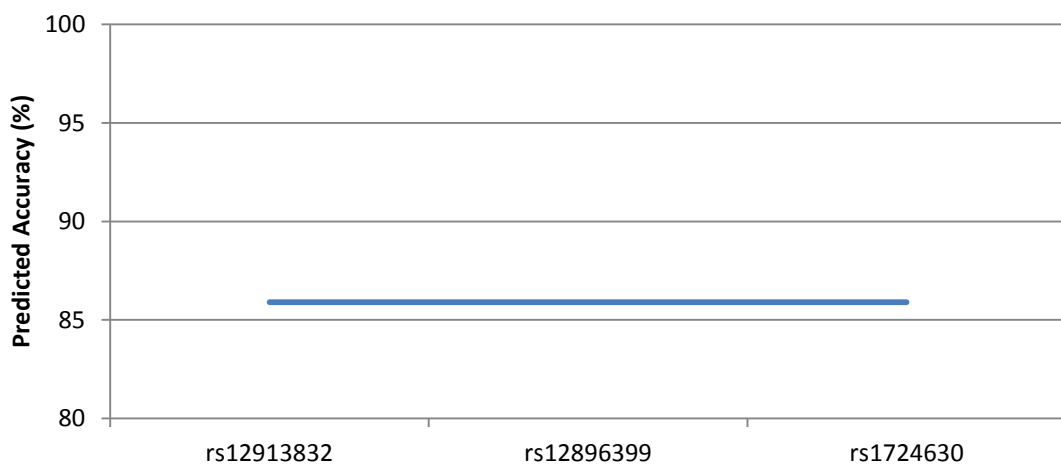
A. Blue Eyes



B. Brown Eyes



C. Green Eyes



D. Hazel Eyes

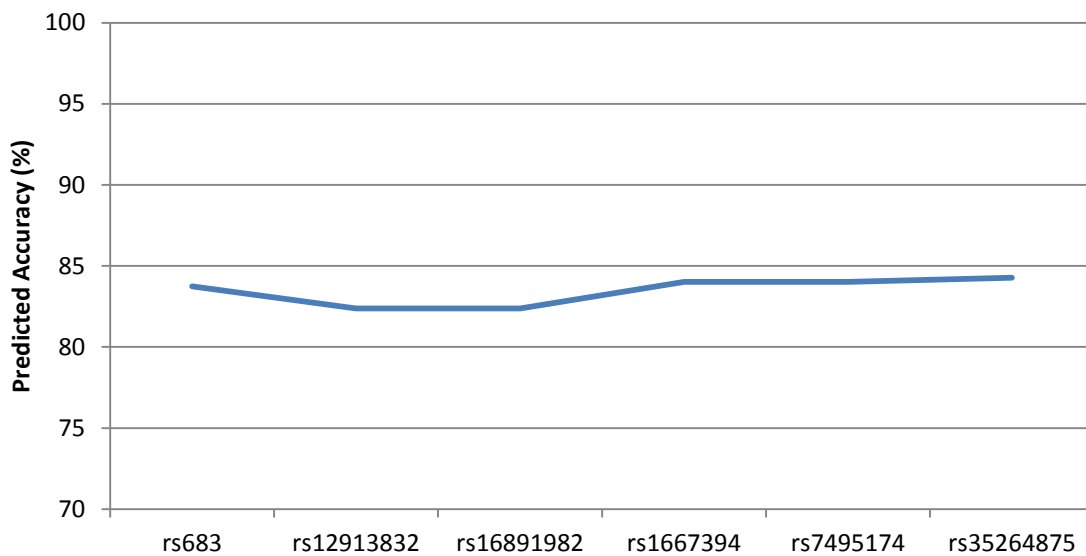


Figure 4.10 Statistical models for the prediction of eye colour.

The accuracy predicted by logistic regression analysis for A) Blue eyes, B) Brown eyes, C) Green eyes and D) Hazel eyes.

Of the 31 SNPs reported in key studies to be most strongly associated with eye colour variation, only 19 were included in the 96-plex panel tested in this study, and a further 5 were excluded from statistical analysis (Appendix 11). The fact that less than half of the SNPs currently known to be most predictive for eye colour were included in this study may explain the lower predictive accuracy and R^2 values obtained (Fig. 4.9) than seen in those previous works [155, 158, 373]. Five of the six SNPs reported to be key predictive indicators of eye colour (included in the IrisPlex [159] and HirisPlex [160] assays) were included in the 96-plex assay, but one (rs1800407) was excluded due to poor performance).

The rs1129038 and rs12913832 SNPs in the HERC2 gene have been reported as the most informative SNPs for eye colour [154, 374, 375], with rs12913832 being ranked as the single highest predictor [158, 161]. In fact rs12913832 has been reported to have strong predictive power for human pigmentation in general [149, 162, 163, 368].

Both SNPs (rs1129038 and rs12913832) are included in the same “h-1” haplotype spanning 166kB on chromosome 15, found in homozygous state (C allele, [376]) in 97%

of Caucasian individuals with blue eyes [377]. Although these SNPs were the two most strongly associated with blue and brown eye colours ($p < 0.0001$) in this study (Appendix 9), the algorithm used for predictive models would select only one of the two SNPs. These two SNPs are linked, and therefore a reasonable approach would be to use one of these as a tag SNP for predictive purposes. One of these SNPs, rs12913832 was included in the predictive models for hazel and green eyes, whilst the other, rs1129038 was used to predict blue and brown eyes.

Prediction using a broader colour category such as 'blue eyes' versus 'not blue eyes', and 'brown' versus 'not brown' may also improve the accuracy rates for eye colour. In this study, that approach decreased the predicted accuracy for blue and brown eyes (blue; 83% to 79% and brown; 86% to 74%), but increased the accuracy predicted for 'not blue' and 'not brown' eyes (blue; 83% to 85% and brown; 86% to 93%) (Fig. 4.11).

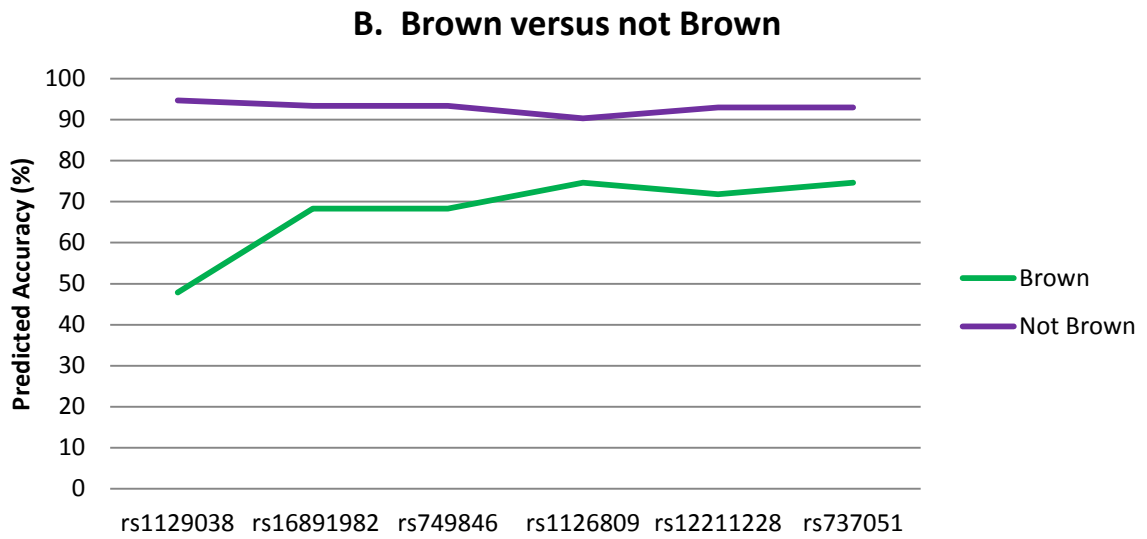
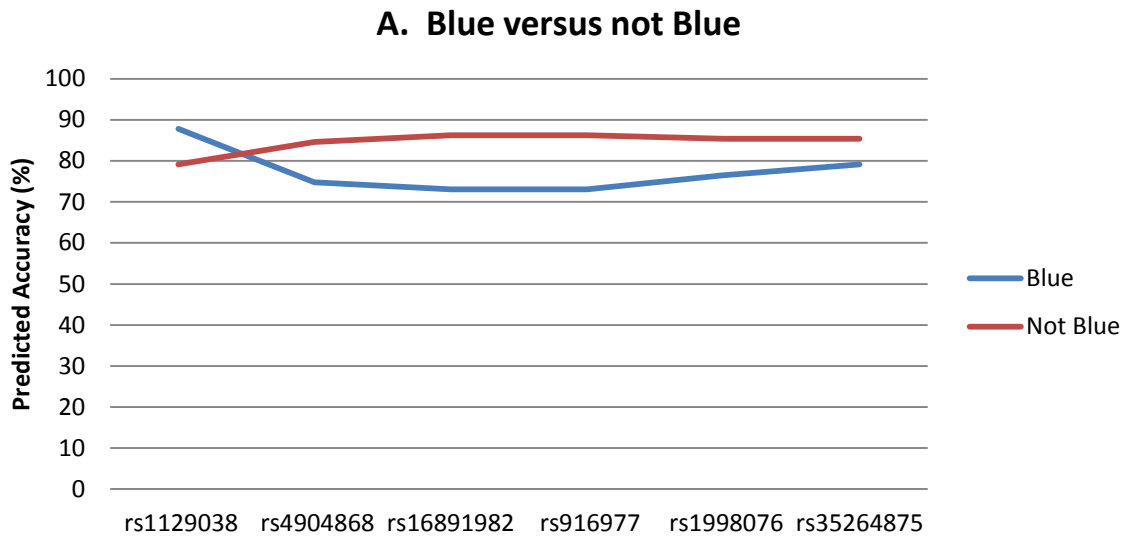


Figure 4.11 Statistical models for the prediction of eye colour.

The accuracy predicted by logistic regression analysis for A) Blue eyes versus not blue eyes, B) Brown eyes versus not brown eyes.

4.3.5.1.2 Skin Colour

Less is known about the genetic determination of skin colour than eye colour. However a generalisation can be made that populations further from the equator tend to have lighter shades of skin [367]. Statistical models were generated to predict four shades of skin colour (fair, average, olive and dark) in this study (Fig. 4.12). The model for dark skin used the most SNPs (20) and also predicted the highest accuracy (97.1%). The SNP model for dark skin was also the strongest with an R^2 value of 0.917 (Fig. 4.12). The next most informative model was the average skin with a predicted accuracy of 89.4%. However, the pseudo- R^2 values with the predictive models for average, fair and olive skin colours were low (0.287, 0.287 and 0.382 respectively) indicating weaker associations.

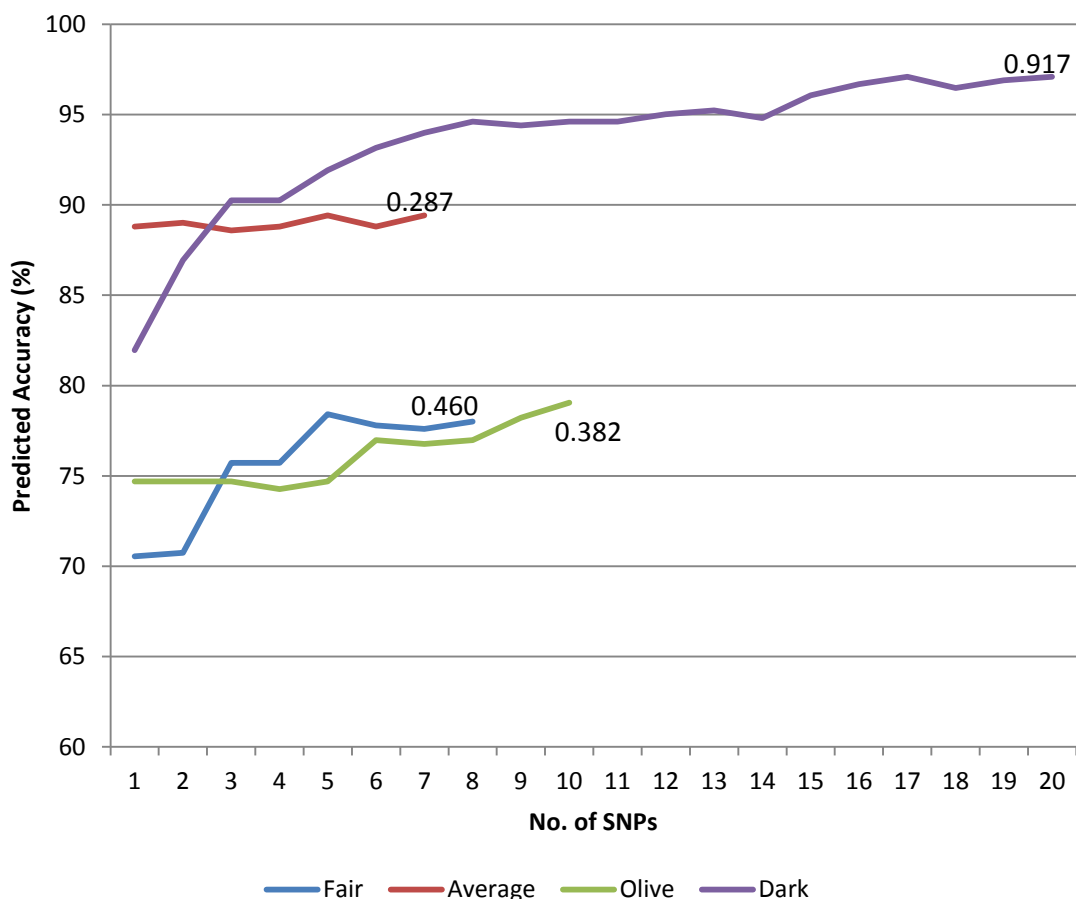


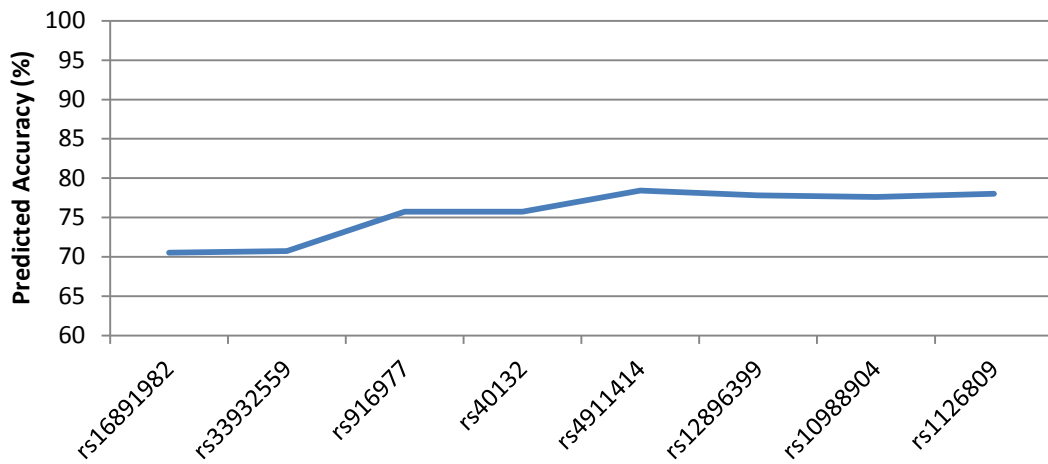
Figure 4.12 Comparison of the statistical models for the prediction of skin colour.

The predicted accuracy of each statistical model for each skin colour is compared. Values displayed are Nagelkerke R^2 values for each model indicating the goodness-of-fit.

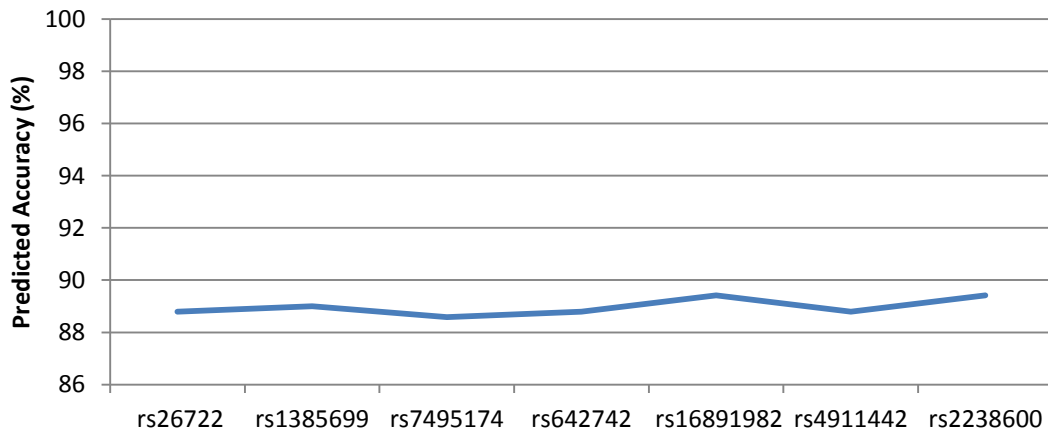
Of the 17 SNPs reported in various studies to be informative of skin colour (Appendix 11), six were not included in the 96-plex panel, and another three were removed from analysis. Of the remaining 8 SNPs, only three (rs12896399, rs16891982, rs7495174) were used to model skin colour in this study. However, five SNPs which are known to be strongly associated with eye colour, but not skin colour in particular, were used to build the statistical models in this study. rs1129038, rs1015362 and rs4778138 were used in the dark skin model, rs26722 in both average and dark skin, and rs916977 for light skin (Fig. 4.13).

There is a lack of concordance between those SNPs reported in literature as being highly associated with skin colour, and those used to generate the predictive models in this study (Appendix 11). A SNP panel for the prediction of skin colour highlighted seven informative SNPs [162]. Of these seven, two (rs6119471 and rs1545397) were not included in the assay, and one (rs885479) was excluded from statistical analysis. Of the four remaining SNPs, only two (rs16891982 and rs12203592) were found to be strongly associated with skin colour ($p < 0.5$) (Appendix 9). One (rs16891982) of those seven SNPs was used to build the statistical models for all four skin shades. In addition, one of the seven SNPs (rs1426654 in the SLC24A5 gene), reported as highly associated with eye, hair, skin colour and ancestry was not included in any predictive model in this study (Appendix 11). The omission of such a high number of SNPs reported to be highly indicative of skin colour from the predictive SNP models generated in this study suggests that the predictive power and accuracy of these phenotype models is comparatively low.

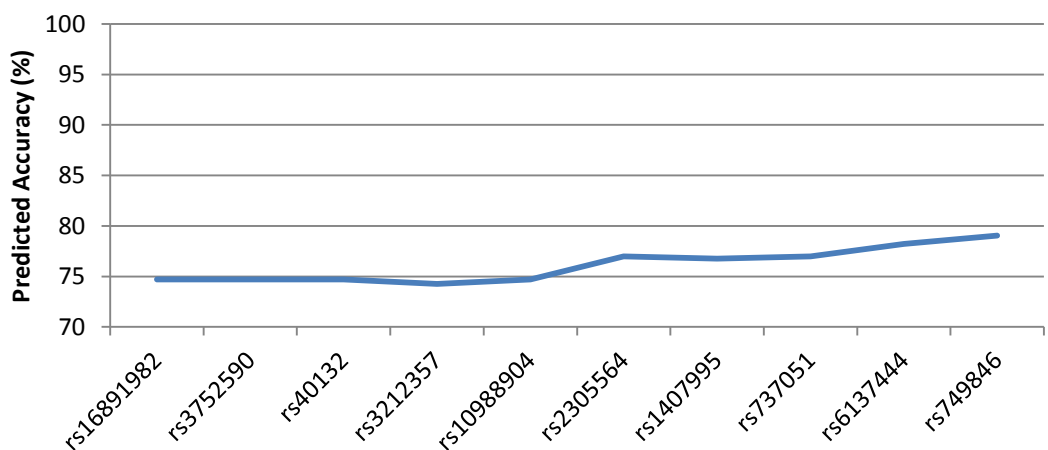
A. Fair Skin



B. Average Skin



C. Olive Skin



D. Dark Skin

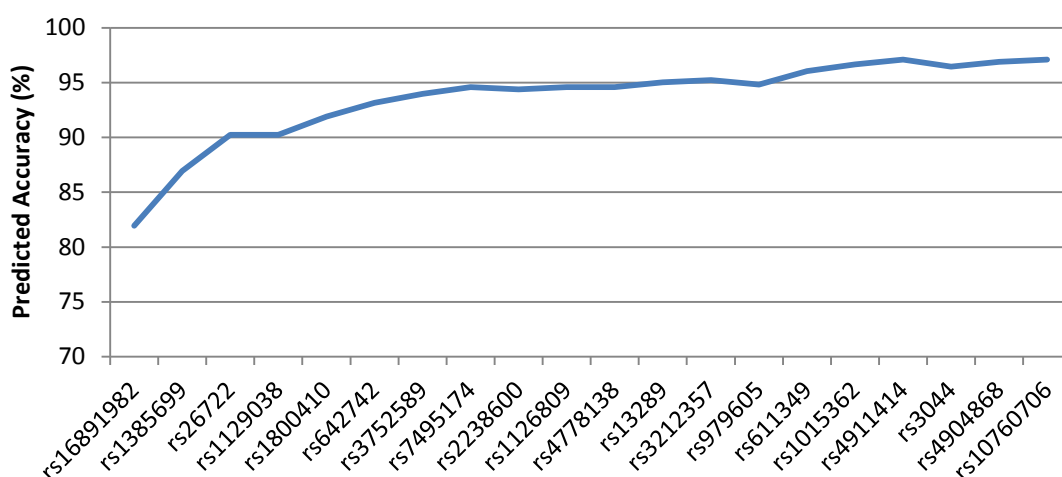


Figure 4.13 Statistical models for the prediction of skin colour.

The accuracy predicted by logistic regression analysis for A) Fair skin, B) Average skin, C) Olive Skin and D) Dark skin.

The statistical model for the prediction of dark skin versus ‘not dark’ skin was robust (Fig. 4.14). Dark skin is predicted with 95% accuracy, and ‘not dark’ skin would be expected to be correct 97% of the time.

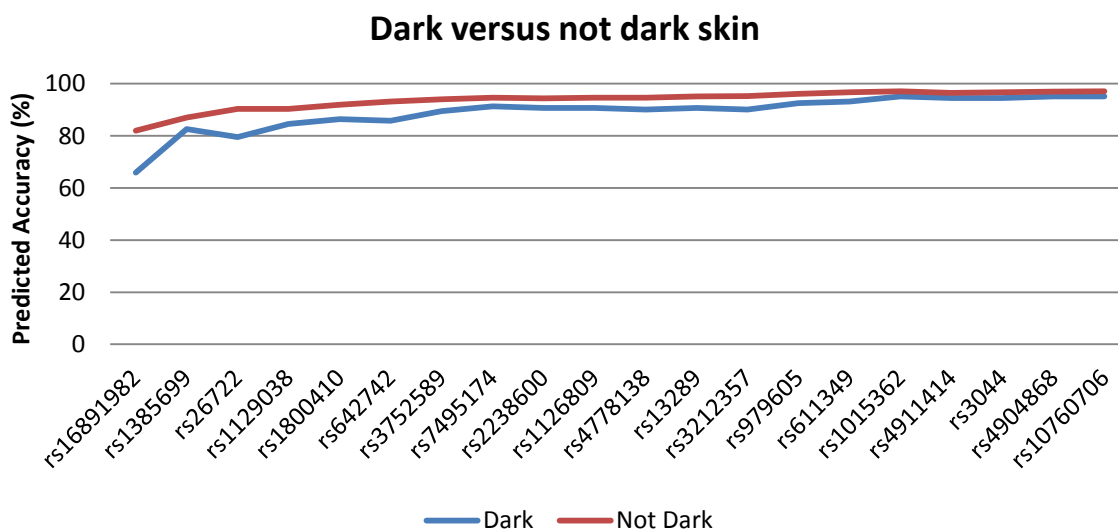


Figure 4.14 Statistical models for the prediction of skin colour.

The accuracy predicted by logistic regression analysis for dark versus ‘not dark’ skin.

4.3.5.1.3 Hair Colour

The ability of the 96-plex SNP panel (described in section 4.2.3) to predict four common shades of hair colour (blonde, brown, red and black) were investigated. For the prediction of hair colour, the same genes contributing to eye and skin colour (OCA2, HERC2, SLC24A5, SLC45A2, MC1R and TYR) are involved. The most notable are SNPs within the MC1R gene which are tightly associated red hair and fair skin [141, 142, 374]. The predictability of hair colour has been reported with mixed levels of accuracy, being generally reported as either lower (<80%) than eye colour predictions [374], or equal to those for eye colour (>90%)[149].

A set of 10 SNPs was found to be a highly predictive (94%) and robust model (R^2 value = 0.835) for the prediction of black hair (Fig. 4.15). A comparably high accuracy was predicted for red hair using five SNPs (Fig. 4.16) despite no SNP being identified as strongly associated ($p < 0.05$) with red hair in this study (Appendix 9). This model also showed a weaker association with a R^2 value of 0.311. These low values and lack of SNPs showing strong association is not surprising, as no MC1R SNPs were included in the analyses due to poor performance (as previously discussed in section 4.3.5, Table 4.10). Sensitivities for predicting blonde and brown hair had lower rates of accuracy with 88% and 73% respectively (Fig 4.16). Interestingly, no significant SNPs ($p < 0.05$) for either blonde or brown hair were identified in this study (Appendix 9).

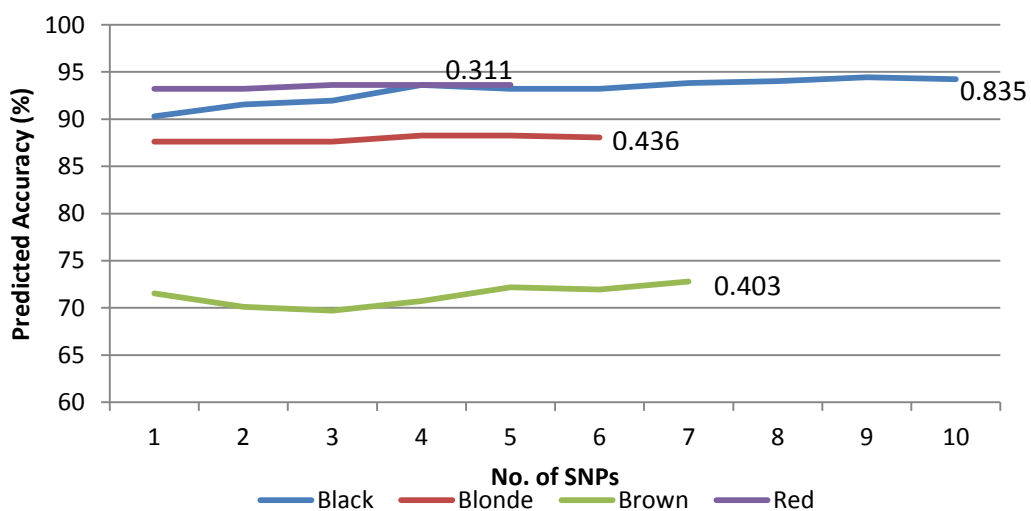
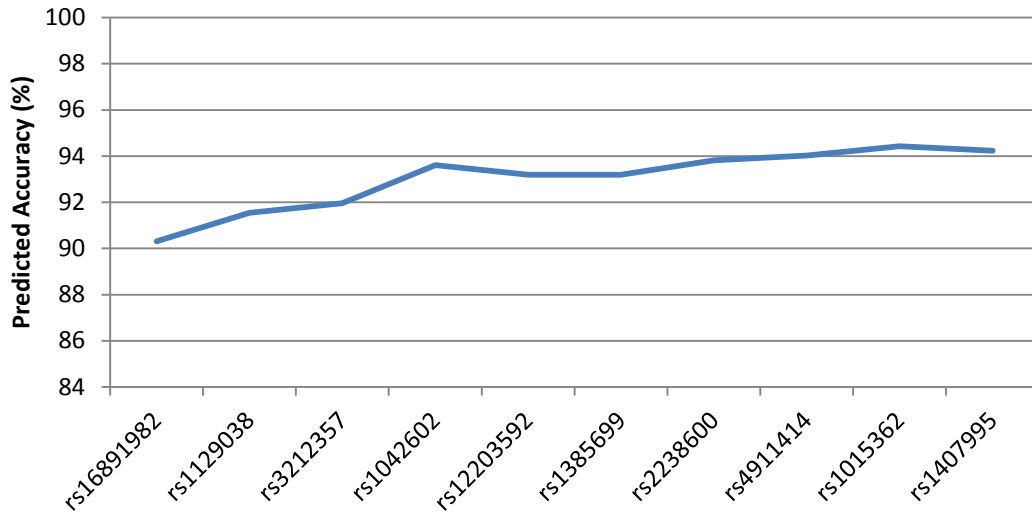


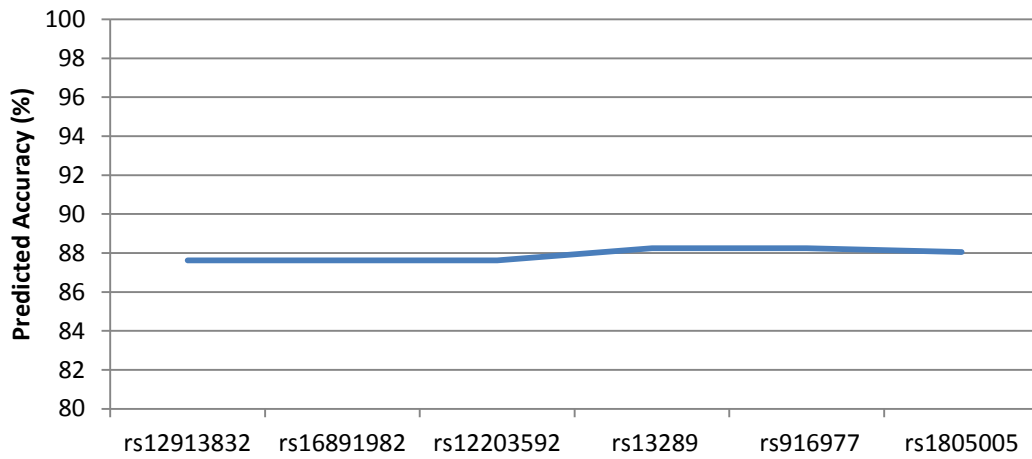
Figure 4.15 Comparison of the statistical models for the prediction of hair colour.

The predicted accuracy of each statistical model for each hair colour is compared. Values displayed are Nagelkerke R^2 values for each model indicating the goodness-of-fit.

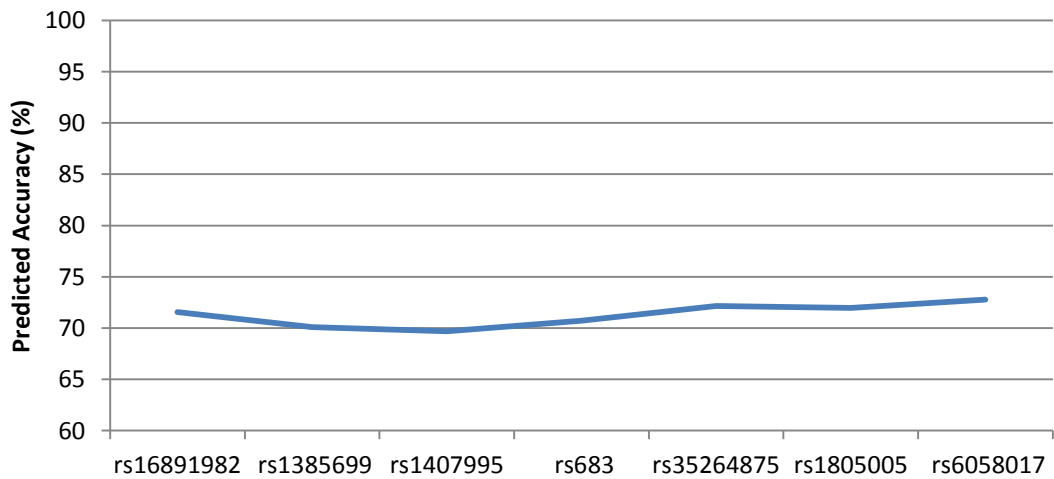
A. Black Hair



B. Blonde Hair



C. Brown Hair



D. Red Hair

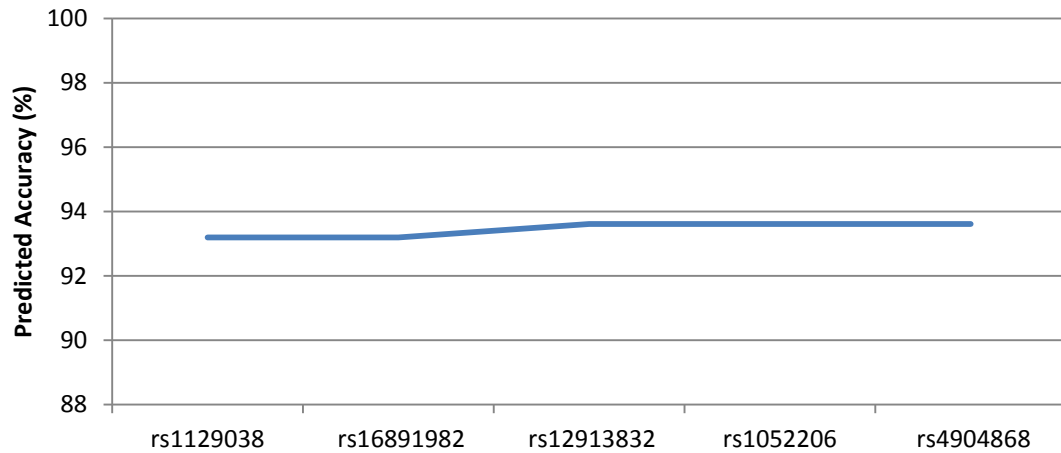


Figure 4.16 Statistical models for the prediction of hair colour.

The accuracy predicted by logistic regression analysis for A) black hair, B) blonde hair, C) brown hair and D) red hair.

Several studies [141, 142, 149, 160, 374, 378] have identified SNPs significantly associated with hair colour (Table 4.11). Of those 46 SNPs, 17 were not included in the 96-plex assay, 6 were removed from analysis and another 5 were not found to be predictive of the pigmentation phenotypes (Table 4.11). Of the remaining 18 SNPs, 6 were found to be associated ($p < 0.5$) with hair colour (Appendix 9). Three of those six SNPs (rs11547464, rs1805008 and rs1800407) were excluded from predictive analyses due to $>5\%$ missing data, and the remaining three SNPs were included in the predictive models for skin colour, eye colour and/or ancestry. The 10 SNPs which were used to predict hair colour were, in general, not closely associated with the same hair colour as reported in the literature [149, 374]. As only a few of the known SNPs strongly associated with hair colour were used to generate the predictive models, the actual accuracy of the prediction models may be expected to be relatively low.

Table 4.11 Information on 46 DNA variants reported to be strongly associated with hair colour.

SNP	Gene	96-plex SNP Panel	Used for Predictive Model ¹	
rs1015362	ASIP	I	None	
rs2378249		N	N/A	
rs4959270	EXOC2	I	None	
rs6918152		I	African American	
rs916977	HERC2	I	Blonde Hair	
rs8039195		N	N/A	
rs1667394		N	N/A	
rs7183877		N	N/A	
rs11636232		N	N/A	
rs1129038		I	Blue & Brown eyes, Dark skin, Caucasian and Hispanic	
rs12913832		I	Hazel and Green, Blonde and Red Hair	
rs1667394		I	Caucasian	
rs12203592		IRF4	I	Black Hair
rs12203592			I	Black and Blonde hair
rs1540771	I		Hispanic	
rs12821256	KITLG	I	Hispanic	
rs1805005	MC1R	I	Blonde hair	
rs885479		I	Excluded	
rs2228479		I	Excluded	
rs11547464		I	Excluded	
rs1805007		N	N/A	
rs1805008		I	Excluded	
rs1805009		N	N/A	
rs1805006		N	N/A	
rs1110400		I	Excluded	
Y152OCH		N	N/A	
N29insA		N	N/A	
rs1805005		I	Blonde and Brown hair	
rs4778138		OCA2	I	None
rs1800407	I		Excluded	
rs7495174	I		Hazel eyes, Average and Dark skin	
rs7170989	N		N/A	
rs11855019	N		N/A	
rs7174027	N		N/A	
rs4778211	N		N/A	
rs4904868	SLC24A4	I	Red hair	
rs2402130		I	None	

rs12896399		I	Green eyes
rs16891982		I	Black Hair
rs28777	SLC45A2	N	N/A
rs26722		I	None
rs1393350	TYR	N	N/A
rs35264875	TPCN2	I	Brown hair, Hazel & Blue eyes
rs3829241		N	N/A
rs1042602	TYR	I	Caucasian
rs683	TYRP1	I	Hazel eyes, Brown Hair, Caucasian and Hispanic

¹ The predictive models for which this SNP was used to generate.

I = Included in the 96-plex assay

N =- Not included in the 96-plex assay

N/A = not applicable, as the SNP was not included in the assay

4.3.5.1.4 Ancestry Prediction

As pigmentation phenotypes vary across population groups and geographical areas, it might be expected that pigmentation SNPs may also be predictive of ancestry to some degree. The probability of determining the ancestry of an individual based on the same 96-plex pigmentation SNP panel was investigated. Predictive models were generated for the three major US population groups (Caucasian, African American and Hispanic). The predicted accuracy for all three population groups was high, with African American being the highest with 96%, Caucasian at 95% and Hispanic at 92%. The strength of the association was moderate for the Hispanic model ($R^2=0.647$) and higher with both the African American and Caucasian models ($R^2=0.88$) (Fig. 4.17).

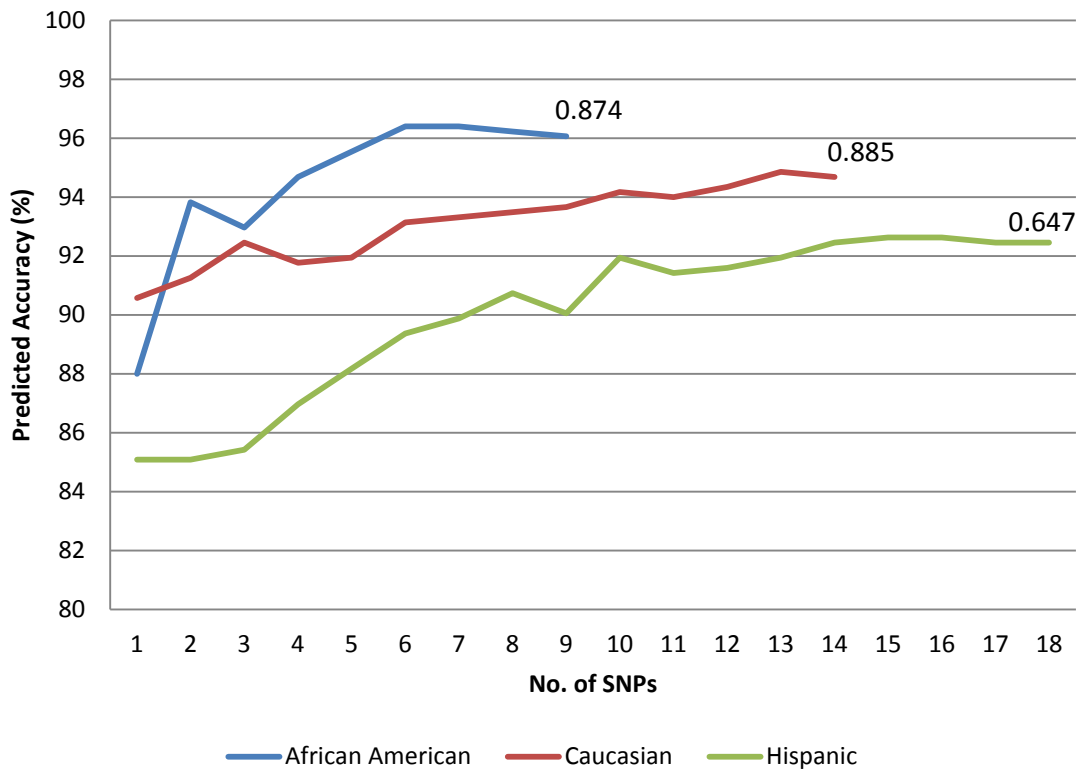
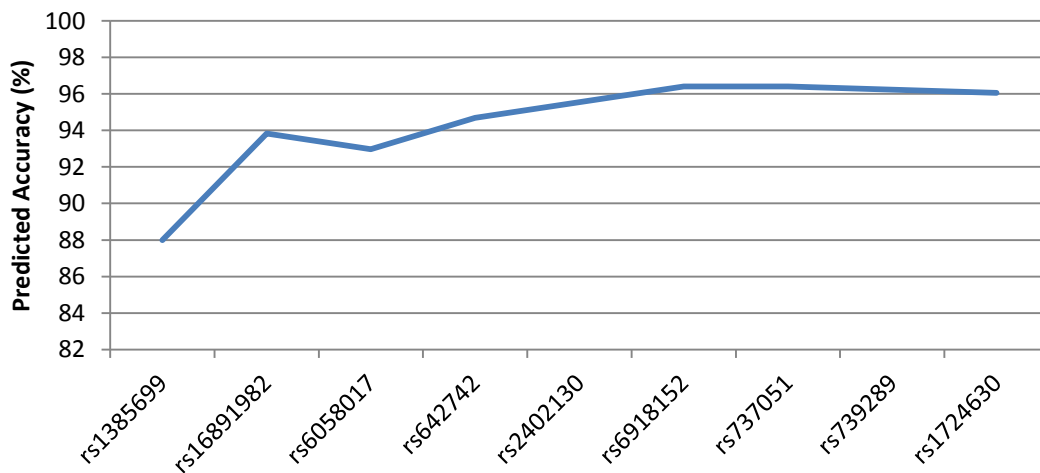


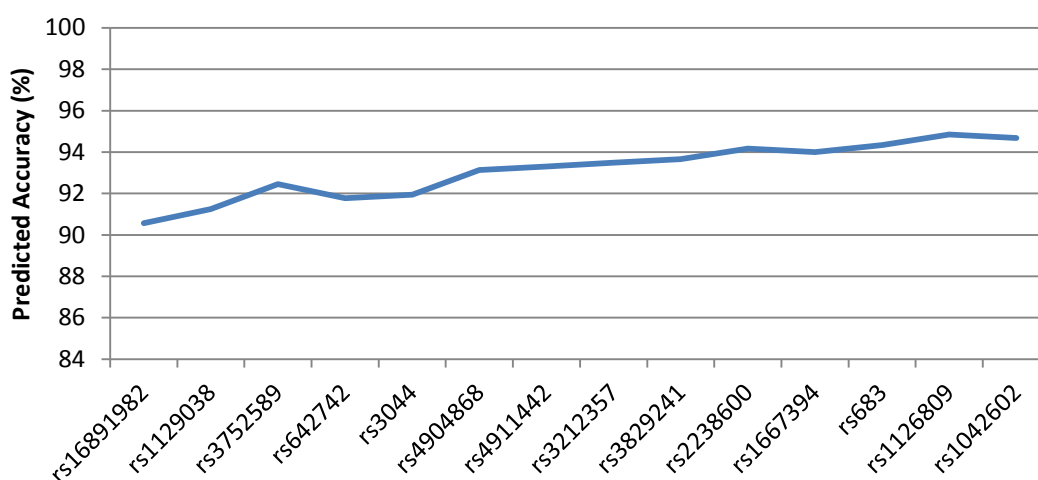
Figure 4.17 Comparison of the statistical models for the prediction of ancestry

The predicted accuracy of each statistical model for each population group is compared. Values displayed are Nagelkerke R² values for each model indicating the goodness-of-fit.

A. African American



B. Caucasian



C. Hispanic

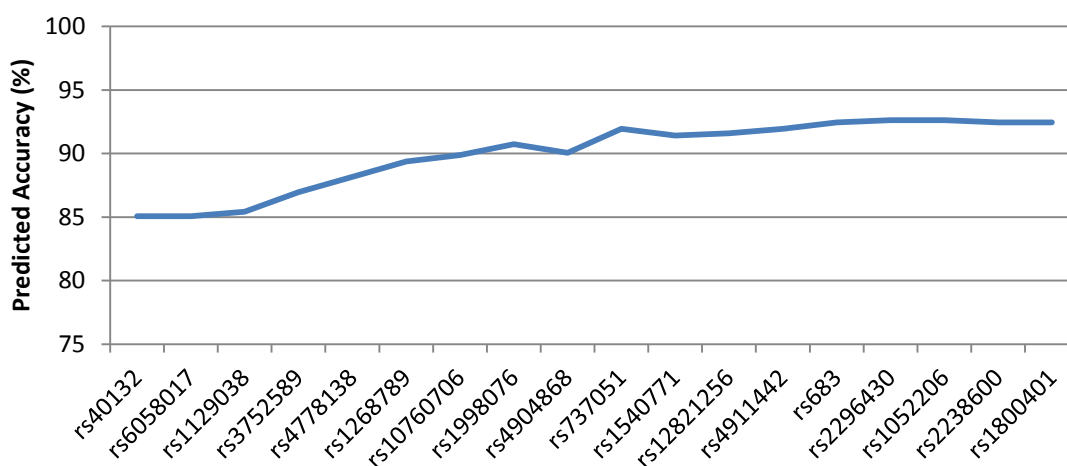


Figure 4.18 Statistical models for the prediction of ancestry.

The accuracy predicted by logistic regression analysis for A) African American, B) Caucasian and C) Hispanic populations.

Phillips et al. (2007) developed a 34-plex SNP assay which infers ancestral origin from a DNA sample with a ~99% accuracy for Caucasian, African and Asian populations. They also proposed that more than half the SNPs included were not critical for correct assignment of ancestry, but rather increased the probability in samples from an admixed population. The same authors subsequently used the 34-plex assay to predict ancestry for the major US population groups (Caucasian, African American, Hispanic and Asian) [379]. All four groups were able to be reliably assigned, but the

classification power for the Hispanic group was much lower than the other three and was presumed to be due to the higher degree of admixture within that population.

Of the 15 highest ranked SNPs in the 34-plex [135], only three were part of the 96-plex SNP assay investigated in this study (Appendix 11). This is because pigmentation SNPs, rather than AIMs, were selected for the assay. Of the three fixed difference SNPs (rs1426654, rs2814778 and rs16891982) found by Phillips *et al.* to be most informative for ancestry, rs1426654 and rs16891982 were included in the assay tested in this study. Both SNPs (rs1426654 and rs16891982) were found to be strongly associated with Caucasian ancestry with p-values of 0.005 and 7.21E-08 respectively. SNP rs1426654 was excluded from the predictive analysis due to >5% missing data, whilst rs16891982 was included in the predictive models for Caucasian and African American ancestry (Fig. 4.18), in addition to all skin colours, all hair colours and all eye colours except green.

Although the accuracy rates for the prediction of ancestry were quite high (>92%), several SNPs found to be very strongly associated in this study were excluded from the ancestry predictive models due to >5% missing data (Appendix 9). The first and second ranked SNPs for African American and Hispanic predictions (1:rs4827380; 2:rs1485682 and 1:rs1805008; 2:rs3212355 respectively) and, the second and third ranked SNPs (rs1800407 and rs1426654 respectively) for the Caucasian group were removed from analyses. If these strongly significant SNPs were included in models for the prediction of ancestry, even higher accuracies might be expected.

4.3.5.2 Accuracy of Prediction for each Phenotype

To ascertain the validity of the model predictions for each phenotype (section 4.3.5.1), logistic regressions were run on an additional 100 blind samples. The percentage of false positives, false negatives and prediction-accuracies were calculated.

In 11 of the 15 phenotype categories, the actual accuracy obtained when blind testing was lower than the accuracy predicted by the statistical model (Table 4.12). The two different accuracy predictions for olive skin and black hair were comparable (approximately 80% and 94% respectively), and the actual accuracy for hazel and green eyes was slightly higher (87.4% and 88.9% respectively) than predicted.

Table 4.12 Blind testing of the predictive models for each phenotype.

Trait	Phenotype	Predicted Accuracy (%)	Actual Accuracy (%)	False Negatives (%)	False Positives (%)
Ancestry	Caucasian	94.7	91.8	3.7	4.5
	African American	96.1	95.7	0.0	4.3
	Hispanic	92.5	89.1	6.5	4.3
Hair Colour	Black	94.2	94.3	1.9	3.8
	Blonde	88.0	80.9	9.1	10.0
	Brown	72.8	70.3	12.6	17.1
	Red	93.6	90.2	6.3	3.6
Skin Colour	Fair	78.0	69.2	14.0	16.8
	Average	89.4	72.3	25.9	1.8
	Olive	79.0	80.6	9.7	9.7
	Dark	97.1	94.1	3.0	3.0
Eye Colour	Blue	83.5	79.7	6.3	14.0
	Brown	85.9	67.4	5.1	27.5
	Hazel	84.3	87.4	7.7	4.9
	Green	85.9	88.9	11.1	0.0

* Based on predicted accuracy values in section 4.3.5.1 and 4.3.5.2
n=100 individuals

Of the four traits investigated in this study, the statistical models for ancestry had the highest accuracy rates for predictions (92.5% – 96.1%) (Table 4.12). When tested with 100 blind samples, these predictions were accurate for the three population groups. On average the actual accuracy was 2.2% lower than predicted. The percentage of false negatives and false positives assigned was the lowest in the African American population and the highest with the Hispanic samples. These findings might be expected given that the statistical model for the African American prediction was generally more robust (R^2 value = 0.874 compared to 0.647). In addition to the smaller number of Hispanic samples used to predict the statistical model, the Hispanic ethnic group is a heterogeneous population with a high level of admixture, which may also contribute to the higher error rates. These findings support those of Phillips *et al.* (2011), who reported a higher number of miscalls for Hispanic samples.

The strength of association of the Caucasian and African American models were similar ($R^2=0.885$ and 0.874 respectively), and the level of miscalls were moderate (8.2% and 4.3%) (Table 4.12). However, the actual accuracy of the Caucasian samples was slightly lower than that with the African American samples (91.8% compared to 95.7% respectively).

The predicted accuracy for all four eye colours were similar (83%-85%). The actual accuracy for green and hazel eyes when tested with the blind samples was well predicted by the models (84-86%). However the correct call rates for blue eyes and brown eyes were 3.8 and 18.5% less than predicted. This result was surprising as blue eye prediction has been reported as high (90-99%) [154, 155, 373]. However most of these studies have been performed on large datasets of mostly European populations. It has also been reported that the highest predictive values may be obtained by dividing eye colour into light (blue and green) and dark (brown and hazel) groups [154]. Although this approach may yield less miscalls, from a forensic perspective it is less discriminatory.

The predicted accuracy for skin colour was more variable with a strong prediction for dark skin (97.1%), 89% for average, and 78-79% for fair and olive skin. The actual accuracy rate when tested was notably lower for all skin colours except olive skin (Table 4.12). The determination of dark skin was the most successful with 94.1%,

followed by olive skin with 80.6%. It must be noted that the determination of average skin also resulted in an unacceptably high number of false negative (26%) calls. A high level of miscalls was also observed for fair skin using the 8-SNP model in this study yielding a 64.2% accuracy.

A similar approach to the broad eye colour classification groups (eg. blue eyes versus 'not blue') has also been used for skin colour. With a method classifying skin pigmentation as 'not white' and 'not dark', skin colour was predicted with high accuracy and a low error rate (0.5%)[162]. However, due to the conservative methods used (only homozygote genotypes were used for prediction), and the choice of SNP markers being more strongly associated with European populations, more than 50% of samples from other populations had insufficient genotyping data to predict the skin colour. This method, whilst accurate, is not robust enough for forensic use without the addition of more SNPs associated with skin pigmentation variance in population groups other than Caucasians.

Blind testing of the hair colour statistical models proved to be moderately accurate. The logistic regression analysis suggested that black and red hair could be accurately predicted ~94% of the time, and blonde and brown colours 88% and 72.8% of the time respectively. The actual accuracy for black hair was as predicted (94%), whilst those for blonde (81%), red (90%) and brown (70%) hair were all lower. The HIrisPlex is a recently developed single multiplex assay targeting 24 SNPs (6 Irisplex SNPs included) to predict hair and eye colour across worldwide populations [160]. The HIrisPlex yielded a higher accuracy than this pilot study for brown hair (78.5% versus 70%), and lower for the other three hair colours (blonde; 69.5%, red; 80% and black hair; 87.5%).

4.4 CONCLUSION

The utility of a custom designed 96-plex GoldenGate® Genotyping SNP Assay on the BeadExpress (Illumina) for application in the field of forensic science was investigated. This assay comprised SNPs known to have a strong association with hair, eye or skin colour. It was evaluated for performance with optimal genomic samples (250ng good quality template), samples of low quantity (0.5-10ng), whole genomic amplified samples, and degraded and environmentally challenged samples.

Overall the assay performed extremely well with pristine genomic samples. Seven of the 96 SNPs have been identified as routinely requiring exclusion from data analysis. Sensitivity studies have shown that the assay is quite tolerant to less DNA template than recommended by the manufacturer. The SNP multiplex has reproducibly generated complete and accurate SNP profiles for genomic samples 50-250ng. Complete SNP profiles were also observed at 10ng and 20ng. However poorer clustering (lower confidence) and low levels of miscalls are also seen at these template amounts.

A substantial reduction in SNP typing performance was observed with samples of low quality and quantity. Despite the short length of amplicons (<121bp), SNP typing of degraded bone samples exposed to certain environmental insults (freshwater, burial and surface exposed) had low success rates due to the possible combination of low amounts of degraded and damaged DNA. It appears that sub-optimal genomic samples are not suitable templates for the Illumina GoldenGate® SNP assay. The combination of time-consuming bench work, low call rates, unacceptably high miscall rates and complex (and often subjective) data analysis makes this platform undesirable for the analysis of poor quality casework samples. However, as an investigative tool, the SNP multiplex is able, to varying degrees, to predict phenotype.

External visible characteristics such as eye, hair and skin colour are complex polygenetic traits. Many genes and DNA polymorphisms are associated with variations in human pigmentation. As population groups vary in pigmentation phenotypes,

pigmentation SNPs may be expected to also infer ancestral origin of a sample. The probability of determining the ancestry of an individual based on the 96-plex pigmentation SNP panel was investigated. In this pilot study, a significant number of samples (~20%) and SNPs (27 out of 96) did not meet the strict requirements for predictive analysis due to poor performance or missing data. However, this SNP panel does hold potential for predicting traits such as hair, skin and eye colour in addition to ancestry. In fact, the most robust predictions were obtained when determining ancestry. For the three main US population groups (African American, Caucasian and Hispanic) accurate assignment of ancestry was made 89-96% of the time. The prediction of hair colour was reasonably accurate for black and red (94% and 90% accuracy), but was not as high for blonde (81%) and brown hair (70%). In general, the ability of this SNP panel to predict eye and skin colour was variable (67-89% and 69-94% respectively). The comparatively low predictive and actual accuracy of most of the traits investigated in this study were due to three main reasons:

1. Several SNPs known to be highly associated with the various pigmentation traits investigated in this study were not included in the assay because most of these more informative SNPs were reported in the literature after the candidate SNPs were selected for inclusion in the 96-plex panel tested in this study.
2. The database samples used in this pilot study were of mixed DNA quality and quantity which led to more incomplete genotypes than would have been obtained if a homogeneous sample source was used (250ng of HMW DNA).
3. An unacceptably high number of SNPs and samples were removed from the statistical analysis due to poor performance or missing data. The fact that the algorithm used to generate and test the predictive models rejects any sample with even one missing datum point was restrictive.

Although this SNP panel may provide some reliable information regarding the ancestry, eye, skin and hair colour of the donor of a DNA sample, caution must be exercised as the accuracy rates obtained were not as high as reported in literature. To improve the discriminatory value of this assay, monomorphic SNPs, and SNPs which failed to genotype should be removed, and more markers (or more tightly associated SNPs) should be included. A stronger statistical prediction for eye colour may also

result if a larger sample set from each phenotype was used to generate the predictive models. The 96-plex SNP panel genotyped using the GoldenGate® technology was not robust with sub-optimal samples such as low DNA amounts, whole genome amplified samples or even slightly degraded samples, and therefore may make this assay unsuitable for molecular anthropology and many forensic applications.

Because the majority of database and forensic samples are below the optimal concentration for direct SNP analysis (50-250ng/sample), most samples would require WGA to produce sufficient quantities of DNA. The results of this study demonstrate that although the application of WGA prior to SNP typing produces reliable results if the template for WGA is of high quality and quantity (10-80ng), the clustering of samples at each locus is more diffuse, requiring greater scrutiny during data analysis. In an effort to improve allelic imbalance during WGA prior to SNP analysis, several alterations to the standard WGA protocol were investigated. Little difference in SNP performance was observed with high quality samples. However, the split-and-pooled WGA reaction (eight aliquots) was considered the method of choice for WGA of all database samples. Although not investigated in this study, improvement in the specificity of template amplification and a reduction in amplification bias may also be achieved using a reduced MDA reaction volume [380, 381] or a modified template denaturation process [268].

Poor SNP-typing performance was worsened by WGA prior to SNP typing for sub-optimal samples. It has been noted that the amplification bias during the MDA process may have differing effects on downstream genotyping results depending on the markers used, with multiallelic STRs and SNPs appearing to be particularly problematic [268]. The amplification bias inherent in the WGA process is significantly exaggerated with samples of low quality and quantity making these samples unsuitable templates for WGA methods used in this study prior to SNP-typing. The data from this study confirm that neither direct SNP-typing (with Illumina GoldenGate® platform) nor WGA prior to genotyping is the optimal solution for genotyping highly degraded samples. Alternate SNP and DNA sequencing platforms, and methods of DNA repair may give improved results and warrant investigation.

5 Chapter Five

DNA Repair

5.1 INTRODUCTION

This chapter outlines investigations into six methods of DNA repair prior to STR-typing of highly damaged and degraded DNA samples. A selection of DNA repair techniques such as linear and circular ligation, enzymatic repair cocktails and an alternative DNA polymerase were used prior to, or in conjunction with whole genome amplification (WGA). A commercial WGA kit (FFPE REPLI-g, Qiagen) which has been designed specifically to amplify fragmented DNA from formalin-fixed paraffin embedded samples was also investigated.

DNA degradation results in fragmentation of the double helix into smaller and smaller pieces [13]. This process also effectively decreases the amount of amplifiable DNA for downstream genotyping. Once the average DNA fragment length is reduced to below 300bp, a significant loss of genetic information occurs due to lack of suitable template DNA for amplification [29]). The concept of restoring the template length in order to improve PCR or WGA (via multiple displacement amplification method (MDA) from fragmented DNA was investigated.

Degraded DNA may also exhibit various forms of damage which can significantly interfere with PCR amplification and therefore decrease genotyping success. Forms of DNA damage include nicks, oxidation, hydrolysis, pyrimidine dimers, cytosine deamination and DNA-DNA and DNA-protein cross-linkages [17, 18, 21, 27]. Oxidative damage mediated by free radicals also results in modified bases [17]. The major sites of oxidative attack on the DNA bases are the carbon-carbon double bonds in the pyrimidine rings, and the imidazole ring of purines, both leading to DNA fragmentation. Hydrolysis of the N-glycosyl bond that attaches the base to the deoxyribose backbone results in the loss of a base leaving an apurinic/apyrimidinic (AP) site that eventually forms a nick [21]. The breakdown of AP sites create nicks in the DNA, which accumulate and eventually leads to double strand breakages. Pyrimidine dimers are pairs of adjacent thymine or cytosine bases that crosslink when DNA is exposed to ultraviolet light. Photochemical exposure induces the formation of covalent linkages by localised reactions on the C=C, or T=T double bonds which stall DNA polymerase and arrest replication during PCR.

Several repair technologies such as bead hybridisation [298], ligase detection reaction with PCR [297], and pre-PCR reaction assays [299, 300] aiming to improve DNA profiling from degraded samples have been described. These methods have resulted in some improvements in genotyping. This study will focus on DNA repair methods involving linear ligation and circularisation of DNA prior to WGA and STR-typing. Such methods have been explored for forensic application [290, 296] and warrant further research. In addition, several proprietary DNA repair products have been investigated by forensic laboratories seeking improvement in the DNA typing of highly degraded, damaged and low template samples [44, 303, 382]. These initial studies had limited success, but show some potential for forensic application and warrant further investigation.

Five different DNA repair methods were investigated (Fig. 5.1). The techniques aimed to improve the degraded DNA template prior to amplification with MDA and/or STR-typing.

Table 5.1 DNA repair methods used in this study.

Treatment		Mode of Repair
1	T4 DNA ligase	Nick repair and linear ligation
2	CirLigase™ + MDA	Circularisation and MDA
3	PreCR™	Repair of abasic sites, nicks, thymidine dimer, blocked 3'-ends, oxidized guanine and pyrimidines, deaminated cytosine
4	Restorase® DNA polymerase	Modification of damaged sites by a blend of polymerases and repair enzymes
5	REPLI-g FFPE	Random ligation of fragmented DNA template and WGA

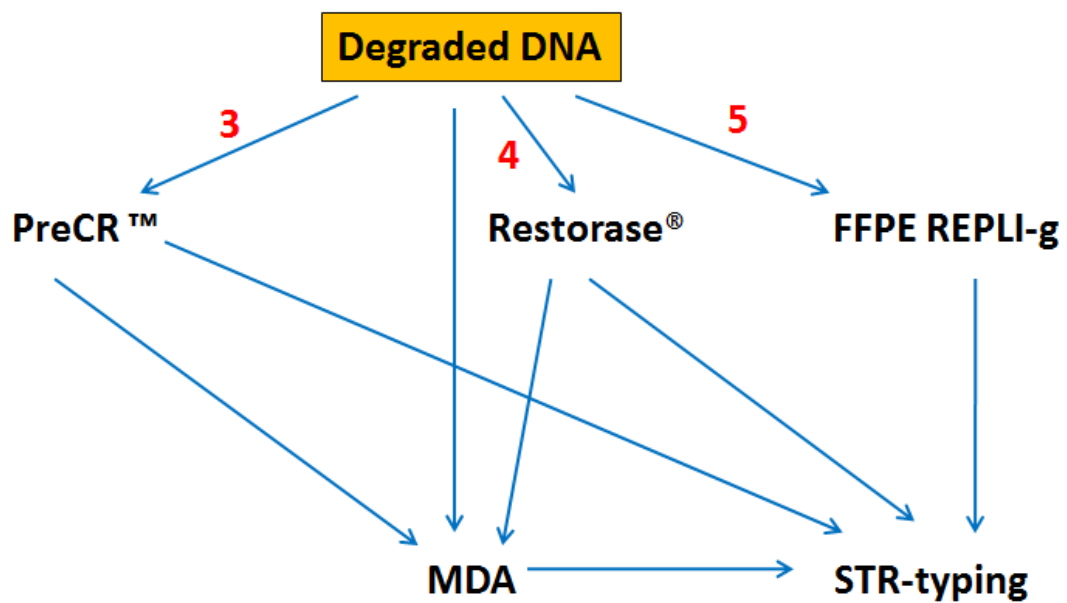
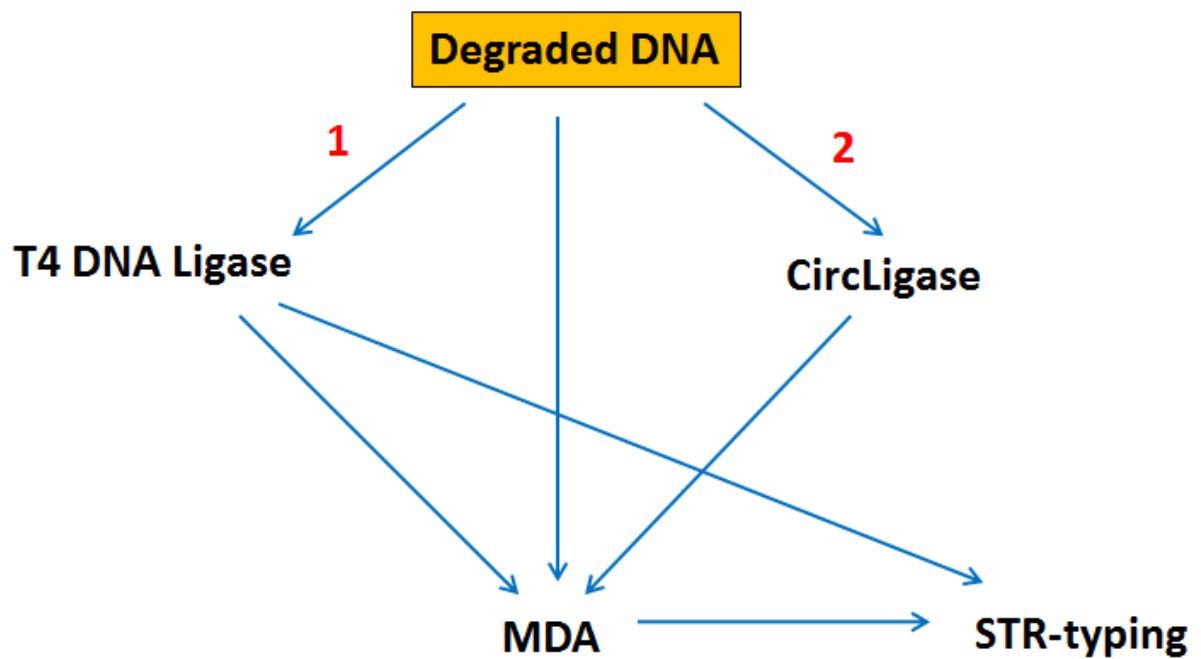


Figure 5.1 Overview of the six DNA repair methods investigated in this thesis prior to MDA and/or STR typing.

5.2 General Materials and Methods

5.2.1 DNA Extraction and Quantitation

DNA was purified from whole blood using one of two methods. Blood was extracted on the QIAGEN BioRobot EZ1 using the EZ1 DNA Blood kit (350µL) (Qiagen, Hilden, Germany). Alternatively, DNA from 10mL whole blood was extracted using QIAamp® Blood Maxi kits (Qiagen, Hilden, Germany).

The DNA extracts were quantified using a real-time quantitative PCR (qPCR) assay. This assay amplified a 63bp region of the *hTERT* locus. The primer sequences were 5'-CAGCTTCCTTCGTTGAGGAG-3' (forward primer) and 5'-GAACAGCAATGACAGGCAGA-3' (reverse primer) at a final concentration of 200mM.

The assay was performed with 4µL of 1:10 dilution DNA extract on the Rotor-Gene 6000 (Qiagen) real-time thermocycler in a 25µL reaction volume using SensiMix HRM Master Mix (Bioline). The three-step qPCR protocol consisted of an initial 15 minute 95°C *Taq* DNA polymerase activation step, followed by 40 cycles of 15 seconds of denaturation (95°C), 10 seconds of annealing (60°C) and 10 seconds extension (72°C). HMW human genomic male DNA of known concentration (Promega, Madison, WI) was used as a qPCR quantification standard (0.0254 - 25.4ng/µL). Standard curves with good linearity (R^2 values above 0.99) were accepted for analysis. No template controls were included to monitor contamination.

5.2.2 DNA Degradation

Degraded samples were generated by sonication, DNase treatment or UV irradiation. For sonicated DNA samples, the sonic probe (Branson SLPt Sonifier®, Danbury, CT, USA) was soaked in 10% bleach for 5 minutes, rinsed with sterile water and UV irradiated before and after sonication of each sample. DNA extract (0.5-1mL) was sonicated on ice with 3/32" Microtip at 30% amplitude for up to 25 minutes in cycles of 30 seconds.

A second set of samples were degraded using DNase I (New England BioLabs, Australia). Neat DNA extracts (450µL) were added to 50µL DNase I buffer. DNase I enzyme was added (0.5µL) to the DNA and incubated at 37°C. Aliquots were removed at various time intervals from 30 seconds to 5 minutes. The reaction was stopped by inactivation of the enzyme (65°C; 10 minutes). DNA samples were also fragmented using UV radiation (254nm UV lamp) for 10-120 minutes. The most degraded sample (average fragment size of 200bp) was used.

Degraded DNAs were screened to identify samples with fragments below the desired size threshold of ~300bp. DNA (2-5µL) was visualised on a 1% agarose gel as described in section 5.2.3.1.

5.2.3 Assessment of DNA Repair

DNA repair and/or WGA yield were assessed using agarose gel electrophoresis and/or STR typing.

5.2.3.1 Agarose Gel Electrophoresis

WGA products were separated using 1% (m/v) Tris-acetate-EDTA (TAE) agarose gels. Electrophoresis was performed at 110V for approximately 35 minutes in a BioRad gel system. Gels were post-stained with 2µg/mL ethidium bromide for 10 minutes, destained in distilled water for 10 minutes and then visualised with UV illumination using a GelDoc system (Bio-Rad, Richmond, CA, USA).

5.2.3.2 STR-typing

Two STR systems were used to measure any improvement in downstream genotyping after repair treatments:

1. Polymerase Chain Reaction (PCR) Quadruplex Assay

An STR quadruplex was used as a screening tool to assess any improvement in STR results prior to further downstream analysis. The four targets were TH01, TPOX, CSF1PO and amelogenin (Table 5.2). Primers were synthesised by Geneworks, Australia.

PCR was performed using a GeneAmp 9700 thermocycler (Applied Biosystems) in a 20µL reaction volume using the HotStar Taq® Master Mix Kit (Qiagen). Cycling conditions consisted of denaturation at 95°C for 15 minutes, followed by 35 cycles of 94°C for 30 seconds, 60°C for 30 seconds and 72°C for 30 seconds, with a final extension at 72°C for 10 minutes.

PCR product was analysed via capillary electrophoresis using a DNA High Resolution gel cartridge on a QIAxcel system (Qiagen, Hilden, Germany). Aliquots (1-3µL) of DNA extract were combined with DNA dilution buffer (Qiagen) to 10µL total volume and electrophoresed using the OM500 method (5kV per 500 seconds separation time). The QIAxcel system produces a digital gel image for fragment analysis.

Table 5.2 PCR amplicon length and primer sequences and concentrations of each target sequence included in the quadruplex PCR assay.

Target	Amplicon Length (bp)	Primer Concentration (nM)	Primer sequences (5' – 3')
TPOX	226-254	200	Fwd: ACTGGCACAGAACAGGCACTTAGG Rvs: GGAGGAACTGGGAACCACACAGGT
CSF1PO	296-328	400	Fwd: AACCTGAGTCTGCCAAGGACTAGC Rvs: TTCCACACACCACTGGCCATCTTC
TH01	180-204	200	Fwd: GTGGGCTGAAAAGCTCCCGATTAT Rvs: ATTCAAAGGGTATCTGGGCTCTGG
Amelogenin	106, 112	200	Fwd: CCCTGGGCTCTGTAAAGAATAGTG Rvs: ATCAGAGCTTAACTGGGAAGCTG

2. Commercial Forensic STR PCR Amplification Kits

The PowerPlex® ESI 16 PCR Amplification kit (Promega) was used for STR analysis. PCR was performed in 25µL reaction volumes on a GeneAmp 9700 thermocycler (Applied Biosystems). The cycling protocol consisted of two minutes activation at 96°C, 30 cycles of 94°C for 30 sec, 59°C for 2 min and 72°C for 90 sec with a 45 minute final extension at 60°C. Capillary electrophoresis was performed on a 3130 Genetic Analyser (Applied Biosystems). Samples were prepared for fragment analysis according to the PowerPlex® ESI 16 PCR Amplification kit instructions. Data analyses were performed using Gene Mapper ID v 3.2.1 software (Applied Biosystems) with a 50 relative fluorescence units (RFU) peak amplitude threshold for heterozygote loci and 100 RFU for homozygote loci. The stutter threshold was 15%. A partial profile was defined as the loss of one or more allele.

5.3 Whole Genome Amplification

Forensic casework samples may contain insufficient amounts of DNA template for analysis. Low amounts of DNA (<100pg) are known to be associated with problems such as exaggerated stochastic effects such as allele drop-out/drop-in, increased peak height imbalance and stutter [224, 228, 229]. One possible solution to this problem is whole genome amplification (WGA) as a means to produce sufficient quantities of DNA for reliable STR and SNP typing. WGA would also provide enough sample for additional testing and subsequent archiving. The major limitation of the WGA process is amplification bias. This may result from the under-amplification of certain regions of the genome such as centromeres, telomeres [258, 272] or regions containing a high G-C content [363], or repetitive elements [362]. This uneven amplification may result in locus and/or allelic imbalance, which may lead to sub-optimal genotyping downstream. Of the different types of WGA, multiple displacement amplification (MDA) represents the most reliable and efficient WGA protocol developed to date [272]. MDA relies on isothermal amplification utilising the high processivity and strand displacement abilities of Φ 29 DNA polymerase and the use of random hexamer

primers. The amplification bias observed with MDA is much lower compared to other WGA methods [257, 364]

5.3.1 *Materials and Methods*

WGA was performed using the GenomiPhi V2 DNA Amplification Kit (GE Healthcare, Buckinghamshire, UK).

DNA or repair product (1, 3, or 5 μ L) was diluted with sample buffer to a final volume of 10 μ L. This mix was denatured at 95°C for 3 minutes and cooled on ice. After the addition of 9 μ L of reaction buffer and 1 μ L of enzyme mix, samples were incubated at 30°C for 90 minutes followed by heat inactivation of enzyme at 65°C for 10 minutes. Degraded DNA was pre-treated with one of the repair methods described in 5.2.5.

HMW DNA template (10ng and 1ng) were each whole genome amplified in duplicate and combined. Ethanol precipitation was performed on half of the pooled reaction volume (20 μ L each). MDA product was precipitated with 2 μ L 3M sodium acetate (pH 5.2) and 40 μ L of 100% ethanol. Tubes were vortexed and incubated at -20°C for 40 minutes to precipitate the product. Tubes were centrifuged for 40 minutes at 14,000g, and the supernatant discarded. The DNA pellet was rinsed with 120 μ L of 70% ethanol and centrifuged again at 14,000g for 10 minutes. The supernatant was removed and the pellet was vacuum dried on a Speedvac (Thermo Scientific, Inc., Bremen, Germany) at medium heat for 4 minutes.

Samples were made to a final volume of 500 μ L with sterile water and centrifuged in Ultracel YM-30 columns (Millipore) at 14,000g for 8 minutes. The filter insert was inverted and centrifuged at 1,000g for 3 minutes to elute approximately 8 μ L DNA volume.

5.3.2 Results and Discussion

It has been suggested that a reduction in MDA reaction volume may decrease amplification bias and improve the specificity of template amplification [380, 381]. Because the maximum volume of repair product needs to be added to the WGA reaction, the recommended 20 μ L WGA reaction volume was used. However, the tolerance of the GenomiPhi V2 kit for using less sample buffer was tested. The recommended ratio of 1 μ L DNA with 9 μ L of sample buffer was varied to add 3 μ L and 5 μ L of DNA to 7 μ L and 5 μ L of sample buffer respectively. The same amount of DNA (1ng or 10ng) template was added to each reaction.

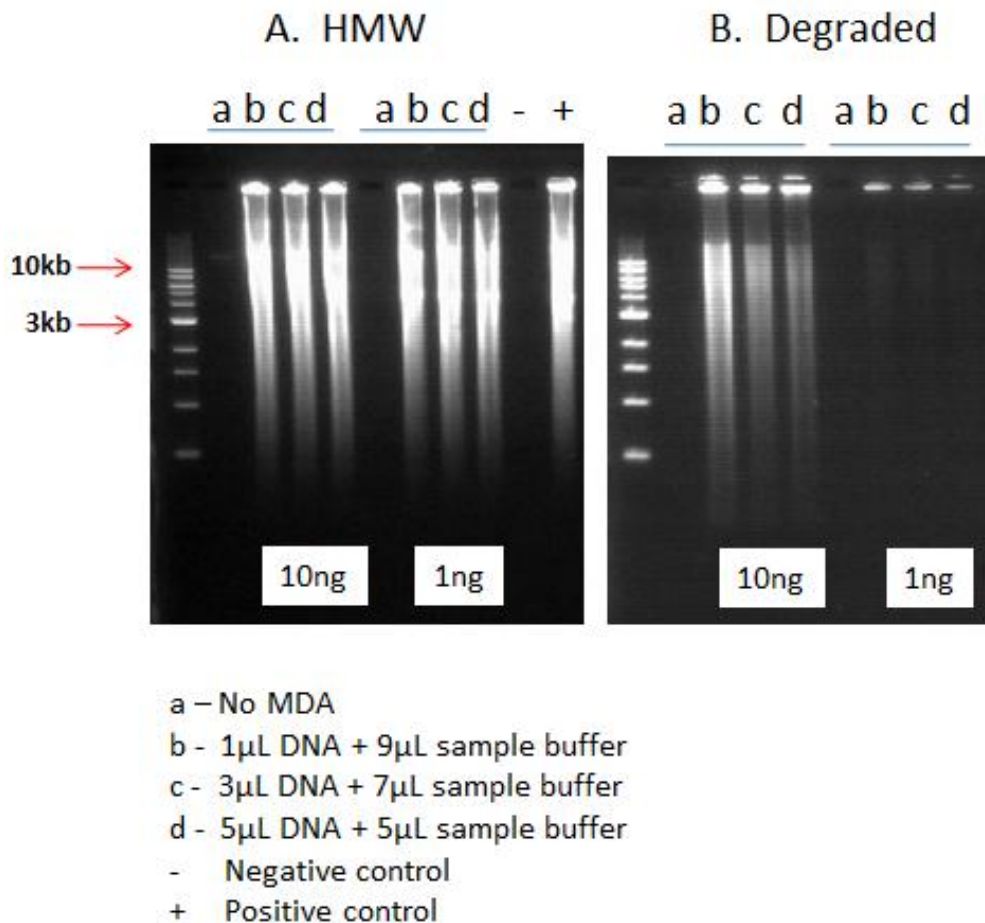


Figure 5.2 MDA product from varying DNA template volumes.

The end product (3 μ L) of GenomiPhi V2 MDA reactions using both A) HMW, and B) degraded DNA was visualised on a 1% agarose gel. To challenge the tolerance of the sample buffer, 10ng and 1ng of DNA was whole genome amplified with input volumes of 1 μ L, 3 μ L and 5 μ L. A negative control (sterile water) and positive control (10ng HMW DNA) was included in each reaction.

Decreasing the sample buffer to half volume resulted in successful WGA. Using HMW template, similarly large amounts of MDA product were seen with each combination of buffer strength (Fig. 5.2). However with degraded DNA, MDA only worked well with 10ng input. Noticeably less HMW product was visualised with 1ng of degraded template (Fig. 5.2B). This was not a surprising result as the amount of sufficient template for MDA would be greatly reduced in the degraded DNA. MDA seemed to perform slightly better with the 1µL:9µL DNA: buffer ratio showing a higher yield than the two alternate ratios tested (Fig. 5.2B Lane b).

A positive control (10ng HMW DNA) was included with each degraded DNA reaction series. Large amounts of HMW product (10kb) were generated with every set of reactions (Fig. 5.2A). A negative control (sterile water) was also included with each set of reactions and no product was visualised via gel electrophoresis in these controls (Fig. 5.2A).

Although high yields of HMW DNA after MDA were produced (Fig. 5.2), downstream STR typing did not always result in complete profiles.

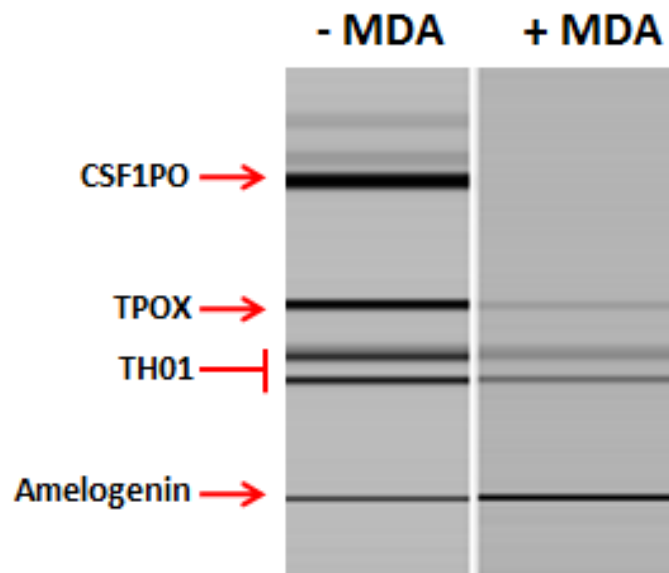


Figure 5.3 STR-typing of HMW DNA with and without MDA

Multiplex PCR amplification of HMW DNA (10ng) yielded a full 4-locus STR profile (CSF1PO, TPOX, TH01 and Amelogenin) and visualised using the QIAxcel electrophoresis system (Qiagen). However following MDA of the same HMW DNA (10ng), two loci (TPOX and TH01) showed fainter bands, and one locus (CSF1PO) was not amplified.

MDA of 10ng of HMW DNA template resulted in differential amplification since PCR analysis of four loci showed bias. Two of the four loci (TPOX and TH01) showed fainter bands, and one locus (CSF1PO) was not amplified (Fig. 5.3). This observation could be from amplification bias during WGA. Alternatively, it could reflect amplification bias in the PCR due to inhibition in the WGA reaction mix. The latter possibility was tested by adding MDA product to HMW DNA during amplification of the quadruplex STR assay (Fig. 5.4). When 10ng HMW DNA was spiked with 1 μ L of the MDA no template control (NTC), the PCR reaction showed a significantly reduced yield (Fig. 5.4). However, when the PCR reaction was spiked with a 1:100 dilution of the MDA reaction, the PCR reaction was not inhibited (Fig. 5.4). This suggests that neat MDA reagents are causing inhibition of PCR. Other studies [250, 268, 315] used 1 μ L of neat MDA product successfully in downstream STR genotyping. However, those used a previous version of the MDA kit (GenomiPhi). More importantly, the MDA product was ethanol purified prior to STR-typing (as recommended with the original GenomiPhi kit), which perhaps removed any inhibitors.

Attempts were made to overcome the PCR inhibition by purifying MDA product (via columns, ethanol precipitation or simple dilution) prior to PCR. Purification of MDA product by ethanol precipitation has been used to purify MDA product prior to PCR [250, 268, 315]. HMW DNA samples (10ng and 1ng) were whole genome amplified in duplicate and then pooled to ensure consistency. Ethanol precipitation was performed on half of the product prior to amplification with the STR quadruplex (as described in section 5.2.4).

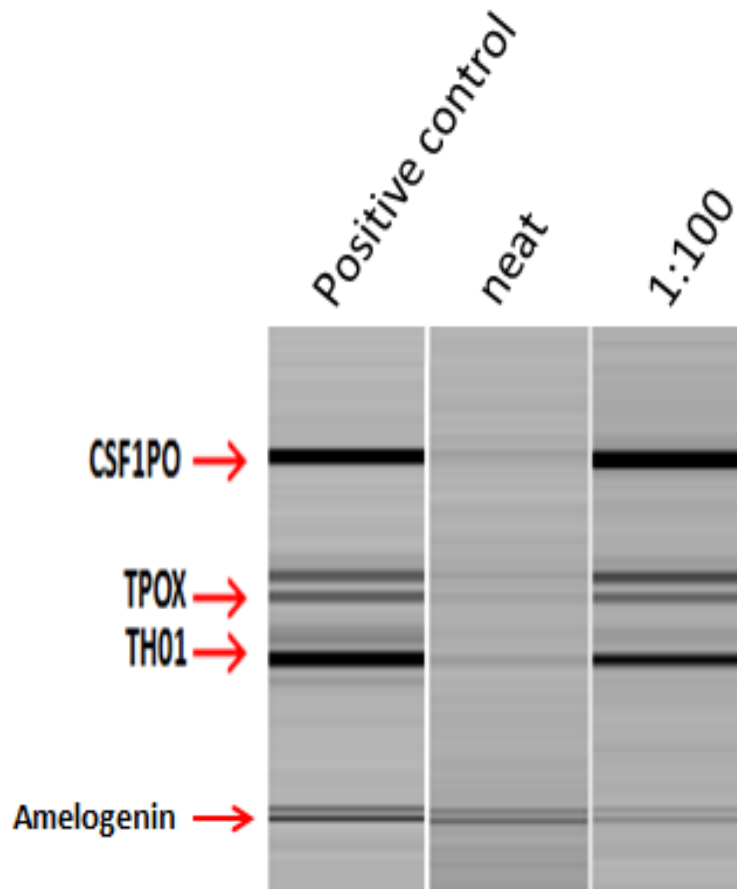


Figure 5.4 Testing for PCR inhibition due to excessive MDA reagents.

HMW DNA (10ng) was STR typed using the quadruplex PCR assay without MDA amplification (positive control). To test for PCR inhibition, the same DNA sample (10ng) was spiked with one of two agents for STR-typing: 1 μ L of the neat MDA no template control, and a 1:100 dilution of the MDA no template control.

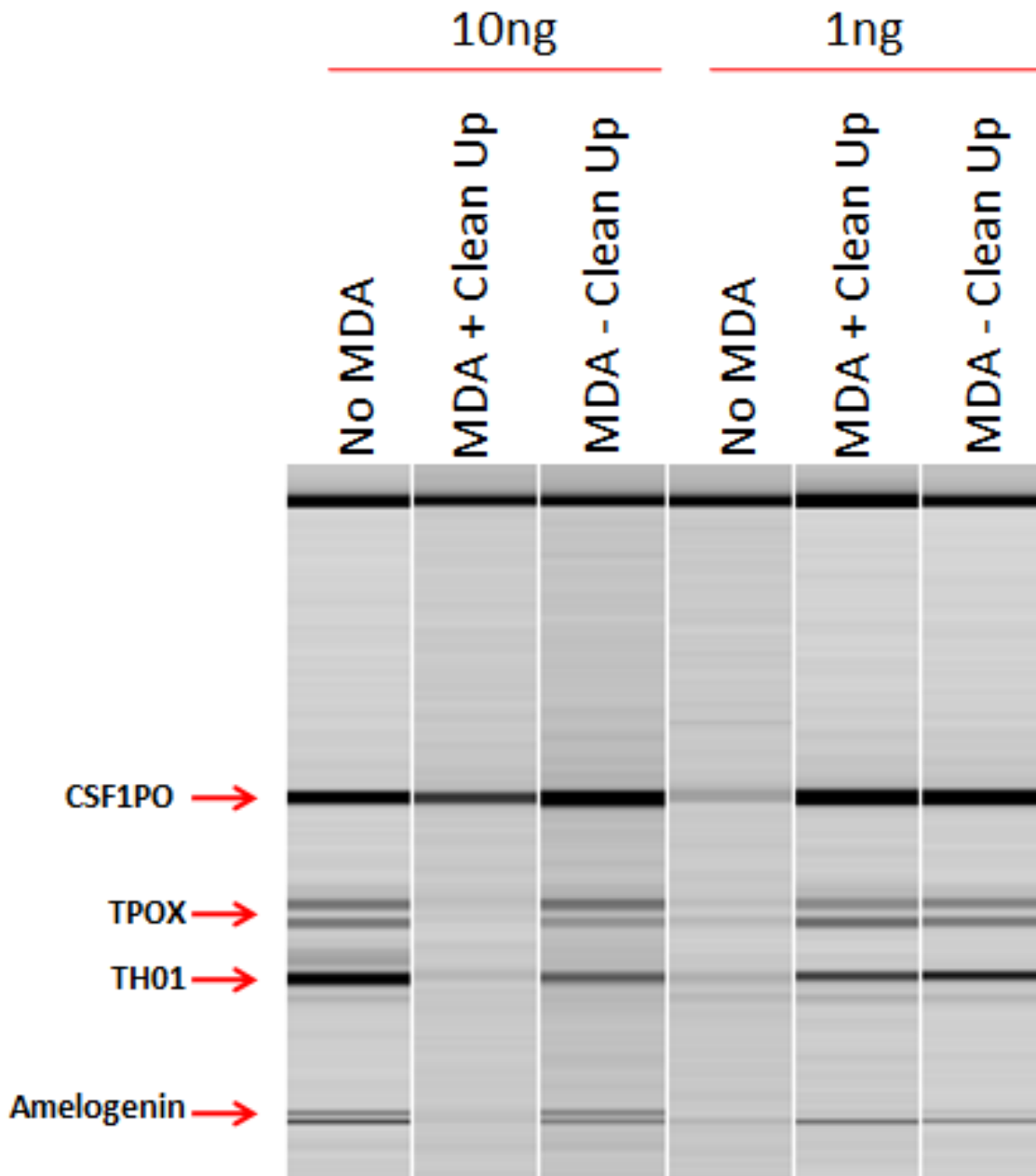


Figure 5.5 The effect of ethanol precipitation of MDA product prior to STR amplification.

HMW DNA (10ng and 1ng) was STR-typed using the quadruplex assay. The same samples were added to the GenomiPhi V2 MDA kit. The MDA product of duplicate reactions was pooled to create one homogenous sample. One half of the product was purified via ethanol precipitation, the other was not. The same amount of MDA product (with or without ethanol precipitation) was then added to the PCR reactions.

Results of the STR quadruplex (Fig. 5.5) show that in general ethanol precipitation after MDA did not improve the downstream STR typing. In fact, successful STR amplification was observed without any purification. Surprisingly with 10ng of DNA, STR results were worse than with 1ng of template. This result was repeatable but is not readily explained.

Spin columns are recommended by the GenomiPhi V2 kit manufacturer as the method of choice to purify MDA product if downstream results are poor due to inhibition [365]. MDA product was purified using Ultracel YM-30 (Millipore) spin columns or were diluted 1:100 or 1:1000 prior to STR typing to minimise PCR inhibitors. Results indicate that no significant improvement in STR profiles was obtained by filtering MDA products using columns prior to PCR (Fig. 5.6). In fact, with lower MDA template amounts more complete STR profiles were seen without filtration. This may be due to product loss during filtration. These data suggest that any PCR inhibition due to excessive MDA product or inhibitory reagents is most efficiently overcome by a 1:100 dilution of the MDA product prior to genotyping as opposed to filtration or ethanol precipitation.

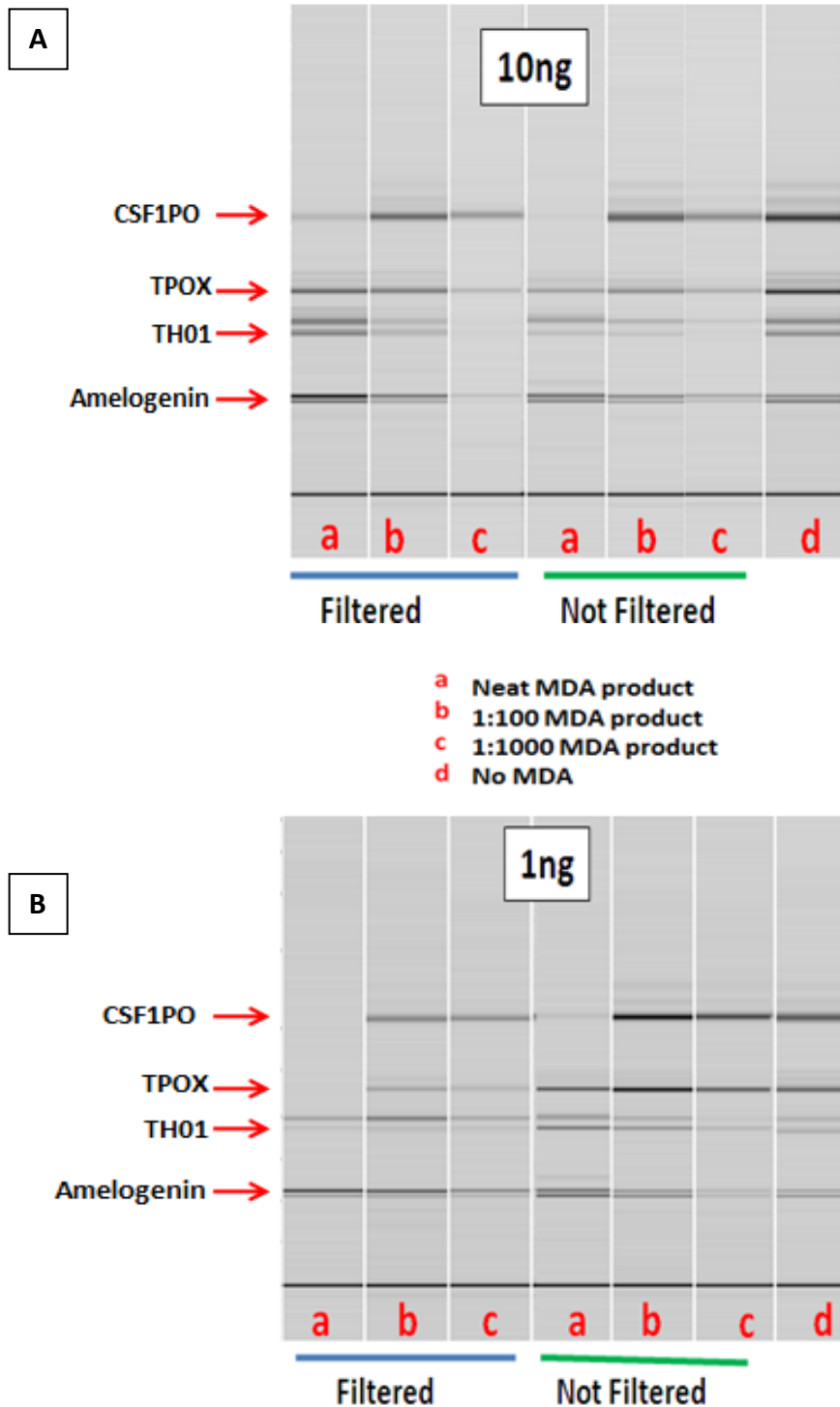


Figure 5.6 STR results of MDA product with and without spin column filtration and sample dilution prior to PCR.

A) 10ng and B) 1ng of HMW DNA was used to test the effect of spin columns and sample dilution on PCR inhibition due to MDA product or reagents. HMW DNA was STR-typed without MDA (d), or whole genome amplified prior to PCR (a-c). Half of the MDA product was purified using YM-30 spin columns. All MDA samples (filtered or not) were added to the PCR reaction a) neat, with a b) 1:100 dilution, or c) 1:1000 dilution.

MDA of degraded DNA template was unsuccessful (Fig. 5.7). This was as expected, and the average size of MDA product was smaller than prior to MDA (Fig. 5.7). Downstream genotyping of MDA treated degraded template also failed. The results of this study support previously reported MDA data [383, 384]. Yan *et. al.* report that significant genotyping errors occurred in 25% of degraded samples when whole genome amplified prior to genotyping. Another study [383] reports that MDA of artificially degraded samples (<200bp fragments) generated ample HMW product as visualised on a gel, but downstream PCR failed. It was hypothesised that small DNA fragments were too short to allow the multiple random hexamer primers to anneal and maintain MDA reaction kinetics, and that primers in the reaction served as templates for the DNA polymerase leading to primer-directed DNA synthesis. However, no NTC reactions in this study generated HMW product.

5.4 Linear Ligation + MDA

Fragments of DNA <2kb provide unsuitable templates for WGA [289]. The inability of Φ 29 DNA polymerase to prime from short fragments may be the predominant reason that MDA fails to amplify such highly degraded samples. The T4 DNA ligase repairs nicks and ligates dsDNA through the formation of a phosphodiester bond between a 5' phosphate and a 3' hydroxyl group. The enzyme can be used to ligate fragments with staggered or blunt ends. T4 DNA ligase can also ligate small fragments of dsDNA together forming concatamers. Use of T4 DNA ligase should increase the length of the DNA molecules which may then be a suitable template for MDA. However, initial studies have shown that T4 ligation of both double and single stranded template to be inefficient [290, 291]. This study investigates the utility of T4 DNA Ligase treatment to improve fragmented DNA template prior to MDA and STR-typing.

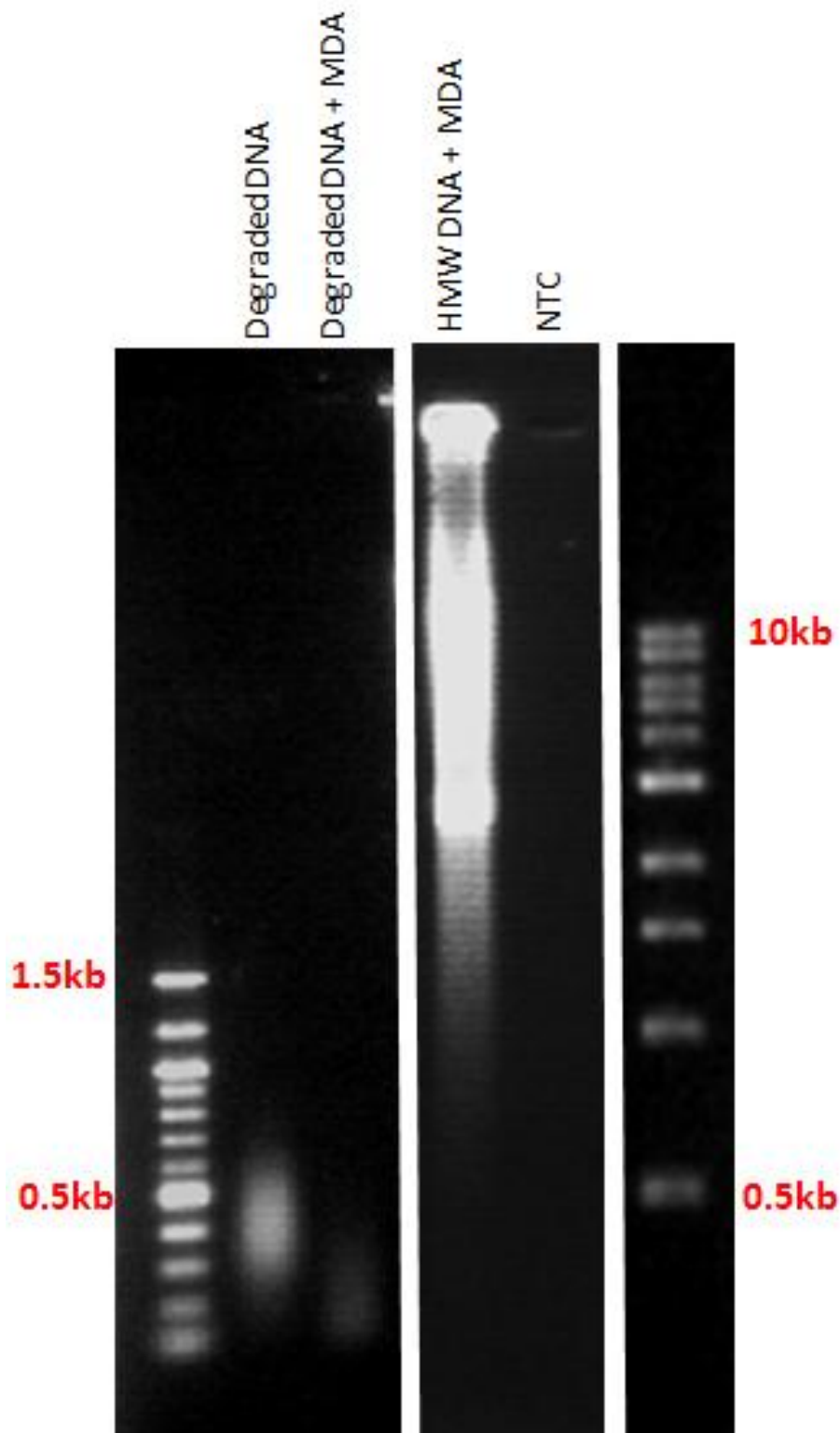


Figure 5.7 Agarose gel electrophoresis of MDA product from degraded and HMW DNA template.

Degraded DNA samples before and after MDA were visualised via gel electrophoresis. HMW DNA (10ng) was used as a positive control, and sterile water was added as an NTC during MDA.

5.4.1 Material and Methods

T4 DNA ligase reactions were performed with 10 and 100ng of degraded DNA template (n=2) in a 10 μ L reaction volume. T4 DNA ligase (1 or 5 units) (Life Technologies, Carlsbad, CA) was added to reaction buffer (50mM Tris-HCl (pH 7.6), 10mM MgCl₂, 1mM ATP, 1mM DTT and 5% (w/v) polyethylene glycol-8000) and incubated at 14°C for 18 or 21 hours (Fig 5.8). Ligated product was purified prior to MDA or STR-typing using Ultracel YM-30 columns (Millipore) as described in 5.3.1. 10ng of DNA (with or without T4 DNA ligation) was loaded onto a 1% agarose gel.

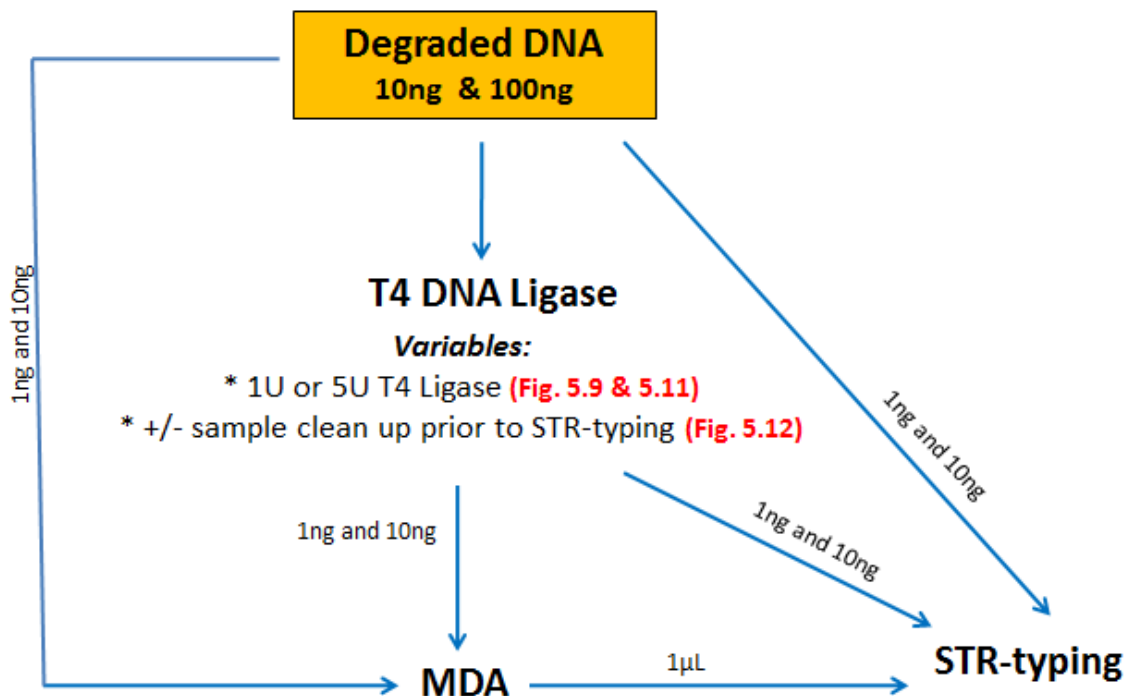


Figure 5.8 Workflow overview of the linear ligation of degraded DNA samples prior to MDA and STR-typing.

Degraded DNA (10ng and 100ng) was added to a T4 DNA Ligase reaction with 1U or 5U of enzyme. Samples were either purified with spin columns or added directly to MDA or the STR quadruplex assay. Degraded DNA (1ng and 10ng) was also added directly to the MDA and PCR. MDA product (1 μ L) was added directly to the STR PCR.

5.4.2 Results and Discussion

Linear ligation of highly fragmented dsDNA was attempted in order to increase template length prior to MDA. The recommended T4 DNA ligase input for blunt end ligation is 1U per reaction, or for difficult to ligate substrates an increase to 5U is suggested by the manufacturer. After ligation, the samples (10ng and 1ng) were whole genome amplified to determine if the increased ligase concentration had any benefit (Fig. 5.8).

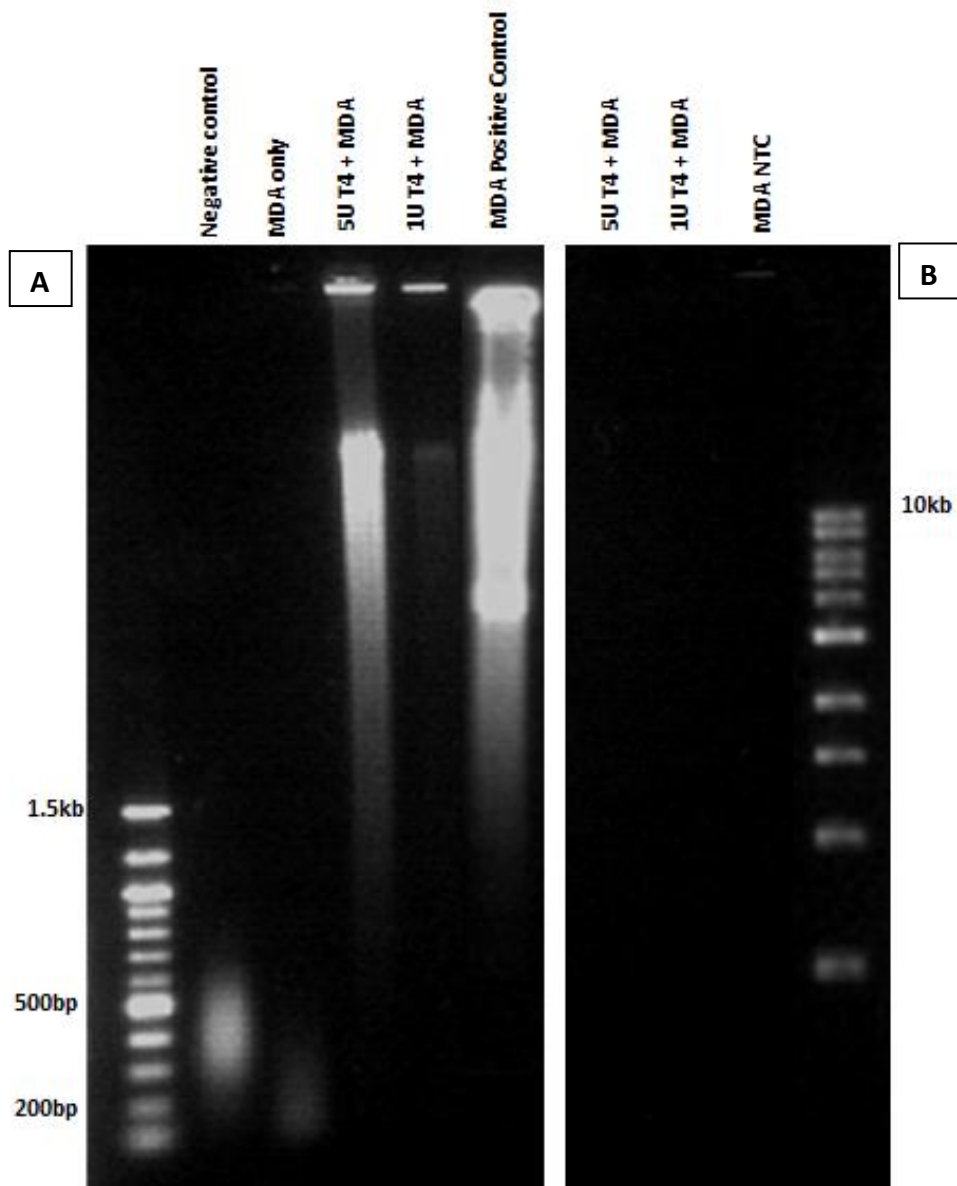


Figure 5.9 Gel Electrophoresis of degraded samples treated with T4 DNA ligase and whole genome amplified.

Linear ligation and MDA of A) 10ng and B) 1ng of degraded DNA template. T4 DNA ligation was performed with 1U and 5U of enzyme. 10ng of the degraded DNA was also added to the MDA reaction without prior T4 DNA ligation. The untreated DNA sample was added directly to the gel as a negative control. The MDA positive control was 10ng HMW DNA and sterile water was used as the NTC.

After MDA of 10ng template, HMW product was detected for samples treated with 1U or 5U of T4 DNA ligase. The yield was significantly higher using 5U enzyme. MDA of the degraded DNA sample without ligation was unsuccessful (Fig. 5.9A).

The high amount of MDA product may be due to addition of the large amounts of degraded DNA (10ng). Sufficient copies of larger less degraded fragments may have been available and acted as DNA template for MDA. Input of 1ng of the same degraded failed to produce any HMW DNA following the same T4 and MDA treatments (Fig. 5.9B). No spurious product was seen in the MDA negative controls.

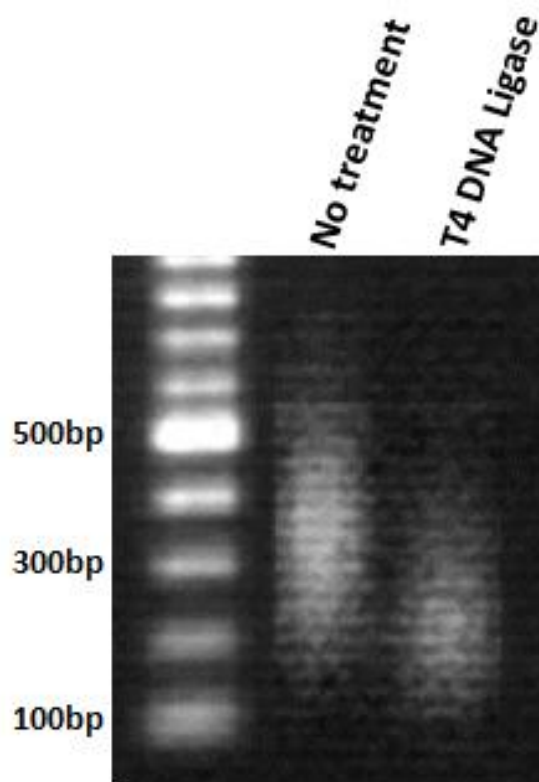


Figure 5.10 The average fragment lengths of the degraded sample before and after linear ligation

T4 DNA ligation was performed with 100ng of degraded DNA. 10ng of DNA from each sample (with and without T4 DNA ligase treatment) was visualised using a 1% agarose gel stained with ethidium bromide.

As previously discussed (section 5.3.2), the average size of fragments after MDA was smaller than before MDA (Fig. 5.7 and 5.9A). Surprisingly, this result also occurred with the ligase treatment. The average size of DNA fragments was 350bp before ligase treatment, compared to 250bp after ligation (Fig. 5.10). This is not an artefact due to dilution of the reduced amount of DNA in the ligation reaction, as this was compensated for prior to electrophoresis (Section 5.4.1). A possible explanation is contamination of reagents with DNases. The experiment was repeated using a different batch of reagents, but the same end result was observed. This failure of T4 DNA ligase to increase template could not be readily explained.

A quadruplex STR assay was used to screen for any improvement in genotyping after ligation and/or MDA of the degraded template. Degraded DNA (10ng and 100ng) was added to 10 μ L T4 DNA ligase reactions. One tenth of the reaction volume (1 μ L) was used for downstream STR and MDA reactions (~1ng and 10ng DNA input amounts). Degraded DNA (1ng and 10ng) was also used directly in MDA and STR reactions for comparison.

The genotype of the sample was heterozygotic at all four loci. All eight alleles were amplified in all HMW samples (10ng and 1ng). MDA with 10ng input was also successful in generating a complete STR profile. However, amplification bias was observed during MDA of 1ng of template as amplification of the three largest loci in the quadruplex (CSFP10, TPOX and TH01) resulted in allele drop out (Fig. 5.11B).

PCR of the degraded samples produced partial profiles. T4 ligation did not improve downstream STR typing of these samples. Ligation of 100ng of DNA using both 1U and 5U of DNA ligase produced STR profiles with one less allele (CSF1PO) than direct PCR of the untreated degraded sample (Fig. 5.11A). STR results from T4 DNA ligase treated samples with less DNA (10ng) were also poor. No alleles were amplified with 1U of T4 DNA ligase (Fig. 5.11B).

STR results were significantly worse when T4 DNA ligase treated samples were whole genome amplified prior to STR typing. Significant amplification bias resulted from MDA as evidenced by differences in band intensities, allele and locus dropout (Fig. 5.11A).

Control MDA reactions with 1ng and 10ng of HMW DNA showed full STR profiles indicating successful MDA amplification (Fig. 5.11A and B). However, PCR of the whole genome amplified degraded templates (10ng and 1ng) resulted in failure to amplify a single allele. Both negative controls (MDA+PCR and STR) generated blank STR profiles (Fig. 5.11A and B).

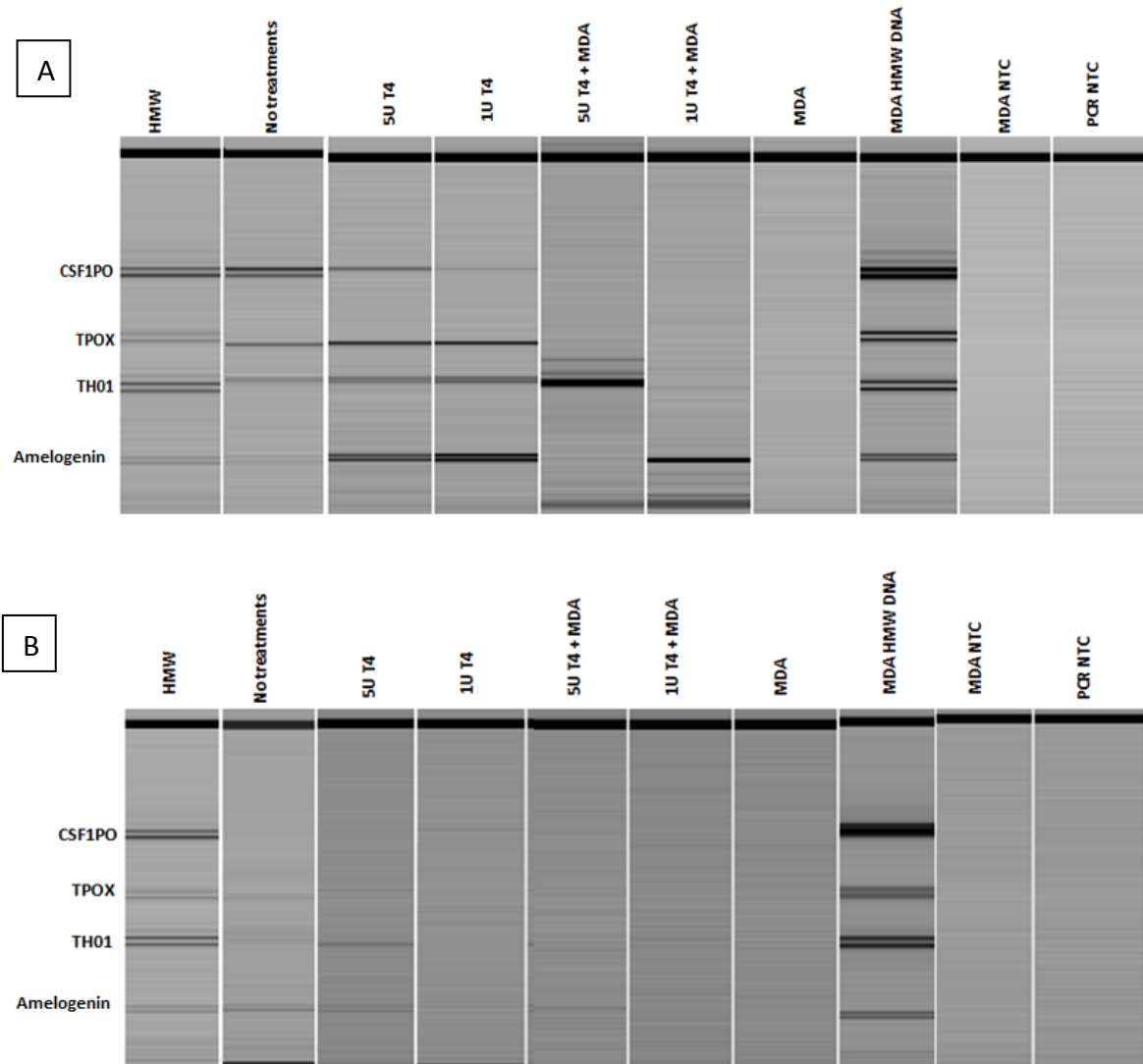


Figure 5.11 STR results of MDA and T4 DNA ligated samples with A) 10ng and B) 1ng DNA template.

HMW DNA was used as positive controls for STR-typing with and without MDA prior to the PCR. This same DNA sample was artificially degraded, and subsequently treated with T4 DNA ligase (1U and 5U). These ligated samples were then added directly to the PCR, or whole genome amplified using the GenomiPhi V2 MDA kit prior to STR-typing. Degraded DNA was also added directly to both the MDA and multiplex PCR reactions. MDA and PCR NTC (sterile water) controls were included.

These data suggest that 5U of T4 ligase enzyme per reaction does not improve the template yield for MDA or STR typing of degraded samples. However, ligation with 5U T4 DNA ligase generated slightly better results than ligation with 1U of enzyme.

Neither T4 ligase, nor MDA of DNA, improved the STR typing of the degraded sample. Although DNA of T4 ligase treated samples generated sufficient amounts of HMW DNA after MDA (Fig. 5.9), improved downstream STR genotyping did not occur. Possible explanations include not enough T4 'repaired' product is being generated or added to the MDA reaction (maximum of 5 μ L) for successful amplification. Alternatively, the MDA product or reagents themselves may be inhibiting PCR. However simple dilution of the MDA product has been shown to minimise any PCR inhibition due to MDA reagents (section 5.3.2). Lastly, by-products or residual proteins in the T4 DNA ligase reaction may be inhibiting the MDA reaction. Polyethylene glycol (PEG)-8000 is a component of the high concentration T4 DNA ligase reaction buffer. Carry-over of high amounts of PEG from the ligase reaction may interfere PCR but this species is 8,000 Daltons in size and should be eliminated by the 30,000 Dalton size exclusion filter in the Millipore spin columns. Spin columns (YM-30, Millipore) were used to investigate whether any carry-over products from the T4 ligation were hindering MDA.

The most complete STR profile from degraded DNA was obtained without MDA (Fig. 5.12). Three out of four loci were successfully amplified from degraded samples without any treatment (lane 1). The largest locus, CSF1PO (~300bp) did not amplify. MDA only (lane 2) showed poor amplification results. Very faint bands at the middle two loci demonstrate significant amplification bias.

Treatment with T4 ligase only (without MDA) (lanes 3 and 4) yielded similar STR results than untreated DNA with three out of four loci amplified. However, amplification was not balanced with less DNA (1ng) showing a significant decrease in amplification of the larger locus (TPOX at ~250bp). T4 DNA ligase did not lead to an improvement in STR results (i.e. could not resolve the missing 300bp locus).

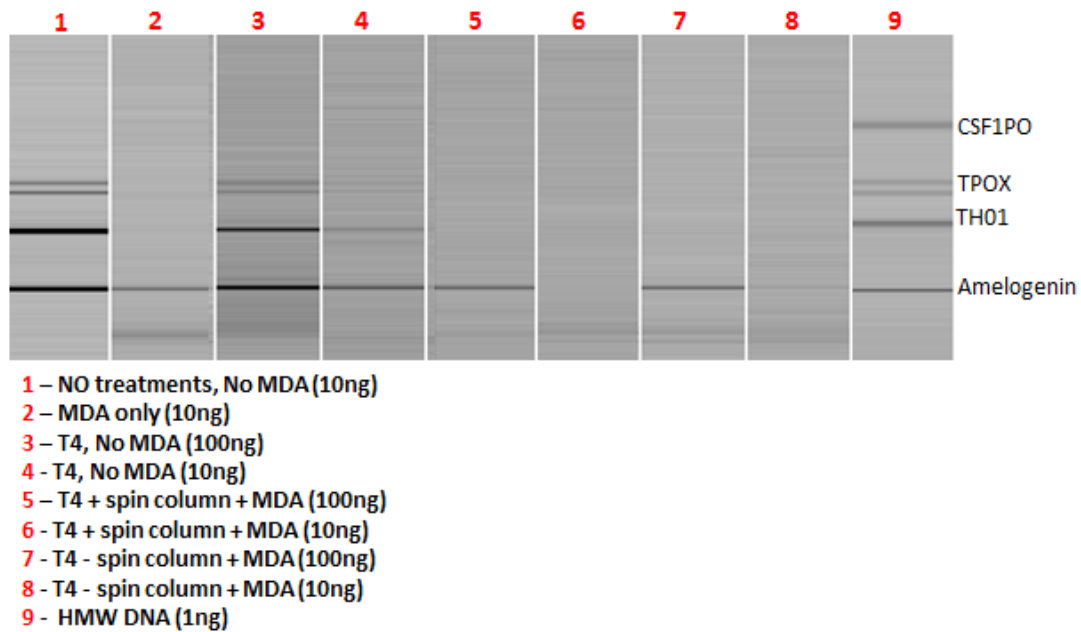


Figure 5.12 Quadruplex PCR results of degraded DNA samples repaired with T4 DNA Ligase prior to MDA and STR-typing.

Degraded DNA (100ng and 10ng) was added to T4 DNA ligase reactions. The ligation product was either added directly to the PCR, or filtered using a spin column prior to PCR. Degraded DNA was also added directly to MDA and PCR reaction for comparison. A HMW control was also included for STR-typing.

All T4 ligase + MDA (regardless of filtration) performed poorly. With 100ng of degraded DNA, only one of the four loci was amplified, whilst no loci at all were amplified with 10ng DNA. Filtration of T4 ligation products prior to MDA did not improve STR results. Additional concerns with filtration of products include inconsistent volume yield, loss of DNA template, extra sample handling and increased risk for contamination.

The results indicate an inherent failure of MDA to amplify highly degraded DNA samples. In addition, linear ligation of fragmented DNA templates was unsuccessful in improving downstream MDA or STR-typing.

5.5 CirLigase™

The bacteriophage has a circular single stranded viral genome, which is replicated by a Φ 29 DNA polymerase. Therefore the circularization of highly fragmented DNA (<200bp) may provide a more suitable template for Φ 29 DNA polymerase via Rolling Circle Amplification (RCA). CirLigase™ (Epicentre® Biotechnologies) efficiently circularises short ssDNA templates (>30 bases) with almost no formation of linear or circular concatamers. CirLigase™ has been shown to successfully circularise ssDNA fragments prior to RCA for applications such as genome walking [292], RNA sequencing [293] and WGA [294]. Studies optimising CirLigase™ conditions for low amounts of fragmented DNA have shown promising results [295, 296].

5.5.1 *Materials and Methods*

Double stranded degraded DNA (n=3) were denatured by heating at 95°C for 3 minutes and then snap cooled on ice prior to circularisation. Various CirLigase™ conditions were investigated (Fig. 5.13). Ligase reactions were performed in 10 μ L or 20 μ L reaction volumes using the CirLigase™ II ssDNA ligase enzyme (EPICENTRE, Madison, Wisconsin). Degraded DNA template (1-150ng) was added to 50U of enzyme in 1X CirLigase™ II reaction buffer and 2.5mM MnCl₂. The manufacturer's 55-nucleotide (nt) single-stranded oligodeoxynucleotide was included with each assay as a positive control. CirLigase™ product was visualised via polyacrylamide gel electrophoresis (PAGE). 15% TBE-Urea Ready Gels (Biorad) were electrophoresed at 150V for 50 minutes. CirLigase™ reactions were purified prior to MDA or STR-typing using Ultracel YM-30 columns (Millipore) as described in 5.3.1.

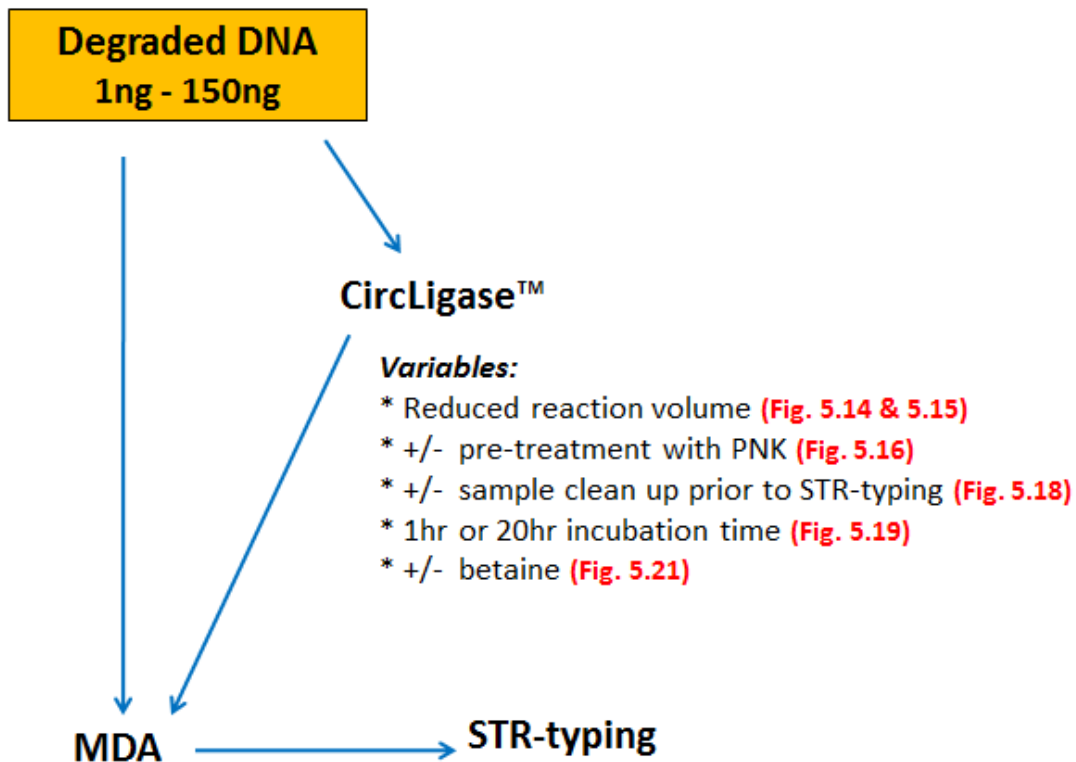


Figure 5.13 Workflow overview of circular ligation of degraded DNA samples.

5.5.2 Results and Discussion

It was important to add the maximum volume of each CirLigase™ reaction (and therefore maximum DNA) into the MDA reaction. Although 1µL input of sample is recommended by the manufacturer, as demonstrated in section 5.3.2, the GenomiPhi V2 MDA kit can tolerate a DNA input volume of 5µL (section 5.3.2). In order to maximise the amount of CirLigase™ product being added to the MDA reaction, a reduced CirLigase™ reaction volume was tested. The recommended reaction volume was halved to 10µL. The 55nt control single stranded oligo supplied in the kit was circularised and then visualised using PAGE. The results showed that circularisation was not only successful with a reduced volume, but also a greater proportion of the DNA can be loaded into any downstream reactions (Fig. 5.14).

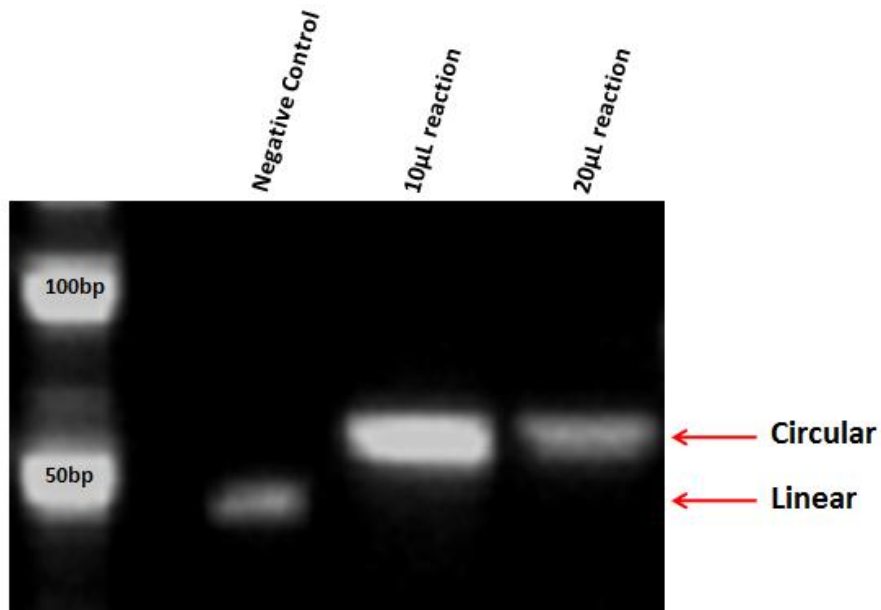


Figure 5.14 Circularisation of the control oligo provided in the CirLigase™ kit.

Circularisation was performed in a 10µL and 20µL reaction using the 55nt synthetic ss-oligo provided. The ligated product was visualised via PAGE. The control ss-oligo was added directly to the gel as a negative control.

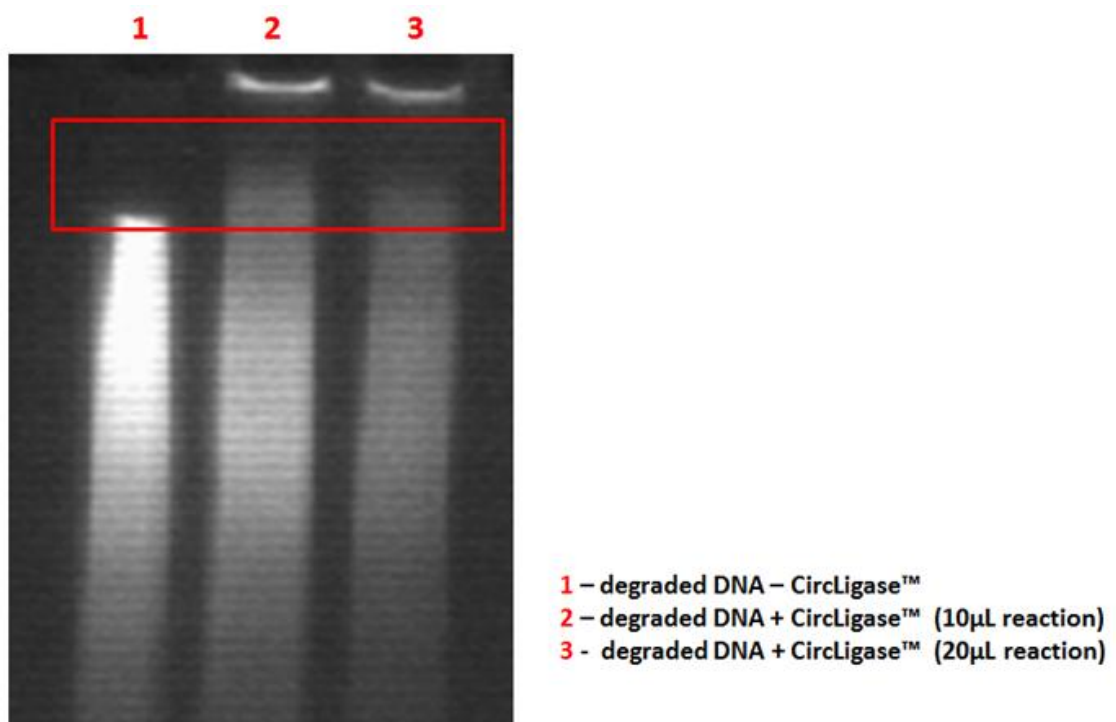


Figure 5.15 Circularisation of highly degraded DNA

Artificially degraded DNA (150ng) was added to 10µL and 20µL reactions and visualised via PAGE. The degraded sample was also added directly to the gel for comparison.

The increase in the size of the fragments, shown in Fig. 5.15, may indicate circularisation of degraded DNA. Successful circularisation of each degraded sample was difficult to assess due to the small size shift, and the heterogeneous nature of the sample (a smear of DNA comprised of various fragment lengths). In addition, DNA samples below 10ng were unable to be visualised via PAGE, and routine screening of CirLigase™ product prior to MDA would result of a significant loss of product. Therefore, any improvement in template quality was assessed by product yield after MDA. However this is not confirmation that CirLigase™ had worked with the degraded samples. Successful circularisation of the ssDNA oligo (55nt) was used as an indication that the reaction chemistry and conditions were working for the control template.

CirLigase™ requires linear substrates that have both a 5'-phosphate and a 3'-hydroxyl group. The artificially degraded samples used in this study may have lost the 5'-phosphate group. Therefore phosphorylation of both the degraded DNA and T4 ligated products was performed with T4 polynucleotide kinase (PNK) to ensure that the 5' ends of the linear ssDNA templates were fully phosphorylated prior to ligation. Phosphorylation of DNA prior to circularisation did not improve the template for MDA. As before, no MDA product was produced following any of the CirLigase™ treatments with or without PNK pre-treatment.

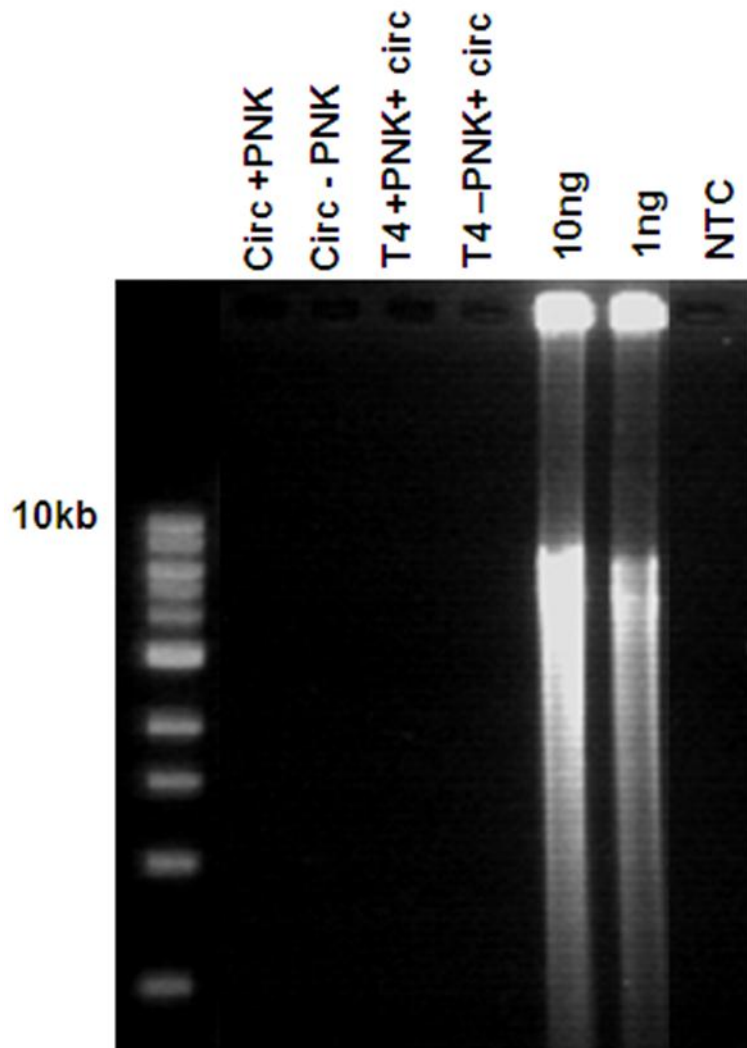


Figure 5.16 The effect of T4 polynucleotide kinase (PNK) treatment of degraded DNA and T4 DNA ligated templates prior to circularisation and MDA.

CirLigase™ was performed with 10ng of degraded DNA, and 10ng of T4 DNA ligated product. These templates were, or were not pretreated with PNK prior to circularisation. All circularised samples were added directly to the downstream MDA reactions. HMW DNA (10ng and 1ng) was added to the MDA as positive controls. Sterile water was used as a NTC during MDA.

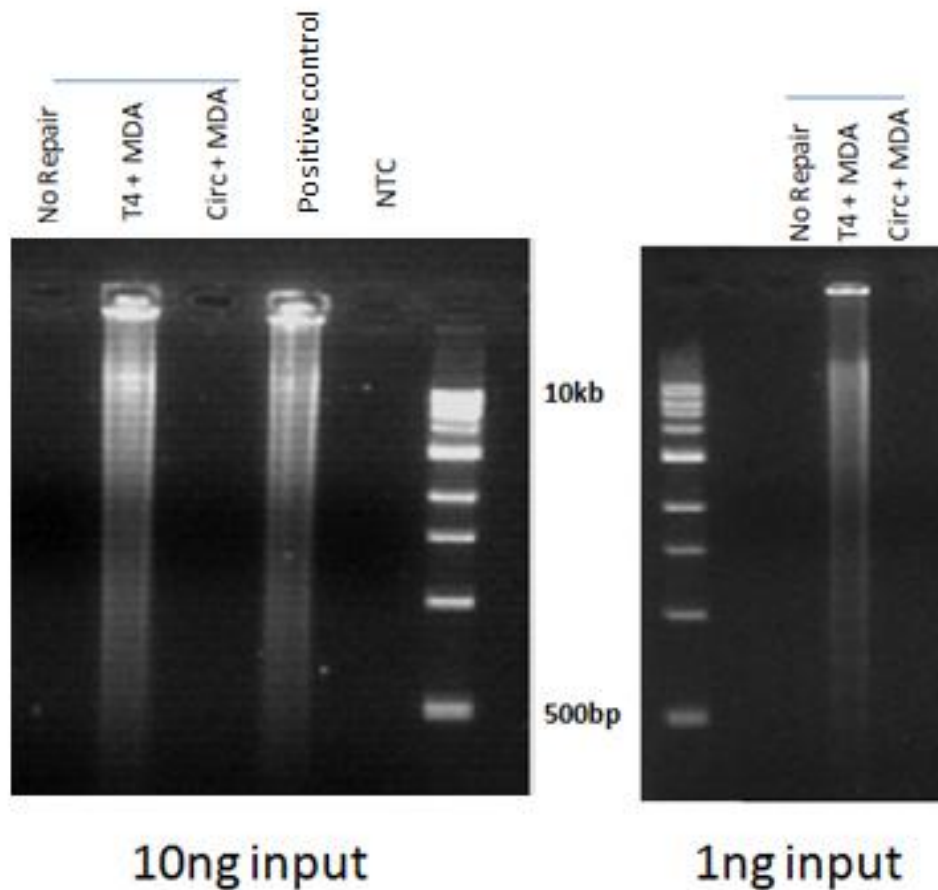


Figure 5.17 MDA yield using linear and circular ligated samples as templates.

Degraded DNA (10ng and 1ng) was added directly to MDA and visualised via agarose gel electrophoresis. The same DNA sample was pretreated with T4 DNA ligase or CirLigase™ prior to MDA. HMW DNA (10ng) was whole genome amplified as positive controls. Sterile water was used as a NTC during MDA.

When 10ng and 1ng of degraded DNA was circularised prior to MDA, no visible product was observed (Fig. 5.17). It was thought that reagents from the CirLigase™ reaction may be inhibiting the MDA reaction. The CirLigase™ reaction was filtered using Microcon YM-30 spin columns prior to MDA to assess any difference in MDA yield after sample clean-up was performed prior to MDA.

Results showed that filtration after CirLigase™ product prior to MDA resulted in HMW product. To confirm inhibition of MDA by CirLigase™ reaction elements, HMW control DNA (10ng) was spiked with CirLigase™ product (lane 11, Fig. 5.18) prior to MDA resulting in significant inhibition.

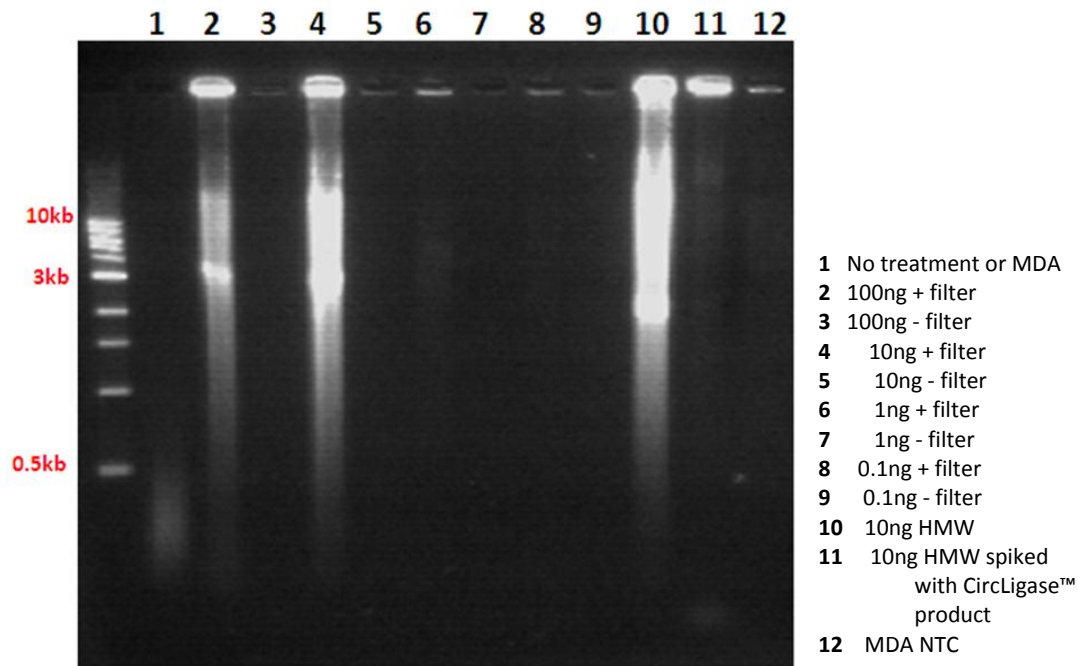


Figure 5.18 MDA yield of Circligase™ treated template with and without filtration prior to amplification.

DNA (100ng, 10ng and 0.1ng) was added to Circligase™ reactions. Circularised product was, or was not purified using YM-30 spin columns prior to WGA. HMW DNA (10ng) was whole genome amplified as a positive control (Lane 10). The same HMW positive control was also spiked with 4µL of the Circligase™ NTC reaction (Lane 11). Degraded DNA was added directly to the agarose gel as a negative control (Lane 1).

As with the T4 DNA ligase treatments, an increased yield of HMW DNA product after MDA does not necessarily indicate an improvement due to circularisation. With an input of large amounts of degraded DNA (>10ng), enough copies of longer DNA fragments may be available as templates for MDA. This result was consistent across all repair methods and MDA performed with 10ng in this study. Some HMW product was observed with ≤1ng DNA, the yield was significantly reduced (Lanes 6 and 8, Fig. 5.18). The amount of DNA available for analysis with degraded forensic casework samples is often less than 1ng.

The effect of a longer incubation time on circularisation of highly degraded samples was also investigated. The manufacturer recommends a one hour incubation, but also suggests that a prolonged incubation (up to 16-20 hours) may improve yield [290]. The incubation time was found to not affect yield for 150ng DNA. However, with less template (1.5ng), a slightly improved yield of HMW DNA was produced after MDA (Fig. 5.19).

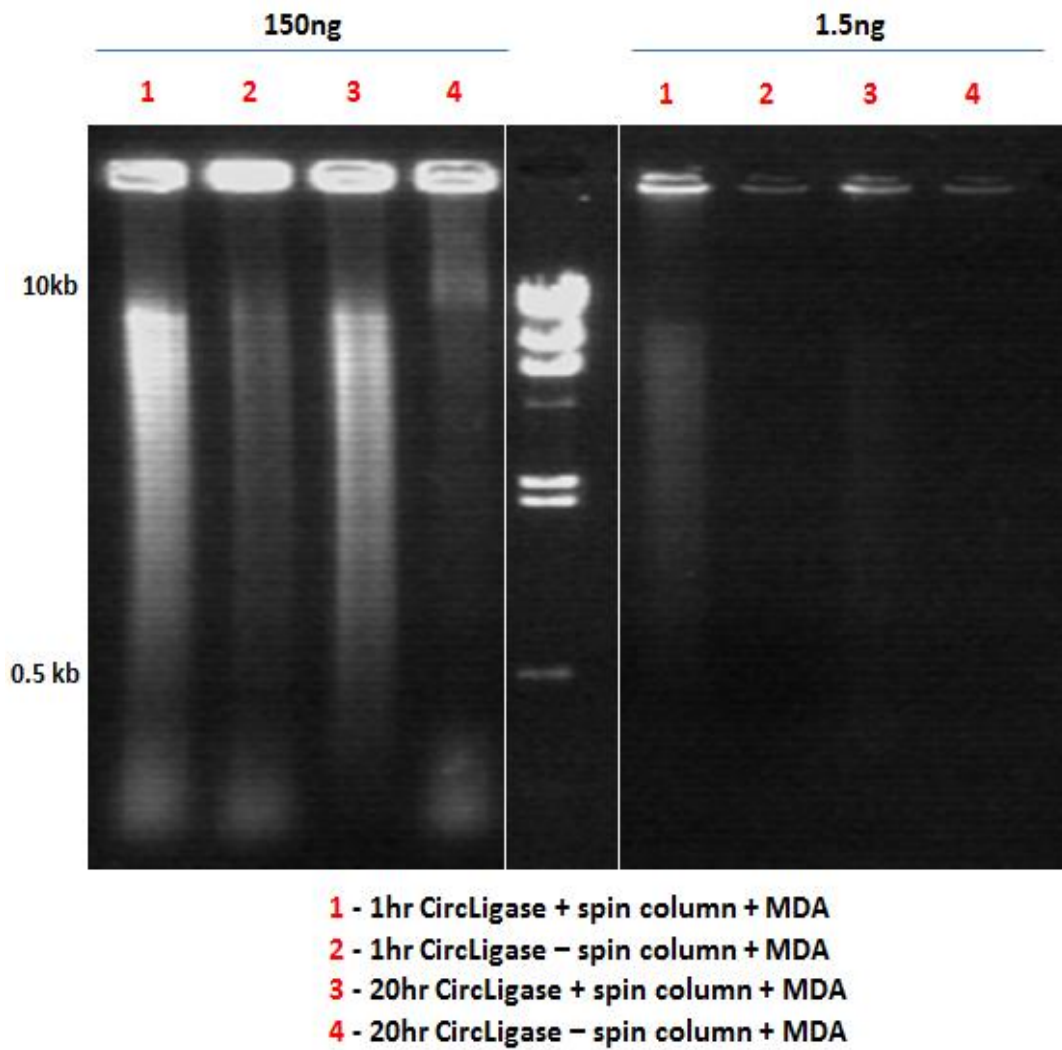


Figure 5.19 MDA yield of Circligase™ product with and without sample purification prior to a 1 hour or 20 hour incubation.

Degraded DNA (150ng and 1.5ng) was added to each Circligase™ reaction and incubated for 1 or 20 hours. Sample purification was performed on half the samples using YM-30 spin columns. The same amount of sample was added to each MDA reaction. MDA product was visualised on a 1% agarose gel.

Although sufficient HMW product is observed via gel electrophoresis after MDA (Fig. 5.19), STR-typing was not successful. STR typing of T4 DNA ligase and Circligase™ treated degraded samples prior to MDA (Fig. 5.20) was poor.

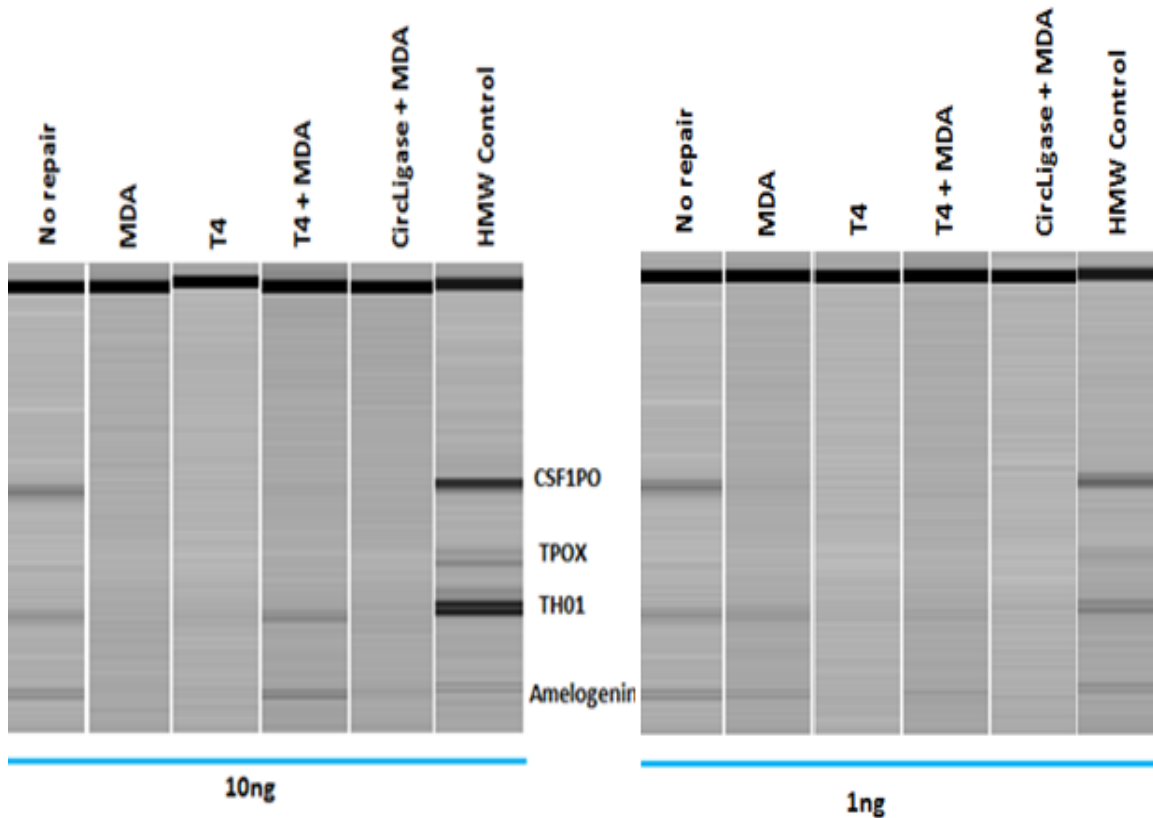


Figure 5.20 STR-typing of degraded DNA samples treated with T4 DNA Ligase, Circligase™ and MDA prior to PCR.

Degraded DNA (10ng and 1ng) was added to T4 DNA ligase, Circligase™ or MDA reactions prior to STR-typing. Degraded DNA was added directly to the PCR and MDA reactions as negative controls (no repair). HMW DNA was also amplified as a positive control and confirmation of the STR genotype. Fragment analysis was performed on the QIAxcel electrophoresis system (Qiagen).

The addition of betaine (1M final concentration) to the CirLigase™ reaction has been reported to improve the circularisation of difficult to ligate fragments [385]. The CirLigase™ reactions were performed with and without betaine on either 50ng of fragmented DNA or the same DNA pre-treated with T4 DNA ligase. The sample was purified using YM-30 filters (as described 5.2.4) and then whole genome amplified. There was no improvement in the STR typing. It therefore appears that MDA did not work with these suboptimal templates.

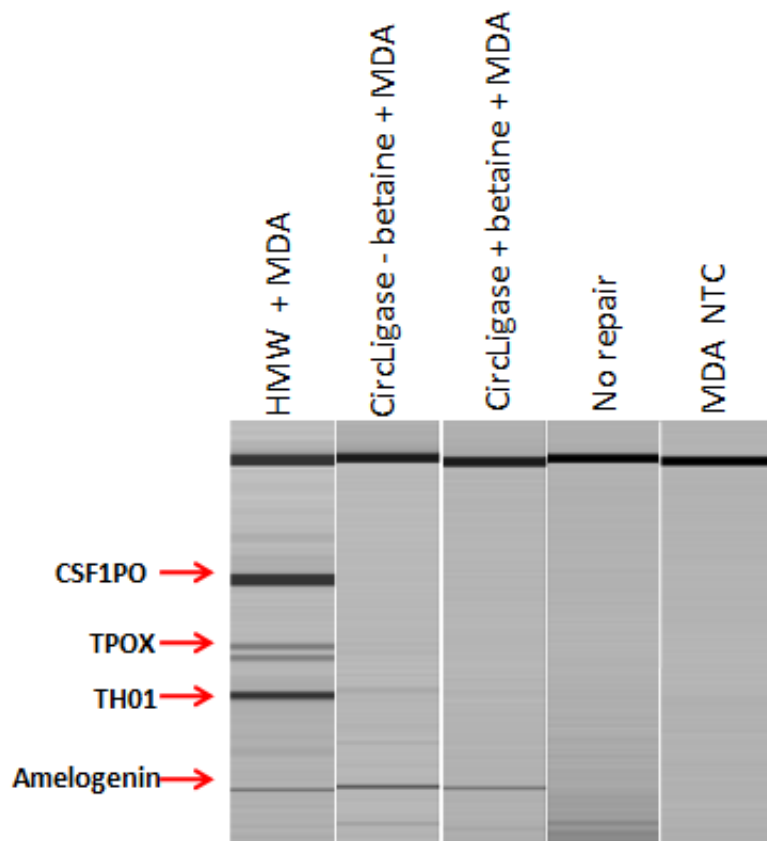


Figure 5.21 Results of PCR amplification of CirLigase™ treatment with and without the addition betaine prior to MDA.

Degraded DNA was added to the CirLigase™ reaction with and without the addition of betaine (1M final concentration). All circularised samples were whole genome amplified prior to genotyping with the quadruplex STR assay. Degraded DNA was also added directly to the PCR reaction as a negative control (no repair). HMW DNA (10ng) was added to the MDA reaction as a positive control. A MDA NTC consisted of adding sterile water instead of DNA during MDA. This MDA NTC reaction was subsequently added to the STR PCR reaction.

5.6 PreCR®

PreCR® Repair Mix (New England BioLabs®) is a commercial cocktail of enzymes that repairs DNA lesions such as nicks, abasic sites, thymidine dimers and oxidative damage (Table 5.3) [301]. The repair mix contains *Taq* DNA Ligase, Endonuclease IV, *Bst* DNA Polymerase, Fpg, Uracil-DNA Glycosylase (UDG), T4 Endonuclease V and Endonuclease VIII [301]. PreCR® will not repair all damage (eg. fragmentation) which interfere with PCR. The ligase (*Taq* DNA ligase) will seal nicks, but cannot ligate blunt ends. Hydrolysis (resulting in AP sites and nicks), oxidation (pyrimidine dimers and oxidised bases) and UV radiation (thymidine dimers) are forms of damage that are common in environmentally challenged samples. Previous studies evaluating the effect of PreCR® treatment on UV damaged samples have been mixed [302, 382]. Some have shown moderate increases in the retrieval of STR loci and peak height values, but the general consensus is that inconsistent results are observed when used with forensic samples [303].

Table 5.3 Types of damage repaired by PreCR®. [301]

DNA Damage	Cause	Can it be repaired by the PreCR Repair Mix?
abasic sites	hydrolysis	yes
nicks	hydrolysis nucleases shearing	yes
thymidine dimers	UV radiation	yes
blocked 3'-ends	multiple	yes
oxidized guanine	oxidation	yes
oxidized pyrimidines	oxidation	yes
deaminated cytosine	hydrolysis	yes
fragmentation	hydrolysis nucleases shearing	no
Protein-DNA cross-links	formaldehyde	no

5.6.1 *Materials and Methods*

DNA (n=4) was artificially degraded using DNase I treatment and UV exposure as described in section 5.2.2. and visualised by agarose gel electrophoresis (Fig. 5.22). The degraded samples (in duplicate) were repaired using the PreCR[®] mix prior to WGA and STR-typing (Fig. 5.23).

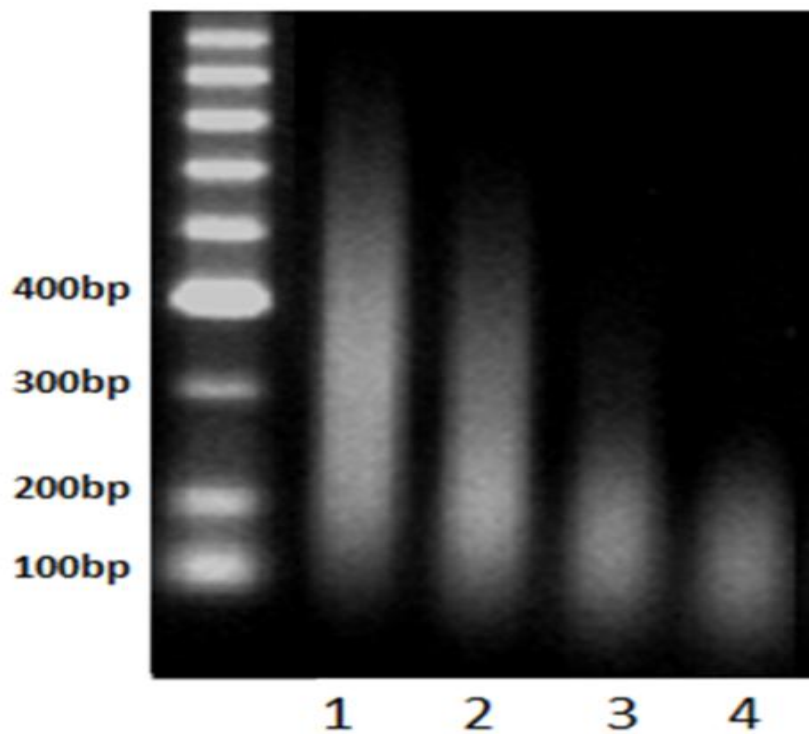


Figure 5.22 Artificially degraded samples used for PreCR[®] treatment prior to MDA and/or STR typing.

HMW DNA was artificially degraded using DNase I to create four samples with different levels of fragmentation. DNA was visualised via electrophoresis on a 1% agarose gel. Samples 1-4 show increasing levels of degradation as measured by a decreasing in average fragment length.

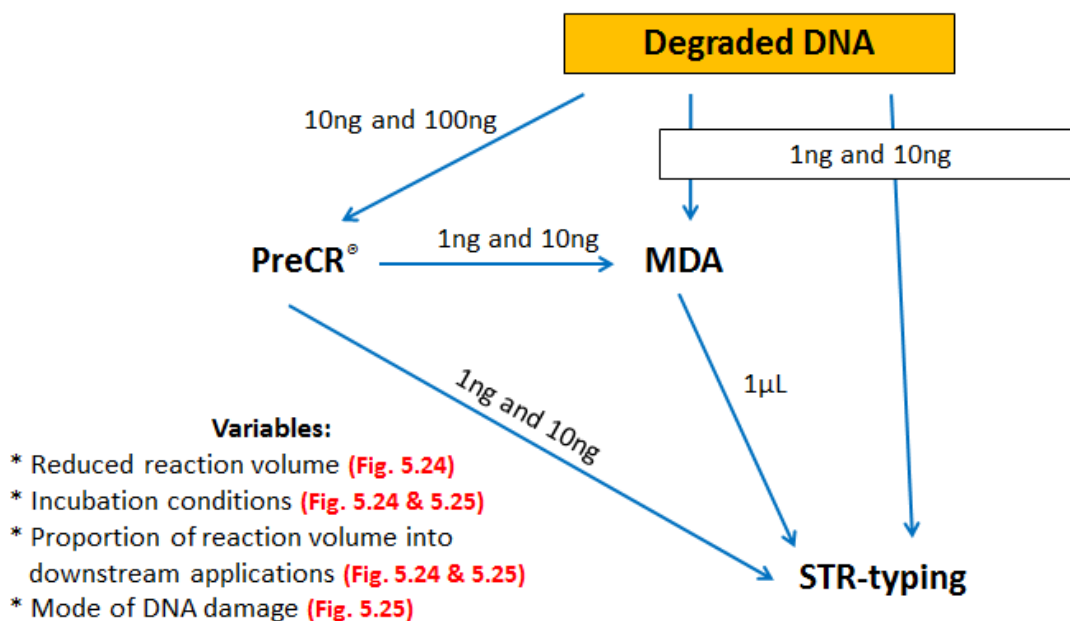


Figure 5.23 Workflow overview for the repair of degraded samples using PreCR prior to MDA and STR-typing.

Following the sequential reaction protocol, artificially degraded DNA (10ng and 100ng) was added to ThermoPol buffer, 100µM dNTPs, 1X NAD⁺ and sterile water to a total reaction volume of 24.5µL. This protocol is recommended if PreCR product is to be used in a downstream PCR reaction using a PCR buffer other than the ThermoPol buffer provided in the PreCR repair kit. The PreCR repair mix containing a cocktail of repair enzymes was then added (0.5µL) and incubated at 37°C for 20 minutes or at 4°C overnight. The repaired DNA (10% reaction volume) was added to MDA (GenomiPhi V2) or downstream STR genotyping assays (Powerplex ESI 16 STR amplification kit) (Fig. 5.23). MDA product (1µL) was amplified using the Powerplex ESI kit as per the manufacturer instructions.

Untreated degraded DNA (1ng and 10ng) was added to both the MDA and STR reactions for comparison. A positive control reaction was performed using the UV degraded Lambda DNA provided in the PreCR repair kit. The Lambda DNA was treated with the PreCR repair mix and amplified using the primers provided in the kit according to manufacturer instructions. A negative control reaction was performed by adding the damaged DNA to the ThermoPol buffer, dNTPs and NAD⁺ mastermix, but

the repair cocktail was substituted with sterile water. A no template control was also performed.

5.6.2 Results and Discussion

The PreCR[®] repair mix includes a control reaction using UV damaged Lambda DNA and primers. This control reaction was used to test three variables prior to using the PreCR[®] repair mix on degraded samples:

- a) A reduction of the manufacturer's protocol from a 50 μ L to a 25 μ L reaction volume.
- b) Whether adding 10% of the PreCR[®] product (as recommended by the manufacturer), or adding the maximum PreCR[®] volume to the downstream STR reaction would yield better results.
- c) Whether a prolonged incubation (overnight) at 4°C would improve DNA repair over the standard 20 minutes at 37°C.

Successful repair of the damaged Lambda DNA yielded a PCR amplicon of approximately 1000bp. Results of the control test showed that repair was just as efficient at the reduced volume (25 μ L) and that adding 10% of the repair product into a downstream PCR yielded a positive result (Fig. 5.24). The addition of the maximum amount of PreCR[®] product (12 μ L) into a 25 μ L PCR reaction led to PCR inhibition.

No difference in repair was seen between the two incubation conditions. This result is not surprising, as the increased incubation time of overnight at 4°C was suggested by the manufacturer for improved repair of only some types of DNA damage (the types of damage are not specified).

DNA template (100ng and 10ng) which was degraded using either UV radiation or DNase I was used to test for any difference in repair at 4°C or 37°C due to a different mode of damage.

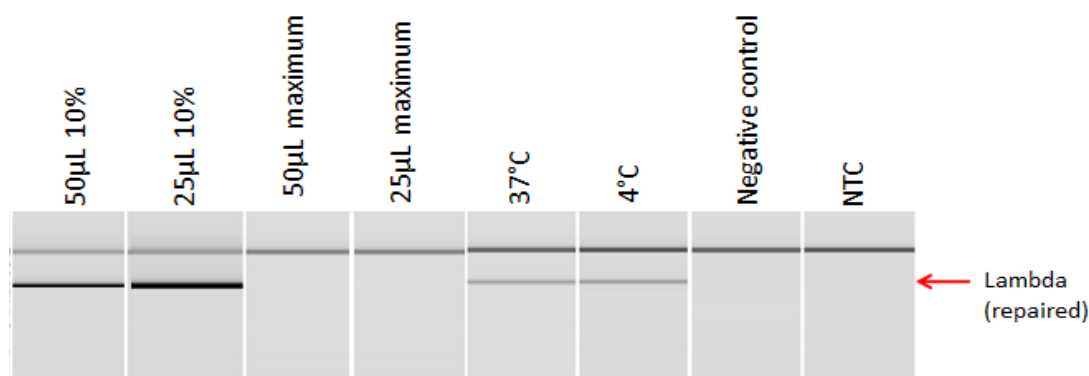


Figure 5.24 Optimisation of PreCR® repair conditions.

Lambda DNA was treated with the PreCR® repair mix at either 37°C for 20 minutes or 4°C overnight. PreCR® was performed in a 50µL or 25µL reaction volume. 10% or maximum volume (12µL) of the PreCR® reaction product was added to the downstream PCR. A negative control reaction was performed by adding the damaged DNA to the ThermoPol buffer, dNTPs and NAD⁺ mastermix, but the repair cocktail was substituted with sterile water. A no template control (NTC) was also performed. Amplification of a 10kb amplicon indicated successful repair.

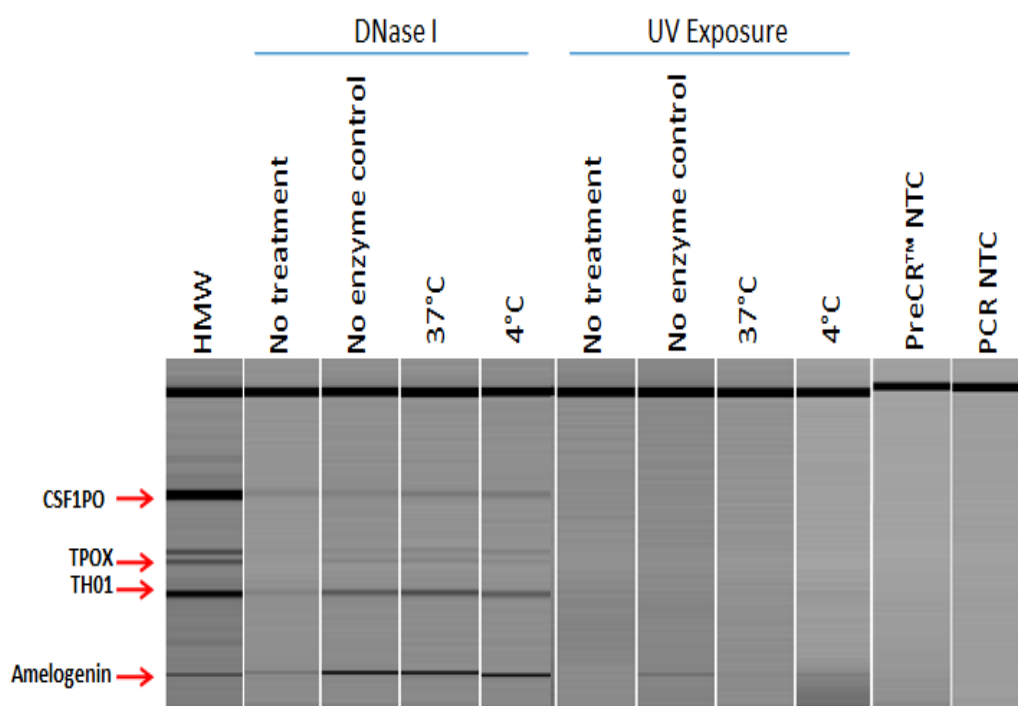


Figure 5.25 STR amplification of DNase I and UV degraded samples pretreated with PreCR® repair mix.

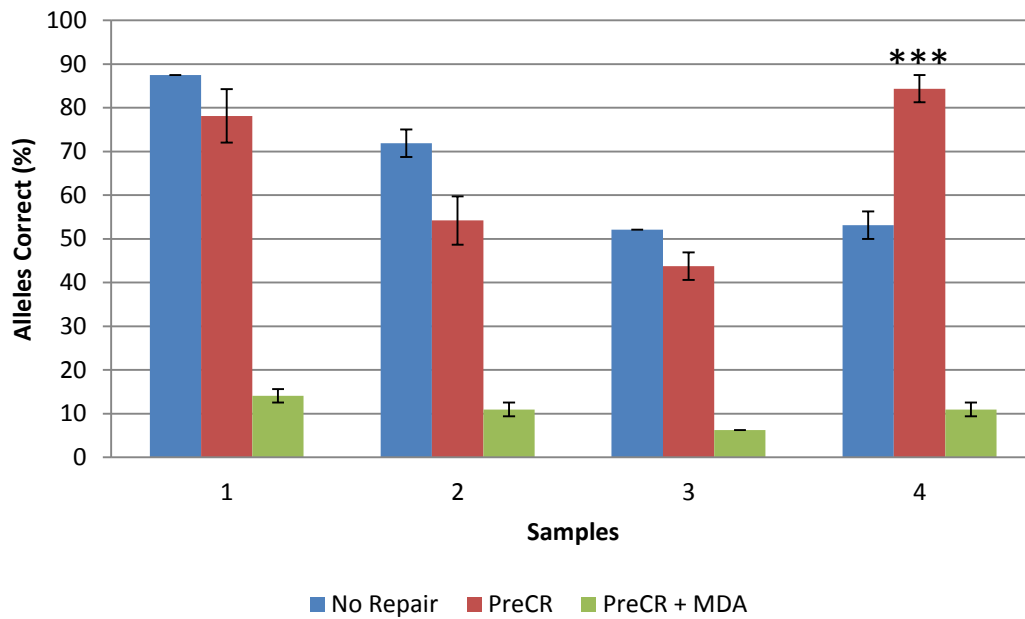
DNA was artificially degraded by DNase I and UV exposure. Degraded DNA (100ng) was added to a 25µL PreCR® repair mix and incubated at 37°C for 20min or 4°C overnight. A no enzyme control reaction was performed by adding the damaged DNA to the ThermoPol buffer, dNTPs and NAD⁺ mastermix, but the repair cocktail was substituted with sterile water. Degraded DNA samples were added directly to the STR PCR (no treatment). No template controls (sterile water) were included in both PreCR® and PCR reactions.

An aliquot (10% of reaction volume) of each PreCR[®] reaction was added to the PCR reaction (final input of 10ng DNA). 10ng of untreated degraded DNA was included as a negative control. No improvement in STR-typing was observed for the UV degraded samples (Fig. 5.25). Slightly more promising results were seen with the repair of samples degraded with DNase I. Although all four loci were amplified without PreCR[®] treatment, the amplicons were very faint (particularly the TPOX locus). After PreCR[®] treatment, all four loci were amplified to a greater degree. Interestingly, this improvement in amplification was also seen in the sample which was incubated without the PreCR[®] repair mix (no enzyme control). This improvement in STR-typing was reproducible with all no enzyme control reactions performed on DNase I treated samples. Therefore, the ThermoPol buffer which includes Tris-HCl, (NH₄)₂S₄, KCl, MgSO₄ and Triton X-100 may be having a non-enzymatic (molecular crowding) effect that improved the PCR.

Although both the UV damaged and DNase I treated samples were of similar sizes (average 200-300bp) they have different damage. DNase I cleaves DNA into 5' phosphodinucleotide fragments [386], whereas UV exposure forms modified bases and base-base crosslinks (thymidine dimers) [381]. These data are interesting as the manufacturer claims that PreCR[®] can repair DNA damage due to UV exposure, but not DNA fragmentation. The UV damaged Lambda control DNA was successfully repaired during the PreCR[®] reaction (data not shown). This indicates that the UV degraded sample used in this study may have been more severely UV damaged than the control DNA, and therefore too badly damaged for PreCR[®] repair.

More discriminating analysis was required to further assess any repair of degraded samples after PreCR[®] treatment. The more sensitive STR amplification kits were used to better assess the genotyping success. DNase I degraded samples (n = 4) (Fig. 5.22) were repaired using the PreCR[®] mix prior to WGA and STR-typing.

A. 10ng Degraded DNA



B. 1ng Degraded DNA

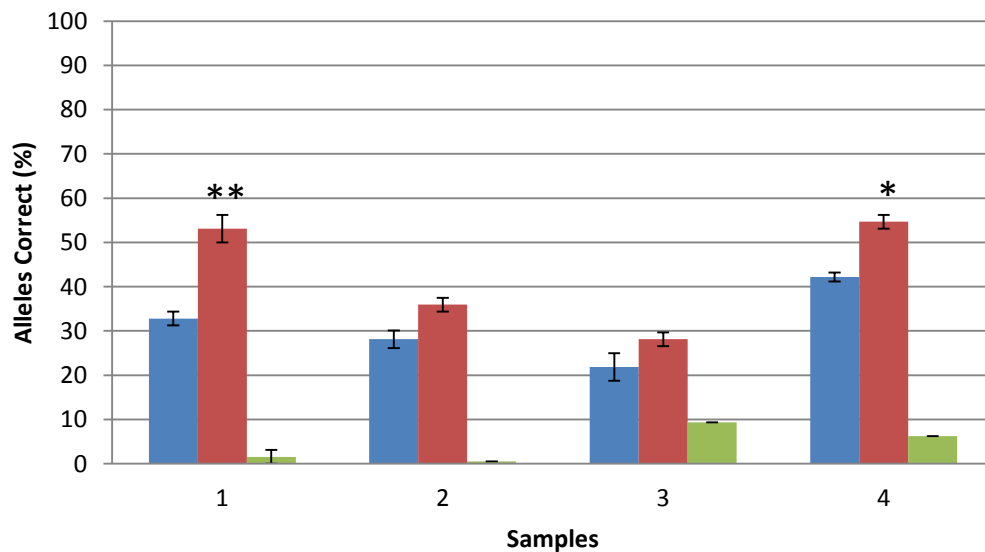


Figure 5.26 STR results of PreCR[®] and MDA treated samples using the PowerPlex ESI 16 STR Amplification kit.

Highly degraded DNA samples (10ng and 1ng) were added to PreCR[®] repair reactions. 10% of the reaction volume (2.5 μ L) was added to a downstream MDA reaction, or directly into the PCR. 1 μ L of each MDA reaction was added to the Powerplex[®] ESI reaction. Degraded DNA was directly STR-typed as negative controls (no repair). Genotyping success was measured by the average percentage of correct alleles detected. Data presented as means \pm SEM. Student's two-tailed paired *t*-test performed on all No repair–PreCR paired data (with ** = $p < 0.01$, * = $p < 0.05$). All other analyses were not significantly different).

Not surprising, STR typing was more successful with 10ng of degraded DNA template than with 1ng (Fig. 5.26). The number of alleles amplified in all non-treated samples was significantly more with 60-85% compared to 0-30% respectively. In general samples repaired with PreCR[®] prior to STR typing also generated more complete profiles with 10ng of DNA than with 1ng DNA (55-78% compared to 28-52% of alleles).

The most degraded sample (sample 4; Fig. 5.22) showed a significant ($p=0.01$) increase in the average number of alleles (84% vs 53%) after PreCR[®] repair. However, the other three less degraded samples (Fig. 5.22) yielded more complete STR profiles without repair. Inconsistent results with STR typing of PreCR[®] treated samples have also been reported in previous studies [382].

With a lower amount of DNA (1ng), all four samples showed more complete STR profiles with PreCR[®] treatment prior to amplification (Fig. 5.26). However, only two of the four were significantly different (Fig. 5.26). Between 5 and 30% more alleles were recovered by repairing the degraded DNA with PreCR[®] prior to STR-typing. The effect of DNA repair was more evident with the lesser amount of DNA (1ng) as fewer intact DNA templates were available for amplification in the untreated degraded DNA.

Whole genome amplification did not successfully amplify degraded samples which were pre-treated with the PreCR[®] repair mix. This result is most likely due to PreCR[®] failing to repair the highly degraded samples to a level which would provide a suitable template for MDA. Reagents in the PreCR[®] reaction mix (ligases, polymerases and buffer species) may also interfere with the whole genome amplification.

The PreCR[®] repair protocol recommends 50-500ng of damaged template. However, this amount of DNA is usually not available in forensic samples. This study used 10ng and 100ng DNA during the repair reaction with 10% of the reaction (1ng and 10ng) added to the STR and MDA reactions. Although not investigated in this study, some promising results have recently been reported with a modified PreCR[®] protocol for UV degraded forensic samples [303]. This improved method involved the addition of the PreCR[®] repair cocktail directly to the AmpFISTR Identifier and MiniFiler STR amplification kits (Applied Biosystems) with ~2ng of degraded DNA. The alternate method also reduced cost, loss of sample, sample handling and risk of contamination.

This study investigated the use of PreCR® on ≥10ng of artificially degraded DNA. However forensic casework samples may possess a broader spectrum of damage. To evaluate the utility of this repair mix with forensic samples, a wider testing of environmentally challenged samples with lower amounts of template would be required.

5.7 Restorase®

Restorase® (Sigma-Aldrich) is a commercial cocktail designed to facilitate repair and provide reliable amplification of damaged DNA. Restorase® combines a DNA repair enzyme with a high-quality Long and Accurate (LA) PCR *AccuTaq* DNA polymerase and mesophilic polymerase to repair damaged DNA sites, which improves amplicon specificity and yield [387]. Restorase™ is designed to amplify long DNA fragments from damaged template DNA that is unable to be amplified using standard PCR enzymes [304]. Restorase® modifies damaged sites to allow subsequent amplification of PCR product from 0.2-20kb in length [387]. This product has been used as an alternate polymerase for DNA typing of very difficult forensic samples with moderate success [305, 306]. However, while Restorase® may be able to restore the quality of damaged DNA, some templates may be irretrievably damaged [387].

5.7.1 Materials and Methods

DNase I degraded DNA (n=6) (Fig. 5.27) was added to a Restorase® repair cocktail (Sigma) prior to MDA and/or STR-typing (Fig. 5.28).

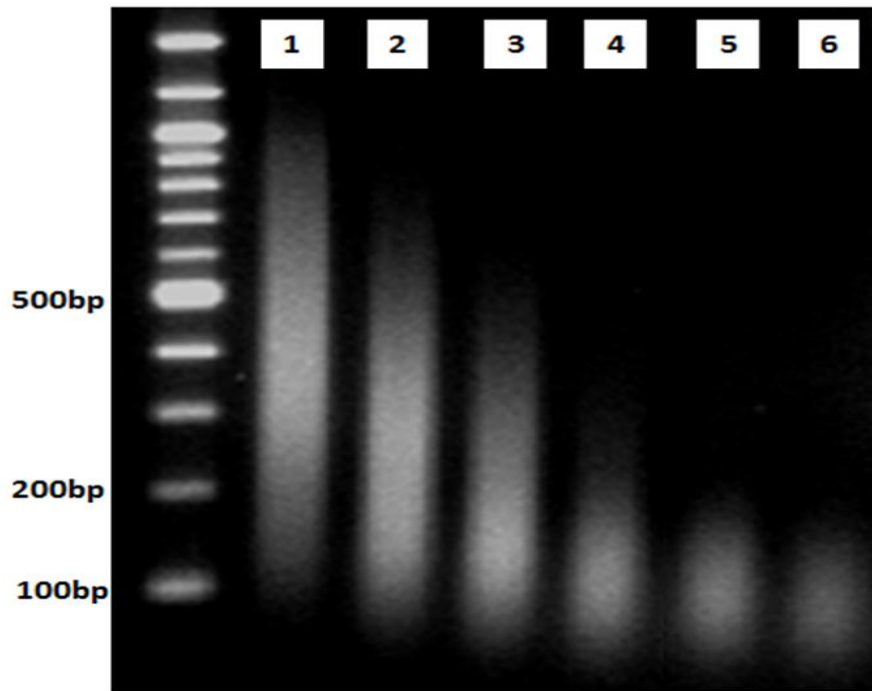


Figure 5.27 Degraded DNA samples used for Restorase® treatment prior to MDA and/or STR typing.

HMW DNA was fragmented using DNase I digestion to generate differentially degraded samples. Artificially degraded samples were visualised via agarose gel electrophoresis. Samples 1- 6 show a decrease in fragment length indicating an increase in the level of DNA degradation.

DNA (5ng and 50ng in 10 μ L) was added to 2.5 μ L 10x Restorase® reaction buffer, 0.5 μ L Restorase® enzyme and 0.5 μ L dNTP mix (final concentration 200 μ M each) in a 25 μ L final reaction volume. Incubation was performed at 37°C for 10 minutes and then 72°C for 5 minutes. An aliquot (5 μ L) of each repaired sample was then added to downstream MDA (GenomiPhi V2) or STR profiling reactions (Powerplex® ESI 16) (Fig. 5.28). MDA and STR-typing were performed as described in section 5.2. HMW DNA was added to both MDA and STR reactions as positive controls. No template controls were also performed to monitor contamination.

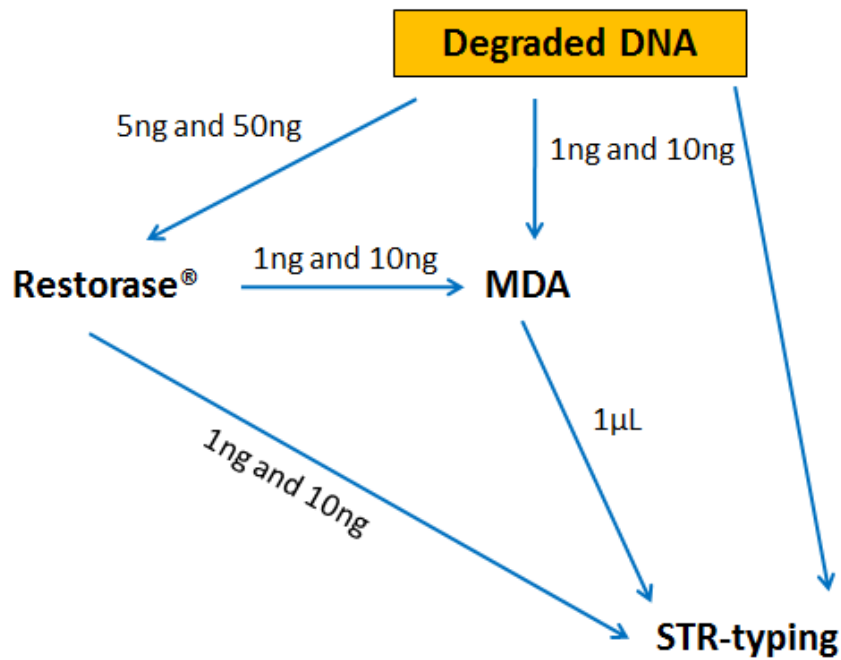


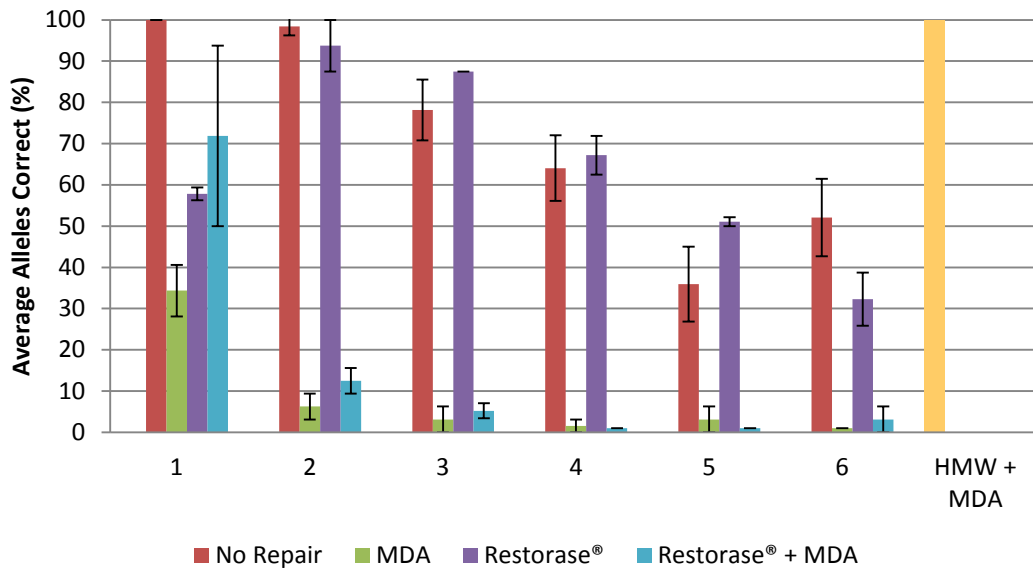
Figure 5.28 Sample workflow overview of the DNA repair using Restorase® DNA polymerase prior to MDA and STR-typing.

Degraded DNA (5ng and 50ng) was repaired with Restorase® repair cocktail. One fifth of the Restorase® reaction (1ng and 10ng DNA) was added to downstream MDA and STR reactions. Degraded DNA (1ng and 10ng DNA) was also added directly to the Powerplex® ESI PCR as negative (no repair) controls.

5.7.2 Results and Discussion

Degraded DNA samples (n=6 in duplicate) (5ng and 50ng/reaction) were pre-incubated with the Restorase® repair cocktail prior to MDA and/or STR typing with the Powerplex® ESI 16 amplification kit. One fifth of each Restorase® sample (1ng and 10ng respectively) was added to MDA or STR PCR reactions.

A. 10ng DNA



B. 1ng DNA

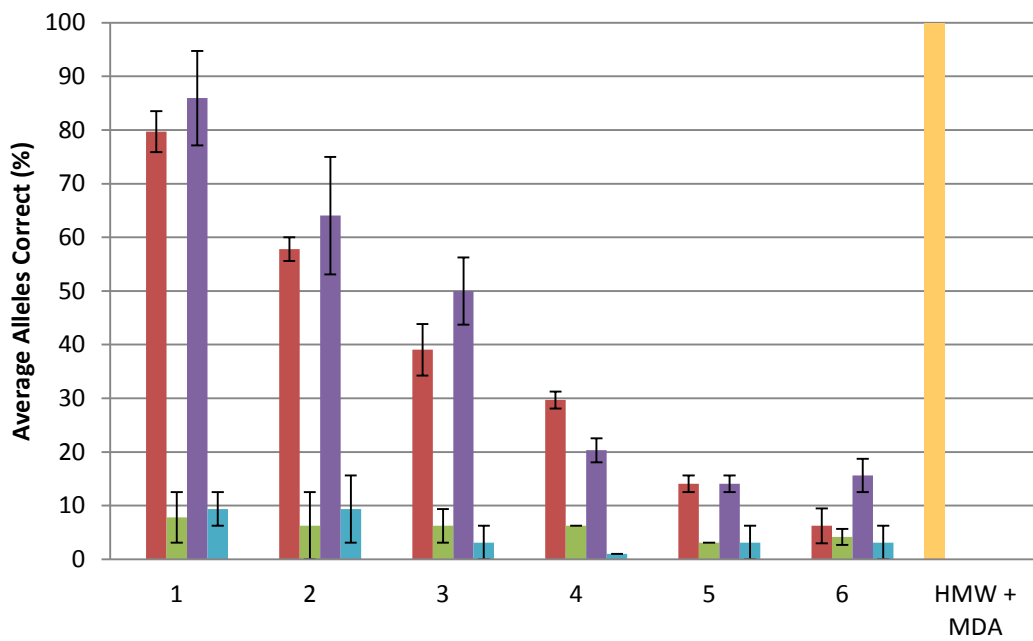


Figure 5.29 STR genotyping success of degraded samples with and without Restorase® treatment.

Degraded DNA (5ng and 50ng) was repaired with Restorase® repair cocktail. One fifth of the Restorase® reaction (1ng and 10ng DNA) was added to downstream MDA and STR reactions. Degraded DNA (1ng and 10ng DNA) was also added directly to the Powerplex® ESI PCR as negative controls (no repair). HMW DNA (10ng and 1ng) was whole genome amplified and subsequently STR-typed. Genotyping success was measured by the average percentage of correct alleles detected. Data presented as means ± SEM

The degraded samples all yielded more complete STR profiles with 10ng of DNA compared to 1ng. STR-typing success decreases as the level of DNA degradation increases. This trend was observed with both template amounts (10ng and 1ng). However, the percentage of alleles detected was 20-45% less with 1ng compared to 10ng of DNA.

Restorase® treatment prior to STR-typing showed little improvement in the average percentage of alleles detected compared to standard Powerplex® ESI analysis. In 7 of the 12 samples tested, a slight increase in the number of alleles detected was seen. However, the results were inconsistent. Due to large standard deviations in the STR results, it cannot be concluded that the Restorase® repair cocktail was successful in improving highly degraded DNA template prior to STR-typing. These results confirm previous studies [382] which show slightly improved, but variable and inconsistent STR-typing results using Restorase® prior to AmpFISTR SGM Plus® (Applied Biosystems) amplification.

Full STR profiles were obtained from WGA samples when HMW DNA (1ng and 10ng) was used as MDA template (Fig. 5.29). However, when degraded DNA or Restorase® 'repaired' samples were whole genome amplified, downstream STR amplification was unsuccessful (Fig. 5.29). One exception was sample 1 when Restorase® treatment was followed by 10ng DNA into the MDA reaction prior to STR-typing (Fig. 5.29A). This sample generated an average of 72% of alleles detected, but a wide standard deviation between replicates was seen. Sample 1 was the least degraded of the six DNA samples (Fig. 5.29) and therefore with 10ng added to the MDA reaction, it is presumed that a sufficient number of intact templates were available for MDA to be relatively successful.

PCR inhibition due to MDA reagents has been observed previously in this study (section 5.3.2). However, with a 1:100 dilution of MDA product prior to STR-typing, interference of the PCR by MDA components was not the cause of the poor STR results. In addition, the positive MDA control yielded a full profile (Fig. 5.29). Alternatively, insufficient MDA product was added to the PCR for successful STR typing. However, when neat or a 1:10 dilution of MDA product was added to the STR reaction the resulting profiles were overloaded with off scale peaks (data not shown).

These data suggest that degraded DNA samples with or without Restorase® treatment are suboptimal templates for MDA prior to STR-typing. Although some improvement in STR typing was seen with Restorase® treatment, the results were unreliable. It appears that Restorase® cannot adequately repair these highly degraded DNA samples.

5.8 REPLI-g-FFPE

Formalin-fixed paraffin-embedded (FFPE) tissues have been successfully used as a viable source of DNA for clinical analysis [307] and forensic cases [308, 309]. DNA within biological tissues which are formalin-fixed undergo chemical modifications that degrade and fragment DNA [310] to lengths often shorter than 300bp [311]. Genotyping and DNA sequence analysis of these samples can also be limited by the small amount of sample available. A process which can amplify small amounts of highly degraded template to yield enough HMW product for successful analysis would be of great benefit to the molecular, medical and forensic sciences. A commercial WGA kit (REPLI-g FFPE, Qiagen) has been developed to amplify such highly damaged and fragmented samples. The REPLI-g FFPE kit is recommended for use with genomic DNA with average DNA fragments >500bp in length. The reaction consists of two steps: a ligation reaction which randomly joins DNA fragments, and a WGA reaction (Fig. 1.10). The WGA master mix contains a proprietary REPLI-g Midi DNA Polymerase and undergoes a two or eight hour isothermal reaction. The end product is suitable for most downstream genotyping methods such as STR, SNP and sequencing assays. This study investigated whether the REPLI-g FFPE kit could repair and amplify degraded samples with fragments ranging from 500bp to <100bp.

5.8.1 Materials and Methods

Artificially degraded DNA samples (n=6) were directly amplified via WGA using the Formalin-Fixed Paraffin Embedded (FFPE) REPLI-g kit (Qiagen, Hilden, Germany) according to manufacturer's instructions.

DNA samples (100ng in 10 μ L) were denatured at 95°C for 5 minutes and cooled to 4°C. The denatured DNA was added to a reaction mastermix consisting of 8 μ L FFPE buffer, 1 μ L FFPE enzyme and 1 μ L ligation enzyme. The reaction mix (20 μ L) was incubated at 24°C for 30 minutes. The reaction was stopped by heating to 95°C for 5 minutes. The REPLI-g master mix (29 μ L REPLI-g midi reaction buffer and 1 μ L REPLI-g midi DNA polymerase) was added to the denatured samples and incubated at 30°C for two or eight hours. REPLI-g product (1 μ L) was added to the STR quadruplex assay and performed as described in section 5.2.4. Alternatively a 1:100 dilution of the REPLI-g product was added to the more sensitive Powerplex ESI 16 STR amplification kit.

Several controls were performed during the REPLI-g-FFPE reactions including a HMW positive control, no template control (NTC) and a ligation only control (subsequent WGA step was omitted). In addition, positive (HMW DNA), negative (degraded DNA) and NTC controls were included in all downstream PCR reactions.

5.8.2 Results and Discussion

Differentially degraded DNA (100ng) (Fig. 5.30A) was added to each FFPE reaction (n=6). A smear of HMW product was visualised via agarose gel electrophoresis after the REPLI-g amplification (Fig. 5.30B). No HMW product was observed in the negative control or the FFPE ligase only reaction.

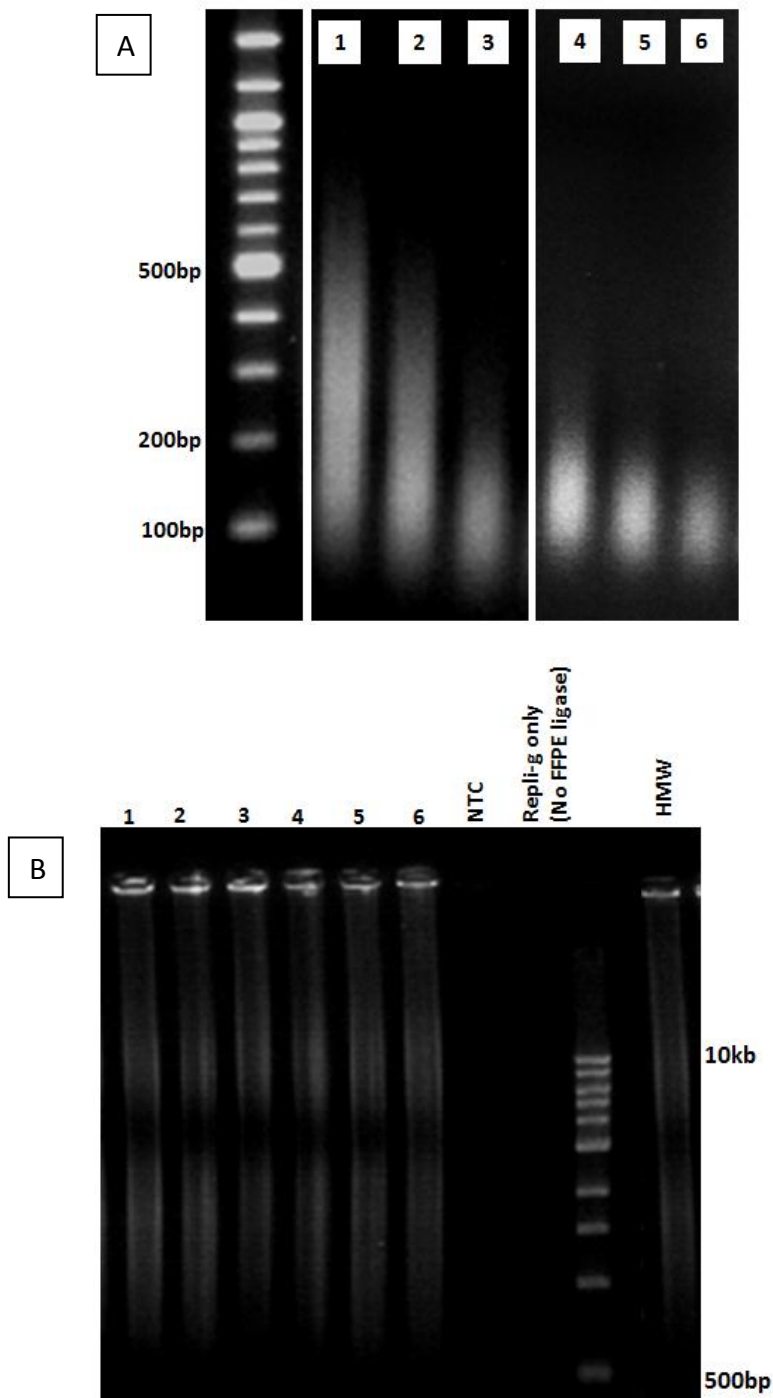


Figure 5.30 Agarose gel electrophoresis of degraded samples before and after FFPE REPLI-g amplification.

A) Degraded DNA samples (n=6) were visualised via agarose gel electrophoresis. Samples show variation in the level of degradation with average fragment lengths of <500bp, <400bp, <300bp and <200bp. B) Degraded DNA (100ng) was added to each Formalin-Fixed Paraffin Embedded (FFPE) and 2 hour REPLI-g whole genome amplification reaction. A positive FFPE REPLI-g control (100ng of HMW DNA) and no template control (sterile water) was included. Degraded DNA (100ng) was whole genome amplified (REPLI-g) without pretreatment with the FFPE repair cocktail. FFPE REPLI-g product was visualised on a 1% agarose gel.

STR-typing of FFPE product with the quadruplex assay was performed on a subset of three samples showing various degrees of degradation (no. 2, 4 & 6; Fig 5.34) to determine if an eight hour incubation would generate more complete STR results than the standard two hour incubation.

The samples which were incubated for two hours generated better quadruplex STR results than eight hour incubated samples (Fig. 5.31). In fact not a single locus was amplified from degraded samples with an eight hour REPLI-g-FFPE reaction. However, the reaction did not fail, as the HMW positive control was successfully STR-typed (Fig. 5.31). The longer incubation time may allow up to four-fold increase ($\leq 10\mu\text{g}$ versus $\leq 40\mu\text{g}$) in the final amount of DNA product per reaction. However, if the majority of this DNA product is the result of amplification of damaged or 'junk' template, the few copies of intact target template may be masked, interfering with successful STR typing. It must be noted that significant amplification bias was observed with the control as the CSF1PO amplicon is extremely faint compared to the other three loci (Fig. 5.31).

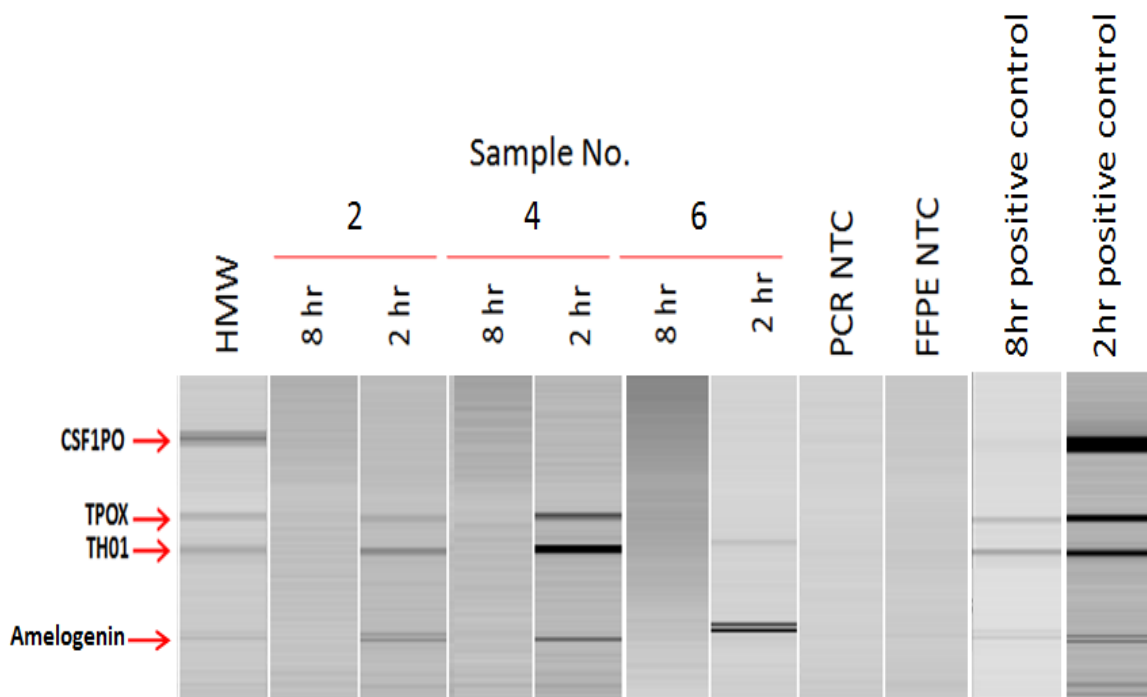


Figure 5.31 STR quadruplex results comparing a two and eight hour FFPE REPLI-g incubation.

FFPE REPLI-g was performed with a 2 hour and 8 hour incubation time using three degraded DNA samples (Samples 2, 4 and 6). FFPE REPLI-g product (1 μL) was added to the quadruplex STR assay. FFPE REPLI-g and PCR no template controls (NTC) were included. HMW DNA was added to both 8 hour and 2 hour FFPE REPLI-g reactions as positive controls. HMW DNA was also added to the STR PCR reaction as a PCR positive control for confirmation of the genotype at each locus.

STR typing of the two hour REPLI-g FFPE samples resulted in the detection of up to three of the four loci (Fig. 5.31). However these results varied depending on the sample with amplification bias seen in both samples 4 and 6. None of the REPLI-g-FFPE reactions were able to recover the CSF1PO locus in degraded samples.

To gain a more complete assessment of whether the REPLI-g-FFPE kit can improve the STR success of degraded samples, the same six degraded samples were STR-typed using the Powerplex® 16 ESI (Promega) amplification kit with a two hour FFPE incubation. The addition of neat FFPE product (1µL) to the PCR resulted in overloaded STR profiles, necessitating a 1:100 dilution prior to genotyping.

Results show that the most complete STR profiles were obtained with a 10ng input of highly degraded sample directly into the STR reaction (Fig. 5.32). As expected, there was a significant decrease in the number of alleles called when the input of degraded template decreased to 1ng (an approximate 50% reduction). However, more alleles were detected in REPLI-g-FFPE samples than the amplification of 1ng degraded DNA without repair (10-30%). More complete STR profiles may be obtained by directly adding more template (>10ng) to the PCR. However, standard STR amplification kits recommend an input amount of DNA between 0.5ng and 2ng. More importantly, the amount of DNA in difficult forensic samples is often much less than 10ng. It is therefore often not possible to simply add more degraded template to counteract the loss of alleles due to the relatively few intact copies available for PCR. Moreover, the FFPE repair reactions were performed with 100ng of degraded DNA. Forensic casework samples most commonly present in much lower amounts of DNA, making these methods (as described here) impractical for forensic use.

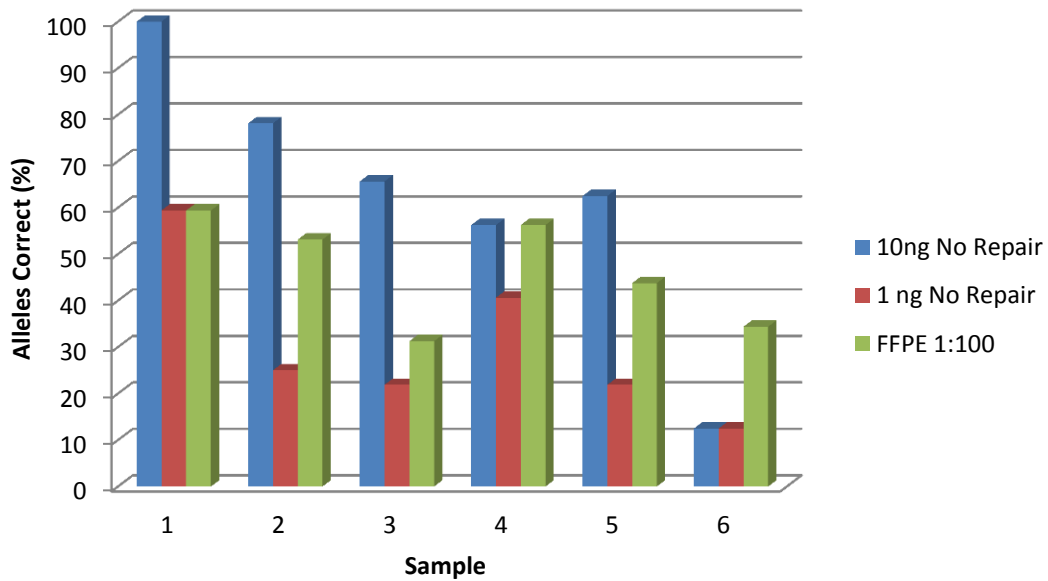


Figure 5.32 STR profile success of degraded samples with and without REPLI-g-FFPE amplification.

Six degraded DNA samples (10ng and 1ng) were amplified using the Powerplex® ESI 16 STR amplification kit without FFPE REPLI-g repair. FFPE REPLI-g product was diluted 1:100 and added to the STR PCR reaction. Genotyping success was measured as the percentage of alleles correct.

The manufacturer claims that REPLI-g-FFPE end product is suitable for most downstream genotyping methods such as STR, SNP and sequencing assays [312]. However, they also note that the most successful genotyping results are obtained when amplicons of approximately 100bp or smaller in size are targeted [312]. These repaired samples may therefore be better suited for SNP analysis than STR typing. Although comparative SNP, STR and mini-STR typing of WGA samples was not included in this study, it would be interesting for future study.

5.9 Alternative DNA Quantitation

In theory quantification of WGA end product is not required as every reaction should yield the same range of DNA (4–7µg per 20µl reaction when starting with 10ng of purified DNA) [365]. However the manufacturer notes that kinetics will vary if crude samples are amplified. Quantification by UV absorption (spectrophotometry) is not recommended as the presence of unused hexamers will lead to inaccurate results [365]. If accurate quantitation of MDA product is required, the Quant-iT™ PicoGreen® dsDNA quantification reagent (Invitrogen) is recommended as PicoGreen® is a sensitive fluorescent nucleic acid stain for double-stranded DNA [365]. Although able to detect the total quantity of DNA in a sample, PicoGreen® gives no indication of DNA degradation or PCR inhibition. Both factors may result in an overestimation of amplifiable DNA for downstream genotyping.

The Quantifiler® Real-Time Human DNA Quantitation kit™ (Applied Biosystems) is commonly used in forensic laboratories to quantify gDNA samples prior to STR-typing. This kit detects the human telomerase reverse transcriptase (hTERT) locus located on chromosome 5 [193]. In this study, the quantitation values of post-MDA samples using hTERT primers during qPCR assays gave extremely low results. In fact, estimation of the amount of DNA product was sometimes less than the amount of starting template. This was despite high yields of HMW product being observed on agarose gel electrophoresis (Fig. 5.3). A previous study [250] showed extremely low amounts of DNA (or no detectable DNA) when MDA product was quantified using the Quantifiler® Real-Time Human DNA Quantitation kit™. It was therefore hypothesised that the low quantitation values obtained via qPCR analysis was due to under-amplification of the hTERT gene during MDA.

It has been shown that WGA does not amplify the entire genome evenly, having an amplification bias up to sixfold between loci [258]. Methods such as comparative genomic hybridisation to evaluate copy number variations [363], high-density SNP arrays [388, 389] and genome-wide STR scans [390] have identified particular areas of the genome susceptible to amplification bias. Telomeric and centromeric regions tend not to amplify during MDA, as these areas possess high levels of repetitive DNA [259].

Long interspersed elements (LINEs) and short interspersed elements (SINEs) have also been shown to routinely under-amplify during MDA [362] along with regions of higher than average G-C content [363]. The hTERT locus is telomeric in location (5p15.33) and may therefore be expected to under-amplify during MDA (Fig. 5.33).

In order to determine whether amplification bias during MDA was leading to under-representation of the hTERT locus, four alternative loci were used for comparative quantification post-MDA: TH01, CSF1PO and SRY (loci amplified in the degradation assay; Chapter 2) and OCA2. The non-telomeric OCA2 locus was chosen since it is located away from areas of the chromosome known to under-amplify with WGA (Fig. 5.33).

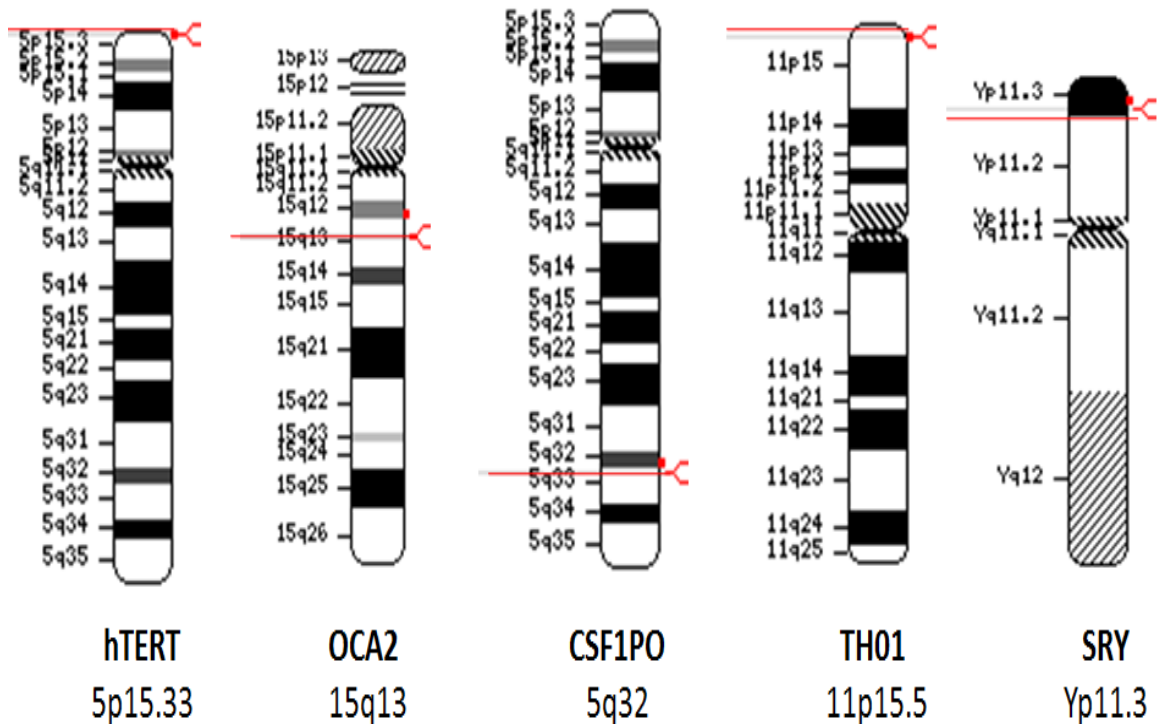


Figure 5.33 Schematic representation of the chromosomal locations of each locus used for quantitation of MDA product.

Ideograms show the chromosomal location of each locus detected in the three qPCR assays used in this study to quantify genomic DNA and MDA end product. The hTERT and OCA2 loci were amplified in separate, single-plex qPCR reactions with identical reaction conditions. The CSF1PO, TH01 and SRY loci were simultaneously detected in a quadruplex qPCR assay (described in section 2.2.3). (Sourced from NCBI Map Viewer)

5.9.1 *Materials and Methods*

Four HMW DNA samples (2 male and 2 female; 1:100 dilutions) were quantified in triplicate using three different qPCR assays:

1. Standard quantitation assay (hTERT locus) described in section 5.2.1.
2. Identical assay conditions as the standard quantitation assay, but substituting the hTERT primers with OCA2 primers [(5' – 3') Fwd: GCT GCA GGA GTC AGA AGG TT and (5' – 3') Rvs: CAT TTG GCG AGC AGA ATC C].
3. The degradation quadruplex assay. Three of the four loci (TH01, CSF1PO and SRY) are used for quantification purposes (as described in section 2.2.3). The fourth locus is an IPC used to monitor PCR inhibition.

DNA (1ng or 10ng) from each individual was added to the MDA reaction and performed as per the recommended protocol (described in section 4.2.2).

Comparative post-MDA quantification was performed on each sample (1:200 dilution, in triplicate) using the same three qPCR assays.

5.9.2 *Results and Discussion*

All three assays (5 loci) resulted in similar quantity values within an acceptable range of precision (0.5ng/ μ L) for each genomic sample prior to MDA (Fig. 5.34A). However significant differences were seen in the quantity values after MDA.

Of the five loci used to measure the amount of amplifiable DNA post MDA, the hTERT locus generated the lowest quantities (Fig. 5.34A and B). TH01 also generated quantitation values substantially lower than the other four loci. These results can be explained by the fact that both of these loci (hTERT and TH01) are telomeric, and therefore likely to be underrepresented during the MDA process. Studies measuring changes in DNA copy number have shown a >3-fold under-amplification of the regions at the ends of chromosomes during MDA [363].

The DNA quantity measured using the OCA2 and CSF1PO loci (both located away from telomeres) resulted in comparable values for each sample. The total amount of amplifiable DNA detected post-MDA was slightly higher in all samples when MDA was performed with 10ng of DNA as compared to 1ng (Fig. 5.34B and C). It should be noted that regardless of the input amount of template DNA (1ng or 10ng), the pattern of amplification coverage of the five loci tested did not alter (Fig. 5.34B and C). These results suggest that although overall MDA yield may be slightly lower with less DNA template (1ng), the degree of amplification bias is not greatly affected.

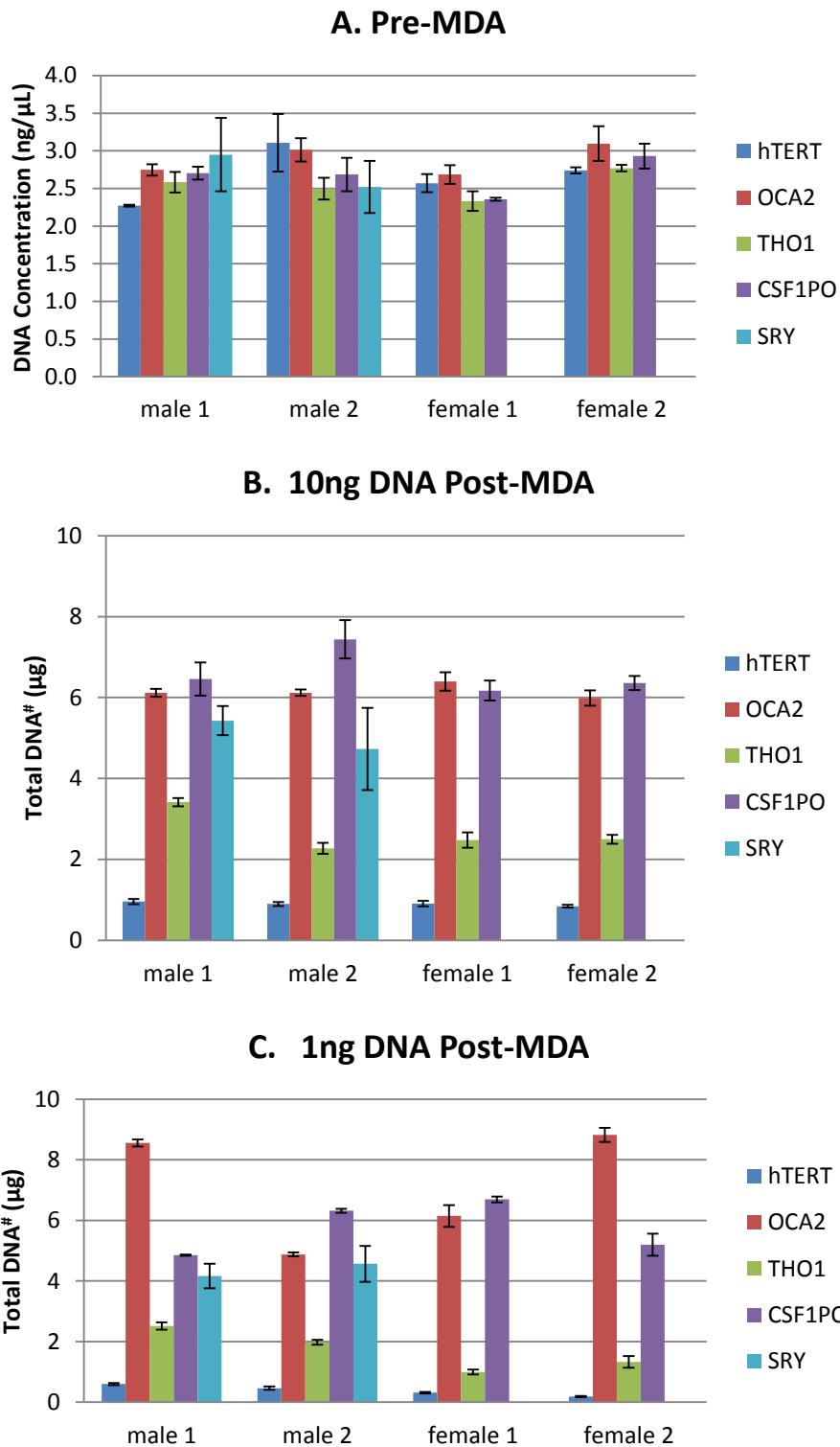


Figure 5.34 Comparative quantitation results using different loci for detection of DNA before and after MDA.

HMW gDNA (n=4) was quantified in triplicate using three qPCR assays; two identical single-plex reactions each with different primers (hTERT and OCA2), and a multiplex assay simultaneously detecting THO1, CSF1PO and SRY loci. DNA from each sample (10ng and 1ng) was added to a standard MDA reaction. 1:200 dilutions of MDA product was re-quantified in triplicate using the same three qPCR assays (5 loci). Data presented as means \pm SEM. (# Total amount of amplifiable DNA)

The quality of a DNA sample can be assessed using a multiplex qPCR assay designed to amplify targets of two different lengths (described in chapter 2). The degradation ratios generated by the assay used in this study are an indication of the differences in the amplification of TH01 (170-190bp) and a shorter (67bp) CSF1PO target. In this study all samples quantified prior to MDA generated ratios of approximately 1, reflecting an even amplification of both targets and no DNA degradation (Fig. 5.35). However, a substantial increase (2-6.5fold) in the degradation ratio after MDA was observed (Fig. 5.35). These results appear to suggest that the WGA product is moderately degraded, but data more likely indicate significant amplification imbalance between the two loci during MDA. The results show that the TH01 locus is under-amplified during MDA in comparison to the CSF1PO locus which would explain the increase in degradation ratios after MDA.

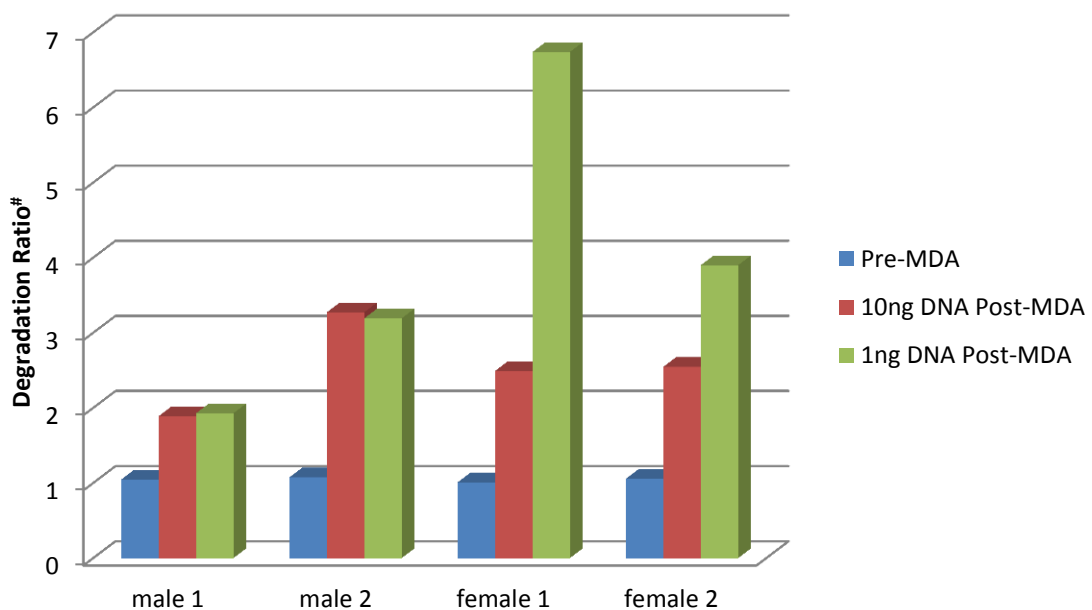


Figure 5.35 Comparative degradation ratios before and after MDA.

The degradation ratio was used to assess the level of amplification bias during MDA with 10ng and 1ng of HMW DNA template. Four samples were amplified with the degradation qPCR assay (as described in 2.2.3) both before and after MDA. MDA product was diluted 1:200 prior to quantification. (# The degradation ratio is calculated by dividing the quantity of short (67bp) CSF1PO target detected by the amount of TH01 (170-190bp) target detected).

The level of inter-locus balance was not consistent across the samples tested in this study. No significant difference in the degradation ratios was seen between 10ng and 1ng DNA template for MDA in the two male samples (Fig. 5.35). However, a substantial increase in the degradation ratio was seen with the female 1ng template (Fig. 5.35). As both targets are autosomal, this result was surprising. A lack of competition for the SRY-primers in the female samples may be contributing to the overamplification of the CSF1PO locus. Alternatively, the exaggerated amplification bias with the 1ng female samples occurred during MDA.

Two more recently developed DNA quantitation kits which are commonly used in forensic laboratories do not detect the hTERT locus. The Quantifiler® Duo DNA Quantification Kit (Applied Biosystems) amplifies a 140bp region of the Ribonuclease P RNA Component H1 (RPPH1) gene (Fig. 5.36) [391]. The Plexor® HY System (Promega) amplifies a 99bp sequence from the human RNU2 locus (Fig. 5.36) [392]. Neither locus is located in areas that are known to be routinely under-amplified during MDA and therefore may be more appropriate assays for the DNA quantitation of MDA product. Although not investigated in this study, these two human DNA quantification kits may generate a more accurate measure of the amount of WGA product prior to genotyping.

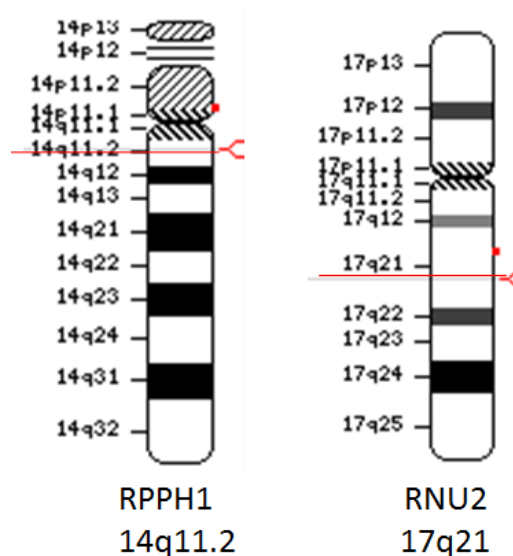


Figure 5.36 Ideograms indicating the chromosome locations of RPPH1 and RNU loci.

The Quantifiler® Duo DNA Quantification Kit (Applied Biosystems) detects the RPPH1 locus, whilst the RNU2 locus is amplified by the Plexor® HY System (Promega) to quantify the amount of gDNA in a sample. (Sourced from NCBI Map Viewer)

5.10 Conclusions

Forensic casework samples can be highly degraded due to the age of the material and/or harsh environmental insults such as UV exposure, extreme heat and microbial activity. DNA from such samples is often highly fragmented with chemical modifications and damage which make poor templates for PCR. Degraded samples often lead to partial or no STR profiles making the identification of individuals more challenging. However, some improvement in the profiling success of such samples may result if the DNA could be partially repaired prior to genotyping.

MDA has been used to successfully whole genome amplify HMW DNA samples prior to genetic analysis [393, 394] and has also shown some potential with forensic [250, 395] clinical [259, 396], and single cell samples [247, 254]. However, MDA has produced variable genotyping results with these difficult samples, and poor SNP and STR genotyping has been reported with degraded templates [384]. As a result, this study investigated several repair strategies which might improve the quality of DNA template for WGA and STR-typing.

In this study, MDA of HMW DNA produced sufficient template for successful downstream STR-typing. However, significant MDA amplification bias was observed in the STR-typing. This bias increases with lower starting amounts of template [396, 397]. In addition, PCR inhibition resulted in locus dropout or complete amplification failure when undiluted MDA product was amplified. The effects of any PCR inhibitors in the GenomiPhi V2 MDA reaction product could be avoided using a 1:100 dilution rather than purification by ethanol precipitation or spin columns. In general, MDA of the highly degraded samples used in this study was unsuccessful.

In order to repair nicks and increase the length of DNA template prior to MDA and STR-typing, linear ligation of fragmented DNA was attempted using T4 DNA ligase. The methods used in this study did not lead to an increase in the length of template, nor did the quality of MDA end product or STR profiles improve. As an alternative approach, DNA fragments were circularised (with CirLigase™) in order to create a template for rolling circle amplification. RCA of CirLigase™ treated samples (>1ng)

produced HMW product if the CircLigase™ reaction was purified with spin columns prior to amplification. However, downstream STR typing of the MDA product failed. The combination of linear ligation and circularization of degraded samples prior to MDA and genotyping was also investigated. No improvement in MDA yield or STR typing was achieved with this approach. Results indicate an inherent failure of MDA to amplify highly degraded and damaged samples.

The ability of two commercial DNA products (PreCR® and Restorase®) to repair highly degraded samples prior to MDA and forensic STR-typing was investigated. The PreCR® Repair Mix is a cocktail of enzymes which repairs a variety of DNA lesions. In general, an increase in the number of STR alleles was detected from degraded samples pretreated with PreCR®. However this improvement was inconsistent across the samples and replicates tested. MDA of PreCR® treated DNA consistently failed, and led to poor STR profiles.

Restorase® combines a DNA repair enzyme with a Long and Accurate (LA) PCR *AccuTaq* DNA polymerase and mesophilic polymerase to repair damaged DNA. A similar trend to that seen with PreCR® was observed with Restorase® treatment. Results showed a slight increase in the number of alleles detected when degraded samples were treated with Restorase®. However, these results were inconsistent and unreliable. Restorase® repair of degraded samples prior to MDA did not lead to improved STR profiles.

A commercial WGA kit (FFPE REPLI-g) specifically designed for the amplification of highly fragmented DNA was also tested in this study. Ample quantities of HMW product was obtained from the amplification of highly degraded samples. FFPE REPLI-g amplified product consistently yielded more alleles (10-30%) than STR-typing of 1ng degraded template directly.

Several products and DNA repair strategies to improve genotyping success from degraded samples were tested in this study. A concern when performing any DNA repair treatment prior to forensic genotyping is the creation of 'false alleles' or increased contamination. No increase in spurious alleles or contamination was observed with treatments tested in these studies.

An interesting observation to come from this study was the difficulty in quantifying the amount of MDA end product. Using three different qPCR assays, a wide variation in the amount of amplifiable DNA measured was seen depending on the locus used for detection. Significant amplification bias during MDA has been previously reported with telomeres, centromeres, highly repetitive and high G-C content regions under-amplified, or not amplified at all [362, 363]. The locus amplified in a DNA quantification kit (Quantifiler Real-Time Human DNA Quantitation kit™) commonly used by the forensic community is hTERT. This gene is telomeric in location and is therefore expected to amplify poorly during MDA. The very low post-MDA quantification values using the hTERT locus in this study supported that notion. As confirmation, another telomeric locus tested in this work (TH01) also yielded poor quantitation results from MDA product. Alternative loci (OCA2, CSF1PO and SRY) were used for comparative qPCR quantification of MDA product due to their chromosomal locations away from areas which are known to under-amplify during the MDA process. All three of these loci resulted in more realistic estimates of the amount of MDA product.

These results highlight the importance of knowing the positions of likely under-amplification during MDA. Although not exhaustive, several studies have started characterising the uniformity of the MDA process [362, 363, 398, 399], and allow for the selection of better qPCR amplicons. Results of this study suggest that the hTERT locus is not a suitable method of quantitation of WGA product. However, newer DNA quantification assays (Quantifiler® Duo DNA Quantification Kit, and the Plexor® HY System) which use different loci away from such difficult chromosomal regions (RPPH1 and RNU2) may be expected to more accurately measure the amount of amplifiable DNA present in whole genome amplified samples.

6 Chapter Six

General Discussion

6.1 Introduction

Research in the field of forensic genetics is continually expanding in order to achieve greater powers of discrimination for identification, explore alternate sources of genetic data that may be of investigative interest, and improve the genotyping success of the most challenging samples. Successful genotyping of DNA samples that are extremely degraded and/or in low amounts is very challenging. Such samples are encountered in forensic casework, particularly fires, aircraft crashes, mass disasters and missing persons cases when skeletal remains are used for identification.

Artificially degraded DNA samples were used in this study to investigate the comparative genotyping success of highly degraded samples using industry standard STR markers, mini-STRs specifically designed to improve DNA typing success of degraded samples and SNPs. Additionally, bone and teeth were used to create a set of environmentally challenged samples to investigate various genotyping and PCR enhancement methods. These samples more closely mimic the types of forensic samples which may result from exposure to damaging conditions such as heat, burial, UV and water exposure. In addition, skeletal remains from a 200 year old shipwreck were used as a historical case study to assess the genotyping success from such degraded samples.

Although recent advances in forensic DNA typing methods have greatly improved the genotyping success of degraded samples, some samples still fail to amplify. Methods which repair damaged and/or degraded DNA template prior to genotyping may enable identification from a sample which would otherwise fail. This research investigated several methods of DNA repair and PCR enhancement in order to improve the downstream genotyping success of highly fragmented DNA samples.

SNPs have been used within the forensic field as alternate markers to STRs for identification purposes [11, 115-121]. This approach has been successful in genotyping extremely degraded samples when STR analysis failed. This is due to the much shorter regions of the genome targeted. However, SNPs have also provided other information useful to forensic investigations such as ancestral origin and

pigmentation (eye, skin and hair colour) [143-154, 156, 157]. The Illumina 96-plex GoldenGate® Genotyping SNP assay was the tool used in this study to investigate the SNP-typing success of a variety of samples. These difficult samples included environmentally challenged and degraded DNA, template in low amount, and whole genome amplified samples. In addition, a pilot study served as a 'first-pass' assessment of whether this SNP panel could predict the hair, eye, skin colour and broad ethnic origin of an individual.

6.2 Comparative Genotyping of Degraded Samples

The amount of total human DNA, male DNA, level of DNA degradation and presence of PCR inhibitors in a sample were simultaneously assessed using a quadruplex qPCR assay. By considering the amount of DNA and the degradation ratio of a sample, a general prediction of genotyping success using AmpFISTR® Profiler Plus®, MiniFiler™ kits and SNP analysis could be made. This assay could act as a screening tool to help in determining which genotyping method may be more informative, thereby maximising the evidentiary value of each sample. For good quality and moderately degraded samples in amounts within the recommended range for PCR (>0.5ng), STR profiling was the most appropriate choice. The extent of DNA degradation could be assessed with reasonable accuracy to 62.5pg and genomic targets could be quantified to a lower limit of 15.6pg. The qPCR assay was able to detect male DNA to a lower limit of 20pg in a 1:1000 background of female DNA. However in cases of extreme degradation and/or template amounts below 250pg, mini-STR or SNP analysis yielded significantly more complete profiles and generated lower match probabilities. Although not currently used for routine human identification by the forensic community, this study confirms previous suggestions that SNP typing would be the most beneficial adjunct to traditional STR and mini-STR profiling for analysis of highly degraded samples [9, 324].

6.3 Genotyping of Environmentally Challenged Samples

Skeletal samples were exposed to one of five environmental insults in order to create a set of mock forensic samples similar to those resulting from mass disasters or missing person cases. Bone and tooth samples were subjected to surface exposure, burial, immersion in saltwater and freshwater, or extreme heat which produced skeletal samples of varying levels of preservation. Samples which were exposed to the surface for up to 24 months were the most heavily degraded as measured by the highest qPCR degradation ratios and loss of STR alleles. Buried samples were heavily infested with mould growth and grass root infiltration, but were relatively well preserved. Samples exposed to low (150°C) to intense (550°C) temperatures destroyed the bone surfaces, but enough of the underlying osseous tissue was protected to obtain full STR profiles. Only when samples were left at extreme temperatures (700°C) for long periods of time (30 minutes) were bone and tooth samples burnt to the point of calcination, and DNA extraction failed.

Decomposition of remains in aquatic environments is poorly understood and there is a lack of comprehensive research into the comparative success of STR typing following fresh or saltwater immersion. Samples submerged in freshwater decomposed more rapidly than those in saltwater, presumably due to the more favourable saline environment for microbial and algal growth. Saltwater samples were well preserved and DNA from these samples showed low levels of degradation and allele loss. Samples incubated in freshwater decomposed more rapidly and were more heavily infested with various microbial growths. DNA extracted from these samples showed moderate levels of degradation but STR results were successful. Overall, this study suggests that DNA was most susceptible to degradation from three elements: UV exposure, extensive microbial activity and extreme heat.

Two commercial STR kits (AmpFISTR[®] NGM[™] and PowerPlex[®] ESI 16) were used to assess the amplification of environmentally challenged samples. Both kits perform well with low and moderately degraded samples. However, with highly degraded samples, on average 10-15% more alleles were recovered from samples using the PowerPlex[®] ESI 16 kit. No statistical correlation between the time of exposure, DNA

degradation and profiling success was observed. However, data suggest that the majority of DNA damage occurs early (first time period tested) and then plateaus. In addition, no correlation to the visual appearance or degree of decomposition of the bone samples and the STR-typing success was evident.

6.3.1 Comparative Dentine Extraction from Teeth

An alternative method to grinding the entire tooth root prior to DNA extraction was investigated. This technique involved filing the inside of the root canal with endodontic files for dentine as opposed to grinding the entire root prior for DNA extraction. Although a more laborious process, which resulted in less dentine powder recovery, the amount of amplifiable DNA per milligram of powder was significantly higher with the filing method. In addition, the quality of the DNA was superior since the number of alleles detected and the peak height ratios of the STR profiles were also higher. Although several other methods of extracting DNA-rich tissue from the pulp chamber of teeth have been previously reported [71-73] the new method presented in this study is the least invasive of those techniques, thereby allowing the preservation of tooth and crown morphology.

6.3.2 Skeletal Remains from HMS Pandora

Skeletal samples recovered from the 200 year old ship-wreck *HMS Pandora* provided a case study for the genotyping of degraded skeletal material. Dentine for DNA purification was removed from all teeth using the filing method. Despite low concentrations of DNA in all bone and tooth samples, STR profiles were generated using both AmpFISTR® NGM™ and PowerPlex® ESI 16 amplification kits. All STR profiles showed the classic signs of DNA degradation. However in general, the PowerPlex® ESI 16 kit produced more complete and balanced profiles from the degraded samples. These results suggest that the PowerPlex® ESI 16 amplification kit may be more sensitive to low amounts of template and more tolerant to DNA degradation and/or damage than the AmpFISTR® NGM kit.

The remains were incomplete skeletons of three individuals. Concordance between the STR profiles of the bone and tooth samples from each individual was expected. Tom and Dick samples were concordant across all loci. However the STR profiles from Harry's bone and tooth samples were not a 'match'. Harry's bone sample was in fact concordant with the STR profile from Dick's tooth, and re-sampling confirmed that the bone had been incorrectly re-associated to the wrong individual by the anthropologist over ten years ago. This finding highlights the importance of intra-skeletal DNA profiling to ensure the correct re-association and identification of separated skeletal components. Situations when co-mingled human remains require identification include mass disasters [400], mass graves, war remains [401, 402] and important historical cases such the positive identification of last Russian monarchy (Romanov family) [370].

6.4 Pigmentation SNP Panel

A 96-plex GoldenGate® Genotyping SNP assay comprised SNPs known to have a strong association with hair, eye or skin colour was evaluated for forensic use. Performance was assessed using pristine genomic samples, whole genome amplified samples, environmentally degraded samples and low amounts of DNA template.

The assay performed well with pristine genomic samples. Seven of the 96 SNPs were identified as routinely requiring exclusion from data analysis due to poor performance. Sensitivity studies showed the assay was tolerant to less DNA template than recommended by the manufacturer (250ng) with as little as 20-50ng providing good results. At lower amounts (<20ng) poor clustering (lower confidence) and miscalls were seen. A significant decrease in performance was also observed with samples of low quality and quantity (<20ng). SNP-typing of degraded bone samples exposed to particular environmental insults (freshwater, burial and surface exposed) was not successful, likely because of a combination of low amounts of fragmented and damaged DNA.

Forensic samples may fall below the optimal concentration for direct SNP analysis (50-250ng/sample). The low amounts of DNA for analysis may also prevent multiple testing and archiving for future use. One proposed solution to this problem is whole genome amplification as a means to produce sufficient quantities of DNA prior to SNP typing. However, the results of this study show that although the application of WGA prior to SNP typing produced reliable results if the template for WGA is of high quality and quantity (10-80ng), the clustering of samples at each locus is more diffuse, requiring more scrutiny during data analysis. In an effort to improve allelic balance during WGA prior to SNP analysis, several alterations to the standard WGA protocol were investigated. The split-and-pooled WGA reaction (eight aliquots) produced the tightest clustering patterns (most confident allele calls) and was considered the method of choice for WGA prior to SNP typing.

WGA of degraded samples prior to SNP-typing produced poor results. The amplification bias inherent in the WGA process is significantly exaggerated with samples of low quality and quantity making these samples unsuitable templates for the WGA methods used in this study prior to SNP-typing. This research suggests that neither direct SNP-typing nor WGA prior to genotyping is the solution for genotyping highly degraded samples using the Illumina GoldenGate® assay. Relatively large amounts (>20ng) of good quality DNA is required for accurate analysis. However alternate SNP arrays and next generation DNA sequencing platforms may give improved results. These techniques may also provide the opportunity to multiplex much larger sets of markers from smaller amounts of DNA (<20ng).

Hair, eye and skin colour are visual traits which are vital components of any eyewitness statement. These characteristics are highly heritable with many genes and DNA polymorphisms known to be associated with variations in human pigmentation. As many pigmentation SNPs are also associated with population differences, it may also be possible to determine the ancestry of an individual based on selected pigmentation SNPs. A pilot study was conducted to investigate whether the GoldenGate® 96-plex pigmentation SNP panel was able to predict ancestry in addition to eye, skin and hair colour from a DNA sample.

Due to the variation in DNA quality and quantity of the database samples used, and the notable run-to-run variability of the assay, the completeness of SNP profiles obtained was inconsistent. The algorithm used for logistic regression analysis and the generation of the predictive models for each trait, was not tolerant to missing data. As a result, a significant number of samples (~20%) and SNPs (27 out of 96) did not meet the strict requirements for predictive analysis.

This SNP panel does hold some potential for predicting hair, skin and eye colour in addition to ancestry. In this pilot study, the most robust predictions were obtained when determining ancestry. For the three main US population groups (African American, Caucasian and Hispanic) accurate assignment of ancestry was made 84-94% of the time. The prediction of eye colour was reasonably accurate for brown, green and hazel eyes (83-89%), but surprisingly was not high for blue eyes (71%). The accuracy of this SNP panel to predict hair and skin colour was low and inconsistent (47-85%).

Although the 96-plex SNP panel may provide some information regarding the ancestry, and pigmentation phenotype of the donor of a DNA sample, the accuracy rates for prediction were not as high as would be required for forensic purposes. To improve the discriminatory value of this assay, the suite of SNPs needs refinement to remove failing SNPs, and include more recently reported SNPs which show higher associations with hair, eye and skin colour. The GoldenGate® technology was not robust when genotyping suboptimal samples such as low DNA amounts, whole genome amplified samples or even slightly degraded samples, and therefore may make this particular assay unsuitable for molecular anthropology and many forensic applications. However, future advancement in SNP-typing platforms may alleviate these limitations.

In summary, the results of this research suggest that the Illumina GoldenGate® 96-plex SNP assay would provide reliable and informative analysis when using adequate amounts of good quality DNA. It appears that sub-optimal genomic samples are not suitable templates for the GoldenGate® SNP assay. The combination of time-consuming bench work, low call rates, unacceptably high miscall rates, complex and

often subjective data analysis makes this platform undesirable for the analysis of poor quality casework samples. However, as an investigative tool for phenotype prediction, the SNP multiplex does hold some potential. SNP analysis for forensic identification and phenotypic prediction is a rapidly expanding field of research. More recent (and future) approaches include large microarrays, genome wide association studies and next generation sequencing which may widen the utility of SNP analysis in the field of forensic science.

6.5 DNA Repair

Forensic casework and environmental samples may be highly damaged, degraded or in low amounts. This may lead to partial, or no STR profiles making identification more difficult. However, some improvement in the profiling success of such samples may result if the quality of template DNA could be improved prior to genotyping. This thesis investigated several DNA repair methods in combination with whole genome amplification.

Multiple displacement amplification has shown some success with HMW DNA samples [393, 394], forensic [250, 395] clinical samples [259, 396], and single cells [247, 254] prior to genetic analysis. However, MDA has produced variable genotyping results with difficult samples, particularly poor SNP and STR genotyping has been reported with degraded templates [384]. Therefore, this study investigated several repair strategies which may improve the quality of DNA template for MDA and STR-typing.

The results of this study showed that MDA of HMW DNA produced sufficient template for successful downstream STR-typing. However, significant MDA amplification bias was observed in downstream STR-typing. In addition to bias, PCR inhibition resulted in locus dropout or complete amplification failure when undiluted MDA product was amplified. Any PCR inhibition by the GenomiPhi V2 MDA reaction product was most effectively overcome with a 1:100 dilution compared to ethanol or spin column purification of the reaction.

In general, MDA of the highly degraded samples used in this study was unsuccessful. In order to improve the template quality for MDA and STR-typing, linear ligation of fragmented DNA to increase the length of DNA template was attempted using T4 DNA ligase. This approach did not lead to an increase in the length of template, nor did the quality of MDA end product or STR profiles improve.

Alternatively, circularisation of DNA fragments with CirLigase™ prior to whole genome amplification was tested. MDA of CirLigase™ treated samples (>1ng) produced HMW product if the CirLigase™ reaction was purified with spin columns prior to amplification. However, downstream STR typing of the MDA product failed. The combination of linear ligation and circularisation of degraded samples prior to MDA and genotyping was also investigated. No improvement in MDA yield or STR typing was achieved. Results indicate an inherent failure of MDA to amplify highly degraded and damaged samples.

Two commercial DNA repair products (PreCR® and Restorase®) reported to repair highly degraded samples were investigated in this study. Both products consist of DNA repair enzymes and DNA polymerases which repair a variety of DNA lesions. In general, a slight increase in the number of STR alleles was detected from degraded samples pretreated with PreCR®. However this improvement was inconsistent. A similar trend in downstream MDA and STR-typing was seen with Restorase® treated samples. Results showed a slight increase in the number of alleles detected when degraded samples were treated with Restorase®. However, these results were also inconsistent and unreliable. PreCR® and Restorase® repair of degraded samples prior to MDA did not lead to improved STR profiles.

A combination of random ligation of small DNA fragments and whole genome amplification using the FFPE REPLI-g kit was also tested in this study. Ample quantities of HMW product were obtained from the amplification of highly degraded samples. FFPE REPLI-g amplified product consistently yielded more alleles (10-30%) than STR-typing 1ng of the degraded template directly. However, if more of the degraded

template (10ng) was directly genotyped, more complete STR profiles were obtained than the FFPE REPLI-g treated samples.

The significant amplification bias generated during the MDA process was highlighted when attempting to quantify MDA product using qPCR. A wide variation in the amount of amplifiable DNA was seen depending on the locus used for detection. Significant amplification bias during MDA has been previously reported with telomeres, centromeres, highly repetitive and high G-C content regions under-amplified, or not amplified at all [362, 363]. hTERT is the locus detected in a DNA quantification kit (Quantifiler Real-Time Human DNA Quantitation kit™) commonly used by the forensic community. This gene is telomeric in location, and the comparatively low post-MDA quantification values obtained in this study support that telomeres are under-amplified during MDA.

These results highlight the importance of knowing the regions of under-amplification during MDA. Several studies have characterised the accuracy and uniformity of the MDA process [362, 363, 398, 399]. These data will assist with the choice of suitable loci for STR, SNP typing, and qPCR amplicons for the quantification of MDA product. Newer DNA quantification assays (Quantifiler® Duo DNA Quantification Kit, and the Plexor® HY System) use different loci (RPPH1 and RNU2) away from under-amplified chromosomal regions, and may be expected to more accurately measure the amount of amplifiable DNA present in whole genome amplified samples.

6.6 Future Directions

The repair of highly degraded and damaged DNA is a complex problem which has proved difficult to solve. This thesis briefly investigated several repair strategies for fragmented DNA prior to STR typing. Although the approaches investigated in this thesis were not successful, future methods worthy of further investigation may include alternative repair enzymes which more efficiently ligate nicked templates and double

stranded breaks, and WGA methods optimised to amplify much shorter DNA fragments and low amounts of DNA.

The results of this study were consistent with other studies showing the potential of SNP analysis to generate equivalent or greater powers of discrimination to STR and mini-STR typing of highly degraded samples for DNA identification. Coupled with the ability to obtain genetic information regarding ancestral origin and phenotypic characteristics, SNPs could become a valuable addition to human identification testing, molecular archaeology and forensic investigation. Future investigations into the utility of the 96-plex SNP panel presented in this thesis would require a larger set of samples in order to strengthen the statistical predictive models for ancestry, hair, eye, and skin colour. Sequencing of samples would also be recommended to ensure correct SNP typing was obtained. Future SNP research, including genome wide association studies and next generation sequencing may improve SNP analysis for forensic identification and assist in the understanding of SNP involvement in traits such as face shape and a person's height and weight.

6.7 Final Conclusions

The overarching aim of this research was to investigate various genotyping approaches for highly degraded DNA samples such as those resulting from natural, mass and missing person cases. Forensic markers such as STRs, mini-STRs and SNPs were used to examine the genotyping success of degraded samples, and a custom SNP panel was used to assess the potential for predicting phenotypic information from suboptimal DNA samples. In addition, this study explored the potential of several DNA repair and PCR enhancement strategies in order to improve downstream genotyping of such degraded samples.

The specific outcomes of this thesis were:

- 1) The real-time qPCR quadruplex assay was able to reliably assess the level of DNA degradation in a sample to a lower level of 62.5pg and generally indicate downstream STR, mini-STR or SNP genotyping success.

- 2) Low and moderately degraded samples were successfully genotyped using conventional STR typing, but highly degraded samples were most successfully genotyped with SNP analysis.
- 3) A collection of mock forensic skeletal samples mimicking the types of samples that often result from a mass disaster or missing person case was created by subjecting bone and tooth samples to burial or surface exposure for up to 24 months, various degrees of heat or submerged in fresh or salt water for up to six months.
- 4) Skeletal samples subjected to surface exposure showed the highest level of DNA degradation and loss of alleles due to the damaging effects of UV damage.
- 5) Both commercial STR kits (AmpFISTR[®] NGM[™] and PowerPlex[®] ESI 16) performed well with low and moderately degraded samples but when genotyping highly degraded skeletal samples, the PowerPlex[®] ESI 16 kit was more robust, generating significantly more complete STR profiles.
- 6) Better quality DNA was obtained from teeth using a new technique to extract dentine powder from tooth roots as measured by more complete downstream STR profiles.
- 7) STR profiles were obtained from 200 year old bones and teeth recovered from the *HMS Pandora* shipwreck. PowerPlex[®] ESI 16 kit produced significantly more complete and evenly balanced profiles from the degraded samples than the AmpFISTR[®] NGM[™] kit.
- 8) A custom 96-plex pigmentation SNP assay was used to successfully genotype HMW genomic and whole genome amplified samples. However, genotyping success was poor for DNA samples which were whole genome amplified, low in quantity or damaged and/or degraded.
- 9) A pilot study testing the predictive power of the 96-plex pigmentation SNP panel found that ancestry determination for the three major population groups (Caucasian, African American and Hispanic) was robust (84-94% accuracy). The prediction of eye colour was reasonably accurate for brown, green and hazel eyes (83-89%), but not as high for blue eyes (71%). The ability to predict hair and skin colour was lower and inconsistent (47-85%).
- 10) DNA repair using linear and/or circularisation of fragmented template prior to STR typing or whole genome amplification was not successful.

- 11) MDA failed to amplify highly degraded genomic samples. Downstream STR analysis of MDA product from degraded DNA templates, or degraded samples which were pre-treated with 'repair' enzymes was also not successful.
- 12) A small improvement in STR genotyping was seen when highly degraded samples were pre-treated with PreCR™ or Restorase® DNA repair cocktails. However these slight increases in the number of alleles detected was inconsistent and unreliable.
- 13) REPLIg-FFPE amplification of highly degraded samples resulted in a 10-30% increase in the number of alleles detected than the amplification of 1ng degraded DNA without repair.

6.8 Summary

In conclusion, forensic casework such as missing persons and mass disasters often require DNA analysis from bone and tooth samples. STRs are the traditional marker used for DNA identification and they work well with routine forensic samples. Improvements to commercial forensic STR and mini-STR kits have enabled more successful amplification from samples with degraded and low amounts of DNA. However, some extremely degraded samples or very low amounts of DNA still prove to be problematic. The use of SNPs may be a more successful approach for the identification of such challenging samples. SNPs may also provide additional genetic data of interest such as ancestry and phenotypic information from degraded skeletal material such as missing person cases and ancient historical remains.

This research will contribute to the current body of knowledge regarding the amplification of degraded DNA samples. Further understanding of degraded DNA amplification is of particular significance for the forensics science and ancient DNA communities which routinely encounter such compromised skeletal samples. The current methods for human identification from degraded DNA are not sufficient and therefore improvements are necessary.

7. REFERENCES

1. Hsu, C.M., et al., *Identification of victims of the 1998 Taoyuan Airbus crash accident using DNA analysis*. Int J Legal Med, 1999. **113**(1): p. 43-6.
2. Leclair, B., et al., *Enhanced kinship analysis and STR-based DNA typing for human identification in mass fatality incidents: the Swissair flight 111 disaster*. J Forensic Sci, 2004. **49**(5): p. 939-53.
3. Holland, M.M., et al., *Development of a quality, high throughput DNA analysis procedure for skeletal samples to assist with the identification of victims from the World Trade Center attacks*. Croatian medical journal, 2003. **44**(3): p. 264-72.
4. Budimlija, Z.M., et al., *World Trade Center human identification project: experiences with individual body identification cases*. Croat Med J, 2003. **44**(3): p. 259-63.
5. Rohland, N. and M. Hofreiter, *Ancient DNA extraction from bones and teeth*. Nature protocols, 2007. **2**(7): p. 1756-62.
6. Pizzamiglio, M., et al., *The use of mini-STRs on degraded DNA samples*. International Congress Series, 2006. **1288**: p. 498-500.
7. Butler, J.M., *Short tandem repeat typing technologies used in human identity testing*. Biotechniques, 2007. **43**(4): p. ii-v.
8. Alonso, A., et al., *Challenges of DNA profiling in mass disaster investigations*. Croatian medical journal, 2005. **46**(4): p. 540-8.
9. Budowle, B., *SNP typing strategies*. Forensic science international, 2004. **146 Suppl**: p. S139-42.
10. Budowle, B., et al., *SNPs and microarray technology in forensic genetics: development and application to mitochondrial DNA*. Forens. Sci. Rev., 2004. **16**: p. 22-36.
11. Kidd, K.K., et al., *Developing a SNP panel for forensic identification of individuals*. Forensic science international, 2006. **164**(1): p. 20-32.
12. Burger, J., et al., *DNA preservation: a microsatellite-DNA study on ancient skeletal remains*. Electrophoresis, 1999. **20**(8): p. 1722-8.
13. Fondevila, M., et al., *Challenging DNA: Assessment of a range of genotyping approaches for highly degraded forensic samples*. Forensic Science International: Genetics Supplement Series, 2008. **1**(1): p. 26-28.
14. Bogas, V., et al., *Genetic identification of degraded DNA samples buried in different types of soil*. Forensic Sci Int: Gen Supp, 2009. **Series 2**: p. 169-171.
15. Levy-Booth, D., et al., *Cycling of extracellular DNA in the soil environment*. Soil Biol. Biochem., 2007. **39**: p. 2977-2991.
16. Blum, S.A.E., M.G. Lorenz, and W. Wackernagel, *Mechanism of retarded DNA degradation and prokaryotic origin of DNases in nonsterile soils*. Syst. Appl. Microbiol., 1997. **20**: p. 513-521.
17. Lindahl, T., *Instability and decay of the primary structure of DNA*. Nature, 1993. **362**(6422): p. 709-15.
18. Poinar, H.N., *The top 10 list: criteria of authenticity for DNA from ancient and forensic samples*. International Congress Series, 2003. **1239**: p. 575-579.

19. Alaeddini, R., S.J. Walsh, and A. Abbas, *Forensic implications of genetic analyses from degraded DNA--a review*. Forensic science international. Genetics, 2010. **4**(3): p. 148-57.
20. Evans, J., et al., *Thymine ring saturation and fragmentation products: lesion bypass, misinsertion and implications for mutagenesis*. Mutat Res, 1993. **299**(3-4): p. 147-56.
21. Evans, T.C., *DNA Damage*, in *NEB Expressions2007*, New England BioLabs inc. p. 1-3.
22. Bruskov, V.I., et al., *Heat-induced formation of reactive oxygen species and 8-oxoguanine, a biomarker of damage to DNA*. Nucleic Acids Res, 2002. **30**(6): p. 1354-63.
23. Sikorsky, J.A., et al., *DNA damage reduces Taq DNA polymerase fidelity and PCR amplification efficiency*. Biochem Biophys Res Commun, 2007. **355**(2): p. 431-7.
24. Van Der Schans, G.P., *Gamma-ray induced double-strand breaks in DNA resulting from randomly-inflicted single-strand breaks: temporal local denaturation, a new radiation phenomenon?* International journal of radiation biology and related studies in physics, chemistry, and medicine, 1978. **33**(2): p. 105-20.
25. Lindahl, T. and B. Nyberg, *Rate of depurination of native deoxyribonucleic acid*. Biochemistry, 1972. **11**(19): p. 3610-8.
26. Ballantyne, J., *Assessment and In Vitro repair of Damaged DNA Templates*, 2006, National Institute of Justice, US Department of Justice.
27. Goodsell, D.S., *The molecular perspective: ultraviolet light and pyrimidine dimers*. Oncologist, 2001. **6**(3): p. 298-9.
28. Chandrasekhar, D. and B. Van Houten, *In vivo formation and repair of cyclobutane pyrimidine dimers and 6-4 photoproducts measured at the gene and nucleotide level in Escherichia coli*. Mutation research, 2000. **450**(1-2): p. 19-40.
29. Bender, K., M.J. Farfan, and P.M. Schneider, *Preparation of degraded human DNA under controlled conditions*. Forensic science international, 2004. **139**(2-3): p. 135-40.
30. Jennings, R.B., C.E. Ganote, and K.A. Reimer, *Ischemic tissue injury*. The American journal of pathology, 1975. **81**(1): p. 179-98.
31. Alaeddini, R., *Forensic implications of PCR inhibition-A review*. Forensic science international. Genetics, 2012. **6**(3): p. 297-305.
32. Collan, Y. and M. Salmenpera, *Electron microscopy of postmortem autolysis of rat muscle tissue*. Acta neuropathologica, 1976. **35**(3): p. 219-33.
33. Hofreiter, M., et al., *Ancient DNA*. Nature reviews. Genetics, 2001. **2**(5): p. 353-9.
34. Shutler, G.G., et al., *Removal of a PCR inhibitor and resolution of DNA STR types in mixed human-canine stains from a five year old case*. J Forensic Sci, 1999. **44**(3): p. 623-6.
35. Tsai, Y.L. and B.H. Olson, *Rapid method for separation of bacterial DNA from humic substances in sediments for polymerase chain reaction*. Appl Environ Microbiol, 1992. **58**(7): p. 2292-5.
36. von Wurmb-Schwark, N., et al., *A simple Duplex-PCR to evaluate the DNA quality of anthropological and forensic samples prior short tandem repeat typing*. Legal medicine (Tokyo, Japan), 2004. **6**(2): p. 80-8.

37. Akane, A., et al., *Identification of the heme compound copurified with deoxyribonucleic acid (DNA) from bloodstains, a major inhibitor of polymerase chain reaction (PCR) amplification*. J Forensic Sci, 1994. **39**(2): p. 362-72.
38. Eckhart, L., et al., *Melanin binds reversibly to thermostable DNA polymerase and inhibits its activity*. Biochem Biophys Res Commun, 2000. **271**(3): p. 726-30.
39. Jacobsen, C.S. and O.F. Rasmussen, *Development and application of a new method to extract bacterial DNA from soil based on separation of bacteria from soil with cation-exchange resin*. Applied and environmental microbiology, 1992. **58**(8): p. 2458-62.
40. Biosystems, A., *AmpFISTR® IProfiler Plus® PCR Amplification Kit. Users Manual*. 2006.
41. Parsons, T.J., et al., *Application of novel "mini-amplicon" STR multiplexes to high volume casework on degraded skeletal remains*. Forensic Science International: Genetics, 2007. **1**(2): p. 175-179.
42. Hedman, J., et al., *Improved forensic DNA analysis through the use of alternative DNA polymerases and statistical modeling of DNA profiles*. Biotechniques, 2009. **47**(5): p. 951-8.
43. Radstrom, P., et al., *Pre-PCR processing: strategies to generate PCR-compatible samples*. Mol Biotechnol, 2004. **26**(2): p. 133-46.
44. Le, L., et al. *Recovering DNA profiles from low quantity and low quality forensic samples*. Available from: <http://www.biomatrica.com/media/pcrboost/Italy%20Poster.pdf>.
45. Kontanis, E.J. and F.A. Reed, *Evaluation of real-time PCR amplification efficiencies to detect PCR inhibitors*. Journal of forensic sciences, 2006. **51**(4): p. 795-804.
46. Budowle, B., F.R. Bieber, and A.J. Eisenberg, *Forensic aspects of mass disasters: Strategic considerations for DNA-based human identification*. Legal Medicine, 2005. **7**(4): p. 230-243.
47. Mundorff, A.Z., E.J. Bartelink, and E. Mar-Cash, *DNA preservation in skeletal elements from the World Trade Center disaster: recommendations for mass fatality management*. Journal of forensic sciences, 2009. **54**(4): p. 739-45.
48. Biesecker, L.G., et al., *Epidemiology. DNA identifications after the 9/11 World Trade Center attack*. Science, 2005. **310**(5751): p. 1122-3.
49. Olaisen, B., M. Stenersen, and B. Mevag, *Identification by DNA analysis of the victims of the August 1996 Spitsbergen civil aircraft disaster*. Nat Genet, 1997. **15**(4): p. 402-5.
50. Pereira, R., et al., *A new multiplex for human identification using insertion/deletion polymorphisms*. Electrophoresis, 2009. **30**(21): p. 3682-90.
51. Brenner, C.H. and B.S. Weir, *Issues and strategies in the DNA identification of World Trade Center victims*. Theoretical population biology, 2003. **63**(3): p. 173-8.
52. Milos, A., et al., *Success rates of nuclear short tandem repeat typing from different skeletal elements*. Croatian medical journal, 2007. **48**(4): p. 486-93.
53. Loreille, O.M., et al., *High efficiency DNA extraction from bone by total demineralization*. Forensic Science International: Genetics, 2007. **1**(2): p. 191-195.
54. Salamon, M., et al., *Relatively well preserved DNA is present in the crystal aggregates of fossil bones*. Proc Natl Acad Sci U S A, 2005. **102**(39): p. 13783-8.

55. Campos, P.F., et al., *DNA in ancient bone - where is it located and how should we extract it?* Ann Anat, 2012. **194**(1): p. 7-16.
56. Soler, M.P., et al., *Morphological and DNA analysis in human skeletal remains exposed to environmental conditions in Brazil.* Forensic Sci Int: Gen Supp, 2011. **Series 3**: p. e339-340.
57. Hagelberg, E. and J.B. Clegg, *Isolation and characterization of DNA from archaeological bone.* Proc Biol Sci, 1991. **244**(1309): p. 45-50.
58. Alonso, A., et al., *DNA typing from skeletal remains: evaluation of multiplex and megaplex STR systems on DNA isolated from bone and teeth samples.* Croatian medical journal, 2001. **42**(3): p. 260-6.
59. Davoren, J., et al., *Highly effective DNA extraction method for nuclear short tandem repeat testing of skeletal remains from mass graves.* Croatian medical journal, 2007. **48**(4): p. 478-85.
60. Yang, D.Y., et al., *Technical note: improved DNA extraction from ancient bones using silica-based spin columns.* Am J Phys Anthropol, 1998. **105**(4): p. 539-43.
61. Rohland, N. and M. Hofreiter, *Comparison and optimization of ancient DNA extraction.* BioTechniques, 2007. **42**(3): p. 343-52.
62. Lalueza-Fox, C., et al., *Mitochondrial DNA from Myotragus balearicus, an extinct bovid from the Balearic Islands.* J Exp Zool, 2000. **288**(1): p. 56-62.
63. Irwin, J.A., et al., *Characterization of a modified amplification approach for improved STR recovery from severely degraded skeletal elements.* Forensic Sci Int Genet, 2012.
64. Malaver, P.C. and J.J. Yunis, *Different dental tissues as source of DNA for human identification in forensic cases.* Croat Med J, 2003. **44**(3): p. 306-9.
65. Alvarez Garcia, A., et al., *Effect of environmental factors on PCR-DNA analysis from dental pulp.* Int J Legal Med, 1996. **109**(3): p. 125-9.
66. Marjanovic, D., et al., *DNA identification of skeletal remains from the World War II mass graves uncovered in Slovenia.* Croatian medical journal, 2007. **48**(4): p. 513-9.
67. Gaytmenn, R. and D. Sweet, *Quantification of forensic DNA from various regions of human teeth.* J Forensic Sci, 2003. **48**(3): p. 622-5.
68. Adler, C.J., et al., *Survival and recovery of DNA from ancient teeth and bones.* Journal of Archaeological Science, 2011. **38**: p. 956-964.
69. Corte-Real, A., et al., *The DNA extraction from the pulp dentine complex of both with and without carious.* International Congress Series, 2006. **1288**: p. 710-712.
70. Sweet, D. and D. Hildebrand, *Recovery of DNA from human teeth by cryogenic grinding.* J Forensic Sci, 1998. **43**(6): p. 1199-202.
71. Smith, B.C., et al., *A systematic approach to the sampling of dental DNA.* J Forensic Sci, 1993. **38**(5): p. 1194-209.
72. Trivedi, R., P. Chattopadhyay, and V.K. Kashyap, *A new improved method for extraction of DNA from teeth for the analysis of hypervariable loci.* Am J Forensic Med Pathol, 2002. **23**(2): p. 191-6.
73. Tilotta, F., et al., *A comparative study of two methods of dental pulp extraction for genetic fingerprinting.* Forensic Sci Int, 2010. **202**(1-3): p. e39-43.
74. Bolnick, D.A., et al., *Nondestructive sampling of human skeletal remains yields ancient nuclear and mitochondrial DNA.* Am J Phys Anthropol, 2011. **147**(2): p. 293-300.

75. Budowle, B. and R.C. Allen, *Electrophoresis reliability: I. The contaminant issue*. J Forensic Sci, 1987. **32**(6): p. 1537-50.
76. Budowle, B. and A. van Daal, *Forensically relevant SNP classes*. Biotechniques, 2008. **44**(5): p. 603-8, 610.
77. Budowle, B. and F.S. Baechtel, *Modifications to improve the effectiveness of restriction fragment length polymorphism typing*. Appl Theor Electrophor, 1990. **1**(4): p. 181-7.
78. Jeffreys, A.J., V. Wilson, and S.L. Thein, *Hypervariable 'minisatellite' regions in human DNA*. Nature, 1985. **314**(6006): p. 67-73.
79. Thompson, R., S. Zoppis, and B. McCord, *An overview of DNA typing methods for human identification: past, present, and future*. Methods in molecular biology, 2012. **830**: p. 3-16.
80. Butler, J., *Fundamentals of Forensic DNA Typing* 2009, Burlington, MA, USA: Academic Press.
81. Thymann, M., et al., *Analysis of the locus D1S80 by amplified fragment length polymorphism technique (AMP-FLP). Frequency distribution in Danes. Intra and inter laboratory reproducibility of the technique*. Forensic Sci Int, 1993. **60**(1-2): p. 47-56.
82. Rand, S., et al., *Population genetics and forensic efficiency data of 4 AMPFLP's*. Int J Legal Med, 1992. **104**(6): p. 329-33.
83. Butler, J.M., ed. *Forensic DNA Typing: Biology, Technology, and Genetics of STR Markers*. 2nd ed. 2005, Elsevier Academic Press: New York.
84. Opel, K.L., et al., *The application of miniplex primer sets in the analysis of degraded DNA from human skeletal remains*. Journal of forensic sciences, 2006. **51**(2): p. 351-6.
85. Coble, M.D. and J.M. Butler, *Characterization of new miniSTR loci to aid analysis of degraded DNA*. Journal of forensic sciences, 2005. **50**(1): p. 43-53.
86. Wiegand, P. and M. Kleiber, *Less is more--length reduction of STR amplicons using redesigned primers*. International journal of legal medicine, 2001. **114**(4-5): p. 285-7.
87. Chung, D.T., et al., *A study on the effects of degradation and template concentration on the amplification efficiency of the STR Miniplex primer sets*. Journal of forensic sciences, 2004. **49**(4): p. 733-40.
88. Biosystems, A. *AmpFISTR® MiniFiler™ PCR amplification kit. Product Bulletin*. 2007; Available from: http://www3.appliedbiosystems.com/cms/groups/applied_markets_marketing/documents/generaldocuments/cms_043658.pdf.
89. Welch, L., et al., *A comparison of mini-STRs versus standard STRs--results of a collaborative European (EDNAP) exercise*. Forensic Sci Int Genet, 2011. **5**(3): p. 257-8.
90. Senge, T., et al., *STRs, mini STRs and SNPs--a comparative study for typing degraded DNA*. Leg Med (Tokyo). **13**(2): p. 68-74.
91. Fondevila, M., et al., *Case report: Identification of skeletal remains using short-amplicon marker analysis of severely degraded DNA extracted from a decomposed and charred femur*. Forensic Science International: Genetics, 2008. **2**(3): p. 212-218.

92. Butler, J.M., Y. Shen, and B.R. McCord, *The development of reduced size STR amplicons as tools for analysis of degraded DNA*. Journal of forensic sciences, 2003. **48**(5): p. 1054-64.
93. Oh, C.S., et al., *Autosomal Short Tandem Repeat Analysis of Ancient DNA by Coupled Use of Mini- and Conventional STR Kits**. J Forensic Sci, 2012.
94. Mulero, J.J., et al., *Development and validation of the AmpFISTR MiniFiler PCR Amplification Kit: a MiniSTR multiplex for the analysis of degraded and/or PCR inhibited DNA*. J Forensic Sci, 2008. **53**(4): p. 838-52.
95. Coble, M.D., et al., *Single nucleotide polymorphisms over the entire mtDNA genome that increase the power of forensic testing in Caucasians*. International journal of legal medicine, 2004. **118**(3): p. 137-46.
96. Ginther, C., L. Issel-Tarver, and M.C. King, *Identifying individuals by sequencing mitochondrial DNA from teeth*. Nat Genet, 1992. **2**(2): p. 135-8.
97. Robin, E.D. and R. Wong, *Mitochondrial DNA molecules and virtual number of mitochondria per cell in mammalian cells*. J Cell Physiol, 1988. **136**(3): p. 507-13.
98. Holland, M.M., et al., *Mitochondrial DNA sequence analysis of human skeletal remains: identification of remains from the Vietnam War*. J Forensic Sci, 1993. **38**(3): p. 542-53.
99. Budowle, B., et al., *Forensics and mitochondrial DNA: applications, debates, and foundations*. Annu Rev Genomics Hum Genet, 2003. **4**: p. 119-41.
100. Hall, T.A., et al., *Base composition analysis of human mitochondrial DNA using electrospray ionization mass spectrometry: A novel tool for the identification and differentiation of humans*. Analytical Biochemistry, 2005. **344**(1): p. 53-69.
101. Giles, R.E., et al., *Maternal inheritance of human mitochondrial DNA*. Proc Natl Acad Sci U S A, 1980. **77**(11): p. 6715-9.
102. Anderson, S., et al., *Sequence and organization of the human mitochondrial genome*. Nature, 1981. **290**(5806): p. 457-65.
103. Turchi, C., et al., *Italian mitochondrial DNA database: results of a collaborative exercise and proficiency testing*. Int J Legal Med, 2008. **122**(3): p. 199-204.
104. Loogvali, E.L., et al., *Disuniting uniformity: a pied cladistic canvas of mtDNA haplogroup H in Eurasia*. Mol Biol Evol, 2004. **21**(11): p. 2012-21.
105. Gabriel, M.N., et al., *Improved MtDNA sequence analysis of forensic remains using a "mini-primer set" amplification strategy*. J Forensic Sci, 2001. **46**(2): p. 247-53.
106. Loreille, O., et al., *Application of next generation sequencing technologies to the identification of highly degraded unknown soldiers' remains*. Forensic Sci Int: Gen Supp, 2011. **3**: p. e540-541.
107. Hall, T.A., et al., *Base Composition Profiling of Human Mitochondrial DNA Using Polymerase Chain Reaction and Direct Automated Electrospray Ionization Mass Spectrometry*. Anal Chem, 2009.
108. Ivanov, P.L., *[A new approach to forensic medical typing of human mitochondrial DNA with the use of mass-spectrometric analysis of amplified fragments: PLEX-ID automated genetic analysis system]*. Sud Med Ekspert, 2010. **53**(3): p. 46-51.
109. Wang, D.G., et al., *Large-scale identification, mapping, and genotyping of single-nucleotide polymorphisms in the human genome*. Science, 1998. **280**(5366): p. 1077-82.

110. Altshuler, D., et al., *An SNP map of the human genome generated by reduced representation shotgun sequencing*. Nature, 2000. **407**(6803): p. 513-6.
111. Collins, F.S., L.D. Brooks, and A. Chakravarti, *A DNA polymorphism discovery resource for research on human genetic variation*. Genome Res, 1998. **8**(12): p. 1229-31.
112. Reich, D.E., et al., *Human genome sequence variation and the influence of gene history, mutation and recombination*. Nat Genet, 2002. **32**(1): p. 135-42.
113. Weber, J.L. and C. Wong, *Mutation of human short tandem repeats*. Hum Mol Genet, 1993. **2**(8): p. 1123-8.
114. Daniel, R. and S.J. Walsh, *The continuing evolution of Forensic DNA profiling - from STRs to SNPs*. Australian Journal of Forensic Sciences, 2006. **38**(2): p. 59-74.
115. Dixon, L.A., et al., *Validation of a 21-locus autosomal SNP multiplex for forensic identification purposes*. Forensic science international, 2005. **154**(1): p. 62-77.
116. Sanchez, J.J., et al., *A multiplex assay with 52 single nucleotide polymorphisms for human identification*. Electrophoresis, 2006. **27**(9): p. 1713-24.
117. Sanchez, J.J., et al., *Development of a multiplex PCR assay detecting 52 autosomal SNPs*. International Congress Series, 2006. **1288**: p. 67-69.
118. Borsting, C., C. Tomas, and N. Morling, *Typing of 49 autosomal SNPs by single base extension and capillary electrophoresis for forensic genetic testing*. Methods Mol Biol, 2012. **830**: p. 87-107.
119. Pakstis, A.J., et al., *Candidate SNPs for a universal individual identification panel*. Hum Genet, 2007. **121**(3-4): p. 305-17.
120. Tomas, C., et al., *Autosomal SNP typing of forensic samples with the GenPlex HID System: results of a collaborative study*. Forensic Sci Int Genet, 2010. **5**(5): p. 369-75.
121. Lou, C., et al., *A SNaPshot assay for genotyping 44 individual identification single nucleotide polymorphisms*. Electrophoresis. **32**(3-4): p. 368-78.
122. Musgrave-Brown, E., et al., *Forensic validation of the SNPforID 52-plex assay*. Forensic Sci Int Genet, 2007. **1**(2): p. 186-90.
123. Biosystems, A., *AmpFISTR® Identifiler® PCR Amplification Kit. Product Bulletin*. 2006.
124. Borsting, C., E. Rockenbauer, and N. Morling, *Validation of a single nucleotide polymorphism (SNP) typing assay with 49 SNPs for forensic genetic testing in a laboratory accredited according to the ISO 17025 standard*. Forensic Sci Int Genet, 2009. **4**(1): p. 34-42.
125. Underhill, P.A. and T. Kivisild, *Use of y chromosome and mitochondrial DNA population structure in tracing human migrations*. Annu Rev Genet, 2007. **41**: p. 539-64.
126. Phillips, C., et al., *Resolving relationship tests that show ambiguous STR results using autosomal SNPs as supplementary markers*. Forensic Science International: Genetics. **In Press, Corrected Proof**.
127. Pitterl, F., et al., *Increasing the discrimination power of forensic STR testing by employing high-performance mass spectrometry, as illustrated in indigenous South African and Central Asian populations*. Int J Legal Med, 2010. **124**(6): p. 551-8.
128. Oki, T., et al., *Development of multiplex assay with 16 SNPs on X chromosome for degraded samples*. Leg Med (Tokyo), 2011. **14**(1): p. 11-6.

129. Tomas, C., et al., *Forensic usefulness of a 25 X-chromosome single-nucleotide polymorphism marker set*. Transfusion, 2010. **50**(10): p. 2258-65.
130. Chiaroni, J., P.A. Underhill, and L.L. Cavalli-Sforza, *Y chromosome diversity, human expansion, drift, and cultural evolution*. Proc Natl Acad Sci U S A, 2009. **106**(48): p. 20174-9.
131. Kohnemann, S., et al., *A rapid mtDNA assay of 22 SNPs in one multiplex reaction increases the power of forensic testing in European Caucasians*. Int J Legal Med, 2008. **122**(6): p. 517-23.
132. Vallone, P.M., *Capillary electrophoresis of an 11-plex mtDNA coding region SNP single base extension assay for discrimination of the most common Caucasian HV1/HV2 mitotype*. Methods Mol Biol. **830**: p. 159-67.
133. Butler, K., et al., *Molecular "eyewitness": Forensic prediction of phenotype and ancestry*. Forensic Sci Int Genet, 2011. **Series 3**: p. e498-499.
134. Kayser, M. and P. de Knijff, *Improving human forensics through advances in genetics, genomics and molecular biology*. Nat Rev Genet, 2011. **12**(3): p. 179-92.
135. Phillips, C., et al., *Inferring ancestral origin using a single multiplex assay of ancestry-informative marker SNPs*. Forensic Science International: Genetics, 2007. **1**(3-4): p. 273-280.
136. Frudakis, T., et al., *A classifier for the SNP-based inference of ancestry*. J Forensic Sci, 2003. **48**(4): p. 771-82.
137. Rosenberg, N.A., et al., *Genetic structure of human populations*. Science, 2002. **298**(5602): p. 2381-5.
138. Phillips, C., M. Fondevila, and M.V. Lareau, *A 34-plex autosomal SNP single base extension assay for ancestry investigations*. Methods Mol Biol, 2012. **830**: p. 109-26.
139. Clark, P., et al., *A twin study of skin reflectance*. Ann Hum Biol, 1981. **8**(6): p. 529-41.
140. Silventoinen, K., et al., *Heritability of adult body height: a comparative study of twin cohorts in eight countries*. Twin Res, 2003. **6**(5): p. 399-408.
141. Sulem, P., et al., *Genetic determinants of hair, eye and skin pigmentation in Europeans*. Nat Genet, 2007. **39**(12): p. 1443-52.
142. Han, J., et al., *A genome-wide association study identifies novel alleles associated with hair color and skin pigmentation*. PLoS Genet, 2008. **4**(5): p. e1000074.
143. Voisey, J., N.F. Box, and A. van Daal, *A polymorphism study of the human Agouti gene and its association with MC1R*. Pigment Cell Res, 2001. **14**(4): p. 264-7.
144. Sturm, R.A., *A golden age of human pigmentation genetics*. Trends Genet, 2006. **22**(9): p. 464-8.
145. Graf, J., et al., *Promoter polymorphisms in the MATP (SLC45A2) gene are associated with normal human skin color variation*. Hum Mutat, 2007. **28**(7): p. 710-7.
146. Lao, O., et al., *Signatures of positive selection in genes associated with human skin pigmentation as revealed from analyses of single nucleotide polymorphisms*. Ann Hum Genet, 2007. **71**(Pt 3): p. 354-69.
147. Grimes, E.A., et al., *Sequence polymorphism in the human melanocortin 1 receptor gene as an indicator of the red hair phenotype*. Forensic science international, 2001. **122**(2-3): p. 124-9.

148. Rees, J.L., *The melanocortin 1 receptor (MC1R): more than just red hair*. *Pigment Cell Res*, 2000. **13**(3): p. 135-40.
149. Branicki, W., et al., *Model-based prediction of human hair color using DNA variants*. *Hum Genet*, 2011. **129**(4): p. 443-54.
150. Frudakis, T., et al., *Sequences associated with human iris pigmentation*. *Genetics*, 2003. **165**(4): p. 2071-83.
151. Rebbeck, T.R., et al., *P gene as an inherited biomarker of human eye color*. *Cancer Epidemiol Biomarkers Prev*, 2002. **11**(8): p. 782-4.
152. Walsh, S., et al., *IrisPlex: a sensitive DNA tool for accurate prediction of blue and brown eye colour in the absence of ancestry information*. *Forensic Sci Int Genet*. **5**(3): p. 170-80.
153. Sturm, R.A. and M. Larsson, *Genetics of human iris colour and patterns*. *Pigment Cell Melanoma Res*, 2009. **22**(5): p. 544-62.
154. Mengel-From, J., et al., *Human eye colour and HERC2, OCA2 and MATP*. *Forensic Sci Int Genet*, 2010. **4**(5): p. 323-8.
155. Ruiz, Y., et al., *Further development of forensic eye color predictive tests*. *Forensic science international. Genetics*, 2012.
156. Lango Allen, H., *Hundreds of variants clustered in genomic loci and biological pathways affect human height*. *Nature*, 2010. **467**: p. 832-838.
157. Aulchenko, Y.S., et al., *Predicting human height by Victorian and genomic methods*. *Eur J Hum Genet*, 2009. **17**(8): p. 1070-5.
158. Walsh, S., et al., *IrisPlex: a sensitive DNA tool for accurate prediction of blue and brown eye colour in the absence of ancestry information*. *Forensic Sci Int Genet*, 2011. **5**(3): p. 170-80.
159. Walsh, S., et al., *Developmental validation of the IrisPlex system: determination of blue and brown iris colour for forensic intelligence*. *Forensic Sci Int Genet*, 2010. **5**(5): p. 464-71.
160. Walsh, S., et al., *The HirisPlex system for simultaneous prediction of hair and eye colour from DNA*. *Forensic science international. Genetics*, 2012.
161. Pneuman, A., et al., *Verification of eye and skin color predictors in various populations*. *Leg Med (Tokyo)*, 2012. **14**(2): p. 78-83.
162. Spichenok, O., et al., *Prediction of eye and skin color in diverse populations using seven SNPs*. *Forensic Sci Int Genet*, 2010. **5**(5): p. 472-8.
163. Valenzuela, R.K., et al., *Predicting phenotype from genotype: normal pigmentation*. *J Forensic Sci*, 2010. **55**(2): p. 315-22.
164. Sturm, R.A., *Molecular genetics of human pigmentation diversity*. *Hum Mol Genet*, 2009. **18**(R1): p. R9-17.
165. Bulbul, O., et al., *A SNP multiplex for the simultaneous prediction of biogeographic ancestry and pigmentation type*. *Forensic Sci Int Genet*, 2011. **Series 3**: p. e500-501.
166. Castel, C. and A. Piper, *Development of a SNP multiplex assay for the inference of biogeographical ancestry and pigmentation phenotype*. *Forensic Sci Int Genet*, 2011. **Series 3**: p. e411-412.
167. Phillips, C., et al., *The SNPfor ID consortium, inferring ancestral origin using a single multiplex assay of autosomal ancestry-informative mark SNPs*. *Forensic Sci Int Genet*, 2007. **1**: p. 273-280.
168. Borsting, C., B.B. Hjort, and N. Morling, *SNP typing of crime scene samples with the SNPforID multiplex assay*. *Forensic Sci Int Genet*, 2011. **Series 3**: p. e99-e100.

169. Comey, C.T. and B. Budowle, *Validation studies on the analysis of the HLA DQ alpha locus using the polymerase chain reaction*. Journal of forensic sciences, 1991. **36**(6): p. 1633-48.
170. Gill, P., *An assessment of the utility of single nucleotide polymorphisms (SNPs) for forensic purposes*. Int J Legal Med, 2001. **114**(4-5): p. 204-10.
171. Chakraborty, R., et al., *The utility of short tandem repeat loci beyond human identification: implications for development of new DNA typing systems*. Electrophoresis, 1999. **20**(8): p. 1682-96.
172. Sobrino, B., M. Brion, and A. Carracedo, *SNPs in forensic genetics: a review on SNP typing methodologies*. Forensic science international, 2005. **154**(2-3): p. 181-94.
173. Dixon, L.A., et al., *Analysis of artificially degraded DNA using STRs and SNPs--results of a collaborative European (EDNAP) exercise*. Forensic science international, 2006. **164**(1): p. 33-44.
174. Gill, P., et al., *An assessment of whether SNPs will replace STRs in national DNA databases--joint considerations of the DNA working group of the European Network of Forensic Science Institutes (ENFSI) and the Scientific Working Group on DNA Analysis Methods (SWGDM)*. Sci Justice, 2004. **44**(1): p. 51-3.
175. Hall, T.A., et al., *Base composition profiling of human mitochondrial DNA using polymerase chain reaction and direct automated electrospray ionization mass spectrometry*. Anal Chem, 2009. **81**(18): p. 7515-26.
176. Gill, P., *Role of short tandem repeat DNA in forensic casework in the UK--past, present, and future perspectives*. Biotechniques, 2002. **32**(2): p. 366-8, 370, 372, passim.
177. Butler, J.M., *Genetics and genomics of core short tandem repeat loci used in human identity testing*. Journal of forensic sciences, 2006. **51**(2): p. 253-65.
178. Gill, P., et al., *The evolution of DNA databases--recommendations for new European STR loci*. Forensic Sci Int, 2006. **156**(2-3): p. 242-4.
179. Freire-Aradas, A., et al., *A new SNP assay for identification of highly degraded human DNA*. Forensic Sci Int Genet, 2011.
180. Luger, K., et al., *Crystal structure of the nucleosome core particle at 2.8 A resolution*. Nature, 1997. **389**(6648): p. 251-60.
181. Galea, A.M. and V. Murray, *The influence of chromatin structure on DNA damage induced by nitrogen mustard and cisplatin analogues*. Chem Biol Drug Des. **75**(6): p. 578-89.
182. Mir, M.A., S. Das, and D. Dasgupta, *N-terminal tail domains of core histones in nucleosome block the access of anticancer drugs, mithramycin and daunomycin, to the nucleosomal DNA*. Biophys Chem, 2004. **109**(1): p. 121-35.
183. Romanini, C., et al., *Typing short amplicon binary polymorphisms: Supplementary SNP and Indel genetic information in the analysis of highly degraded skeletal remains*. Forensic Sci Int Genet, 2011.
184. Larue, B.L., et al., *A validation study of the Qiagen Investigator DIPplex(R) kit; an INDEL-based assay for human identification*. International journal of legal medicine, 2012. **126**(4): p. 533-40.
185. Pereira, R., et al., *Insertion/deletion polymorphisms: a multiplex assay and forensic applications*. Forensic Sci Int Genet, 2009. **Series 2 (Suppl.)**: p. 513-515.
186. Wayne, J.S., et al., *A simple and sensitive method for quantifying human genomic DNA in forensic specimen extracts*. Biotechniques, 1989. **7**(8): p. 852-5.

187. Hopwood, A., et al., *Rapid quantification of DNA samples extracted from buccal scrapes prior to DNA profiling*. Biotechniques, 1997. **23**(1): p. 18-20.
188. Alonso, A., et al., *Real-time PCR designs to estimate nuclear and mitochondrial DNA copy number in forensic and ancient DNA studies*. Forensic Science International, 2004. **139**(2-3): p. 141-149.
189. Andreasson, H., U. Gyllensten, and M. Allen, *Real-time DNA quantification of nuclear and mitochondrial DNA in forensic analysis*. Biotechniques, 2002. **33**(2): p. 402-4, 407-11.
190. Higuchi, R., et al., *Kinetic PCR analysis: real-time monitoring of DNA amplification reactions*. Biotechnology (N Y), 1993. **11**(9): p. 1026-30.
191. Karlen, Y., et al., *Statistical significance of quantitative PCR*. BMC Bioinformatics, 2007. **8**: p. 131.
192. Holland, P.M., et al., *Detection of specific polymerase chain reaction product by utilizing the 5'----3' exonuclease activity of Thermus aquaticus DNA polymerase*. Proc Natl Acad Sci U S A, 1991. **88**(16): p. 7276-80.
193. Green, R.L., et al., *Developmental validation of the quantifiler real-time PCR kits for the quantification of human nuclear DNA samples*. J Forensic Sci, 2005. **50**(4): p. 809-25.
194. Barbisin, M., et al., *Developmental validation of the Quantifiler Duo DNA Quantification kit for simultaneous quantification of total human and human male DNA and detection of PCR inhibitors in biological samples*. J Forensic Sci, 2009. **54**(2): p. 305-19.
195. Swango, K.L., et al., *A quantitative PCR assay for the assessment of DNA degradation in forensic samples*. Forensic Science International, 2006. **158**(1): p. 14-26.
196. Hudlow, W.R., et al., *A quadruplex real-time qPCR assay for the simultaneous assessment of total human DNA, human male DNA, DNA degradation and the presence of PCR inhibitors in forensic samples: A diagnostic tool for STR typing*. Forensic Science International: Genetics, 2008. **2**(2): p. 108-125.
197. Timken, M.D., et al., *A duplex real-time qPCR assay for the quantification of human nuclear and mitochondrial DNA in forensic samples: implications for quantifying DNA in degraded samples*. J Forensic Sci, 2005. **50**(5): p. 1044-60.
198. Walker, J.A., et al., *Multiplex polymerase chain reaction for simultaneous quantitation of human nuclear, mitochondrial, and male Y-chromosome DNA: application in human identification*. Analytical Biochemistry, 2005. **337**(1): p. 89-97.
199. Fregel, R., et al., *Reliable nuclear and mitochondrial DNA quantification for low copy number and degraded forensic samples*. Forensic Sci Int: Gen Supp, 2011. **Series 3**: p. e303-304.
200. von Wurmb-Schwark, N., et al., *A new multiplex-PCR comprising autosomal and y-specific STRs and mitochondrial DNA to analyze highly degraded material*. Forensic Science International: Genetics, 2009. **3**(2): p. 96-103.
201. Nicklas, J.A. and E. Buel, *Development of an Alu-based, real-time PCR method for quantitation of human DNA in forensic samples*. J Forensic Sci, 2003. **48**(5): p. 936-44.
202. Nicklas, J.A. and E. Buel, *Simultaneous determination of total human and male DNA using a duplex real-time PCR assay*. J Forensic Sci, 2006. **51**(5): p. 1005-15.

203. Nicklas, J.A., T. Noreault-Conti, and E. Buel, *Development of a real-time method to detect DNA degradation in forensic samples**. J Forensic Sci, 2011. **57**(2): p. 466-71.
204. LaSalle, H.E., G. Duncan, and B. McCord, *An analysis of single and multi-copy methods for DNA quantitation by real-time polymerase chain reaction*. Forensic Sci Int Genet, 2011. **5**(3): p. 185-93.
205. Kim, K., et al., *Technical note: improved ancient DNA purification for PCR using ion-exchange columns*. Am J Phys Anthropol, 2008. **136**(1): p. 114-21.
206. Rompler, H., et al., *Multiplex amplification of ancient DNA*. Nature protocols, 2006. **1**(2): p. 720-8.
207. d'Abbadie, M., et al., *Molecular breeding of polymerases for amplification of ancient DNA*. Nature biotechnology, 2007. **25**(8): p. 939-43.
208. Gilbert, M.T. and E. Willerslev, *Rescuing ancient DNA*. Nat Biotechnol, 2007. **25**(8): p. 872-4.
209. Schmerer, W.M., S. Hummel, and B. Herrmann, *Optimized DNA extraction to improve reproducibility of short tandem repeat genotyping with highly degraded DNA as target*. Electrophoresis, 1999. **20**(8): p. 1712-6.
210. Huel, R., et al., *DNA extraction from aged skeletal samples for STR typing by capillary electrophoresis*. Methods in molecular biology, 2012. **830**: p. 185-98.
211. Jakubowska, J., A. Maciejewska, and R. Pawlowski, *Comparison of three methods of DNA extraction from human bones with different degrees of degradation*. Int J Legal Med, 2011. **126**(1): p. 173-8.
212. Vanek, D., et al., *Genomic DNA extraction protocols for bone samples: The comparison of Qiagen and Zymo research spin columns*. Forensic Sci Int: Gen Supp, 2011. **Series 3**: p. e397-398.
213. Hughes, A., T.L. Stewart, and V. Mann, *Extraction of nucleic acids from bone*. Methods Mol Biol, 2012. **816**: p. 249-59.
214. Ludwikowska-Pawlowska, M., et al., *[Application of the QIAamp DNA Investigator Kit and Prepfiler Forensic DNA Extraction Kit in genomic DNA extraction from skeletal remains]*. Arch Med Sadowej Kryminol, 2009. **59**(4): p. 289-94.
215. Seo, S.B., et al., *Technical note: Efficiency of total demineralization and ion-exchange column for DNA extraction from bone*. Am J Phys Anthropol, 2009. **141**(1): p. 158-62.
216. Lee, H.Y., et al., *Simple and highly effective DNA extraction methods from old skeletal remains using silica columns*. Forensic Sci Int Genet, 2010. **4**(5): p. 275-80.
217. Amory, S., et al., *Automatable full demineralization DNA extraction procedure from degraded skeletal remains*. Forensic science international. Genetics, 2012. **6**(3): p. 398-406.
218. Barnett, R. and G. Larson, *A phenol-chloroform protocol for extracting DNA from ancient samples*. Methods Mol Biol, 2012. **840**: p. 13-9.
219. Courts, C. and B. Madea, *Full STR profile of a 67-year-old bone found in a fresh water lake*. J Forensic Sci, 2011. **56 Suppl 1**: p. S172-5.
220. Kitayama, T., et al., *Evaluation of a new experimental kit for the extraction of DNA from bones and teeth using a non-powder method*. Leg Med (Tokyo), 2010. **12**(2): p. 84-9.

221. Schwark, T., A. Heinrich, and N. von Wurmb-Schwark, *Genetic identification of highly putrefied bodies using DNA from soft tissues*. *Int J Legal Med*, 2011. **125**(6): p. 891-4.
222. Schwark, T., et al., *Reliable genetic identification of burnt human remains*. *Forensic Sci Int Genet*, 2010. **5**(5): p. 393-9.
223. Liu HD, R.F., Xing RX, Pei LG., *Progress in individual identification of burned bones*. *Fa Yi Xue Za Zhi.* , 2009. **25**(1): p. 61-62.
224. Whitaker, J.P., E.A. Cotton, and P. Gill, *A comparison of the characteristics of profiles produced with the AMPFISTR(R) SGM Plus(TM) multiplex system for both standard and low copy number (LCN) STR DNA analysis*. *Forensic Science International*, 2001. **123**(2-3): p. 215-223.
225. Anjos, M.J., et al., *Low copy number: Interpretation of evidence results*. *International Congress Series*, 2006. **1288**: p. 616-618.
226. Tvedebrink, T., et al., *Performance of two 17 locus forensic identification STR kits-Applied Biosystems's AmpFISTR((R)) NGMSElect and Promega's PowerPlex((R)) ESI17 kits*. *Forensic science international. Genetics*, 2012.
227. Romano, C., et al., *A novel approach for genotyping of LCN-DNA recovered from highly degraded samples*. *International Congress Series*, 2006. **1288**: p. 577-579.
228. Gill, P., *Application of low copy number DNA profiling*. *Croatian medical journal*, 2001. **42**(3): p. 229-32.
229. Gill, P., et al., *An investigation of the rigor of interpretation rules for STRs derived from less than 100 pg of DNA*. *Forensic Science International*, 2000. **112**(1): p. 17-40.
230. Caragine, T., et al., *Validation of testing and interpretation protocols for low template DNA samples using AmpFISTR Identifier*. *Croat Med J*, 2009. **50**(3): p. 250-67.
231. Buckleton, J., *Validation issues around DNA typing of low level DNA*. *Forensic Sci Int Genet*, 2009. **3**(4): p. 255-60.
232. Budowle, B., A.J. Eisenberg, and A. van Daal, *Validity of low copy number typing and applications to forensic science*. *Croat Med J*, 2009. **50**(3): p. 207-17.
233. Wiegand, W., K. Trubner, and M. Kleiber, *STR Typing of Biological Stains on Strangulation Tools*. *Progress in Forensic Genetics*, 2000. **8**: p. 508-13.
234. Sewell, J., et al., *Recovery of DNA and fingerprints from touched documents*. *Forensic Science International: Genetics*, 2008. **2**(4): p. 281-285.
235. van Oorschot, R.A. and M.K. Jones, *DNA fingerprints from fingerprints*. *Nature*, 1997. **387**(6635): p. 767.
236. Balogh, M.K., et al., *STR genotyping and mtDNA sequencing of latent fingerprint on paper*. *Forensic Science International*, 2003. **137**(2-3): p. 188-195.
237. Barbaro, A., G. Falcone, and A. Barbaro, *DNA typing from hair shaft*. *Progress in Forensic Genetics*, 2000. **8**: p. 523-5.
238. Pizzamiglio, M., et al., *Identifying the culprit from LCN DNA obtained from saliva and sweat traces linked to two different robberies and use of a database*. *International Congress Series*, 2004. **1261**: p. 443-445.
239. Kloosterman, A.D. and P. Kersbergen, *Efficacy and limits of genotyping low copy number DNA samples by multiplex PCR of STR loci*. *International Congress Series*, 2003. **1239**: p. 795-798.

240. Budowle, B., et al. *Low Copy Number - consideration and caution*. in *Proceedings of the Twelfth International Symposium on Human Identification*. 2001. Madison, Wisconsin.
241. Forster, L., J. Thomson, and S. Kutranov, *Direct comparison of post-28-cycle PCR purification and modified capillary electrophoresis methods with the 34-cycle "low copy number" (LCN) method for analysis of trace forensic DNA samples*. *Forensic Science International: Genetics*, 2008. **2**(4): p. 318-328.
242. Gross, T., J. Thomson, and S. Kutranov, *A review of low template STR analysis in casework using the DNA SenCE post-PCR purification technique*. *Forensic Sci Int Genet*, 2009. **Suppl Series 2**: p. 5-7.
243. Smith, P.J. and J. Ballantyne, *Simplified low-copy-number DNA analysis by post-PCR purification*. *Journal of forensic sciences*, 2007. **52**(4): p. 820-9.
244. Weiler, N.E., A.S. Matai, and T. Sijen, *Extended PCR conditions to reduce drop-out frequencies in low template STR typing including unequal mixtures*. *Forensic Sci Int Genet*, 2012. **6**(1): p. 102-7.
245. Hawkins, T.L., J.C. Detter, and P.M. Richardson, *Whole genome amplification--applications and advances*. *Curr Opin Biotechnol*, 2002. **13**(1): p. 65-7.
246. Sun, G., et al., *Whole-genome amplification: relative efficiencies of the current methods*. *Legal medicine (Tokyo, Japan)*, 2005. **7**(5): p. 279-86.
247. Jiang, Z., et al., *Genome amplification of single sperm using multiple displacement amplification*. *Nucleic Acids Res*, 2005. **33**(10): p. e91.
248. Hanson, E.K. and J. Ballantyne, *Whole genome amplification strategy for forensic genetic analysis using single or few cell equivalents of genomic DNA*. *Analytical biochemistry*, 2005. **346**(2): p. 246-57.
249. Barber, A.L. and D.R. Foran, *The utility of whole genome amplification for typing compromised forensic samples*. *Journal of forensic sciences*, 2006. **51**(6): p. 1344-9.
250. Ballantyne, K.N., R.A.H. van Oorschot, and R.J. Mitchell, *Comparison of two whole genome amplification methods for STR genotyping of LCN and degraded DNA samples*. *Forensic Science International*, 2007. **166**(1): p. 35-41.
251. Kittler, R., M. Stoneking, and M. Kayser, *A whole genome amplification method to generate long fragments from low quantities of genomic DNA*. *Anal Biochem*, 2002. **300**(2): p. 237-44.
252. Lovmar, L. and A.C. Syvanen, *Multiple displacement amplification to create a long-lasting source of DNA for genetic studies*. *Hum Mutat*, 2006. **27**(7): p. 603-14.
253. Handyside, A.H., et al., *Isothermal whole genome amplification from single and small numbers of cells: a new era for preimplantation genetic diagnosis of inherited disease*. *Mol Hum Reprod*, 2004. **10**(10): p. 767-72.
254. Spits, C., et al., *Optimization and evaluation of single-cell whole-genome multiple displacement amplification*. *Hum Mutat*, 2006. **27**(5): p. 496-503.
255. Kumar, G., et al., *Improved multiple displacement amplification with phi29 DNA polymerase for genotyping of single human cells*. *Biotechniques*, 2008. **44**(7): p. 879-90.
256. Ling, J., et al., *Single-nucleotide polymorphism array coupled with multiple displacement amplification: accuracy and spatial resolution for analysis of chromosome copy numbers in few cells*. *Biotechnology and applied biochemistry*, 2012. **59**(1): p. 35-44.

257. Bergen, A.W., et al., *Comparison of yield and genotyping performance of multiple displacement amplification and OmniPlex whole genome amplified DNA generated from multiple DNA sources*. Hum Mutat, 2005. **26**(3): p. 262-70.
258. Dean, F.B., et al., *Comprehensive human genome amplification using multiple displacement amplification*. Proceedings of the National Academy of Sciences of the United States of America, 2002. **99**(8): p. 5261-6.
259. Hosono, S., et al., *Unbiased whole-genome amplification directly from clinical samples*. Genome Res, 2003. **13**(5): p. 954-64.
260. Nelson, D.L., et al., *Alu polymerase chain reaction: a method for rapid isolation of human-specific sequences from complex DNA sources*. Proc Natl Acad Sci U S A, 1989. **86**(17): p. 6686-90.
261. Lucito, R., et al., *Genetic analysis using genomic representations*. Proc Natl Acad Sci U S A, 1998. **95**(8): p. 4487-92.
262. Silander, K. and J. Saarela, *Whole Genome Amplification with Phi29 DNA Polymerase to Enable Genetic or Genomic Analysis of Samples of Low DNA Yield*, in *Genomics Protocols*, M. Starkey and R. Elaswarapu, Editors. 2008, Humana Press Inc.: Totowa, NJ.
263. Zhang, L., et al., *Whole genome amplification from a single cell: implications for genetic analysis*. Proc Natl Acad Sci U S A, 1992. **89**(13): p. 5847-51.
264. Dietmaier, W., et al., *Multiple mutation analyses in single tumor cells with improved whole genome amplification*. Am J Pathol, 1999. **154**(1): p. 83-95.
265. Telenius, H., et al., *Degenerate oligonucleotide-primed PCR: general amplification of target DNA by a single degenerate primer*. Genomics, 1992. **13**(3): p. 718-25.
266. Cheung, V.G. and S.F. Nelson, *Whole genome amplification using a degenerate oligonucleotide primer allows hundreds of genotypes to be performed on less than one nanogram of genomic DNA*. Proc Natl Acad Sci U S A, 1996. **93**(25): p. 14676-9.
267. Esteban, J.A., M. Salas, and L. Blanco, *Fidelity of phi 29 DNA polymerase. Comparison between protein-primed initiation and DNA polymerization*. The Journal of biological chemistry, 1993. **268**(4): p. 2719-26.
268. Ballantyne, K.N., et al., *Decreasing amplification bias associated with multiple displacement amplification and short tandem repeat genotyping*. Analytical biochemistry, 2007. **368**(2): p. 222-9.
269. Garmendia, C., et al., *The bacteriophage phi 29 DNA polymerase, a proofreading enzyme*. J Biol Chem, 1992. **267**(4): p. 2594-9.
270. Esteban, J.A., M. Salas, and L. Blanco, *Fidelity of phi 29 DNA polymerase. Comparison between protein-primed initiation and DNA polymerization*. J Biol Chem, 1993. **268**(4): p. 2719-26.
271. Eckert, K.A. and T.A. Kunkel, *DNA polymerase fidelity and the polymerase chain reaction*. PCR Methods Appl, 1991. **1**(1): p. 17-24.
272. Panelli, S., et al., *Towards the analysis of the genomes of single cells: further characterisation of the multiple displacement amplification*. Gene, 2006. **372**: p. 1-7.
273. Blanco, L., et al., *Highly efficient DNA synthesis by the phage phi 29 DNA polymerase. Symmetrical mode of DNA replication*. J Biol Chem, 1989. **264**(15): p. 8935-40.

274. Lage, J.M., et al., *Whole genome analysis of genetic alterations in small DNA samples using hyperbranched strand displacement amplification and array-CGH*. *Genome Res*, 2003. **13**(2): p. 294-307.
275. Balogh, M.K., et al., *Application of whole genome amplification for forensic analysis*. *International Congress Series*, 2006. **1288**: p. 725-727.
276. Tzvetkov, M.V., et al., *Genome-wide single-nucleotide polymorphism arrays demonstrate high fidelity of multiple displacement-based whole-genome amplification*. *Electrophoresis*, 2005. **26**(3): p. 710-5.
277. Hellani, A., et al., *Multiple displacement amplification on single cell and possible PGD applications*. *Mol Hum Reprod*, 2004. **10**(11): p. 847-52.
278. Maragh, S., et al., *Multiple strand displacement amplification of mitochondrial DNA from clinical samples*. *BMC Med Genet*, 2008. **9**: p. 7.
279. Cunningham, J.M., et al., *Performance of amplified DNA in an Illumina GoldenGate BeadArray assay*. *Cancer Epidemiol Biomarkers Prev*, 2008. **17**(7): p. 1781-9.
280. Kroneis, T., et al., *DNA typing in single cell analysis: Single sperm cells outperform whole genome pre-amplified samples*. *Forensic Sci Int: Gen Supp*, 2011. **Series 3**: p. e465-e466.
281. Lasken, R.S. and M. Egholm, *Whole genome amplification: abundant supplies of DNA from precious samples or clinical specimens*. *Trends Biotechnol*, 2003. **21**(12): p. 531-5.
282. Heid, C.A., et al., *Real time quantitative PCR*. *Genome Res*, 1996. **6**(10): p. 986-94.
283. Silander, K., et al., *Evaluating whole genome amplification via multiply-primed rolling circle amplification for SNP genotyping of samples with low DNA yield*. *Twin Res Hum Genet*, 2005. **8**(4): p. 368-75.
284. Rook, M.S., et al., *Whole genome amplification of DNA from laser capture-microdissected tissue for high-throughput single nucleotide polymorphism and short tandem repeat genotyping*. *Am J Pathol*, 2004. **164**(1): p. 23-33.
285. Dickson, P.A., et al., *Evaluation of multiple displacement amplification in a 5 cM STR genome-wide scan*. *Nucleic Acids Res*, 2005. **33**(13): p. e119.
286. Sorensen, K.J., et al., *Whole-genome amplification of DNA from residual cells left by incidental contact*. *Anal Biochem*, 2004. **324**(2): p. 312-4.
287. Borsting C., M., N., *Multiple Displacement amplification of blood and saliva samples placed on FTA cards*. *International Congress Series*, 2006. **1288**: p. 716-718.
288. Wang, G., et al., *DNA amplification method tolerant to sample degradation*. *Genome Res*, 2004. **14**(11): p. 2357-66.
289. QIAGEN. *REPLI-g Mini/Mid Handbook*. 2005; Available from: <http://www1.qiagen.com/literature/handbooks/literature.aspx?id=1000533>.
290. Nunez-Illas, A., et al., *Application of Circular Ligase to Provide Template for Rolling Circle Amplification of Low Amounts of Fragmented DNA*, in *19th International Symposium on Human Identification 2008*, Promega: Hollywood, California, USA.
291. Kuhn, H. and M.D. Frank-Kamenetskii, *Template-independent ligation of single-stranded DNA by T4 DNA ligase*. *The FEBS journal*, 2005. **272**(23): p. 5991-6000.

292. Gadkar, V.J. and M. Filion, *A novel method to perform genomic walks using a combination of single strand DNA circularization and rolling circle amplification*. J Microbiol Methods, 2011. **87**(1): p. 38-43.
293. Lamm, A.T., et al., *Multimodal RNA-seq using single-strand, double-strand, and CirLigase-based capture yields a refined and extended description of the C. elegans transcriptome*. Genome Res, 2011. **21**(2): p. 265-75.
294. Tate, C.M., et al., *Evaluation of circular DNA substrates for whole genome amplification prior to forensic analysis*. Forensic Sci Int Genet, 2011. **6**(2): p. 185-90.
295. Nunez, A.N., et al., *Application of circular ligase to provide template for rolling circle amplification of low amounts of fragmented DNA*. 19th International Symposium on Human Identification 2008. **Oral Presentation**.
296. Tate, C.M., et al., *Evaluation of circular DNA substrates for whole genome amplification prior to forensic analysis*. Forensic science international. Genetics, 2012. **6**(2): p. 185-90.
297. Zhang, Z., et al., *A LDR-PCR approach for multiplex polymorphisms genotyping of severely degraded DNA with fragment sizes <100 bp*. J Forensic Sci, 2009. **54**(6): p. 1304-9.
298. Wang, J. and B. McCord, *The application of magnetic bead hybridization for the recovery and STR amplification of degraded and inhibited forensic DNA*. Electrophoresis, 2011. **32**(13): p. 1631-8.
299. Rondan Duenas, J.C., et al., *Reparation of degraded DNA improves PCR amplification of larger STR loci*. Forensic Sci Int: Gen Supp, 2009. **Series 2**: p. 522-523.
300. Pusch, C.M., I. Giddings, and M. Scholz, *Repair of degraded duplex DNA from prehistoric samples using Escherichia coli DNA polymerase I and T4 DNA ligase*. Nucleic Acids Res, 1998. **26**(3): p. 857-9.
301. BioLabs, N.E. *PreCR DNA Repair Mix*. Available from: <http://www.neb.com/nebecomm/products/productM0309.asp>.
302. Farr, M., et al., *Examination and Optimization of the PreCR DNA Repair Mix on Damaged DNA for Short Tandem Repeat and Mitochondial DNA Analysis*, in *19th International Symposium on Human Identification 2008*: Hollywood, California, USA.
303. Diegoli, T.M., et al., *An optimized protocol for forensic application of the PreCR Repair Mix to multiplex STR amplification of UV-damaged DNA*. Forensic Sci Int Genet, 2011.
304. Walker, C., et al., *Restorase™: A Novel DNA Polymerase Blend that Repairs Damaged DNA*. SIGMA-ALDRICH Product Poster, 2009.
305. Westen, A.A., et al., *Tri-allelic SNP markers enable analysis of mixed and degraded DNA samples*. Forensic Sci Int Genet, 2009. **3**(4): p. 233-41.
306. Odigie, K., et al., *Repair of damaged DNA using commercially available enzymes*. Society of Advancement of Chicanos and Native Americans in Science, 2007. **Poster Presentation**: p. D43.
307. Gilbert, M.T., et al., *Multiplex PCR with minisequencing as an effective high-throughput SNP typing method for formalin-fixed tissue*. Electrophoresis, 2007. **28**(14): p. 2361-7.

308. Romero, R.L., et al., *The applicability of formalin-fixed and formalin fixed paraffin embedded tissues in forensic DNA analysis*. Journal of forensic sciences, 1997. **42**(4): p. 708-14.
309. Reshef, A., et al., *STR typing of formalin-fixed paraffin embedded (FFPE) aborted foetal tissue in criminal paternity cases*. Science & justice : journal of the Forensic Science Society, 2011. **51**(1): p. 19-23.
310. Li, J., et al., *Improved RNA quality and TaqMan Pre-amplification method (PreAmp) to enhance expression analysis from formalin fixed paraffin embedded (FFPE) materials*. BMC biotechnology, 2008. **8**: p. 10.
311. Cronin, M., et al., *Measurement of gene expression in archival paraffin-embedded tissues: development and performance of a 92-gene reverse transcriptase-polymerase chain reaction assay*. The American journal of pathology, 2004. **164**(1): p. 35-42.
312. QIAGEN, *REPLI-g® FFPE Handbook*, 2007.
313. Pfeiffer, B.H. and S.B. Zimmerman, *Polymer-stimulated ligation: enhanced blunt- or cohesive-end ligation of DNA or deoxyribooligonucleotides by T4 DNA ligase in polymer solutions*. Nucleic Acids Res, 1983. **11**(22): p. 7853-71.
314. Zimmerman, S.B. and B. Harrison, *Macromolecular crowding increases binding of DNA polymerase to DNA: an adaptive effect*. Proc Natl Acad Sci U S A, 1987. **84**(7): p. 1871-5.
315. Ballantyne, K.N., et al., *Molecular crowding increases the amplification success of multiple displacement amplification and short tandem repeat genotyping*. Analytical biochemistry, 2006. **355**(2): p. 298-303.
316. Biomatrix. 2008; Available from: <http://www.biomatrix.com/pcrboost.php>.
317. Biomatrix. *Successful amplification of thermally degraded DNA using PCRboost*. 2008; Available from: <http://www.biomatrix.com/media/pcrboost/Ddegraded%20DNA%20PCRboost.pdf>.
318. Biomatrix, *STRboost™: A Novel STR Amplification Enhancer*. Biomatrix Application Note, 2010.
319. Ho Faix, P. and A. Lee, *Biological evidence analysis: How to improve recovery of DNA profiles*. Evidence Technology Magazine, 2009. **7**(2): p. 28-31.
320. Holland, M.M. and E.F. Huffine, *Molecular analysis of the human mitochondrial DNA control region for forensic identity testing*. Curr Protoc Hum Genet, 2001. **Chapter 14**: p. Unit 14 7.
321. Hellmann, A., et al., *STR typing of human telogen hairs--a new approach*. Int J Legal Med, 2001. **114**(4-5): p. 269-73.
322. Grubwieser, P., et al., *A new "miniSTR-multiplex" displaying reduced amplicon lengths for the analysis of degraded DNA*. International journal of legal medicine, 2006. **120**(2): p. 115-20.
323. Hill, C.R., et al., *Characterization of 26 miniSTR loci for improved analysis of degraded DNA samples*. Journal of forensic sciences, 2008. **53**(1): p. 73-80.
324. Fang R., P.A., Hyland F, Wang D, Shewal J, Kidd JR, Kidd KK, Furtado MR, *Multiplexed SNP detection panels for human identification*. Forensic Sci Int Genet 2, 2009: p. 538-539.
325. Luce, C., et al., *Validation of the AMPFISTR MiniFiler PCR amplification kit for use in forensic casework**. J Forensic Sci, 2009. **54**(5): p. 1046-54.

326. Mulero, J.J., et al., *Development and validation of the AmpFISTR Yfiler PCR amplification kit: a male specific, single amplification 17 Y-STR multiplex system*. Journal of forensic sciences, 2006. **51**(1): p. 64-75.
327. Tilotta, F., et al., *A comparative study of two methods of dental pulp extraction for genetic fingerprinting*. Forensic Sci Int. **202**(1-3): p. e39-43.
328. Manjunath, B.C., et al., *DNA profiling and forensic dentistry--a review of the recent concepts and trends*. J Forensic Leg Med, 2011. **18**(5): p. 191-7.
329. Meyer, E., et al., *Extraction and amplification of authentic DNA from ancient human remains*. Forensic science international, 2000. **113**(1-3): p. 87-90.
330. <http://healthy-lifestyle.most-effective-solution.com/wp-content/uploads/2010/07/human-anatomy-teeth.png>.
331. *Textbook of Endodontology*, ed. G. Bergenholtz, P. Horsted-Bindslev, and C. Reit: Blackwell.
332. Pinchi, V., et al., *Techniques of dental DNA extraction: Some operative experiences*. Forensic Sci Int, 2011. **204**(1-3): p. 111-4.
333. Primorac, D., et al., *Identification of war victims from mass graves in Croatia, Bosnia, and Herzegovina by use of standard forensic methods and DNA typing*. J Forensic Sci, 1996. **41**(5): p. 891-4.
334. Stoner, K.E., *Using a Hedstrom endodontic file to retrieve a root tip*. Journal of the American Dental Association, 2002. **133**(4): p. 473.
335. Available from: http://users.forthnet.gr/ath/abyss/dep1151_1.htm.
336. Steptoe, D., *The Human Skeletal Material from HMS Pandora*, in *Department of Anatomical Sciences 1998*, University of Queensland: St. Lucia, Brisbane. p. 305.
337. Park, M.J., et al., *Y-STR analysis of degraded DNA using reduced-size amplicons*. International journal of legal medicine, 2007. **121**(2): p. 152-7.
338. Vass, A.A., et al., *Time since death determinations of human cadavers using soil solution*. Journal of forensic sciences, 1992. **37**(5): p. 1236-53.
339. Carter, D.O., *Forensic Taphonomy: processes associated with cadaver decomposition in soil.*, in *School of Pharmacy and Molecular Sciences 2005*, James Cook University: Townsville.
340. Hosmer, D.W. and S. Lemeshow, *Applied logistic regression*. 2nd ed. Probability and Statistics 2000: Wiley-Interscience Publication.
341. *Salinity - Dissolved Salts, Measuring Salinity*. Available from: http://www.windows2universe.org/earth/Water/dissolved_salts.html.
342. Carter, D.O., D. Yellowlees, and M. Tibbett, *Cadaver decomposition in terrestrial ecosystems*. Die Naturwissenschaften, 2007. **94**(1): p. 12-24.
343. Benninger, L.A., D.O. Carter, and S.L. Forbes, *The biochemical alteration of soil beneath a decomposing carcass*. Forensic science international, 2008. **180**(2-3): p. 70-5.
344. Cardoso, H.F., et al., *Establishing a minimum postmortem interval of human remains in an advanced state of skeletonization using the growth rate of bryophytes and plant roots*. Int J Legal Med, 2010. **124**(5): p. 451-6.
345. Ubelaker, D.H. and K.M. Zarenko, *Adipocere: what is known after over two centuries of research*. Forensic science international, 2011. **208**(1-3): p. 167-72.
346. Forbes, S.L., B.H. Stuart, and B.B. Dent, *The effect of the burial environment on adipocere formation*. Forensic Sci Int, 2005. **154**(1): p. 24-34.
347. Moses, R.J., *Experimental adipocere formation: implications for adipocere formation on buried bone*. J Forensic Sci, 2012. **57**(3): p. 589-95.

348. Yan, F., et al., *Preliminary quantitative investigation of postmortem adipocere formation*. J Forensic Sci, 2001. **46**(3): p. 609-14.
349. Forbes, S.L., et al., *A preliminary investigation of the stages of adipocere formation*. J Forensic Sci, 2004. **49**(3): p. 566-74.
350. O'Brien, T.G. and A.C. Kuehner, *Waxing grave about adipocere: soft tissue change in an aquatic context*. J Forensic Sci, 2007. **52**(2): p. 294-301.
351. Mellen, P.F., M.A. Lowry, and M.S. Micozzi, *Experimental observations on adipocere formation*. J Forensic Sci, 1993. **38**(1): p. 91-3.
352. Lounsbury, J.A., et al., *An enzyme-based DNA preparation method for application to forensic biological samples and degraded stains*. Forensic science international. Genetics, 2012.
353. Nothnagel, M., et al., *Collaborative genetic mapping of 12 forensic short tandem repeat (STR) loci on the human X chromosome*. Forensic science international. Genetics, 2012.
354. Gittelsohn, S., et al., *Bayesian Networks and the Value of the Evidence for the Forensic Two-Trace Transfer Problem**. Journal of forensic sciences, 2012.
355. Rodriguez III, W.C., *Decomposition of buried and submerged bodies*, in *Forensic Taphonomy*, W.D.H.a.M.H. Sorg, Editor 1997, CRC Press: Boca Raton.
356. Niemcunowicz-Janica, A., et al., *Effect of soil and water environment on typeability of PowerPlex Y (Promega) in selected tissue samples*. Folia Histochem Cytobiol, 2007. **45**(4): p. 393-5.
357. Misner, L.M., et al., *The correlation between skeletal weathering and DNA quality and quantity*. J Forensic Sci, 2009. **54**(4): p. 822-8.
358. Kaestle, F.A. and K.A. Horsburgh, *Ancient DNA in anthropology: methods, applications, and ethics*. American journal of physical anthropology, 2002. **Suppl 35**: p. 92-130.
359. Muruganandhan, J. and G. Sivakumar, *Practical aspects of DNA-based forensic studies in dentistry*. J Forensic Dent Sci, 2011. **3**(1): p. 38-45.
360. Shiroma, C.Y., et al., *A minimally destructive technique for sampling dentin powder for mitochondrial DNA testing*. Journal of forensic sciences, 2004. **49**(4): p. 791-5.
361. Just, R.S., et al., *Toward increased utility of mtDNA in forensic identifications*. Forensic science international, 2004. **146 Suppl**: p. S147-9.
362. Paez, J.G., et al., *Genome coverage and sequence fidelity of phi29 polymerase-based multiple strand displacement whole genome amplification*. Nucleic acids research, 2004. **32**(9): p. e71.
363. Han, T., et al., *Characterization of whole genome amplified (WGA) DNA for use in genotyping assay development*. BMC genomics, 2012. **13**: p. 217.
364. Park, J.W., et al., *Comparing whole-genome amplification methods and sources of biological samples for single-nucleotide polymorphism genotyping*. Clinical chemistry, 2005. **51**(8): p. 1520-3.
365. Healthcare, G., *illustra GenomiPhi V2 DNA Amplification Kit*. , in *Product Web Protocol*2006.
366. Illumina, I., *Using whole-genome amplified (WGA) DNA Samples in the GoldenGate Genotyping Assay*, in http://www.illumina.com/documents/products/technotes/technote_goldengate_genotyping_assay_whole_genome_amplified.pdf2010.

367. Relethford, J.H., *Hemispheric difference in human skin color*. American journal of physical anthropology, 1997. **104**(4): p. 449-57.
368. Visser, M., M. Kayser, and R.J. Palstra, *HERC2 rs12913832 modulates human pigmentation by attenuating chromatin-loop formation between a long-range enhancer and the OCA2 promoter*. Genome research, 2012. **22**(3): p. 446-55.
369. Lipka, A.E., et al., *GAPIT: Genome Association and Prediction Integrated Tool*. Bioinformatics, 2012.
370. Coble, M.D., et al., *Mystery solved: the identification of the two missing Romanov children using DNA analysis*. PloS one, 2009. **4**(3): p. e4838.
371. Rook, M.S., et al., *Whole genome amplification of DNA from laser capture-microdissected tissue for high-throughput single nucleotide polymorphism and short tandem repeat genotyping*. The American journal of pathology, 2004. **164**(1): p. 23-33.
372. Schotsmans, E.M., et al., *The impact of shallow burial on differential decomposition to the body: a temperate case study*. Forensic science international, 2011. **206**(1-3): p. e43-8.
373. Liu, F., et al., *Eye color and the prediction of complex phenotypes from genotypes*. Current biology : CB, 2009. **19**(5): p. R192-3.
374. Kastelic, V. and K. Drobic, *Single multiplex system of twelve SNPs: Validation and implementation for association of SNPs with human eye and hair color*. Forensic Sci Int: Gen Supp 2011. **3**: p. e216-e217.
375. Sturm, R.A., et al., *A single SNP in an evolutionary conserved region within intron 86 of the HERC2 gene determines human blue-brown eye color*. American journal of human genetics, 2008. **82**(2): p. 424-31.
376. Cook, A.L., et al., *Analysis of cultured human melanocytes based on polymorphisms within the SLC45A2/MATP, SLC24A5/NCKX5, and OCA2/P loci*. The Journal of investigative dermatology, 2009. **129**(2): p. 392-405.
377. Eiberg, H., et al., *Blue eye color in humans may be caused by a perfectly associated founder mutation in a regulatory element located within the HERC2 gene inhibiting OCA2 expression*. Human genetics, 2008. **123**(2): p. 177-87.
378. Gerstenblith, M.R., J. Shi, and M.T. Landi, *Genome-wide association studies of pigmentation and skin cancer: a review and meta-analysis*. Pigment cell & melanoma research, 2010. **23**(5): p. 587-606.
379. Phillips, C., et al., *Characterization of U.S. population samples using a 34plex ancestry informative SNP multiplex*. Forensic Sci Int Genet, 2011. **Series 3**: p. 182-183.
380. Hutchison, C.A., 3rd, et al., *Cell-free cloning using phi29 DNA polymerase*. Proceedings of the National Academy of Sciences of the United States of America, 2005. **102**(48): p. 17332-6.
381. Marcy, Y., et al., *Nanoliter reactors improve multiple displacement amplification of genomes from single cells*. PLoS genetics, 2007. **3**(9): p. 1702-8.
382. Westen, A.A. and T. Sijen, *Degraded DNA sample analysis using DNA repair enzymes, mini-STRs and (tri-allelic) SNPs*. Forensic Sci Int: Gen Supp, 2009. **2**: p. 505-507.
383. Muharam, F.A., *Overcoming problems with limiting DNA samples in forensics and clinical diagnostics using Multiple Displacement Amplification*, in *Cooperative Research Centre for Diagnostics, School of Life Sciences, Faculty of Science 2005*, Queensland University of Technology: Brisbane.

384. Yan, J., et al., *Assessment of multiple displacement amplification in molecular epidemiology*. Biotechniques, 2004. **37**(1): p. 136-8, 140-3.
385. Liu, Y., et al., *Whole-genome synthesis and characterization of viable s13-like bacteriophages*. PloS one, 2012. **7**(7): p. e41124.
386. Invitrogen, L.T., *T4 DNA Ligase Manual*, 2002.
387. Sigma-Aldrich, *Restorase DNA Polymerase Product Information*, in <http://www.sigmaaldrich.com/etc/medialib/docs/Sigma/Bulletin/r1028bul.Par.0001.File.tmp/r1028bul.pdf>, Sigma-Aldrich, Editor.
388. Xing, J., et al., *High fidelity of whole-genome amplified DNA on high-density single nucleotide polymorphism arrays*. Genomics, 2008. **92**(6): p. 452-6.
389. Croft, D.T., Jr., et al., *Performance of whole-genome amplified DNA isolated from serum and plasma on high-density single nucleotide polymorphism arrays*. The Journal of molecular diagnostics : JMD, 2008. **10**(3): p. 249-57.
390. Coskun, S. and O. Alsmadi, *Whole genome amplification from a single cell: a new era for preimplantation genetic diagnosis*. Prenatal diagnosis, 2007. **27**(4): p. 297-302.
391. Yang, P., et al., *Purification of the Arabidopsis 26 S proteasome: biochemical and molecular analyses revealed the presence of multiple isoforms*. The Journal of biological chemistry, 2004. **279**(8): p. 6401-13.
392. Hosono, S., et al., *Unbiased whole-genome amplification directly from clinical samples*. Genome research, 2003. **13**(5): p. 954-64.
393. Jasmine, F., et al., *Whole-genome amplification enables accurate genotyping for microarray-based high-density single nucleotide polymorphism array*. Cancer epidemiology, biomarkers & prevention : a publication of the American Association for Cancer Research, cosponsored by the American Society of Preventive Oncology, 2008. **17**(12): p. 3499-508.
394. Barker, D.L., et al., *Two methods of whole-genome amplification enable accurate genotyping across a 2320-SNP linkage panel*. Genome research, 2004. **14**(5): p. 901-7.
395. Giardina, E., et al., *Whole genome amplification and real-time PCR in forensic casework*. BMC genomics, 2009. **10**: p. 159.
396. Lasken, R.S. and M. Egholm, *Whole genome amplification: abundant supplies of DNA from precious samples or clinical specimens*. Trends in biotechnology, 2003. **21**(12): p. 531-5.
397. Binga, E.K., R.S. Lasken, and J.D. Neufeld, *Something from (almost) nothing: the impact of multiple displacement amplification on microbial ecology*. The ISME journal, 2008. **2**(3): p. 233-41.
398. Berthier-Schaad, Y., et al., *Reliability of high-throughput genotyping of whole genome amplified DNA in SNP genotyping studies*. Electrophoresis, 2007. **28**(16): p. 2812-7.
399. Ng, G., I. Roberts, and N. Coleman, *Evaluation of 3 methods of whole-genome amplification for subsequent metaphase comparative genomic hybridization*. Diagnostic molecular pathology : the American journal of surgical pathology, part B, 2005. **14**(4): p. 203-12.
400. Zietkiewicz, E., et al., *Current genetic methodologies in the identification of disaster victims and in forensic analysis*. Journal of applied genetics, 2012. **53**(1): p. 41-60.

401. Zupanic Pajnic, I., et al., *Highly efficient nuclear DNA typing of the World War II skeletal remains using three new autosomal short tandem repeat amplification kits with the extended European Standard Set of loci*. Croatian medical journal, 2012. **53**(1): p. 17-23.
402. Lee, H.Y., et al., *DNA typing for the identification of old skeletal remains from Korean War victims*. Journal of forensic sciences, 2010. **55**(6): p. 1422-9.

8. APPENDICES

Appendix 1. The rs Number, amplicon length and multiplex pools of the 53 SNPs genotyped.

SNP ID Number	Amplicon Length (bp)	Multiplex Reaction
rs3747129	82	1
rs1801243	83	1
rs17782078	84	2
rs3768067	85	1
rs16929374	91	1
rs2014410	92	2
rs1894706	93	2
rs26722	94	1
rs1426654	94	3
rs11883500	94	3
rs2228479	94	4
rs10465613	95	1
rs1042602	96	1
rs17336807	96	2
rs11543848	96	3
rs2276288	97	2
rs16876571	97	2
rs2296434	98	1
rs729421	98	1
rs1800414	98	1
rs14024	98	1
rs3886999	98	2
rs732774	98	2
rs16964944	98	2
rs1800422	99	1
rs2296436	99	1
rs7541041	99	1
rs4468625	99	1
rs3751109	99	2
rs2305253	99	2

rs1805005	99	3
rs1724577	99	3
rs17118154	100	1
rs2634041	100	1
rs1061472	100	1
rs7334118	100	1
rs17470454	100	2
rs71117511	100	2
rs638043	100	3
rs17435026	100	3
rs7128017	100	3
rs5752330	100	4
rs7524261	101	1
rs6107308	101	2
rs1801244	103	1
rs1058219	107	1
rs1894704	110	2
rs28945095	112	1
rs3751107	114	3
rs885479	116	3
rs1052030	118	1
rs6435927	118	1
rs1805007	120	1



JOHN FLYNN
PRIVATE HOSPITAL

HCoA Operations (Australia) Pty Ltd
ABN 85 083 035 661
trading as John Flynn Private Hospital
42 Inland Drive
Tugun QLD 4224
Telephone: (07) 5598 9000
Facsimile: (07) 5598 0173
Web: www.ramsayhealth.com.au

EXPLANATORY STATEMENT

Project Title: Improved DNA Typing Methods for Highly Degraded Samples of Mass and Natural Disasters

BUHREC Protocol Number RO-743. JFHREC Number 08/05

Chief Investigator: *Dr Angela van Daal*
Co-Investigators: *Sheree Hughes-Stamm*
Dr. Kevin Ashton
Other Participants: *Dr. Ray Randle*
Dr. John Cosson


This research aims to develop alternate DNA methods for identifying highly degraded samples commonly encountered in forensic and mass disaster situations. In such cases, often only very fragmented and degraded human remains are available for victim identification. Bone and teeth are commonly the sole tissues remaining from which to extract DNA and obtain an individual DNA profile. Analysis of DNA from these highly degraded samples often results in the inability to gain a reliable identification.

I am seeking participants who are willing to donate their extracted teeth or bone removed during surgery. Two reference buccal swabs are also required. A buccal swab is collected by simply rubbing a small brush firmly against the inside of your cheek. This is completely pain-free. The swab is allowed to dry before returning it to the packaging. This procedure will take approximately five minutes of your time. All samples are labelled with a unique barcode.

The only personal details recorded for this research is name, age and sex. These details will be held in a secure university drive which is password accessible only by the project investigators, and will be stored for five years as prescribed by the university regulations. No findings which could identify any individual participant will be published. **Your anonymity will be preserved.** Your sample will not be used for any other research purposes.

If you agree to participate, you should be aware that your participation is voluntary and that you may withdraw your consent at any time. This can be done by contacting the principle investigator at any time.

If you have any queries or would like to be informed of the aggregate research finding, please contact:

Principal Investigator: Prof. Angela van Daal Signature: 
Telephone: 5595 4433
Fax: 5595 4480
Address: Faculty of Health Sciences, Bond University.

Should you have any complaint concerning the manner in which this research is conducted, please do not hesitate to contact John Flynn Private Hospital and Medical Centre Research Ethics Committee, quoting the Project Number: 08/05

The Secretary
John Flynn Private Hospital and Medical Centre Research Ethics Committee
John Flynn Private Hospital and Medical Centre
42 Inland Drive
TUGUN 4224
Telephone (07) 5598 9008 Fax (07) 5598 0173 E-Mail execsec.ifp@ramsayhealth.com.au

PARTICIPANT INFORMED CONSENT FORM

Improved DNA Typing Methods for Highly Degraded Samples of Mass and Natural Disasters

BUHREC Protocol Number RO-743
JFHREC Project Number 08/05

I agree to take part in the above John Flynn Private Hospital and Medical Centre research project. I have read the Explanatory Statement, which I keep for my records.

I understand that agreeing to take part means that I am willing to:

- provide 2 buccal swab samples
- donate my extracted teeth or bone tissue removed during surgery

I understand that any information I provide is confidential, and that no information that could lead to the identification of any individual will be disclosed in any reports on the project, or to any other party.

I also understand that my participation is voluntary, that I can choose not to participate in part or all of the project, and that I can withdraw at any stage of the project.

Please tick the appropriate box

- The information I provide can be used by other researchers as long as my name and contact information is removed before it is given to them
- The information I provide cannot be used by other researchers without asking me first
- The information I provide cannot be used except for this project
- If visually impaired or cannot read Yes or No
- If yes I have had the form read to me and understand the contents

Name: _____ (please print)

Signature: _____

Date: _____

Appendix 3. Meteorological observations of local area by the Australian Bureau of Meteorology.

Daily Meteorological Observations for Gold Coast Seaway for October 2009

Site Number 040764 - Locality: The Spit - Opened Jan 1987 - Still Open - Latitude 27°58'20"S - Longitude 153°25'42"E - Elevation 3m

Day	6am			9am						3pm			Maximum Wind Gust km/h	Rainfall in 24 hours to 6am mm	Evaporation in 24 hrs to 6am mm	Bright Sunshine hours	Day	
	Maximum Temperature °C	Minimum Temperature °C	Minimum Terrestrial Temperature °C	Temperature °C	Relative Humidity %	Total Cloud oktas	Wind km/h	MSL pressure hPa	Temperature °C	Relative Humidity %	Total Cloud oktas	Wind km/h						MSL pressure hPa
Thu 1	27.8	14.9		24.3	42		NW 28	1019.9	22.9	63		NNE 35	1014.6	NNE 43	0.0			1
Fri 2	28.7	16.9		23.8	50		NW 28	1015.5	23.0	68		NNE 33	1009.5	NNE 39	0.0			2
Sat 3	35.0	19.0		26.1	50		NW 31	1008.3	33.9	16		W 24	1004.2	SSE 72	0.0			3
Sun 4	25.2	17.8		23.9	59		SSE 20	1016.4	22.0	65		SSE 31	1014.5	SE 46	0.0			4
Mon 5	24.1	16.4		21.8	66		ESE 9	1017.5	22.6	69		SE 30	1014.3	SE 41	0.4			5
Tue 6	25.0	15.9		22.4	61		SSE 17	1018.6	23.5	61		ESE 22	1015.3	S 37	0.0			6
Wed 7	27.8	16.9		23.8	59		N 19	1015.3	20.1	70		N 30	1009.7	N 61	0.0			7
Thu 8	23.1	12.3		19.4	32		SSE 15	1015.6	22.2	43		SE 30	1013.2	SSW 48	2.0			8
Fri 9	23.5	14.8		21.8	41		S 28	1021.9	21.5	50		SSE 43	1018.9	SE 56	0.0			9
Sat 10	23.4	14.6		21.2	52		SSE 30	1025.8	20.9	61		SE 39	1022.8	SE 56	0.0			10
Sun 11	21.8	15.4		17.8	60		E 9	1024.0	17.1	84		NW 9	1020.8	S 39	0.2			11
Mon 12	25.9	12.5		21.5	61		NW 24	1017.3	23.7	63		NNE 37	1010.0	N 50	4.6			12
Tue 13	30.3	19.5		25.7	60		N 24	1008.3	28.6	52		N 28	1001.9	N 57	0.4			13
Wed 14	31.1	18.3		27.4	27		NW 26	1008.0	30.6	14		WNW 43	1003.3	NW 72	0.0			14
Thu 15	28.3	15.2		25.9	20		W 15	1013.1	24.1	48		NNE 35	1007.8	NNE 50	0.0			15
Fri 16	30.7	14.5		27.8	19		WNW 15	1012.8	29.7	14			1009.0		0.0			16
Sat 17	24.5	14.9		22.7	28		SSE 31	1019.8	22.9	40		SE 30	1018.2	SSE 43				17
Sun 18	25.4	15.1		23.1	49		SSE 19	1024.6	22.5	55		SE 26	1022.5	SSE 61	0.0			18
Mon 19	23.7	15.2		21.9	63		SSE 26	1026.3	22.2	56		SE 24	1023.5	SE 35	3.2			19
Tue 20	25.0	15.0		23.0	48		SSE 11	1025.9	23.8	49		E 17	1022.4	E 26	0.0			20
Wed 21	27.4	15.0		24.4	48		NNW 22	1024.5	24.6	59		NNE 35	1020.4	NNE 41	0.0			21
Thu 22	27.0	16.5		24.8	50		NNW 22	1022.5	24.7	56		NNE 28	1020.7	NE 37	0.0			22
Fri 23	27.0	16.4		24.6	47		N 17	1022.6	24.6	56		NNE 35	1018.5	NNE 39	0.0			23
Sat 24	28.6	17.1		24.6	43		NW 31	1019.1	24.1	66		NNE 37	1014.0	NW 57	0.0			24
Sun 25	27.2	17.7		25.0	62		ENE 9	1015.3	25.0	64		NNE 35	1011.4	NNE 43	0.0			25
Mon 26	27.5	20.0		26.2	51		N 31	1014.6	23.0	79		ENE 31	1013.8	N 44	0.0			26
Tue 27	26.8	18.8		24.9	67		E 20	1022.9	24.2	64		E 24	1021.3	NE 37	4.4			27
Wed 28	24.5	21.2		24.2	67		ENE 26	1023.6	22.0	72		E 26	1021.3	E 37	0.0			28
Thu 29	25.6	18.5		22.2	63		ESE 11	1023.9	22.5	60		SE 31	1022.4	ESE 37	5.0			29
Fri 30	26.3	17.1		23.3	62		SSE 19	1023.3	24.2	58		ESE 20	1021.4	SE 39	0.6			30
Sat 31	26.8	16.5		24.5	51		ENE 9	1022.8	25.1	55		ENE 20	1020.3	E 31	0.0			31
Mean Daily	26.6	16.4		23.7	50.9		20.7	1019.0	23.9	55.8		29.6	1015.6					
Lowest Daily	21.8	12.3		17.8	19		9	1008.0	17.1	14		9	1001.8					
Highest Daily	35.0	21.2		27.8	80		31	1026.3	33.9	84		42	1023.5	72	5.0			
Total															20.8			



Prepared by Climate Services Centre in the Western Australia Regional Office of the Bureau of Meteorology. Contact us by phone on (08) 9263 2222 by fax on (08) 9263 2233, or by email on climate.wa@bom.gov.au
Copyright © Commonwealth of Australia 2011 Prepared on 1 April 2011
We have taken all due care but cannot provide any warranty nor accept any liability for this information.

Daily Meteorological Observations for Gold Coast Seaway for November 2009

Site Number 040764 - Locality: The Spit - Opened Jan 1987 - Still Open - Latitude 27°58'20"S - Longitude 153°25'42"E - Elevation 3m

Day	6am			9am						3pm			Maximum Wind Gust km/h	Rainfall in 24 hours to 6am mm	Evaporation in 24 hrs to 6am mm	Bright Sunshine hours	Day	
	Maximum Temperature °C	Minimum Temperature °C	Minimum Terrestrial Temperature °C	Temperature °C	Relative Humidity %	Total Cloud oktas	Wind km/h	MSL pressure hPa	Temperature °C	Relative Humidity %	Total Cloud oktas	Wind km/h						MSL pressure hPa
Sun 1	24.4	17.5		20.3	78		SE 13	1024.7	23.1	58		E 20	1021.5	SSE 35	31.4			1
Mon 2	26.3	15.6		23.7	45		ESE 7	1023.0	25.1	53		NNE 30	1018.9	NNE 33	0.2			2
Tue 3	27.7	15.8		24.7	45		NNW 24	1018.7	25.1	67		N 33	1013.6	NNE 41	0.0			3
Wed 4	32.9	19.8		26.6	45		NW 31	1015.5	25.3	70		NNE 31	1011.6	NW 43	0.0			4
Thu 5	28.1	19.7		24.7	71		ENE 6	1016.9	26.7	67		ENE 13	1015.0	W 61	0.0			5
Fri 6	26.0	19.1		21.6	85		ESE 31	1022.1	24.2	81		SE 9	1020.4	E 39	1.2			6
Sat 7	26.7	20.3		25.9	64		E 19	1025.2	25.1	61		ESE 24	1023.9	ESE 35	5.6			7
Sun 8	27.6	20.6		24.3	63		SE 28	1026.9	25.5	58		SE 26	1023.9	E 52	1.4			8
Mon 9	24.9	20.1		23.2	65		E 28	1023.8	23.7	65		ESE 26	1021.0	E 52	6.2			9
Tue 10	25.0	17.7		23.9	58		ESE 26	1021.8	23.6	58		ESE 28	1020.1	ESE 41	3.6			10
Wed 11	26.7	16.5		24.9	58		SE 17	1022.5	25.3	50		E 19	1020.2	ESE 26	0.0			11
Thu 12	27.0	17.1		24.5	56		ESE 15	1021.6	24.8	54		NE 19	1018.4	ENE 28	0.0			12
Fri 13	28.6	17.7		25.1	53		NW 17	1016.8	26.1	57		NNE 22	1014.3	NW 30	0.0			13
Sat 14	27.8	18.6		25.0	60		SE 9	1015.8	25.8	57		NE 22	1013.3	NNE 28	0.0			14
Sun 15	29.6	19.1		26.8	52		NW 20	1012.9	26.1	67		NNE 37	1009.2	NNE 46	0.0			15
Mon 16	29.8	20.9		28.2	56		N 20	1011.0	25.6	72		NNE 37	1006.4	NNE 50	0.0			16
Tue 17	33.8	22.2		29.2	48		NNW 26	1006.0	25.3	71		N 28	1002.1	SSE 74	0.0			17
Wed 18	26.0	20.3		24.1	70		SSE 17	1012.9	24.1	73		ESE 11	1011.8	SSE 46	2.0			18
Thu 19	28.8	19.2		24.4	73		ENE 7	1015.0	27.2	65		NNE 19	1012.4	NE 26	0.0			19
Fri 20	31.7	23.0		28.2	59		NW 20	1014.9	27.2	65		NNE 31	1011.1	NNE 39	0.0			20
Sat 21	30.5	22.2		28.5	57		N 28	1013.9	26.3	71		NNE 35	1010.7	N 43	0.0			21
Sun 22	31.3	22.1		29.6	48		N 26	1014.3	25.7	71		NNE 33	1011.6	N 46	0.0			22
Mon 23	29.4	22.2		27.1	56		N 30	1015.9	26.0	68		NE 30	1013.7	N 41	0.0			23
Tue 24	28.4	21.0		26.5	70		ESE 11	1021.2	27.0	60		ESE 19	1020.0	SE 30	0.4			24
Wed 25	28.0	21.9		27.1	58		E 20	1021.9	26.3	61		ESE 24	1019.0	E 31	0.0			25
Thu 26	28.5	20.4		26.7	63		NE 20	1019.9	27.3	61		NE 28	1016.5	NNE 33	0.0			26
Fri 27	30.6	21.2		28.4	51		N 24	1014.9	26.0	67		NNE 39	1009.8	NNE 46	0.0			27
Sat 28	32.6	22.8		26.1	66		NW 19	1009.7	24.5	81		N 26	1005.7	NNE 33	0.0			28
Sun 29	30.9	22.6		29.2	60		N 35	1005.3	26.2	82		N 28	1002.4	N 56	0.0			29
Mon 30	30.7	21.2		29.3	45		NNW 9	1006.1	25.3	69		N 28	1002.3	SSE 48	0.0			30
Mean Daily	28.7	19.9		25.9	59.2		20.1	1017.0	25.5	65.3		25.8	1014.0					
Lowest Daily	24.4	15.6		20.3	45		5	1005.3	23.1	50		9	1002.1					
Highest Daily	33.6	23.0		29.6	85		35	1026.9	27.3	82		39	1023.9	74	31.4			
Total															52.0			



Prepared by Climate Services Centre in the Western Australia Regional Office of the Bureau of Meteorology. Contact us by phone on (08) 9263 2222 by fax on (08) 9263 2233, or by email on climate.wa@bom.gov.au
Copyright © Commonwealth of Australia 2011 Prepared on 1 April 2011
We have taken all due care but cannot provide any warranty nor accept any liability for this information.

Daily Meteorological Observations for Gold Coast Seaway for December 2009

Site Number 040764 • Locality: The Spit • Opened Jan 1987 • Still Open • Latitude 27°56'20"S • Longitude 153°25'42"E • Elevation 3m

Day	Maximum Temperature			Minimum Temperature			9am			3pm			Maximum Wind Gust	Rainfall in 24 hours to 6am	Evaporation in 24 hrs to 6am	Bright Sunshine	Day
	Temperature	Relative Humidity	Total Cloud	Temperature	Relative Humidity	Total Cloud	Temperature	Relative Humidity	Total Cloud	Temperature	Relative Humidity	Total Cloud					
	°C	%	oktas	°C	%	oktas	°C	%	oktas	°C	%	oktas	km/h	mm	mm	hours	
Tue 1	25.9	19.8		25.1	60		SSE 26	1012.4	23.1	70		SSE 44	1011.0	SSE 57	0.0		1
Wed 2	25.2	18.6		22.0	60		S 31	1018.0	21.0	76		SSE 31	1017.4	S 50	0.0		2
Thu 3	27.1	18.4		25.1	52		SSE 31	1021.2	24.5	61		SE 39	1018.5	SE 52	0.4		3
Fri 4	28.4	18.7		27.1	51		NNE 17	1019.2	27.2	55		NNE 30	1015.6	NNE 37	0.2		4
Sat 5	29.3	19.1		26.9	50		N 26	1016.7	26.1	62		NNE 41	1011.8	NNE 52	0.0		5
Sun 6	29.5	21.7		28.1	51		NNE 17	1014.4	28.1	60		NNE 28	1013.0	NNE 41	0.0		6
Mon 7	30.7	22.2		28.4	52		N 28	1016.3	25.5	68		N 31	1012.4	N 46	0.0		7
Tue 8	28.5	23.0		26.5	60		N 24	1012.8	25.2	72		N 37	1008.5	N 46	0.0		8
Wed 9		22.8		27.1	60		N 31	1011.1	24.5	74		N 37	1007.6		0.0		9
Thu 10	28.5	20.6		27.7	62		NNE 22	1012.0	25.0	76		N 33	1006.1	NNE 41			10
Fri 11	28.7	21.3		28.0	62		N 20	1013.5	24.1	80		N 26	1010.0	SSE 41	0.0		11
Sat 12	28.6	21.2		24.6	75		SSE 24	1016.1	25.7	73		SE 37	1012.8	SE 46	1.6		12
Sun 13	29.2	22.2		26.6	78		E 11	1015.3	27.9	69		NE 22	1012.3	NE 30	1.0		13
Mon 14	30.3	22.1		26.2	76		ENE 11	1017.1	27.5	69		E 15	1015.7	ENE 20	0.0		14
Tue 15	29.5	22.7		26.7	71		E 13	1020.1	27.2	73		SE 13	1018.7	ESE 19	0.0		15
Wed 16	30.1	20.8		28.0	59		SE 13	1021.3	28.0	56		ENE 24	1019.2	ESE 30	0.6		16
Thu 17	29.4	23.0		27.6	52		N 11	1021.2	27.3	62		NNE 33	1017.8	NNE 41	0.0		17
Fri 18	30.7	22.7		27.7	56		N 17	1016.9	27.1	61		NNE 39	1013.5	NNE 48	0.0		18
Sat 19	28.2	22.7		26.1	70		NNE 17	1015.5	26.4	70		NNE 30	1012.3	NNE 37	0.0		19
Sun 20	28.4	21.7		25.0	70		E 11	1016.0	22.2	87		S 30	1015.0	S 43	0.0		20
Mon 21	28.6	20.9		25.5	72		SSE 17	1015.4	26.4	64		SE 28	1013.9	SE 43	2.0		21
Tue 22	28.9	20.1		27.1	69		ESE 13	1014.9	27.0	71		ENE 11	1011.9	ESE 24	0.0		22
Wed 23	30.0	21.3		25.9	73		SSE 17	1015.4	26.5	71		SE 16	1013.8	SE 31	0.8		23
Thu 24	30.0	21.3		26.1	75		SSE 19	1015.7	26.5	60		ENE 17	1013.1	ENE 28	2.2		24
Fri 25	30.1	22.0		26.7	79		NE 17	1013.3	29.0	66		NE 30	1011.2	NNE 43	1.2		25
Sat 26	29.2	22.7		25.3	86		N 9	1014.0	27.6	72		NE 28	1012.4	NE 52	10.4		26
Sun 27	28.8	22.8		25.2	90		NE 24	1016.4	26.9	76		NE 20	1014.2	NE 41	4.6		27
Mon 28	27.0	22.9		23.4	100		NNE 15	1015.8	25.1	95		ENE 17	1013.1	NE 35	28.2		28
Tue 29	28.1	23.0		25.8	85		NNE 17	1016.7	23.0	100		SSE 20	1015.7	ENE 39	8.2		29
Wed 30	28.9	22.1		26.8	81		SSE 15	1019.2	28.0	65		E 17	1017.0	ESE 33	48.4		30
Thu 31	28.8	23.5		27.2	63		E 22	1018.1	28.4	61		E 17	1016.0	E 39	0.0		31
Mean Daily	28.9	21.5		26.3	67.7		18.8	1016.2	26.1	70.2		27.0	1013.7				
Lowest Daily	25.2	18.4		22.0	50		9	1011.1	21.0	55		11	1007.6				
Highest Daily	30.7	23.5		28.4	100		31	1021.3	29.0	100		44	1019.2	57	48.4		
Total															107.8		



Australian Government
Bureau of Meteorology

Prepared by Climate Services Centre in the Western Australia Regional Office of the Bureau of Meteorology. Contact us by phone on (08) 9263 2222 by fax on (08) 9263 2233, or by email on climate.wa@bom.gov.au
Copyright © Commonwealth of Australia 2011 Prepared on 1 April 2011
We have taken all due care but cannot provide any warranty nor accept any liability for this information.

Page 1 of 1

Daily Meteorological Observations for Gold Coast Seaway for January 2010

Site Number 040764 • Locality: The Spit • Opened Jan 1987 • Still Open • Latitude 27°56'20"S • Longitude 153°25'42"E • Elevation 3m

Day	Maximum Temperature			Minimum Temperature			9am			3pm			Maximum Wind Gust	Rainfall in 24 hours to 6am	Evaporation in 24 hrs to 6am	Bright Sunshine	Day
	Temperature	Relative Humidity	Total Cloud	Temperature	Relative Humidity	Total Cloud	Temperature	Relative Humidity	Total Cloud	Temperature	Relative Humidity	Total Cloud					
	°C	%	oktas	°C	%	oktas	°C	%	oktas	°C	%	oktas	km/h	mm	mm	hours	
Fri 1	29.7	22.4		26.8	67		NNE 15	1016.2	26.1	74		NNE 20	1013.6	NE 31	1.8		1
Sat 2	30.7	23.2		27.0	70		N 15	1012.4	27.0	73		NNE 31	1008.8	N 43	0.8		2
Sun 3	31.5	24.7		29.8	59		W 11	1010.4	24.0	100		SE 31	1010.8	SE 56	0.0		3
Mon 4	27.1	23.3		25.7	73		SE 33	1015.9	25.4	73		SE 41	1015.3	SSE 59	15.4		4
Tue 5	28.4	21.6		26.5	64		SSE 30	1017.7	26.1	63		SE 33	1016.0	S 39	0.2		5
Wed 6	29.1	21.8		24.7	84		SSE 17	1015.7	28.1	72		SE 17	1013.5	SSE 33	1.2		6
Thu 7	28.9	22.5		26.6	78		SSE 19	1015.0	28.1	69		ESE 20	1013.4	SE 35	1.6		7
Fri 8	30.2	22.7		25.6	76		SSE 28	1017.7	28.4	65		SE 28	1016.9	ESE 43	0.2		8
Sat 9	30.0	21.7		27.2	71		SSE 22	1019.2	28.0	63		ESE 22	1017.6	SSE 33	3.4		9
Sun 10	30.1	21.4		27.9	59		NE 9	1017.5	29.3	55		ENE 19	1014.8	ENE 26	0.0		10
Mon 11	29.6	20.8		27.9	62		SSE 15	1017.0	28.7	62		ESE 22	1014.7	ESE 30	0.0		11
Tue 12	30.1	21.4		28.4	62		SSE 22	1015.0	28.6	62		ESE 22	1012.9	SSE 31	0.0		12
Wed 13	30.4	20.9		28.0	56		NNE 15	1014.7	28.8	54		NNE 33	1011.3	NNE 39	0.0		13
Thu 14	30.7	21.6		28.2	59		ESE 9	1015.5	29.2	57		ENE 24	1012.9	ENE 30	0.0		14
Fri 15	30.7	23.1		28.3	60		SE 17	1015.9	28.6	54		SE 28	1013.6	SE 33	0.0		15
Sat 16	30.0	22.2		26.8	56		SSE 7	1012.6	28.9	55		E 17	1009.6	SE 31	0.0		16
Sun 17	31.6	21.3		28.1	54		NNW 15	1007.8	27.5	64		NNE 39	1003.7	NNE 48	0.2		17
Mon 18	37.9	23.0		30.2	52		NW 24	1003.5	27.2	70		N 37	999.1	N 54	0.0		18
Tue 19	28.6	19.6		26.7	62		SSE 19	1007.9	26.3	58		SE 33	1006.7	SE 41	0.0		19
Wed 20	29.6	20.0		27.1	56		ENE 13	1011.9	29.0	56		NNE 24	1009.2	NE 31	0.0		20
Thu 21	30.5	21.1		29.0	54		N 17	1012.8	27.9	63		NNE 24	1010.5	NNE 31	0.0		21
Fri 22	29.7	21.6		27.2	65		NNE 13	1014.7	28.3	61		NNE 24	1013.6	NNE 31	0.0		22
Sat 23	30.3	21.2		28.8	60		NE 9	1014.2	29.4	59		NE 22	1011.4	NE 30	0.0		23
Sun 24	31.2	21.6		28.3	59		NNE 15	1014.1	29.1	61		NE 28	1012.3	NE 33	0.0		24
Mon 25	31.9	22.3		28.6	62		NE 15	1014.9	30.6	57		NNE 30	1012.5	NNE 33	0.0		25
Tue 26	33.1	23.6		29.6	54		NNW 20	1013.4	29.4	64		NE 33	1011.2	NE 44	0.0		26
Wed 27	31.0	23.5		29.5	55		NW 11	1012.8	27.7	68		N 31	1009.2	S 69	0.0		27
Thu 28	31.6	22.8		27.7	66		N 13	1011.1	28.1	68		NNE 31	1007.8	NNE 37	0.0		28
Fri 29	29.9	20.5		26.0	74		NW 13	1009.4	27.1	71		NNE 11	1007.7	W 39	35.0		29
Sat 30	29.4	22.3		28.1	67		SSE 31	1012.4	25.4	92		S 24	1011.4	SSE 54	0.0		30
Sun 31	28.0	22.7		26.3	81		E 33	1011.3	26.0	79		ESE 31	1006.5	ENE 59	14.0		31
Mean Daily	30.4	22.0		27.6	63.8		17.6	1013.6	27.8	65.8		26.9	1011.3				
Lowest Daily	27.1	19.6		24.7	52		8	1003.5	24.0	54		11	999.1				
Highest Daily	37.9	24.7		30.2	84		33	1019.2	30.6	100		41	1017.6	68	35.0		
Total															73.8		



Australian Government
Bureau of Meteorology

Prepared by Climate Services Centre in the Western Australia Regional Office of the Bureau of Meteorology. Contact us by phone on (08) 9263 2222 by fax on (08) 9263 2233, or by email on climate.wa@bom.gov.au
Copyright © Commonwealth of Australia 2011 Prepared on 1 April 2011
We have taken all due care but cannot provide any warranty nor accept any liability for this information.

Page 1 of 1

Gold Coast, Queensland
February 2010 Daily Weather Observations
 Observations from the Gold Coast Seaway, at the northern end of Southport Spit.



Date	Day	Temps		Rain	Evap	Sun	Max wind gust			9am						3pm						
		Min	Max				Dirn	Spd	Time	Temp	RH	Cld	Dirn	Spd	MSLP	Temp	RH	Cld	Dirn	Spd	MSLP	
		°C	°C																			km/h
1	Mo	23.2	27.1	6.2			E	63	01:23	25.9	72		ESE	46	1010.1	25.5	71		ESE	46	1008.8	
2	Tu	22.8	28.5	0.8			SE	57	05:47	25.9	67		SE	37	1009.7	27.9	64		SSE	31	1007.9	
3	We	21.9	28.7	7.2			E	43	18:18	25.1	79		ESE	30	1010.0	28.1	65		ESE	20	1008.7	
4	Th	21.2	29.8	3.2			NE	30	17:22	27.0	72		SE	11	1011.2	28.6	61		NE	22	1009.0	
5	Fr	23.3	30.9	0.4			NW	28	11:41	25.0	78		WSW	7	1011.4	29.8	60		ENE	20	1009.3	
6	Sa	23.9	30.5	1.6			ESE	57	23:31	28.2	75		SE	11	1012.7	29.1	72		E	13	1011.6	
7	Su	21.1	26.0	93.6			ESE	48	02:40	21.3	100		SSW	19	1018.1	24.8	99		SSE	20	1016.0	
8	Mo	21.1	28.9	55.0			SE	46	04:55	26.0	77		ESE	28	1019.1	28.1	61		SE	31	1017.6	
9	Tu	21.8	27.6	8.2			SSE	44	00:26	23.5	99		S	22	1020.1	27.2	68		SE	30	1018.5	
10	We	21.5	28.7	6.6			SE	46	13:15	27.2	68		SSE	30	1019.0	28.0	65		SSE	30	1017.1	
11	Th	21.1	29.7	0			SE	26	14:13	27.6	64		SSE	17	1018.2	28.3	62		ESE	17	1015.5	
12	Fr	21.2	30.6	0			NNE	41	18:12	27.5	59		N	13	1015.2	28.9	61		NNE	33	1012.0	
13	Sa	21.8	31.1	0			NNE	41	13:24	28.1	57		NW	19	1013.0	29.8	62		NNE	30	1011.1	
14	Su	23.0	31.8	0			NNW	44	12:27	28.0	62		NNW	22	1012.6	27.5	71		NNE	28	1008.6	
15	Mo	24.5	31.9	0			W	50	21:05	30.1	62		NNW	19	1010.1	27.3	79		N	30	1006.4	
16	Tu	23.3	28.4	19.4			SSE	54	20:36	27.0	81		NNE	11	1010.0	24.0	100		SSE	20	1008.9	
17	We	21.5	28.5	34.0			S	43	04:34	24.0	73		S	26	1013.5	26.6	70		SSE	24	1012.1	
18	Th	22.6	30.0	0.2			S	59	16:57	26.0	59		S	37	1016.7	27.5	59		S	37	1016.1	
19	Fr	21.1	29.2	0.8			SSE	57	21:35	25.7	67		S	30	1019.6	27.8	57		SE	31	1018.0	
20	Sa	21.6	30.2	0.4			SE	57	02:29	27.1	65		SSE	28	1019.2	27.2	65		SE	31	1017.3	
21	Su	22.0	30.0	4.4			SSE	33	03:26	25.6	76		ENE	24	1019.7	27.9	62		ESE	13	1017.4	
22	Mo	20.9	30.1	0			SSE	28	08:37	28.5	61		SSE	22	1019.0	29.5	63		ENE	13	1016.0	
23	Tu	22.4	31.3	0			ENE	26	11:58	28.7	66		N	7	1015.2	30.7	61		NE	15	1012.1	
24	We	24.6	27.7	0			SSE	57	14:03	27.3	70		S	37	1017.2	24.4	80		SSE	39	1017.5	
25	Th	22.0	27.9	16.6			SSE	61	11:42	25.3	77		SSE	31	1021.4	23.8	78		S	30	1020.9	
26	Fr	21.1	28.4	3.6			SE	59	01:34	23.4	84		S	31	1022.3	26.1	62		SE	37	1019.4	
27	Sa	21.0	27.7	4.8			SE	52	12:47	25.3	82		S	31	1018.8	23.1	99		SE	39	1016.9	
28	Su	21.7	28.0	32.8			SE	31	02:19	25.8	80		SSE	20	1017.2	25.9	78		SE	15	1014.1	
Statistics for February 2010																						
	Mean	22.1	29.3							26.3	72			23	1015.7	27.3	69			26	1013.7	
	Lowest	20.9	26.0							21.3	57		#	7	1009.7	23.1	57		#	13	1006.4	
	Highest	24.6	31.9	93.6			E	63		30.1	100		ESE	46	1022.3	30.7	100		SE	46	1020.9	
	Total			299.8																		

Observations were drawn from Gold Coast Seaway (station 040784).

The Gold Coast Seaway site is an Automatic Weather Station (AWS) at the northern end of Southport Spit. If you are interested in the southern end of the Gold Coast, see the observations from Coolangubra.

DC/DW/4050/201002 Prepared at 13:20 GMT on 13 Mar 2011

Copyright © 2011 Bureau of Meteorology
 Users of this product are deemed to have read the information and accepted the conditions described in the notes at <http://www.bom.gov.au/climate/dwo/DC/DW0000.pdf>

Gold Coast, Queensland
March 2010 Daily Weather Observations
 Observations from the Gold Coast Seaway, at the northern end of Southport Spit.



Date	Day	Temps		Rain	Evap	Sun	Max wind gust			9am						3pm						
		Min	Max				Dirn	Spd	Time	Temp	RH	Cld	Dirn	Spd	MSLP	Temp	RH	Cld	Dirn	Spd	MSLP	
		°C	°C																			km/h
1	Mo	22.8	24.5	13.4			SE	59	23:55	24.5	98		S	15	1013.5	22.9	87		S	31	1010.5	
2	Tu	21.0	25.6	106.8			SE	63	12:19	22.6	98		SE	43	1011.0	23.3	89		SE	43	1008.7	
3	We	22.1	27.4	13.4			SE	72	17:19	25.6	81		SE	39	1011.4	25.6	78		SE	54	1009.9	
4	Th	23.1	27.7	2.2			SE	57	01:31	25.9	60		SE	37	1013.5	25.9	59		SE	33	1011.5	
5	Fr	23.7	28.0	0			NE	46	17:07	27.3	63		E	28	1012.1	23.9	93		E	26	1009.9	
6	Sa	22.9	26.7	4.2			ENE	41	05:52	25.8	83		ENE	28	1012.1	26.1	73		E	26	1010.8	
7	Su	24.3	29.6	1.8			ENE	41	07:56	24.8	72		E	31	1014.5	28.3	62		E	20	1012.2	
8	Mo	21.8	28.1	3.4			N	24	01:53	23.1	98		WSW	11	1016.1	26.2	74		E	6	1014.1	
9	Tu	21.7	32.8	0.2			NNE	37	15:10	28.0	62		WNW	19	1016.0	29.1	66		NNE	31	1013.3	
10	We	22.4	29.7	0			SSE	44	18:26	27.5	74		SE	9	1017.7	27.5	72		SE	33	1016.3	
11	Th	23.0	30.5	0			S	63	15:24	26.8	62		S	37	1022.2	27.1	53		S	41	1021.7	
12	Fr	20.0	27.2	19.6			SSE	83	10:36	23.5	67		S	37	1027.8	25.1	61		SSE	59	1026.3	
13	Sa	20.1	27.3	0.6			SE	69	22:15	25.6	56		SE	50	1027.5	25.3	62		SSE	50	1025.1	
14	Su	19.8	25.4	3.2			SSE	80	12:25	22.7	79		ESE	37	1024.5	23.0	80		SE	46	1022.2	
15	Mo	19.2	26.9	5.4			SSE	54	09:53	23.7	66		S	35	1022.6	26.1	61		S	24	1019.7	
16	Tu	19.2	27.7	1.6			SSE	70	16:36	25.3	67		S	37	1020.2	26.9	56		SSE	41	1018.4	
17	We	20.7	27.3	1.0			SE	57	21:23	23.7	83		SSE	35	1022.6	26.8	61		SE	35	1021.5	
18	Th	22.4	27.5	0.2			SE	57	09:42	25.1	62		S	30	1024.4	26.3	57		SE	35	1022.6	
19	Fr	22.5	28.1	0.2			ESE	46	04:23	25.3	68		ESE	33	1022.5	27.1	55		SE	24	1020.5	
20	Sa	23.2	28.3	0.2			SE	50	15:45	26.1	60		SSE	28	1021.9	25.5	64		SE	31	1019.7	
21	Su	22.9	29.2	3.2			ESE	37	00:02	26.7	61		ESE	20	1020.7	26.4	63		ESE	17	1017.9	
22	Mo	20.6	29.1	0			NNW	24	10:19	25.9	69		NW	13	1017.9	27.0	73		NNE	17	1016.2	
23	Tu	21.4	29.1	0			SSE	46	14:44	26.6	71		S	17	1018.9	27.7	65		SSE	35	1016.7	
24	We	21.6	28.3	0.2			SE	37	11:31	26.0	63		SSE	26	1020.0	26.9	61		SE	30	1018.2	
25	Th	19.6	28.0	0			SSE	35	09:41	26.5	64		SSE	19	1022.7	26.9	61		SE	22	1019.9	
26	Fr	21.0	28.0	4.0			E	22	14:25	26.0	69		SSE	15	1022.0	27.1	56		E	15	1018.8	
27	Sa	19.3	28.6	0.2			ENE	28	21:02	25.8	61		SSE	11	1020.8	27.9	60		ENE	15	1018.2	
28	Su	21.5	28.6	0			E	33	12:13	26.3	65		SSE	20	1020.1	25.9	65		E	22	1017.4	
29	Mo	22.1	29.6	0			NNE	33	00:42	26.6	61		E	15	1020.6	28.2	55		E	17	1017.8	
30	Tu	20.5	27.9	0			NNE	35	15:08	24.8	72		SSE	7	1019.6	25.6	68		NE	24	1016.5	
31	We	20.4	28.0	0.2			NE	43	21:30	24.5	78		N	15	1017.9	26.7	68		NE	20	1014.1	
Statistics for March 2010																						
	Mean	21.5	28.1							25.4	70			25	1019.2	26.3	66			29	1017.0	
	Lowest	19.2	24.5							22.6	56		SSE	7	1011.0	22.9	53		E	6	1008.7	
	Highest	24.3	32.8	106.8			SSE	83		28.0	98		SE	50	1027.8	29.1	93		SSE	59	1026.3	
	Total			185.2																		

Observations were drawn from Gold Coast Seaway (station 040784).

The Gold Coast Seaway site is an Automatic Weather Station (AWS) at the northern end of Southport Spit. If you are interested in the southern end of the Gold Coast, see the observations from Coolangubra.

DC/DW/4050/201003 Prepared at 13:23 GMT on 12 Mar 2011

Gold Coast, Queensland
April 2010 Daily Weather Observations
 Observations from the Gold Coast Seaway, at the northern end of Southport Spit.



Date	Day	Temps		Rain	Evap	Sun	Max wind gust			9am					3pm							
		Min	Max				Dirn	Spd	Time	Temp	RH	Cld	Dirn	Spd	MSLP	Temp	RH	Cld	Dirn	Spd	MSLP	
		°C	°C				mm	mm	hours	km/h	local	°C	%	eighths	km/h	hPa	°C	%	eighths	km/h	hPa	
1	Th	20.4	26.2	17.2			SSE	41	16:44	23.5	80		S	24	1016.3	25.3	73		SE	28	1013.9	
2	Fr	19.4	27.4	0.2			SSE	50	17:42	23.2	80		S	31	1017.4	26.0	66		SSE	37	1014.4	
3	Sa	19.9	26.9	0			SE	52	15:59	24.2	66		SSE	30	1018.4	25.6	67		SE	35	1015.4	
4	Su	19.9	26.4	0			SSE	54	15:55	24.1	59		S	26	1018.1	25.4	55		S	22	1015.7	
5	Mo	18.0	27.1	0			SSE	50	15:00	25.0	57		S	19	1018.5	24.4	64		SSE	39	1016.0	
6	Tu	18.8	26.6	0			ESE	44	12:49	23.6	62		SSE	20	1020.1	23.8	61		Calm		1018.4	
7	We	18.7	27.8	0			NNE	30	17:23	22.9	69		WSW	7	1021.2	25.5	60		NE	19	1017.9	
8	Th	19.1	29.8	0			NW	43	09:41	25.6	62		WNW	22	1018.0	29.1	53		NW	20	1012.4	
9	Fr	21.3	28.1	0			S	35	04:17	26.5	61		SSE	20	1013.9	26.5	60		E	15	1010.2	
10	Sa	20.3	29.9	0			NNE	35	17:09	24.8	71		NNW	9	1012.3	28.0	68		NNE	30	1008.4	
11	Su	22.8	30.6	0			NNE	39	15:48	26.2	75		NW	13	1012.4	28.5	72		NNE	30	1009.0	
12	Mo	23.8	28.4	0			SE	41	12:55	26.3	76		NW	19	1011.7	25.2	74		SSE	24	1010.3	
13	Tu	21.6	26.0	0.4			SSE	59	12:41	22.3	61		S	28	1017.9	25.3	54		SSE	39	1016.5	
14	We	18.6	27.2	0			SE	54	17:52	24.1	58		S	31	1020.1	24.7	60		SE	33	1018.3	
15	Th	17.5	27.4	0			SE	44	13:41	24.4	57		S	30	1020.3	24.8	59		SE	37	1018.2	
16	Fr	19.0	26.2	1.2			SSE	54	11:50	22.3	70		SSE	41	1022.8	24.2	50		SSE	35	1021.3	
17	Sa	18.9	27.3	0.4			SSE	48	02:04	24.5	65		S	30	1024.2	25.9	59		SSE	31	1021.8	
18	Su	18.9	26.6	3.4			SSE	52	12:37	23.5	75		S	30	1023.8	24.9	64		SSE	31	1021.1	
19	Mo	20.1	26.8	3.4			SE	57	18:09	24.1	63		SE	37	1022.8	25.6	56		SSE	35	1020.2	
20	Tu	19.6	24.7	0.6			SE	54	23:43	23.3	74		S	19	1021.3	24.4	70		SE	33	1018.6	
21	We	19.6	24.0	17.2			SE	56	02:14	21.9	81		ESE	24	1021.5	21.4	94		S	17	1019.4	
22	Th	18.6	26.1	4.0			SSE	39	05:06	24.0	71		S	19	1022.2	25.1	67		SSE	17	1019.9	
23	Fr	17.8	26.6	8.2			SE	30	13:41	23.1	86		S	15	1021.7	25.0	72		SE	26	1018.4	
24	Sa	19.0	27.2	0			NNW	30	20:05	22.1	89		N	17	1019.6	25.0	67		NW	9	1016.1	
25	Su	19.3	30.0	0.2			S	52	23:23	24.0	71		NW	26	1016.3	27.0	71		NNE	22	1012.0	
26	Mo	18.2	25.7	0			S	52	01:03	21.7	48		S	30	1021.0	24.4	44		SSE	20	1020.2	
27	Tu	15.4	25.4	0			S	28	09:16	22.3	57		S	15	1022.3	24.2	61		ESE	13	1019.5	
28	We	17.3	27.8	0			NE	28	13:31	23.0	65		NW	11	1021.8	25.8	60		NNE	22	1018.6	
29	Th	18.1	29.8	0			NNW	30	10:40	23.9	68		NW	13	1021.1	28.3	38		WNW	15	1017.4	
30	Fr	15.8	27.2	0			SSE	43	12:28	22.0	57		S		1021.9	25.4	58		SSE	35	1020.2	
Statistics for April 2010																						
	Mean	19.2	27.2							23.7	67				22	1019.4	25.5	62			25	1016.7
	Lowest	15.4	24.0							21.7	48		WSW	7	1011.7	21.4	36			Calm		1008.4
	Highest	23.8	30.6	17.2			SSE	59		26.5	89		SSE	41	1024.2	29.1	94		SSE	39	1021.8	
	Total			56.4																		

Observations were drawn from Gold Coast Seaway (station 040764)
 The Gold Coast Seaway site is an Automatic Weather Station (AWS) at the northern end of Southport Spit. If you are interested in the southern end of the Gold Coast, see the observations from Coolangatta.

IDCJDW4050.201004 Prepared at 13:21 GMT on 11 Mar 2011
 Copyright © 2011 Bureau of Meteorology
 Users of this product are deemed to have read the information and accepted the conditions described in the notes at <http://www.bom.gov.au/climate/dwo/IDCJDW0000.pdf>

Gold Coast, Queensland
May 2010 Daily Weather Observations
 Observations from the Gold Coast Seaway, at the northern end of Southport Spit.



Date	Day	Temps		Rain	Evap	Sun	Max wind gust			9am					3pm							
		Min	Max				Dirn	Spd	Time	Temp	RH	Cld	Dirn	Spd	MSLP	Temp	RH	Cld	Dirn	Spd	MSLP	
		°C	°C				mm	mm	hours	km/h	local	°C	%	eighths	km/h	hPa	°C	%	eighths	km/h	hPa	
1	Sa	18.6	26.7	0			SE	41	13:18	24.4	61		S	24	1025.2	24.2	68		SE	31	1023.1	
2	Su	17.4	26.9	0			SE	28	18:36	24.2	65		SSE	17	1026.0	25.4	64		SSE	17	1023.3	
3	Mo	18.0	26.6	0			SSE	48	17:04	24.0	64		SSE	28	1025.0	25.3	56		SSE	35	1021.8	
4	Tu	18.8	21.9	115.2			ENE	46	03:33	19.1	99		NE	31	1021.7	19.0	99		W	11	1017.9	
5	We	16.2	27.5	23.0			WNW	30	10:21	21.9	80		NW	19	1016.3	27.4	49		NW	17	1012.8	
6	Th	15.4	24.3	0.2						22.4	59		S	31	1017.8	22.8	57		SSE	39	1016.5	
7	Fr	14.5	24.8				S	39	10:37	21.1	48		SSW	19	1019.8	24.3	40		SSE	15	1016.7	
8	Sa	14.1	25.7	0			SSE	48	14:33	22.2	58		S	17	1019.0	23.6	55		SSE	39	1017.0	
9	Su	16.4	26.0	0			SSE	48	13:39	21.1	58		S	19	1020.3	24.0	57		SSE	30	1017.2	
10	Mo	18.1	24.2	0.8			SSE	41	04:16	20.5	78		SE	24	1019.9	23.3	65		SE	19	1016.5	
11	Tu	16.3	27.1	0			NW	30	19:26	22.7	64		WNW	7	1016.7	25.6	58		NE	13	1012.9	
12	We	15.8	27.9	0			SSE	43	13:08	23.3	54		W	13	1014.7	23.5	59		SE	31	1012.5	
13	Th	13.5	24.3	0			S	35	00:45	19.6	32		S	13	1019.1	23.7	31		WNW	13	1014.7	
14	Fr	12.4	25.1	0			ESE	24	14:59	19.0	48		WNW	15	1016.7	22.3	46		ESE	17	1013.3	
15	Sa	12.9	23.6	0			SSE	35	18:38	19.4	51		W	9	1015.9	22.6	46		ESE	17	1013.7	
16	Su	13.2	23.3	0			SSE	35	12:19	19.5	51		S	11	1018.9	21.0	50		S	19	1016.3	
17	Mo	13.7	21.8	0			SE	44	18:04	18.9	66		WSW	4	1017.9	20.0	61		S	20	1014.6	
18	Tu	12.3	23.5	0			WNW	26	11:24	18.3	65		NW	9	1015.7	20.7	52		ESE	13	1012.9	
19	We	12.1	24.3	0			S	43	10:28	19.2	55		SSW	9	1017.9	23.4	49		S	22	1016.7	
20	Th	14.6	24.2	0			S	33	09:05	20.0	63		S	19	1020.4	21.6	65		SE	22	1018.2	
21	Fr	16.6	19.5	0.8			S	35	16:27	18.4	88		W	6	1019.2	17.6	99		S	15	1015.5	
22	Sa	12.4	23.3	68.6			SSE	39	15:07	18.4	68		SW	9	1016.5	22.1	51		SSE	30	1014.4	
23	Su	13.5	22.5	0.2			S	56	11:32	19.6	64		S	31	1018.3	20.4	61		S	30	1016.9	
24	Mo	17.0	23.6	0			S	37	03:03	20.7	66		SSE	26	1019.3	21.7	53		ESE	17	1016.0	
25	Tu	16.6	21.6	5.6			NW	33	12:06	17.8	95		W	7	1013.4	20.8	76		NW	19	1008.0	
26	We	16.8	24.0	0			WNW	54	12:36	21.4	68		NW	17	1006.1	22.6	37		W	20	1004.2	
27	Th	14.8	23.3	0			S	50	12:43	19.9	49		W	13	1011.6	18.1	86		SSW	17	1011.8	
28	Fr	16.5	22.7	1.0			SSE	43	14:05	19.9	71		S	17	1019.1	21.4	61		SSE	30	1017.3	
29	Sa	16.3	22.2	9.2			NW	69	13:13	20.0	93		NNE	39	1012.1	18.9	75		NW	22	1007.8	
30	Su	13.1	20.4	12.4			WNW	54	12:36	16.9	61		NW	31	1010.2	18.1	41		WNW	28	1008.0	
31	Mo	12.6	22.0	0			NW	39	09:06	16.5	61		NW	30	1012.2	21.2	45		W	22	1009.9	
Statistics for May 2010																						
	Mean	15.2	24.0							20.3	64				18	1017.5	22.1	58			22	1014.8
	Lowest	12.1	19.5							16.5	32		WSW	4	1006.1	17.6	31		W	11	1004.2	
	Highest	18.8	27.9	115.2			NW	69		24.4	99		NNE	39	1026.0	27.4	99		SSE	39	1023.3	
	Total			237																		

Gold Coast, Queensland
June 2010 Daily Weather Observations
 Observations from the Gold Coast Seaway, at the northern end of Southport Spit.



Date	Day	Temps		Rain	Evap	Sun	Max wind gust			9am						3pm					
		Min	Max				Dirn	Spd	Time	Temp	RH	Cld	Dirn	Spd	MSLP	Temp	RH	Cld	Dirn	Spd	MSLP
1	Tu	12.5	22.0	0			S	26	13:06	19.2	58		W	9	1016.3	19.1	77		WNW	17	1014.6
2	We	16.3	21.0	2.0			SSE	35	11:30	19.2	84		SSW	13	1016.2	19.7	76		S	15	1014.2
3	Th	14.9	22.9	0			S	37	10:19	19.6	71		NW	13	1016.3	21.5	51		WSW	13	1013.5
4	Fr	11.4	22.3	0			WNW	37	11:56	16.5	76		NW	17	1012.6	20.6	52		W	20	1008.6
5	Sa	14.4	24.9	0			S	37	10:41	19.9	60		NW	11	1009.7	23.6	43		S	17	1008.4
6	Su	12.9	22.3	0			W	31	11:21	18.9	45		WSW	9	1013.4	22.0	32		WNW	15	1012.2
7	Mo	10.9	22.3	0			S	46	09:14	18.4	50		S	22	1019.9	20.2	50		S	24	1018.6
8	Tu	12.1	21.8	0			SE	35	13:12	18.5	62		S	17	1022.0	20.1	66		SE	26	1018.7
9	We	13.2	23.6	0			NW	37	13:49	17.2	79		WNW	15	1018.0	23.2	46		NW	15	1012.1
10	Th	11.9	21.8	0			WNW	41	08:16	15.6	36		W	31	1017.9	18.9	38		ESE	9	1016.6
11	Fr	11.6	21.1	0			SW	17	00:58	14.1	67		W	11	1021.6	19.7	51		N	13	1017.7
12	Sa	7.3	20.4	0			SSE	41	17:39	13.9	53		NW	13	1019.2	18.6	44		SSE	13	1017.4
13	Su	11.8	21.0	0			S	50	11:06	17.2	49		S	24	1025.0	19.2	56		SSE	33	1024.6
14	Mo	14.8	21.4	0.2			SE	59	18:10	18.1	74		SSE	30	1029.6	19.8	63		SSE	31	1027.5
15	Tu	15.1	22.2	0			S	48	02:38	18.0	63		S	35	1029.0	20.9	54		SSE	37	1025.8
16	We	14.7	21.9	0			SSE	41	11:29	19.4	55		SSE	30	1027.3	19.8	54		SE	30	1024.3
17	Th	12.2	22.9	0			SW	19	01:51	17.5	65		WSW	9	1022.6	20.8	66		NE	11	1018.7
18	Fr	16.1	20.2	2.2			NW	19	11:45	17.7	95		WSW	7	1018.4	19.3	74		NNW	9	1015.1
19	Sa	14.6	21.7	0.2			NE	17	12:29	17.8	59		W	9	1018.9	20.3	54		ENE	13	1017.9
20	Su	11.7	21.7	0			SSE	26	10:57	17.1	65		SW	11	1024.8	19.9	60		ESE	19	1023.5
21	Mo	12.9	22.4	0			SE	43	14:47	18.0	65		S	17	1029.0	20.4	59		SE	37	1027.9
22	Tu	14.5	22.4	0			SSE	59	15:36	19.2	68		S	31	1031.5	20.4	60		SSE	43	1029.5
23	We	14.9	20.4	4.8			SE	59	13:11	16.2	99		S	33	1030.4	19.0	77		SE	46	1028.1
24	Th	14.6	21.5	2.6			S	43	07:20	17.7	74		S	26	1028.8	19.9	61		SE	28	1025.6
25	Fr	12.2	21.6	0			ESE	30	15:12	17.5	65		SSW	13	1026.7	19.6	65		SE	22	1023.7
26	Sa	13.4	21.1	0			N	31	14:30	16.7	73		W	9	1022.9	19.8	68		N	26	1018.9
27	Su	14.6	20.4	0			NNW	24	02:50	17.5	82		NW	15	1018.1	19.8	70		ENE	9	1015.4
28	Mo	10.0	20.0	0			SE	20	14:02	15.3	63		NW	11	1018.8	19.0	60		ESE	15	1016.7
29	Tu	10.6	17.9	0			NW	24	15:20	12.8	72		WNW	13	1020.0	15.9	50		NW	15	1018.0
30	We	9.8	20.1	0.4			NNW	28	15:30	13.7	75		NW	9	1020.7	19.1	58		NNW	13	1017.9
Statistics for June 2010																					
Mean		12.9	21.6							17.3	66			17	1021.5	20.0	57			21	1019.1
Lowest		7.3	17.9							12.8	36		WSW	7	1009.7	15.9	32		#	9	1008.4
Highest		16.3	24.9	4.8			#	59		19.9	99		S	35	1031.5	23.6	77		SE	46	1029.5
Total				12.4																	

Observations were drawn from Gold Coast Seaway (station 040784)
 The Gold Coast Seaway site is an Automatic Weather Station (AWS) at the northern end of Southport Spit. If you are interested in the southern end of the Gold Coast, see the observations from Coolangatta.
 ID:DJW4050.201006 Prepared at 13:21 GMT on 9 Mar 2011
 Copyright © 2011 Bureau of Meteorology
 Users of this product are deemed to have read the information and accepted the conditions described in the notes at <http://www.bom.gov.au/climate/dw/IDCJDW0000.pdf>

Gold Coast, Queensland
July 2010 Daily Weather Observations
 Observations from the Gold Coast Seaway, at the northern end of Southport Spit.



Date	Day	Temps		Rain	Evap	Sun	Max wind gust			9am						3pm					
		Min	Max				Dirn	Spd	Time	Temp	RH	Cld	Dirn	Spd	MSLP	Temp	RH	Cld	Dirn	Spd	MSLP
1	Th	12.9	20.3	0			S	41	10:36	15.5	74		WNW	7	1023.7	18.8	54		S	24	1022.3
2	Fr	12.2	17.6	0			SSE	37	17:09	15.4	75		SSW	9	1025.9	17.0	70		SSE	24	1023.6
3	Sa	13.7	19.4	8.2			SSE	41	16:16	15.8	67		W	15	1023.9	19.0	30		WSW	15	1022.0
4	Su	7.8	21.0	0.2			S	39	11:03	14.4	55		WSW	9	1026.8	18.4	54		S	24	1023.6
5	Mo	11.6	21.3	0			SSE	37	09:27	17.5	64		S	20	1024.7	20.0	58		SE	22	1021.3
6	Tu	14.1	21.6	0.2			NW	33	11:25	18.4	76		NW	11	1019.7	19.2	75		N	13	1015.4
7	We	12.7	18.5	0.2			W	39	00:28	15.4	53		WNW	13	1020.0	16.8	56		WNW	13	1018.0
8	Th	13.3	20.9	1.4			S	63	13:21	17.3	70		S	20	1020.4	19.1	62		SSE	46	1018.1
9	Fr	14.7	21.5	0			SSE	72	14:47	17.9	64		S	39	1022.8	17.7	76		SSE	43	1021.8
10	Sa	14.9	21.6	0			S	46	06:01	19.5	66		SSE	28	1026.7	19.6	67		SSE	26	1023.8
11	Su	13.6	22.1	0			S	26	09:41	16.8	75		SW	11	1026.0	20.4	64		E	11	1023.6
12	Mo	13.2	23.0	0			NE	31	13:56	19.1	68		W	9	1023.7	20.9	68		NNE	28	1020.5
13	Tu	13.2	24.0	0.2			NNE	28	13:01	19.1	74		NW	9	1022.6	21.9	63		NNE	24	1018.9
14	We	15.1	23.5	0			NW	54	12:14	19.3	72		NNW	26	1017.0	21.7	44		WNW	24	1014.3
15	Th	8.9	22.5	0			NW	35	12:03	15.3	49		NW	22	1019.0	22.2	30		WNW	20	1014.8
16	Fr	9.7	20.2	0			S	37	09:34	16.5	44		S	19	1023.4	18.3	51		SE	31	1021.3
17	Sa	10.1	20.5	0			SE	37	13:41	17.0	58		SSE	15	1026.2	18.9	55		SE	31	1023.5
18	Su	10.2	21.4	0			WSW	20	05:26	16.4	60		WSW	9	1025.2	20.9	52		ENE	15	1021.3
19	Mo	11.0	22.2	0			N	33	16:35	17.0	76		WNW	6	1020.0	20.5	61		NNW	13	1015.6
20	Tu	12.7	20.1	15.8			SE	37	14:56	16.1	87		SSW	7	1018.6	18.5	54		SE	30	1017.6
21	We	11.6	19.8	0.2			S	41	10:08	15.9	54		SSW	17	1022.2	18.5	47		SSE	28	1019.8
22	Th	9.6	20.0	0			SSE	48	15:41	15.9	48		S	24	1024.9	19.3	42		SSE	24	1023.1
23	Fr	10.5	21.0	0			S	48	09:29	17.2	55		S	28	1027.8	19.4	53		S	35	1026.1
24	Sa	14.2	21.5	0			SE	41	15:13	17.9	61		S	20	1027.7	20.1	63		SSE	31	1024.7
25	Su	14.7	21.7	0			SSE	31	16:12	18.5	65		S	7	1027.5	20.3	63		SE	24	1024.6
26	Mo	14.0	21.8	1.6			SSE	50	15:38	17.8	77		S	13	1029.2	20.2	64		SSE	37	1027.6
27	Tu	15.3	22.1	0.4			SSE	48	09:44	18.9	67		SSE	35	1030.9	17.8	82		SSE	30	1028.2
28	We	15.6	21.3	29.8			N	48	12:34	20.2	77		NE	35	1026.3	18.7	86		N	19	1022.6
29	Th	17.2	23.1	10.2			NNE	30	04:23	18.3	100		W	7	1022.2	21.6	80		N	17	1018.4
30	Fr	15.4	24.2	0			NNE	35	16:31	19.6	89		WNW	9	1020.7	23.0	77		NNE	24	1017.4
31	Sa	18.5	25.9	0			NW	48	14:08	21.7	78		NNW	22	1019.0	24.8	59		NW	26	1015.5
Statistics for July 2010																					
Mean		13.0	21.5							17.5	67			16	1023.7	19.8	60			24	1020.9
Lowest		7.8	17.6							14.4	44		WNW	6	1017.0	16.8	30		E	11	1014.3
Highest		18.5	25.9	29.8			SSE	72		21.7	100		S	39	1030.9	24.8	86		SSE	46	1028.2
Total				68.4																	

Observations were drawn from Gold Coast Seaway (station 040784)
 The Gold Coast Seaway

Gold Coast, Queensland
August 2010 Daily Weather Observations
 Observations from the Gold Coast Seaway, at the northern end of Southport Spit.



Date	Day	Temps		Rain	Evap	Sun	Max wind gust			9am						3pm					
		Min °C	Max °C				Dirn	Spd km/h	Time local	Temp °C	RH %	Cld eighths	Dirn	Spd km/h	MSLP hPa	Temp °C	RH %	Cld eighths	Dirn	Spd km/h	MSLP hPa
1	Su	14.5	24.3	0.2			NW	31	13:26	19.8	51		W	15	1023.2	24.0	36		NW	15	1018.6
2	Mo	11.3	22.2	0			WNW	46	22:12	17.4	41		WNW	24	1020.4	21.8	23		WNW	20	1014.6
3	Tu	9.6	22.6	0			WNW	41	10:48	15.4	44		WSW	24	1013.3	22.6	35		S	11	1011.2
4	We	9.1	21.3	0			SSW	24	09:56	16.9	49		WSW	7	1018.9	19.9	48		E	17	1016.6
5	Th	9.2	22.2	0			N	26	12:29	16.3	68		NW	7	1019.7	20.1	57		NNE	17	1016.1
6	Fr	12.2	21.7	0			SE	33	16:27	18.0	51		SSE	11	1018.8	19.5	42		SE	26	1016.1
7	Sa	8.1	20.1	0			S	37	10:21	15.4	42		S	15	1022.6	18.7	54		SE	28	1019.5
8	Su	8.9	21.6	0			NE	26	16:09	15.6	58		NW	11	1021.8	20.5	53		ENE	15	1018.6
9	Mo	11.4	24.1	0			NE	54	21:31	18.9	56		SW	9	1023.5	22.0	48		NE	24	1020.8
10	Tu	16.4	20.5	12.0			NNE	63	06:25	20.3	75		NE	41	1020.7	18.4	99		W	7	1017.3
11	We	16.8	18.7	56.2			NNE	52	07:40	17.0	91		NW	20	1013.5	17.3	45		WNW	26	1010.0
12	Th	11.6	20.3	0			WNW	67	16:14	14.9	56		N	19	1011.3	18.7	34		W	43	1006.9
13	Fr	11.0	21.6	0			SE	41	16:24	15.8	46		W	19	1012.5	20.9	31		WNW	13	1011.0
14	Sa	8.6	21.6	0			N	35	17:02	16.1	56		NW	13	1018.1	20.7	43		N	19	1015.1
15	Su	11.1	23.8	0			NW	44	12:38	17.2	62		NW	20	1014.9	22.5	45		N	24	1009.8
16	Mo	11.7	23.8	0			NW	39	11:41	18.5	37		W	22	1016.6	23.6	30		NW	19	1013.0
17	Tu	10.3	21.2	0			W	41	01:00	17.9	35		S	7	1021.3	19.7	56		SSE	30	1019.5
18	We	11.4	23.4	0			NNE	33	16:53	18.9	51		S	9	1023.3	22.1	46		NNE	24	1019.0
19	Th	14.1	27.5	0			NW	48	10:07	21.1	65		WNW	17	1017.6	26.4	47		NW	15	1012.9
20	Fr	17.2	18.0	6.2			NW	37	13:45	17.8	99		NNW	19	1017.1	17.1	94		NNW	17	1013.6
21	Sa	9.6	20.2	2.0			WNW	26	03:45	16.3	44		WSW	13	1019.2	19.4	47		ENE	17	1016.2
22	Su	8.5	21.3	0			SSE	31	11:01	16.8	53		S	9	1022.8	19.9	56		SE	24	1020.0
23	Mo	13.7	18.5	0			NW	31	22:05	18.2	70		NW	11	1018.9	17.3	84		NW	11	1014.8
24	Tu	14.5	21.6	6.8			WNW	41	23:56	18.5	61		WNW	13	1014.4	19.7	41		WNW	19	1010.9
25	We	13.8	17.0	0			WNW	41	00:01	14.8	66		NNW	13	1013.5	16.4	62		NNW	15	1009.5
26	Th	14.3	22.0	0			NW	57	14:06	15.7	48		WNW	24	1011.5	21.2	28		WNW	33	1007.7
27	Fr	10.1	23.3	0			WNW	48	10:44	17.0	45		NW	19	1015.2	23.0	28		WNW	26	1012.1
28	Sa	9.7	22.0	0			W	30	09:23	18.7	34		W	15	1021.1	20.7	40		E	15	1019.1
29	Su	13.1	21.9	0			SE	46	12:41	18.9	51		S	28	1026.1	20.6	59		SSE	33	1023.6
30	Mo	11.5	21.9	0			SE	37	13:30	19.3	58		S	19	1025.9	19.2	62		SE	28	1022.9
31	Tu	12.2	23.1	0			NNE	28	21:01	18.8	70		SSE	13	1025.9	21.3	58		NE	15	1023.2
Statistics for August 2010																					
Mean		11.8	21.7							17.5	55			16	1018.8	20.5	49			20	1015.5
Lowest		8.1	17.0							14.8	34		#	7	1011.3	16.4	23		W	7	1006.9
Highest		17.2	27.5	56.2			WNW	67		21.1	99		NE	41	1026.1	26.4	99		W	43	1023.6
Total				83.4																	

Observations were drawn from Gold Coast Seaway (station D40764)
 The Gold Coast Seaway site is an Automatic Weather Station (AWS) at the northern end of Southport Spit. If you are interested in the southern end of the Gold Coast, see the observations from Coolangatta.

IDCJDW050 201008 Prepared at 16:22 GMT on 7 Mar 2011
 Copyright © 2011 Bureau of Meteorology
 Users of this product are deemed to have read the information and accepted the conditions described in the notes at <http://www.bom.gov.au/climate/dwo/IDCJDW0000.pdf>

Gold Coast, Queensland
September 2010 Daily Weather Observations
 Observations from the Gold Coast Seaway, at the northern end of Southport Spit.



Date	Day	Temps		Rain	Evap	Sun	Max wind gust			9am						3pm					
		Min °C	Max °C				Dirn	Spd km/h	Time local	Temp °C	RH %	Cld eighths	Dirn	Spd km/h	MSLP hPa	Temp °C	RH %	Cld eighths	Dirn	Spd km/h	MSLP hPa
1	We	12.5	25.9	0			NW	41	12:41	20.7	60		NW	13	1023.9	22.6	48		N	24	1019.3
2	Th	14.0	28.0	0			NW	46	09:30	21.5	54		NW	35	1020.4	25.4	45		N	22	1015.7
3	Fr	16.8	25.0	0			SSE	48	10:13	23.0	71		SSE	28	1020.7	22.3	77		SSE	31	1019.5
4	Sa	20.5	25.9	0			NNE	46	13:57	23.7	69		N	24	1021.1	22.6	76		NNE	35	1016.8
5	Su	19.7	23.2	3.4			NNE	39	00:16	21.7	92		NNW	15	1017.8	21.9	91		NW	22	1015.6
6	Mo	18.0	21.9	15.6			SE	30	11:42	20.0	79		SSE	9	1020.0	21.4	50		SE	17	1017.6
7	Tu	12.7	22.6	0			E	22	14:54	19.1	61		SSE	11	1022.9	21.6	63		E	17	1019.8
8	We	15.2	22.9	0			SSE	41	15:08	21.3	61		SSE	28	1024.4	21.1	63		SSE	33	1021.4
9	Th	14.6	25.3	0			NNW	43	22:54	22.2	64		WNW	6	1020.3	22.6	67		N	28	1015.0
10	Fr	19.0	23.4	0.4			NNW	39	00:23	20.4	79		NW	13	1011.0	22.7	76		NNW	19	1007.4
11	Sa	13.3	23.0	0.4			W	31	03:27	21.0	41		SSE	20	1017.3	21.5	46		SE	24	1016.7
12	Su	13.9	24.3	0			NE	24	14:50	21.5	53		SSE	13	1022.4	22.6	50		NE	19	1019.4
13	Mo	16.9	24.5	0			NNE	30	16:20	19.7	64		NW	13	1019.3	23.3	68		NE	19	1014.9
14	Tu	15.6	24.6	0			N	35	21:58	20.9	80		NE	13	1016.0	20.8	79		NNE	19	1012.0
15	We	18.6	26.8	0			WNW	59	11:10	22.6	37		WNW	30	1011.4	25.7	29		W	37	1009.6
16	Th	14.1	26.5	0			WNW	37	22:40	23.3	27		SW	11	1017.5	22.2	31		WNW	19	1014.2
17	Fr	15.1	23.0	0			SE	33	13:40	20.7	40		NNW	4	1019.8	19.7	61		SSE	19	1019.0
18	Sa	13.7	24.0	0			NW	31	12:36	19.3	48		NW	11	1019.3	21.1	45		N	20	1015.3
19	Su	15.1	20.7	0			S	30	18:04	19.2	42		WNW	9	1020.2	20.3	42		S	17	1018.7
20	Mo	14.1	21.1	11.4			SSE	37	15:11	18.2	99		S	19	1020.8	18.8	99		SSE	28	1019.1
21	Tu	17.6	23.8	17.0			S	41	17:18	18.3	100		SSW	17	1020.9	22.4	69		S	28	1018.6
22	We	18.2	21.3	1.2			SE	46	06:53	20.4	77		SSE	20	1024.2	20.6	68		SSE	28	1021.9
23	Th	15.7	25.3	3.4			ENE	26	12:19	21.1	67		SW	6	1022.7	21.8	66		NE	17	1020.3
24	Fr	17.5	25.5	0			NNE	31	20:20	22.5	68		SSE	4	1023.2	24.1	60		NNE	22	1020.0
25	Sa	18.8	23.6	0			N	39	14:25	21.2	72		NW	20	1021.4	21.8	68		NNE	24	1018.0
26	Su	16.6	26.2	0			NE	28	13:02	22.0	66		NNW	13	1019.7	23.8	63		NE	20	1017.0
27	Mo	16.6	26.2	0.4			NNE	41	15:49	23.2	70		NNE	13	1018.7	24.0	72		NNE	31	1013.9
28	Tu	20.3	28.1	2.0			NNE	39	13:56	23.7	80		NW	13	1015.4	20.4	87		NE	26	1011.1
29	We	18.5	24.9	34.8			S	54	19:56	23.1	84		SE	13	1012.6	20.9	86		SE	31	1011.5
30	Th	15.9	22.4	4.2			S	59	04:09	18.5	65		S	37	1021.2	21.0	59		SSE	41	1021.3
Statistics for September 2010																					
Mean		16.3	24.3							21.1	65			16	1019.6	22.0	63			24	1016.7
Lowest		12.5	20.7							18.2	27		#	4	1011.0	18.8	29		#	17	1007.4
Highest		20.5	28.1	34.8			#	59		23.7	100		S	37	1024.4	25.7	99		SSE	41	1021.9
Total				94.2																	

Observations were drawn from Gold Coast Seaway (station D40764)
 The Gold Coast Seaway site is an Automatic Weather Station (AWS) at the northern end of Southport Spit. If you are interested in the southern end of the Gold Coast, see the observations from Coolangatta.

IDCJDW050 201009 Prepared at 13:21 GMT on 20 Mar 2011
 Copyright © 2011 Bureau of Meteorology
 Users of this product are deemed to have read the information and accepted the conditions described in the notes at [http://www.bom.gov.au/climate/dwo/IDCJDW](http://www.bom.gov.au/climate/dwo/IDCJDW0000.pdf)

Gold Coast, Queensland October 2010 Daily Weather Observations

Observations from the Gold Coast Seaway, at the northern end of Southport Spit.



Date	Day	Temps		Rain	Evap	Sun	Max wind gust			9am						3pm					
		Min	Max				Dirn	Spd	Time	Temp	RH	Cld	Dirn	Spd	MSLP	Temp	RH	Cld	Dirn	Spd	MSLP
		°C	°C	mm	mm	hours	km/h	km/h	local	°C	%	eighths	km/h	hPa	°C	%	eighths	km/h	hPa		
1	Fr	15.9	22.2	0.6			SE	50	12:51	21.7	50		SE	31	1026.5	18.9	71		SSE	30	1024.2
2	Sa	15.6	19.7	2.2			ESE	56	00:49	18.9	77		SE	22	1026.5	17.4	95		S	13	1022.9
3	Su	16.3	23.0	34.6			S	39	18:42	17.9	100		SSW	11	1023.9	19.3	100		S	28	1020.6
4	Mo	17.3	25.7	118.6			NE	26	14:17	23.0	82		ENE	11	1017.4	24.5	77		NE	20	1014.3
5	Tu	17.6	25.4	0			S	48	18:01	23.0	68		NNE	7	1018.8	22.5	83		SE	26	1014.5
6	We	17.3	27.0	0			SE	46	15:57	24.6	65		ENE	7	1017.8	23.4	75		SE	31	1015.1
7	Th	17.1	29.5	0			NE	41	15:02	25.1	62		NW	19	1016.9	21.7	98		NNE	33	1013.5
8	Fr	19.5	22.1	20.6			SE	63	14:09	21.9	79		S	30	1019.2	19.5	93		SSE	50	1017.8
9	Sa	17.6	19.8	41.4			SSE	69	13:27	18.3	89		S	37	1022.0	17.3	90		SSE	39	1020.1
10	Su	16.1	20.6	24.2			SSE	80	18:04	17.3	99		S	44	1023.1	17.0	96		SSE	61	1022.8
11	Mo	15.7	21.4	79.2			ESE	78	06:26	20.4	77		SE	54	1027.0	20.6	76		SE	46	1025.8
12	Tu	18.7	22.8	2.6			ESE	57	08:43	20.5	74		ESE	44	1028.1	21.4	75		E	28	1025.1
13	We	16.8	24.2	0.6			ENE	43	08:01	21.1	63		ENE	26	1023.1	22.6	54		NE	17	1019.3
14	Th	15.5	24.4	0.4			NNE	37	14:56	23.0	58		N	17	1017.6	21.9	70		NNE	31	1013.6
15	Fr	18.4	25.0	0			N	65	23:24	21.7	82		NNW	13	1010.7	22.3	79		N	35	1005.6
16	Sa	14.9	22.1	18.8			WNW	67	11:14	18.2	46		W	13	1007.3	21.6	29		WNW	35	1005.9
17	Su	9.5	21.5	0			NE	37	14:18	17.7	45		NE	15	1015.8	19.2	54		NE	31	1013.5
18	Mo	12.0	23.4	0			ENE	22	15:33	20.4	52		ESE	9	1020.4	21.9	52		ENE	17	1017.9
19	Tu	13.1	24.5	0			SSE	46	16:15	22.4	48		NW	7	1021.7	21.6	74				1020.5
20	We	16.7	22.8	3.4			SE	50	09:23	20.2	81		E	31	1026.7	22.0	63		SE	28	1024.7
21	Th	16.9	22.7	0			SE	33	00:26	22.3	56		SSE	17	1025.8	20.8	56		E	15	1022.4
22	Fr	13.9	24.8	0			ESE	20	11:38	22.3	54		SSE	13	1023.2	23.1	53		E	15	1019.3
23	Sa	15.3	25.0	0			NE	31	14:00	23.8	62		ENE	11	1020.2	24.2	59		NE	28	1016.3
24	Su	16.6	26.1	0			NNE	39	13:34	24.2	60		N	17	1018.0	24.5	66		NNE	31	1014.3
25	Mo	17.5	24.3	27.0			SSE	30	19:09	20.9	91		SSE	9	1017.9	23.5	71		ENE	19	1015.1
26	Tu	17.9	24.5	0			SSE	30	04:59	22.0	74		SE	13	1019.2	22.5	76		ESE	15	1016.0
27	We	18.7	26.1	0			E	26	12:17	23.4	73		E	13	1017.0	23.5	69		E	19	1014.0
28	Th	17.6	25.4	0			SE	41	10:55	23.9	71		SSE	13	1017.4	22.1	75		SE	26	1015.8
29	Fr	17.5	25.4	0.2			E	26	15:49	23.7	68		SSE	17	1018.9	24.4	58		E	17	1017.1
30	Sa	17.1	26.4	0			NE	26	14:45	23.9	59		SE	9	1019.2	25.3	58		NE	20	1016.3
31	Su	17.2	25.3	0			NE	20	14:47	22.5	62		NE	9	1017.3	23.7	57		NE	17	1014.6

Statistics for October 2010

Mean	16.4	24.0								21.6	68			19	1020.1	21.7	71			27	1017.4	
Lowest	9.5	19.7								17.3	45		#	7	1007.3	17.0	29		S	13	1005.6	
Highest	19.5	29.5	118.6				SSE	80		25.1	100		SE	54	1028.1	25.3	100		SSE	61	1025.8	
Total			374.4																			

Observations were drawn from Gold Coast Seaway (station D40764)

The Gold Coast Seaway site is an Automatic Weather Station (AWS) at the northern end of Southport Spit. If you are interested in the southern end of the Gold Coast, see the observations from Coolangub.

DC/JDW050/201011 Prepared at 13:22 GMT on 19 Mar 2011

Copyright © 2011 Bureau of Meteorology

Users of this product are deemed to have read the information and accepted the conditions described in the notes at <http://www.bom.gov.au/climate/dwo/IDCJDW0000.pdf>

Gold Coast, Queensland November 2010 Daily Weather Observations

Observations from the Gold Coast Seaway, at the northern end of Southport Spit.



Date	Day	Temps		Rain	Evap	Sun	Max wind gust			9am						3pm					
		Min	Max				Dirn	Spd	Time	Temp	RH	Cld	Dirn	Spd	MSLP	Temp	RH	Cld	Dirn	Spd	MSLP
		°C	°C	mm	mm	hours	km/h	km/h	local	°C	%	eighths	km/h	hPa	°C	%	eighths	km/h	hPa		
1	Mo	17.2	24.9	0			N	28	14:51	22.0	67		E	6	1015.6	21.8	65		N	24	1012.7
2	Tu	18.4	28.7	0			WNW	41	12:52	24.3	42		WNW	9	1014.4	27.8	27		W	26	1011.1
3	We	15.7	25.2	0			SSE	37	08:04	23.8	52		SSE	28	1018.4	24.4	52		E	19	1016.2
4	Th	19.7	22.7	2.6			E	41	21:57	22.4	70		ENE	20	1018.1	20.6	80		N	13	1015.1
5	Fr	16.9	24.5	8.2			ESE	48	10:57	22.3	75		SSE	30	1016.1	22.3	73		SSE	31	1013.6
6	Sa	15.6	26.4	0			S	61	22:50	23.2	61		ENE	13	1016.5	25.6	45		S	17	1014.1
7	Su	17.2	25.7	0.8			S	48	00:42	23.3	68		SSE	20	1020.0	24.2	66		ESE	19	1018.8
8	Mo	20.8	26.6	2.2			ENE	31	21:06	23.7	71		NE	19	1022.3	24.6	63		NE	17	1020.7
9	Tu	20.1	25.6	3.2			ENE	39	00:25	23.0	79		ENE	19	1025.3	24.6	67		ENE	20	1023.6
10	We	19.8	26.3	1.2			ENE	33	10:26	24.7	62		SE	9	1024.1	24.5	61		ENE	17	1020.6
11	Th	17.3	26.7	0.2			NNE	39	14:58	25.3	60		NNE	9	1018.1	24.5	70		NNE	33	1014.5
12	Fr	20.2	26.9	0.6			NNE	39	07:48	24.0	72		N	22	1017.1	24.2	74		NNE	28	1015.4
13	Sa	21.1	26.8	0			NE	26	13:22	25.1	60		NE	19	1021.1	25.3	63		NE	19	1019.4
14	Su	20.0	27.6	0			NE	30	09:26	26.2	66		NE	13	1020.9	25.0	70		NE	24	1018.1
15	Mo	18.1	28.4	0			NNE	35	13:08	25.7	57		NE	13	1017.0	26.3	64		NNE	28	1013.5
16	Tu	21.5	28.2	0			NNE	37	11:54	25.4	68		NE	19	1013.6	26.4	61		NNE	33	1010.3
17	We	19.9	28.6	0			SSE	41	16:05	27.0	49		NNW	20	1013.2	26.0	66		NE	22	1010.6
18	Th	19.5	23.3	0.4			SSE	31	16:15	22.8	80		SE	19	1013.9	21.5	99		SSE	20	1012.3
19	Fr	18.9	24.7	12.0			SSE	61	23:49	20.9	94		SSE	30	1015.8	22.4	85		SSE	35	1015.8
20	Sa	18.8	26.4	2.0			SSE	61	16:52	24.0	63		SSE	43	1022.1	22.1	84		SSE	37	1021.0
21	Su	19.1	24.4	1.0			SSE	48	07:02	22.9	65		SSE	33	1021.9	22.7	58		SSE	33	1020.3
22	Mo	18.7	24.8	3.6			ESE	59	21:48	22.5	81		SE	35	1021.9	22.8	64		ESE	43	1020.8
23	Tu	20.2	25.6	1.4			ESE	57	02:20	23.1	64		ESE	41	1024.2	24.7	56		SE	28	1022.6
24	We	18.5	24.6	4.4			ESE	56	01:47	19.5	93		ENE	11	1024.5	22.9	66		ESE	30	1022.0
25	Th	18.4	26.8	1.2			ESE	57	02:36	23.8	56		E	31	1021.9	25.2	54		E	26	1020.0
26	Fr	18.5	27.9	0			E	35	06:41	25.6	53		E	19	1019.2	26.1	57		E	19	1017.0
27	Sa	22.0	27.3	0			E	37	06:45	26.0	49		E	22	1018.2	25.9	53		ENE	22	1015.5
28	Su	19.9	26.9	0.6			NE	41	03:00	24.3	57		NE	22	1015.7	23.8	56		NE	19	1012.4
29	Mo	17.6	28.1	0.2			NE	33	20:44	25.8	61		ESE	13	1012.8	26.6	61		E	19	1010.8
30	Tu	21.2	28.0	0.6			NE	48	22:18	25.9	62		ENE	19	1013.1	26.3	62		ENE	17	1011.2

Statistics for November 2010

Mean	19.0	26.3								23.9	65			20	1018.6	24.4	64			24	1016.3
Lowest	15.6	22.7								19.5	42		E	6	1012.8	20.6	27		N	13	1010.3

**Gold Coast, Queensland
December 2010 Daily Weather Observations**

Observations from the Gold Coast Seaway, at the northern end of Southport Spit.



Australian Government
Bureau of Meteorology

Date	Day	Temps		Rain mm	Evap mm	Sun hours	Max wind gust			9am						3pm					
		Min °C	Max °C				Dirn	Spd km/h	Time local	Temp °C	RH %	Cld eighths	Dirn	Spd km/h	MSLP hPa	Temp °C	RH %	Cld eighths	Dirn	Spd km/h	MSLP hPa
1	We	21.8	27.1	1.4			NE	48	01:02	24.3	76		ENE	28	1014.3	24.7	75		ENE	26	1012.6
2	Th	21.0	26.4	5.4			ENE	39	18:08	25.0	77		ENE	13	1017.3	24.5	79		ENE	22	1015.4
3	Fr	20.9	23.4	4.4			E	50	16:40	22.3	80		ENE	15	1017.2	22.3	81		E	20	1013.9
4	Sa	20.9	23.1	6.2			NE	54	00:19	22.8	81		ENE	28	1012.0	23.0	81		ENE	37	1008.9
5	Su	19.9	26.0	23.8			E	41	15:40	21.7	98		ENE	15	1010.6	23.6	83		E	24	1008.7
6	Mo	20.5	24.6	22.8			E	46	18:52	22.5	92		SE	33	1011.6	22.3	92		SE	31	1010.1
7	Tu	20.9	26.5	48.6			SE	41	00:07	23.6	93		SSE	20	1014.1	22.6	93		SE	35	1012.9
8	We	22.3	28.3	2.4			ENE	33	19:22	25.9	78		ENE	19	1017.1	26.4	70		E	17	1015.8
9	Th	22.1	28.4	0			NNE	33	17:34	26.3	69		NE	17	1017.2	27.5	68		NNE	24	1014.6
10	Fr	21.6	30.5	0			NNE	44	14:20	28.0	57		NNW	22	1012.7	27.2	73		NNE	35	1007.8
11	Sa	24.1	29.7	0			NNW	37	11:43	29.1	65		NNW	20	1007.6	22.9	99		ENE	9	1005.4
12	Su	20.6	26.8	45.8			NNE	31	14:40	23.0	83		NW	13	1008.6	23.5	87		NNE	26	1007.0
13	Mo	21.8	28.3	0.4			ESE	37	15:57	25.9	72		SE	9	1010.9	26.0	76		ESE	24	1009.7
14	Tu	21.1	29.1	0.6			SSE	46	16:49	26.6	66		S	30	1011.7	24.9	84		SSE	26	1009.9
15	We	20.0	28.6	0.8			E	28	13:06	26.5	62		ESE	11	1011.1	26.5	65		E	17	1007.5
16	Th	21.7	31.3	0			SE	52	13:49	28.0	64		NW	20	1007.7	23.6	87		SE	22	1006.8
17	Fr	22.1	29.9	2.0			NNE	61	18:54	27.1	71		SE	17	1006.5	26.5	77		N	30	1002.7
18	Sa	22.0	28.3	1.4			NW	31	20:58	26.3	67		SE	9	1006.2	23.1	78		NW	13	1005.2
19	Su	21.0	23.4	2.2			SSE	37	15:33	21.9	76		SW	9	1006.7	18.8	91		SSE	24	1005.4
20	Mo	17.9	30.0	53.0			W	56	12:06	23.2	69		NW	20	1001.6	29.4	25		W	43	1002.4
21	Tu	15.1	27.2	0			SSE	33	09:17	26.1	38		SSE	28	1011.7	26.5	54		ESE	19	1010.4
22	We	18.4	25.0	0			SSE	54	20:38	23.1	70		SSE	26	1016.7	20.4	89		S	28	1015.2
23	Th	19.3	26.5	18.6			SE	43	16:32	25.0	82		SSE	24	1016.7	25.4	78		SSE	24	1015.5
24	Fr	22.7	25.6	4.2			SSE	63	13:23	25.5	81		SSE	44	1017.1	23.7	93		SSE	43	1015.7
25	Sa	22.2	24.8	71.0			SE	41	00:05	23.1	100		S	17	1015.3	24.5	92		SE	20	1012.3
26	Su	21.5	24.0	17.4			NE	52	20:47	22.7	99		WNW	6	1010.0	21.6	99		NE	17	1005.8
27	Mo	21.4	25.6	112.2			S	65	14:34	23.4	100		NNW	13	1002.2	21.5	100		SSE	46	1000.2
28	Tu	21.2	25.6	45.4			SSE	78	13:16	23.0	80		SE	56	1012.9	23.7	73		SE	54	1013.3
29	We	21.6	28.3	0.4			SSE	61	00:06	25.1	62		SSE	44	1015.9	24.5	75		SE	44	1013.8
30	Th	21.1	29.3	0			SE	52	14:27	27.3	58		SSE	24	1015.3	27.0	71		SSE	41	1014.0
31	Fr	21.3	28.4	0			SSE	54	15:57	26.3	61		SSE	26	1015.2	27.4	63		SSE	39	1014.1

Statistics for December 2010

	Mean	Min	Max	Rain	Evap	Sun	Dirn	Spd	Time	Temp	RH	Cld	Dirn	Spd	MSLP	Temp	RH	Cld	Dirn	Spd	MSLP	
Mean	21.0	27.1								24.9	75			21	1012.0	24.4	79			28	1010.1	
Lowest	15.1	23.1								21.7	38		WNW	6	1001.6	18.8	25		ENE	9	1000.2	
Highest	24.1	31.3	112.2				SSE	78		29.1	100		SE	56	1017.3	29.4	100		SE	54	1015.8	
Total			490.4																			

Observations were drawn from Gold Coast Seaway (Station 040764)

The Gold Coast Seaway site is an Automatic Weather Station (AWS) at the northern end of Southport Spit. If you are interested in the southern end of the Gold Coast, see the observations from Coolangatta.

IDCJDW4050 201012 Prepared at 13:24 GMT on 17 Mar 2011

Copyright © 2011 Bureau of Meteorology
Users of this product are deemed to have read the information and accepted the conditions described in the notes at <http://www.bom.gov.au/climate/dw/IDCJDW0000.pdf>

**Gold Coast, Queensland
January 2011 Daily Weather Observations**

Observations from the Gold Coast Seaway, at the northern end of Southport Spit.



Australian Government
Bureau of Meteorology

Date	Day	Temps		Rain mm	Evap mm	Sun hours	Max wind gust			9am						3pm					
		Min °C	Max °C				Dirn	Spd km/h	Time local	Temp °C	RH %	Cld eighths	Dirn	Spd km/h	MSLP hPa	Temp °C	RH %	Cld eighths	Dirn	Spd km/h	MSLP hPa
1	Sa	21.8	28.0	0.4			SSE	52	09:21	23.6	89		SSE	37	1014.9	23.0	99		S	30	1013.3
2	Su	22.8	29.5	10.8			NE	26	04:22	27.6	72		NE	13	1014.3	28.0	68		ENE	15	1011.4
3	Mo	22.8	29.1	0.6			SE	50	17:29	27.3	76		SE	15	1009.9	27.9	69		SE	33	1006.6
4	Tu	21.9	30.2	0			SE	61	14:49	26.6	61		SSE	31	1007.6	26.3	76		SE	48	1006.1
5	We	21.9	28.5	0.4			SSE	39	23:42	26.4	67		SSE	11	1008.4	27.3	64		NE	17	1004.7
6	Th	20.3	25.5	29.6			N	61	21:50	22.7	94		SE	13	1006.1	20.7	91		NNW	2	1004.5
7	Fr	19.2	26.8	37.0			N	56	09:10	23.8	89		N	31	1007.7	25.5	69				1007.8
8	Sa	22.6	27.7	0.8						23.1	88				1008.4	26.0	77				1005.3
9	Su	23.0	26.6	1.2						26.4	82				1007.7	25.5	84				1006.7
10	Mo	23.5	26.4	22.0			E	56	18:19	25.2	93				1007.6	25.0	99				1006.1
11	Tu	24.3	27.7	14.6			E	54	03:37	25.1	90		E	37	1009.4	24.8	97		E	31	1006.6
12	We	23.8	29.3	6.2			E	39	02:33	27.5	76		E	20	1011.2	28.1	71		ENE	31	1010.3
13	Th	23.8	28.2	0			ESE	52	22:41	25.9	66		SE	30	1013.5	27.3	64		SE	28	1011.6
14	Fr	22.6	28.4	1.4			ESE	39	00:08	26.3	66		SE	30	1011.8	26.1	69		ESE	26	1009.8
15	Sa	21.4	28.5	0.8			S	37	07:58	25.3	71		ESE	26	1009.2	28.0	56		SE	24	1007.2
16	Su	20.3	29.1	0.2			SE	54	14:53	27.2	62		SSE	31	1007.3	26.9	66		SE	41	1005.0
17	Mo	18.3	29.9	0			ENE	24	13:37	28.0	54		SSE	9	1004.9	28.9	54		NE	19	1001.8
18	Tu	23.1	30.4	0			SE	37	10:01	28.3	72		SSE	17	1004.3	27.7	78		SSE	20	1005.1
19	We	24.4	30.6	0.8			ENE	30	16:19	28.0	75		ESE	17	1008.0	29.0	71		ENE	20	1006.4
20	Th	21.5	27.9	13.8			SSE	56	01:33	26.6	75		SSE	28	1009.4	26.6	68		SSE	31	1009.4
21	Fr	20.8	27.6	16.4			SE	59	04:10	21.4	88		ESE	43	1012.7	26.6	66		SE	35	1011.2
22	Sa	20.4	28.4	1.8			SE	54	14:16	26.5	80		S	33	1013.1	26.9	56		SE	39	1012.5
23	Su	19.5	28.4	0			SE	56	16:04	26.5	54		SSE	33	1011.2	26.6	63		SE	39	1009.2
24	Mo	18.4	28.7	0			ENE	28	13:15	26.2	54		SSE	9	1010.2	27.1	57		NE	22	1007.5
25	Tu	20.9	29.1	0			NNE	41	13:19	27.1	56		N	17	1011.2	27.3	61		NNE	35	1009.9
26	We	21.7	29.7	0			ENE	24	12:00	28.0	59		NE	9	1015.3	28.9	58		ENE	17	1014.2
27	Th	21.6	29.7	0			ENE	22	13:11	27.2	61		SSE	11	1015.8	28.7	60		ENE	15	1013.0
28	Fr	23.7	29.0	0			S	63	21:55	27.3	64		SSE	15	1013.9	28.0	67		SE	33	1013.5
29	Sa	22.6	29.0	2.2			S	61	01:47	25.3	66		SSE	46	1018.0	27.5	62		SSE	39	1016.8
30	Su	22.8	28.6	0			SE	43	01:20	26.5	67		SE	31	1020.1	27.5	65		SE	28	1018.3
31	Mo	22.9	30.1	0			ENE	26	15:51	26.8	67		E								

Gold Coast, Queensland
February 2011 Daily Weather Observations

Observations from the Gold Coast Seaway, at the northern end of Southport Spit.

Date	Day	Temps		Rain	Evap	Sun	Max wind gust			9am						3pm					
		Min	Max				Dirn	Spd	Time	Temp	RH	Cld	Dirn	Spd	MSLP	Temp	RH	Cld	Dirn	Spd	MSLP
		°C	°C																		
1	Tu	23.7	30.4	0			NNE	31	16:18	26.3	82		SSE	13	1017.8	29.0	69		NE	20	1015.0
2	We	24.5	30.4	1.4			NNE	33	18:46	27.9	81		NE	15	1017.7	30.0	73		NE	19	1016.6
3	Th	24.4	30.8	0			NE	31	14:26	28.2	74		NNE	13	1018.2	29.2	70		NNE	28	1015.6
4	Fr	24.7	30.6	0			NNE	39	13:39	28.3	73		NNE	15	1017.1	29.4	68		NNE	33	1014.8
5	Sa	24.7	31.3	0			NNE	35	16:54	28.1	75		NNE	15	1017.5	30.1	69		NNE	28	1015.0
6	Su	24.7	30.0	0			N	37	09:13	28.9	80		NNE	17	1018.3	28.7	76		NNE	24	1015.4
7	Mo	22.9	28.4	5.8			S	61	10:55	24.9	75		S	39	1017.8	26.9	70		SSE	44	1015.6
8	Tu	22.0	26.0	0			SSE	52	22:44	22.0	83		S	24	1015.9	22.9	85		S	26	1014.7
9	We	20.7	28.8	7.4			SSE	54	11:51	26.0	66		SSE	31	1019.9	27.4	56		SSE	37	1019.6
10	Th	20.5	28.8	2.0			SSE	48	04:50	24.5	74		S	33	1020.6	27.2	61		SE	30	1018.4
11	Fr	20.7	27.5	1.8			SSE	41	05:30	24.5	71		S	13	1018.6	26.8	53		ESE	13	1015.5
12	Sa	20.2	29.8	0.4			ENE	28	14:20	27.0	61		E	7	1015.9	28.6	61		ENE	20	1013.0
13	Su	21.1	29.9	0			SE	33	23:45	28.4	61		SSE	19	1015.9	28.8	64		E	19	1013.6
14	Mo	23.4	30.4	0			SSE	50	20:16	27.9	67		SSE	31	1016.5	28.5	64		SE	33	1015.1
15	Tu	22.0	29.2	9.4			SSE	56	14:36	25.2	85		S	22	1017.8	24.7	97		SSE	31	1016.4
16	We	21.2	28.5	16.6			ESE	41	13:02	27.5	71		SSE	30	1017.0	27.0	72		ESE	26	1014.7
17	Th	23.1	28.9	7.2			ENE	30	03:35	26.0	81		S	15	1014.9	28.3	72		ESE	19	1012.7
18	Fr	21.3	29.6	0.2			ESE	37	18:58	27.8	72		SSE	17	1013.8	28.0	70		ESE	22	1012.3
19	Sa	23.1	29.9	7.8			ENE	20	15:18	27.4	72		E	13	1014.3	29.2	64		ENE	15	1011.8
20	Su	23.2	34.8	0			N	39	16:06	26.7	59		NW	20	1011.1	29.8	66		NNE	28	1007.2
21	Mo	24.5	31.8	0			S	67	17:17	29.4	72		SE	9	1008.3	27.1	82		SE	35	1005.9
22	Tu	21.2	30.5	34.2			SE	80	20:29	25.6	63		SSE	56	1014.5	25.5	60		SSE	54	1015.2
23	We	18.0	27.0	3.8			SSE	65	13:57	21.7	80		S	43	1017.3	24.0	72		SE	43	1015.6
24	Th	19.4	27.7	7.0			SSE	57	10:00	24.8	70		SSE	37	1017.1	25.0	61		SSE	19	1015.0
25	Fr	18.7	28.2	0.2			ESE	24	12:41	26.0	61		SSE	11	1015.2	27.7	57		ENE	17	1012.7
26	Sa	19.7	28.9	0			ENE	28	14:02	26.9	54		WNW	6	1014.2	27.8	61		NE	20	1011.4
27	Su	21.6	29.9	0			NNE	39	16:26	27.6	55		N	17	1013.4	28.3	60		NNE	33	1010.6
28	Mo	22.9	32.3	0			NNE	41	15:10	28.0	56		NW	19	1012.8	28.9	64		NNE	35	1009.4
Statistics for February 2011																					
Mean		22.1	29.7							26.6	70			21	1016.0	27.7	67			27	1013.9
Lowest		18.0	26.0							21.7	54		WNW	6	1008.3	22.9	53		ESE	13	1005.9
Highest		24.7	34.8	34.2			SE	80		29.4	85		SSE	56	1020.6	30.1	97		SSE	54	1019.6
Total				105.2																	

Observations were drawn from Gold Coast Seaway (station 040764). The Gold Coast Seaway site is an Automatic Weather Station (AWS) at the northern end of Southport Spit. If you are interested in the southern end of the Gold Coast, see the observations from Coolangatta.

IDCJDW4050.201102 Prepared at 13:20 GMT on 21 Mar 2011
Copyright © 2011 Bureau of Meteorology
Users of this product are deemed to have read the information and accepted the conditions described in the notes at <http://www.bom.gov.au/climate/dwo/IDCJDW000.pdf>

Gold Coast, Queensland
March 2011 Daily Weather Observations

Observations from the Gold Coast Seaway, at the northern end of Southport Spit.

Date	Day	Temps		Rain	Evap	Sun	Max wind gust			9am						3pm					
		Min	Max				Dirn	Spd	Time	Temp	RH	Cld	Dirn	Spd	MSLP	Temp	RH	Cld	Dirn	Spd	MSLP
		°C	°C																		
1	Tu	23.1	32.7	0			NNE	41	16:12	28.2	63		NNW	22	1010.9	29.8	67		NNE	30	1007.7
2	We	22.4	29.2	5.0			SE	56	01:11	24.9	81		WNW	7	1012.9	28.4	63		SE	17	1011.0
3	Th	22.9	32.5	73.2			S	48	19:26	27.3	79		NNW	15	1011.4	29.4	71		NNE	31	1007.7
4	Fr	21.0	25.8	30.2			S	26	02:43	23.5	97		ENE	6	1011.8	24.7	83		ESE	7	1009.3
5	Sa	21.2	27.8	8.0			SSE	80	17:02	25.2	74		S	30	1014.0	23.8	77		S	46	1014.9
6	Su	20.1	27.2	13.6			SE	70	18:12	23.0	70		S	31	1020.9	25.9	58		SSE	43	1019.9
7	Mo	21.3	27.2	2.2			SE	67	06:51	24.6	58		SE	46	1020.4	25.3	53		SE	37	1018.4
8	Tu	19.3	26.5	6.8			ESE	54	09:39	24.6	68		ENE	20	1018.6	25.4	61		ESE	26	1016.6
9	We	19.2	26.6	0.2			E	35	00:20	25.0	61		S	15	1017.9	24.6	62		E	17	1015.7
10	Th	19.7	28.3	2.4			NE	37	18:15	25.5	64		SSE	13	1016.0	27.6	60		ENE	17	1013.6
11	Fr	21.1	29.3	1.6			ENE	33	19:03	26.5	71		ENE	6	1016.7	28.4	58		ENE	17	1015.9
12	Sa	21.9	29.3	0			ENE	50	07:14	25.9	68		E	15	1020.5	28.0	62		E	22	1019.4
13	Su	22.7	27.8	0			ESE	37	14:53	25.2	85		SSE	28	1021.8	25.4	82		ESE	30	1018.8
14	Mo	24.0	28.1	0.6			E	31	02:43	26.5	68		ESE	20	1020.9	27.0	61		SE	19	1017.8
15	Tu	20.4	28.7	0			SE	33	00:45	25.5	69		SSE	22	1019.3	27.3	64		SE	20	1016.3
16	We	21.1	29.4	0			NE	24	15:45	27.3	69		SSE	11	1017.9	27.8	64		NE	17	1015.4
17	Th	23.1	29.8	0			ENE	20	13:03	26.6	68		ENE	4	1018.7	27.8	63		ENE	15	1015.4
18	Fr	22.2	27.9	0			NNE	19	16:32	24.8	76		NW	2	1014.8	26.3	69		S	13	1011.3
19	Sa	22.0	23.5	8.4			SE	52	19:03	22.2	99		S	22	1012.4	21.5	95		SSE	9	1008.9
20	Su	20.1	26.8	31.8			SSE	43	15:48	22.6	99		S	24	1008.0	24.3	86		S	31	1004.8
21	Mo	22.1	28.7	3.6			SSW	22	00:10	26.5	82		SSE	19	1004.8	28.0	75		SE	19	1002.3
22	Tu	23.3	30.7	0.2			NNE	31	14:25	27.6	79		N	13	1002.8	29.9	76		NNE	22	1000.0
23	We	20.2	33.2	0			NW	41	13:55	28.7	44		W	19	1006.0	32.8	34		NW	24	1002.8
24	Th	20.5	32.1	0			NW	50	12:19	28.4	41		W	15	1009.1	31.4	33		NW	15	1005.8
25	Fr	17.2	30.8	0			WNW	41	13:46	26.5	38		NW	17	1011.0	29.8	30		NW	24	1007.9
26	Sa	20.0	28.4	0			S	56	20:58	25.7	60		SSE	37	1015.0	27.1	52		SSE	33	1014.5
27	Su	21.1	28.5	0			S	61	14:03	24.0	59		S	41	1020.1	24.8	57		S	50	1018.6
28	Mo	19.6	28.1	0.6						25.2	63		SSE	30	1022.8	22.7	76		SSE	44	1021.1
Statistics for the first 28 days of March 2011																					
Mean		21.2	28.8							25.6	69			19	1014.9	27.0	64			24	1012.6
Lowest		17.2	23.5							22.2	38		NW	2	1002.8	21.5	30		ESE	7	1000.0
Highest		24.0	33.2	73.2			SSE	80		28.7	99		SE	46	1022.8	32.8	95		S	50	1021.1
Total				188.4																	

Observations were drawn from Gold Coast Seaway (station 040764). The Gold Coast Seaway site is an Automatic Weather Station (AWS) at the northern end of Southport Spit. If you are interested in the southern end of the Gold Coast, see the observations from Coolangatta.

IDCJDW4050.201103 Prepared at 08:29 GMT on 28 Mar 2011
Copyright © 2011 Bureau of Meteorology
Users of this product are deemed to have read the information and accepted the conditions described in the notes at <http://www.bom.gov.au/climate/dwo/IDCJDW000.pdf>

Gold Coast, Queensland
April 2011 Daily Weather Observations

Observations from the Gold Coast Seaway, at the northern end of Southport Spit.



Australian Government
Bureau of Meteorology

Date	Day	Temps		Rain	Evap	Sun	Max wind gust			9am						3pm						
		Min	Max				Dirn	Spd	Time	Temp	RH	Cld	Dirn	Spd	MSLP	Temp	RH	Cld	Dirn	Spd	MSLP	
		°C	°C				mm	mm	hours	°C	%	eighths	km/h	local	°C	%	eighths	km/h	hPa	°C	%	eighths
1	Fr	20.2	25.6	1.2			SE	61	10:12	21.7	89		SSE	31	1021.7	24.5	66		SSE	41	1019.4	
2	Sa	18.6	27.5	6.2			S	33	23:59	25.3	62		S	19	1020.2	26.4	61		S	15	1016.5	
3	Su	18.5	25.8	24.8			SE	70	00:30	21.3	81		S	39	1022.2	24.4	63		SSE	31	1020.2	
4	Mo	19.2	27.2	0.8			S	59	15:25	24.4	57		S	30	1023.1	25.9	51		SSE	35	1020.8	
5	Tu	18.0	25.9	2.2			SSE	72	14:42	19.5	88		S	22	1024.1	22.9	77		SSE	39	1022.5	
6	We	17.6	25.5	8.6			SSE	56	15:26	20.5	77		S	30	1024.3	24.7	55		SSE	39	1022.4	
7	Th	17.6	25.7	1.0			SSE	69	20:20	22.1	66		S	33	1025.0	23.7	71		SE	37	1023.0	
8	Fr	18.1	23.5	22.2			ESE	67	00:17	20.2	93		ESE	31	1026.3	22.5	74		SE	46	1023.5	
9	Sa	17.2	26.6	3.4			SSE	56	01:15	23.4	67		S	30	1023.6	25.0	57		SSE	31	1020.1	
10	Su	16.8	26.9	0			NNE	30	17:04	23.7	63		WSW	9	1018.4	25.4	61		NE	20	1013.6	
11	Mo	18.9	27.4	0			N	41	12:31	24.2	66		NNW	17	1013.2	25.1	48		N	22	1010.1	
12	Tu	17.9	26.5	4.2			ENE	28	14:48	23.1	72		SSE	7	1015.8	23.4	71		ENE	19	1013.3	
13	We	17.4	26.6	0			E	26	13:40	24.4	67		E	6	1017.4	24.9	67		E	20	1013.6	
14	Th	17.2	28.4	0			SE	26	13:38	24.2	60		NW	15	1014.5	25.7	64		ESE	22	1010.1	
15	Fr	17.4	26.5	0			E	30	21:22	23.7	69		SSE	9	1014.3	26.0	58		E	17	1011.9	
16	Sa	20.2	26.3	0.2			S	43	17:23	22.8	70		SW	9	1015.2	22.4	73		SSE	28	1013.2	
17	Su	18.9	24.4	0			S	50	20:26	21.8	68		SSW	20	1017.7	23.1	69		S	26	1016.8	
18	Mo	18.0	22.5	11.6			SE	69	03:16	19.8	91		S	39	1020.0	18.8	99		S	28	1017.4	
19	Tu	18.2	24.5	43.8			S	46	01:32	22.0	77		S	26	1019.3	22.7	79		SSE	31	1017.2	
20	We	19.2	26.3	8.4			S	33	04:08	24.0	76		S	22	1019.5	25.2	67		ESE	17	1016.2	
21	Th	19.3	27.4	0.2			ENE	22	14:42	24.9	66		Calm		1015.1	25.9	64		NE	17	1011.8	
22	Fr	19.2	27.0	0			SE	20	11:54	25.4	73		S	7	1013.9	23.7	81		E	13	1011.4	
23	Sa	18.8	27.1	0.6			SE	52	15:41	24.2	73		S	11	1016.7	25.4	71		SSE	37	1015.4	
24	Su	18.7	26.2	0			S	56	21:16	24.3	64		S	28	1021.3	23.6	66		S	22	1019.5	
25	Mo	19.2	26.5	0			SSE	50	18:13	23.0	66		S	28	1022.7	24.5	54		SSE	35	1020.7	
26	Tu	18.3	24.9	2.8			SSE	74	15:55	22.4	77		S	28	1022.7	20.7	86		SE	50	1020.4	
27	We	17.2	22.6	24.4			SSE	76	21:53	18.1	97		S	41	1022.9	20.8	75		SE	52	1020.1	
28	Th	16.7	22.6	23.6			SSE	67	02:18	19.0	94		S	24	1020.3	21.8	70		S	33	1017.7	
29	Fr	17.0	24.8	10.0			S	57	13:18	21.0	72		S	39	1018.4	19.2	88		S	35	1016.3	
30	Sa	17.0	25.9	5.6			S	52	14:24	22.3	71		S	30	1017.0	22.7	68		SSW	17	1014.6	
Statistics for April 2011																						
Mean		18.2	25.8							22.6	73			22	1019.6	23.7	68			29	1017.0	
Lowest		16.7	22.5							18.1	57		Calm		1013.2	18.8	48		E	13	1010.1	
Highest		20.2	28.4	43.8			SSE	76		25.4	97		S	41	1026.3	26.4	99		SE	52	1023.5	
Total				205.8																		

Observations were drawn from Gold Coast Seaway (station 040764)

The Gold Coast Seaway site is an Automatic Weather Station (AWS) at the northern end of Southport Spit. If you are interested in the southern end of the Gold Coast, see the observations from Coolangatta.

ICJDW4060 201104 Prepared at 16:21 GMT on 7 Nov 2011

Copyright © 2011 Bureau of Meteorology
Users of this product are deemed to have read the information and accepted the conditions described in the notes at <http://www.bom.gov.au/climate/dwo/ICJDW0000.pdf>

Gold Coast, Queensland
May 2011 Daily Weather Observations

Observations from the Gold Coast Seaway, at the northern end of Southport Spit.



Australian Government
Bureau of Meteorology

Date	Day	Temps		Rain	Evap	Sun	Max wind gust			9am						3pm					
		Min	Max				Dirn	Spd	Time	Temp	RH	Cld	Dirn	Spd	MSLP	Temp	RH	Cld	Dirn	Spd	MSLP
		°C	°C				mm	mm	hours	°C	%	eighths	km/h	local	°C	%	eighths	km/h	hPa	°C	%
1	Su	16.3	26.3	0			S	33	13:42	22.3	52		SSW	11	1014.7	25.2	50		SSE	22	1011.7
2	Mo	14.2	24.9	0			ESE	26	13:27	22.0	56		SSE	4	1014.9	23.5	70		ESE	19	1012.4
3	Tu	16.8	25.6	0			SW	37	15:53	21.8	75		ESE	9	1014.3	23.2	70		NE	19	1010.9
4	We	15.0	24.2	4.6			SSE	30	10:29	20.0	70		S	17	1013.7	23.6	59		SSE	17	1011.5
5	Th	15.3	24.8	0			SSE	59	14:03	21.0	57		S	28	1015.8	23.2	59		SSE	35	1014.9
6	Fr	15.9	24.3	0			S	54	01:48	20.8	51		S	30	1019.8	23.4	45		S	28	1016.6
7	Sa	12.7	23.3	0			SSE	31	17:14	19.9	45		SW	9	1017.6	22.3	49		SE	17	1014.3
8	Su	13.5	24.9	0			N	28	13:22	18.9	57		WNW	13	1016.4	22.6	53		N	17	1012.4
9	Mo	16.3	19.7	2.2			NNW	30	02:57	17.0	91		WNW	11	1012.9	19.2	69		S	2	1009.2
10	Tu	13.9	21.7	1.6			SSE	50	13:00	17.5	67		WNW	11	1011.1	19.2	57		N	11	1009.8
11	We	10.6	22.0	3.6			WNW	41	12:04	17.2	61		NW	13	1014.1	21.5	34		NW	22	1009.8
12	Th	11.3	21.8	0			W	50	12:42	16.8	38		W	33	1013.7	20.7	34		W	31	1009.9
13	Fr	9.9	22.3	0			N	28	11:48	16.4	44		W	9	1016.0	21.4	43		NNE	15	1012.0
14	Sa	10.4	22.0	0			WNW	24	06:56	18.6	45		W	11	1015.5	21.3	39		E	11	1014.5
15	Su	12.7	22.5	0			S	52	09:28	18.3	43		S	33	1025.6	21.8	39		S	19	1025.0
16	Mo	11.9	23.6	0			S	33	09:43	19.9	56		S	19	1028.9	21.6	59		SE	30	1026.1
17	Tu	14.0	23.8	0			SSE	48	18:09	20.3	64		SSW	9	1027.0	22.0	61		SSE	30	1024.5
18	We	13.7	24.4	0			SSE	52	14:32	19.3	67		S	26	1028.6	21.8	55		S	33	1026.1
19	Th	16.2	21.5	0.8			SSE	52	13:47	18.9	84		S	26	1028.2	18.7	88		S	28	1026.5
20	Fr	14.9	21.8	18.0			S	48	09:26	20.3	68		SSE	35	1027.1	21.2	63		SSE	19	1024.4
21	Sa	15.5	22.3	3.0			SSE	33	04:28	19.5	84		S	13	1025.5	21.4	74		SSE	11	1022.5
22	Su	17.2	22.1	7.8			NW	26	14:02	18.9	93		SSW	11	1022.6	19.1	96		SW	4	1018.7
23	Mo	17.0	22.5	7.2			WNW	57	13:35	19.4	93		N	9	1014.0	17.8	91		NW	17	1010.5
24	Tu	14.0	23.0	5.4			NW	41	13:55	18.9	65		WNW	15	1008.8	22.2	41		NW	26	1004.8
25	We	11.8	20.3	0.2			W	46	13:23	16.4	53		W	28	1008.0	18.6	45		W	24	1005.5
26	Th	12.1	22.1	0			SSW	37	10:43	17.5	50		WNW	15	1012.8	21.1	44		S	24	1012.2
27	Fr	10.0	22.7	0			SE	28	17:13	17.0	62		WNW	9	1018.4	21.2	56		ESE	15	1015.7
28	Sa	12.5	22.5	0			S	50	17:07	18.5	69		S	17	1021.0	20.8	61		SSE	33	1019.4
29	Su	13.7	23.2	0.6			SE	46	14:10	18.8	76		S	17	1022.7	20.3	69		E	30	1019.5
30	Mo	14.2	19.7	3.4			S	33	20:23	16.3	88		SSE	19	1017.9	19.2	65		SE	15	1013.8
31	Tu	10.9	21.1	7.0			SE	54	20:04	16.0	72		SSW	9	1014.9	18.9	61		SSE	28	1012.8
Statistics for May 2011																					
Mean		13.7	22.8							18.9	64			16	1018.1	21.2	58			21	1015.4
Lowest		9.9	19.7							16.0	38		SSE	4	1008.0	17.8	34		S	2	1004.8
Highest		17.2	26.3	18.0			SSE	59		22.3	93										

Gold Coast, Queensland
June 2011 Daily Weather Observations

Observations from the Gold Coast Seaway, at the northern end of Southport Spit.



Australian Government
Bureau of Meteorology

Date	Day	Temps		Rain	Evap	Sun	Max wind gust			9am						3pm						
		Min	Max				Dirn	Spd	Time	Temp	RH	Cld	Dirn	Spd	MSLP	Temp	RH	Cld	Dirn	Spd	MSLP	
		°C	°C																			km/h
1	We	11.6	20.4	1.4			S	26	23:09	14.5	90		Calm	1014.3	20.1	68		S	13	1014.6		
2	Th	14.4	23.4	0.6			S	59	15:28	20.2	63		S	28	1016.9	22.1	56		S	30	1015.3	
3	Fr	12.8	23.1	0			SSW	24	00:01	18.7	59		S	9	1018.2	21.5	55		ESE	13	1015.1	
4	Sa	11.3	24.3	0			WNW	30	14:14	17.2	74		NW	15	1018.0	23.6	37		WNW	15	1014.8	
5	Su	11.8	23.0	0			NW	22	10:05	15.9	72		WNW	13	1018.1	21.9	45		NNW	13	1014.3	
6	Mo	11.6	25.4	0			ESE	19	15:31	18.6	64		WNW	7	1016.8	22.9	53		E	13	1014.5	
7	Tu	15.1	20.5	0			S	19	10:51	17.7	78		SSW	6	1019.6	20.2	69		SSW	6	1015.9	
8	We	13.6	18.5	0			WNW	28	09:00	16.8	52		WNW	20	1018.3	17.8	48		NNW	13	1014.8	
9	Th	13.1	14.5	0			NW	33	06:21	14.1	31		W	17	1016.5	13.2	41		WNW	17	1014.0	
10	Fr	7.3	19.2	0			NW	28	00:30	13.3	46		W	11	1016.9	18.5	40		NNE	13	1015.7	
11	Sa	10.6	18.5	0			S	44	18:02	15.9	59		SSW	11	1019.8	16.9	62		S	20	1016.9	
12	Su	14.6	19.9	10.2			S	39	23:20	15.8	99		SSW	11	1016.3	17.9	69		S	15	1013.3	
13	Mo	13.8	21.3	2.8			S	46	06:06	18.3	72		S	28	1013.5	20.3	59		S	17	1009.7	
14	Tu	12.4	20.7	0			NW	46	09:45	15.8	73		NW	31	1010.7	19.6	52		NW	24	1008.6	
15	We	11.2	20.3	0			NNW	28	00:28	15.0	72		NW	15	1015.4	19.5	55		NNE	17	1013.3	
16	Th	10.4	21.5	0			SSW	31	15:45	15.5	70		WNW	17	1014.7	20.9	52		SSW	9	1011.9	
17	Fr	11.3	22.1	0			W	50	13:50	17.2	59		NW	22	1013.3	21.2	41		WNW	24	1008.5	
18	Sa	10.1	21.1	0			W	28	01:13	15.8	42		W	20	1012.4	20.5	28		W	17	1010.0	
19	Su	8.4	20.4	0			NW	19	09:05	14.1	58		NW	13	1016.9	19.4	42		NE	13	1014.8	
20	Mo	8.4	21.1	0			NE	26	13:50	13.9	66		NW	13	1018.2	20.7	38		NW	15	1014.7	
21	Tu	10.0	22.3	0			NNW	35	10:43	14.8	65		NW	13	1015.5	21.9	42		NNW	19	1009.6	
22	We	11.7	20.2	0			WNW	41	13:05	15.5	55		WNW	26	1014.8	19.2	25		W	22	1013.1	
23	Th	8.2	19.4	0			ENE	20	14:05	13.4	51		WNW	7	1019.8	18.8	39		ENE	15	1018.0	
24	Fr	10.6	22.2	0			S	43	17:47	15.4	64		SSW	7	1025.0	19.8	51		S	20	1023.3	
25	Sa	15.0	22.2	0			S	41	23:25	19.6	66		S	28	1028.4	20.7	53		SSE	33	1026.3	
26	Su	14.7	22.7	0			SSE	35	05:10	19.2	67		S	15	1028.4	20.2	65		SE	11	1025.2	
27	Mo	11.4	22.6	0			SW	19	00:43	16.9	64		SSW	7	1026.8	21.8	50		ENE	13	1024.3	
28	Tu	12.7	22.7	0			SSE	50	15:25	18.3	54		S	28	1029.4	20.2	58		SSE	31	1026.8	
29	We	14.2	20.0	2.2			SE	70	20:02	16.1	99		SSE	41	1030.8	18.9	65		SSE	48	1029.0	
30	Th	14.0	20.3	3.2			SE	72	01:15	17.7	61		S	30	1030.7	18.8	63		S	44	1027.6	
Statistics for June 2011																						
Mean		11.9	21.1								16.4	64		16	1019.1	20.0	50			19	1016.5	
Lowest		7.3	14.5							13.3	31		Calm	1010.7	13.2	25		SSW	6	1008.5		
Highest		15.1	25.4	10.2			SE	72		20.2	99		SSE	41	1030.8	23.6	69		SSE	48	1029.0	
Total				20.4																		

Observations were drawn from Gold Coast Seaway (station 040764)

The Gold Coast Seaway site is an Automatic Weather Station (AWS) at the northern end of Southport Spit. If you are interested in the southern end of the Gold Coast, see the observations from Coolangatta.

ICJDW4060.201106 Prepared at 13:22 GMT on 5 Nov 2011
 Copyright © 2011 Bureau of Meteorology
 Users of this product are deemed to have read the information and accepted the conditions described in the notes at <http://www.bom.gov.au/climate/dwo/ICJDW0000.pdf>

Gold Coast, Queensland
July 2011 Daily Weather Observations

Observations from the Gold Coast Seaway, at the northern end of Southport Spit.



Australian Government
Bureau of Meteorology

Date	Day	Temps		Rain	Evap	Sun	Max wind gust			9am						3pm					
		Min	Max				Dirn	Spd	Time	Temp	RH	Cld	Dirn	Spd	MSLP	Temp	RH	Cld	Dirn	Spd	MSLP
		°C	°C																		
1	Fr	13.2	20.7	2.6			S	48	08:16	16.4	72		SSW	20	1025.8	19.5	60		SSE	30	1022.8
2	Sa	12.8	20.7	0			S	46	12:48	17.5	65		S	20	1024.0	19.8	55		S	28	1021.4
3	Su	13.8	20.6	0			S	37	00:56	16.8	75		WSW	7	1023.0	20.1	60		Calm		1021.0
4	Mo	12.3	22.9	0			NW	31	11:53	16.6	78		NW	11	1021.8	22.6	41		NW	17	1016.9
5	Tu	14.2	22.7	0			WNW	54	21:27	19.7	54		W	20	1016.4	21.9	26		WNW	31	1012.3
6	We	11.4	22.2	0			W	39	00:26	15.2	45		NW	17	1015.9	21.3	28		NNW	15	1011.9
7	Th	9.6	21.5	0			W	57	21:36	15.2	43		NW	22	1017.2	20.7	29		WNW	28	1015.0
8	Fr	9.5	19.7	0			W	19	01:02	15.6	45		SSW	7	1024.1	19.1	45		ENE	13	1020.9
9	Sa	6.9	21.5	0			WNW	41	10:50	11.8	50		NNW	19	1019.6	21.1	24		W	13	1016.0
10	Su	7.4	19.9	0			W	44	23:57	12.5	49		NW	19	1018.1	19.4	28		NW	28	1014.0
11	Mo	10.0	20.6	0			W	52	00:06	16.0	36		W	13	1018.0	19.4	37		ESE	11	1017.9
12	Tu	7.9	20.8	0			NW	30	11:20	14.5	55		NW	15	1024.2	20.2	34		NNW	17	1020.9
13	We	8.6	20.9	0			NW	39	09:50	13.5	56		NW	19	1021.2	20.0	31		NW	17	1018.3
14	Th	9.0	22.2	0			SSE	57	16:41	17.2	50		WNW	7	1023.0	20.8	53		E	17	1021.6
15	Fr	14.3	19.7	0			SSE	69	20:40	16.9	57		S	31	1029.4	16.6	68		S	28	1027.3
16	Sa	12.6	17.1	20.6			S	48	02:03	13.5	87		S	26	1028.3	14.9	84		S	22	1024.4
17	Su	13.1	20.5	2.6			SSE	37	09:23	16.9	75		S	28	1022.5	19.4	71		SSE	26	1019.3
18	Mo	10.7	22.0	0.2			ENE	20	11:00	16.5	72		NW	9	1018.6	20.1	62		ENE	17	1014.9
19	Tu	9.7	20.9	0			WNW	41	12:02	16.5	45		W	19	1015.6	20.0	26		NNW	24	1011.5
20	We	9.3	21.2	0			NE	57	15:05	12.9	55		WNW	31	1010.3	19.5	43		NW	30	1007.5
21	Th	12.0	22.5	0.2			WNW	28	00:23	17.7	51		WNW	17	1011.3	21.5	50		ENE	15	1008.1
22	Fr	10.9	22.7	0.2			S	46	12:48	18.5	53		SSW	24	1011.3	21.9	42		S	24	1009.1
23	Sa	10.9	21.6	0			S	46	11:38	17.1	50		SSW	24	1014.2	20.6	36		S	22	1013.6
24	Su	9.2	20.4	0			S	30	09:54	16.1	52		NW	6	1018.6	18.7	56		SE	24	1016.5
25	Mo	9.3	21.9	0			NE	22	13:02	16.3	69		NW	13	1020.7	20.7	46		E	13	1017.9
26	Tu	7.7	24.0	0			NW	31	13:56	15.5	63		NNW	11	1023.1	21.5	41		N	17	1019.6
27	We	10.0	21.1	0			SSE	43	17:26	16.3	52		WSW	7	1025.0	19.2	49		SE	30	1023.2
28	Th	8.6	21.6	0			SSE	50	20:14	16.5	51		S	17	1027.2	20.0	52		SSE	31	1024.3
29	Fr	12.9	21.4	0			SSE	43	12:07	18.4	66		S	28	1026.1	19.9	58		SSE	24	1023.8
30	Sa	11.9	21.1	0			SSE	33	09:32	17.9	62		S	20	1024.5	19.3	50		SE	24	1021.8
31	Su	11.3	21.5	0			SE	26	13:15	17.8	56		SW	11	1023.4	19.9	54		SE	17	1020.5
Statistics for July 2011																					
Mean		10.7	21.2								16.1	57		17	1020.7	20.0	46			21	1017.9
Lowest		6.9	17.1							11.8	36		NW	6	1010.3	14.9	24		Calm		1007.5
Highest		14.3	24.0	20.6			SE	69		19.7	87		#	31	1029.4	22.6	84		#	31	10

Gold Coast, Queensland
August 2011 Daily Weather Observations

Observations from the Gold Coast Seaway, at the northern end of Southport Spit.



Date	Day	Temps		Rain mm	Evap mm	Sun hours	Max wind gust			9am						3pm						
		Min °C	Max °C				Dirn	Spd km/h	Time local	Temp °C	RH %	Cld eighths	Dirn	Spd km/h	MSLP hPa	Temp °C	RH %	Cld eighths	Dirn	Spd km/h	MSLP hPa	
1	Mo	11.2	21.1	0			ESE	22	15:37	17.5	65		SW	7	1023.8	20.2	60		E	13	1021.6	
2	Tu	11.3	21.5	0			ESE	26	13:39	17.6	67		SW	9	1024.8	19.8	67		ESE	19	1022.6	
3	We	12.1	22.1	0			SE	33	14:57	18.0	65		SSW	9	1026.0	20.1	63		SE	28	1024.6	
4	Th	11.9	22.0	0			SSE	28	13:29	18.5	65		S	15	1028.9	20.2	54		SE	20	1027.3	
5	Fr	13.5	22.0	0			SE	35	11:04	18.7	61		SSW	13	1029.1	20.6	60		SSE	13	1026.1	
6	Sa	11.9	22.9	0			NNE	28	15:23	18.8	60		W	6	1025.8	21.5	60		NE	20	1021.4	
7	Su	14.1	24.9	0			NNE	31	13:27	20.4	59		NW	9	1020.5	22.4	57		NNE	26	1015.5	
8	Mo	15.5	24.0	0			NW	50	15:13	17.8	69		NNW	13	1013.6	23.1	26		NW	31	1008.6	
9	Tu	9.8	21.9	0			WNW	44	14:57	15.9	45		NW	13	1012.0	20.4	26		WNW	33	1007.3	
10	We	8.2	22.3	0			NW	46	15:30	15.1	48		NW	15	1012.0	22.1	26		NW	26	1006.7	
11	Th	11.3	21.0	0			S	37	17:17	19.1	41		S	19	1009.4	18.3	69		SE	20	1006.6	
12	Fr	9.7	21.8	0			SSE	41	20:15	16.7	44		SW	9	1014.9	21.0	41		SE	17	1013.5	
13	Sa	10.9	21.9	0			S	43	10:38	18.8	59		S	30	1023.0	19.7	58		SE	33	1020.7	
14	Su	11.9	21.5	0			S	41	20:11	18.9	59		S	13	1024.8	20.1	58		ESE	13	1021.3	
15	Mo	10.8	20.8	0.2			SSE	37	18:08	16.9	68		SSW	9	1023.7	19.2	61		SE	26	1020.0	
16	Tu	12.2	21.1	0			ESE	28	12:48	18.5	62		S	17	1021.2	19.3	62		ESE	20	1017.8	
17	We	12.4	22.2	0			N	43	23:49	18.7	69		S	9	1020.2	19.1	70		NE	26	1018.0	
18	Th	15.7	21.5	0.4			WNW	59	13:29	19.3	65		NW	26	1014.5	21.0	32		W	24	1011.6	
19	Fr	9.0	21.6	0			WNW	41	13:09	16.0	40		WNW	19	1017.1	20.1	31		W	20	1013.7	
20	Sa	7.9	21.2	0			S	61	15:23	16.4	54		SSW	9	1021.0	19.0	59		S	28	1018.7	
21	Su	12.8	20.4	22.4			SSE	76	14:42	13.8	99		SSW	17	1025.7	18.9	62		SSE	52	1024.5	
22	Mo	13.3	19.8	26.4			SSE	81	14:28	15.9	78		S	39	1028.2	18.3	74		S	50	1026.4	
23	Tu	14.7	20.6	30.8			SSE	93	00:44	19.4	84		SE	46	1026.9	19.8	73		SE	43	1024.8	
24	We	14.6	21.3	2.2			S	61	13:52	18.1	69		S	35	1025.7	20.2	65		SSE	39	1023.1	
25	Th	15.8	22.2	0			S	48	09:09	19.6	67		S	35	1024.9	21.1	70		SSE	22	1022.9	
26	Fr	13.9	22.4	0			ESE	30	14:12	20.9	73		SSE	13	1025.3	21.0	68		ESE	24	1022.3	
27	Sa	16.2	20.1	4.2			NNE	41	18:53	18.0	88		NE	28	1022.4	18.6	100		NE	28	1016.6	
28	Su	15.4	22.6	27.8			SE	35	16:12	20.1	71		Calm		1019.2	20.6	72		SE	24	1016.8	
29	Mo	13.5	24.9	0			N	35	17:51	19.8	70		NW	11	1020.4	23.1	55		NNE	26	1017.2	
30	Tu	14.9	22.1	0.2			N	33	19:03	18.4	82		NNE	20	1020.5	20.6	71		SE	17	1017.5	
31	We	12.6	21.3	11.0			SSE	31	00:01	18.7	69		SSW	6	1022.4	21.0	62		SE	19	1019.9	
Statistics for August 2011																						
Mean		12.5	21.8							18.1	65			16	1021.5	20.3	58			25	1018.6	
Lowest		7.9	19.8							13.8	40			Calm	1009.4	18.3	26		#	13	1006.6	
Highest		16.2	24.9	30.8			SSE	93		20.9	99			SE	46	1029.1	23.1	100		SSE	52	1027.3
Total				125.6																		

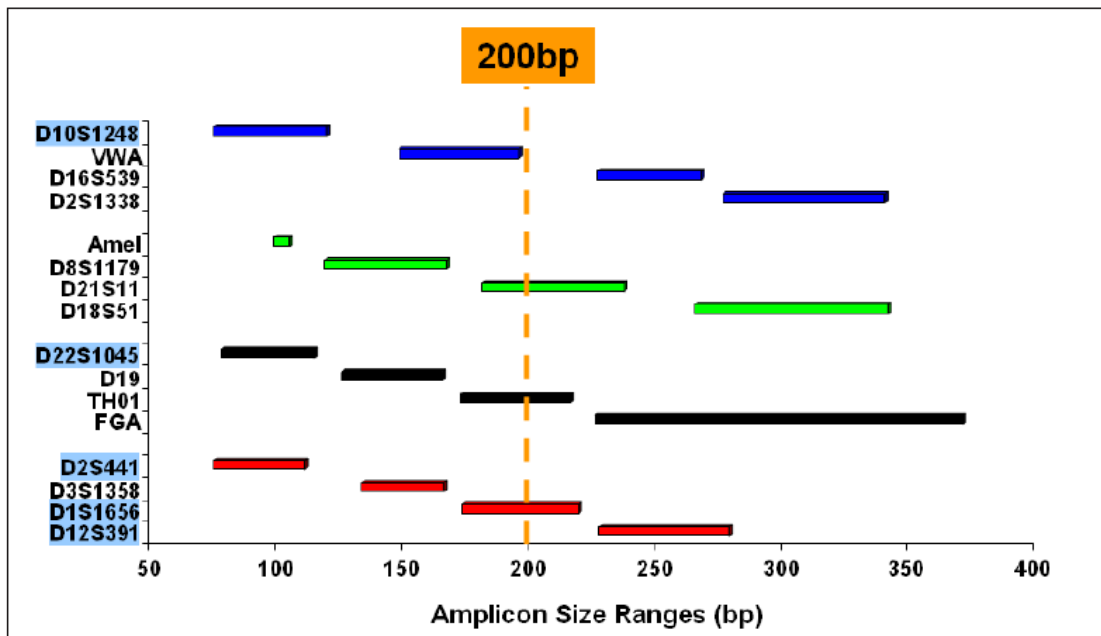
Observations were drawn from Gold Coast Seaway (Station 040764)

The Gold Coast Seaway site is an Automatic Weather Station (AWS) at the northern end of Southport Spit. If you are interested in the southern end of the Gold Coast, see the observations from Coolangubra.

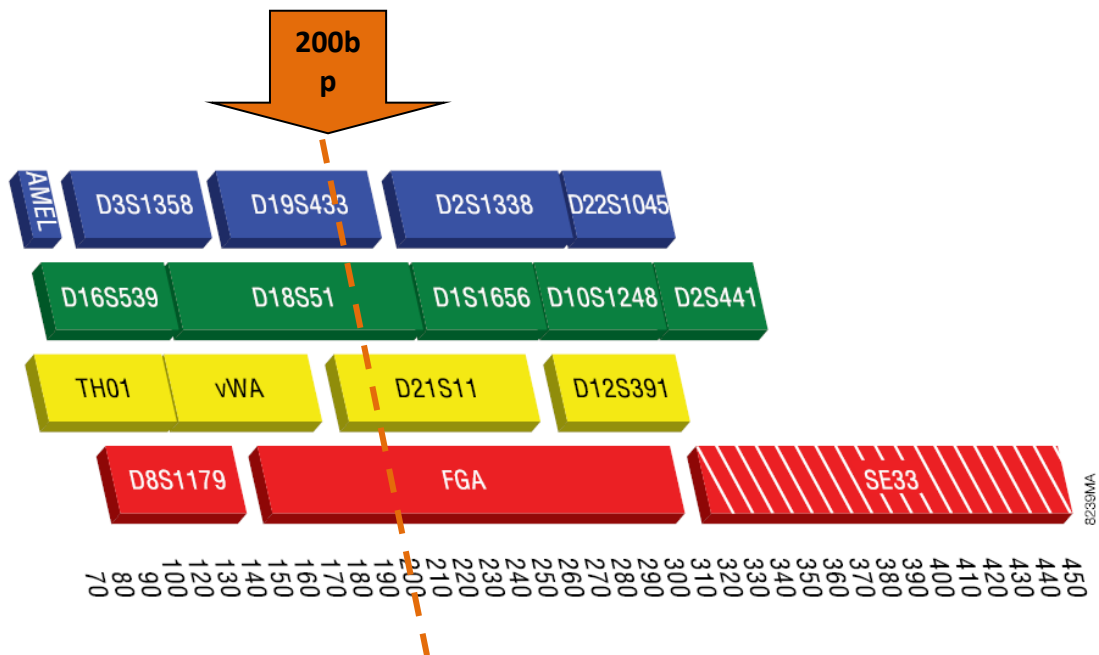
IDCJ.DW000_201108 Prepared at 13:21 GMT on 3 Nov 2011
 Copyright © 2011 Bureau of Meteorology
 Users of this product are deemed to have read the information and accepted the conditions described in the notes at <http://www.bom.gov.au/climate/dwo/IDCJ.DW0000.pdf>

Appendix 4. Forensic STR Amplification Kit Configurations

AmpFISTR® NGM™ (Applied Biosystems)

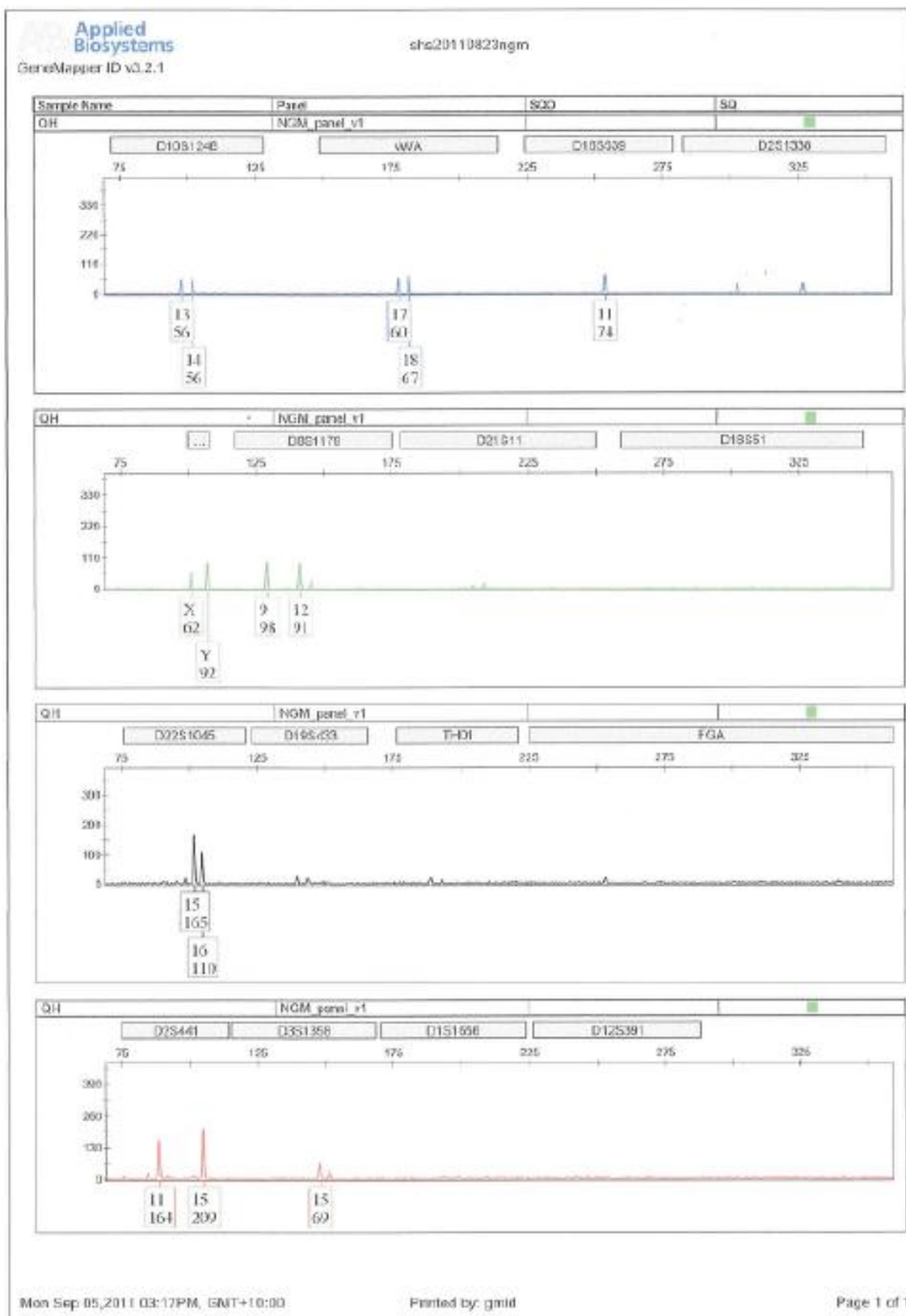


PowerPlex® ESI 16 (Promega)

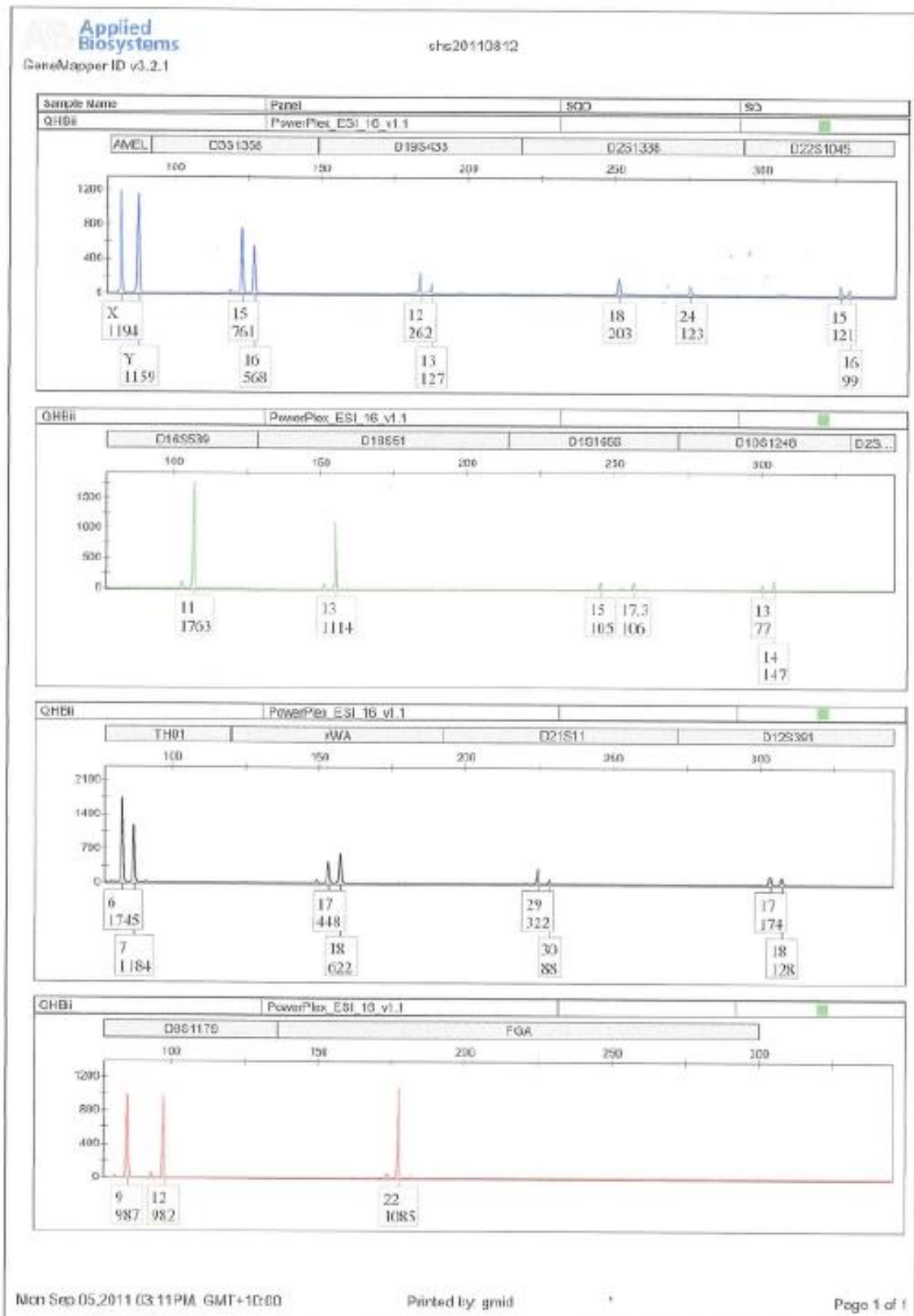


Appendix 5. STR Profiles of the Pandora Remains

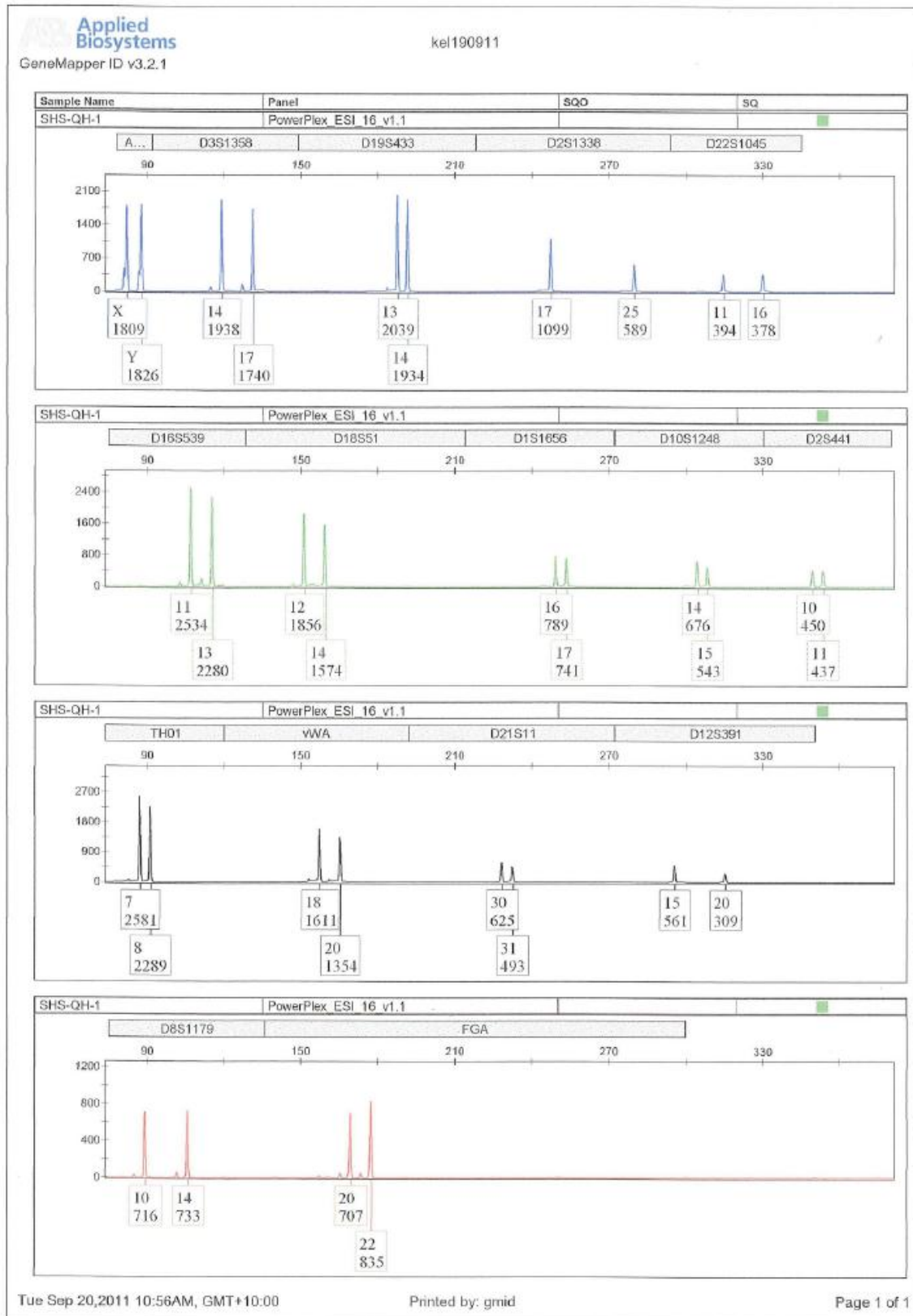
A. STR profile from 'Harry's' bone using the NGM kit



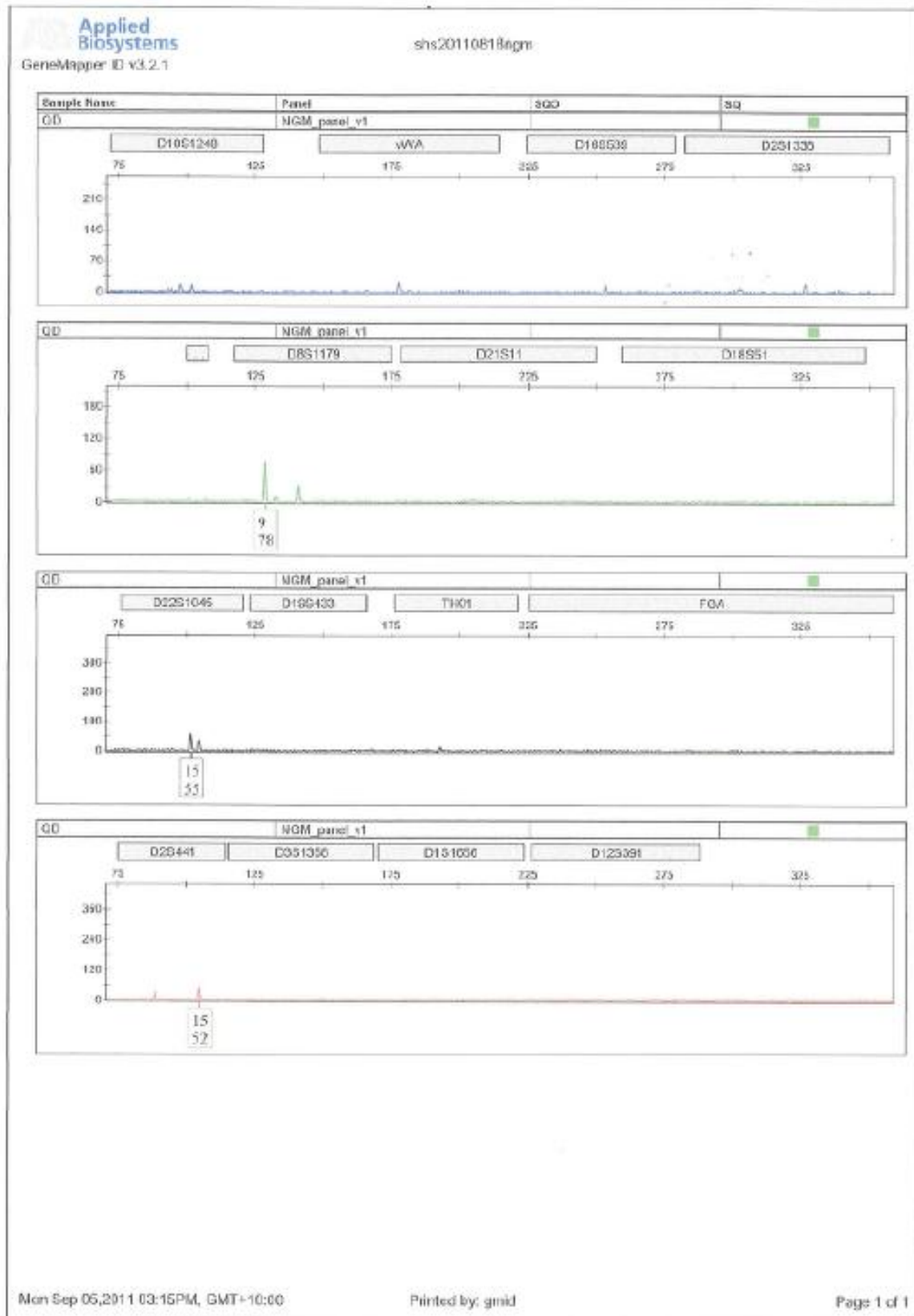
B. STR profile from 'Harry's' bone sample using the Powerplex ESI 16 kit.



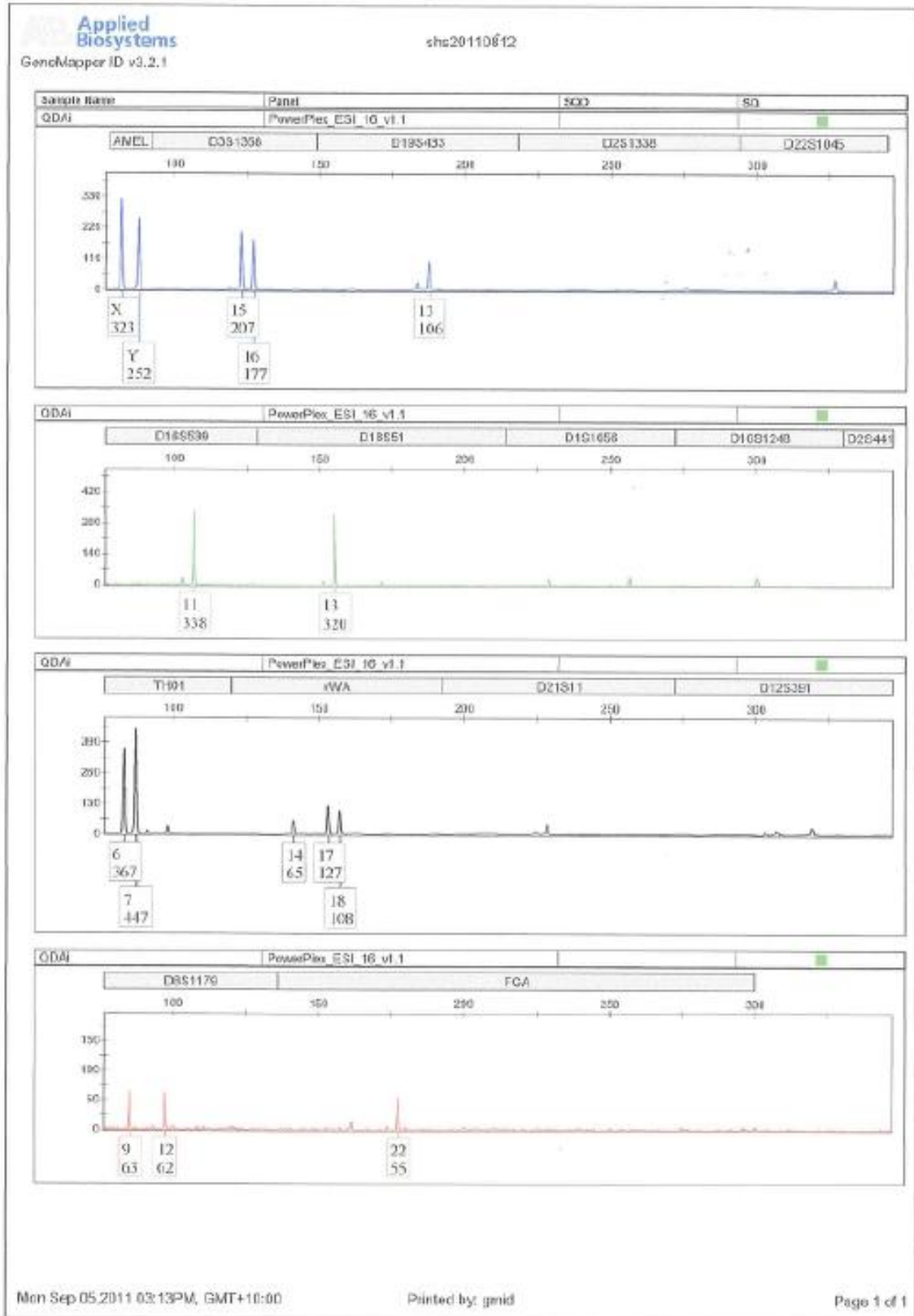
C. STR profile from 'Harry's' tooth using the Powerplex ESI 16 kit



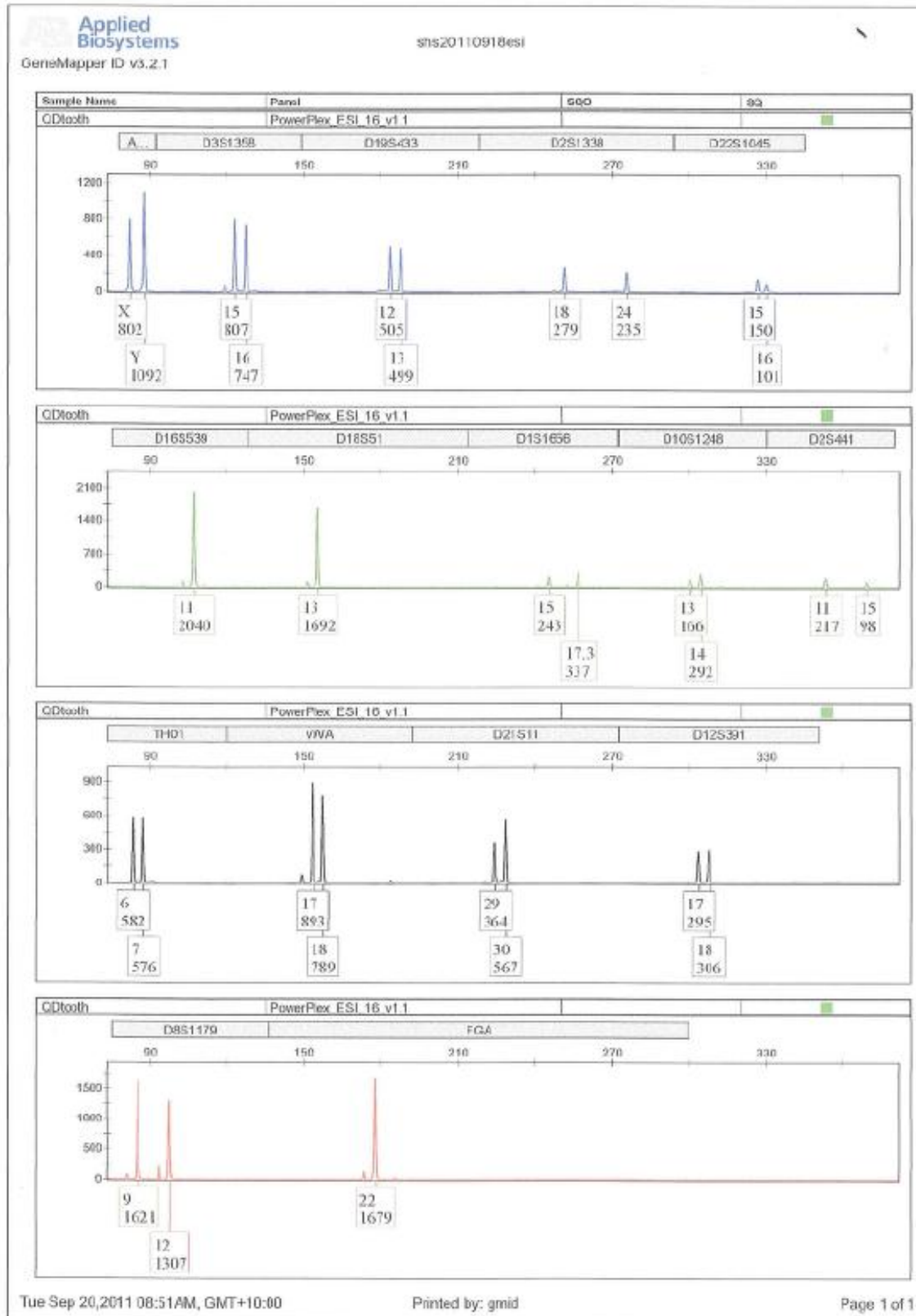
D. STR profile from 'Dick's' bone using the NGM kit



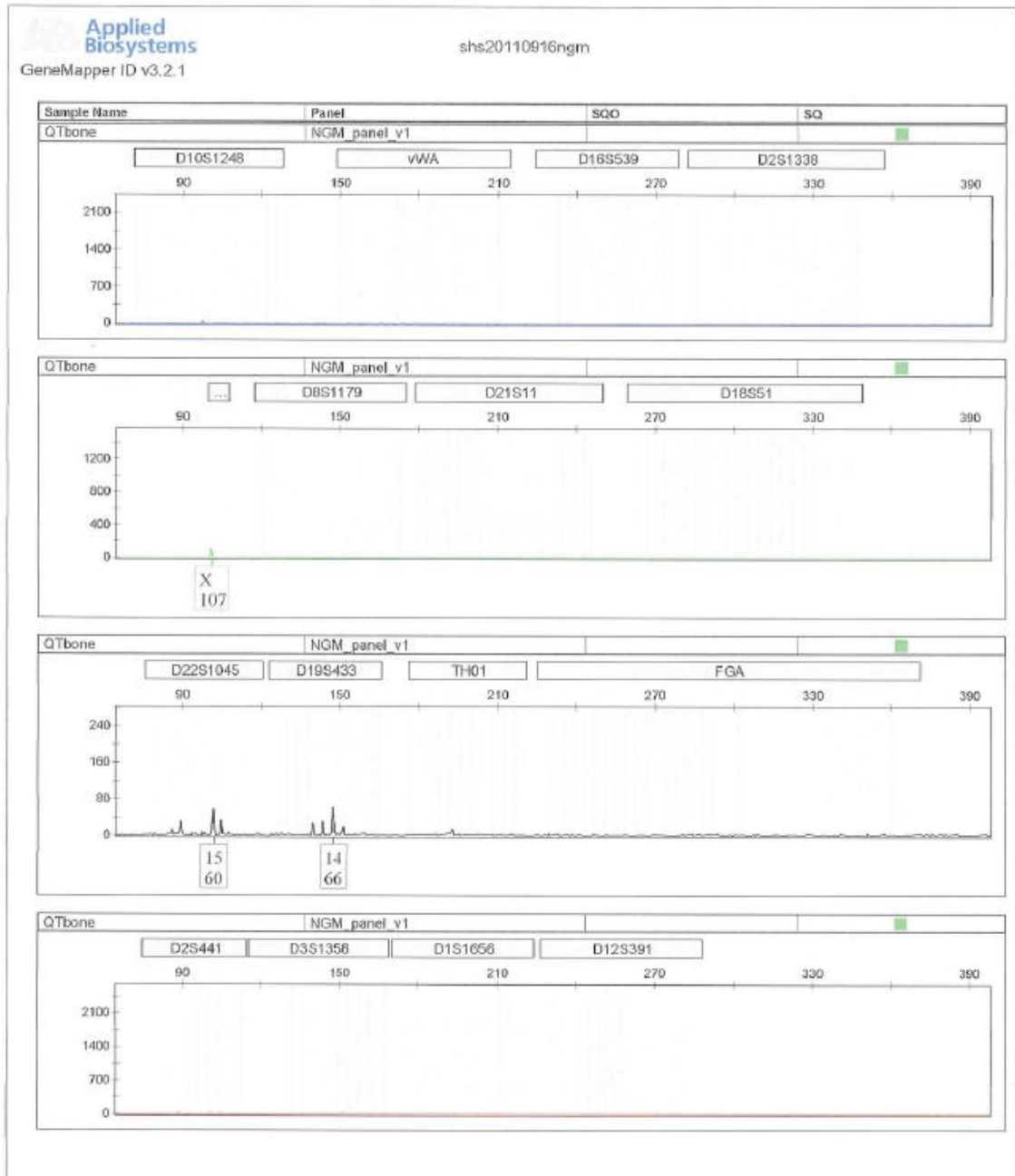
E. STR profile from 'Dick's' bone using the Powerplex ESI 16 kit.



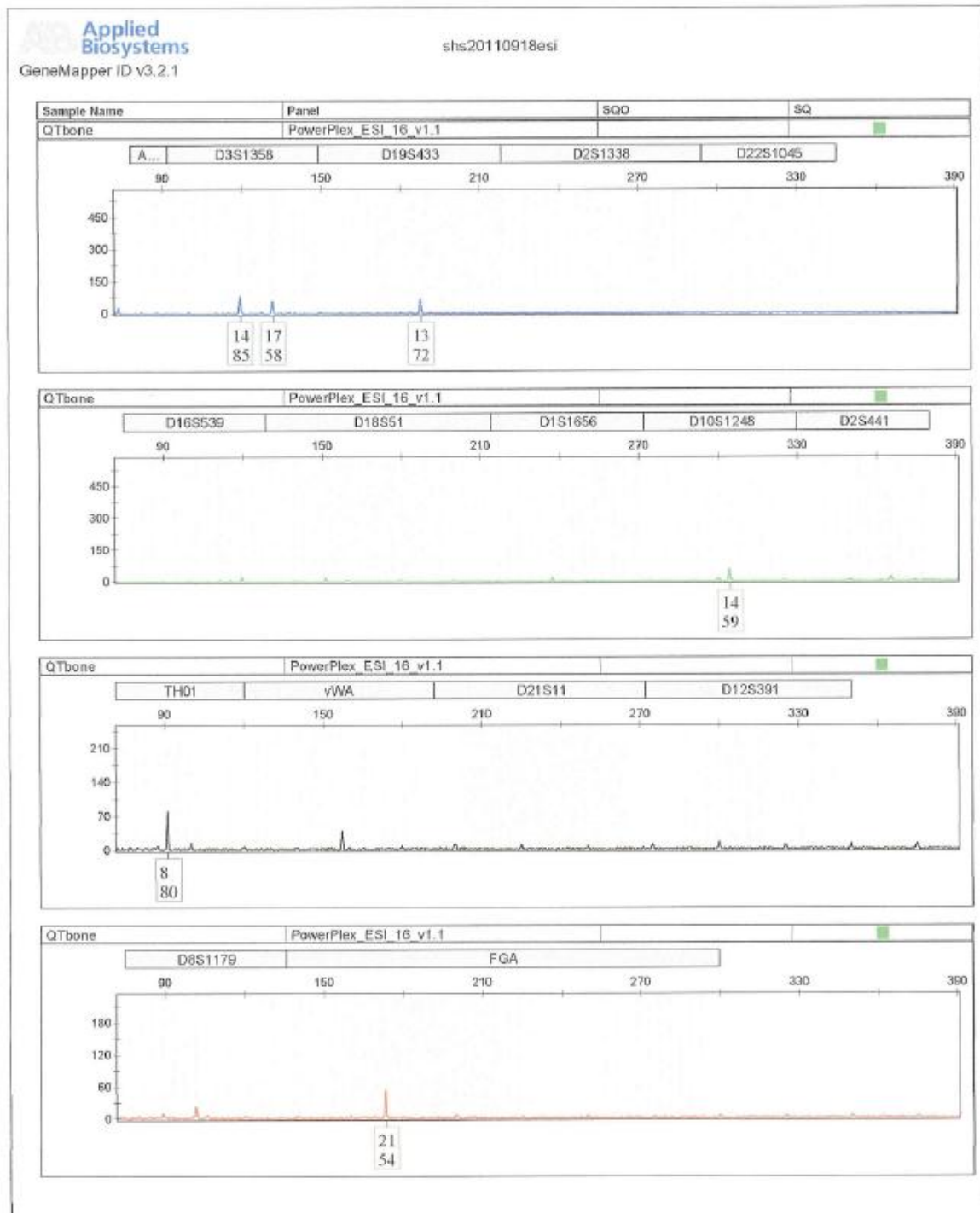
F. STR profile from 'Dick's' tooth using the Powerplex ESI 16 kit



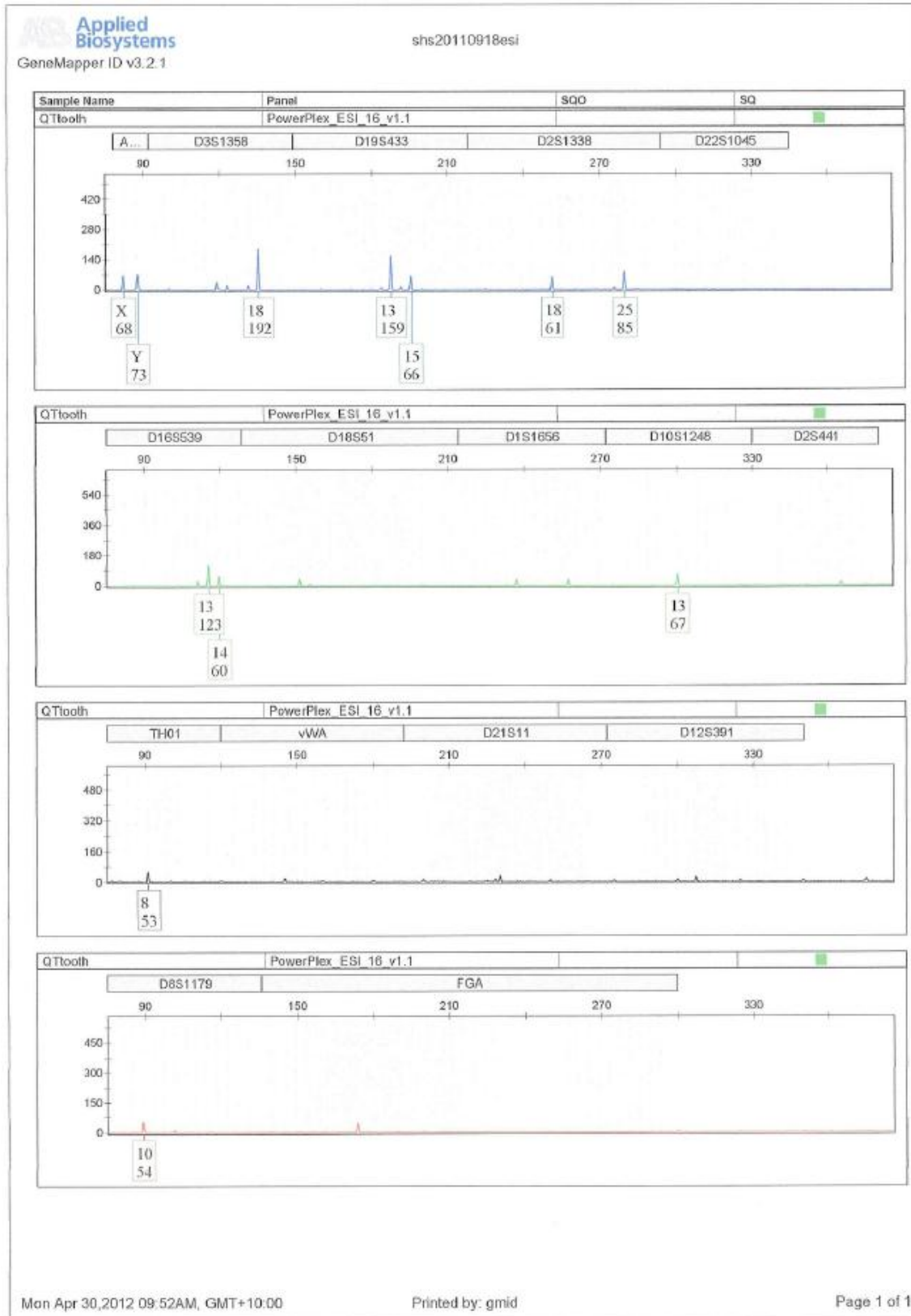
G. STR profile from 'Tom's' bone using the NGM kit.



H. STR profile from 'Tom's' bone using the Powerplex ESI 16 kit.



I. STR profile from 'Tom's' tooth using the Powerplex ESI 16 kit.



**Appendix 6. Volunteer Questionnaire, Consent Form and Explanatory Statement for
Pigmentation Research Project.**



BOND UNIVERSITY

QUESTIONNAIRE

Name: _____
Date of Birth: _____ Email/Phone: _____

Please answer the following questions for your appearance as at about 20 years of age by circling the most appropriate category.

Ancestry	Caucasian	Asian	Indian	Indigenous Australian	African	Other
Ancestry Details						
Face/Head measurements	v-gn (craniofacial height)		eu-eu (head width)		g-op (head length)	
HAIR						
Natural Colour & Shade:	RED	Auburn	Orange	Carrot	Strawberry	
	BLONDE	Light Blonde		Dark Blonde		
	BROWN	Light Brown	Medium Brown	Dark Brown	Brown with red	
	BLACK	Light Black		Dark Black		
	<i>Significant hair colour change from child to adult?</i>			No		Yes
				got much darker		got lighter
Curliness	VERY CURLY	CURLY		HAS BODY		STRAIGHT
Beard	Red	Blonde	Brown	Black	Mixture	
Eyebrows	Red	Blonde	Brown	Black	Mixture	
Grey Hair	Approximate age you commenced going grey?					
Baldness	Approximate age you commenced going bald?					
Was the hair loss	From the crown		From the forehead		Both	
EYES	Eyes lid single/double					
Colour & Shade	BLUE	Light Blue	Medium Blue		Dark Blue	
	GREEN	Light Green	Medium Green		Dark Green	
	GRAY	Light Gray	Medium Gray		Dark Gray	
	HAZEL	Light Hazel	Medium Hazel		Dark Hazel	
	BROWN	Light Brown	Medium Brown		Dark Brown	
SKIN						
Colour & Freckling	FAIR	Extensive Freckling	Medium Freckling	Light Freckling	No Freckling	
	AVERAGE	Extensive Freckling	Medium Freckling	Light Freckling	No Freckling	
	DARK	Olive	Light Brown	Dark Brown	Black	
Ear lobes	attached			non - attached		
Height	Your height (cm or feet, inches)					
Weight	Your current weight (kg or stones, pounds)					
Weight	Your weight at 20-25 years of age (kgs, stones, pounds)					
Have you had any severe facial injuries or facial surgery? If yes, please provide general details.					No	



BOND UNIVERSITY

STATEMENT OF CONSENT

I, (Name, please print) _____

agree to participate in this study.

I have read the attached explanatory information.

I understand that this study will be of no direct benefit to me.

I understand that participation in this study is voluntary and that I am free to withdraw at any time without penalty or comment.

- I am happy for a blood/saliva sample to be taken.
- I am happy for an image of my face to be taken
- I am happy for my sample to be used for other studies in the future.
- I am happy to complete the questionnaire.

Please tick the appropriate boxes.

If you are under 18, a parent/guardian signature is required.

I understand that my anonymity will be strictly preserved and photographs will be used only to classify my facial features and colouring.

Signature of Participant _____

Date _____

Signature of parent/guardian _____



BOND UNIVERSITY

EXPLANATORY STATEMENT

Chief Investigator: Dr Angela van Daal
Faculty of Health Sciences and Medicine
Bond University
Gold Coast
Queensland 4229
Ph: 07 5595 4433
e-mail: avandaal@staff.bond.edu.au

Project Title: Inheritance of complex physical characteristics such as hair colour

Bond University is committed to research in various forms. In order to conduct some research projects biological samples from individuals are required.

This project aims to investigate the inheritance of complex physical characteristics (eg hair colour, height) by analysing genes identified as associated with the particular physical trait. To carry out this research biological samples from individuals of families or groups with a high incidence of the particular physical characteristic are required (eg families containing many individuals with red hair).

Your involvement will be limited to a buccal swab sample (swab from inner cheek) or blood sample. A buccal swab is collected by simply rubbing a cotton bud (or something similar) firmly against the inside of your cheek. This is allowed to dry before placing it in the plastic sleeve. Alternatively or additionally a blood sample will be collected.

If you do not wish your sample to be used for these purposes, then you must not volunteer for this study.

Before signing this consent form you should be aware that your participation is voluntary. If you decide to take part you may also discontinue your participation at any time without comment or penalty.

If you are under 18, a parent/guardian signature is required

The results of this research may be published at a future date. Your anonymity will be preserved.

You may contact the Chief Investigator about any matter of concern (see address and contact details above) should you wish to raise any concern. If you have any concerns about the ethical conduct of this research, please contact the Bond University Human Research Ethics Committee located at Level 2, Central Building, Bond University QLD 4229 Phone: 5595 4194 Fax: 5595 4122 E-mail: buhrec@bond.edu.au

Appendix 7. 96 pigmentation SNPs

SNP	Gene
rs13289	AMACR
rs2238600	AP3D1
rs6152	AR
rs6625163	
rs6058017	ASIP
rs2296151	
rs2424984	
rs1015362	
rs4911414	
rs1325611	DCT
rs1407995	
rs12855916	EDA2R
rs1041668	
rs1385699	
rs1485682	
rs4827380	
rs6918152	EXOC2
rs1268789	FRAS1
rs3810741	GPR143
rs3044	
rs2521667	
rs1667394	HERC2
rs916977	
rs1129038	
rs12913832	
rs2296430	HPS1
rs1894704	HPS4
rs3752589	HPS4
rs3752590	HPS4
rs739289	HPS4
rs2305564	HPS5
rs12203592	IRF4
rs12211228	
rs1540771	
rs4959270	

SNP	Gene	
rs642742	KITLG	
rs3768051	LYST	
rs41273937	MAF	
rs979605	MAOA	
rs3212359	MC1R	
rs3212355		
rs1110400		
rs2228479		
rs3212361		
rs33932559		
rs885479		
rs3212360		
rs1805005		
rs3212357		
rs3212346		
rs11547464		
rs1805008	MYO18A	
rs11080078		
rs1724630		MYO5A
rs4911442		NCOA6
rs10988904		NR4A3
rs4778138		OCA2
rs7495174		
rs4778241		
rs1800410		
rs749846		
rs10852218		
rs1800407		
rs1800411		
rs1800401		
rs11638265		
rs737051	rs1800404	
rs1800404		
rs1900758		

SNP	Gene
rs2180439	PAX1
rs1160312	
rs913063	
rs1998076	
rs6137444	
rs611349	RFXDC1
rs1052206	SILV
rs2402130	SLC24A4
rs12896399	
rs4904868	
rs4904864	SLC24A5
rs1426654	
rs6867641	SLC45A2
rs26722	
rs40132	
rs16891982	
rs35388	
rs35414	STX17
rs10760706	
rs11803731	TCHHL1
rs35264875	TPCN2
rs12821256	
rs1126809	TYR
rs1042602	
rs1408799	TYRP1
rs2733832	
rs683	

Appendix 8. SNP Details and Performance in the 96-Plex Phenotype Assay

SNP	Chr	Coordinate	NCBI_Gene_Id	Gene	Location	Final_Score	Amplicon length (bp)	Minor Allele Frequency	
								Caucasian	African
SNPs to Exclude									
rs1805008	16	88513644	4157	MC1R	coding	0.332	121	0.065	0.042
rs3212359	16	88512677	4157	MC1R	5UTR	0.344	121	0.348	0.457
rs3212355	16	88511878	4157	MC1R	flanking_5UTR	0.362	121	0	0.143
rs1110400	16	88513630	4157	MC1R	coding	0.412	121	0	0
rs2228479	16	88513440	4157	MC1R	coding	0.489	121	0.081	0
rs3212361	16	88512722	4157	MC1R	5UTR	0.622	121	0.239	0.37
rs6867641	5	34021613	51151	SLC45A2	flanking_5UTR	0.837	121	-	-
Poorly Performing SNPs									
rs33932559	16	88513525	4157	MC1R	coding	0.762	93	0	0
rs35264875	11	68602974	219931	TPCN2	coding	0.966	121	-	-
rs6152	X	32314035	367	AR	coding	1.1	121	0.184	0.278
SNPs Requiring Further Investigation									
rs885479	16	88513654	4157	MC1R	coding	0.486	121	0.08	0.042
rs1408799	9	12662096	7306	TYRP1	flanking_5UTR	0.949	121	0.3	0.225
rs3212360	16	88512717	4157	MC1R	5UTR	0.421	121	0	0.022

rs6625163	X	66427708	367	AR	flanking_5UTR	0.994	121	0.202	0
rs12855916	X	65734246	60401	EDA2R	3UTR	0.1	121	0.191	0.377
Well performing SNPs									
rs6058017	20	32320658	434	ASIP	3UTR	0.267	121	0.208	0.478
rs11803731	1	150349948	126637	TCHHL1	flanking_5UTR	0.322	121	0.263	0
rs3810741	X	9693948	4935	GPR143	flanking_5UTR	0.334	121	-	-
rs4778138	15	26009414	4948	OCA2	intron	0.344	121	0.092	0.267
rs2402130	14	91870955	123041	SLC24A4	intron	0.352	121	0.167	0.333
rs1800410	15	25903778	4948	OCA2	intron	0.491	121	0.095	0.322
rs1805005	16	88513344	4157	MC1R	coding	0.531	121	0.1	0
rs3212357	16	88512104	4157	MC1R	flanking_5UTR	0.554	121	0.452	0.009
rs2180439	20	21801099	5075	PAX1	flanking_3UTR	0.58	121	0.408	0.442
rs1426654	15	46213775	283652	SLC24A5	coding	0.628	121	0	0.025
rs1667394	15	26203776	8924	HERC2	intron	0.65	121	0.133	0.05
rs1800401	15	25933647	4948	OCA2	coding	0.698	121	0.04	0.021
rs3212346	16	88509858	4157	MC1R	flanking_5UTR	0.703	121	0.075	0.425
rs4911442	20	32818706	23054	NCOA6	intron	0.763	121	0.07	0
rs7495174	15	26017832	4948	OCA2	intron	0.769	121	0.05	0.15
rs11547464	16	88513591	4157	MC1R	coding	0.778	121	0	0
rs4778241	15	26012307	4948	OCA2	intron	0.778	121	0.125	0.383
rs1052206	12	54634294	6490	SILV	coding	0.787	121	0.192	0.492

rs26722	5	33999626	51151	SLC45A2	coding	0.791	121	0	0.05
rs642742	12	87823876	728084	LOC728084	flanking_3UTR	0.794	121	0.136	0.078
rs41273937	9	101753252	55014	STX17		0.798	121	-	-
rs11080078	17	24480380	399687	MYO18A	intron	0.81	121	-	-
rs40132	5	33986459	51151	SLC45A2	intron	0.812	121	0	0.079
rs16891982	5	33987449	51151	SLC45A2	coding	0.818	121	0.017	0
rs916977	15	26186958	8924	HERC2	intron	0.818	121	0.125	0.217
rs1129038	15	26030453	8924	HERC2	3UTR	0.819	121	0.24	-
rs749846	15	25942584	4948	OCA2	intron	0.824	121	0.125	0.217
rs3044	X	9653651	4935	GPR143	3UTR	0.849	121	0.233	0.195
rs35388	5	34019126	51151	SLC45A2	intron	0.855	121	0.35	0.275
rs1126809	11	88657608	7299	TYR	coding	0.859	121	0.396	0.065
rs12896399	14	91843415	123041	SLC24A4	flanking_5UTR	0.873	121	0.4	0.008
rs611349	6	117354910	222546	RFXDC1	coding	0.879	121	0.2	0.283
rs10852218	15	25905387	4948	OCA2	intron	0.887	121	0.142	0.433
rs4904868	14	91850753	123041	SLC24A4	flanking_5UTR	0.894	121	0.308	0.2
rs1160312	20	21998502	5075	PAX1	flanking_3UTR	0.9	121	0.458	0.208
rs12913832	15	26039212	8924	HERC2	intron	0.901	121	0.208	0
rs1800411	15	25885515	4948	OCA2	coding	0.904	121	0.375	0.227
rs35414	5	34005384	51151	SLC45A2	intron	0.905	121	0.308	0
rs2305564	11	18274033	11234	HPS5	intron	0.91	121	0.367	0.3
rs3768051	1	233926336	1130	LYST	intron	0.912	121	0.117	0.058

rs11638265	15	25876167	4948	OCA2	intron	0.925	121	-	-
rs12203592	6	341320	3662	IRF4	intron	0.927	121	0.167	0
rs1724630	15	50495291	4644	MYO5A	intron	0.937	121	0.273	0.378
rs913063	20	21990417	5075	PAX1	flanking_3UTR	0.938	121	0.458	0.331
rs10988904	9	101635505	8013	NR4A3	coding	0.94	121	-	-
rs1540771	6	411032	730077	LOC730077	flanking_3UTR	0.957	121	0.425	0.05
rs737051	15	25599430	4948	OCA2	flanking_3UTR	0.958	121	0.208	0.039
rs1042602	11	88551343	7299	TYR	coding	0.959	121	0.417	0
rs12211228	6	353832	3662	IRF4	3UTR	0.966	121	-	-
rs4904864	14	91834271	123041	SLC24A4	flanking_5UTR	0.972	121	0.225	0.4
rs2238600	19	2091033	8943	AP3D1	intron	0.973	121	0.009	0
rs1268789	4	79499716	80144	FRAS1	intron	0.982	103	0.309	0.296
rs1015362	20	32202272	729547	LOC729547	flanking_3UTR	0.983	121	0.233	0.167
rs13289	5	34022165	23600	AMACR	flanking_3UTR	0.984	121	0.317	0.267
rs12821256	12	87852465	728084	LOC728084	flanking_3UTR	0.994	121	0.142	0
rs1041668	X	66682351	60401	EDA2R	flanking_5UTR	1.1	121	0.117	0
rs10760706	9	101763512	55014	STX17	intron	1.1	121	0.325	0.267
rs1325611	13	93892385	1638	DCT	intron	1.1	121	0.142	0.192
rs1385699	X	65741710	60401	EDA2R	coding	1.1	121	0.211	0
rs1407995	13	93894013	1638	DCT	intron	1.1	121	0.142	0.192
rs1485682	X	65732315	60401	EDA2R	3UTR	1.1	121	0.183	0.35
rs1800404	15	25909367	4948	OCA2	coding	1.1	121	0.136	0.092

rs1800407	15	25903912	4948	OCA2	coding	1.1	121	0.097	0
rs1894704	22	25183904	89781	HPS4	coding	1.1	121	0.05	0.275
rs1900758	15	25903691	4948	OCA2	intron	1.1	121	0.233	0.11
rs1998076	20	21828044	5075	PAX1	flanking_3UTR	1.1	121	0.408	0.2
rs2296151	20	32311878	434	ASIP	coding	1.1	121	0	0
rs2296430	10	100185572	3257	HPS1	intron	1.1	121	0.293	0.433
rs2424984	20	66002680	434	ASIP	intron	1.1	121	-	-
rs2521667	X	9690837	4935	GPR143	intron	1.1	121	0.222	0.044
rs2733832	9	12694724	7306	TYRP1	intron	1.1	121	0.438	0.196
rs3752589	22	25177585	89781	HPS4	3UTR	1.1	121	0.042	0.267
rs3752590	22	25177811	89781	HPS4	3UTR	1.1	121	0	0
rs4827380	X	65734464	60401	EDA2R	3UTR	1.1	121	0.211	0.356
rs4911414	20	32193104	729547	LOC729547	flanking_3UTR	1.1	121	0.275	0.133
rs4959270	6	402747	730077	LOC730077	flanking_5UTR	1.1	121	0.455	0.217
rs6137444	20	21733638	5075	PAX1	flanking_3UTR	1.1	121	0.342	0.242
rs683	9	12699304	7306	TYRP1	3UTR	1.1	121	0.396	0.217
rs6918152	6	487158	642335	LOC642335	flanking_5UTR	1.1	121	0.405	0.112
rs739289	22	25192152	89781	HPS4	intron	1.1	121	0.083	0.342
rs979605	X	43486306	4128	MAOA	intron	1.1	121	0.233	0.35

Appendix 9. The SNPs showing statistical association (p-value <0.5) for each trait

I = Included in the model, N = Not included in the Model, Excluded = Removed from statistical analysis due to >5% missing data

Ancestry

	SNP	p-value	Model
Caucasian	rs16891982	7.21E-08	I
	rs1800407	1.40E-04	Excluded
	rs1426654	0.005	Excluded
	rs916977	0.006	N
	rs1667394	0.014	I
	rs3212355	0.029	Excluded
	rs1325611	0.030	N
	rs1042602	0.035	I
	rs1407995	0.035	N
	rs4911442	0.047	I
	rs737051	0.051	N
African American	rs4827380	2.20E-05	Excluded
	rs1485682	5.51E-04	Excluded
	rs1998076	0.001	N
	rs26722	0.024	N
	rs1015362	0.027	N
	rs3212360	0.035	Excluded
Hispanic	rs1805008	1.13E-05	Excluded
	rs3212355	8.03E-05	Excluded
	rs35264875	1.34E-04	N
	rs40132	4.40E-04	I
	rs2424984	0.002	Excluded
	rs4827380	0.002	Excluded
	rs12913832	0.003	N
	rs1540771	0.003	I
	rs1268789	0.005	I
	rs3768051	0.005	N
	rs611349	0.006	N
	rs2521667	0.008	N
	rs1052206	0.014	I
	rs2228479	0.017	Excluded
	rs3752589	0.018	I
	rs13289	0.031	N
	rs6058017	0.034	I
	rs4959270	0.041	N
rs6918152	0.043	N	
rs3212359	0.044	Excluded	
rs6625163	0.049	Excluded	

Eye Colour

	SNP	p-value	Model
Blue Eyes	rs1129038	3.29E-09	I
	rs12913832	1.63E-04	N
Brown Eyes	rs1129038	7.45E-07	I
	rs12913832	3.24E-05	N
	rs16891982	8.40E-04	I
	rs1800411	0.003	N
	rs11638265	0.006	N
	rs1800407	0.007	Excluded
	rs13289	0.009	N
	rs35388	0.022	N
	rs1408799	0.041	Excluded
Hazel Eyes	rs1129038	2.64E-08	N
	rs12913832	5.23E-07	I
	rs11547464	0.005	N
	rs1426654	0.010	Excluded
	rs683	0.020	I
	rs4904868	0.031	N
	rs885479	0.046	Excluded
	rs737051	0.048	N
	rs1998076	0.049	N
	rs2180439	0.050	N
Green Eyes	rs12896399	0.001	I
	rs12913832	0.004	I
	rs1129038	0.009	N
	rs11638265	0.013	N
	rs1800411	0.015	N
	rs1800404	0.018	Excluded
	rs4904868	0.032	N
	rs1110400	0.046	Excluded

Skin Colour

	SNP	p-value	Model
Dark Skin	rs16891982	4.44E-08	I
	rs7495174	0.002	I
	rs26722	0.003	I
	rs3212355	0.004	N
	rs1800410	0.006	I
	rs3752590	0.012	N
	rs12896399	0.031	N
	rs1800411	0.033	N
	rs6867641	0.035	Excluded
	rs916977	0.056	N
Fair Skin	rs16891982	0.030	I
Olive Skin	rs1805005	0.012	N
	rs16891982	0.014	I
	rs12211228	0.025	N
	rs6058017	0.029	N
	rs3752590	0.048	I
Average Skin	rs1900758	0.026	N
	rs6137444	0.033	N
	rs12203592	0.050	N
	rs2238600	0.052	I

Hair Colour

	SNP	p-value	Model
Black Hair	rs16891982	1.26E-07	Y
	rs33932559	0.001	N
	rs3212355	0.003	N
	rs1667394	0.011	N
	rs1800401	0.014	N
	rs1805008	0.021	Excluded
	rs1800411	0.023	N
	rs11547464	0.025	N
	rs916977	0.029	N
	rs3212359	0.031	Excluded
	rs1800407	0.035	Excluded
Brown Hair	None		
Blonde Hair	None		
Red Hair	None		

Appendix 10. Nagelkerke R² values of the SNP Predictive Models for each Trait

Ancestry

	SNP	Nagelkerke R ²	SNP significance in model
African American	rs1385699	.518	1.69E-07
	rs16891982	.712	1.86E-05
	rs6058017	.763	1.05E-06
	rs642742	.804	9.31E-05
	rs2402130	.830	9.53E-05
	rs6918152	.849	.008
	rs737051	.861	.004
	rs739289	.868	.026
	rs1724630	.874	.029
Caucasian	rs16891982	.733	6.31E-11
	rs1129038	.783	.026
	rs3752589	.808	.001
	rs642742	.823	.001
	rs3044	.835	.009
	rs4904868	.844	.001
	rs4911442	.853	.003
	rs3212357	.861	.019
	rs3829241	.867	.021
	rs2238600	.870	.013
	rs1667394	.875	.017
	rs683	.878	.053
	rs1126809	.881	.020
	rs1042602	.885	.027
Hispanic	rs40132	.222	4.19E-10
	rs6058017	.300	1.16E-06
	rs1129038	.362	5.57E-08
	rs3752589	.398	2.15E-05
	rs4778138	.441	.014
	rs1268789	.470	2.74E-05
	rs10760706	.494	.001
	rs1998076	.519	.002
	rs4904868	.537	.002
	rs737051	.552	.036
	rs1540771	.566	.009
	rs12821256	.581	.008
	rs4911442	.598	.018
	rs683	.610	.021
	rs2296430	.620	.007
	rs1052206	.627	.009
	rs2238600	.637	.024
rs1800401	.647	.027	

Eye Colour

	SNP	Nagelkerke R Square	SNP significance in model
Blue Eyes	rs1129038	.489	7.37E-06
	rs4904868	.532	1.65E-04
	rs16891982	.570	0.001
	rs916977	.591	0.014
	rs1998076	.602	0.042
	rs35264875	.610	0.050
Hazel Eyes	rs683	.096	6.05E-04
	rs12913832	.159	1.03E-08
	rs16891982	.205	0.003
	rs1667394	.237	.016
	rs7495174	.262	.022
	rs35264875	.279	.051
Brown Eyes	rs1129038	0.525	4.17E-09
	rs16891982	0.615	2.98E-07
	rs749846	0.63	0.007
	rs1126809	0.64	0.035
	rs12211228	0.648	0.023
	rs737051	0.655	0.050
Green Eyes	rs12913832	.142	3.68E-06
	rs12896399	.193	.001
	rs1724630	.222	.015

Skin Colour

	SNP	Nagelkerke R ²	SNP significance in model
Fair Skin	rs16891982	.361	5.66E-06
	rs33932559	.380	.999
	rs916977	.401	.015
	rs40132	.414	.022
	rs4911414	.428	.018
	rs12896399	.440	.006
	rs10988904	.451	.025
	rs1126809	.460	.033
Average Skin	rs26722	.111	4.41E-08
	rs1385699	.179	.001

	rs7495174	.220	.007
	rs642742	.241	.002
	rs16891982	.261	.002
	rs4911442	.273	.037
	rs2238600	.287	.035
Olive Skin	rs16891982	.248	7.29E-07
	rs3752590	.269	.017
	rs40132	.288	.012
	rs3212357	.310	.001
	rs10988904	.326	.012
	rs2305564	.341	.008
	rs1407995	.352	.014
	rs737051	.362	.025
	rs6137444	.372	.030
	rs749846	.382	.041
Dark Skin	rs16891982	.589	1.87E-04
	rs1385699	.703	.011
	rs1129038	.771	9.52E-06
	rs1800410	.801	6.34E-05
	rs642742	.823	.002
	rs3752589	.842	.003
	rs7495174	.852	2.73E-05
	rs2238600	.863	.013
	rs1126809	.869	.014
	rs4778138	.876	.005
	rs13289	.880	.045
	rs3212357	.886	.006
	rs979605	.891	.021
	rs611349	.896	.003
	rs1015362	.901	.001
	rs4911414	.906	.026
	rs3044	.911	.020
	rs4904868	.913	.027
	rs10760706	.917	.055

Hair Colour

	SNP	Nagelkerke R Square	SNP significance in model
Blonde Hair	rs12913832	.249	3.48E-04
	rs16891982	.315	.001
	rs12203592	.382	4.64E-05
	rs13289	.398	.012
	rs916977	.422	.019
	rs1805005	.436	.040
Brown Hair	rs16891982	.340	7.53E-09
	rs1385699	.354	.022
	rs1407995	.366	.015
	rs683	.376	.023
	rs35264875	.386	.026
	rs1805005	.395	.027
	rs6058017	.403	.047
Black Hair	rs16891982	.737	2.58E-09
	rs1129038	.775	3.77E-04
	rs3212357	.789	.001
	rs1042602	.799	.008
	rs12203592	.806	.007
	rs1385699	.813	.034
	rs2238600	.819	.023
	rs4911414	.825	.003
	rs1015362	.830	.034
	rs1407995	.835	.043
Red Hair	rs1129038	.150	.001
	rs16891982	.231	.992
	rs12913832	.269	.007
	rs1052206	.290	.037
	rs4904868	.311	.037

Appendix 11. SNPs previously identified in literature as most closely related to pigmentation phenotypes and ancestry.

SNP	Gene	Eye Colour									Ancestry	96-plex ¹¹	Predictive Model ¹²
		Liu Rank ¹	Ruiz <i>et al.</i> ²	Mengel-From <i>et al.</i> ³	Walsh <i>et al.</i> ⁴	Spichenok <i>et al.</i> ⁵	Sulem <i>et al.</i> ⁶	Valenzuela <i>et al.</i> ⁷	Kasteli & Drobnic ⁸	Walsh <i>et al.</i> ⁹	Phillips Rank ¹⁰		
rs1800407	OCA2		X	X	X				X	X		I	Excluded
rs12896399	SLC24A4	3	X		X		X			X		I	Green eyes Fair skin
rs1393350	TYR	5	X		X		X		X	X		N	N/A
rs12913832	HERC2	1	X	X	X	X		X	X	X	9	I	Hazel and Green, Blonde and Red Hair
rs16891982	SLC45A2	4	X	X	X	X		X	X	X	2	I	Brown, Blue and Hazel eyes, All skin colours, All Hair Colours, AA and Caucasian
rs12203592	IRF4	6	X		X	X				X		I	Black and Blonde Hair
rs885479	MC1R					X				X		I	Excluded
rs6119471	ASIP					X						N	N/A
rs1545397	OCA2					X						N	N/A

rs1426654	SLC24A5					X		X	X		1	I	None
rs12821256	KITLG						X		X			N	N/A
rs1540771	IRF4/6p2 5.3						X					I	Hispanic
rs1042602	TYR						X		X			I	Caucasian
rs1667394	HERC2	9	X				X		X			N	N/A
rs7495174	OCA2	8					X		X			I	Hazel eyes, Average and Dark skin
rs1805008	MC1R		X				X		X	X		I	Excluded
rs1805007	MC1R						X	X		X		N	N/A
rs1129038	HERC2		X	X					X			I	Blue and brown eyes, Dark skin, Caucasian and Hispanic
rs7170989	OCA2								X			N	N/A
rs1805005	MC1R								X	X		I	Blonde and Brown hair
rs2424984	ASIP							Y				I	Excluded
rs11636232	HERC2		X	X								N	N/A
rs916977	HERC2	10	X	X								I	Blue eyes, Fair Skin
rs2238289	HERC2			X								N	N/A
rs7170852	HERC2			X								N	N/A
rs1800401	OCA2			X								I	Hispanic
rs12592730	HERC2	7	X									N	N/A
rs1408799	TYRP1	12	X									I	Excluded

rs4778232	OCA2	11	X									N	N/A
rs6058017	ASIP	14	X									I	Brown eyes, AA and Hispanic
rs683	TYRP1	15	X						X			I	Hazel eyes, Brown Hair, Caucasian and Hispanic
rs26722	SLC45A2		X									I	Average and Dark skin
rs4778138	OCA2		X									I	Dark Skin, Hispanic
rs4778241	OCA2		X									I	None
rs1015362	ASIP		X									I	Dark Skin, Black Hair
rs7183877	HERC2		X									N	N/A
rs11547464	MC1R								X			I	None
rs1805006	MC1R								X			N	N/A
rs1805009	MC1R								X			N	
rs2228479	MC1R								X			I	Excluded
rs1110400	MC1R								X			I	Excluded
rs28777	SLC45A2								X			N	N/A
rs4959270	EXOC2								X			N	
rs2402130	SLC24A4								X			I	African American
Y152OCH	MC1R								X			N	N/A
N29insA	MC1R								X			N	
rs2378249	ASIP/PIG U								X			N	

rs8024968	OCA2		X									N
rs1375164	OCA2		X									N
rs2814778	DARC									3		N
rs182549	MCM6									4		N
rs4540055	TLR1									5		N
rs881929	ZNF668									6		N
rs239031	LINC0047 8									7		N
rs2065982	LINC0047 8									8		N
rs3785181	GAS8									10		N

¹ [155, 373] Ranked from most informative 1 to 15

² [155]

³ [154]

⁴ IrisPlex [158, 159]

⁵ [161, 162]

⁶ [141, 161]

⁷ [163]

⁸ [374]

⁹ HIrisPlex [160]

¹⁰ [135] The 10 most informative SNPs from the 34-plex assay (Ranked 1 to 10)

¹¹ The 96-plex SNP panel used in this study to predict phenotype and ancestry. I = SNP was included in the assay, N = SNPs (highlighted in red) were not included in the assay.

¹² The statistical models in which a particular SNP was included for phenotype prediction in this study. Excluded = SNPs removed from statistical analysis (highlighted yellow) due to >5% missing data.